



UNIVERSITÀ
DEGLI STUDI
DI PALERMO



Università degli Studi di Palermo
Dottorato in
Scienze Molecolari e Biomolecolari
Dipartimento STEBICEF
S.S.D. -- Chim/08

Westfälische Wilhelms-Universität Münster
PhD in
Pharmaceutical and Medicinal Chemistry
Department of
Pharmaceutical and Medicinal Chemistry

“Stereoselective Synthesis and Pharmacological Evaluation of
2,4-Bridged Piperidine Derivatives Designed to Activate the
 κ -Opioid Receptor”

PhD STUDENT
HENDRIK JONAS

COORDINATOR
PROF. PATRIZIA DIANA

TUTOR
PROF. PATRIZIA DIANA

TUTOR
PROF. DR. BERNHARD WÜNSCH
PROF. DR. MATTHIAS LEHR

CICLO XXXIII

2021

Pharmaceutical and Medicinal Chemistry

Pharmazeutische und Medizinische Chemie

**Stereoselective Synthesis and Pharmacological Evaluation of
2,4-Bridged Piperidine Derivatives Designed to Activate the
 κ -Opioid Receptor**

Inaugural-Dissertation

to obtain the Doctoral degree in

“Science Molecolari e Biomolecolari”

from the Faculty of Pharmacy

of the Università degli Studi di Palermo

and

zur Erlangung des Doktorgrades

der Naturwissenschaften im Fachbereich Chemie und Pharmazie

der Mathematisch-Naturwissenschaftlichen Fakultät

der Westfälischen Wilhelms-Universität Münster

vorgelegt von

Hendrik Jonas

aus Ochtrup

2021

For the Università degli Studi di Palermo

Rector: Prof. Fabrizio Micari

First supervisor: Prof.ssa Patrizia Diana

For the Westfälische Wilhelms-Universität

Dekan: Prof. Dr. Joachim Jose

Erster Gutachter: Prof. Dr. Bernhard Wunsch

Zweiter Gutachter: Prof. Dr. Matthias Lehr

Tag der mündlichen Prüfung: 29. September 2021

Tag der Promotion:

Parts of this work have been already published.

Conference contribution:

H. Jonas, B. Wunsch, P. Diana.

Synthesis of novel bicyclic KOR ligands with piperidine substructure.

DPHG Annual Meeting 2019, Heidelberg, Germany. (Poster presentation)

H. Jonas, B. Wunsch, P. Diana.

Chiral pool synthesis of KOR agonists with 2-azabicyclo[3.2.1]octane scaffold.

Frontiers in Medicinal Chemistry 2021, Darmstadt (online), Germany. (Poster presentation)

I have completed this work at the Institut für Pharmazeutische und Medizinische Chemie, Westfälische Wilhelms-Universität Münster and at the department of Scienze e Tecnologie Biologiche Chimiche e Farmaceutiche, Università degli Studi di Palermo under the supervision of

Herrn Prof. Dr. Bernhard Wunsch

I would like to extend my sincere gratitude to him for giving me the chance to be a member of his great research group. Without his patience, brilliant ideas, constant motivation and support this work would not have been achievable. His guidance, encouragement and optimism motivated me to become a thorough and conscientious scientist.

and

Prof.ssa Dr. Patrizia Diana

I would like to extend my earnest gratitude to her for giving me the chance to be a part of her research group. I thank her for the tremendous academic support and providing me with intellectual freedom in my work. Without her support, commitment and patience this work would not have been achievable.

Mein besonderer Dank gilt:

- **Prof. Matthias Lehr** für die freundliche Übernahme des Koreferats.
- **Dr. Jens Köhler, Claudia Thier** und **Thomas Meiners** für die Aufnahmen der NMR Spektren, besonders **Dr. Jens Köhler** für die NOESY Langzeitmessungen und die Reperaturen an der HPLC Anlage.
- **Bastian Frehland** für die Durchführung der Rezeptor-Bindungsstudien und **Dr. Dirk Schepmann** für die Auswertung und Diskussion der Ergebnisse.
- **Dr. Constantin Daniliuc** für die Anfertigung der Röntgenstrukturanalysen.
- **Dr. Jörg Fabian** und **Thomas Meiners** für die Aufnahmen der Massespektren.
- **Kirstin Lehmkuhl** für die durchführung der Reinheitsbestimmungen, die Bestellungen von Chemikalien, die Hilfestellung beim Umgang mit der chiralen HPLC und die schöne Zeit in ihrem Büro während meiner Schreibphase.
- **Laura Prause, Sarah Berling** und **Dr. Peter Dziemba** für die organisatorische Unterstützung, besonders **Laura Prause** für die vielen Gespräche zwischendurch.
- **Sarah Maskri** für die Berechnungen der Diederwinkel, sowie **Janosch Menke** für seine Fähigkeiten in der Statistik.
- **Ulrich Heczko** und **Alfred Gerber** für die unterhaltsamen Einkäufe in der Chemikalien- und Glasausgabe.
- **Michael Janning, Helmut Gausepohl, Christoph Kozjan, Annemarie Erdt, Karsten Suwelack** und **Heribert Wennemer** für die schnelle und kompetente Hilfe bei allen handwerklichen Belangen.
- **Elena Bechthold** für ihre Hilfe beim Auswerten der pharmakologischen Daten.
- **Ruben Steigerwald, Tobias Winge, Dr. Daniele Aiello, Marvin Korff,** und **Lukas Imberg** für die gewissenhafte Durchsicht dieser Arbeit und die vielen nützlichen Vorschläge.
- dem Labor 336: **Dr. Donglin Gao** – meinem Kappa-Mitstreiter - für die lustige Zeit im Labor, die langen Radtouren während der Pandemie, sowie den interkulturellen sowie kulinarischen Austausch; **Anastasia Pica** – mia vecchia confusa - für das tägliche Quatschen im Labor und den tollen Kochabenden; **Lukas Imberg** - meinem Thunfisch Weggefärten - für mehr als zwei Jahre Spiel, Spaß und Spannung im Labor, den vielen Gesprächen über Wissenschaft und Nicht-Wissenschaft, sowie einer schönen Zeit in Heidelberg; **Marvin Korff** - dem nettesten Menschen der Welt - für die aufschlussreichen Diskussionen

über Stereochemie, den tollen Spieleabenden zusammen mit **Jenny** und **Zelda**, sowie seinem Molekülbaukasten, der mir das Leben erleichtert hat; **Tobias Winge** - dem Terraforming Mars König – für die vielen Niederlagen und wenigen Siege im selbigen Spiel und der Hilfe bei Problemen mit Word; **Simon Platte** - meinem Nachfolger - für die Zeit im Campus Gym, die hoffentlich noch etwas andauern wird.

- meiner Praktikantin **Lea Flämig** für die große Unterstützung im Labor, für die sie ihren Koffeinkonsum erhöhen musste, wenn es mal wieder länger wurde. Es tut mir leid.
- allen ehemaligen und jetzigen Assistenten des 3. Semester und dem Praktikumsleiter **Dr. Jens Köhler** für die gute Zusammenarbeit im Labor und die entspannten Pizza- und Grillabende.
- allen ehemaligen und jetzigen Mitarbeitern der Arbeitskreise Wünsch, Junker und Koch für die tolle Arbeitsatmosphäre und die schöne gemeinsame Zeit.
- **Dr. Daniele Aiello** für seine Hilfe, sich einen Weg durch den Urwald italienischer Bürokratie zu schlagen, die lustige Zeit im Labor im 3. Stock in Palermo und seine Freundschaft.
- meinen italienischen Kollegen im Labor in Palermo: **Ale, Virginia, Stella, Marilia, Angela** and **Giovanna**.
- meinen Freunden aus Sizilien: **Gabriella, Giulia, Dario, Flora** und **Oriana**.
- meinem ersten Mitbewohner **Timo** für großartige sechs Jahre in Münster, super Reisen auf den Seychellen und in Europa, die Einführung ins Kochen und seine lange Freundschaft.
- meinen jetzigen Mitbewohnerinnen **Elena** und **Philine** für ein entspanntes letztes Jahr, den ein oder anderen Spiele- und Kochabend und den vielen Spaziergängen durch den Stadtpark und anderswo.
- meinen Freunden aus der Studienzeit: **Jonathan, Verena, Toni, Fritz, Niko, Jan, Sophia, Kevin, Tobi, Rike, Eva, Alex, Edde** und **Charly**.
- meiner Familie für ihr Verständnis, ihre Unterstützung und, dass sie mich so akzeptieren wie ich bin.
- a **Giordano**: L'amore non conosce distanze; non ha continenti; i suoi occhi sono le stelle. Grazie per essermi stato accanto in ogni situazione.

Für meine Familie

Table of contents

1. Introduction	1
1.1 Analgesics and pain management.....	1
1.2 Opioid receptors	2
1.3 Structure of KOR	4
1.4 KOR agonists	6
1.4.1 Opioid peptides.....	6
1.4.2 Terpenoids	7
1.4.3 Morphinoids.....	7
1.4.4 Ethylenediamines	8
2. Aim of the project	11
3. Synthesis plan	12
4. Synthesis	13
4.1 Part 1: Synthesis of 2-azabicyclo[3.3.1]nonanes 19a and 19b	14
4.1.1 Synthesis of 2-azabicyclo[3.3.1]nonane 25	14
4.1.1.1 Esterification of 4-oxopiperic acid 24	14
4.1.1.2 Incorporation of C ₃ side chain	15
4.1.1.3 Synthesis of <i>cis</i> - 37 and <i>trans</i> - 37 and assignment of relative configuration.....	19
4.1.1.4 Ring closure by Dieckmann condensation	21
4.1.2 Introduction of KOR pharmacophoric structural elements	24
4.1.3 Separation of enantiomers and determination of the absolute configuration of 2-azabicyclo [3.3.1]nonanes 19a	33
4.2 Part 2: Synthesis of 2-azabicyclo[3.3.1]nonanes 20 and 21 with an ethyl ester in 3-position	36
4.2.1 Synthesis of 2,6-disubstituted piperidine 56	36
4.2.2 Synthesis of <i>endo</i> - and <i>exo</i> -configured 2-azabicyclo[3.3.1]nonanes with an ethyl ester in 3-position	43

4.2.2.1	Synthesis of bicyclic enol ester 75	43
4.2.2.2	Krapcho reaction of enol esters and formation of tricyclic compounds.....	48
4.2.2.3	Introduction of the pyrrolidine ring as the second KOR pharmacophoric element	55
4.3	Part 3: Synthesis of 7-azabicyclo[4.3.1]decane 22 with an ethyl ester in 8-position.....	58
4.3.1	Oxidation of piperidine 56	58
4.3.2	Four-carbon homologation and formation of bicyclic ketone 22	61
4.4	Excursus: Synthesis of 1,2,3,4-tetrahydropyridine derivatives as analogs of betalaines.....	65
4.5	Part 4: Synthesis of 2-azabicyclo[3.2.1]octanes 23a,b	69
4.5.1	Synthesis of piperidinones with an ester moiety in 2-position.....	69
4.5.2	Incorporation of C ₂ side chain.....	75
4.5.3	Synthesis of 2-azabicyclo[3.2.1]octanes 23a,b	78
4.5.4	Determination of the enantiomeric purity of 23a,b and absolute configuration of 2-azabicyclo[3.2.1]octanes 23a,b	81
4.5.5	Separation of 2-azabicyclo[3.2.1]octanamines 23a and 23b	82
4.6	Part 5: Synthesis of 2-azabicyclo[3.2.1]octanes V with different substituents in 3-position	85
4.6.1	Synthesis of bicyclic amides 140 and 141	85
4.6.2	Synthesis of bicyclic amines 142a,b and 143a,b and derivatives.....	91
5.	Pharmacological evaluation	96
5.1	Receptor binding studies	96
5.2	Assays.....	96
5.2.1	KOR binding assay.....	96
5.2.2	MOR binding assay	97
5.2.3	DOR binding studies.....	97
5.2.4	σ_1 binding assay	98

5.2.5	σ_2 binding assay	99
5.3	Receptor affinity	100
5.3.1	KOR affinity and selectivity of bicyclic compounds with an ester moiety in 3-position	100
5.3.2	KOR affinity and selectivity of unsubstituted bicyclic compounds.....	102
5.3.3	Discussion of the dihedral angle.....	104
6.	Summary	107
7.	Experimental Part.....	113
7.1	General remarks.....	113
7.1.1	General working techniques.....	113
7.1.2	Solvents.....	113
7.1.3	Thin layer chromatography	114
7.1.4	Flash column chromatography	114
7.1.5	Melting points	114
7.1.6	HPLC.....	114
7.1.6.1	Method A (Chromni).....	114
7.1.6.2	Method B (Chromni).....	115
7.1.6.3	Method C (chiral HPLC to determine the enantiomeric purity)	116
7.1.6.4	Method D (chiral HPLC to determine the enantiomeric purity)	116
7.1.6.5	Method E (preparative chiral HPLC)	116
7.1.6.6	Method F (preparative chiral HPLC).....	117
7.1.6.7	Method G (preparative chiral HPLC)	117
7.1.7	NMR spectroscopy	118
7.1.8	IR spectroscopy.....	118
7.1.9	Mass spectrometry	119
7.2	Synthetic procedures.....	120
7.3	Crystallography section	207
7.3.1	X-ray crystal structure of enol ester 80	207

7.3.2	X-ray crystal structure of tricyclic alcohol 82	214
7.3.3	X-ray crystal structure of tricyclic bis(enol) 84	223
7.3.4	X-ray crystal structure of triester 144	230
7.3.5	X-ray crystal structure of bicyclic amine 143a	237
7.4	Receptor binding studies	245
7.4.1	Materials.....	245
7.4.2	Preparation of membrane homogenates from guinea pig.....	245
7.4.3	Preparation of membrane homogenates from rat brain	245
7.4.4	Preparation of membrane homogenates from rat liver	246
7.4.5	Protein determination	246
7.4.6	General procedures for the binding assays	246
7.4.7	Performance of the binding assays	247
8.	Appendices	249
8.1	List of abbreviations.....	249
8.2	NOESY spectra	252
8.3	Compound list	263
8.4	Bibliography.....	270

1. Introduction

1.1 Analgesics and pain management

Pain is an unpleasant feeling affecting every human several times throughout their lives. Depending on the duration, pain can be distinguished into an acute (damage of body tissue) and chronic phenomenon (autoimmune diseases).¹ Acute pain is a warning signal leading to fast recognition and localization of tissue damage, which allows the prompt treatment of the origin of pain. However, the manifestation of chronic pain can tremendously reduce the quality of life leading to bad mood, depression or anxiety.² Slight to medium pain can be treated by non-steroidal anti-inflammatory drugs (e.g. ibuprofen or acetylsalicylic acid), which show low side effects if used correctly.³ Treatment of severe pain, however, requires strong analgesics such as opioids. The term opioid derives from opium, which is the dried latex obtained from unripe seed capsules of the opium poppy *papaver somniferum*. The analgesic effect of opium and its alkaloids is used since centuries. In the early 19th century, the active compound of opium was isolated, which was termed morphine (**1**).⁴ (Figure 1) At the beginning of the 20th century, a diacetylated derivative of morphine named heroine (**2**) and other semisynthetic opioids such as oxycodone (**3**) were synthesized and clinically used as analgesic and antitussive drugs.

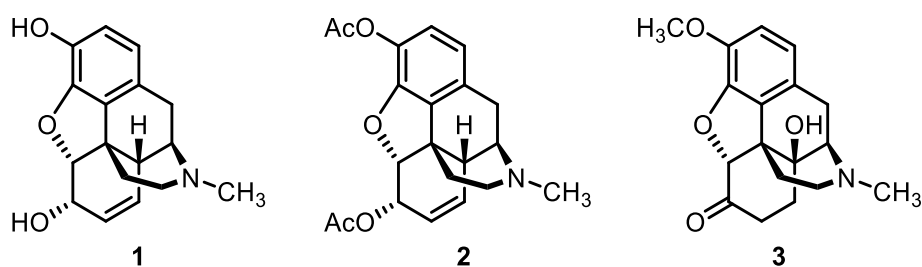


Figure 1: Opiate morphine (**1**) extracted from opium and semisynthetic derivatives heroine (**2**) and oxycodone (**3**).

In addition to the desired pain relief, opioids cause serious adverse effects including euphoria, physical and psychic dependency and respiratory depression.^{5,6} Despite these side effects, opiates are still indispensable in severe pain management since alternatives are not available.

1.2 Opioid receptors

The discovery of opioid receptors started in the second half of the 20th century.^{7–11} At first, three different opioid receptors were differentiated based on a nondependent chronic spinal dog experiment. Opioid agonists with different pharmacological profiles were detected, which led to the names of the corresponding receptors. Morphine (**1**) binds predominantly at the μ -opioid receptor (MOR), ketocyclazocine (**4**) binds at the κ -opioid receptor (KOR) and SKF-10,047 (**5**) binds at the σ receptor.¹¹ (Figure 2)

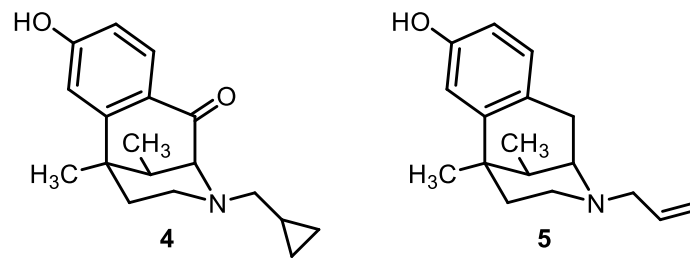


Figure 2: Opioid agonist ketocyclazocine (**4**) and SKF-10,047 (**5**).

In 1977, the δ -opioid receptor (DOR) was identified by Lord *et al.* and added to the list of opioid receptors. The receptor was named after the tissue *vas deferens* in which it was found in the mouse model.¹² Six years later, however, the list of opioid receptors was reduced by one, since it was shown that naloxone, a classical opioid antagonist, did not bind at the σ receptor.¹³ Further investigations revealed steroid binding at the σ receptor and no relationship to opioid receptors.¹⁴ In 1994, the nociceptin opioid receptor (NOR), named after its endogenous ligand nociceptin, was cloned and added to the opioid receptor family.^{15–17}

All four opioid receptors belong to the class A (rhodopsin-like) superfamily of G_i/G_o protein-coupled receptors (GPCR).^{18,19} In general, these receptors consist of seven transmembranal α -helices (TM I - VII), which are connected by three intracellular (IL 1 - 3) and three extracellular loops (EL 1 - 3). The C-terminal tail is located intracellularly and the N-terminal tail is located extracellularly. (Figure 3)

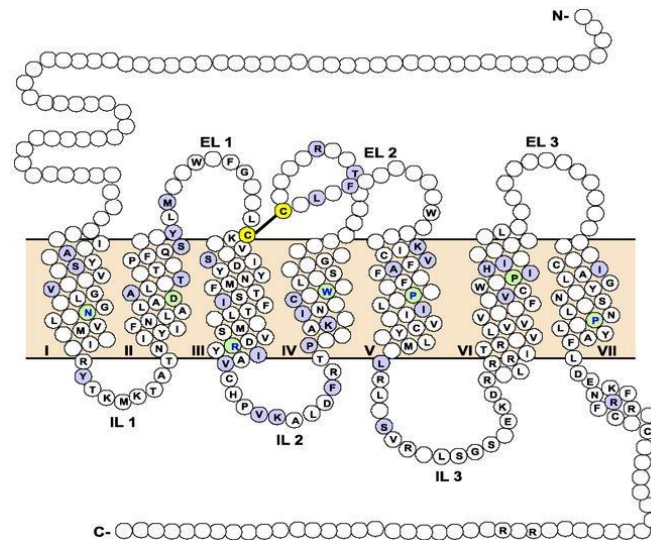


Figure 3: Serpentine model of opioid receptors. The transmembrane helices (TM) are labeled with roman numbers (I - VII). The three intracellular loops (IL 1 - 3) and the three extracellular loops (EL 1 - 3) are labeled with arabic numbers. White empty circles: nonconserved amino acids among the opioid receptors. White circles with a letter: identical amino acids among all four opioid receptors. Violet circles: identical amino acids among the classical opioid receptors MOR, KOR and DOR. Green circles: highly conserved fingerprint residue of class A receptors. Yellow circles: disulfide bridge between Cys75 (TM III) and Cys118 (EL2).¹⁹

All four opioid receptors show a high sequence homology of around 60% in the transmembranal domains. The homology for the classical opioid receptors MOR, KOR and DOR is even higher. As a consequence, the development of ligands with high selectivity towards a specific opioid receptor subtype is very ambitious.²⁰

Reaction of a GPCR with an agonist leads to a conformational change at the intracellular side allowing the binding of the heterotrimeric G-protein. Upon binding, GDP at the G_{α} -subunit of the G-protein is exchanged by GTP. The G_{α} (GTP)-subunit dissociates from the G_{β}/G_{γ} -dimer and starts the second messenger cascade.²¹ The released G_{α} -monomer inhibits the adenylyl cyclase leading to a reduction of the intracellular cAMP level.²² The G_{β}/G_{γ} -dimer interacts with different ion channels in the cell membrane increasing the conductivity of postsynaptically located K^{+} channels,²³ while reducing the conductivity of presynaptically located Ca^{2+} channels.²⁴ The change of conductivity results in a hyperpolarization of the membrane which reduces the release of neurotransmitters and, thus, inhibits the signal transmission.

All four opioid receptors are located in the central nervous system (CNS). The three classical opioid receptors MOR, KOR and DOR are also found in the periphery.^{19,25} In

addition to the localization, the different endogenous opioid peptides and physiological effects of the opioid receptors are summarized in Table 1.

Table 1: Localization, endogenous peptides and response on activation of the opioid receptors.¹⁹

receptor	localization	endogenous peptides	response on activation
MOR	brain, spinal cord, peripheral sensory neurons, intestinal tract	endomorphin-1, endomorphin-2, β -endorphin	analgesia, euphoria, respiratory depression, physical dependence, obstipation
KOR	brain, spinal cord, peripheral sensory neurons	dynorphin A, dynorphin B	analgesia, sedation, dysphoria, diuresis, immunomodulation
DOR	brain, peripheral sensory neurons	Met-enkephalin, Leu-enkephalin	analgesia, antidepressant effects, seizures, physical dependence
NOR	brain, spinal cord	nociceptin	anxiety, depression, increased appetite

As already mentioned in chapter 1.1, the administration of opioids can cause severe side effects. Opioids like morphine (**1**) or oxycodone (**2**) preferably bind at MOR and the activation of MOR is connected with side effects like euphoria, respiratory depression and obstipation. (Table 1) Therefore, the interest in the development of subtype selective opioid agonists was consistently growing during the last decades with the aim of designing novel opioid analgesics with less side effects.^{26,27} In particular, KOR came into focus, since activation of KOR does not lead to euphoria or respiratory depression. However, dysphoria, sedation and strong diuresis are associated with activation of KOR.

1.3 Structure of KOR

In the last ten years, the structure of KOR and its binding site have been thoroughly investigated. Che *et al.* reported the first crystal structure of the human KOR in complex with the KOR antagonist JD₁Tic (**6**) which was synthesized in 2001.^{28,29} (Figure 4) The structure showed seven transmembrane domains and an additional eighth intracellular α -helix parallelly oriented to the membrane. Moreover, the dimeric character of KOR was confirmed.

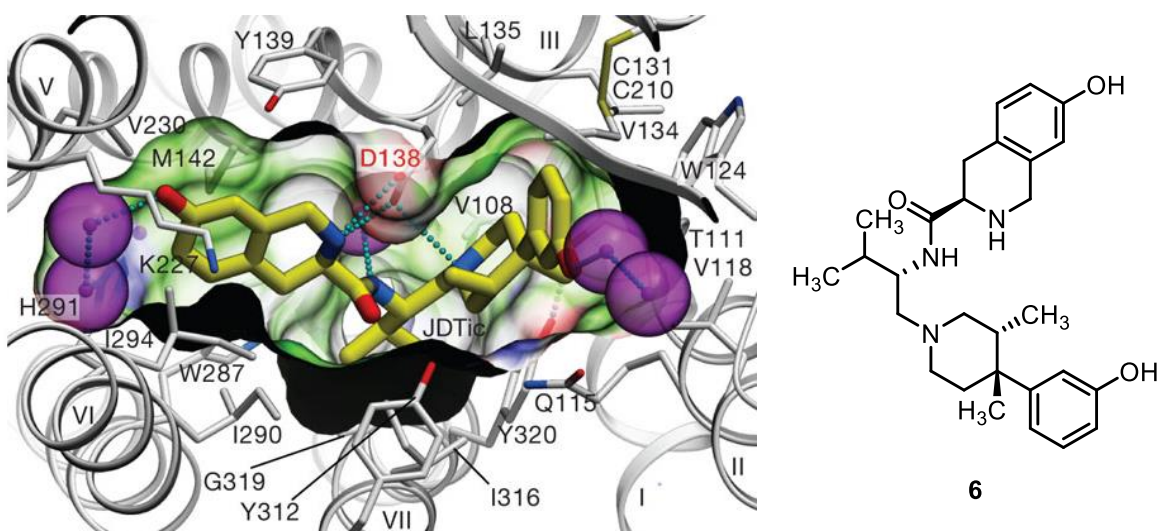


Figure 4: Left: Complex of KOR with KOR antagonist JDtic (**6**); right: JDtic (**6**).²⁹

The most important interaction between KOR and JDtic (**6**) is the salt bridge of Asp138 with the protonated amino moieties of the tetrahydroisoquinoline and piperidine ring. This interaction anchors the ligand in a V-like shape deep inside the receptor. The high KOR selectivity of the antagonist JDtic is caused by hydrophobic interactions with the amino acid residues of Ile294, Tyr312, Val108 and Val118, which exists only in KOR.²⁹

In 2018, Wu *et al.* were able to crystallize the human KOR in its active state binding to the KOR agonists MP1104 (**7**). (Figure 5) The complex was stabilized by the nanobody Nb39.³⁰

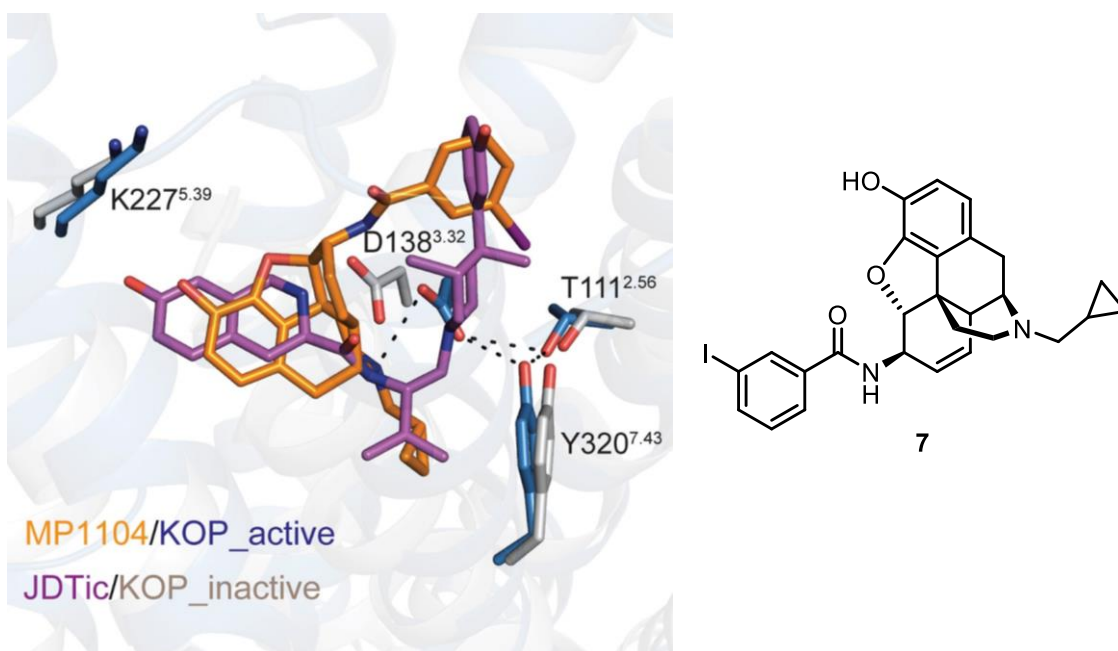


Figure 5: Left: ionic interaction of KOR antagonist JDtic (**6**, purple) and KOR agonist MP1104 (**7**, orange) with Asp138 in the binding pocket of KOR; right: MP1104 (**7**).³⁰

Similar to the KOR/JDTic complex, the ionic interaction of Asp138 with the protonated amino moiety fixes the KOR agonist MP1104 (**7**) in the binding pocket of KOR. In addition, a water-mediated H-bond of the backbone carbonyl O-atom of Lys227 with the phenolic OH group of MP1104 (**7**) is formed.³⁰

1.4 KOR agonists

According to their structures, KOR agonists are classified in four different subclasses: opioid peptides, terpenoids, morphinoids (morphinans and benzomorphans) and ethylenediamines.

1.4.1 Opioid peptides

The class of opioid peptides is derived from the endogenous ligand dynorphin A, which was discovered in the 1970s.³¹ Generally, these peptides show high KOR affinity and selectivity over the other opioid receptors.^{32,33} A particular feature of peripheric KOR agonists is their low ability to pass the blood brain barrier due to their hydrophilicity and size. This property reduces the centrally mediated side effects associated with activation of KOR in the CNS. However, enzymes can quickly hydrolyze opioid peptides into smaller fragments, which can interact with various pathways not related to the opioid-pathway.³³ Moreover, fast hydrolysis reduces the half-live and thus the time of action.

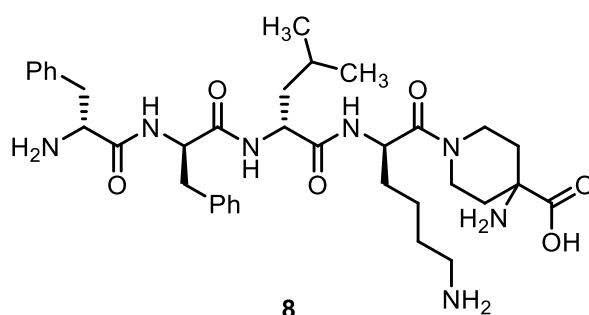


Figure 6: KOR agonist difelikefalin (**8**) belonging to the class of opioid peptides.

The opioid peptide difelikefalin (**8**) is under investigation for the treatment of chronic kidney disease associated pruritus. (Figure 6) A phase III clinical trial showed the ability of difelikefalin (**8**) to reduce chronic itching of hemodialysis patients.³⁴ Recently, the European Medicines Agency (EMA) started an approval procedure. The decision is expected for 2022.

1.4.2 Terpenoids

The second class of KOR agonists are terpenoids such as naturally occurring salvinorin A (**9**, R = Ac).³⁵ (Figure 7)

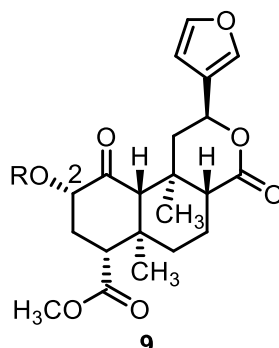


Figure 7: KOR agonists belonging to the class of terpenoids: salvinorin A (**9**, R = Ac) and its semisynthetic analogs (R = Et, (CO)NH₂, CH₂OCH₃, CH₂OEt).

In contrast to the other classes of KOR agonists, terpenoids do not contain a basic N-atom, which was thought to be crucial to form the ionic interaction with Asp138.^{29,30} Nevertheless, salvinorin A (**9**, R = Ac) and some semisynthetic analogs with different functional groups in 2-position (R = Et, (CO)NH₂, CH₂OCH₃, CH₂OEt) show very high KOR affinity.^{36,37} Interestingly, a free hydroxy group (salvinorin B, R = H) leads to significantly reduced KOR affinity.³⁶ The result may indicate an additional hydrophobic pocket inside KOR.³⁷

1.4.3 Morphinoids

Morphinans like nalfurafine (**10**) and benzomorphans like (-)-pentazocine ((-)-**11**) belong to the class of morphinoids, which derive from morphine (**1**). (Figure 8)

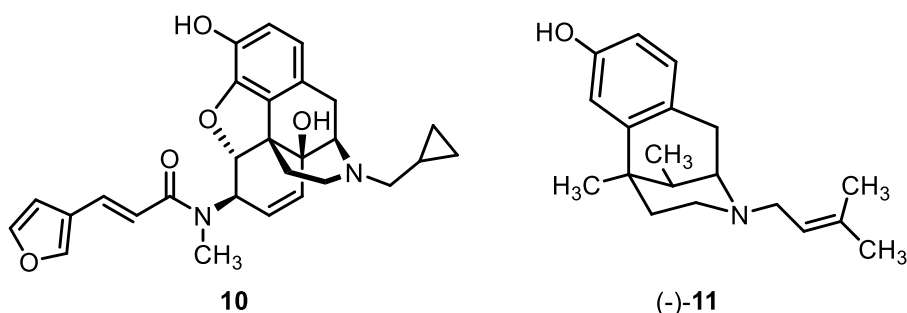


Figure 8: KOR agonists belonging to the class of morphinoids: nalfurafine (**10**) and pentazocine ((-)-**11**, partial KOR agonists, partial MOR antagonists).

In addition to their high KOR affinity, morphinoids show often low selectivity over MOR, DOR and NOR. The KOR agonist nalfurafine (**10**) was approved in Japan for the

treatment of uremic pruritus of hemodialysis patients.^{38,39} The racemic benzomorphone pentazocine ((-)-**11**) was approved as potent analgesic, despite its psychotomimetic effects including hallucinations and delusions.^{40,41} Pentazocine is a partial KOR agonist / partial MOR antagonist.⁴²

1.4.4 Ethylenediamines

The last class of KOR agonists are ethylenediamines. Here, an ethylene moiety connects an amino group and an arylacetamide, the two KOR pharmacophoric elements. U-50,488 (**12**) was first synthesized by Szmuszkovicz in 1975 and pharmacologically evaluated by von Voigtlander. It is the first member of this class displaying high KOR affinity and selectivity over the other opioid receptors.^{43,44} (Figure 9)

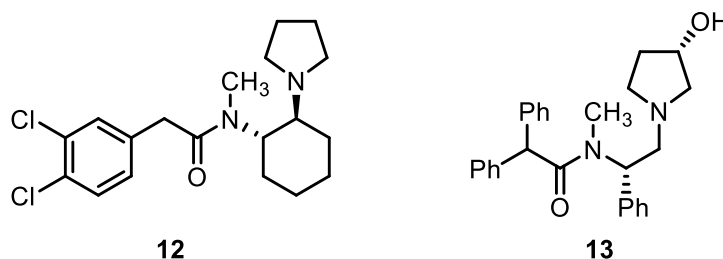


Figure 9: KOR agonists belonging to the class of ethylenediamines: U-50,488 (**12**) and asimadoline (**13**).

In addition to U-50,488 (**12**), asimadoline (**13**) was developed which contains a rather flexible ethylene moiety compared to the more rigid cyclohexane ring of U-50,488 (**12**).⁴⁵ Due to the hydroxy group at the pyrrolidine ring, asimadoline (**13**) has a low potential to pass the blood-brain barrier and, consequently, to elicit centrally mediated side effects like dysphoria, sedation and diuresis.⁴⁶ Therefore, it is used for the symptomatic treatment of patients suffering from an irritable bowel syndrome⁴⁷ or pulmonary or vascular diseases.⁴⁸

In Figure 10 the main interactions between KOR agonist U-50,488 (**12**) and the KOR binding pocket are highlighted.⁴⁹

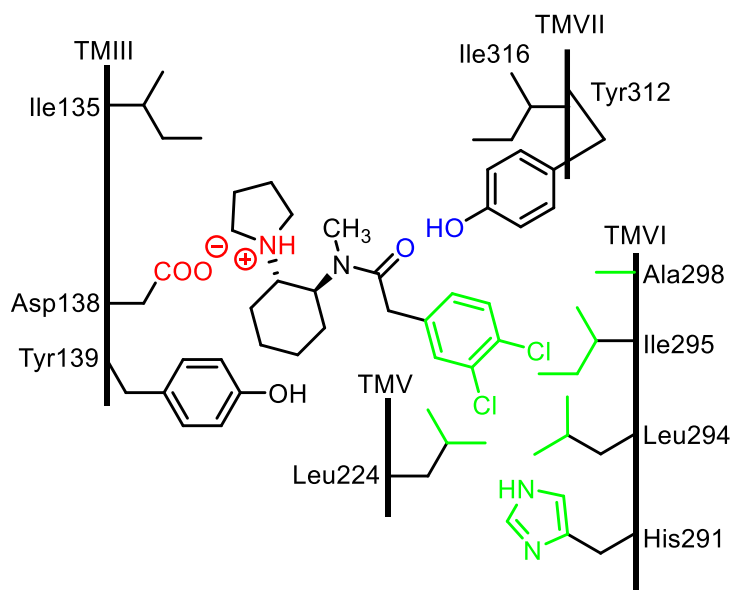


Figure 10: Interactions between KOR agonist U-50,488 (**12**) and the KOR binding pocket. Red: ionic interaction between Asp138 and protonated amino group; blue: H-bond between Tyr312 and carbonyl O-atom of amide moiety; Green: hydrophobic interactions between the aryl ring and Leu224, His291, Leu294, Ile295 and Ala298.⁴⁹

The protonated N-atom of the pyrrolidine ring forms an ionic interaction with the carboxylate group of Asp138 anchoring the ligand into the KOR binding pocket. An H-bond is formed between the OH moiety of Tyr312 with the carbonyl O-atom of the amide group.³⁰ Additionally, several lipophilic interactions of the aryl ring with various amino acid residues stabilize the binding of U-50,488 in the KOR binding pocket. Moreover, they are responsible for the selectivity over MOR, DOR and NOR.⁴⁹

All four isomers of U-50,488 (**12**) were synthesized and pharmacologically evaluated. Interestingly, the (1*R*,2*S*)- and (1*S*,2*R*)-*cis*-configured and (1*R*,2*R*)-*trans*-configured isomers display lower affinity towards KOR than the (1*S*,2*S*)-*trans*-configured isomer U-50,488.⁵⁰

A similar result was obtained for the (*R*)-configured piperazine derivative GR-89,696 (**14**) which is considerably more potent than its (*S*)-configured enantiomer.⁵¹ (Figure 11)

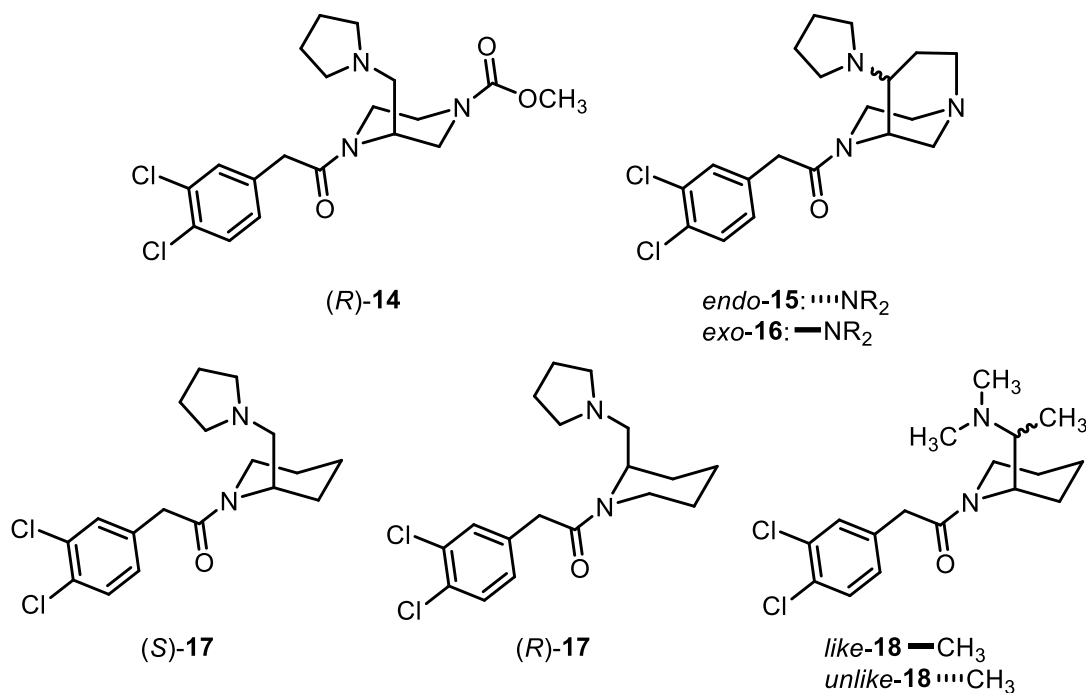


Figure 11: KOR agonists with an ethylenediamine moiety based on U50,488 (12).

In an attempt to investigate the bioactive conformation, the bicyclic piperazine-based KOR agonist *endo*-15 was synthesized which showed a reduced KOR affinity compared to GR-89,696 (14). Interestingly, the *exo*-configured diastereomer *exo*-16 showed very low KOR affinity in the micromolar range.⁵²

In 1990, Vecchietti *et al.* reported the synthesis and pharmacological evaluation of piperidine-based ethylenediamines.⁵³ While the (*S*)-configured bicyclic amine 17 shows 64-fold higher KOR affinity than the (*R*)-configured enantiomer (*R*)-17, the difference between the diastereomeric dimethylamines *like*-18 and *unlike*-18 is extraordinary high (1667-fold affinity towards KOR).

Therefore, the stereochemistry of KOR agonists with an ethylenediamine substructure plays a crucial role for high KOR affinity and needs further investigation to understand the bioactive conformation.

2. Aim of the project

The aim of the project is the synthesis of conformationally restricted ethylenediamines **I** derived from piperidine **18** and rigid 1,4-diazabicyclo[3.3.1]nonanes **15a,b** (Figure 12).

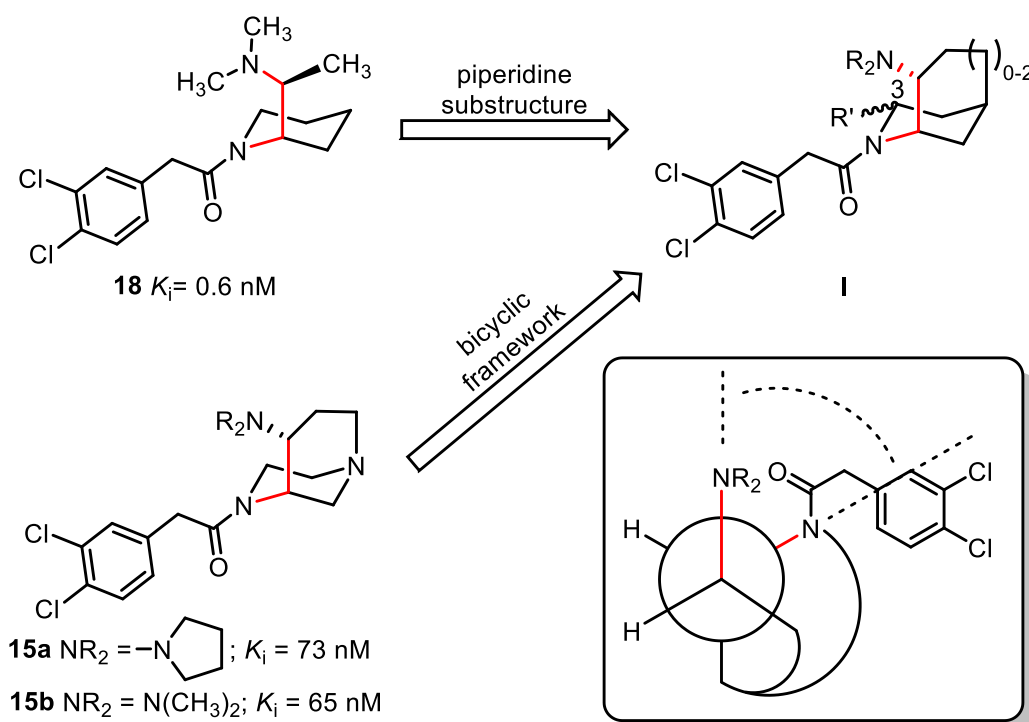


Figure 12: Novel rigid *endo*-configured KOR agonists **I** derived from **18** and **15a,b**.

While the monocyclic compound **18** shows high KOR affinity ($K_i = 0.6$ nM), the affinity of bicyclic piperazine analogs **15a,b** is reduced ($K_i = 73$ nM and 65 nM). To develop novel high-affinity KOR agonists, the bridgehead N-atom of **15a,b** will be replaced by a CH moiety in analogy to piperidine **18** leading to a bicyclic piperidine-based scaffold. The size of the bicyclic system will be modified (**I**: $n = 0,1,2$) to further investigate the significance of the dihedral angle of the ethylenediamine moiety (N-C-C-N) for high KOR affinity. Moreover, different substituents will be introduced in 3-position of the bicyclic system to affect the polarity of the final compounds. The KOR affinity and selectivity of all obtained bicyclic amines of type **I** will be tested and the enantiomers of promising racemic and nonracemic ($ee \sim 50\%$) KOR agonists will be separated *via* chiral HPLC, respectively.

3. Synthesis plan

In Figure 13 the retrosynthetic analysis of the potential bicyclic KOR agonists of type **I** is displayed.

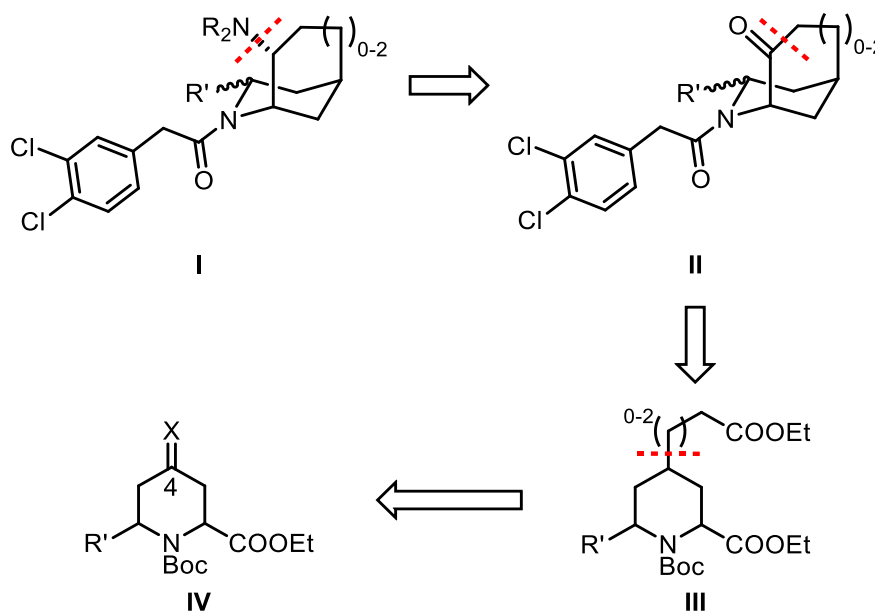


Figure 13: Retrosynthetic analysis of conformationally restricted KOR agonists **I**.

Since *endo*-configuration of the bicyclic amines is indispensable for high KOR affinity,^{52,54} a key step is the reductive amination of ketones **II**. A sterically demanding reducing agent should transfer the hydride from the backside leading to the desired *endo*-configured amines. The bicyclic systems **II** can be obtained by Dieckmann condensation of diesters **III**. Side chains with different length will be introduced into 4-position of piperidines **IV** to get the desired bicyclic frameworks. Piperidines **IV** are either commercially available or can be synthesized by modifying already published procedures from the literature.^{55–62}

4. Synthesis

The description of the synthesis of the different bicyclic amines **19 - 23** and **V** deriving from intermediate **IV** is divided into five main parts. (Figure 14)

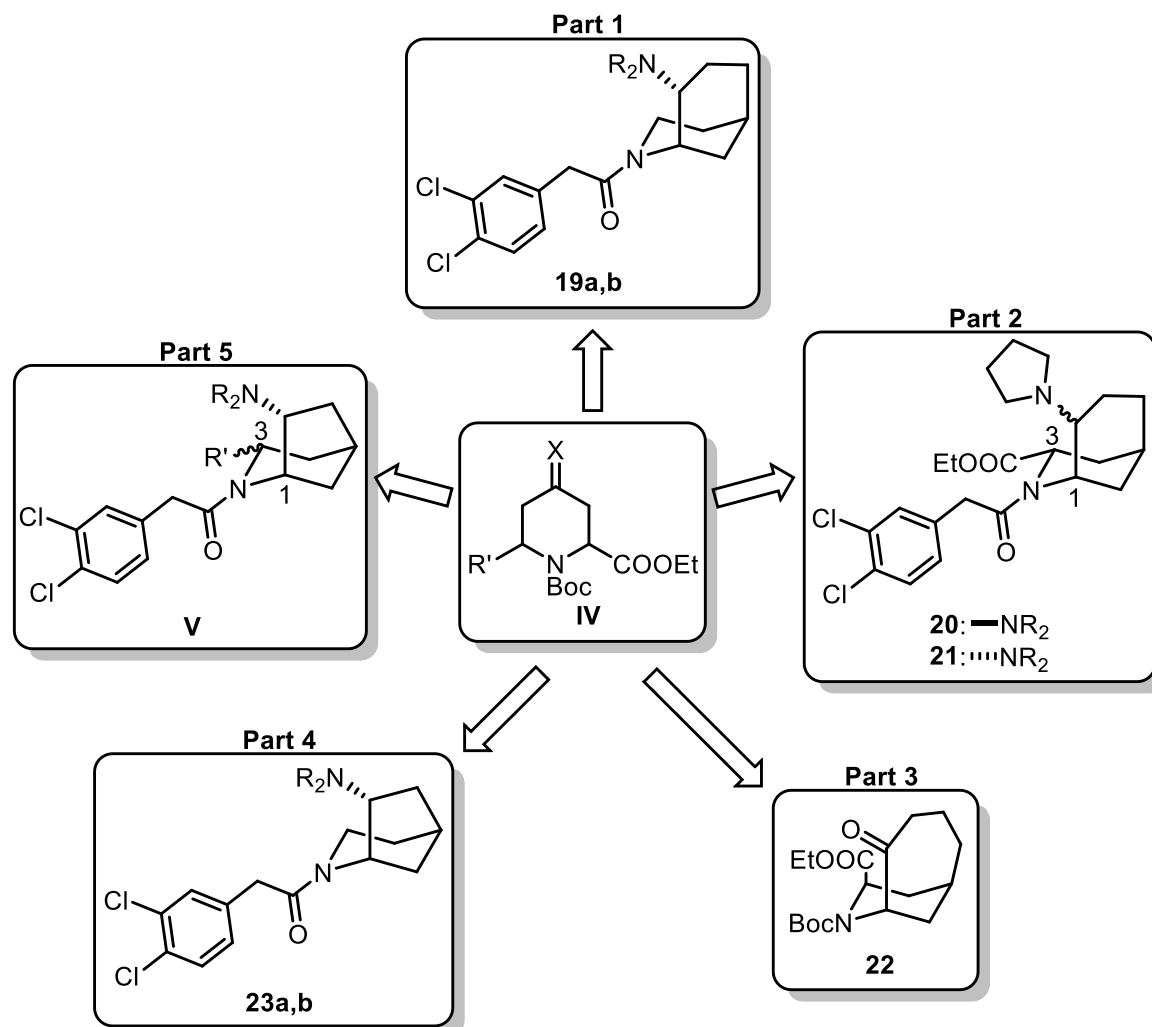
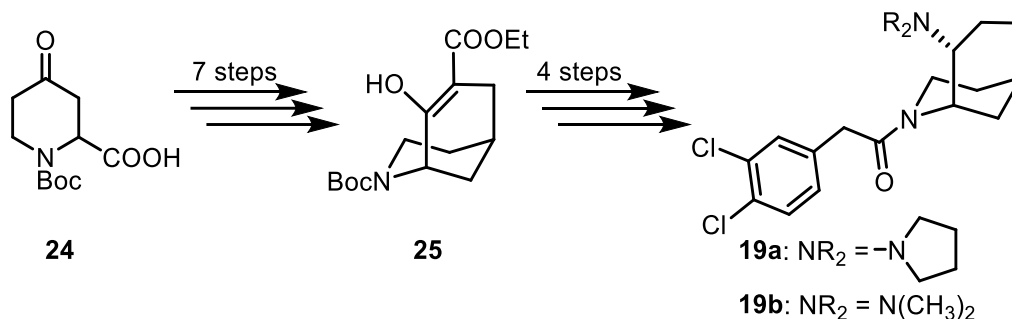


Figure 14: Synthesized bicyclic amines **19 - 23** and **V** originate from piperidine derivatives **IV**.

First, the synthesis of *endo*-configured 2-azabicyclo[3.3.1]nonanes **19a,b** will be presented, which show high similarities towards 1,4-diazabicyclo[3.3.1]nonanes **15a,b**. This will be followed by the synthesis of bicyclic analogs **20** and **21** with an additional ester moiety in 3-position. The third part will focus on the preparation of 7-azabicyclo[4.3.1]decane **22** with an enlarged bicyclic ring system. Then, the synthesis of ethylenediamines **23a,b** with an ethano bridged bicyclic ring system will be presented and finally, the formation of the corresponding substituted bicyclic amines **V** will be shown.

4.1 Part 1: Synthesis of 2-azabicyclo[3.3.1]nonanes **19a** and **19b**

The ethylenediamines **19a** and **19b** were prepared in an eleven step diastereoselective synthesis starting with 4-oxopiperidine-2-carboxylic acid **24**. (Scheme 1)



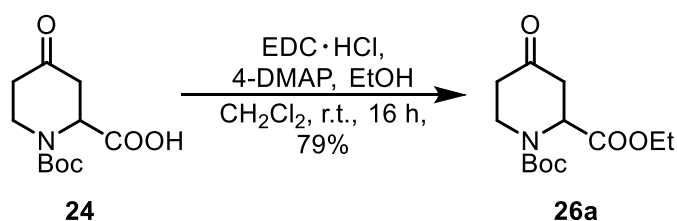
Scheme 1: Plan for the synthesis of KOR agonists **19a** and **19b** with a 2-azabicyclo[3.3.1]nonane scaffold.

The description of the synthesis of **19a** and **19b** is divided into two parts: At first, enol ester **25** was synthesized starting from piperidinone **24**; then, the two KOR pharmacophoric structural elements were introduced.

4.1.1 Synthesis of 2-azabicyclo[3.3.1]nonane **25**

4.1.1.1 Esterification of 4-oxopiperidone **24**

The synthesis started with a racemic mixture of commercially available 1-(*tert*-butoxycarbonyl)-4-oxopiperidine-2-carboxylic acid (**24**). At first, the carboxylic acid was protected as an ethyl ester. (Scheme 2)



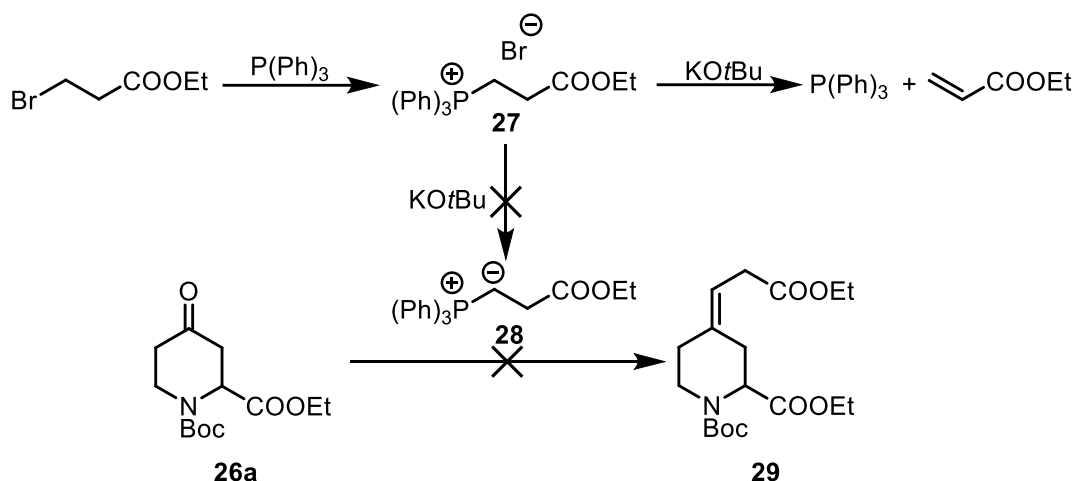
Scheme 2: Mild esterification of 4-oxopiperidone **24**.

To generate the ester **26a**, neither a reaction with EtOH/H₂SO₄ (Fischer esterification)⁶³ nor EtOH/thionyl chloride (SOCl₂)⁶⁴ could be performed, due to the acid-labile Boc group. Therefore, the coupling agent 1-ethyl-3-[3-(dimethylamino)propyl]carbodiimide hydrochloride (EDC · HCl)⁶⁵ and a catalytic amount of 4-(dimethylamino)pyridine (4-DMAP) in EtOH and CH₂Cl₂ were used leading to ester **26a** in 79% yield. In the ¹H NMR spectrum of **26a**, a triplet at 1.25 ppm (CH₃

group) and a quartet at 4.17 ppm (CH₂ group) proved the successful esterification of carboxylic acid **24**.

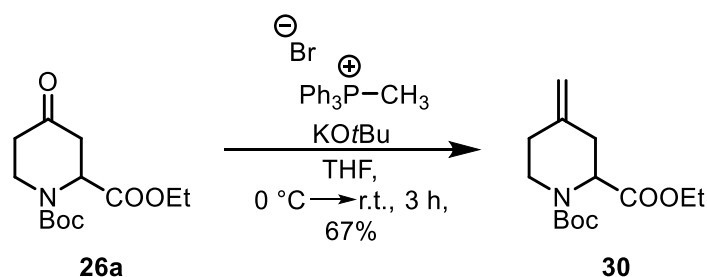
4.1.1.2 Incorporation of C₃ side chain

For the synthesis of a compound with a 2-azabicyclo[3.3.1]nonane scaffold, a C₃ side chain had to be introduced in 4-position of piperidinone **26a**. At first, a Wittig reaction should be performed using *in situ* generated ylide **28**. (Scheme 3)



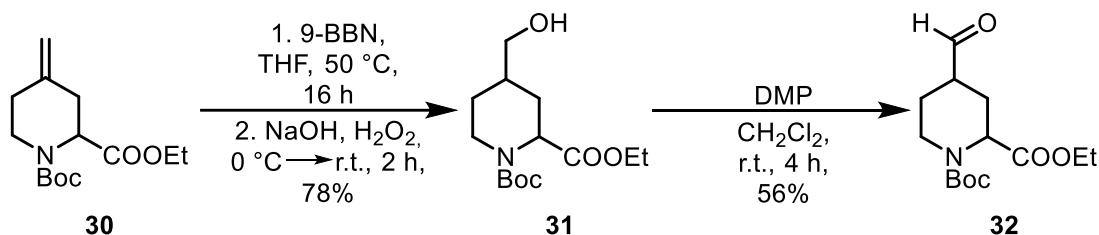
Scheme 3: Synthesis⁶⁶ and elimination reaction^{66–68} of phosphonium bromide **27**.

Therefore, ethyl 3-bromopropanoate and triphenylphosphane (PPh_3) were heated without solvent to 110 °C.⁶⁶ Afterwards, the phosphonium bromide **27** should be deprotonated with potassium *tert*-butoxide ($\text{KO}t\text{Bu}$) to form the ylide **28**. Although some methods are described in the literature using ylide **28**,^{67–70} a conversion of piperidinone **26a** into β,γ -unsaturated ester **29** could not be observed. Since both CH₂ groups between the ester moiety and the phosphonium group of compound **27** show similar pK_a -values (~ 25), the elimination reaction (E1cB) is entropically favored compared to the formation of ylide **28**. Therefore, under basic conditions a proton in α -position to the ester group is more likely to be removed leading to the elimination products PPh_3 and ethyl acrylate, as described in the literature.^{66–68} For this reason, an alternative synthesis was developed. Instead of incorporating a C₃ building block, a C₁ and C₂ subunit should be introduced sequentially. First, a methylenation of ketone **26a** was performed to insert a C₁ subunit. (Scheme 4)



Scheme 4: Conversion of ketone **26a** into piperidine **30** via Wittig reaction.

Hence, methyltriphenylphosphonium bromide was deprotonated with KO^tBu⁷¹ and subsequently reacted with piperidinone **26a** to form piperidine **30** with an exocyclic double bond in 4-position in 67% yield. The successful conversion was shown by the loss of the signal at 206.1 ppm in the ¹³C NMR spectrum for the carbonyl C-atom of the ketone and new signals for the methylene group in the ¹H NMR spectrum at 4.74 – 4.82 ppm. Also, in the IR spectrum a band at 1655 cm⁻¹ indicates the presence of the C=C double bond.



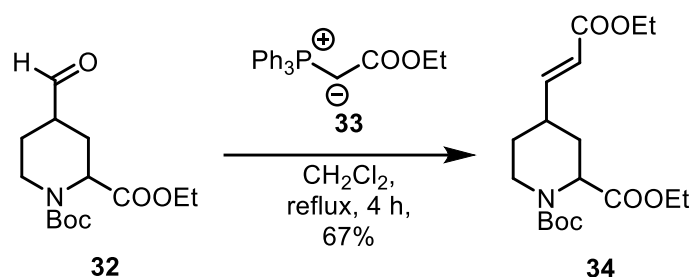
Scheme 5: Functionalization of the methylene group of piperidine **30** via hydroboration-oxidation reaction followed by Dess-Martin oxidation.

Next, the double bond was functionalized to allow the establishment of the C₂ subunit. Therefore, a hydroboration of piperidine **30** with 9-borabicyclo[3.3.1]nonane (9-BBN) followed by oxidative work-up^{72–74} with H₂O₂ and NaOH was performed to obtain the primary alcohol **31**. (Scheme 5) A band at 3463 cm⁻¹ in the IR spectrum caused by a stretching vibration of the O-H group confirmed the successful functionalization of the double bond. The hydroboration is highly regioselective due to the electronic nature of 9-BBN leading to the anti-Markovnikov product. After the addition of borane, however, a chiral center was generated in 4-position leading to diastereomers *cis*-**31** and *trans*-**31** after oxidative work-up. ¹H NMR spectra analysis confirmed the formation of two diastereomers with the ratio 6:4. The diastereomers were not separated.

Primary alcohol **31** was oxidized with Dess-Martin periodinane (DMP). Although high yields of ≥90% are described for this type of oxidation in the literature,⁷⁵ the aldehyde

32 was isolated in only 56% yield. The work-up with NaOH could have caused a partial hydrolysis of the ester decreasing the yield of aldehyde **32**. The formation of the aldehydes *cis*-**32** and *trans*-**32** was proven by two singlets in the ^1H NMR spectrum at 9.64 ppm and 9.68 ppm and two signals in the ^{13}C NMR spectrum at 202.3 ppm and 202.6 ppm. Moreover, the band for the OH group in the IR spectrum had disappeared confirming the oxidation of alcohol **31**.

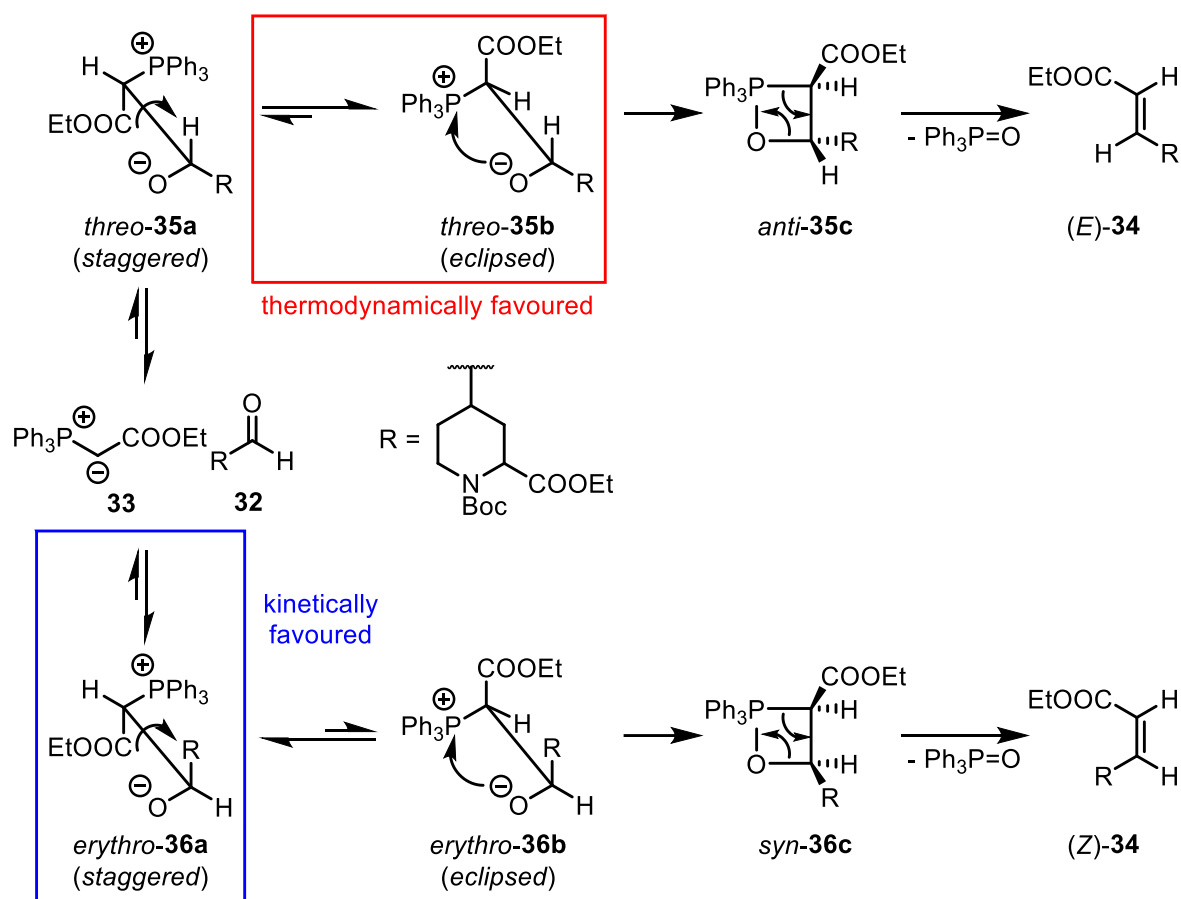
The next step was the introduction of the C₂-subunit by a Wittig reaction. Aldehyde **32** reacted with ylide **33** providing the α,β -unsaturated ester **34** in 67% yield. (Scheme 6)



Scheme 6: Incorporation of a C₂ subunit by Wittig reaction generating **34**.

The configuration of the formed double bond can be determined by analysis of the ^1H NMR spectrum of compound **34**. A multiplet at 5.78 – 5.85 ppm is caused by the overlap of the CH signal in α -position of the α,β -unsaturated ester of both diastereomers which does not give any information about the configuration of the double bond. However, the signal for the CH group in β -position of the α,β -unsaturated ester is presented by two dd's at 6.85 ppm ($J = 15.8 / 6.6$ Hz) for the major diastereomer and 6.90 ppm ($J = 15.9 / 6.5$ Hz) for the minor diastereomer. The large coupling constants indicate (*E*)-configured double bonds for both diastereomers.

The mechanism of the Wittig reaction allows the synthesis of (*E*)- and (*Z*)-configured alkenes.^{76,77} (Scheme 7)



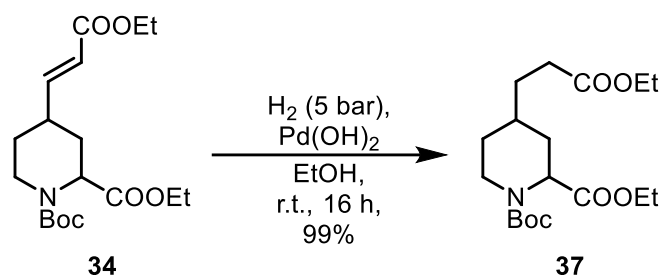
Scheme 7: Reaction mechanism^{76,77} of stabilized Wittig reagent **33** with aldehyde **32**.

At first, an addition of ylide **33** at aldehyde **32** forms the betaines *threo*-**35a** and *erythro*-**36a**. The generated alcoholate and the phosphonium moiety adopt the antiperiplanar conformation. Due to geometrical restrictions, the kinetically controlled addition favors the formation of betaine **36a** over **35a**. In the next step, a rotation around the newly formed C-C σ-bond transforms the *staggered* conformation into the *eclipsed* conformation. Lower activation energy favors the rotation of **35a** to **35b** over **36a** to **36b**. The rotation leads to transition states **35b** and **36b** which will immediately react to oxaphosphetanes *anti*-**35c** and *syn*-**36c**. Finally, a [2+2] reversed cycloaddition with the elimination of triphenylphosphine oxide leads to (E)-**34** and (Z)-**34**. According to the literature, carbonyl compounds react with stabilized ylides preferably to (E)-configured alkenes due to the reversible formation of betaines **35a** and **36a**.^{76,77} The betaines **35a** and **36a** are in a dynamic equilibrium with ylide **33** and aldehyde **32**. Since the rotation along the σ-bond of betaine **35a** is faster than the rotation of **36a**, formation of (E)-**34** is thermodynamically more favored. In case of non-stabilized Wittig reagents, the formation of betaines is not reversible and the kinetically more favored *erythro*-adduct **36a** will be formed leading to (Z)-configured

alkenes. In addition to this general idea of the mechanism, many reaction conditions can influence the (*E*)/(*Z*) ratio, like Li-additives, ligands bound to the P-atom, temperature and solvent.⁷⁸

4.1.1.3 Synthesis of *cis*-**37** and *trans*-**37** and assignment of relative configuration

The saturated diester **37** was obtained by hydrogenation of α,β -unsaturated ester **34** with H₂ (5 bar) and Pd(OH)₂ as catalyst in quantitative yield. (Scheme 8)



Scheme 8: Hydrogenation of α,β -unsaturated ester **34**.

Mass spectrometry and the loss of the band of the stretching vibration of the C=C double bond in the IR spectrum indicate the successful hydrogenation. Moreover, the methyne signals of the alkene in the ¹H NMR spectrum of diester **37** have vanished, whilst two new multiplets - each with an integral of 2H - appear in the aliphatic region at 1.41 – 1.50 ppm and 2.24 – 2.31 ppm. Two diastereomers were obtained in the ratio 6:4. (Figure 15)

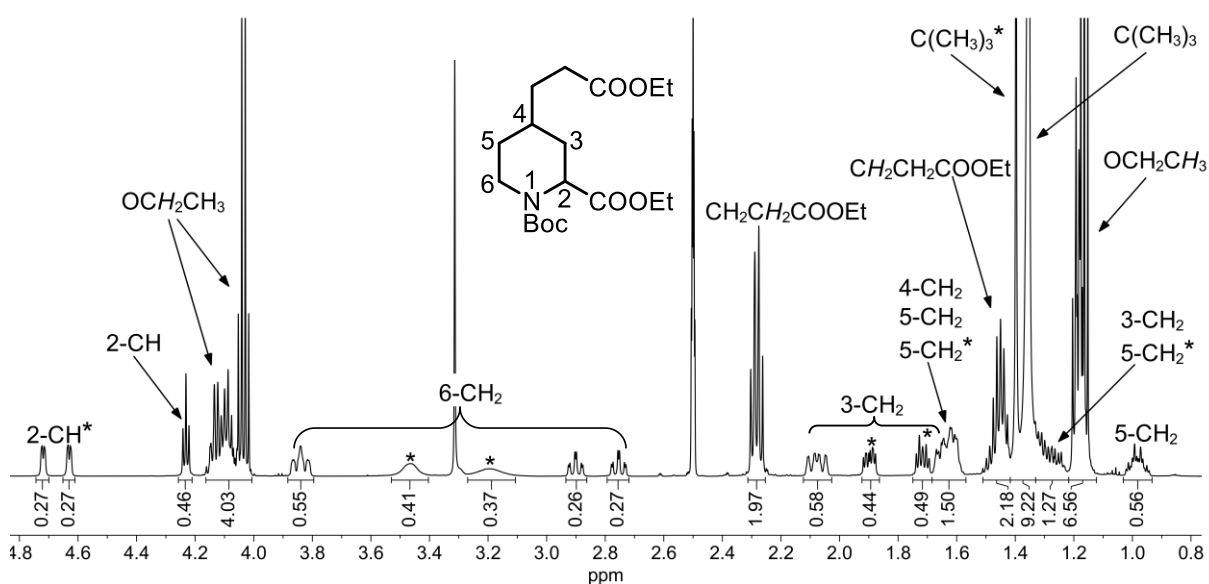


Figure 15: ¹H NMR spectrum (DMSO-*d*₆) of diester **37** showing two diastereomers in the ratio 6:4. The signals for the minor diastereomer are marked with an asterisk (*).

Due to rotational isomerism along the Boc group, the signals for the major diastereomer are split, while the signals for the minor diastereomer are broadened. The configuration of the diastereomers cannot be assigned by analysis of the coupling constants of the two sets of signals. Therefore, the assignment of the two sets of signals to *trans*-**37** and *cis*-**37** was achieved by nuclear Overhauser enhancement spectroscopy (NOESY). (Figure 16) The complete NOESY spectrum is displayed in Figure S1. (Appendix)

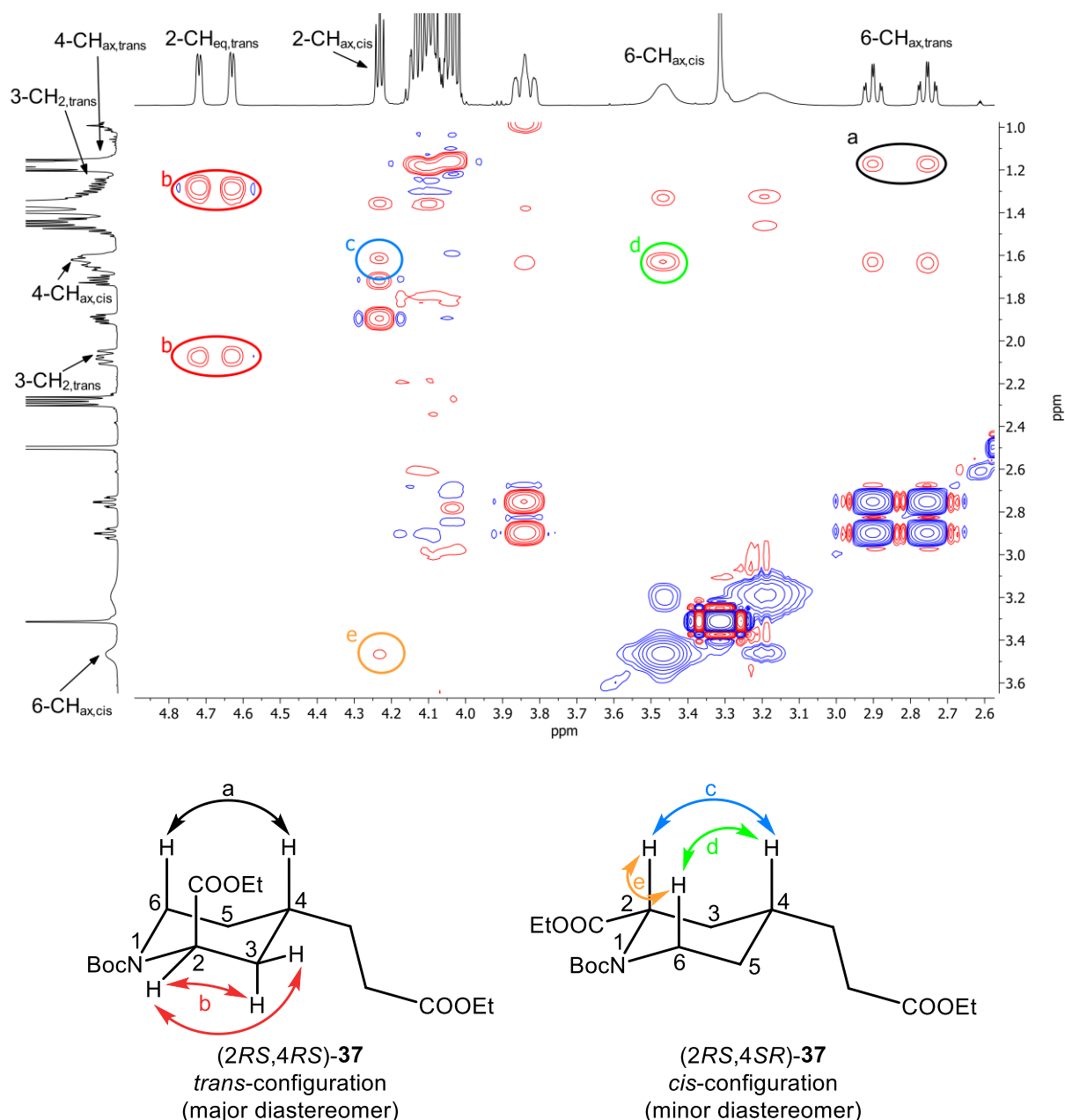
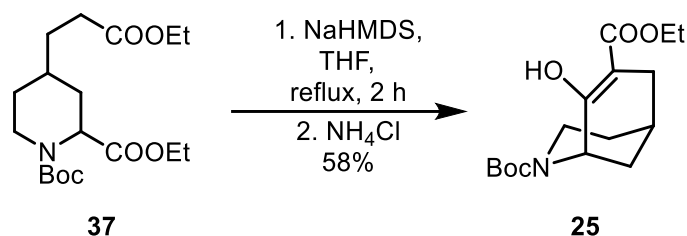


Figure 16: Part of the NOESY spectrum (top) and NOE (bottom) of *trans*- and *cis*-configured diester **37**.

The set of signals of the major diastereomer shows a cross peak of one methylene proton in 6-position at 2.75 ppm and 2.90 ppm and a methyne proton in 4-position at 1.13 – 1.32 ppm. (Figure 16, mark a) This indicates an axial orientation of both protons and consequently, the side chain in 4-position is equatorially oriented. A proximity with the methyne proton in 2-position (4.63 and 4.72 ppm) cannot be observed. However, a correlation of 2-CH with both methylene protons in 3-position (1.13 – 1.21 ppm and 2.03 – 2.07 ppm) can be seen. (Figure 16, mark b) This indicates an equatorial orientation of the proton in 2-position and an axial orientation of the ester group in 2-position. As a result, the major diastereomer is *trans*-configured. The set of signals for the minor diastereomer is showing proximities of three protons in 2- (4.23 ppm), 4- (1.57 – 1.68 ppm) and 6-position (3.39 – 3.53 ppm) which are marked in Figure 16 with c, d and e. The three protons are axially orientated and thus, the corresponding substituents in 2- and 4-position adopt the equatorial orientation. As a result, the minor diastereomer is *cis*-configured. In summary, the ^1H NMR spectrum of **37** is showing a mixture of *trans*-**37** and *cis*-**37** in the ratio 6:4.

4.1.1.4 Ring closure by Dieckmann condensation

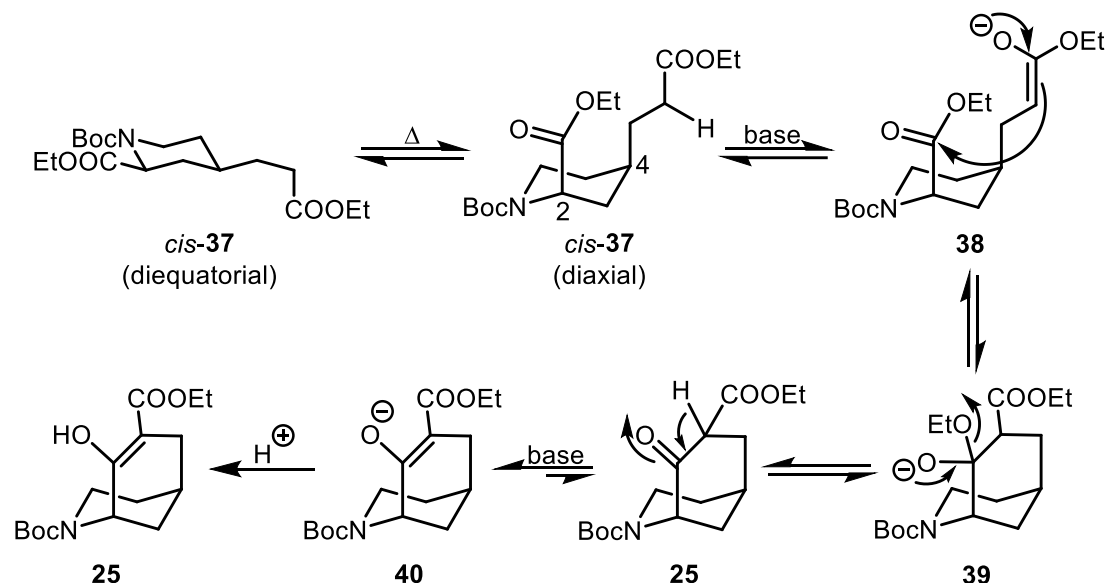
A cyclocondensation - first published by Dieckmann⁷⁹ in 1894 - was performed with diester **37** to obtain 2-azabicyclo[3.3.1]nonane **25** in 58% yield. (Scheme 9)



Scheme 9: Dieckmann condensation of diester **37**.

Several procedures are described in the literature to synthesize bicyclic compounds by Dieckmann condensation.^{80–85} A method developed by Kaiser *et al.*⁸² was modified by our group,⁸⁶ using sodium bis(trimethylsilyl)amide (NaHMDS) instead of potassium metal as base. A highly diluted solution ($c = 0.02$ M) of diester **37** in THF was used to prevent intermolecular side reactions (Ziegler-Ruggli dilution principle).^{87,88} At room temperature, both side chains in 2- and 4-position of compound *cis*-**37** are equatorially orientated. Since the Dieckmann condensation is only possible, if both substituents in 2- and 4-position adopt the axial orientation, an elevated temperature was necessary

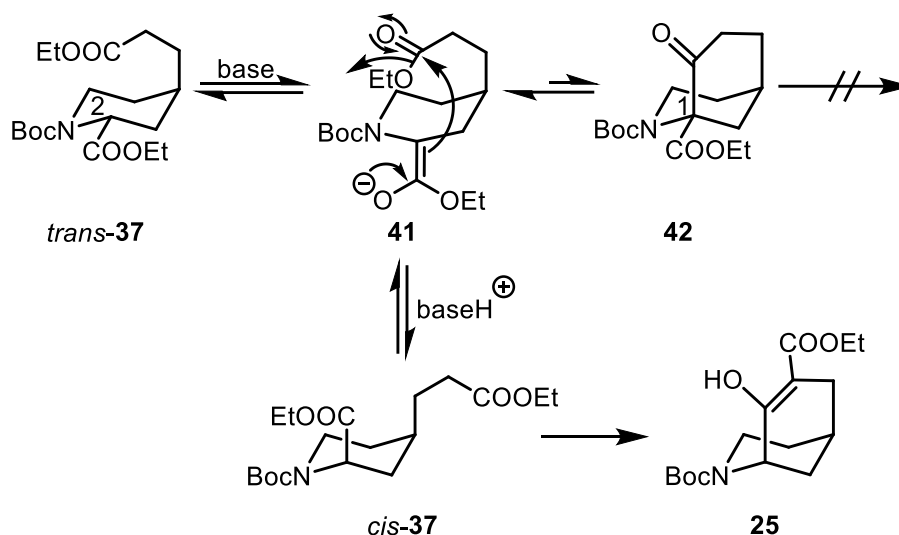
to accelerate the ring inversion. The mechanism for the Dieckmann condensation is well understood.^{89,90} (Scheme 10)



Scheme 10: Mechanism of Dieckmann condensation of diester *cis*-37.^{89,90}

A proton in α -position to the ester moiety in the C₃ side chain (4-position) is removed. Then, the formed enolate **38** undergoes an addition-elimination reaction attacking the carbonyl C-atom of the ester in 2-position. In 1955, Carrick and Fry found by measuring ¹⁴C isotope effects that the rate-determining step is the ring closure.⁹¹ During the cyclization, one molecule of ethanolate is eliminated from the tetrahedral intermediate **39**, forming the β -keto ester **25**. Finally, the proton between the ketone and ester moiety is removed, leading to the enolate **40**. The formation of the enolate **40** is the driving force of the Dieckmann condensation, since the preceding reaction steps are in an equilibrium.⁹⁰ The final deprotonation of β -keto ester **25** shifts the equilibrium towards the product side. In order to isolate enol ester **25** the reaction mixture was treated with NH₄Cl to protonate the enolate **40**.

The *trans*-configured diastereomer *trans*-37 cannot undergo the cyclization reaction due to geometrical restrictions. Theoretically, the proton in 2-position can be removed leading to enolate **41** and induce the formation of the bicyclic system **42**. (Scheme 11) However, due to the missing proton between the ester and the ketone moiety in **42**, a stabilized enolate cannot be formed which is essential to shift the equilibrium to the product side.



Scheme 11: Theoretical ring formation of *trans-37* to β -keto ester **42** and epimerization into *cis-37*.

Still, the stereocenter in 2-position of diester *trans-37* can be inverted, which changes the *trans*-configuration of *trans-37* into *cis*-configuration via enolate **41**. *cis-37* can form the bicyclic product **25** as shown in Scheme 10. The idea of epimerization was confirmed by the yield of enol ester **25**. According to the ^1H NMR spectrum of **37** (Figure 15), 40% of the diester is *cis*-configured. Thus, a quantitative conversion of only *cis-37* would lead to a yield of 40%. The obtained yield of 58%, is only possible by epimerization of *trans-37* into *cis-37* and subsequent cyclization.

Since the centers of chirality of the bridgehead atoms in 1- and 5-position are connected with each other due to the rigidness of the bicyclic system, only one pair of enantiomers of enol ester **25** could be formed. As a result, the *trans*- and *cis*-configured diastereomers *trans-37* and *cis-37* were converted into diastereomerically pure enol ester **25**.

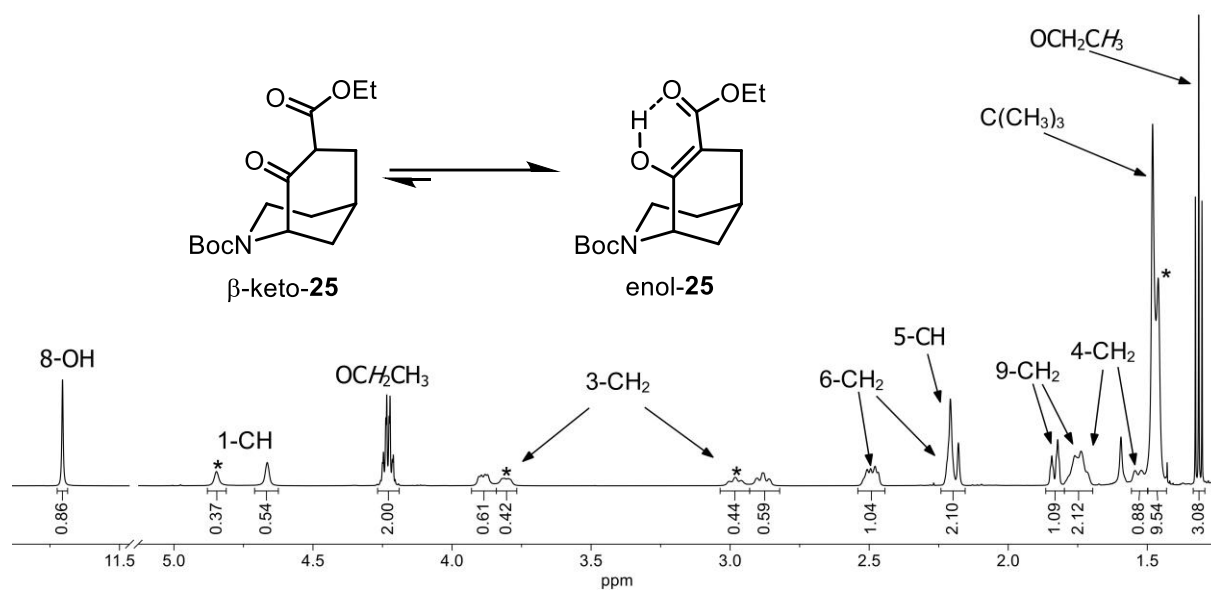
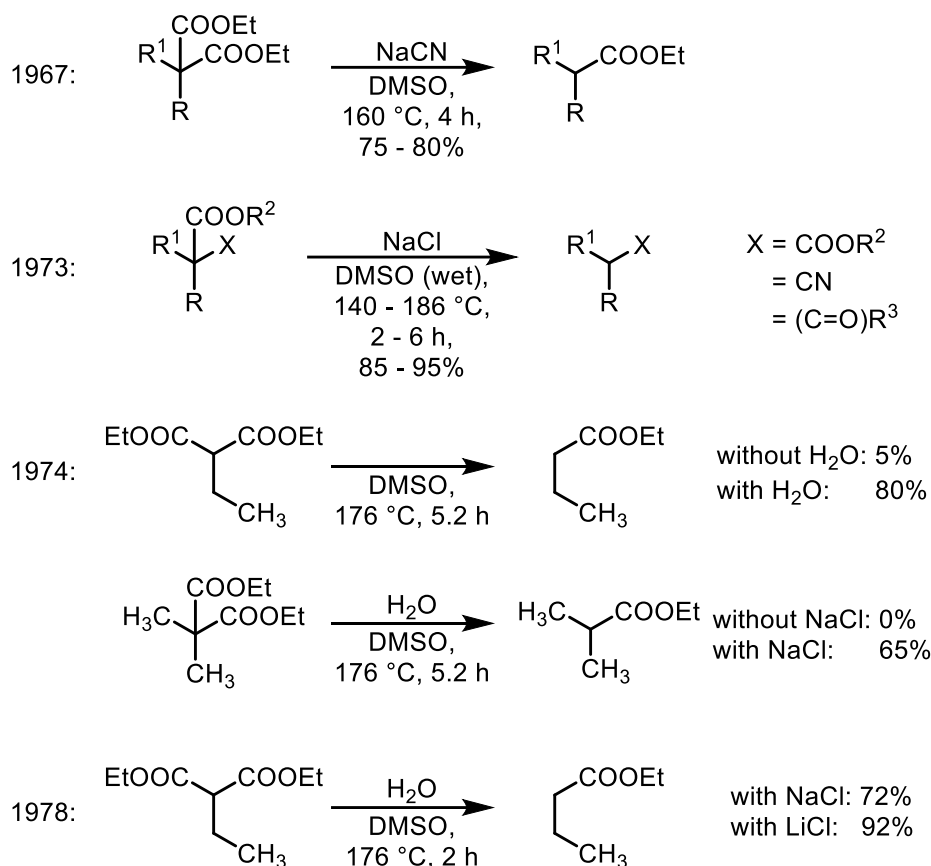


Figure 17: ^1H NMR spectrum (CDCl_3) of enol ester **25**. The signals for the minor rotamer are marked with an asterisk (*).

The successful cyclocondensation was confirmed by NMR and IR spectra. Due to the Boc group, the ^1H NMR spectrum of enol ester **25** shows rotational isomers in the ratio of 6:4. (Figure 17) A low field shifted singlet at 11.70 ppm (OH, 1H) and a missing signal for the CH group in 7-position indicate the exclusive existence of the enol form. The enol ester tautomer is stabilized by an intramolecular H-bond between the hydroxy group and the carbonyl O-atom of the ester moiety. In the IR spectrum, the formed H-bond is lowering the wave number of the $\text{C}=\text{O}_{\text{ester}}$ stretching vibration to 1659 cm^{-1} . This hypothesis was confirmed by similar observations in the literature.^{85,86} The integrals of the methylene (4.20 – 4.26 ppm, 2H) and methyl signals (1.31 ppm, 3H) of the ester moiety are halved compared to diester **37** and confirm the successful condensation.

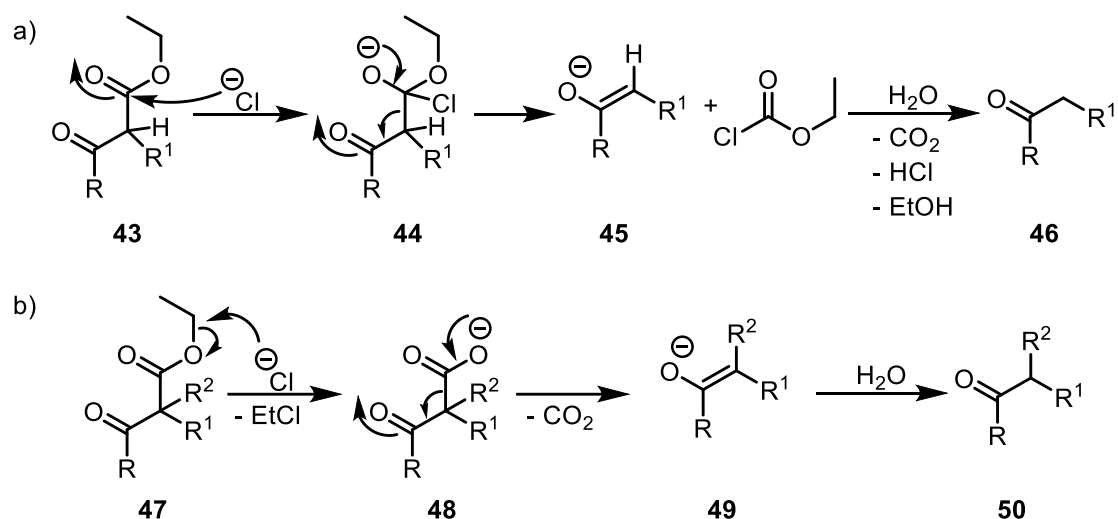
4.1.2 Introduction of KOR pharmacophoric structural elements

The next reaction step was the removal of the ester group in 7-position. Usually, the reaction of an enol/ β -keto ester to a ketone takes place in two steps: the first step is the acid- or base-induced hydrolysis of the ester into a carboxylic acid and the second step is the thermal-induced decarboxylation of the *in situ* formed, unstable β -keto acid.^{92,93} An acid-induced hydrolysis was unfavorable, due to the acid-labile Boc group. The base-mediated hydrolysis should be successful, but the Krapcho reaction offered a fast and efficient one-step alternative.⁹⁴



Scheme 12: Different conditions for the dealkoxycarbonylation of esters and the effect of H₂O and salts as additives.^{95–97}

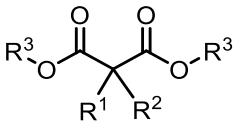
In 1967, Krapcho described the deethoxycarbonylation of several geminal diesters to afford the corresponding monoesters in high yields using NaCN as an additive.⁹⁵ (Scheme 12) Seven years later, he expanded the application of this type of reaction to a variety of substrates with an electron withdrawing group in α -position to the ester (β -keto ester, α -cyano ester).⁹⁶ The addition of H₂O and salts can be helpful to enhance the reaction rate especially for α,α -disubstituted malonic esters. Due to their enhanced solubility in DMSO, Li-salts became the preferred additives.⁹⁷ In 1977, Krapcho described two different mechanisms for the dealkoxycarbonylation reaction depending on the substitution pattern in α -position to the ester.⁹⁸ (Scheme 13)



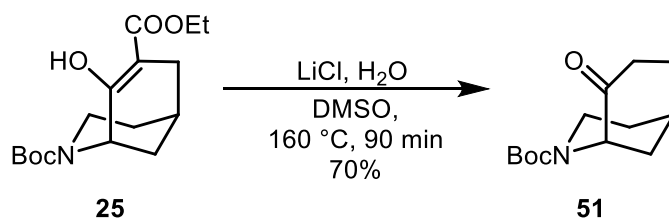
Scheme 13: Two different mechanisms of the Krapcho deethoxycarbonylation of (a) α -monosubstituted and (b) α,α -disubstituted β -keto esters.⁹⁸

For α -monosubstituted β -keto ester **43**, an addition-elimination mechanism was proposed. (Scheme 13a) At first, the chloride (or hydroxide ion if no salt additive is used) attacks nucleophilically the β -keto ester **43** forming the tetrahedral intermediate **44**. Then, the carbonyl double bond is reformed, transforming intermediate **44** into enolate **45** and ethyl chloroformate. Enolate **45** reacts with H_2O to give the ketone **46** while ethyl chloroformate decomposes into CO_2 , HCl and EtOH . For α,α -disubstituted β -keto ester **47**, a nucleophilic substitution ($\text{S}_{\text{N}}2$) was proposed. (Scheme 13b) The chloride ion attacks the methylene group of the ethyl ester forming ethyl chloride and β -keto carboxylate **48**. After the release of CO_2 , the obtained enolate **49** was protonated to afford the ketone **50**. To investigate the dealkoxycarbonylation mechanism, Krapcho used various diesters and determined the ratio of formed side products by gas liquid chromatography (GLC). (Table 2) In his study, NaCN was used as an additive.⁹⁸

Table 2: Nitrile/alcohol ratios after dealkoxycarbonylation reaction with NaCN.⁹⁸

Substitution pattern	R ¹	R ²	R ³	Ratio nitrile/alcohol
	Et	H	Et	3:7
	CH ₃	H	Et	1:2
α,α-disubstituted	CH ₃	CH ₃	Et	6:4
	Et	Et	Et	4:1
	Et	Et	CH ₃	only CH ₃ CN

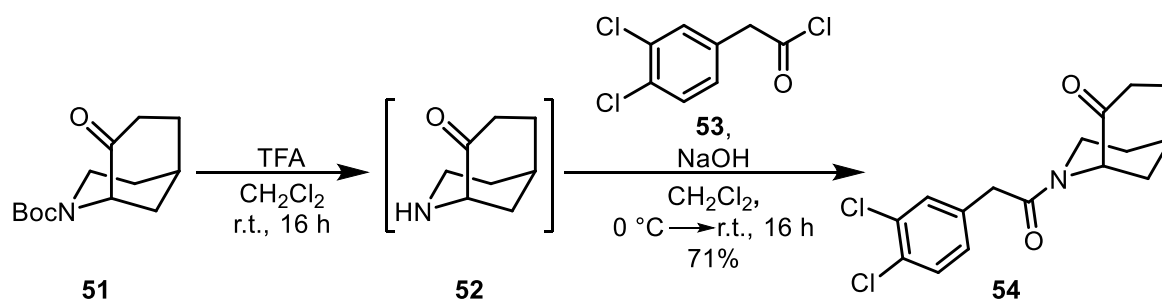
During the addition-elimination reaction (mechanism a), an alcohol was formed as side product, whilst after the S_N2 reaction (mechanism b) a nitrile was obtained. Thus, the formation of the side product (nitrile or alcohol) gave insight into the mechanism. Almost all starting materials and reaction conditions led to nitrile and alcohol indicating that both mechanisms took place simultaneously. However, two substituents at the α-position to the ester led to a higher nitrile/alcohol ratio. Methyl esters favour the S_N2 reaction. In general, it can be concluded, that α-monosubstituted β-keto esters favor the addition-elimination mechanism, whilst α,α-disubstituted β-keto esters and methyl esters react preferably *via* a S_N2 reaction.

**Scheme 14:** Krapcho deethoxycarbonylation reaction of enol ester **25**.

The deethoxycarbonylation reaction was performed, by stirring a solution of enol ester **25** and LiCl in DMSO and H₂O at 160 °C. (Scheme 14). Due to the fast decomposition of DMSO at elevated temperature, the reaction mixture was added into a pre-heated oil bath. Moreover, the reaction was controlled by TLC (KMnO₄ staining) every 30 min. The reaction was stopped after 90 min providing the ketone **51** in 70% yield. The successful deethoxycarbonylation can be recognized by the loss of the band at 1659 cm⁻¹ (C=O_{ester}) and the formation of a new band at 1721 cm⁻¹ (C=O_{ketone}) in the IR spectrum. A new signal at 210.5 ppm in the ¹³C NMR spectrum indicates the existence of a ketone, whilst the signal for the carbonyl C-atom of the ester had

disappeared. In the ^1H NMR spectrum signals for the ethyl group of the ester moiety can no longer be observed.

The next step was the introduction of the first KOR pharmacophoric element. The Boc group was cleaved off with trifluoroacetic acid (TFA) and without further purification the obtained secondary amine **52** was acylated with (3,4-dichlorophenyl)acetyl chloride (**53**). (Scheme 15)



Scheme 15: Introduction of the dichlorophenylacetyl moiety as the first KOR pharmacophoric structural element.

The successful removal of the Boc group could be seen on the TLC (KMnO_4 staining). The spot of **51** vanished during the transformation, while a new spot for a more polar compound appeared close to the baseline. After 16 h, the dichlorophenylacetyl moiety was introduced by basifying the reaction mixture with NaOH (2 M) and adding a solution of acyl chloride **53** in CH_2Cl_2 . The overall yield of the one-pot reaction forming amide **54** was 71%. The method for the acylation of amines with acyl chlorides in a two-phase solvent system was described by Carl Schotten and Eugen Baumann in 1883.^{99,100} The starting materials as well as the product are dissolved in the organic layer, due to their low solubility in H_2O . The generated HCl reacts with the base in the aqueous phase. The acid/base reaction prevents the protonation of the amine, which would inhibit the acylation reaction.

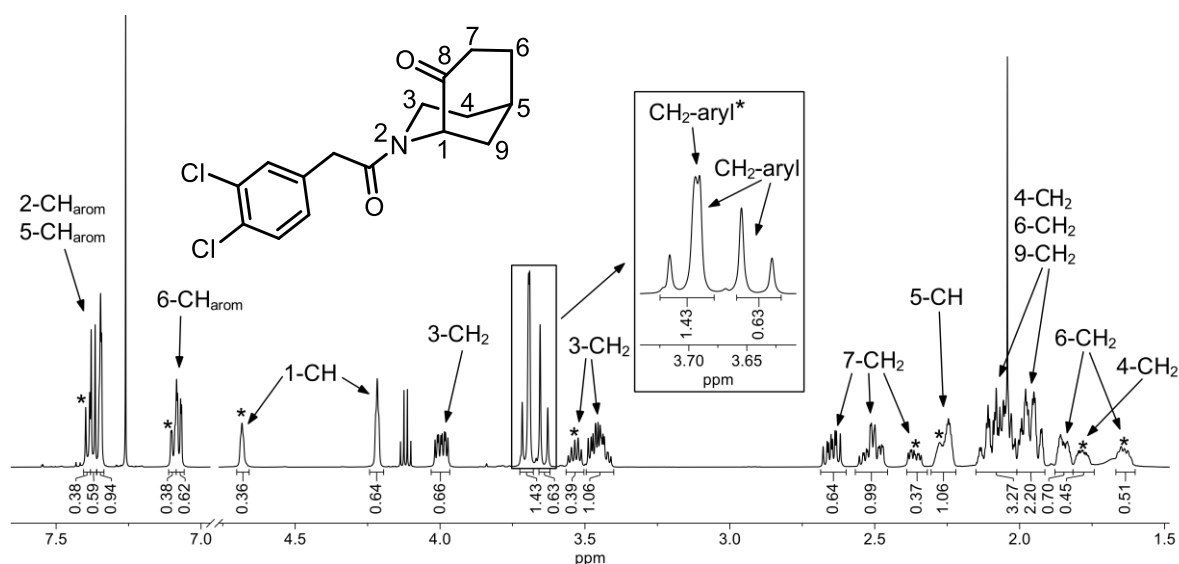
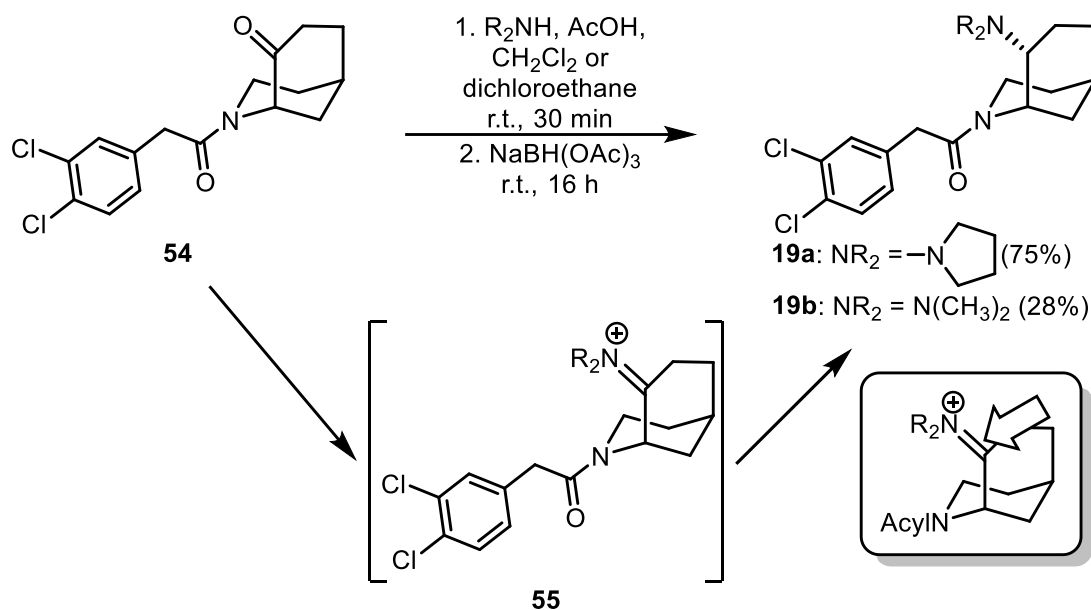


Figure 18: ^1H NMR spectrum (CDCl_3) of amide **54**. The signals for the minor rotamer are marked with an asterisk (*).

The exchange of the Boc group by the dichlorophenylacetyl moiety was shown in the ^1H NMR spectrum of amide **54**. (Figure 18) Due to rotational isomerism along the amide C-N-bond, two sets of signals in the ratio 6:4 are observed. Whereas the singlet for the Boc group with an integral of 9H disappeared, new signals for the acyl side chain are detected. A doublet at 3.64 ppm with an integral of 0.6H and an overlapping singlet and doublet at 3.68 – 3.73 ppm with an integral of 1.4H represent the benzylic CH_2 group. The protons of the major rotamer are diastereotopic leading to two doublets. However, the singlet of the benzylic CH_2 group of the minor rotamer overlap with one doublet of the major rotamer resulting into an overlapped signal with an integral of 1.4H. The aromatic proton in 6-position shows two dd's at 7.07 ppm (major rotamer) and 7.10 ppm (minor rotamer). The $2\text{-CH}_{\text{arom}}$ signals of both rotamers overlap in a multiplet at 7.34 – 7.36 ppm and two doublets at 7.37 ppm (major rotamer) and 7.39 ppm (minor rotamer) represent the protons in 5-position. In the IR spectrum, a stretching vibration band at 1639 cm^{-1} underlines the formation of an amide. Mass spectrometry also confirms the successful exchange of the Boc group by the acyl moiety.

The final reaction step to obtain conformationally restricted ethylenediamines **19a** and **19b**, was the reductive amination of ketone **54**. (Scheme 16)



Scheme 16: Diastereoselective reductive amination of ketone **54**.

For this purpose, a solution of amide **54**, pyrrolidine or $HN(CH_3)_2$ and AcOH was stirred for 30 min, inducing the formation of the iminium ion **55**. Then, $NaBH(OAc)_3$ was added to obtain the desired bicyclic pyrrolidine **19a** and dimethylamine **19b** in 75% and 28% yield, respectively. The bulky reducing agent $NaBH(OAc)_3$ led to diastereoselective hydride transfer from the sterically less hindered backside. As a result, only the *endo*-configured bicyclic amines **19a** and **19b** were isolated.

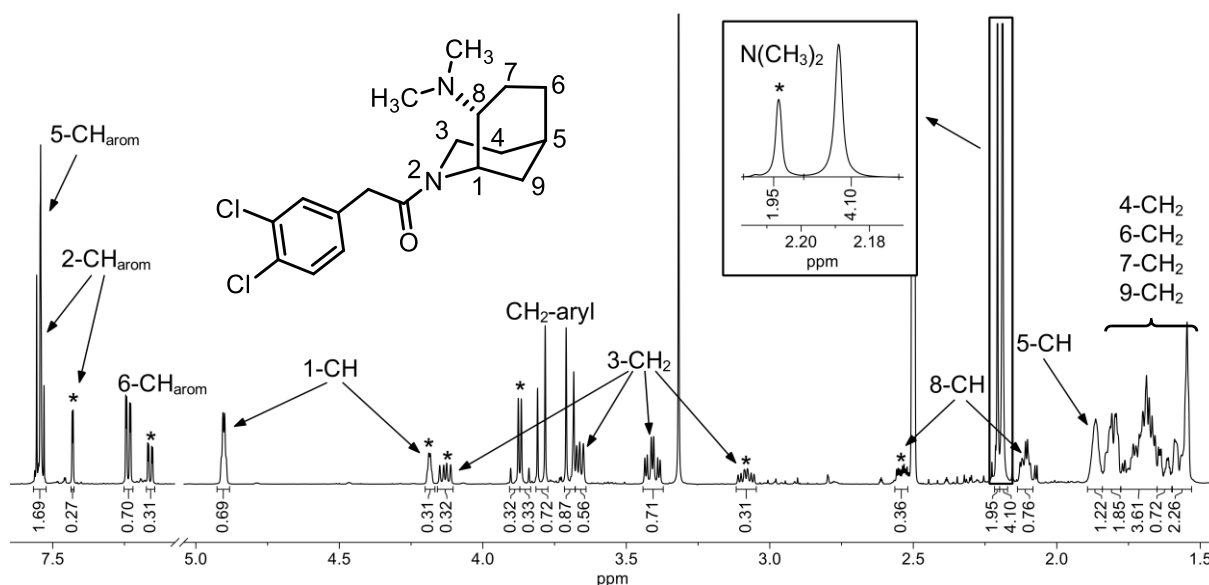


Figure 19: 1H NMR spectrum ($CDCl_3$) of bicyclic dimethylamine **19b**. The signals for the minor rotamer are marked with an asterisk (*).

The ^1H NMR spectrum of the bicyclic dimethylamine **19b** shows two sets of signals in the ratio 7:3, due to rotational isomerism along the C-N bond of the amide group. (Figure 19) The introduction of the dimethylamino moiety is demonstrated by two singlets at 2.19 ppm (major rotamer) and 2.21 ppm (minor rotamer). Furthermore, the two multiplets at 2.08 – 2.13 ppm and 2.51 – 2.56 ppm belong to the newly formed methyne proton in 8-position. In the ^{13}C NMR spectrum the signal for the carbonyl C-atom of the ketone has disappeared. Also, in the IR spectrum a band for the stretching vibration of the C=O group cannot be observed anymore. To prove the relative configuration of the bicyclic dimethylamine **19b**, a NOESY experiment was performed. (Figure 20) The complete NOESY spectrum is displayed in Figure S2. (Appendix)

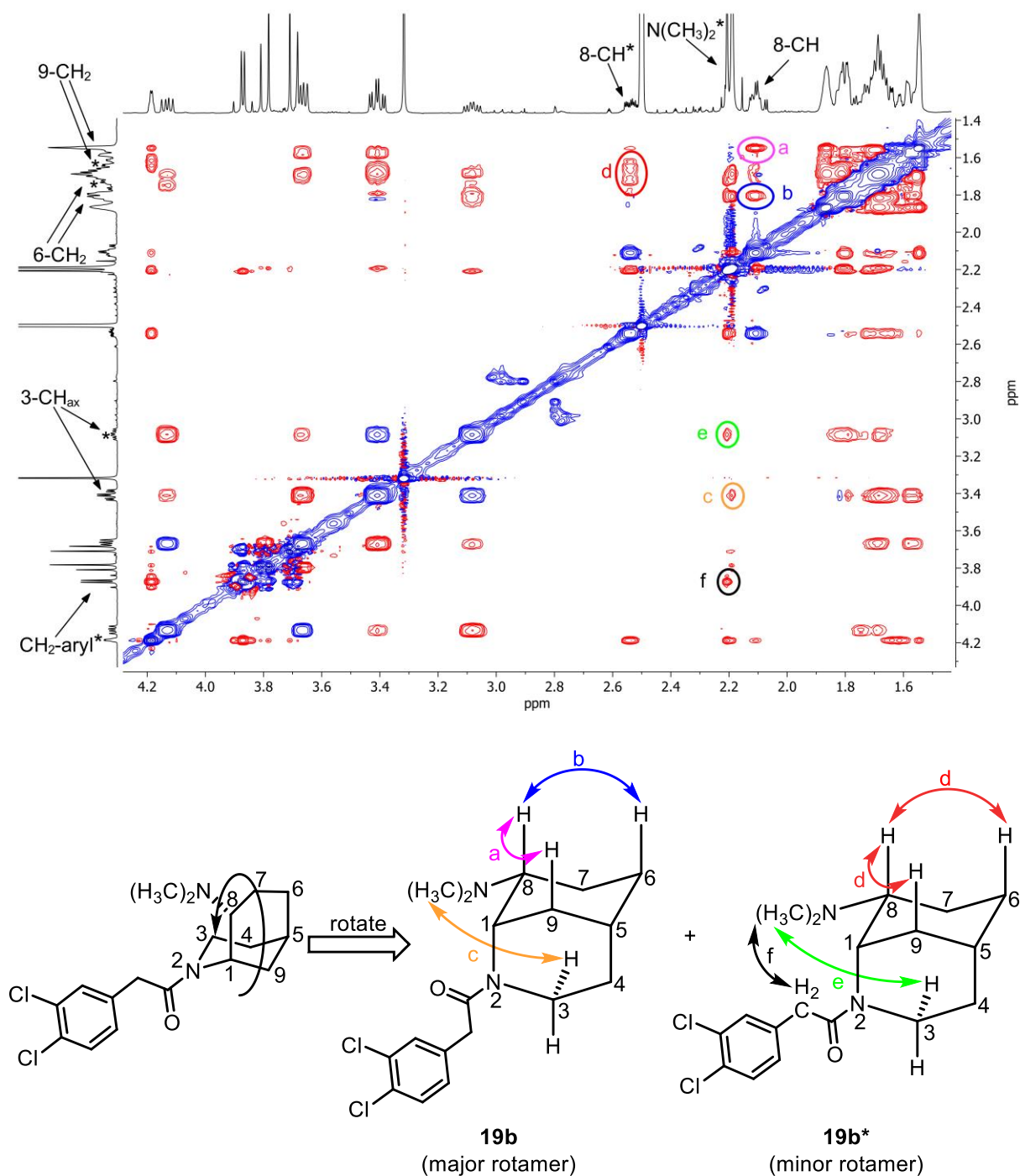


Figure 20: NOESY spectrum of bicyclic dimethylamine **19b**. The signals for the minor rotamer are marked with an asterisk (*).

In the NOESY spectrum, two cross peaks (major rotamer) between the signals of 8-CH (2.09 - 2.14 ppm) and 9-CH (1.53 - 1.57 ppm, mark a) and 8-CH and 6-CH (1.78 - 1.84 ppm, mark b) show *cis*-orientation of the proton in 8-position with the protons in 6- and 9-position. As a result, the *endo*-configuration of the bicyclic dimethylamine **19b** was confirmed. A cross peak of the signals at 2.21 ppm (N(CH₃)₂) and 3.41 ppm (3-CH_{ax, pip}, mark c) shows unequivocally the *endo*-configuration of **19b**. For the minor

rotamer, two cross peaks between the signals at 2.51 - 2.56 ppm (8-CH^{*}) and 1.61 - 1.75 ppm (6-CH^{*} and 9-CH^{*}, mark d) also show *endo*-configuration. Moreover, the methyl groups of the tertiary amine (N(CH₃)₂^{*}) resonating at 2.21 ppm show a cross peak with 3-CH^{*} (3.05 - 3.12 ppm, mark e). These observations correlate with the results for the major rotamer. A special cross peak for the minor rotamer appears between the signals for N(CH₃)₂^{*} and the benzylic protons^{*} (3.85 ppm and 3.89 ppm, mark f). This proximity indicates that for the minor rotamer, the carbonyl O-atom of the amide points to the 3-CH₂^{*} moiety bringing the dichlorobenzyl moiety close to the N(CH₃)₂ group. Thus, the carbonyl O-atom for the major rotamer is orientated towards the 1-CH moiety. Similar results were observed for the bicyclic pyrrolidine analog **19a** with a 85:15 ratio of rotamers. (Figure S3, Appendix)

4.1.3 Separation of enantiomers and determination of the absolute configuration of 2-azabicyclo [3.3.1]nonanes **19a**

Due to the high KOR affinity of the synthesized racemic 2-azabicyclo[3.3.1]nonane **19a**, (chapter 5.3 Receptor affinity) a chiral HPLC method was developed to separate the racemic mixture of pyrrolidine **19a**. Daicel Chiralpak IA was used as chiral stationary phase. The addition of formic acid led to inversion of the peaks. (HPLC method C) The chromatograms in Figure 21 display the enantiomers (1*S*,5*R*,8*R*)-**19a** and (1*R*,5*S*,8*S*)-**19a** (*ent*-**19a**) before (top) and after the chiral separation (middle and bottom) using HPLC methods C (left) and D (right). The preparative chiral HPLC was performed using Daicel Chiralpak IA as stationary phase and *i*-hexane/*i*-propanol 95:5 + 0.1% HNEt₂. (HPLC method G) After the successful separation, the enantiomers **19a** and *ent*-**19a** were investigated performing HPLC methods C and D. Both enantiomers were obtained with high enantiomeric purity. (Figure 21 and Table 3)

The enantiomer, which eluted first using HPLC method C, eluted last when using method D and *vice versa*. Due to the high structural similarity of 2-azabicyclo[3.3.1]nonane **19a** and 2-azabicyclo[3.2.1]octanes **23a,b**, the absolute configuration of the separated enantiomers **19a** and *ent*-**19a** were assigned by correlation with **23a,b**. As described for the separation of the enantiomers of bicyclic amines **23a,b** in chapter 4.5.5, the enantiomer which eluted first using HPLC method D has (1*S*,5*S*,7*R*)-configuration, whereas the enantiomer, which eluted first using HPLC method C has (1*R*,5*R*,7*S*)-configuration. As a consequence, the enantiomer **19a** which

eluted first using method D and last using method C has (1*S*,5*R*,8*R*)-configuration, while the other enantiomer *ent*-**19a** has a (1*R*,5*S*,8*S*)-configuration.

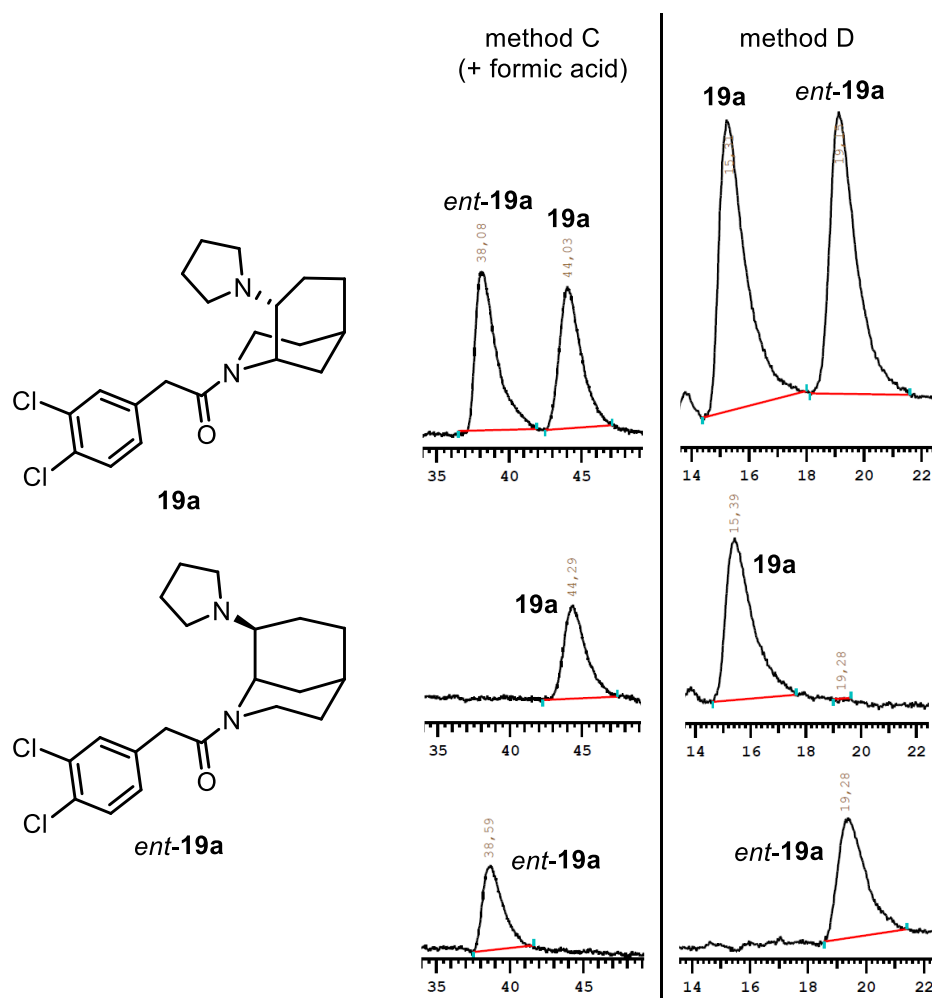
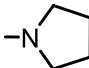
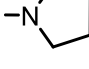


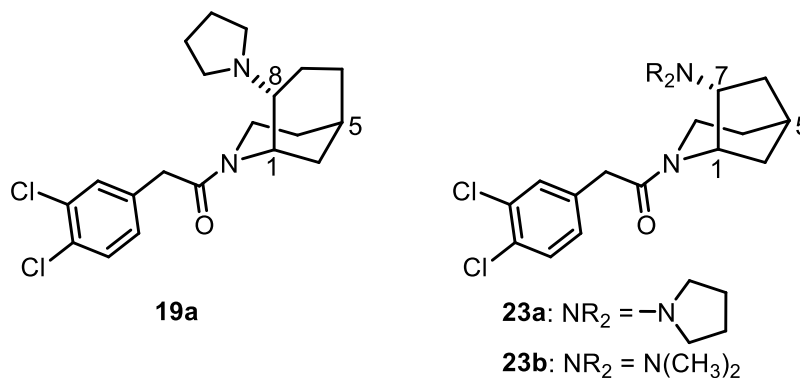
Figure 21: Chiral HPLC chromatograms of **19a** before (top) and after separation. HPLC method C (left) and HPLC method D (right) led to separation of (1*S*,5*R*,8*R*)-**19a** and (1*R*,5*S*,8*S*)-**19a** (*ent*-**19a**). HPLC method C (left): Column: Daicel Chiralpak IA; eluent: *i*-hexane/EtOH = 9:1 + 0.1% HNEt₂ + 0.1% formic acid; HPLC method D (right): *i*-hexane/*i*-propanol = 95:5 + 0.1% HNEt₂. Both HPLC methods C and D: isocratic elution; flow rate: 1.0 mL/min; detection λ = 275 nm. The addition of formic acid led to inversion of the peaks.

Table 3: Enantiomeric excess of the enantiomerically pure test compounds **19a** and *ent*-**19a**.

compd.	configuration	NR ₂	ee [%]
19a	(1 <i>S</i> ,5 <i>R</i> ,8 <i>R</i>)		99.9
<i>ent</i> - 19a	(1 <i>R</i> ,5 <i>S</i> ,8 <i>S</i>)		99.9

This assignment can be affirmed by comparing the specific rotation of 2-azabicyclo[3.3.1]nonanes **19a** and *ent*-**19a** and 2-azabicyclo[3.2.1]octanes **23a,b** and *ent*-**23a,b**. (Table 4)

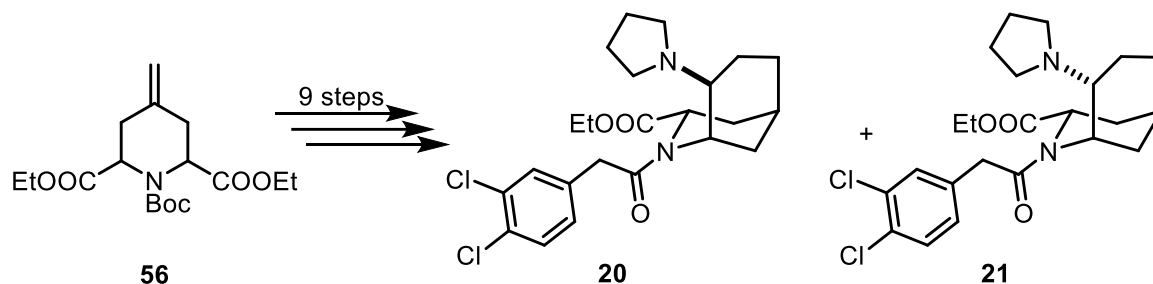
Table 4: Specific rotations of bicyclic amines **19a**, **23a** and **23b**.



compd.	configuration	NR_2	specific rotation $[\alpha]_{20}^{\text{D}}$
19a	(1 <i>S</i> ,5 <i>R</i> ,8 <i>R</i>)		-23.8
<i>ent</i> - 19a	(1 <i>R</i> ,5 <i>S</i> ,8 <i>S</i>)		+22.6
23a	(1 <i>S</i> ,5 <i>S</i> ,7 <i>R</i>)		-70.4
<i>ent</i> - 23a	(1 <i>R</i> ,5 <i>R</i> ,7 <i>S</i>)		+65.9
23b	(1 <i>S</i> ,5 <i>S</i> ,7 <i>R</i>)		-73.8
<i>ent</i> - 23b	(1 <i>R</i> ,5 <i>R</i> ,7 <i>S</i>)	$\text{N}(\text{CH}_3)_2$	+74.3

4.2 Part 2: Synthesis of 2-azabicyclo[3.3.1]nonanes **20** and **21** with an ethyl ester in 3-position

The synthesis of bicyclic KOR agonists **20** and **21** with an ethyl ester in 3-position was planned in analogy to the synthesis of 2-azabicyclo[3.3.1]nonanes **19a** and **19b**. Instead of monoester **30**, diester **56** was used as starting material. (Scheme 17)



Scheme 17: Outline of the synthesis of 2-azabicyclo[3.3.1]nonane **20** and **21** with an additional ethyl ester in 3-position.

The description of the synthesis of **20** and **21** is divided into two parts: the first part describes the preparation of piperidine **56** by adapting different procedures from the literature and second part deals with the transformation of piperidine **56** into bicyclic amines **20** and **21**.

4.2.1 Synthesis of 2,6-disubstituted piperidine **56**

The first idea was to synthesize the benzyl protected piperidinone analog **57** with two ester moieties in 2- and 6-position. (Figure 22)

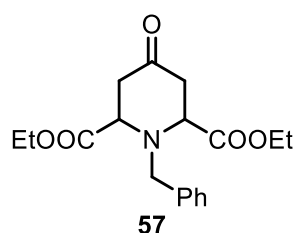
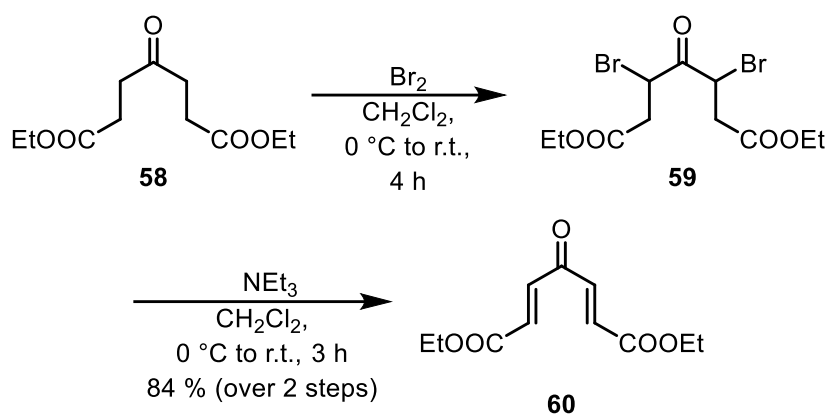


Figure 22: Benzyl protected piperidinone **57** with two ester groups in 2- and 6-position.

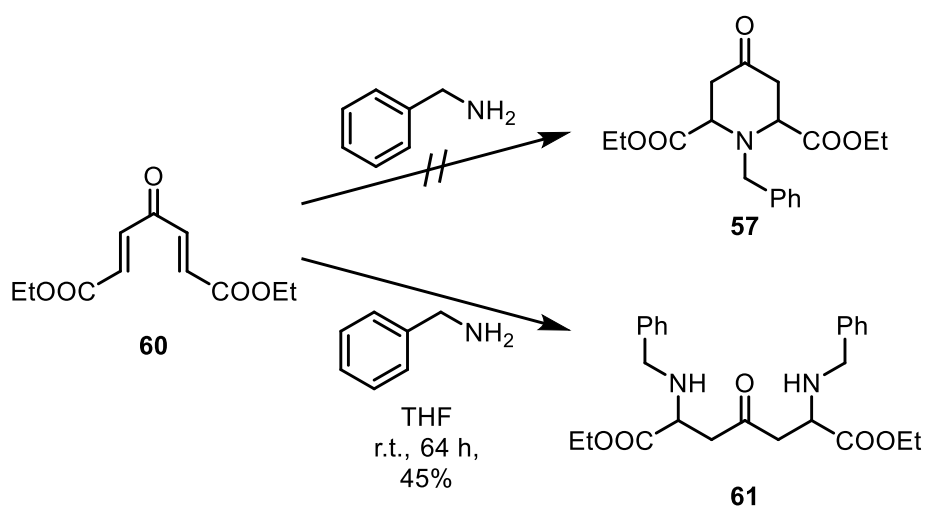
The synthesis of 4-oxopiperidine-2,6-dicarboxylates of type **57** is reported by a tandem aza-Michael addition of amines at the heptadienone **60**.⁵⁹ Dienone **60** was obtained from commercially available diethyl 4-oxopimelate (**58**). (Scheme 18)



Scheme 18: Synthesis of dienone **60** following a reported synthesis by Dreiding *et al.*⁵⁹

After selective bromination with Br_2 at both α -positions of ketone **58**, a dehydrohalogenation with NEt_3 led to dienone **60**. According to the literature^{59,101} alkyl bromide **59** had to be crystallized from petroleum ether and dienone **60** from EtOH. However, conversion of crude **59** into dienone **60** followed by flash column chromatography was faster and very efficient to obtain dienone **60**. The overall yield of **60** from **59** was 84% (lit. 83%⁵⁹, 74%¹⁰¹). The ^1H NMR spectrum of **59** shows the formation of two diastereomers in the ratio 8:2. After dehydrobromination, only the (2*E*,5*E*)-configured dienone **60** was isolated. Both observations are in accordance with the results of Dreiding *et al.*⁵⁹

The next step was the reaction of dienone **60** with benzylamine in a tandem aza-Michael addition. (Scheme 19)



Scheme 19: Aza-Michael addition generating ketone **61** instead of piperidinone **57**.

Although similar cyclization reactions of dienones with amines are described in the literature, piperidinone **57** could not be obtained by this method.^{59,102} Analysis of the

^1H NMR spectrum indicates that two molecules of benzylamine were added to one molecule of dienone **60** forming ketone **61**. (Figure 23)

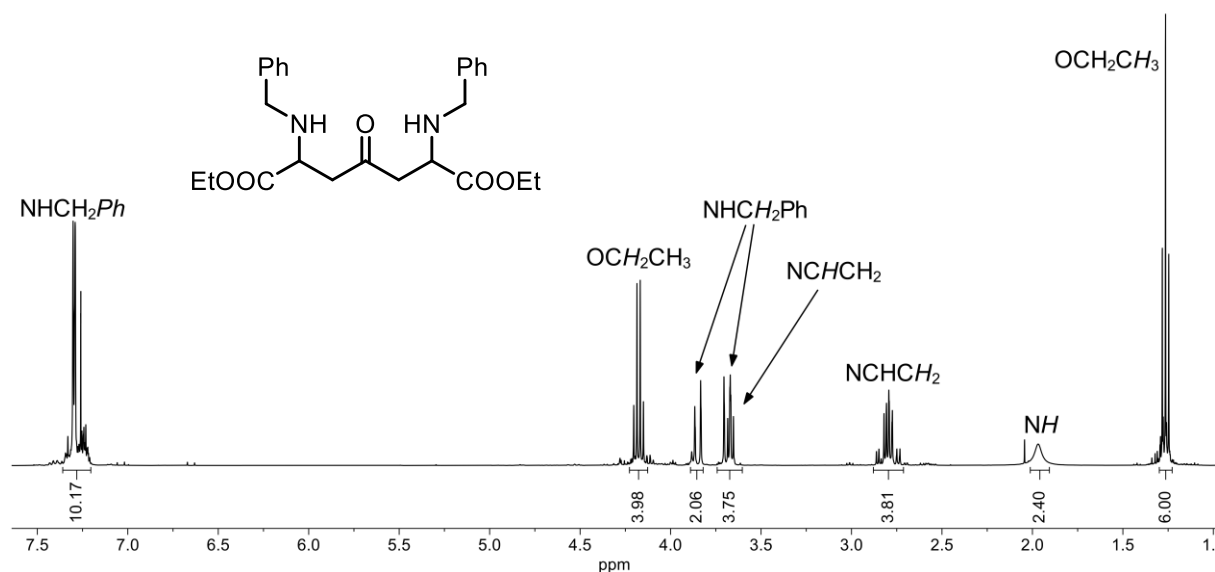
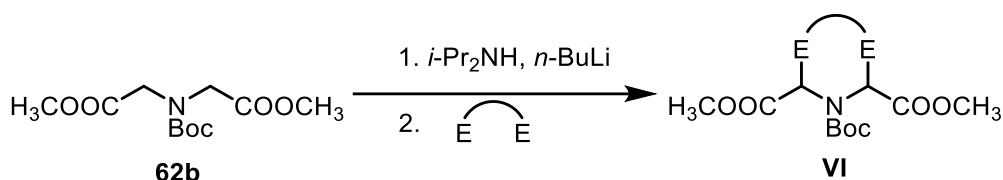


Figure 23: ^1H NMR spectrum (CDCl_3) of ketone **61**.

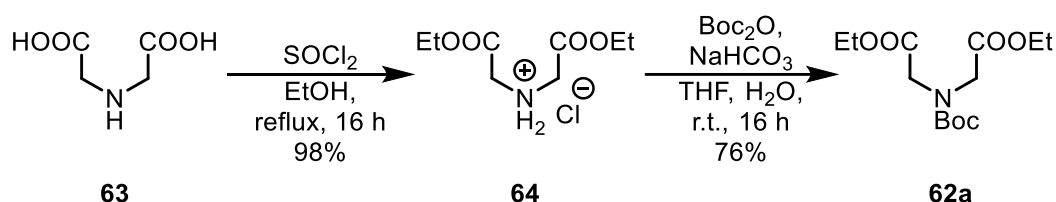
To prove the addition of two molecules of benzylamine, the ratio of the integrals for the phenyl rings and the ester moieties was determined. Since two ester moieties are present in both compounds **57** and **61**, the integrals of the ethyl ester signals were set as 6H for the CH₃ group (t, 1.26 ppm) and 4H for the CH₂ group (q, 4.18 ppm). The integral of the multiplet at 7.19 – 7.45 ppm representing the aromatic protons of the phenyl groups is 10H indicating the presence of two molecules of benzylamine. Furthermore, the integrals of the benzylic protons (3.64 – 3.71 ppm and 3.85 ppm, 4H) and the amine (1.97 ppm, 2H) are doubled proving the structure of **61**. To inhibit the unwanted double addition, a highly diluted solution of dienone **60** in THF ($c = 0.01$ M) was prepared and benzylamine was added slowly to the mixture. Moreover, the reaction was performed at different temperatures. However, the desired product **57** could not be obtained, which was probably caused by fast and uncontrollable side reactions of polyfunctional dienone **60**. As a consequence, a different approach was developed.

In 1994, Einhorn *et al.* reported a method to synthesize different cyclic carbamates **VI** with methyl ester moieties at each α -position to the N-atom.⁶⁰ Therefore, carbamate **62b** was deprotonated and reacted with different dielectrophiles to form a variety of cyclic carbamates **VI**. (Scheme 20)



Scheme 20: Reported method of Einhorn *et al.* to synthesize cyclic carbamates **VI** by reacting carbamate **62b** with different dielectrophiles.⁶⁰

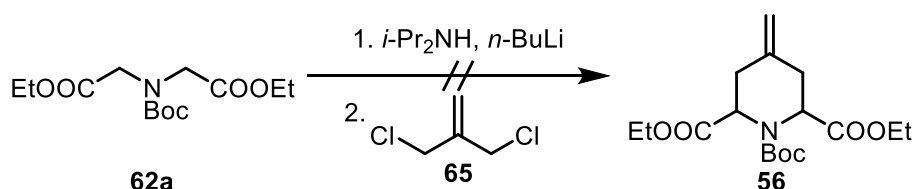
By analogy to piperidine **30** (chapter 4.1.1.2) an ethyl ester derivative was synthesized. The synthesis started with the esterification of iminodiacetic acid (**63**) using SOCl_2 in refluxing EtOH. The HCl salt **64** was obtained in 98% yield. (Scheme 21)



Scheme 21: Synthesis of *N*-Boc protected diester **62a**.

A triplet at 1.24 ppm and a quartet at 4.21 ppm in the ^1H NMR spectrum of **64** represent the signals for the ethyl groups of the esters and confirm the successful esterification. The secondary amine **64** was protected with Boc_2O to obtain carbamate **62a** with a yield of 76%. In the ^1H NMR spectrum of **62a** a singlet at 1.35 ppm with an integral of 9H represents the introduced Boc group. The C=O stretching vibration of the carbamate leads to a band at 1700 cm^{-1} in the IR spectrum.

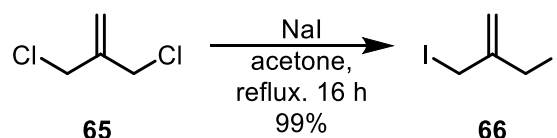
Attempts to react **62a** with allylic dichloride **65** did not lead to 4-methylenepiperidine **56**. (Scheme 22)



Scheme 22: Attempt to synthesize piperidine **56** using allylic dichloride **65**.

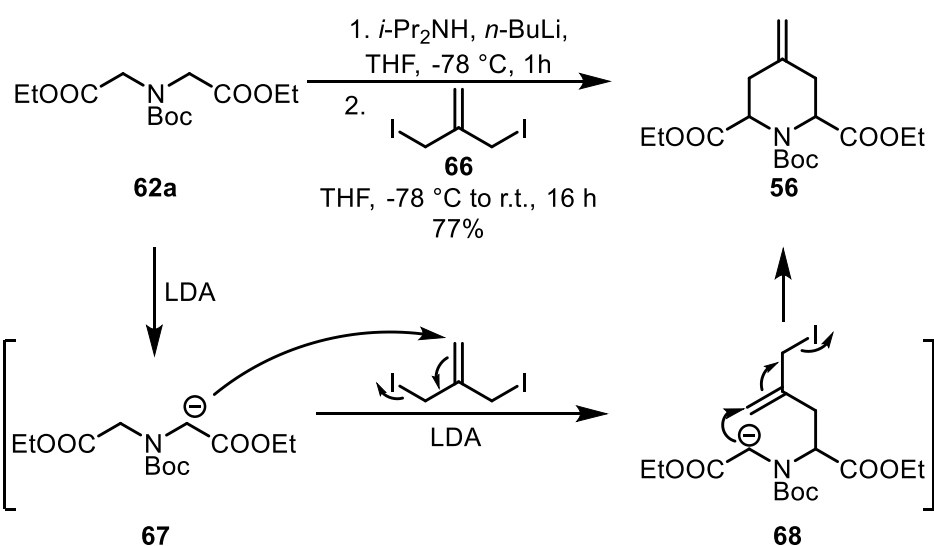
Therefore, **65** was activated by conversion into diiodide analog **66**. Allylic diiodide **66** was freshly synthesized by a Finkelstein reaction¹⁰³ using commercially available 3-chloro-2-(chloromethyl)prop-1-ene (**65**) and NaI. The reaction was performed in refluxing acetone leading to **66** in 99% yield.¹⁰⁴ (Scheme 23) Due to the good solubility

of NaI in acetone (504 g/kg),¹⁰⁵ the Cl-atoms of allylic dichloride **65** were exchanged with I-atoms by a nucleophilic substitution (S_N2). During the reaction, NaCl was generated, which is poorly soluble in acetone (0.00042 g/kg).¹⁰⁵ As a consequence, NaCl precipitated and could not participate in the reaction anymore limiting the backward reaction. Mass spectrometry confirmed the presence of two I-atoms in **66**.



Scheme 23: Halogen exchange (Finkelstein reaction) reaction of allylic dichloride **65** with NaI.¹⁰⁴

The crucial step was the reaction of diester **62a** with 3-iodo-2-(iodomethyl)prop-1-ene (**66**). (Scheme 24)



Scheme 24: Adapted synthesis of piperidine **56** by Einhorn *et al.* and proposed mechanism *via* anionic species **67** and **68**.⁶⁰

For the double allylation of diester **62a**, LDA was prepared *in situ* from *n*-BuLi and *i*-Pr₂NH. After the first removal of a proton in α-position to the ester moiety of carbamate **62a**, anion **67** reacted with the allylic diiodide **66**. A second deprotonation generated anion **68**, which cyclized to piperidine **56**. The methylene piperidine **56** was obtained in 77% yield.

The successful formation of the piperidine ring was shown in the IR and ¹H NMR spectra of piperidine **56**. In the IR spectrum, a band at 1655 cm⁻¹ presents a C=C stretching vibration. In the ¹H NMR spectrum, two sets of signals in the ratio 9:1 are

observed, which is indicated by two singlets for the protons of the exocyclic double bond ($R_2C=CH_2$) at 4.83 ppm and 4.92 ppm and two singlets for the Boc group at 1.42 ppm and 1.47 ppm. (Figure 24)

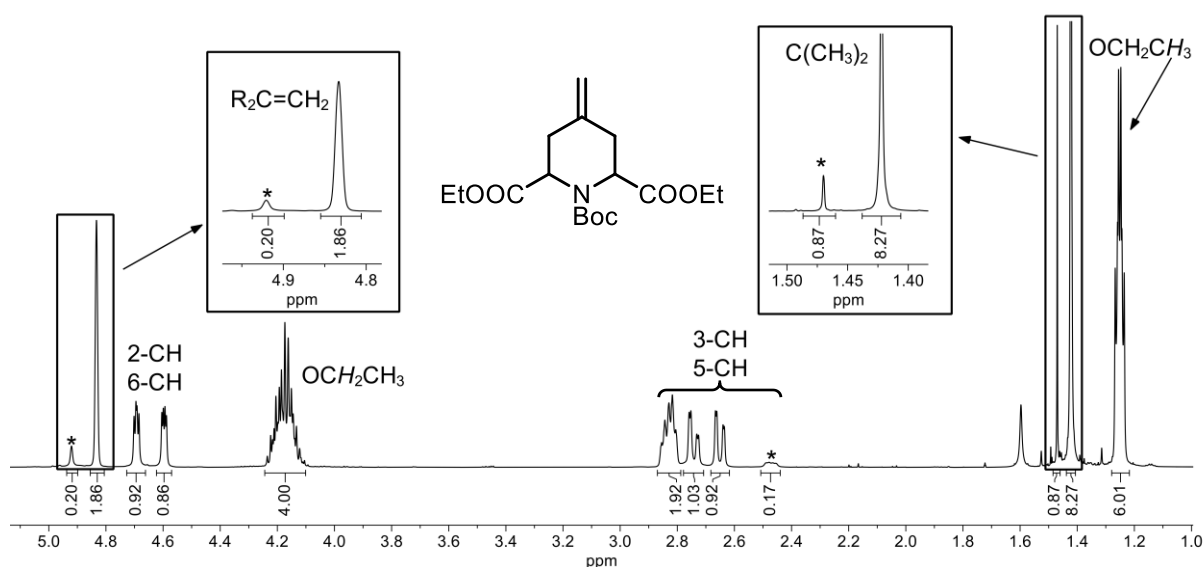
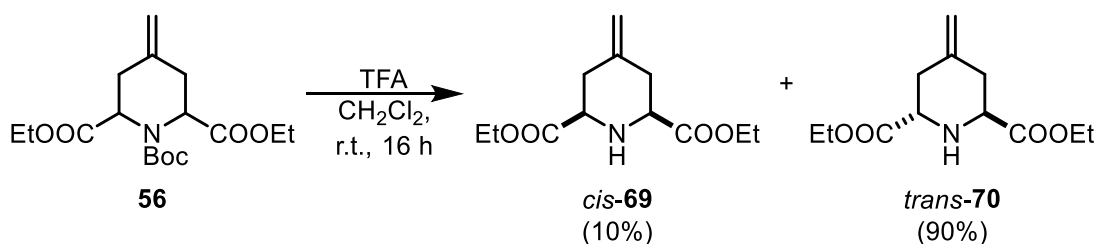


Figure 24: 1H NMR spectrum ($CDCl_3$) of piperidine **56** with a diastereomeric ratio of 9:1. The signals of the minor diastereomer are marked with an asterisk (*).

These pairs of signals prove the formation of *trans*- and *cis*-configured diastereomers *trans*-**56** and *cis*-**56** in the ratio 9:1. The two sets of signals could not be assigned by their J couplings constants to the diastereomers *cis*-**56** and *trans*-**56**. Also, a separation of the diastereomers by flash column chromatography was not possible. Thus, the Boc group of **56** was removed with TFA generating a mixture of *cis*-**69** and *trans*-**70** in quantitative yields. (Scheme 25)



Scheme 25: Removal of the Boc group from piperidine **56** with TFA.

After Boc removal, the 9:1 mixture of diastereomeric secondary amines *cis*-**69** and *trans*-**70** could be separated by flash column chromatography. The relative configuration of the diastereomers **69** and **70** could be assigned by 1H NMR spectroscopy. (Figure 25)

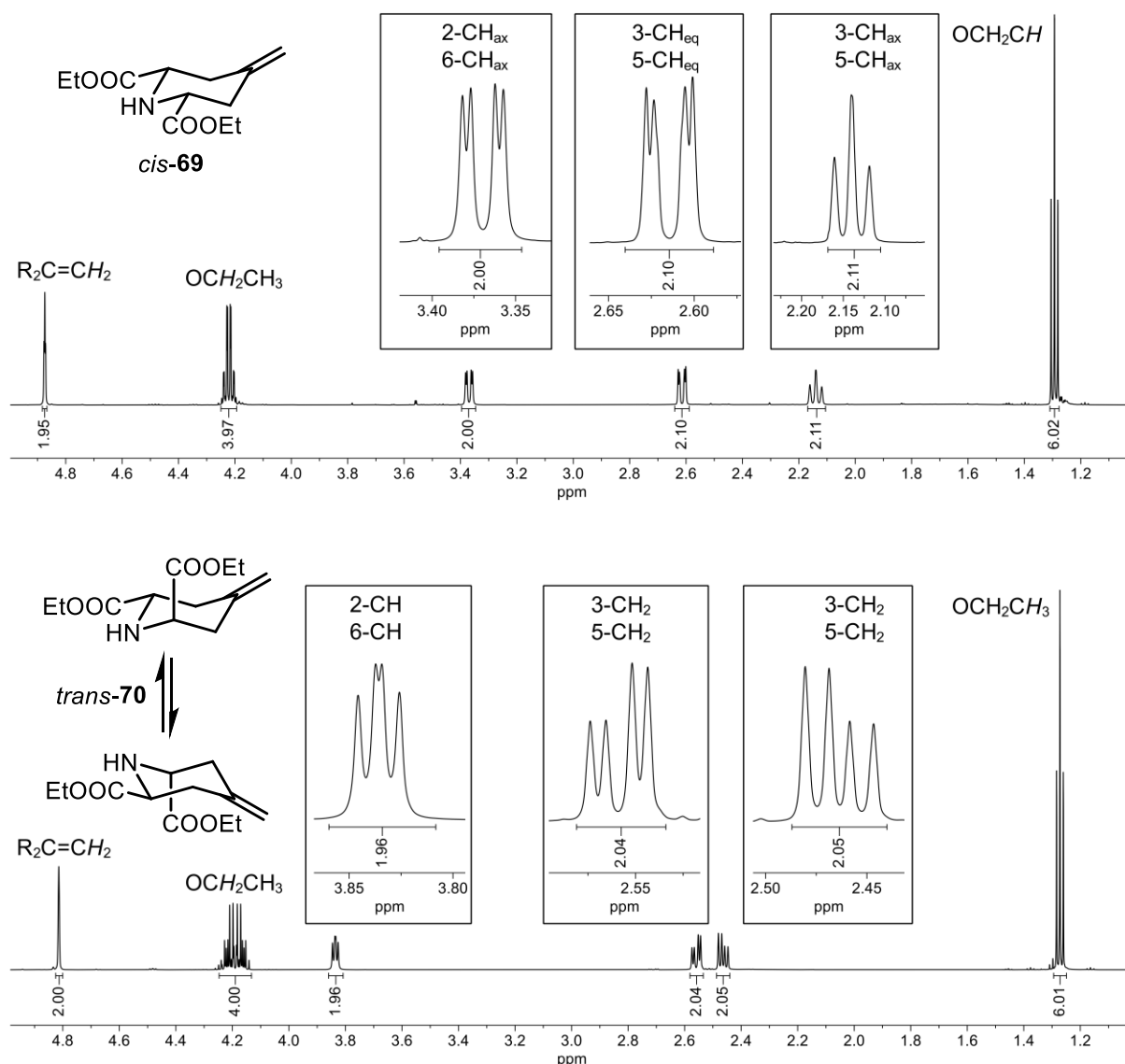


Figure 25: ^1H NMR spectra (CDCl_3) of *cis*-configured *cis*-69 (top) and *trans*-configured *trans*-70 (bottom).

In the ^1H NMR spectrum of the minor diastereomer *cis*-69 (Figure 25 top), the dd ($J = 11.8 / 3.0$ Hz) at 3.37 ppm with an integral of 2H represents the methyne protons in 2- and 6-position. The vicinal coupling constant (3J) depends on the dihedral angle (Karplus equation).¹⁰⁶ According to the Karplus equation, the larger coupling constant (11.8 Hz) indicates a 1,2-diaxial coupling between 2/6- CH_{ax} and 3/5- CH_{ax} (2.10 – 2.17 ppm). Since both methyne protons in 2- and 6-position are axially oriented, consequently, both ester groups are equatorially oriented. Therefore, the minor diastereomer *cis*-69 is *cis*-configured and the major diastereomer *trans*-70 is *trans*-configured.

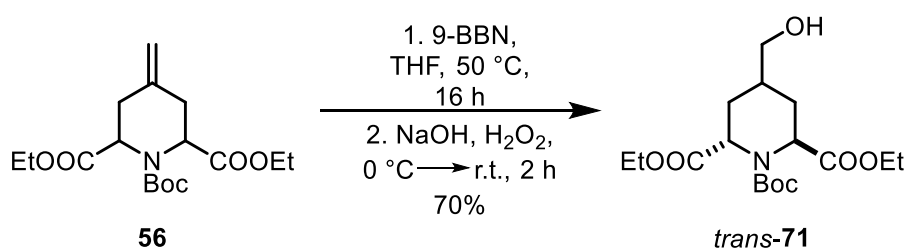
In *trans*-**70** one methyne proton in 2-position is axially oriented while the related methyne proton in 6-position is equatorially oriented. Theoretically, two dd's in the range of 3.2 ppm to 4.0 ppm should be seen in the ^1H NMR spectrum. One of the signals should show a large 1,2-diaxial coupling constant (8 - 12 Hz). However, only one dd at 3.84 ppm with an integral of 2H and two coupling constants of 7.0 and 5.0 Hz appears. (Figure 25 bottom) Due to the fast change of chair conformations of the piperidine ring, the orientation of the methyne protons in 2- and 6-position change rapidly from axial to equatorial and *vice versa*. This equilibrium is faster than the NMR timescale, which results in one signal with averaged coupling constants for both protons. Also, the axially and equatorially oriented methylene protons in 3- and 5-position cannot be distinguished leading to two dd's with similar coupling constants. During the Boc removal, a shift of the ratio of diastereomers did not occur. Therefore, the Boc-protected piperidine **56** consists of *trans*-**56** and *cis*-**56** in the ratio 9:1. This result is in accordance with the reported 92:8 ratio (*trans/cis*) of the methyl ester analog by Einhorn *et al.*⁶⁰

4.2.2 Synthesis of *endo*- and *exo*-configured 2-azabicyclo[3.3.1]nonanes with an ethyl ester in 3-position

With piperidine **56** in hand, we planned to synthesize *endo*-configured bicyclic amine **21** following the developed synthesis for unsubstituted analogs **19a** and **19b**. (chapter 4.1)

4.2.2.1 Synthesis of bicyclic enol ester **75**

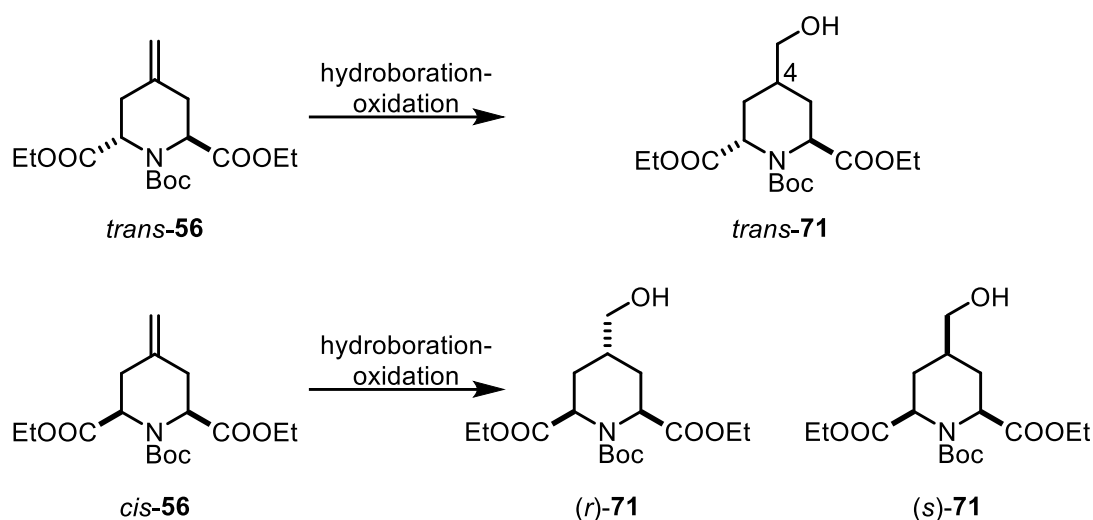
First, piperidine **56** was converted into bicyclic enol ester **75** in five steps. A hydroboration-oxidation with 9-BBN and H_2O_2 led to primary alcohol *trans*-**71** in 70% yield. (Scheme 26)



Scheme 26: Transformation of piperidine **56** into alcohol 2,6-*trans*-**71**.

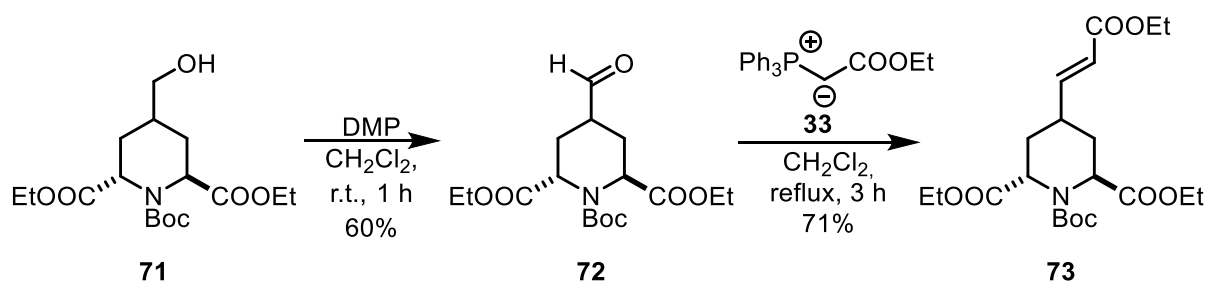
In the IR spectrum of alcohol **71**, a broad band at 3490 cm^{-1} represents the stretching vibration of the OH group, whereas the band for the former C=C double bond of

piperidine **56** has disappeared. The ^1H NMR spectrum of alcohol *trans*-**71** shows signals for only one diastereomer, which had to be the 2,6-*trans*-configured alcohol according to the high yield of the product. Thus, the minor diastereomer 2,6-*cis*-configured (*r/s*)-**71** seems to be lost during the purification process.



Scheme 27: Generation of 2,6-*trans*- and 2,6-*cis*-configured alcohols **71**.

Since a C_2 -axis of symmetry along the N-1-C-4 axis is present, a novel center of chirality in 4-position was not formed during the hydroboration of *trans*-**56**. (Scheme 27) Hydroboration of *cis*-**56**, however, can provide two diastereomers. In (*r*)-**71** the hydroxymethyl moiety is *trans*-oriented towards the ester groups and in (*s*)-**71**, the hydroxymethyl moiety is *cis*-oriented to the ester groups. However, due to the symmetry plane, C-4 is a pseudo-chiral center, which results in (*s*)-configuration for (*s*)-**71** and (*r*)-configuration for (*r*)-**71**.¹⁰⁷

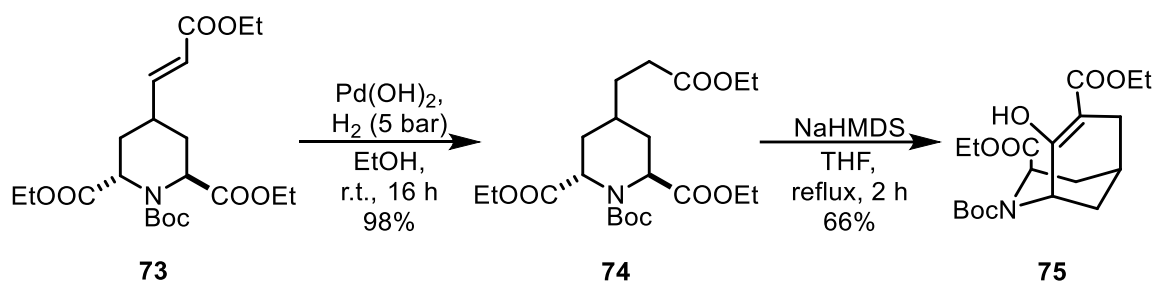


Scheme 28: Oxidation of alcohol **71** and Wittig reaction of the obtained aldehyde **72** with the stabilized ylide **33**.

The alcohol **71** was oxidized with Dess-Martin periodinane to give the aldehyde **72** in 60% yield. (Scheme 28) The yield is in the same range as for the monosubstituted analog **32** (56%). It is possible that the basic work-up of the reaction mixture might lead

to hydrolysis of an ester moiety. The successful oxidation was proven by analysis of the ^1H NMR spectrum. Two singlets at 9.60 ppm and 9.61 ppm in the ratio 6:4 represent the protons of the aldehyde moiety. Two signals appear, due to rotational isomerism along the Boc group. In the IR spectrum, an OH band could not be observed anymore.

The following Wittig reaction with ylide **33** yielded the α,β -unsaturated ester **73** in 71% yield. In the IR spectrum, a band at 1654 cm^{-1} represents the C=C stretching vibration. The alkene protons cause two dd's at 5.80 ppm (15.8 / 1.2 Hz) and 6.80 ppm (15.8 / 6.6 Hz) in the ^1H NMR spectrum. The large coupling constant of 15.8 Hz confirms the (*E*)-configuration of α,β -unsaturated ester **73**. As discussed in chapter 4.1.1.2 Wittig reaction with the stabilized ylide **33** leads to the thermodynamically favoured (*E*)-configured α,β -unsaturated ester **73**.



Scheme 29: Hydrogenation of α,β -unsaturated ester **73** and Dieckmann condensation of triester **74**.

A reduction of the generated double bond with H_2 (5 bar) and $\text{Pd}(\text{OH})_2$ as the catalyst led in almost quantitative yield to the saturated triester **74**. (Scheme 29) Next, a Dieckmann condensation was performed. NaHMDS was added to a refluxing solution of triester **74** in THF, accelerating the necessary ring inversion, which induces the formation of the bicyclic framework in 66% yield. An intramolecular H-bond stabilizes the enol tautomer similar to enol ester **25**. The ^1H NMR spectrum of **75** shows two sets of signals in the ratio 1:1 caused by rotational isomerism along the Boc group. (Figure 26)

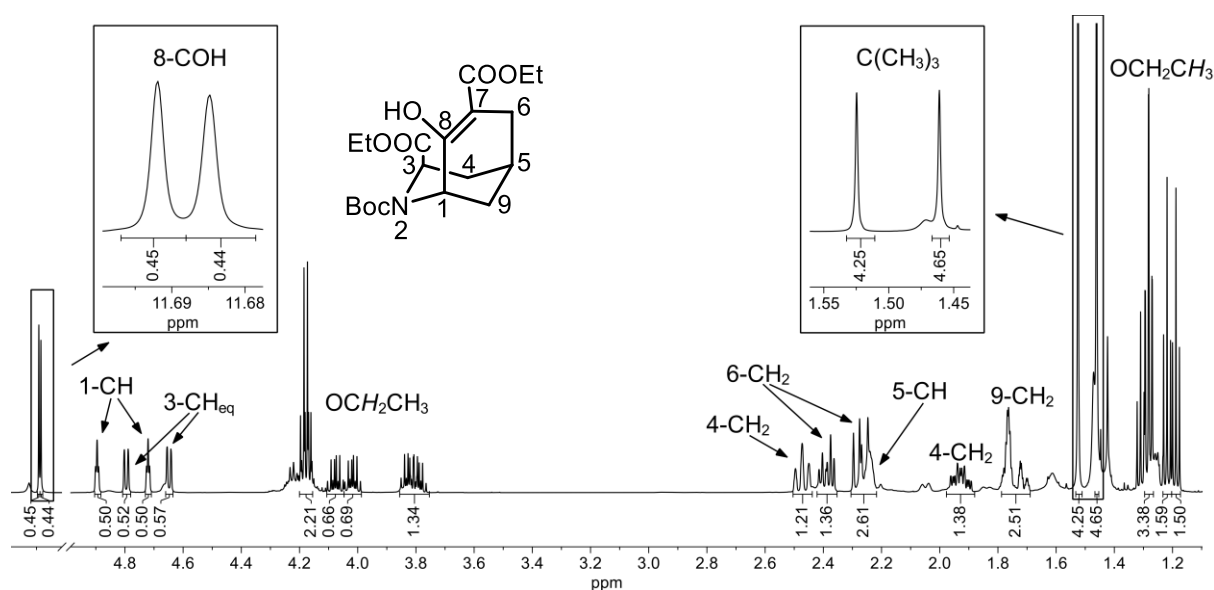
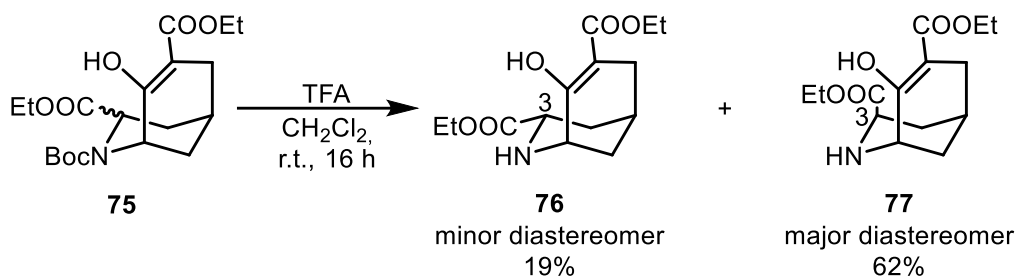


Figure 26: ^1H NMR spectrum (CDCl_3) of enol ester **75** with a presumably axially oriented ester.

The ratio of rotamers was determined by integration of the Boc signals at 1.46 ppm and 1.52 ppm and the OH signals at 11.68 ppm and 11.69 ppm. Two doublets at 4.65 ppm and 4.80 ppm represent the methyne proton in 3-position. With a coupling constant of 7.9 Hz, the orientation of the methyne proton cannot be determined with certainty. Due to steric repulsion, the orientation of the methyne proton can be pseudoequatorial or pseudoaxial, which can lead to similar coupling constants with the neighbouring protons in 4-position. (Karplus equation)¹⁰⁶ Since the Dieckmann condensation was performed with 2,6-*trans*-configured triester **75**, the ester moiety in 3-position should adopt the equatorial orientation. However, two equivalents of base were used during the reaction. Therefore, an epimerization in 3-position could have been occurred transforming the equatorially oriented ester into axial orientation. An axially oriented ester moiety in 3-position is energetically more favoured, due to the sterically demanding Boc group in 2-position (allylic strain).

In an attempt to determine the configuration of enol ester **75**, the Boc group was removed with TFA yielding the diastereomers **76** and **77** in 19% and 62% yield, respectively. (Scheme 30) With respect to the piperidine ring, the ester in 3-position adopts the equatorial orientation in **76** and the axial orientation in **77**.



Scheme 30: Generation of secondary amines **76** and **77** in the ratio 1:3.

The diastereomers were separated by flash column chromatography. Both ^1H NMR spectra are displayed in Figure 27.

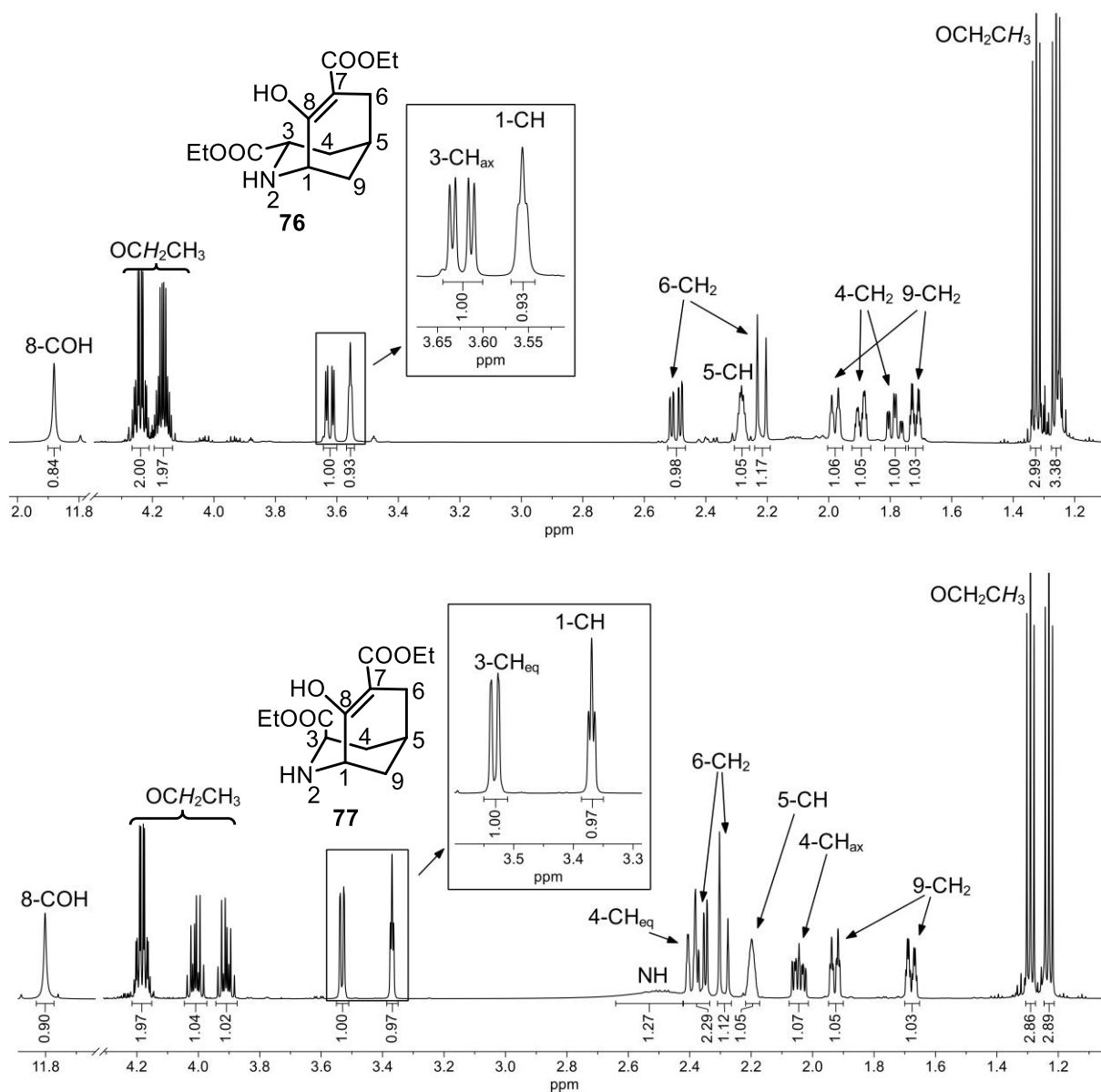


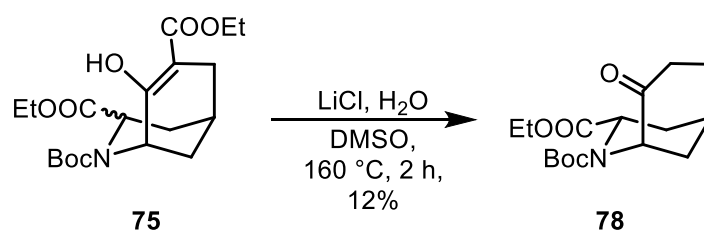
Figure 27: ^1H NMR spectra (CDCl₃) of minor diastereomer **76** (top) and major diastereomer **77** (bottom).

The removal of the Boc group was indicated by the missing singlet with an integral of 9H at a chemical shift of around 1.5 ppm. The orientation of the ester moiety in 3-position was determined by analyzing the coupling constants of the signals for 3-CH. For the minor diastereomer **69** with an equatorial orientation of the ester, the 3-CH signal is a dd at 3.62 ppm ($J = 12.5 / 3.8$ Hz). (Figure 27, top) The large coupling constant of 12.5 Hz is caused by a 1,2-diaxial coupling, hence, an axial oriented proton exists in 3-position. As a consequence, the ethyl ester is in equatorial orientation. The corresponding 3-CH signal for the major diastereomer with an axially oriented ester in 3-position is represented by a doublet at 3.53 ppm ($J = 7.5$ Hz). (Figure 27, bottom) According to the Karplus equation, the vicinal coupling constant between an equatorially oriented proton and an axially or equatorially oriented proton ($dh \sim 60^\circ$) in a six-membered ring should be 2 - 5 Hz.¹⁰⁶ However, steric repulsions between the enol ester moiety and the ester in 3-position lead to a conformational distortion of the chair conformation of the piperidine ring. Thus, the dihedral angle between 3-CH_{eq} and 4-CH_{ax} would be reduced and between 3-CH_{eq} and 4-CH_{eq} increased. Lowering of the dihedral angle ($<60^\circ$) leads to increased coupling constant, whilst an increased dihedral angle ($60^\circ < dh < 90^\circ$) reduces the coupling constant. Consequently, the observed signal for 3-CH_{eq} indicates a substituted bicyclic compound with a pseudoaxially oriented ester moiety.

The 3:1 ratio of the obtained diastereomers cannot be seen in the ¹H NMR spectrum of precursor **75**. (Figure 26) However, 3-CH of **75** results in two doublets ($J = 7.9$ Hz) which corresponds to the signal of the major diastereomer (1*RS*,3*SR*,5*RS*)-**77**. Therefore, an axial orientation of the ester in 3-position is assumed for enol ester **75**.

4.2.2.2 Krapcho reaction of enol esters and formation of tricyclic compounds

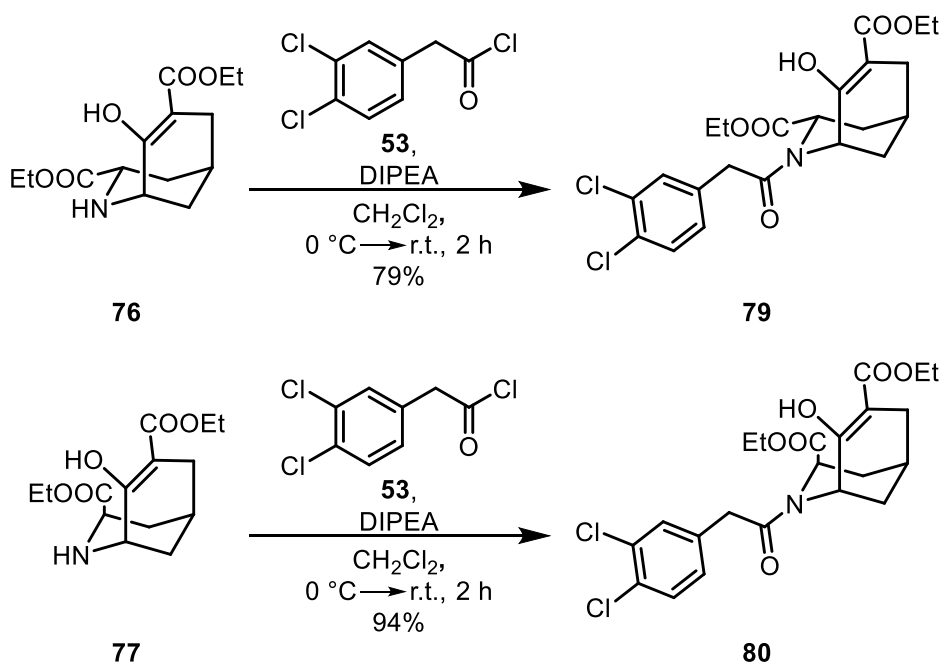
The next step was the Krapcho deethoxycarbonylation of enol ester **75** to obtain the ketone **78** in 12% yield. (Scheme 31)



Scheme 31: Krapcho reaction of enol ester **75**.

The reaction was performed in a preheated oil bath at 160 °C using LiCl as an additive. (chapter 4.1.2) The successful deethoxycarbonylation was shown by a missing band at 1662 cm^{-1} in the IR spectrum of ketone **78** representing the C=O stretching vibration of the enol ester. In the ^{13}C NMR spectrum a signal at 210.8 ppm indicates the ketone moiety, while only one signal for an ester carbonyl C-atom can be seen at 173.8 ppm. The 3-CH resonates as doublet ($J = 8.5$ Hz) at 4.85 ppm in the ^1H NMR spectrum. The coupling constant of 8.5 Hz implies an axially oriented proton in 3-position, thus, the ester is in equatorial orientation. The low yield of the reaction (12%) indicates that only the product of the minor diastereomer (1*RS*,3*RS*,5*RS*)-**75** underwent the deethoxycarbonylation.

To further investigate the Krapcho reaction of the diastereomers, the secondary amines **76** and **77** were acylated separately with (3,4-dichlorophenyl)acetyl chloride (**53**) producing amides **79** and **80** in 79% and 94% yield, respectively. (Scheme 32)



Scheme 32: Acylation of amines **76** and **77** with acyl chloride **53**.

The three characteristic signals of the aromatic protons in the ^1H NMR spectra of **79** and **80** indicate the introduction of the acyl moiety. Two sets of signals in the ratio 3:1 show rotational isomerism along the amide group for **80**. In case of **79** signals for two rotamers are not observed. The crucial signals for 3-CH show coupling constants of 8.7 Hz and 6.0 Hz (**79**) and 7.9 Hz (**80**), respectively, confirming the configuration obtained for the precursors **76** and **77**. To finally prove the postulated configuration of the diastereomers **79** and **80**, an X-ray crystal structure analysis was performed.

(Figure 28) Colorless needles were obtained by recrystallization of **80** from ethyl acetate and cyclohexane using the vapor diffusion method.

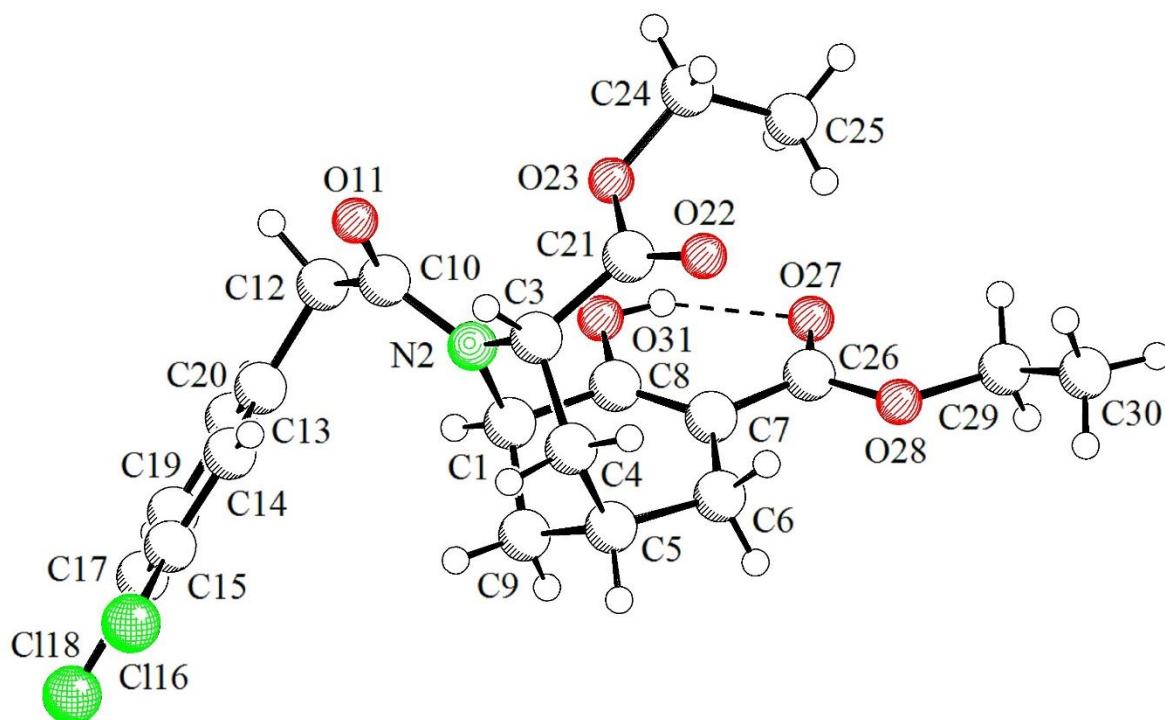
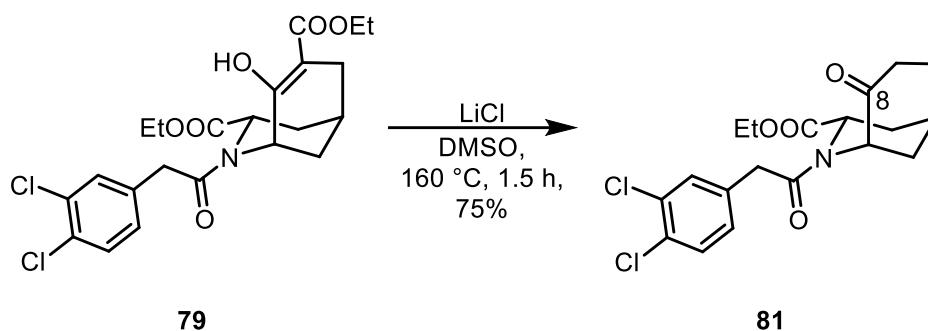


Figure 28: X-ray crystal structure of amide **80**. The ester in 3-position adopts an axial orientation. The piperidine ring consisting of C-1, N-2, C-3, C-4, C-5 and C-9 exists in a chair-like conformation, whilst the cyclohexene ring consisting of C-1, C-9, C-5, C-6, C-7 and C-8 exists in a half-chair conformation. An H-bond is seen between the hydroxy group at C-8 and the carbonyl O-atom of the ester at C-7.

According to the X-ray crystal structure, the relative configuration of **80** is (1*RS*,3*SR*,5*RS*) with an axially oriented ester in 3-position. The equatorial orientation of 3-CH was already derived by analysis of the ¹H NMR spectra. Consequently, the diastereomer **79** is (1*RS*,3*RS*,5*RS*)-configured with the ester moiety in equatorial position.

The following deethoxycarbonylation of diastereomer **79** upon heating with LiCl in DMSO led to ketone **81** in 75% yield. (Scheme 33)



Scheme 33: Krapcho reaction of enol ester **79**.

In the IR spectrum of ketone **81**, a band at 1713 cm^{-1} represents the C=O stretching vibration of the ketone in 8-position. The signal at 209.5 ppm in the ^{13}C NMR spectrum belongs to the carbonyl C-atom of the ketone. Furthermore, one of the two signals for the carbonyl C-atoms of the ester moieties has disappeared indicating the loss of an ester group.

In addition to the bicyclic ketone **81**, the less polar compound **82** was isolated in 10% yield by flash column chromatography. The ^1H NMR spectrum of **82** is shown in Figure 29.

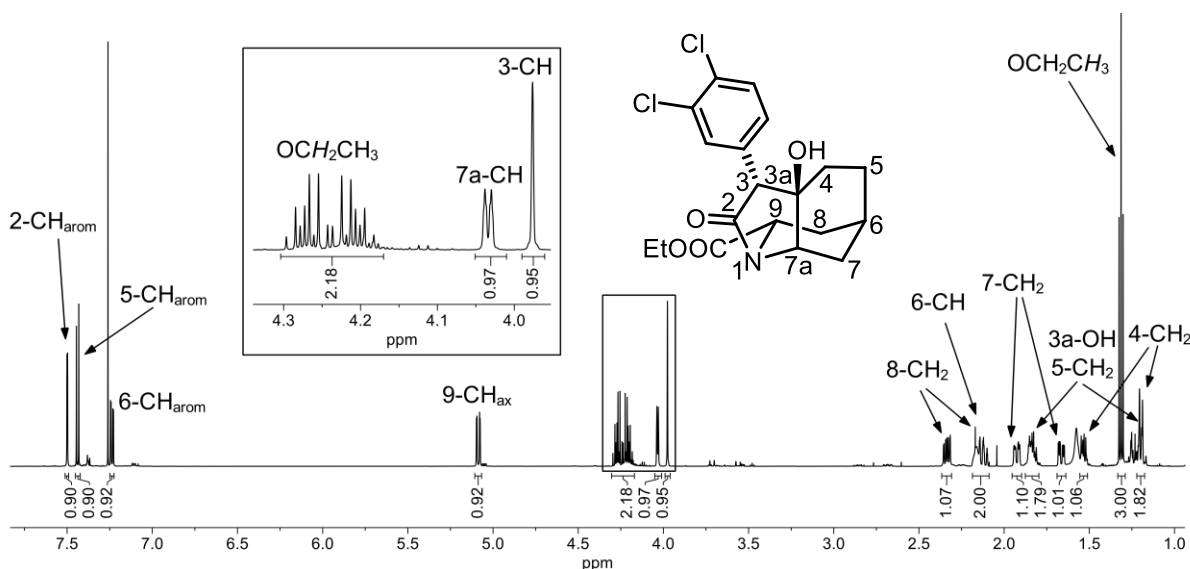


Figure 29: ^1H NMR spectrum (CDCl_3) of tricyclic alcohol **82**.

in the ^{13}C NMR spectrum of compound **82** only one signal for a carbonyl C-atom of an ester moiety is seen at 172.9 ppm. However, a signal for a ketone C-atom does not appear. Moreover, the characteristic two doublets representing the benzylic protons of the phenylacetyl moiety are not observed. Instead, a singlet at 3.98 ppm with an integral of 1H appears. Thus, after the deethoxycarbonylation of enol ester **79**, the obtained ketone **81** had further reacted to the alcohol **82**. Due to the acidity of the

benzylic protons between the phenyl ring and the amide group of ketone **81**, a proton can be removed and the generated enolate can undergo a nucleophilic attack at the carbonyl C-atom of the ketone in 8-position leading to a tricyclic compound **82**. The high temperature during the Krapcho reaction and the coordinating effect of the Li⁺-additive promote the addition reaction. Recrystallization of **82** from ethyl acetate and cyclohexane using the vapor diffusion method provided colorless needles, which were suitable for X-ray crystal structure analysis. The structure of the formed tricyclic product **82** is shown in Figure 30.

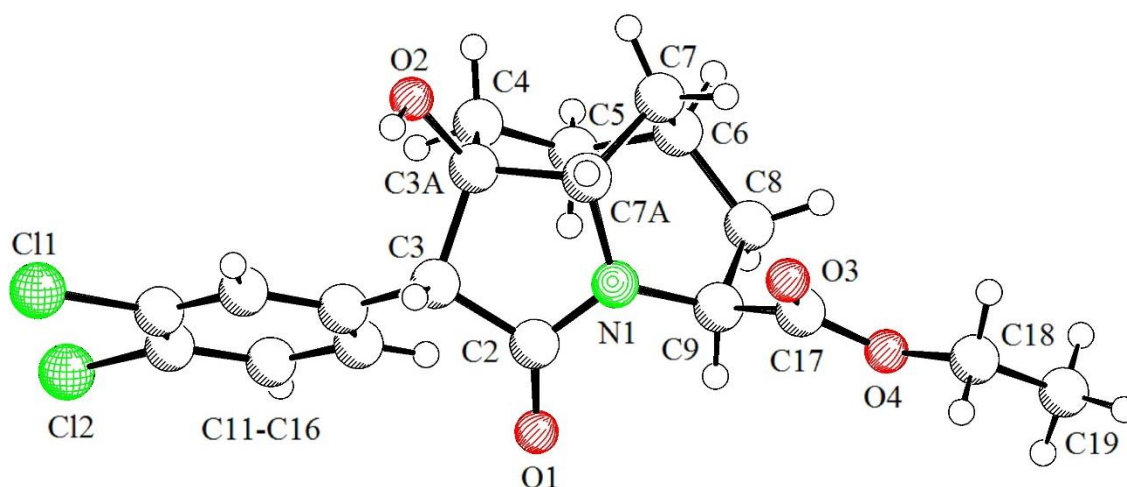
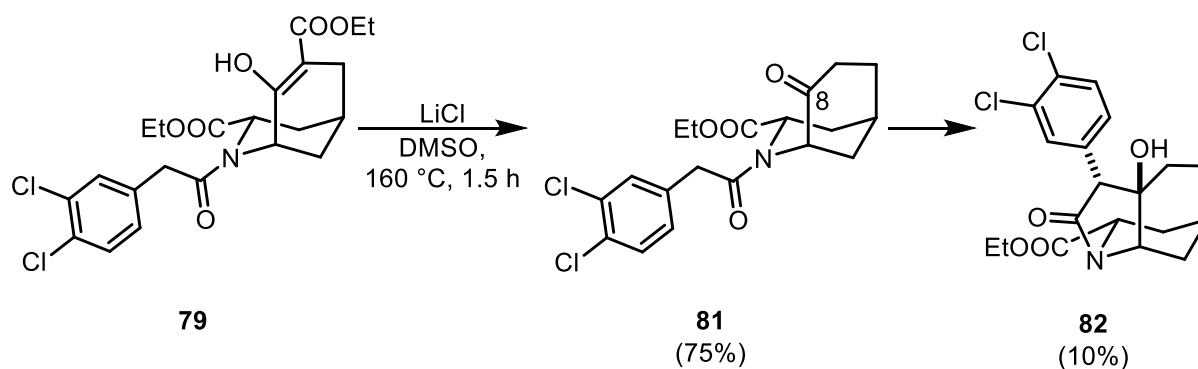


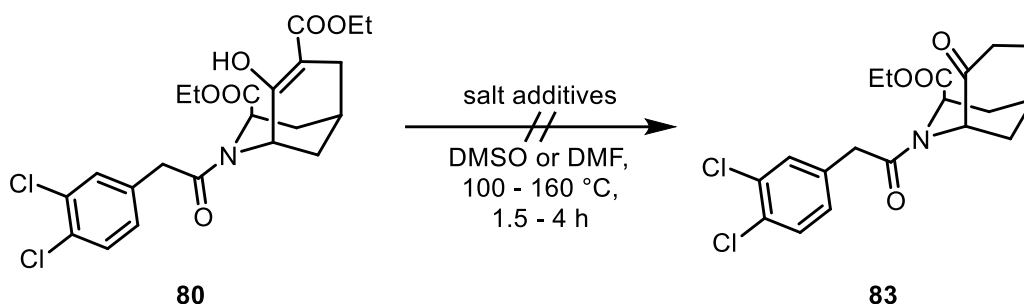
Figure 30: X-ray crystal structure of alcohol **82**. The ester at C-9 is pseudoequatorially oriented and the newly formed γ -butyrolactam consisting of N-1, C-2, C-3, C-3a and C-7a exists in an envelope conformation. Both six-membered rings are highly twisted and the hydroxy group at C-3a and the dichlorophenyl ring at C-3 are *trans*-configured.

In conclusion, enol ester **79** was deethoxycarbonylated with LiCl to afford the ketone **81** (75%). Under these reaction conditions, the formed ketone **81** underwent a cyclization to yield the tricyclic alcohol **82** (10%). (Scheme 34)



Scheme 34: Krapcho reaction of enol ester **79** and subsequent cyclization of ketone **81**.

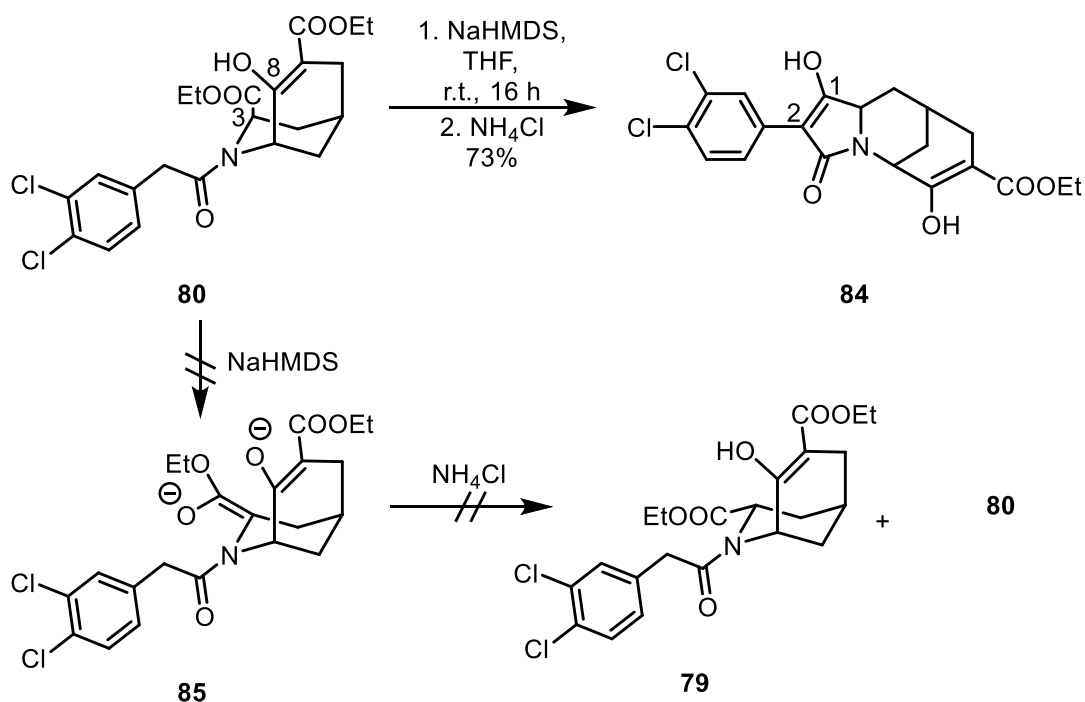
Performing the Krapcho reaction of the main diastereomer **80** under the same conditions used for the diastereomer **79** did not lead to the ketone **83** with an axially oriented ester in 3-position (Scheme 35)



Scheme 35: Attempts to transform enol ester **80** into ketone **83**.

Different reaction conditions were tested by changing the salt additive, solvent, temperature or reaction time. According to TLC (KMnO_4 staining), a consumption of enol ester **80** could be observed, respectively. However, the desired ketone **83** could not be isolated.

During the Dieckmann condensation, a base-induced epimerization had occurred. Therefore, similar reaction conditions were used in an attempt to transform **80** into its diastereomer **79**. (Scheme 36)



Scheme 36: Unexpected cyclization of bicyclic enol ester **80** during treatment with NaHMDS to afford tricyclic bis(enol) **84**.

For this purpose, **80** should be deprotonated with NaHMDS in 3-position. Due to the high acidity of the enol at 8-position, two equivalents of base were used generating dienolate **85**. Protonation from the “axial side” during acidic work-up, should provide **79** with an equatorially oriented ester moiety. Unexpectedly, instead of epimerization the tricyclic product **84** was formed in 73% yield. (Scheme 36) The structure of **84** was determined by X-ray crystal structure analysis. (Figure 31) **84** was formed by nucleophilic attack of the enolate at the axially oriented ester moiety, leading to tricyclic bis(enol) **84** in 73% yield. In the ^1H NMR spectrum of **84** signals for the benzylic protons cannot be observed, whilst the ^{13}C NMR spectrum shows two quaternary C-atoms at 172.4 ppm (C-1) and 101.3 ppm (C-2) indicating the enol tautomer in 1,2-position. X-ray crystal structure analysis confirmed the formation of **84**. Colorless needles were obtained, by recrystallization of **84** from ethyl acetate and cyclohexane using the vapor diffusion method.

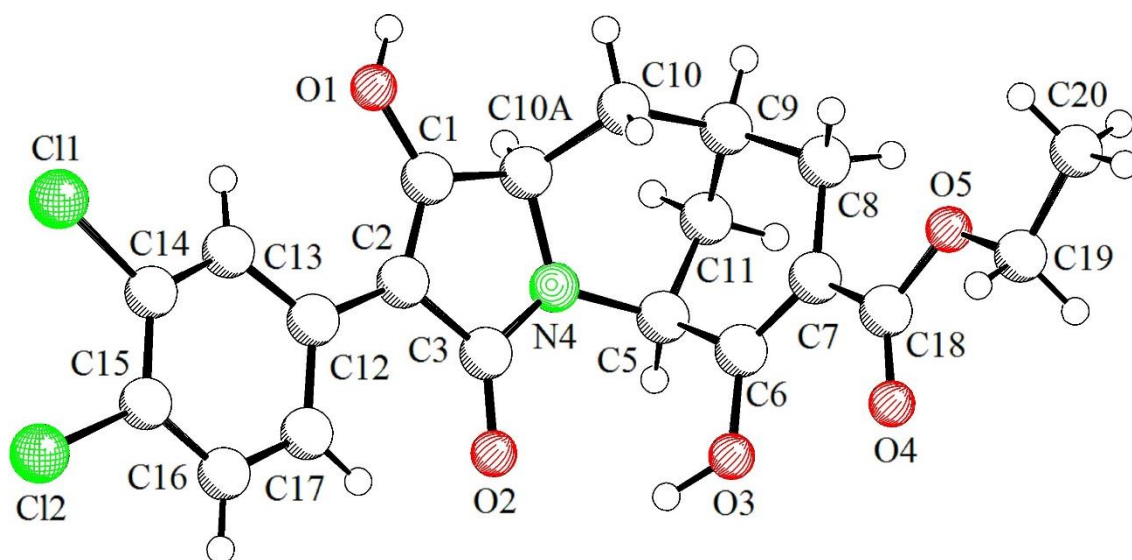
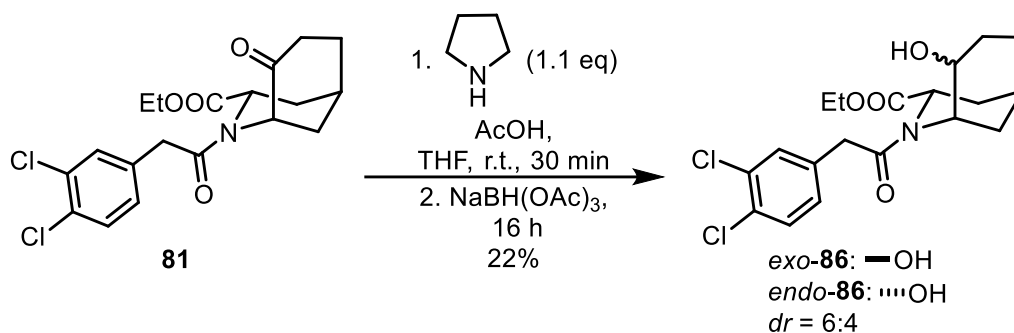


Figure 31: X ray crystal structure of tricyclic bis(enol) **84**. The substituted C-1 is pseudoaxially oriented at the piperidine ring. Due to the four sp^2 -hybridized atoms N-4, C-1, C-2 and C-3, the newly formed γ -butyrolactam consisting of N-4, C-10a, C-1, C-2 and C-3 adopts a flat structure.

It can be concluded that Krapcho deethoxycarbonylation of the minor enol ester **79** with an equatorially oriented ester moiety in 3-position provided the ketone **81** in high yields. The major diastereomer **80** with an axially oriented ester moiety, however, underwent an unexpected side reaction. An attempt to induce an epimerization of **80** to **79** led to tricyclic compound **84**.

4.2.2.3 Introduction of the pyrrolidine ring as the second KOR pharmacophoric element

Finally, reductive amination of the ketone **81** with pyrrolidine and $\text{NaBH}(\text{OAc})_3$ was performed. Different products were obtained depending on the added equivalents of pyrrolidine. Transformation of ketone **81** with 1.1 eq of pyrrolidine led to the secondary alcohol **86** in 22% yield. (Scheme 37)



Scheme 37: Reductive amination of ketone **81** leading to bicyclic alcohol **86**.

In the IR spectrum, the band at 1713 cm^{-1} ($\text{C}=\text{O}_{\text{ketone}}$) disappeared, while a band at 3472 cm^{-1} appeared representing the stretching vibration of the formed O-H group. The ^1H NMR spectrum of bicyclic alcohol **86** shows two sets of signals in the ratio 6:4, which can be recognized by the signals for the OH group at 4.91 ppm (major) and 2.52 ppm (minor) and for 3- H_{ax} at 4.42 ppm (minor) and 4.35 ppm (major). (Figure 32)

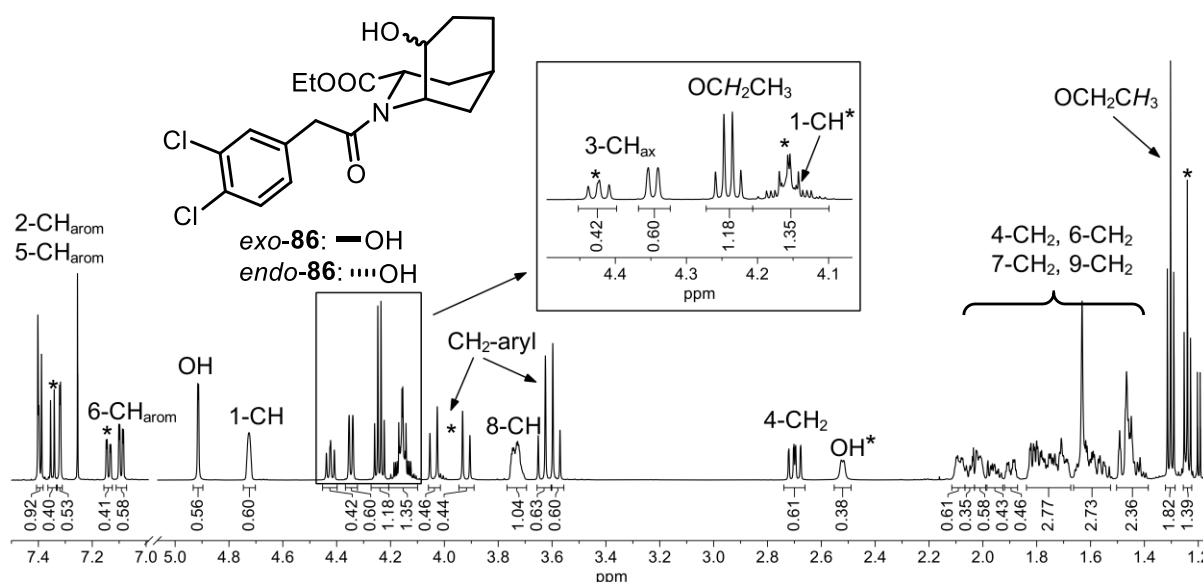
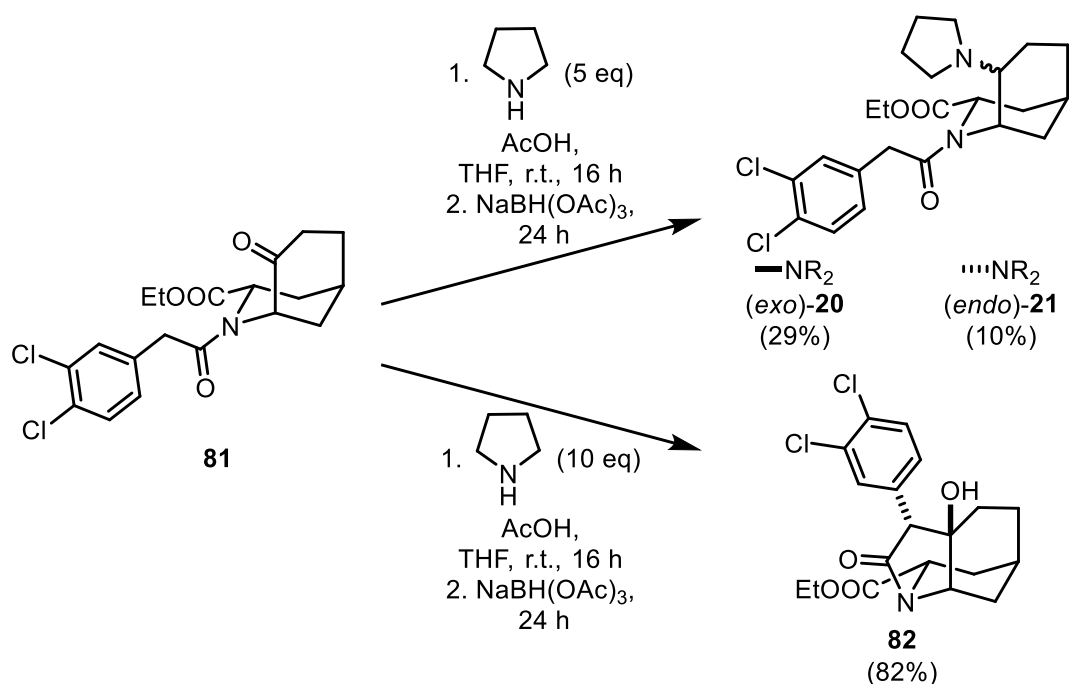


Figure 32: ^1H NMR spectrum (CDCl_3) of bicyclic alcohol *exo*- and *endo*-**86**. The signals for the minor diastereomer are marked with an asterisk (*).

In an attempt to determine the relative configuration of the two diastereomers, a NOESY experiment was performed. However, due to overlapping of crucial signals of 4-CH₂, 6-CH₂, 7-CH₂ and 9-CH₂ the relative configuration could not be assigned unequivocally.

The reduction of a ketone with NaBH(OAc)₃ is rather unlikely due to the steric effects and electron-withdrawing properties of the acetoxy groups.^{108–110} However, reduction of β-hydroxyketones by intramolecular hydride delivery was reported in literature.^{109,111} To prevent the reduction of ketone **81** and promote the formation of the iminium ion, the amount of pyrrolidine was increased (5 eq) and the reducing agent NaBH(OAc)₃ was added only after 16 h leading to *exo*- and *endo*-configured bicyclic amines *exo*-**20** and *endo*-**21** in 29% and 10% yield, respectively. (Scheme 38)



Scheme 38: Reductive amination of ketone **81** and formation of tricyclic alcohol **82**.

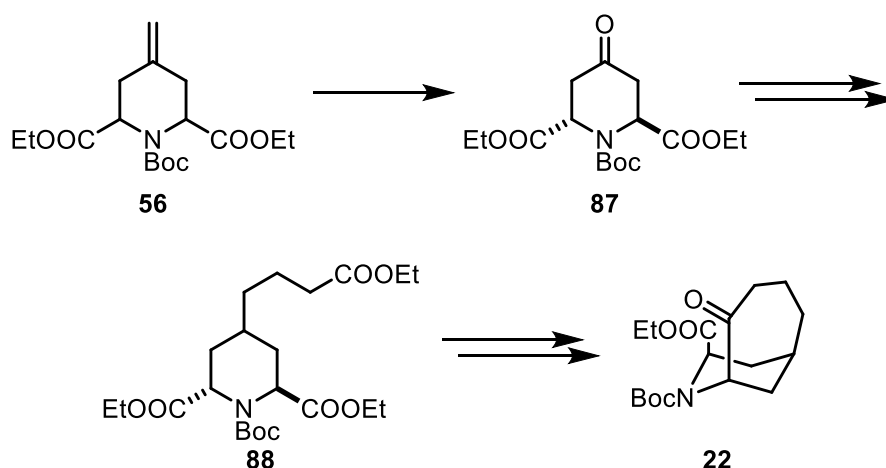
The successful introduction of the pyrrolidine moiety was shown by a new signal for the methyne proton in 8-position in the ¹H NMR spectra of *exo*-**20** (2.31 – 2.34 ppm and 2.50 – 2.76 ppm) and *endo*-**21** (2.57 – 2.63 ppm). Furthermore, the signal for the carbonyl C-atom of the ketone of bicyclic ketone **81** disappeared. The relative configuration was determined by NOESY analysis. Cross peaks between 8-CH and the benzylic protons of the phenylacetyl moiety as well as 1-CH indicate the *exo*-configuration of *exo*-**20**. (Figure S4, Appendix) For *endo*-**21** close proximities are observed between the methylene groups of the pyrrolidine moiety (N(CH₂CH₂)₂) and the

benzylic protons of the phenylacetyl moiety as well as 1-CH proving the *endo*-configuration. (Figure S5, Appendix)

In an attempt to increase the yield of the transformation, an even larger amount of pyrrolidine (10 eq) was used. (Scheme 38) However, neither *exo*- nor *endo*-configured bicyclic amine **20** and **21** were isolated. Instead, tricyclic alcohol **82** was obtained in 82% yield. (Scheme 38) Here, the base pyrrolidine induces the formation of tricyclic compound **82** by deprotonation at the benzylic methylene moiety.

4.3 Part 3: Synthesis of 7-azabicyclo[4.3.1]decane **22** with an ethyl ester in 8-position

This part deals with the synthesis of an enlarged bridge over the piperidine ring. Additionally, an ester was attached at 8-position similar to the bicyclic amines **20** and **21** discussed in the previous chapter 4.2. For this purpose, piperidinone **87** should be synthesized and a C₄-side chain should be introduced in 4-position, which allows the Dieckmann condensation. (Scheme 39)

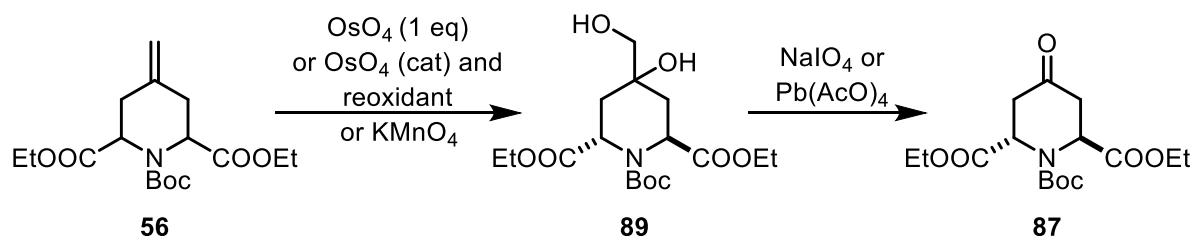


Scheme 39: Plan for the synthesis of 7-azabicyclo[4.3.1]decane **22**.

The synthesis of bicyclic ketone **22** is divided into two parts starting with the transformation of piperidine **56** into piperidinone **87**. Then, the introduction of the four-carbon side chain and finally the Dieckmann condensation are discussed.

4.3.1 Oxidation of piperidine **56**

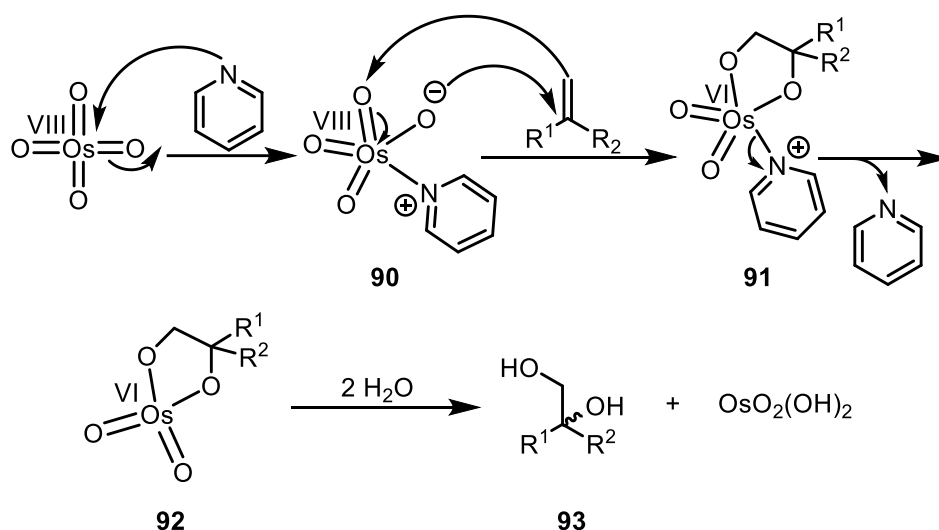
In order to convert the methylene moiety of piperidine **56** into ketone **87**, a dihydroxylation followed by glycol cleavage was performed. (Scheme 40)



Scheme 40: Conversion of alkene **56** into ketone **87**.

OsO_4 can be used to transform an alkene into a vicinal diol. However, OsO_4 should not be used in stoichiometric amounts, due to its high toxicity. Therefore, different

procedures have been developed using only catalytic amounts of OsO_4 and a reoxidant to regenerate OsO_4 . H_2O_2 can be used as reoxidant, but further oxidation of the produced diol could occur.¹¹² The reoxidant *N*-methyl-morpholine-*N*-oxide, does not lead to further oxidation.¹¹³ An asymmetric dihydroxylation (AD) was developed by Sharpless *et al.* using $\text{K}_3[\text{Fe}(\text{CN})_6]$ as reoxidant and quinine $(\text{DHQ})_2\text{PHAL}$ or quinidine derivatives $(\text{DHQD})_2\text{PHAL}$ as chiral ligands. Mixtures containing all required components are commercially available as AD-mix- α and AD-mix- β .¹¹⁴ Sharpless proposed a [2+2] cycloaddition of OsO_4 onto the alkene followed by 1,1-migratory insertion of the ligand. This mechanism was corrected by Corey *et al.* who proposed a [3+2] cycloaddition due to steric repulsion.¹¹⁵ Addition of a nucleophilic base (e.g. pyridine) can accelerate the reaction due to its coordinating properties.^{114,116,117} The mechanism of the oxidation is displayed in Scheme 41.



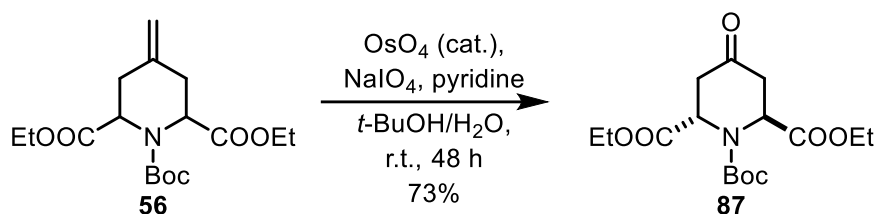
Scheme 41: Ligand accelerated dihydroxylation of a 1,1-disubstituted alkene with OsO_4 and pyridine.^{114,116,117}

The free electron pair of pyridine coordinates with the central Os-atom of OsO_4 leading to a negative charge at one of the O-atoms (**90**). The negatively charged oxygen is involved in the [3+2] cycloaddition with the alkene leading to a five-membered cyclic osmium diester **91**. After dissociation of pyridine from the complex, the diester **92** can be hydrolyzed to obtain diol **93** and osmic(VI) acid. OsO_4 will be regenerated by the reoxidant.

A cheap and less toxic alternative to OsO_4 is KMnO_4 although further oxidation can occur. Ultrasound irradiation can reduce reaction time and improve the yield.¹¹⁸

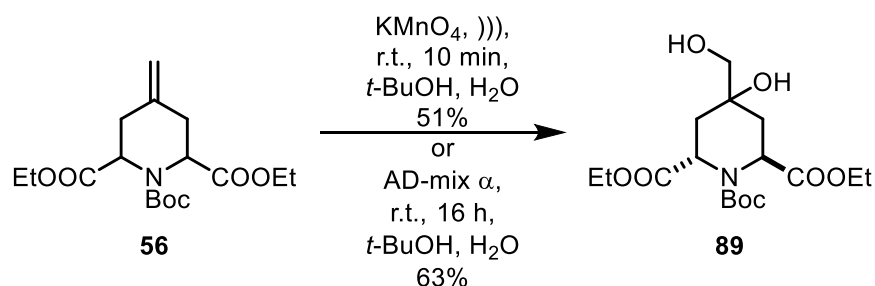
The diol **89** can be oxidatively cleaved to afford the ketone **87** either by Malaprade reaction¹¹⁹ using NaIO_4 or Cingee reaction¹²⁰ using $\text{Pb}(\text{AcO})_4$. In case of a vicinal diol, a five-membered cyclic periodate ester is formed as intermediate followed by fragmentation. The oxidation state of the central I-atom is reduced by two during this cleavage reaction.

The Lemieux-Johnson oxidation combines the dihydroxylation step and glycol cleavage step by using a catalytic amount of OsO_4 , but an excess of NaIO_4 as reoxidant of Os(VI) and diol cleavage reagent.¹²¹ The Lemieux-Johnson oxidation of 4-methylenepiperidine **56** was performed using 1% OsO_4 , five equivalents of NaIO_4 and one equivalent of pyridine leading to piperidinone **87** in 73% yield. (Scheme 42)



Scheme 42: Lemieux-Johnson oxidation of 4-methylenepiperidine **56** to afford piperidinone **87**.

Since two transformations took place, the corresponding intermediate diol **89** should be prepared as reference compound to observe the progress of the transformation. Therefore, dihydroxylation reactions were performed with KMnO_4 and ultrasound and with AD-mix- α . (Scheme 43)



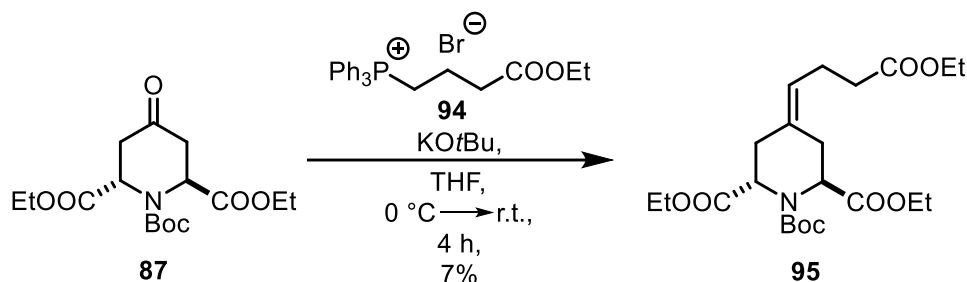
Scheme 43: Dihydroxylation of 4-methylenepiperidine **56**.

Ultrasound irradiation during oxidation with KMnO_4 led after 10 min to diol **89** in 51% yield, while the dihydroxylation with AD-mix- α led after 16 h to diol **89** in 63% yield. After purification, only the 2,6-*trans*-configured diol **89** was isolated similarly to the observations for alcohol **71**. (chapter 4.2.2.1) The successful formation of the ketone **87**, was confirmed by the ^{13}C NMR spectrum showing a signal at 203.8 ppm for the

C-atom of the C=O group. Moreover, the signals of the exocyclic methylene protons disappeared in the ^1H NMR spectrum of ketone **87**.

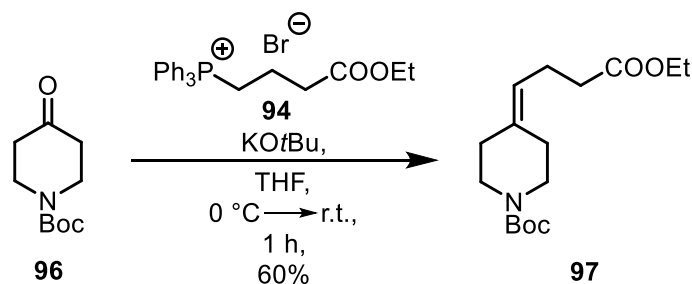
4.3.2 Four-carbon homologation and formation of bicyclic ketone **22**

In the next step, a C₄-side chain was introduced by a Wittig reaction of piperidinone **87** with phosphonium salt **94** and KO t Bu leading to γ,δ -unsaturated ester **95** in 7% yield. (Scheme 44)



Scheme 44: Wittig reaction of piperidinone **87** with phosphonium salt **94**.

Phosphonium salt **94** was synthesized by nucleophilic substitution of ethyl 4-bromobutanoate with PPh₃ according to a procedure of Braddock *et al.*¹²² The ylide was generated *in situ* using KO t Bu as a base. The low yield of the reaction was explained by the rather unreactive ketone **87**. A test reaction with unsubstituted piperidinone **96** led to the corresponding unsaturated ester **97** in 60% yield. (Scheme 45)

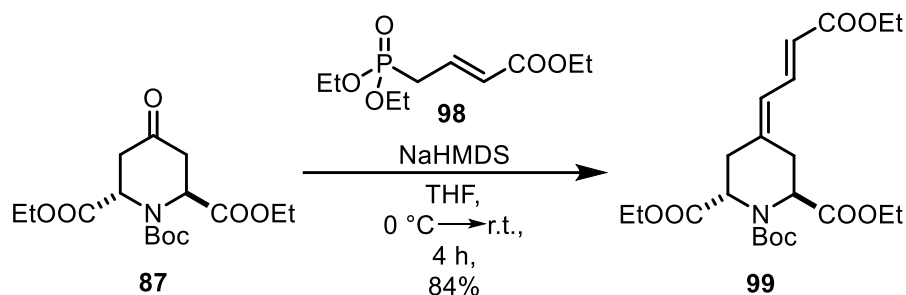


Scheme 45: Test reaction of unsubstituted piperidinone **96** with non-stabilized ylide **97**.

Thus, the ester groups in 2- and 6-position of piperidinone **87** inhibited the reaction with the non-stabilized ylide, which might be due to steric repulsion. An increased reaction temperature led to decomposition of the generated ylide.

In addition to the Wittig reaction, the Horner-Wadsworth-Emmons reaction (HWE) allows the transformation of ketones into alkenes.^{123,124} For the HWE reaction, an *in situ* formed stabilized phosphonate carbanion was used, which is more nucleophilic

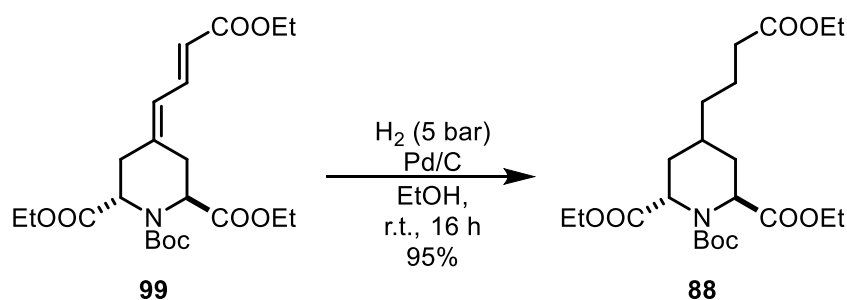
and consequently more reactive than the corresponding phosphonium ylide.¹²⁵ Therefore, piperidinone **87** was reacted with commercially available triethyl 4-phosphonocrotonate (**98**) and NaHMDS leading to diunsaturated ester **99** in 84% yield. (Scheme 46) After the deprotonation of **98**, the generated stabilized anion nucleophilically attacked the carbonyl C-atom in 4-position of ketone **87**.



Scheme 46: HWE-reaction of piperidinone **87** with triethyl 4-phosphonocrotonate (**98**).

Three new signals in the ¹H NMR spectrum of **99** representing the methyne protons of the diene and a loss of the signal for the carbonyl C-atom of the ketone in the ¹³C NMR spectrum demonstrate the presence of the C₄-side chain. In the IR spectrum, the stretching vibration of both alkene groups are represented by two bands at 1640 cm⁻¹ and 1616 cm⁻¹.

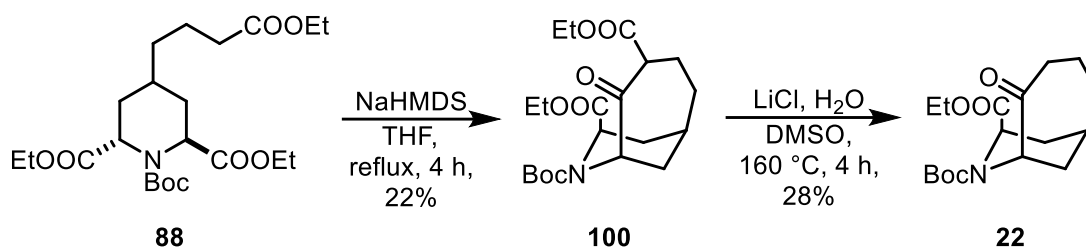
The double bonds of diene **99** were reduced with H₂ using Pd/C as catalyst leading to butanoate **88** in almost quantitative yield. (Scheme 47) In the IR spectrum of triester **88**, both bands representing the C=C moieties have disappeared, which indicate the formation of the desired saturated product.



Scheme 47: Hydrogenation of unsaturated ester **99**.

The bicyclic scaffold should be prepared by a Dieckmann condensation. Already in 1894 Dieckmann himself reported the difficulties of generating seven-membered rings by intramolecular ester condensation. The high flexibility of the butanoate side chain limits the ring formation.¹²⁶ Even performing the reaction in a highly diluted solution

($c = <0.02$ M), according to the Ruggli-Ziegler dilution principle,^{87,88} provided 7-azabicyclo[4.3.1]decane **100** in only 22% yield. (Scheme 48)



Scheme 48: Dieckmann condensation and Krapcho reaction forming ketone **22**.

Due to the existence of various diastereomers, tautomers and rotamers of β -keto ester **100**, the assignment of the signals in the NMR spectra was not possible. However, two signals at 207.1 ppm and 206.9 ppm in the ^{13}C NMR spectrum indicate the presence of a ketone.

The deethoxycarbonylation of β -keto ester **100** with LiCl in DMSO at 160 °C yielded to the bicyclic ketone **22** in 28% yield. The ^1H NMR spectrum of **22** is shown in Figure 33.

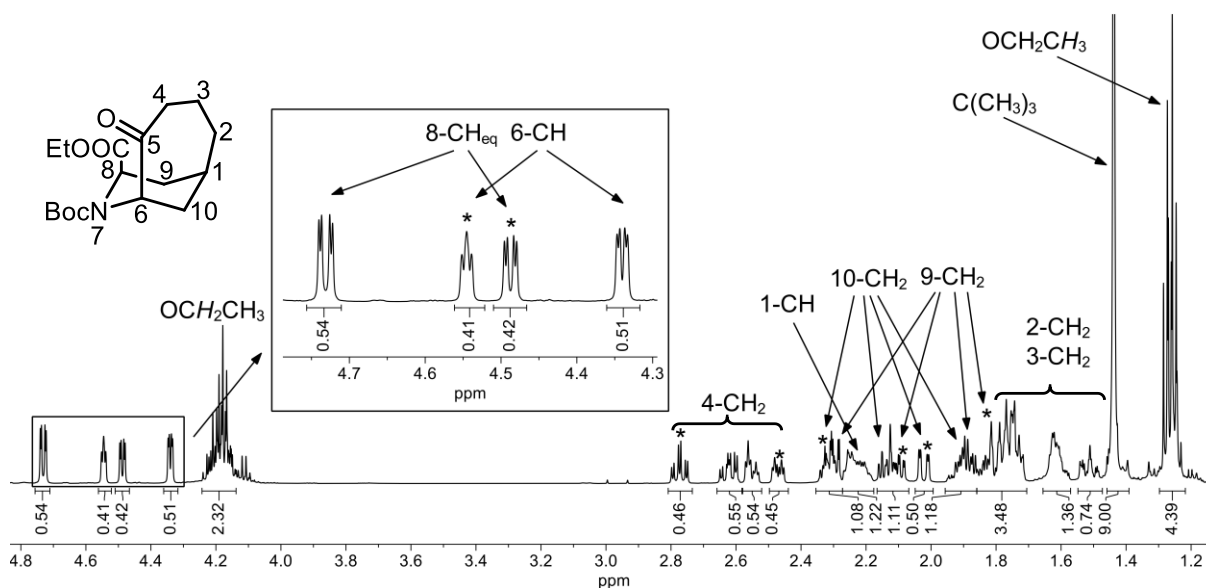


Figure 33: ^1H NMR spectrum (CDCl_3) of bicyclic ketone **22**. The signals for the minor rotamer are marked with an asterisk (*).

Due to rotational isomerism along the Boc group, two sets of signals are observed in the ^1H NMR spectrum in the ratio 55:45. The removal of the ethoxycarbonyl moiety in 4-position is confirmed by reduced integrals of the ester signals at 4.13 – 4.24 ppm (multiplet, OCH_2CH_3) and at 1.27 ppm and 1.26 ppm (two triplets, OCH_2CH_3). Moreover, four signals in the range of 2.40 – 2.80 ppm represent the newly formed methylene protons in 4-position. The methyne protons at the bridgehead atoms in

6- and 8-position are presented by two characteristic dd's at 4.73 ppm ($J = 8.6 / 2.2$ Hz) and 4.49 ppm ($J = 7.4 / 2.4$ Hz) and a triplet at 4.55 ppm ($J = 3.9$ Hz) and a dd at 4.34 ppm ($J = 6.2 / 2.2$ Hz), respectively. Due to a twisted bicyclic system, the larger coupling constants in the 8- H_{eq} signals indicate a pseudo-axially oriented ester in 8-position. A NOESY experiment confirmed this assumption, showing a close proximity of 8- H_{eq} with both protons in 9-position. (Figure S6, Appendix)

Since the products of the Dieckmann condensation and the Krapcho reaction were obtained in only low yields, further investigations were not undertaken to obtain the test compounds with a 7-azabicyclo[4.3.1]decane scaffold.

4.4 Excursus: Synthesis of 1,2,3,4-tetrahydropyridine derivatives as analogs of betalains

Betalains are naturally occurring pigments used as food colorants with antioxidant, anticancer and anti-lipidemic properties.^{127,128} They can be divided into two subclasses: the red-violet betacyanines and the yellow-orange betaxanthines. Their colors are based on large conjugated systems with a positive charge. The pyridinium-2,6-dicarboxylic acid **101** represents the basic structural element of both subclasses. Compounds of type **101** derive from betalamic acid **102** and an amine. (Figure 34) For betacyanins, the used amines are cyclo-DOPA derivatives which are either acylated or glycosylated. In case of betaxanthins, a wide range of amines or amino acids were determined which can condensate at betalamic acid **102**.¹²⁹

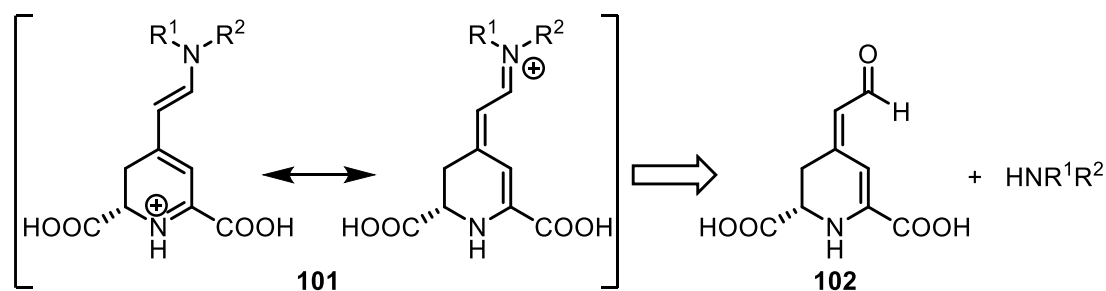
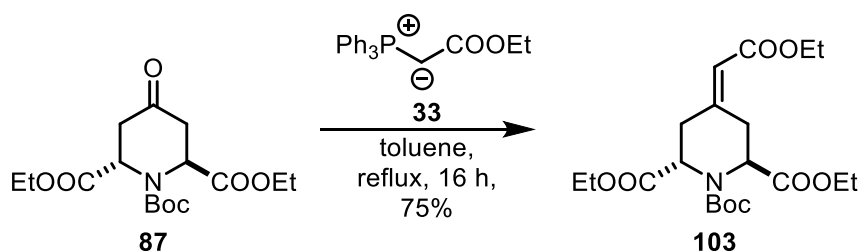


Figure 34: Basic scaffold of betalains **101** which are derived from betalamic acid **102**.

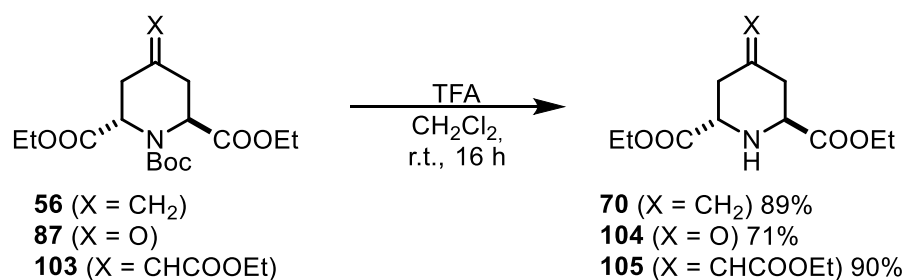
During the syntheses of substituted bicyclic amines **20**, **21** and **22**, *trans*-configured piperidine-2,6-dicarboxylates **56** and **87** were prepared. In order to obtain novel betalamic acid derivatives, a double bond should be introduced in the piperidine-2,6-dicarboxylate scaffold. Hilpert and Dreiding reported the synthesis of racemic mixtures of 1,2,3,4-tetrahydropyridines starting from *cis*-configured piperidine-2,6-dicarboxylic acid derivatives.¹³⁰ In addition to 4-methylenepiperidine **56** and 4-piperidinone **87**, the α,β -unsaturated ester **103** was envisaged for dehydrogenation. Ester **103** was obtained by a Wittig reaction of ketone **78** with ylide **33** in 75% yield. (Scheme 49)



Scheme 49: Wittig reaction of ketone **87** with stabilized ylide **33**.

The introduction of the C₂-side chain was shown by a band at 1651 cm⁻¹ in the IR spectrum of α,β -unsaturated ester **103** representing the C=C moiety. Furthermore, a loss of the signal for the carbonyl C-atom at 203.8 ppm in the ¹³C NMR spectrum proves the structure of **103**.

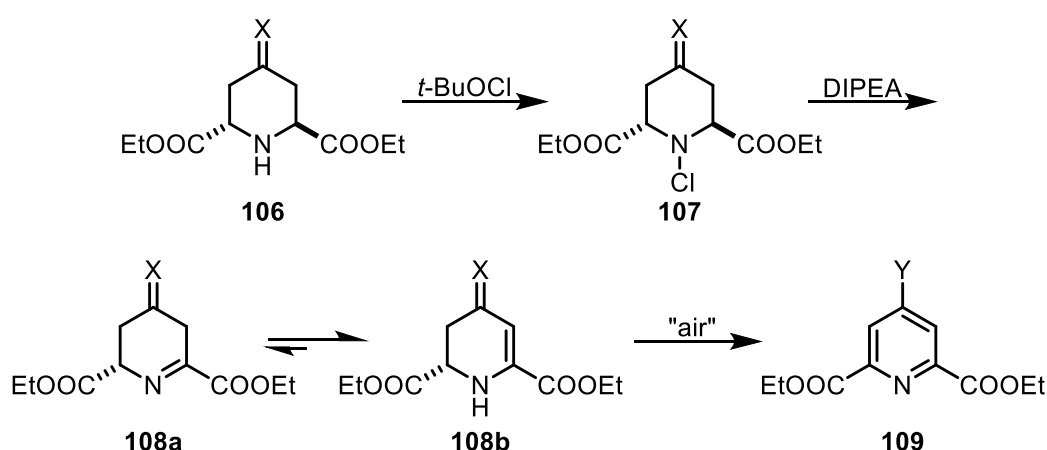
To be able to introduce the double bond, the Boc groups of **56**, **87** and **103** had to be removed. The corresponding secondary amines **70**, **104** and **105** were obtained in 89%, 71% and 90% yield, respectively. (Scheme 50)



Scheme 50: Boc removal of piperidines **56**, **87** and **103**.

The removal of the Boc group can be seen in the ¹H NMR spectra of secondary amines **70**, **104** and **105** by a missing singlet around 1.40 ppm with an integral of 9H. Moreover, due to the absence of a carbamate moiety, rotational isomers do no longer exist resulting in only one set of signals for **70**, **104** and **105**.

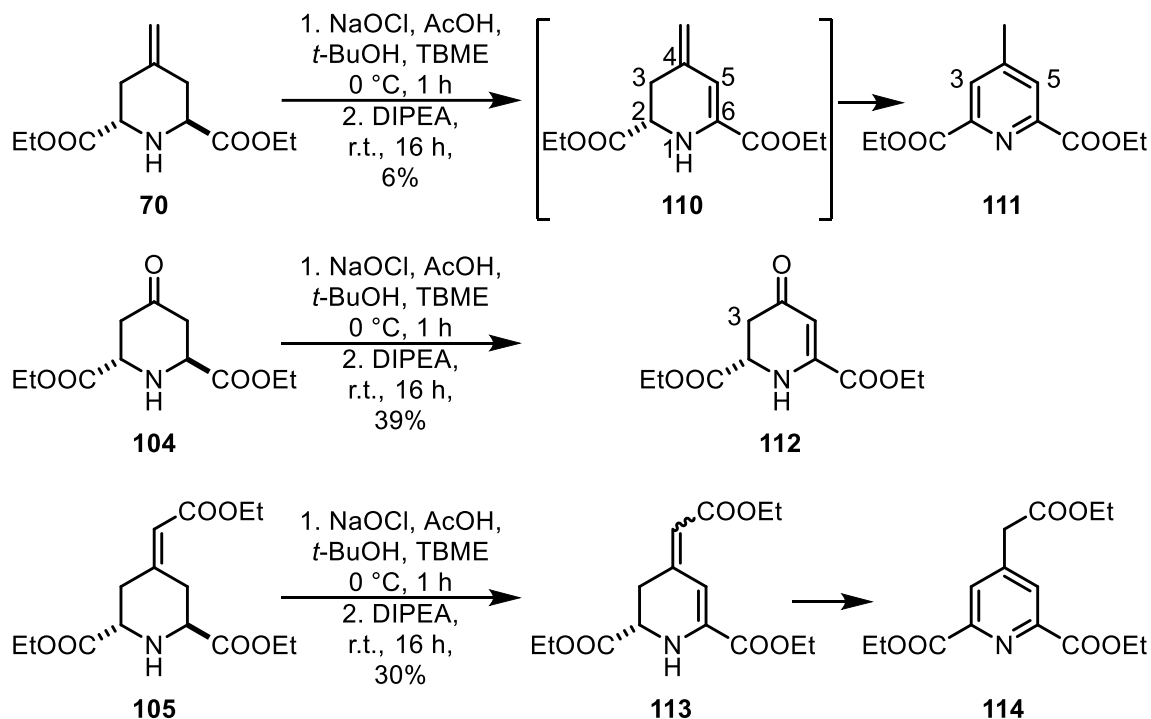
Next, the double bond was introduced in 2,3-position *via* a chloramine intermediate adapting a reported method by Zhong *et al.*¹³¹ (Scheme 51)



Scheme 51: Mechanism of the introduction of a double bond into piperidines and potential oxidation to the corresponding pyridine derivatives.

In general, chloramine **107** was formed by reaction of secondary amine **106** and *t*-BuOCl, which was generated *in situ* by addition of AcOH to a solution of NaOCl in

t-BuOH. After addition of DIPEA, a dehydrohalogenation occurred leading to imine **108a** which tautomerizes to enamine **108b**. Depending on the stability of the unsaturated compound, a second double bond can be introduced in 2,3-position by O₂, which will immediately aromatize into pyridine derivative **109**. Different results were obtained when performing the reaction with secondary amines **70**, **104** and **105**. (Scheme 52)



Scheme 52: Introduction of a double bond in 5,6-position and potential formation of pyridine analogs.

In case of 4-methylenepiperidine **70**, only pyridine **111** was isolated in 6% yield. The ¹H NMR spectrum of **111** displays a singlet at 8.10 ppm for the aromatic protons in 3- and 5-position. Signals for the 1,2,3,4-tetrahydropyridine analog **110** could not be observed, indicating fast oxidation of **110** to pyridine **111** by O₂.

In contrast to the fast oxidation of **110**, the oxidation of piperidinone **104** with *t*-BuOCl led exclusively to 1,2,3,4-tetrahydropyridinone **112**, which was isolated in 39% yield. The methylene protons in 3-position produce two dd's at 2.70 ppm and 2.80 ppm. An oxidation to the 4-hydroxypyridine derivative was not observed. In contrast to the fast oxidation of **110** and the very slow oxidation of **112**, ester **113** was slowly oxidized to pyridine **114**. Thus, oxidation could be observed by measuring ¹H NMR spectra over a period of several days. Selected ¹H NMR spectra are displayed in Figure 35.

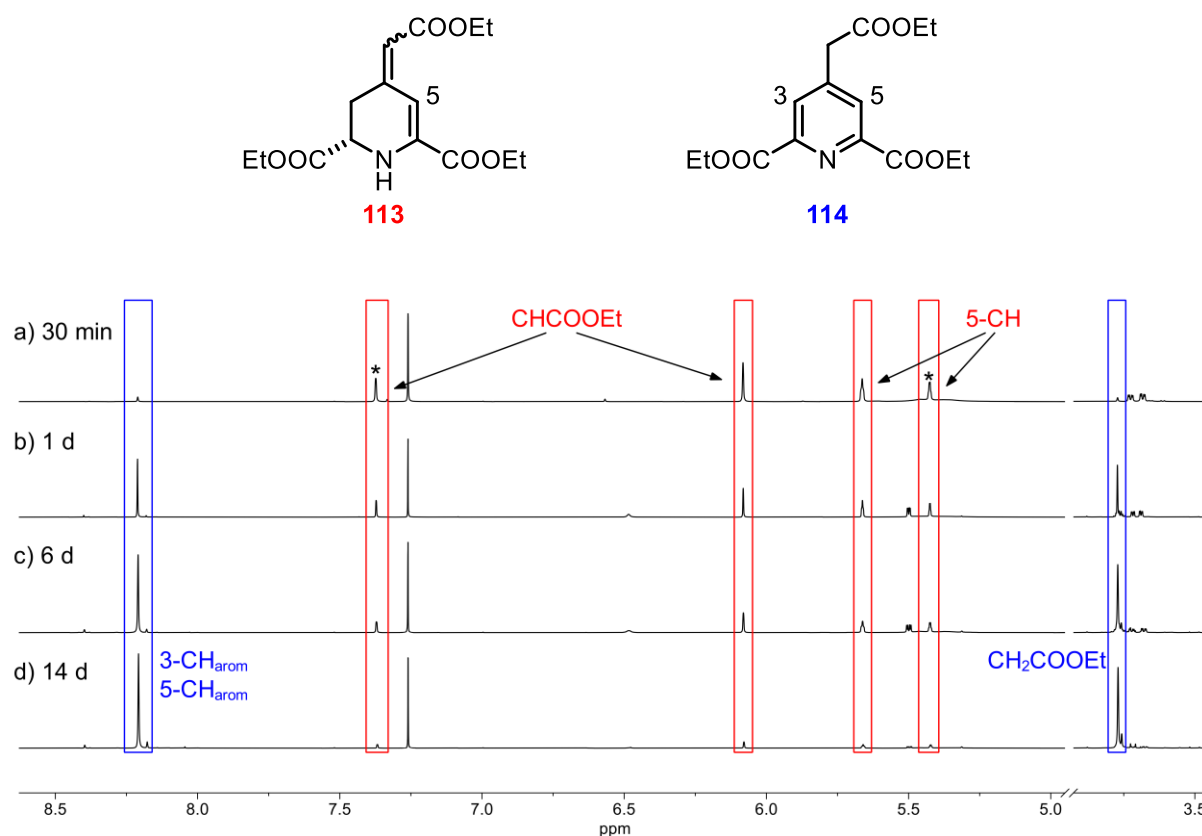


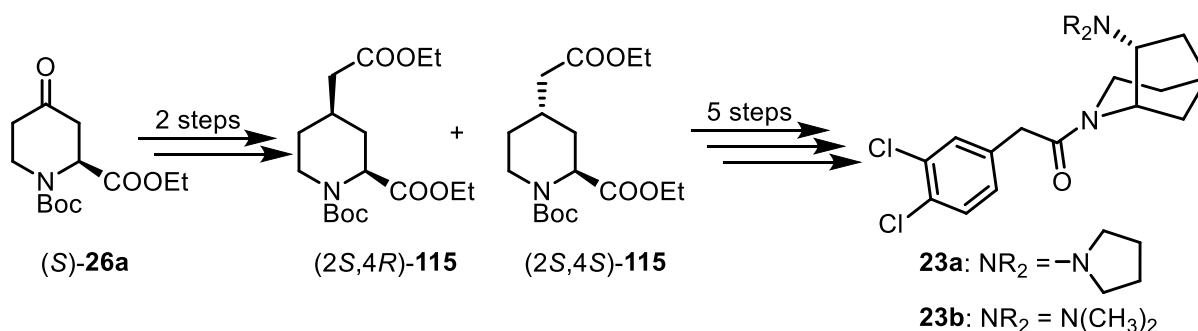
Figure 35: ^1H NMR spectra of 1,2,3,4-tetrahydropyridine **113** after different time intervals. Ratio of diastereomers of *cis*-**113** and *trans*-**113** is 55:45. The signals for the minor diastereomer are marked with an asterisk (*).

The ^1H NMR spectra indicate the formation of 4% of pyridine **114** already after 30 min. (track a) The signals for the oxidation product **114** grew over the time from 4% (30 min) to 44% (1 d, track b) over 62% (6 d, track c) to 84% (14 d, track d). It can be concluded that the methylenepiperidine **110** behaves as potent antioxidant as it is very fast oxidized to afford the pyridine **111**. Enlargement of the *exo*-methylene moiety to an ethoxycarbonylmethylene moiety in **113** reduced the antioxidant properties, as **113** was only slowly oxidized to form the pyridine **114**. A ketone **112**, however, is a rather stable compound with poor antioxidant properties.

The results observed for 1,2,3,4-tetrahydropyridines **112** and **113** correlate well with the reported results by Hilpert and Dreiding.¹³⁰ They observed a steady oxidation of the methyl ester analog of $\alpha,\beta,\gamma,\delta$ -diunsaturated ester **113** into its corresponding pyridine derivative, while the methyl ester analog of ketone **112** was stable.

4.5 Part 4: Synthesis of 2-azabicyclo[3.2.1]octanes **23a,b**

In addition to piperidines with an enlarged C₄-bridge, (chapter 4.3) piperidines with a shorter C₂-bridge were envisaged. A chiral pool synthesis starting with (*S*)-configured piperidine-2-carboxylate (*S*)-**26a** was planned. Altogether, seven reaction steps were performed to obtain **23a,b**. (Scheme 53)

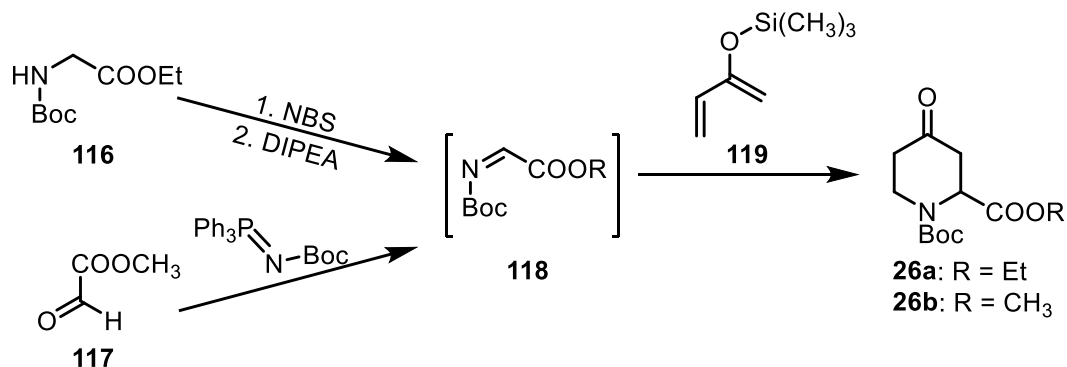


Scheme 53: Outline of the synthesis of 2-azabicyclo[3.2.1]octanes **23a** and **23b**.

The synthesis of bicyclic KOR agonists **23a,b** is described in three parts: the first part deals with the preparation of piperidinone (*S*)-**26a**; the second part describes the generation of *cis*- and *trans*-configured diesters **115** and in the third part the final steps to transform the diesters **115** into bicyclic amines **23a** and **23b** are reported.

4.5.1 Synthesis of piperidinones with an ester moiety in 2-position

Several syntheses of piperidinone derivatives **26a** and **26b** with an ester moiety in 2-position are described in the literature.^{56,58,61,62} An aza-Diels-Alder reaction of *in situ* formed imines **118** with Danishefsky's diene **119** provided the piperidinones **26a** and **26b** (Scheme 54)

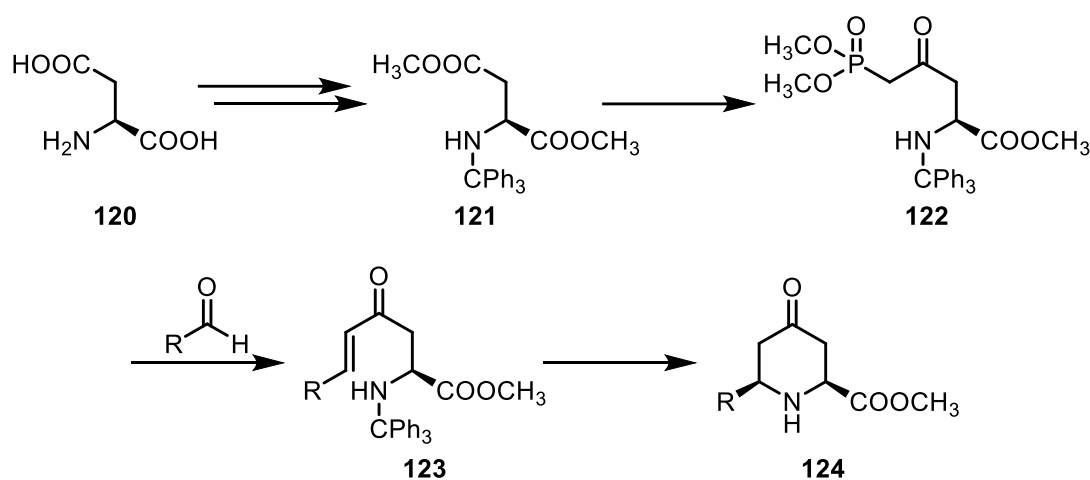


Scheme 54: Synthesis of piperidinones **26a** and **26b** by aza-Diels-Alder reaction.^{58,62}

Imines **118** were prepared either by α -bromination of Boc-protected ethyl glycinate **116** with NBS followed by dehydrohalogenation or by an aza-Wittig reaction of a

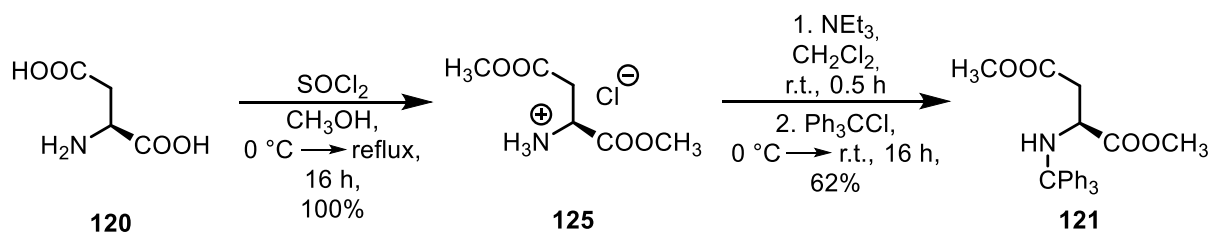
phosphinimine and methyl glyoxylate **117**. In addition to the low yield, the reported methods generated only racemic mixtures of piperidinones **26a** and **26b**.

Enantiomerically pure *cis*-configured 4-oxopiperidine-2-carboxylates (**124**) can be obtained starting with enantiomerically pure (*S*)-aspartic acid (**120**).⁵⁶ Esterification and tritylation provide dimethyl (*S*)-*N*-tritylaspartate (**121**) which reacted with methylenephosphonates and *n*-BuLi to β -oxo-phosphonate **122**. Condensation of phosphonate with aldehydes led to α,β -unsaturated ketones **123**, which underwent an aza-Michael reaction after removal of the trityl protective group to form the desired piperidinones **124**.



Scheme 55: Synthesis of enantiomerically pure *cis*-configured piperidinones **124**.⁵⁶

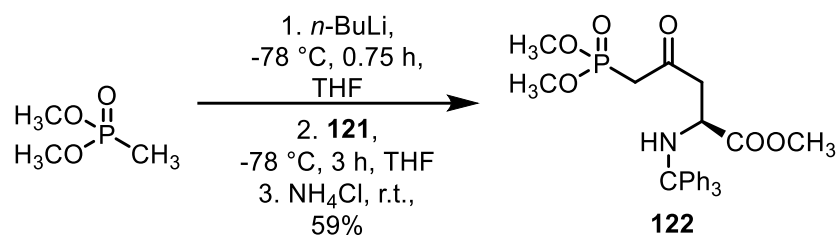
In order to obtain piperidinone **26b**, this strategy was pursued and the phosphonate **122** should react with formaldehyde. Thus, (*S*)-aspartic acid (**120**) was reacted with CH_3OH and $SOCl_2$ to afford the dimethyl ester **125** in quantitative yields. (Scheme 56)



Scheme 56: Synthesis of diester **121** starting from (*S*)-aspartic acid.

Alkylation of **125** with Ph_3CCl led to to tritylamine **121** in 62% yield. The successful tritylation was shown by three multiplets in the range of 7.17 – 7.52 ppm in the 1H NMR spectrum of **121** representing the 15 aromatic protons of the phenyl rings. The next

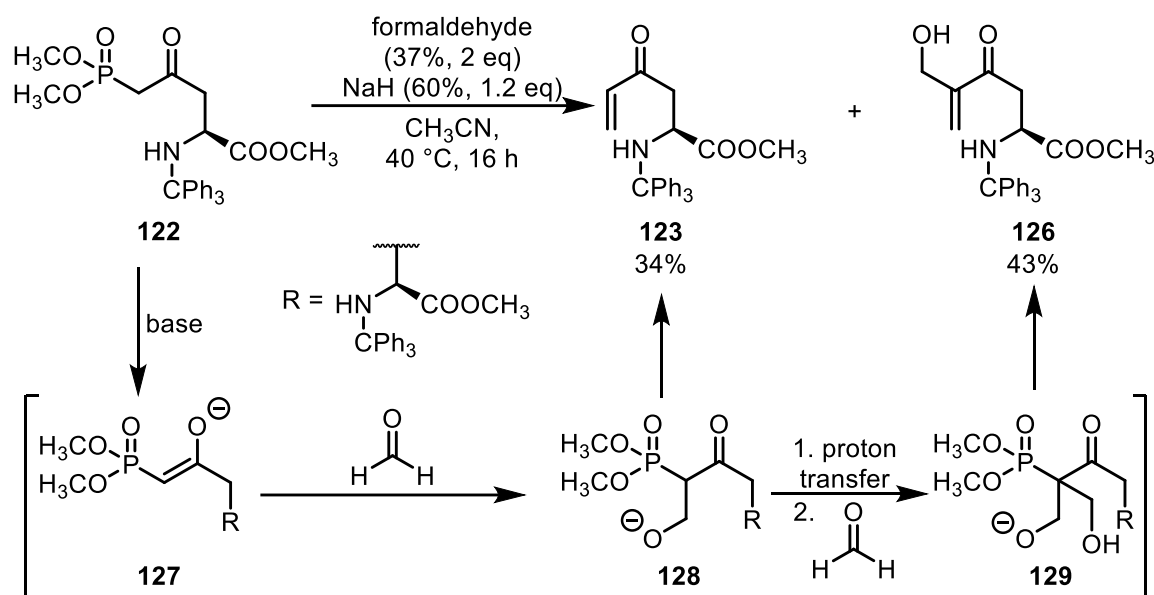
step was the synthesis of phosphonate **122** by Claisen reaction with dimethyl methanephosphonate. (Scheme 57)



Scheme 57: Synthesis of dimethyl phosphonate **122**.

First, $n\text{-BuLi}$ deprotonated dimethyl methanephosphonate generating an anion. After addition of aspartate **121**, the anion attacked selectively the methyl ester in γ -position leading to dimethyl phosphonate **122** in 59% yield. Due to the sterically demanding trityl protective group, the methyl ester in α -position to the amine is not attacked by the phosphonate anion. The formation of phosphonate **122** is proven in the ^{13}C NMR spectrum by a doublet ($J = 127.9\text{ Hz}$, coupling with P-atom) at 42.0 ppm representing the methylene group between the carbonyl moiety and the P-atom. The corresponding signals of the diastereotopic protons in the ^1H NMR spectrum are two doublets at 3.02 ppm and 3.08 ppm. The singlet of the previous methyl ester has disappeared.

Daly *et al.* reported the condensation of phosphonate **122** with different aldehydes to the corresponding enones in yields of 57-96%.⁵⁶ However, the reaction with formaldehyde was not reported. Performing the Horner-Wodswarth-Emmons (HWE) reaction as described in the synthetic procedure⁵⁶ with two equivalents of aldehyde, enones **123** and **126** were obtained in 34% and 43% yield, respectively. (Scheme 58)



Scheme 58: HWE reaction of phosphonate **122** leading to enone **123** and α -(hydroxymethyl)enone **126**.

After deprotonation of the methylene group between the ketone and the phosphonate, the generated enolate **127** attacked the carbonyl C-atom of formaldehyde yielding alcoholate **128**. Then, similar to the Wittig reaction, (chapter 4.1.1.2) an oxaphosphetane was formed, which fragmented by a [2+2] reversed cycloaddition into dimethyl phosphate and enone **123**. In the ¹H NMR spectrum of **123** three dd's at 6.25 ppm, 6.13 ppm and 5.93 ppm represent the protons of the monosubstituted alkene. (Figure 36)

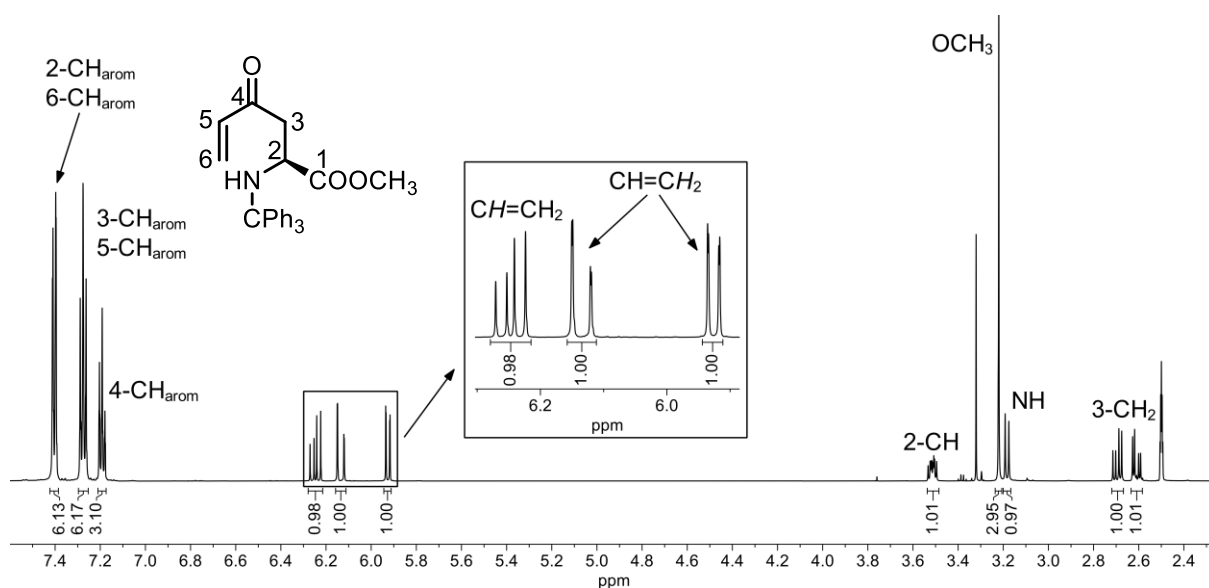
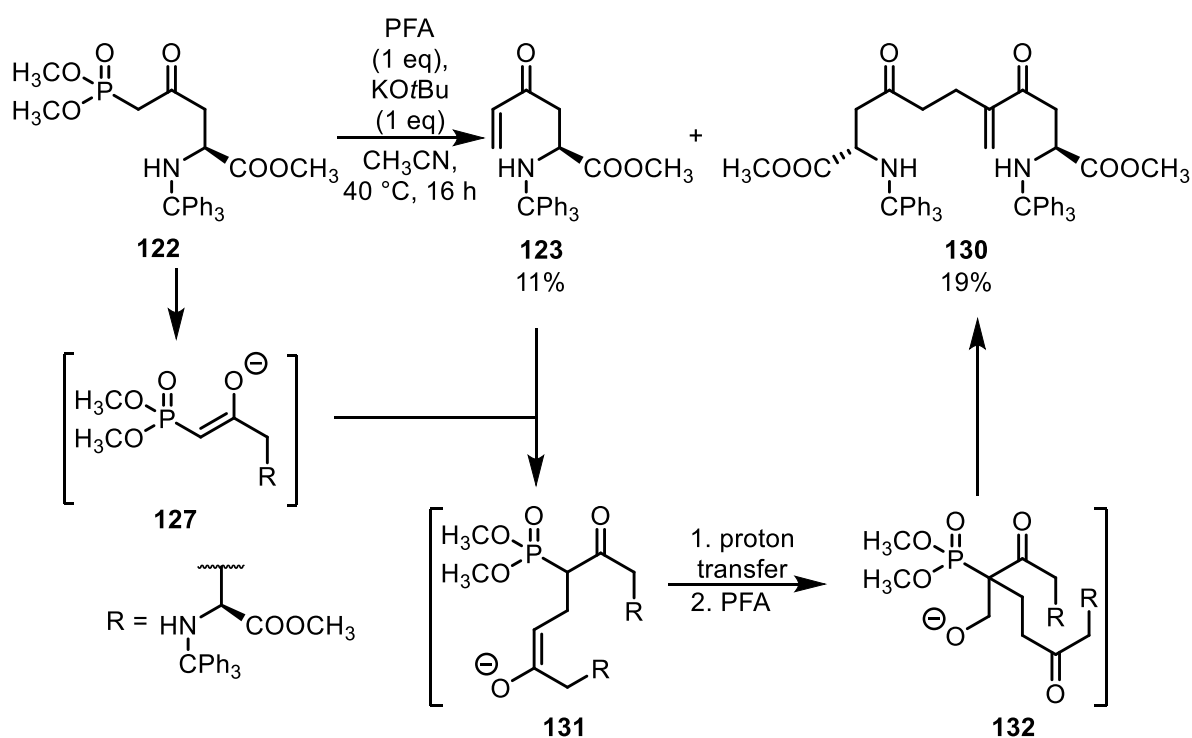


Figure 36: ¹H NMR spectrum (CDCl₃) of enone **123**.

Moreover, doublets caused by a coupling of C-atoms with the P-atom cannot be seen in the ^{13}C NMR spectrum indicating the removal of the phosphonic ester moiety. The hydroxymethyl derivative **126** was formed due to the excess of formaldehyde used in the HWE reaction. Apparently, a second molecule of formaldehyde reacted with the intermediate **128**, before the oxaphosphetane intermediate was formed. The resulting alcoholate **129** cyclized followed by a reversed cycloaddition leading to α -hydroxymethyl ketone **126**. In the IR spectrum of **126**, a band at 3317 cm^{-1} proved the presence of a hydroxy group.

To prevent the double hydroxyalkylation, the amount of formaldehyde was reduced to one equivalent and the base was changed to KO t Bu. Instead of formaline, paraformaldehyde (PFA) was used. (Scheme 59)

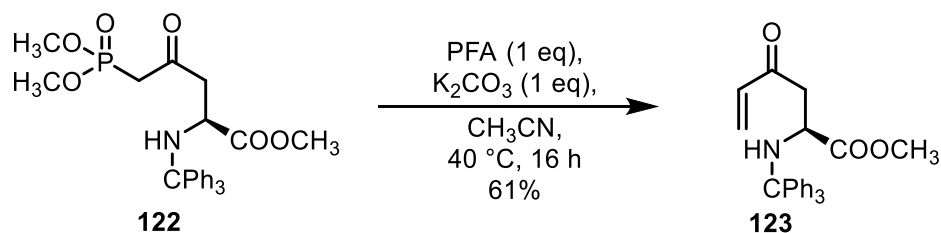


Scheme 59: Reaction of **122** with one equivalent of PFA.

Unexpectedly, the yield of enone **123** dropped down to 11% and the dimeric product **130** was isolated in 19% yield. It is assumed that after formation of a critical amount of desired enone **123**, the *in situ* generated enolate **127** underwent a Michael addition at enone **123** forming enolate **131**. After proton transfer, the corresponding enolate attacked paraformaldehyde, which led to **130** via intermediate **132**. In the ^1H NMR spectrum of enone **130**, two singlets at 5.76 ppm and 5.94 ppm displaying the methylene protons are observed. The existence of two singlets for the methyl esters

at 3.21 ppm and 3.22 ppm and doubling of the integrals of the aromatic protons confirm the proposed structure of the product **130**.

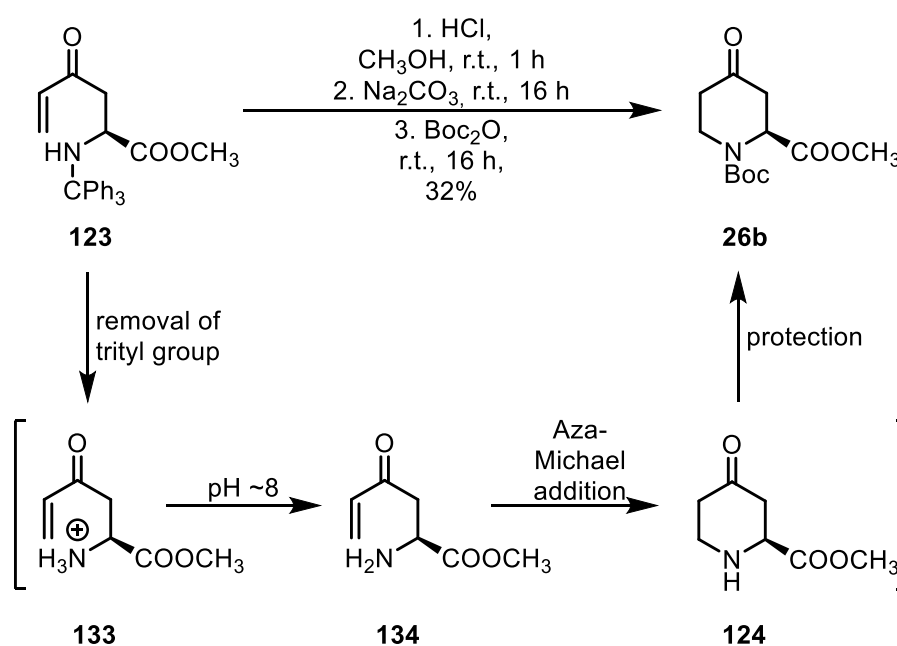
Optimized reaction conditions for the synthesis of enone **123** were obtained by changing the base to K_2CO_3 as originally described by Daly *et al.*⁵⁶ and reducing the concentration of phosphonate **122**. (Scheme 60) Additional side products were not isolated.



Scheme 60: Optimized synthesis of enone **123**.

In conclusion, high yields of enone **123** were obtained with one equivalent of paraformaldehyde and low concentration of phosphonate **122**. Two equivalents of formalin resulted in a double hydroxyalkylation yielding to α -(hydroxymethyl)enone **126**. A high-concentrated solution of **122** with one equivalent of paraformaldehyde led to the dimeric product **130**, which was formed by Michael addition.

The next step was the synthesis of (*S*)-configured piperidinone (*S*)-**26b**. (Scheme 61)

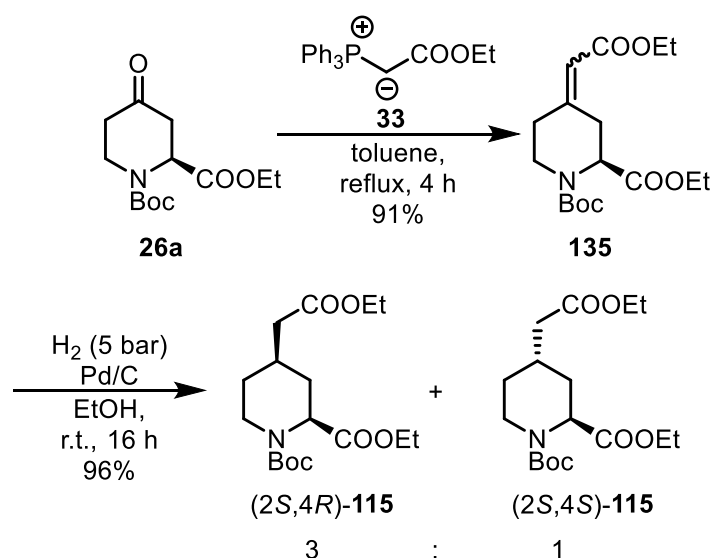


Scheme 61: Overview of ring closure of enone **123**.

The reaction consists of three steps: first, acid-induced removal of the trityl group; second, basifying (pH ~8) the solution to transform ammonium ion **133** into primary amine **134**, which undergoes an aza-Michael reaction; and finally, Boc protection of secondary amine **124**. The desired piperidinone (*S*)-**26b** was isolated in 32% yield. Thus, the ester (*S*)-**26b** can be synthesized starting from (*S*)-aspartic acid in six reaction steps and 7% overall yield. Alternatively, the ethyl ester (*S*)-**26a** is commercially available.

4.5.2 Incorporation of C₂ side chain

In analogy to the described synthesis of 2-azabicyclo[3.3.1]nonanes **19a,b**, (chapter 4.1.1) a C₂ side chain was introduced in 4-position of piperidinone (*S*)-**26a** to obtain compounds with a 2-azabicyclo[3.2.1]octane scaffold. Thus, a Wittig reaction was performed with subsequent hydrogenation. (Scheme 62)



Scheme 62: Wittig reaction of piperidinone **26a** and subsequent hydrogenation.

Stabilized ylide **33** was reacted with piperidinone **26a** leading to α,β-unsaturated ester **135** in 91% yield. A band at 1655 cm⁻¹ in the IR spectrum demonstrates the stretching vibration of the C=C-bond. Although stabilized ylide **33** was used, stereoselectivity considering the configuration of the generated alkene was not observed. (see chapter 4.1.1.2) According to the ¹H NMR spectrum of **135**, the (*E*)- and (*Z*)-isomers were formed in the ratio 1:1. The absence of stereoselectivity is caused by the high symmetry of the two sides of the piperidine ring.

Unsaturated ester **135** was hydrogenated with H₂ (5 bar) using Pd/C as catalyst in almost quantitative yield. The loss of the C=C band in the IR spectrum confirmed the

reduction. Two sets of signals in the ratio 3:1 are seen in the ^1H NMR spectrum of **135** representing the diastereomers (2*S*,4*R*)-**115** and (2*S*,4*S*)-**115**. (Figure 37) The diastereomers could not be separated by flash column chromatography.

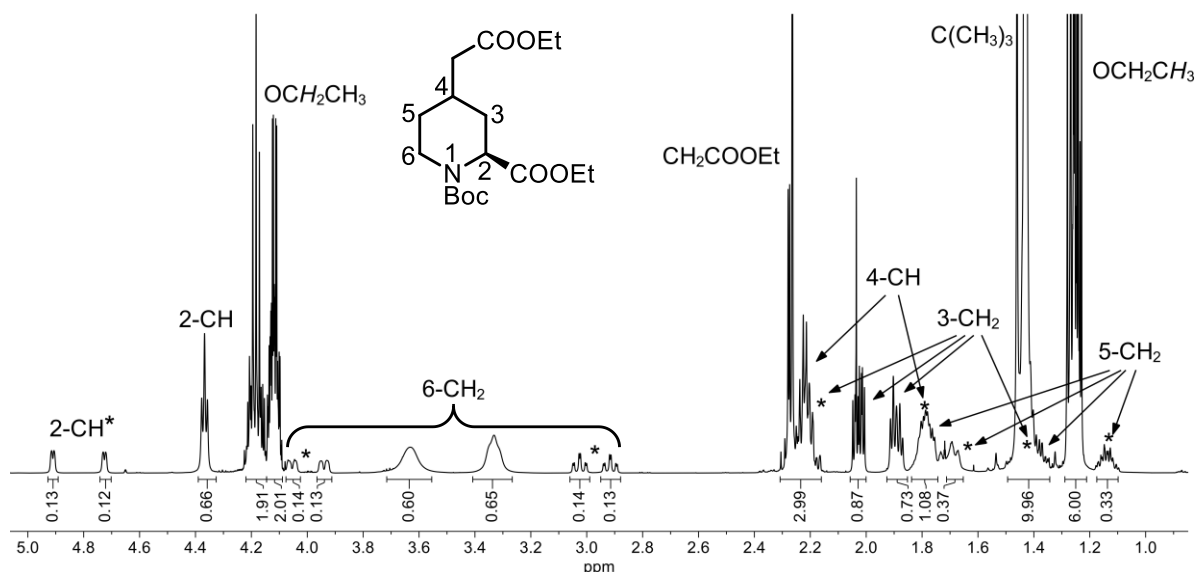


Figure 37: ^1H NMR spectrum (CDCl_3) of diastereomeric diesters **115** existing in the ratio 3:1. The signals for the minor diastereomer are marked with an asterisk (*).

Due to rotational isomerism along the Boc group, a further split of signals for the minor diastereomer is observed, which is shown for the proton signals in 2- and 6-position. The signals of the major diastereomer are broadened. The methyne signal of the alkene at 5.70 – 5.77 ppm has vanished, whilst a new signal at 2.17 – 2.31 ppm appeared representing the newly formed methylene group adjacent to the ester. A NOESY experiment was carried out to determine the relative configuration of the diastereomers. (Figure 38) The complete NOESY spectrum is displayed in Figure S7. (Appendix)

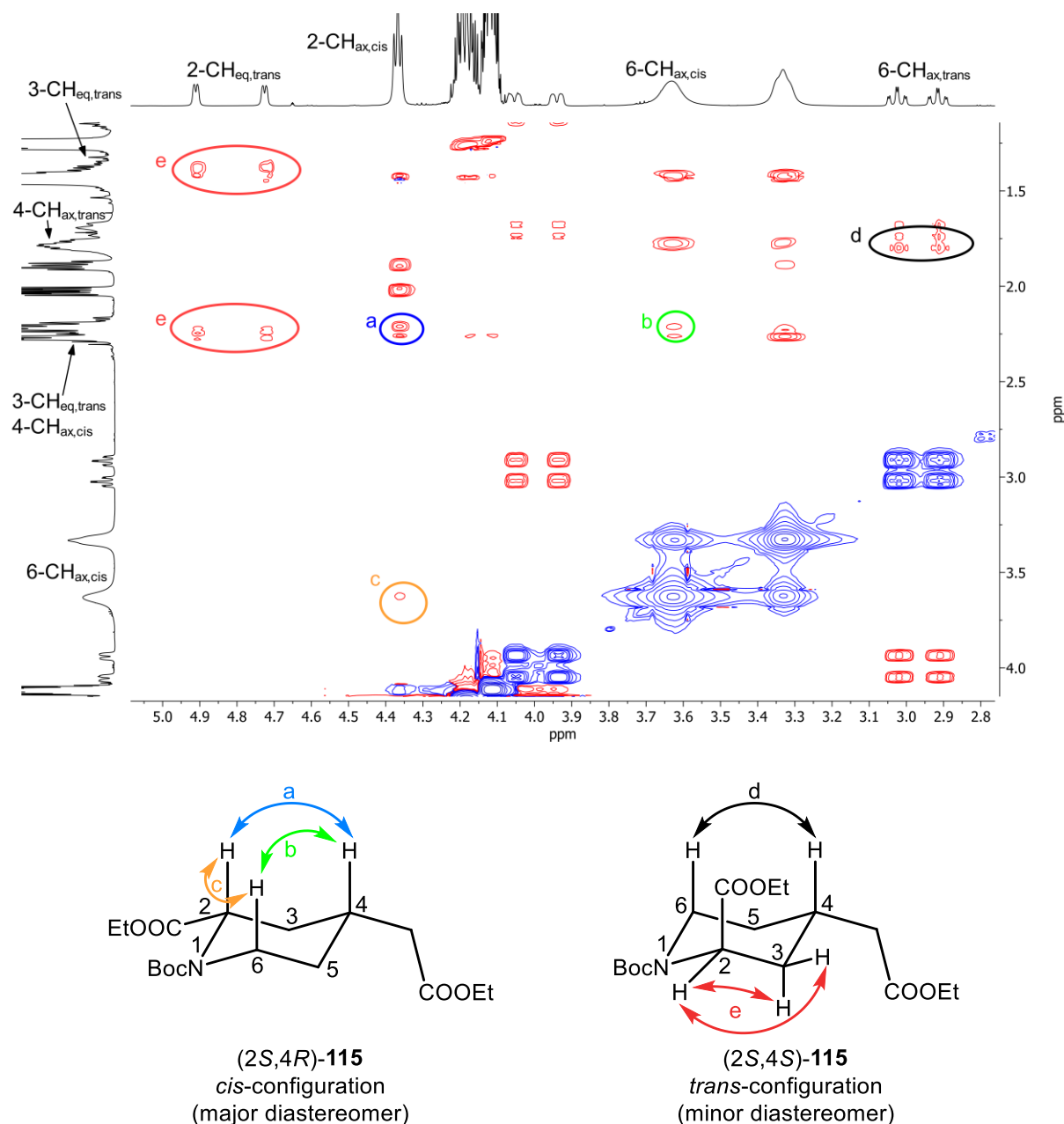


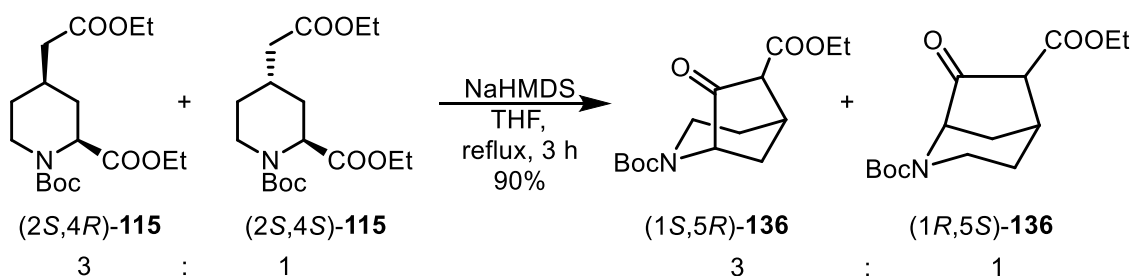
Figure 38: NOESY spectrum (top) and NOE (bottom) of (2*S*,4*R*)-115 and (2*S*,4*S*)-115.

A cross peak between the signals at 2.16 – 2.18 ppm (4-CH) and 4.37 ppm (2-CH) (Figure 38, mark a) for the major diastereomer indicates the *cis*-configuration of these axially oriented protons. Consequently, the ester moiety in 2-position and the ethoxycarbonylmethyl moiety in 4-position are *cis*-configured as well, both in equatorial orientation. Moreover, close proximities are observed between 4-CH and 6-CH₂ (3.63 ppm, mark b) and 2-CH and 6-CH₂ (mark c) confirming the *cis*-configuration. For the minor diastereomer, cross peaks between 4-CH (1.76 – 1.84 ppm) and 6-CH₂ (2.92 ppm and 2.02 ppm) are observed, (mark d) while cross peaks for 2-CH (4.73 ppm and 4.91 ppm) and 4-CH cannot be observed. Thus, a *trans*-configuration

of the protons in 2- and 4-position as well as for the substituents is postulated. Short distances of 2-CH to both protons in 3-position (mark e) further strengthen this assignment. In conclusion, the hydrogenation of α,β -unsaturated ester **135** led to diester (2*S*,4*R*)-**115** (*cis*) and (2*S*,4*S*)-**115** (*trans*) in the ratio 3:1.

4.5.3 Synthesis of 2-azabicyclo[3.2.1]octanes **23a,b**

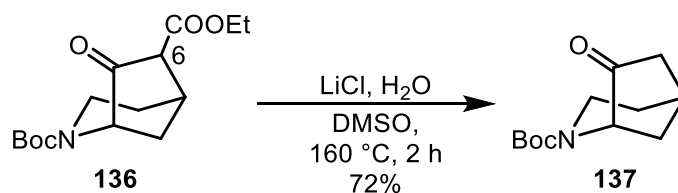
To transform diesters **115** into bicyclic amines **23a,b**, the same reaction procedure was performed as described for 2-azabicyclo[3.3.1]nonanes **19a,b** starting from diester **37**. (chapter 4.1.1.4 and 4.1.2). NaHMDS was added to a refluxing solution of **115** in THF (*c* = 0.02 M) inducing the Dieckmann condensation to provide bicyclic β -keto ester **136**. (Scheme 63)



Scheme 63: Dieckmann condensation of diester **115**.

Whereas the cyclization of *cis*-configured diester (2*S*,4*R*)-**115** into (1*S*,5*R*)-**136** underwent without any difficulties, *trans*-configured diester (2*S*,4*S*)-**115** could not react directly. However, a base-induced epimerization into *cis*-configured diester (2*R*,4*S*)-**115** allowed the cyclization. Thus, the diastereomeric mixture of (2*S*,4*R*)-**115** and (2*S*,4*S*)-**115** was converted into a mixture of enantiomers in the ratio 3:1. The successful condensation was confirmed by the ^1H NMR spectrum of **136**. Reduced integrals of the ester signals at 4.07 – 4.29 (2H, OCH_2CH_3) and 1.23 – 1.32 ppm (3H, OCH_2CH_3) display the loss of one ester moiety. Mass spectrometry confirmed the mass of **136**.

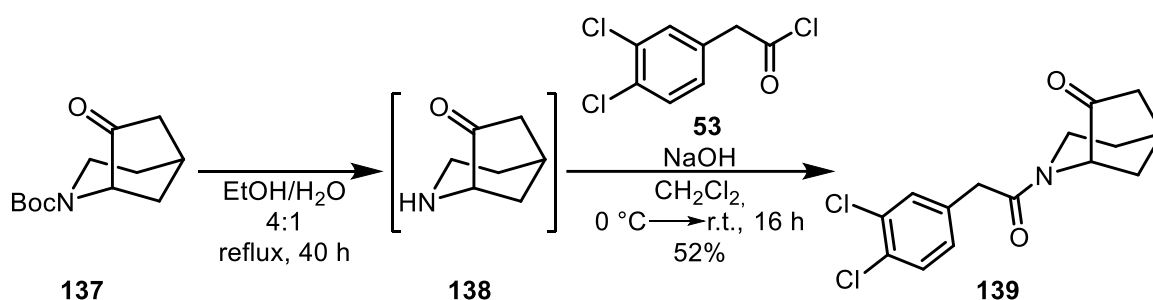
Ketone **137** was synthesized by Krapcho reaction of β -keto ester **136**. (Scheme 64)



Scheme 64: Krapcho reaction of β -keto ester **136**.

Treatment of β -keto ester **136** with LiCl in DMSO led to the bicyclic ketone **137** in 72% yield. The transformation is indicated in the ^1H and ^{13}C NMR spectra of **137**, since signals for the ester moiety in 6-position are no longer present. Instead, a signal representing the newly formed methylene group in 6-position appears at 1.85 ppm in the ^1H NMR spectrum.

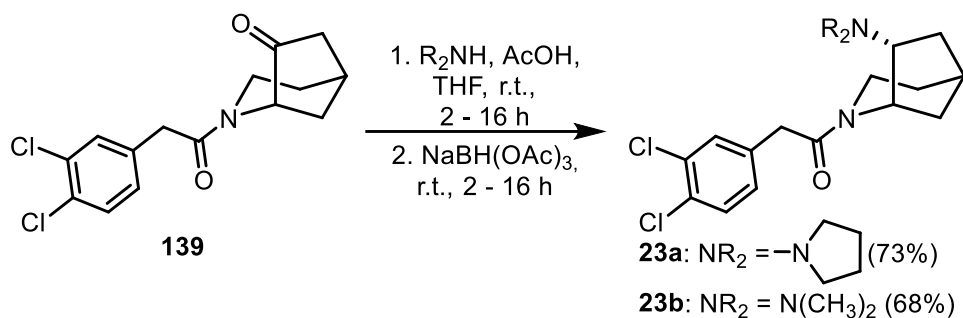
Next, the first KOR pharmacophoric element was introduced, by removal of the Boc group of ketone **137** and subsequent acylation of the *in situ* generated secondary amine **138**. (Scheme 65)



Scheme 65: Removal of the Boc group and subsequent acylation to yield **139**.

In contrast to the Boc removal of ketone **51** with a 2-azabicyclo[3.3.1]nonane scaffold (chapter 4.1.2), secondary amine **138** could not be generated with TFA. Thus, an unconventional method was applied.¹³² The ketone **137** was heated in a mixture of EtOH and H₂O for 40 h. The progress of the Boc removal was controlled by TLC (KMnO₄ staining). While the spot for **137** vanished during the reaction, a novel spot representing a more polar compound appeared close to the baseline. Without isolation and purification, secondary amine **138** was transformed into amide **139** using the Schotten-Baumann method. At 0 °C, NaOH was added followed by a solution of acyl chloride **53** in THF to form bicyclic amide **139** in an overall yield of 52%. The successful exchange of the Boc group by the phenylacetyl moiety of **139** was proven by ^1H NMR spectra analysis. The singlet of the Boc group has disappeared, whilst characteristic signals for aromatic protons of the phenylacetyl group appeared. Due to rotational isomerism along the C-N bond of the amide group, two sets of signals were observed in the ratio 55:45. In the IR spectrum of amide **139**, a band at 1632 cm⁻¹ represents the C=O stretching vibration of the amide group.

A diastereoselective reductive amination of ketone **139** was envisaged to introduce the second KOR pharmacophoric element. As for the 2-azabicyclo[3.3.1]nonanes **19a,b** pyrrolidine and dimethylamine were employed as amines. (Scheme 66)



Scheme 66: Diastereoselective reductive amination of ketone **139**.

The bulky reducing agent $NaBH(OAc)_3$ was used to transfer the hydride selectively from the backside of the generated iminium ion, forming *endo*-configured bicyclic amines **23a** and **23b** in 73% and 68% yield, respectively.

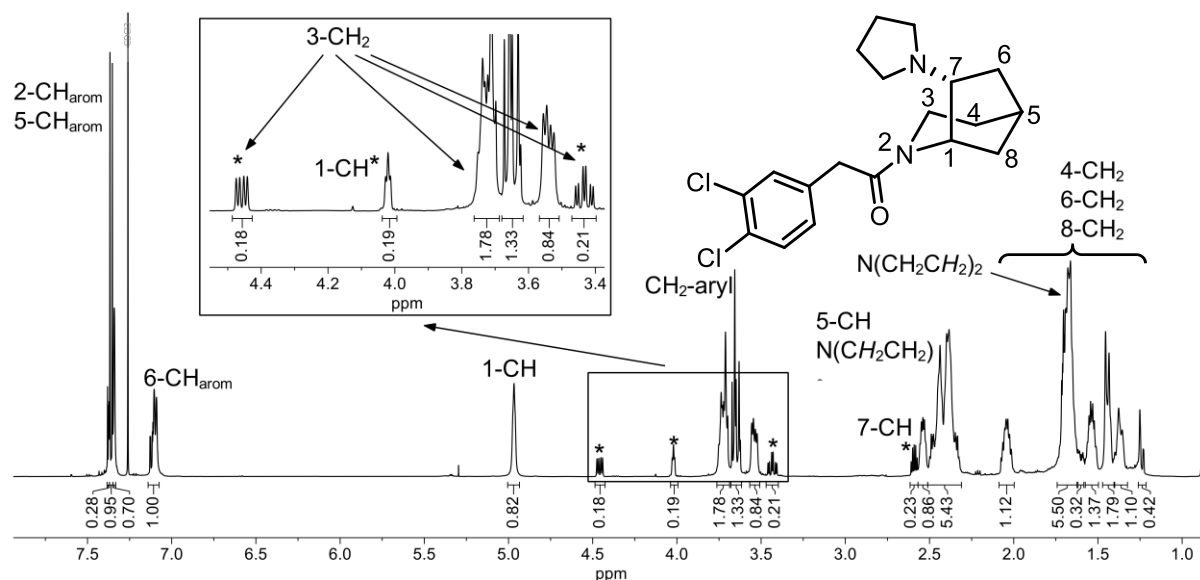


Figure 39: 1H NMR spectrum ($CDCl_3$) of 2-azabicyclo[3.2.1]octane **23a**. The signals for the minor rotamer are marked with an asterisk (*).

Due to rotational isomerism along the C-N bond of the amide group, two sets of signals in the ratio 8:2 are seen in the 1H NMR spectrum of **23a**. (Figure 39) Two signals at 1.62 – 1.74 ppm and 2.28 – 2.51 ppm belong to the pyrrolidine moiety. Moreover, the newly formed methyne proton in 7-position causes two signals at 2.52 – 2.57 ppm and 2.58 – 2.62 ppm. In the ^{13}C NMR spectrum, the signal for the C-atom of the ketone disappeared, whilst new signals for the pyrrolidine C-atoms are observed. To determine the relative configuration of bicyclic amine **23a**, a NOESY experiment was performed. (Figure S8, Appendix) A cross peak between 7-CH and 8- CH_{eq} confirms the *endo*-configuration of **23a**. An interaction of 7-CH and the protons in 3-position

through the space is not observed. Similar results can be seen in the NOESY spectrum of dimethylamine **23b**. (Figure S9, Appendix)

4.5.4 Determination of the enantiomeric purity of **23a,b** and absolute configuration of 2-azabicyclo[3.2.1]octanes **23a,b**

Chiral HPLC methods C and D were developed to determine the enantiomeric purity of the synthesized *endo*-configured bicyclic amines **23a,b**. An inversion of the peaks occurred after addition of formic acid. (HPLC method C) The chromatograms display a ratio of 3:1 for the enantiomers (1*S*,5*S*,7*R*)-**23a,b** and (1*R*,5*R*,7*S*)-**23a,b** (*ent*-**23a,b**). (Figure 40 top)

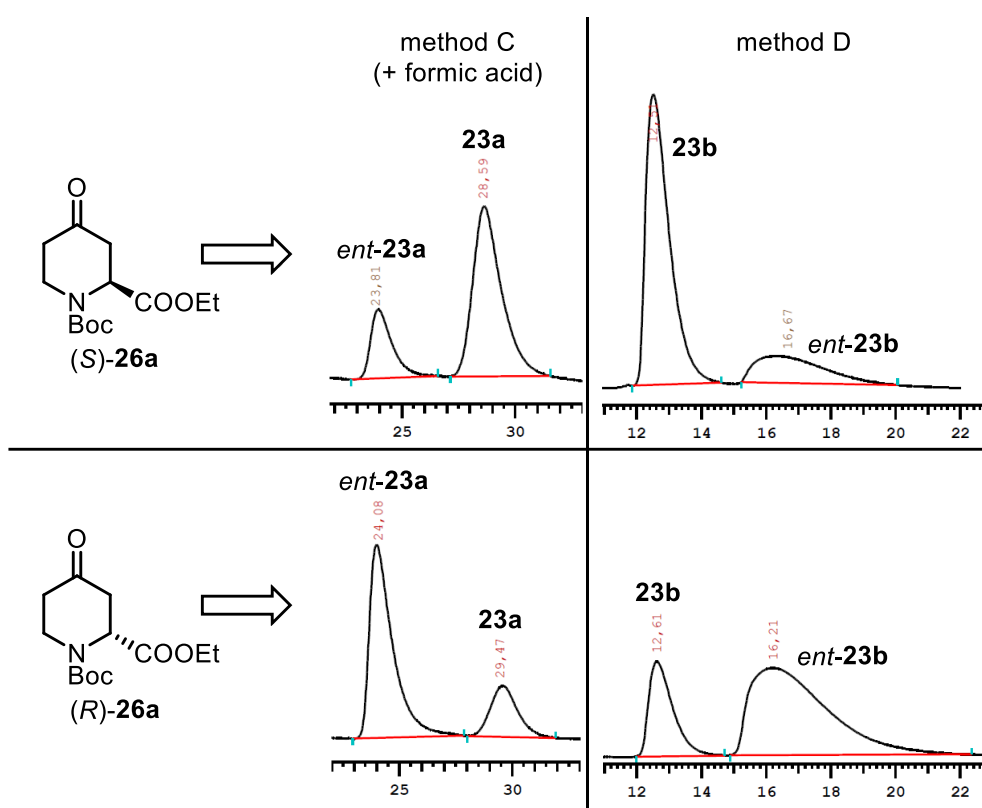


Figure 40: Chiral HPLC chromatograms of bicyclic amines **23a** (left) and **23b** (right) starting from (*S*)-**26a** (top) and (*R*)-**26a** (bottom). HPLC method C (left): Column: Daicel Chiralpak IA; eluent: *i*-hexane/EtOH = 9:1 + 0.1% HNEt₂ + 0.1% formic acid; HPLC method D (right): Column: Daicel Chiralpak IA; *i*-hexane/*i*-propanol = 95:1 + 0.1% HNEt₂. Both HPLC methods C and D: isocratic elution; flow rate: 1.0 mL/min; detection λ = 275 nm. The addition of formic acid led to inversion of the peaks.

The obtained ratio for the mixture of enantiomers correlated well with the ratio of diastereomeric diesters (2*S*,4*R*)-**115** and (2*S*,4*S*)-**115**. These results were validated by repeating the synthesis with commercially available (*R*)-configured piperidinone

(*R*)-**26a**. The ^1H NMR spectrum of the diesters (*2R,4S*)-**115** and (*2R,4R*)-**115**, shows a ratio of 3:1 for the *cis*- and *trans*-configured diastereomers. After transformation of diesters **115** into bicyclic amines *ent*-**23a,b**, chiral HPLC analysis showed the same 3:1 ratio of enantiomers. (Figure 40 bottom) As a consequence, piperidinone (*S*)-**26a** was transformed into bicyclic amines **23a,b** and *ent*-**23a,b** in the ratio 3:1. The corresponding enantiomer (*R*)-**26a** led to bicyclic amines **23a,b** and *ent*-**23a,b** in the ratio 1:3.

4.5.5 Separation of 2-azabicyclo[3.2.1]octanamines **23a** and **23b**

Due to the high KOR affinity of the synthesized nonracemic (*ee* = ~50%) bicyclic amines **23a,b**, (chapter 5.3 Receptor affinity) the enantiomers were separated by preparative chiral HPLC. The separation of pyrrolidino derivatives **23a** was achieved using Daicel Chiralpak IA as stationary phase and *iso*-hexane/EtOH 9:1 + 0.1% HNEt₂ + 0.1% formic acid. (HPLC method E) The addition of formic acid led to inversion of the peaks. Dimethylamino derivatives **23b** were separated using Daicel Chiralpak IA as stationary phase and *i*-hexane/*i*-propanol 95:5 + 0.1% HNEt₂. (HPLC method F) The enantiomers **23a,b** and *ent*-**23a,b** were obtained with high enantiomeric purity. (Figure 41 and Table 5)

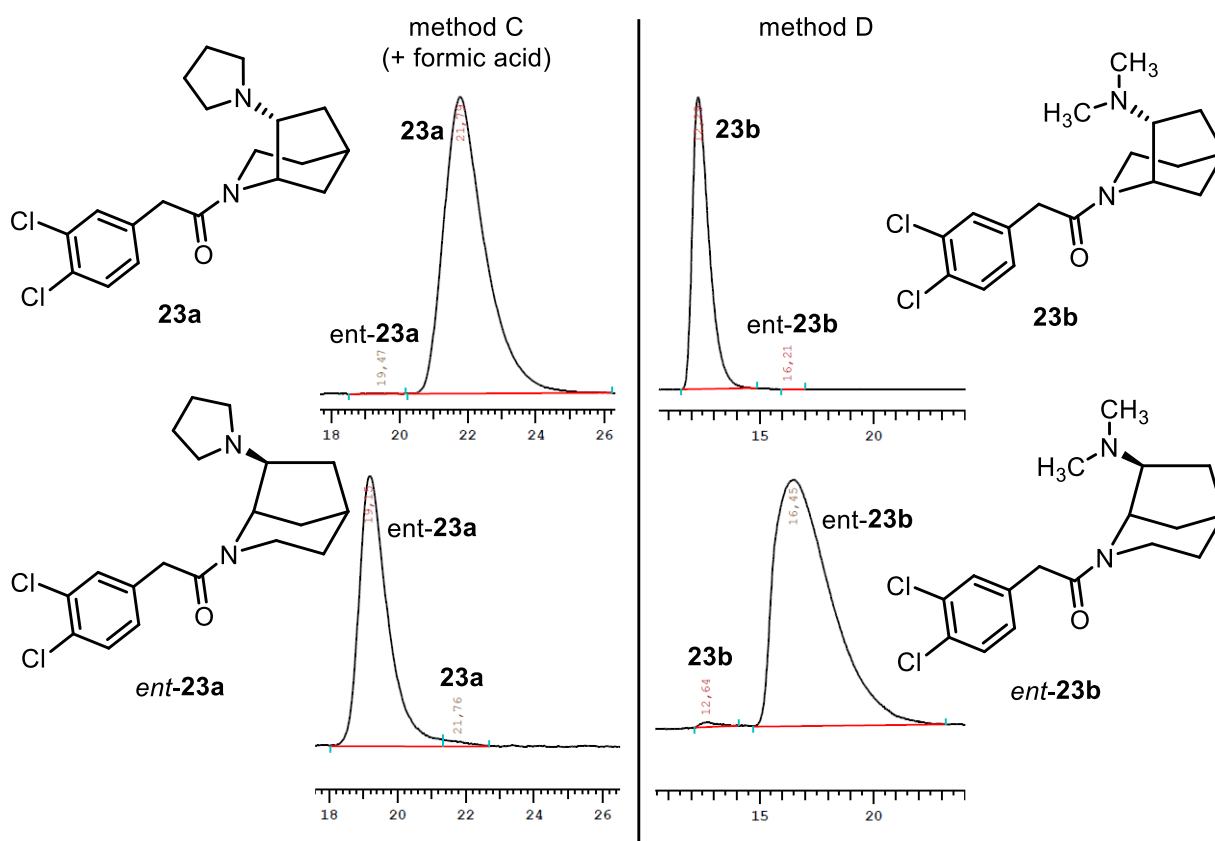
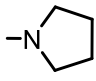


Figure 41: Chiral HPLC chromatograms of bicyclic pyrrolidino derivatives **23a** (left, top) and *ent*-**23a** (left, bottom) and dimethylamino derivatives **23b** (right, top) and *ent*-**23b** (right, bottom) after chiral separation. HPLC method C (left): Column: Daicel Chiralpak IA; eluent: *i*-hexane/EtOH = 9:1 + 0.1% HNEt₂ + 0.1% formic acid; HPLC method D (right): Column: Daicel Chiralpak IA, *i*-hexane/*i*-propanol = 95:1 + 0.1% HNEt₂ (**23b**, HPLC method D), isocratic elution; flow rate: 1.0 mL/min; detection λ = 275 nm. The addition of formic acid led to inversion of the peaks.

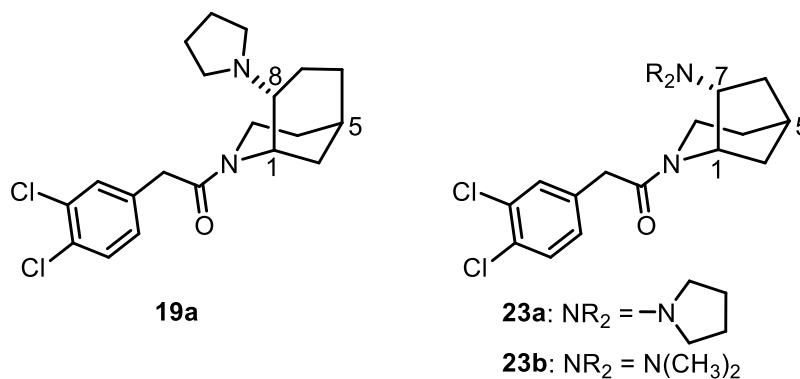
Table 5: Enantiomeric excess of the enantiomerically pure test compounds **23a,b** and *ent*-**23a,b**.

compd.	configuration	NR ₂	ee [%]
23a	(1 <i>S</i> ,5 <i>S</i> ,7 <i>R</i>)		99.9
<i>ent</i> - 23a	(1 <i>R</i> ,5 <i>R</i> ,7 <i>S</i>)		96.3
23b	(1 <i>S</i> ,5 <i>S</i> ,7 <i>R</i>)	N(CH ₃) ₂	99.9
<i>ent</i> - 23b	(1 <i>R</i> ,5 <i>R</i> ,7 <i>S</i>)		98.8

Structural analogy to 2-azabicyclo[3.3.1]nonane **19a**

In an attempt to assign the absolute configuration of the 2-azabicyclo[3.3.1]nonanes **19a** and *ent*-**19a**, the elution orders of the enantiomers using HPLC methods C and D were compared to the results of 2-azabicyclo[3.2.1]octanes **23a** and **23b**. (Table 6)

Table 6: Retention times (t_R) of bicyclic amines **19a**, **23a** and **23b**.

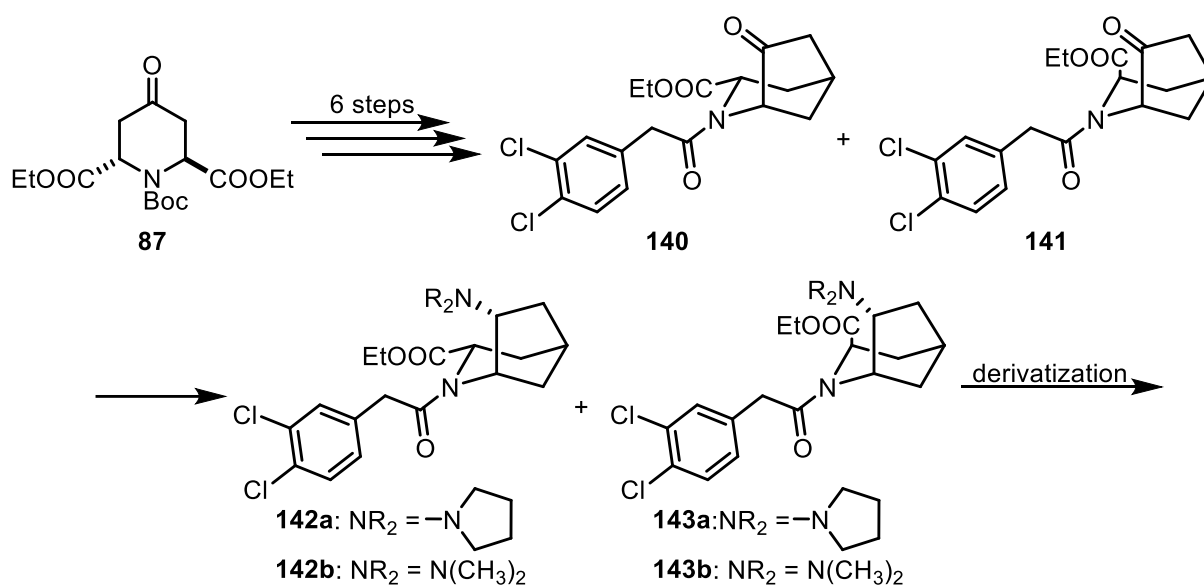


compd.	configuration	NR_2	t_R (HPLC method C) [min]	t_R (HPLC method D) [min]
19a	(1 <i>S</i> ,5 <i>R</i> ,8 <i>R</i>)		44.3	15.4
<i>ent</i> - 19a	(1 <i>R</i> ,5 <i>S</i> ,8 <i>S</i>)		38.6	19.3
23a	(1 <i>S</i> ,5 <i>S</i> ,7 <i>R</i>)		21.8	-
<i>ent</i> - 23a	(1 <i>R</i> ,5 <i>R</i> ,7 <i>S</i>)		19.2	-
23b	(1 <i>S</i> ,5 <i>S</i> ,7 <i>R</i>)		-	12.3
<i>ent</i> - 23b	(1 <i>R</i> ,5 <i>R</i> ,7 <i>S</i>)	$N(CH_3)_2$	-	16.5

After the separation of enantiomers of **19a**, the enantiomer which eluted first using HPLC method C, eluted last using method D and *vice versa*. (chapter 4.1.3, Figure 21) For the 2-azabicyclo[3.2.1]octanes **23a** and **23b**, the (1*S*,5*S*,7*R*)-configured enantiomer **23a** eluted last using HPLC method C and the (1*S*,5*S*,7*R*)-configured enantiomer **23b** eluted first using HPLC method D. Since both bicyclic systems show a high structural similarity, the absolute configuration of **19a** and *ent*-**19a** was assigned by their elution order. Therefore, the enantiomer **19a**, which eluted first using HPLC method D has (1*S*,5*R*,8*R*)-configuration and the enantiomer *ent*-**19a**, which eluted first using HPLC method C has (1*R*,5*S*,8*S*)-configuration.

4.6 Part 5: Synthesis of 2-azabicyclo[3.2.1]octanes **V** with different substituents in 3-position

The final part of the project was the synthesis of 3-substituted 2-azabicyclo[3.2.1]octanes **142a,b** and **143a,b** and subsequent derivatization. The synthesis was performed in analogy to the preparation of **23a,b** described in the previous chapter 4.5. The synthesis started with the racemic mixture of piperidinone **87**. (Scheme 67)

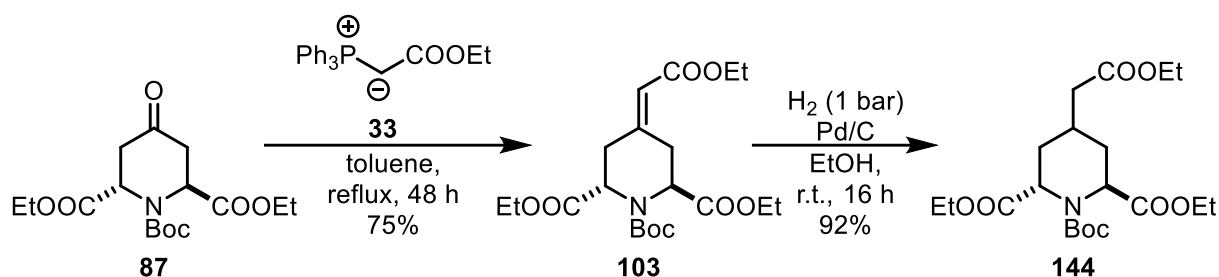


Scheme 67: Outline of the synthesis of bicyclic amines **142a,b** and **143a,b**.

The description of the synthesis is divided into two parts: the first part describes the transformation of piperidinone **87** into amides **140** and **141** and the second part, the formation of bicyclic amines **142a,b** and **143a,b** and subsequent derivatization.

4.6.1 Synthesis of bicyclic amides **140** and **141**

Following the synthetic strategy described in chapter 4.5.2, a two-carbon homologation was performed. Piperidinone **87** was transformed into α,β -unsaturated ester **103** followed by hydrogenation of **103** to obtain triester **144**. (Scheme 68)



Scheme 68: Transformation of piperidinone **87** into diester **144**.

Thus, ketone **87** was reacted with stabilized ylide **33** to afford the α,β-unsaturated ester **103** in 75% yield (chapter 4.4)

The next step was the hydrogenation of **103** with H₂ (1 bar) and Pd/C as catalyst leading to triester **144** in 92% yield. The successful reduction was shown by the loss of the C=C band in the IR spectrum. In the ¹H NMR spectrum of triester **144**, two sets of signals were seen due to rotational isomerism along the Boc group. Instead of the two CH signals of the alkene moiety of the α,β-unsaturated ester **103**, two dd's appear at 2.23 ppm and 2.29 ppm representing the newly formed methylene moiety in α-position to the ester. Due to the same configuration of the centers of chirality in 2- and 6-position of triester **144**, a novel center of chirality was not formed in 4-position. At room temperature, the ethoxycarbonylmethylene moiety in 4-position is equatorially oriented, which was proven by X-ray crystal structure analysis. (Figure 42) Moreover, the X-ray crystal structure confirmed the *trans*-configuration of the ester moieties in 2- and 6-position.

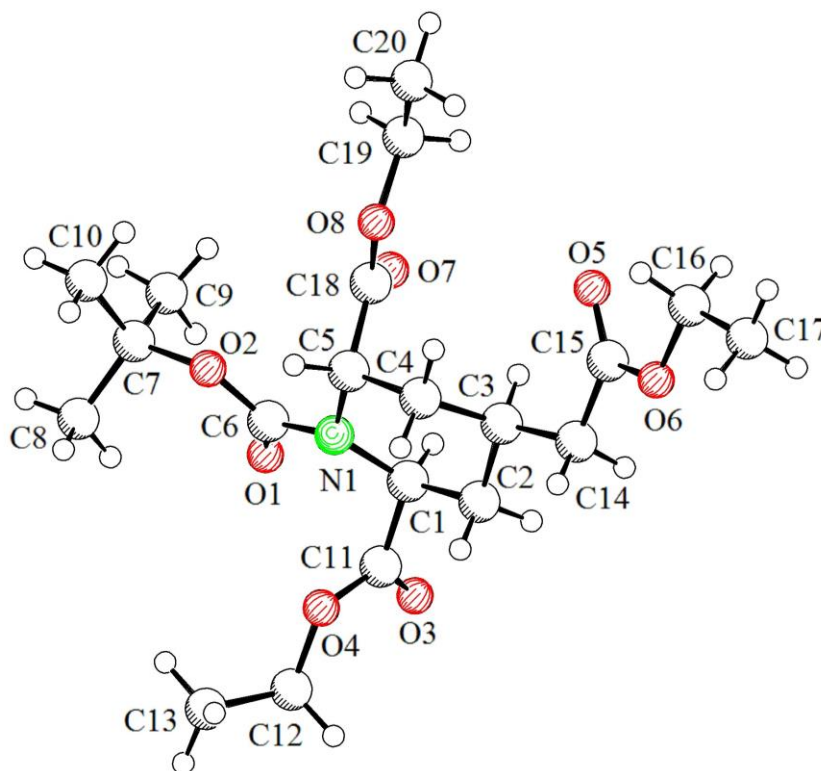
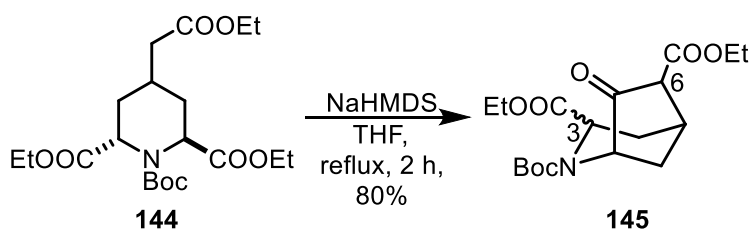


Figure 42: X-ray crystal structure of triester **144**. The ester in 2- and 6-position are *trans*-configured. The ethoxycarbonylmethylene moiety in 4-position is in equatorial orientation.

In the next step, a Dieckmann condensation was performed to obtain bicyclic β -keto ester **145**. (Scheme 69)

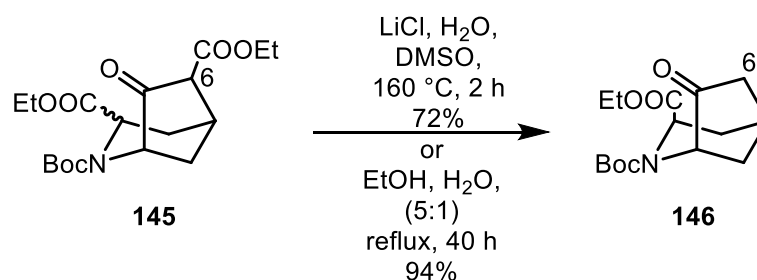


Scheme 69: Dieckmann condensation of triester **144** leading to β -keto ester **145**.

NaHMDS was added to a refluxing solution of triester **144** in THF generating bicyclic β -keto ester **145** in 80% yield. Mass spectrometry confirmed the successful cyclization. The increased temperature was necessary to accelerate the ring inversion and, hence, changing the equatorial orientation of the ethoxycarbonylmethylene moiety in 4-position into an axial orientation. Due to the *trans*-configuration of the ester groups in 2- and 6-position, one ester was always axially oriented independent of the piperidine ring conformation. The side chain in 4-position reacted with the axially oriented ester and, consequently, an equatorially oriented ester moiety should remain

in 3-position. However, a complex mixture of diastereomers, tautomers and rotamers was isolated. Since two equivalents of base were used, it is assumed that the equatorially oriented ester epimerized into an axially oriented ester, similar to the results obtained for the 2-azabicyclo[3.3.1]nonane analog **75**, (chapter 4.2.2.1). Due to the complex nature of the product **145**, the ^1H NMR spectrum does not allow the exact assignment of the configuration of the ester moieties in 3- and 6-position.

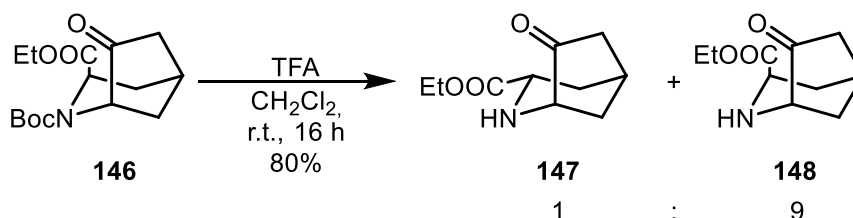
The transformation of the β -keto ester **145** into the bicyclic ketone **146** was achieved in two ways. (Scheme 70)



Scheme 70: Deethoxycarbonylation of β -keto ester **145**.

The deethoxycarbonylation of **145** was performed under Krapcho conditions with LiCl in hot DMSO leading after 2 h to ketone **146** in 72% yield. A higher yield was obtained (94%), upon heating of **145** in a mixture of EtOH and H₂O in the ratio 5:1. However, a 20-fold reaction time was necessary. The presence of the newly formed methylene group in 6-position was documented by two dd's at 1.90 ppm and 1.94 ppm and a multiplet at 2.15 – 2.22 ppm in the ^1H NMR spectrum of **146**. Due to rotational isomerism along the Boc group, two sets of signals are observed.

To introduce the first KOR pharmacophoric element, the Boc group was removed with TFA and the secondary amines **147** and **148** were obtained in 80% yield. (Scheme 71)



Scheme 71: Removal of the Boc group to obtain the secondary amines **147** and **148**.

The ^1H NMR spectrum of the obtained product displays signals for both diastereomers **147** and **148** in the ratio 1:9. (Figure 43) A singlet with an integral of 9H is missing,

which confirms the successful removal of the Boc group. Furthermore, signals for rotational isomers are no longer observed.

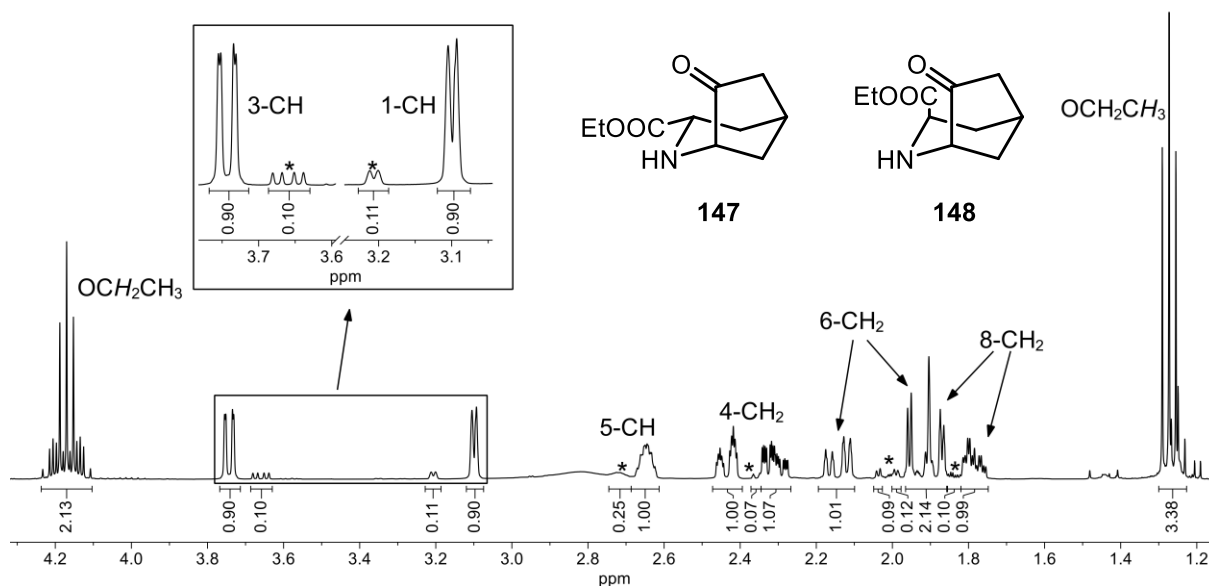
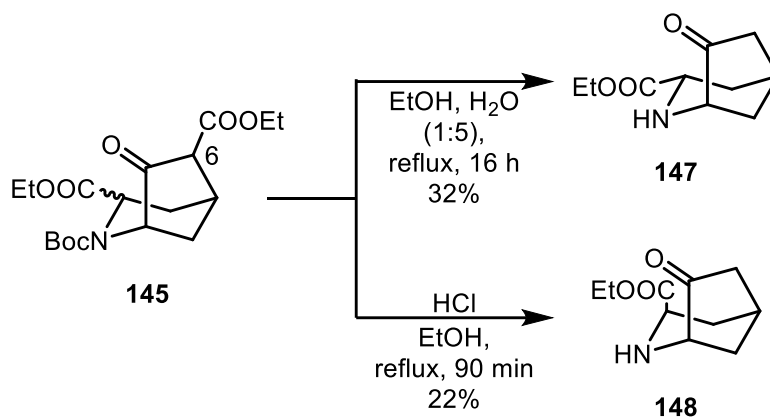


Figure 43: ^1H NMR spectrum (CDCl_3) of secondary amines **147** and **148** in the ratio 1:9. The signals for the minor diastereomer **147** are marked with an asterisk (*).

The fine structure of the signals for 3-CH allows the assignment of the orientation of the attached ester group of diastereomers **147** and **148**. The corresponding signal of the major diastereomer **148** at 3.75 ppm ($J = 8.4 / 1.1$ Hz) is caused by an equatorially oriented proton. As a consequence, the ester moiety in 3-position is axially orientated. The large coupling constant of 8.4 Hz indicates a conformational distortion of the chair conformation for the piperidine ring. This result is in accordance with the observations of the 2-azabicyclo[3.3.1]nonane analogs **76** and **77**. (chapter 4.2) A dd at 3.66 ppm ($J = 11.9 / 4.9$ Hz) represents the axially oriented 3-CH of the minor diastereomer **147**. Thus, the ester moiety is equatorially orientated.

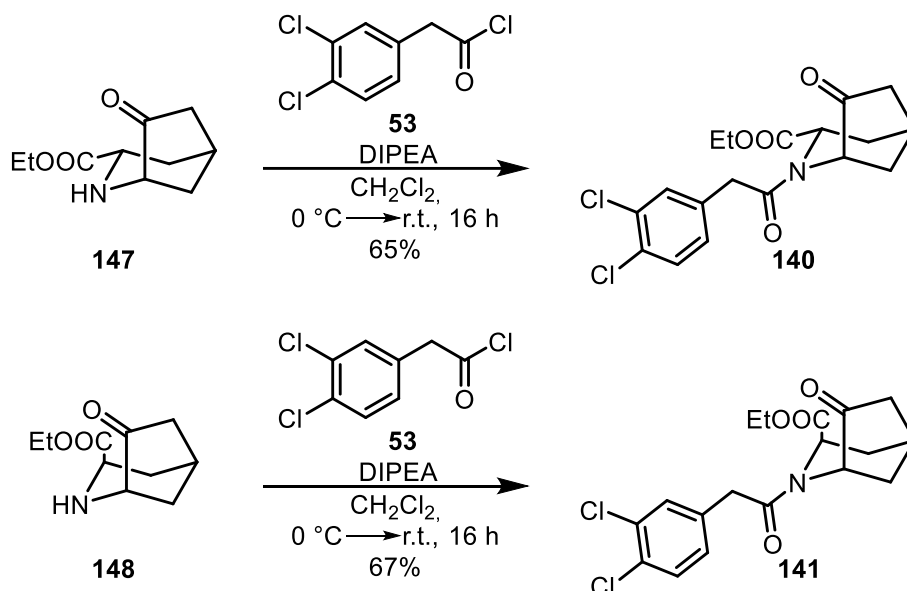
In order to obtain the pure diastereomers **147** and **148** stereoselectively, various reaction conditions were explored starting from the β -keto ester **145**. (Scheme 72) Heating a solution of **145** in EtOH/ H_2O (1:5 instead of 5:1) led to removal of the Boc group in addition to removal of the ester in 6-position, affording secondary amine **147** with an equatorially oriented ester in 32% yield.



Scheme 72: Different reaction conditions to remove the ester in 6-position and the Boc group in 2-position.

In contrast, heating of the β -keto ester **145** in an HCl/EtOH mixture provided selectively diastereomer **148** with an axially oriented ester moiety in 22% yield. In both cases only small signals for the corresponding diastereomer were observed in the ¹H NMR spectra, respectively. The yield of **148** (22%) is twofold higher than the yield obtained when performing the deethoxycarbonylation with EtOH/H₂O (5:1) and subsequent Boc removal with TFA. This result indicates an easy epimerization in 3-position.

The first KOR pharmacophoric element was introduced by acylation of the secondary amines **147** and **148** with (3,4-dichlorophenyl)acetyl chloride (**53**). (Scheme 73)



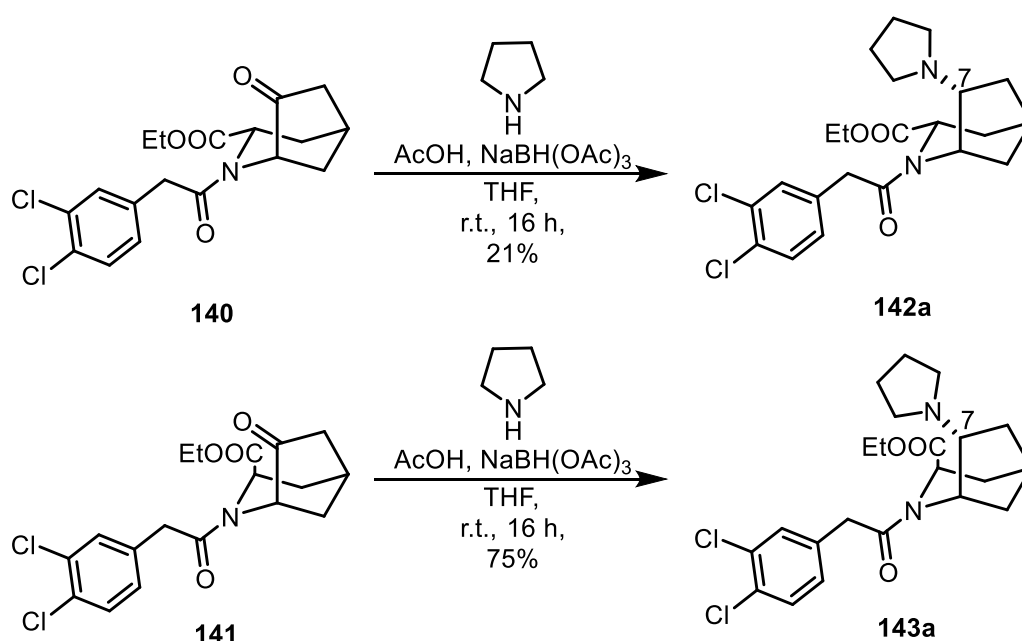
Scheme 73: Acylation of the secondary amines **147** and **148**.

Both reactions were carried out in CH₂Cl₂ with DIPEA leading to bicyclic amides **140** and **141** in 65% and 67% yield, respectively. In the IR spectra, a C=O band at

1651 cm^{-1} for **140** and at 1647 cm^{-1} for **141** confirmed the presence of an amide group. The signals for the aromatic protons of the introduced acyl moiety appear in the ^1H NMR spectra. During the acylation, an epimerization at C-3 was not observed. The crucial signals for 3-CH confirm the equatorial and axial orientation of the ester moiety of **140** and **141**, respectively. The signal structure of 3-CH of **140** and **141** correlates well with the signal structure of 3-CH of **147** and **148**, as described above.

4.6.2 Synthesis of bicyclic amines **142a,b** and **143a,b** and derivatives

Reductive amination of ketones **140** and **141** with pyrrolidine and $\text{NaBH}(\text{OAc})_3$ led to the desired *endo*-configured amines **142a** and **143a** in 21% and 75% yield, respectively. (Scheme 74)



Scheme 74: Synthesis of *endo*-configured bicyclic amines **140** and **141** by diastereoselective reductive amination.

In the ^1H NMR spectra, signals for the protons of the pyrrolidine ring can be observed at 1.59 – 1.69 ppm and 2.17 – 2.53 ppm (**142a**) and at 1.63 – 1.73 ppm and 2.44 – 2.55 ppm (**143a**). The newly formed methyne proton in 7-position is represented by signals at 2.74 ppm (**142a**) and 2.53 – 2.59 ppm (**143a**). Moreover, signals for the ketone carbonyl C-atom at 200 – 210 ppm in the ^{13}C NMR spectra disappeared. A NOESY experiment (Figure S10, Appendix) of **142a** shows a cross peak between 3- CH_{ax} and the methylene groups of the pyrrolidine ring ($\text{N}(\text{CH}_2\text{CH}_2)_2$). (Figure 44) Hence, the pyrrolidino group is *endo*-oriented and the proton in 3-position adopts the

axial orientation. Consequently, the ester moiety is *exo*-oriented, i.e. adopts the equatorial orientation.

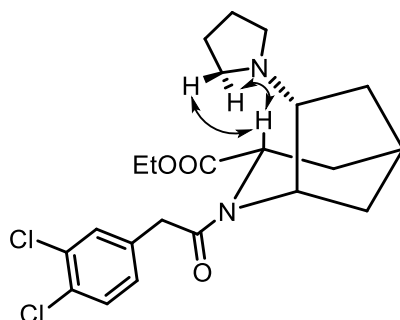


Figure 44: A nuclear Overhauser effect (NOE) between the indicated protons confirms the *endo*-orientation of the pyrrolidino moiety of **142a** and the *exo*-configuration of the ester in 3-position.

The *endo*-configuration of both the pyrrolidino group and the ester moiety of the corresponding diastereomer **143a** was determined unequivocally by X-ray crystal structure analysis. (Figure 45) Colorless needles were obtained, by recrystallization of **143a** from ethyl acetate and cyclohexane using the vapor diffusion method.

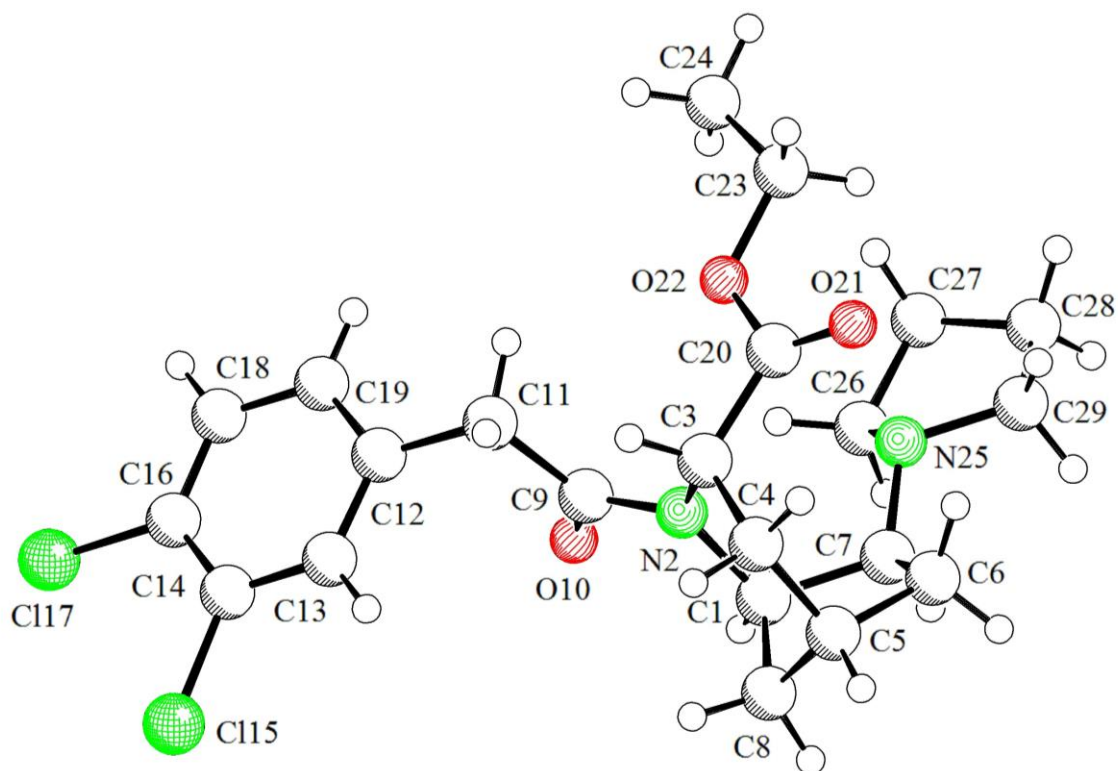
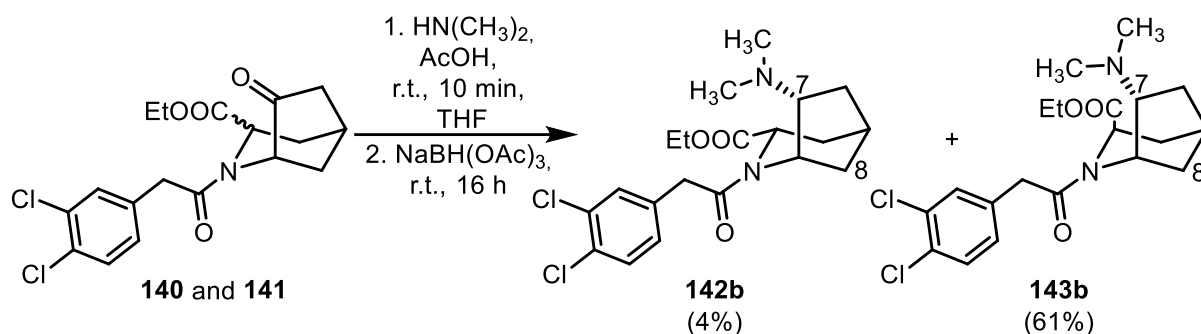


Figure 45: X-ray crystal structure of bicyclic amine **143a**. The pyrrolidine ring is *endo*-configured with a dihedral angle of 40.3° ($N_{\text{pyrrolidine}}\text{-C-C-N}_{\text{amide}}$). The ester moiety in 3-position adopts an axial orientation, i.e. is also *endo*-configured. The piperidine ring consisting of C-1, N-2, C-3, C-4, C-5 and C-8 exists in a chair-like conformation, whilst the cyclopentane ring consisting of C-1, C-8, C-5, C-6 and C-7 exists in an envelope conformation.

In an attempt to investigate the epimerization tendency at the 3-position, a TLC experiment was performed. A solution of pure **142a** and **143a** in CH_3OH was stirred without further additives. After several hours, the formation of a new spot (TLC, KMnO_4 staining) of the corresponding diastereomer was obtained for both diastereomers. Furthermore, a sample of **143a** was dissolved in CD_3OD and ^1H NMR spectra were recorded directly and after different periods of time. The ^1H NMR spectra exhibit increasing signals for the corresponding diastereomer **142a**.

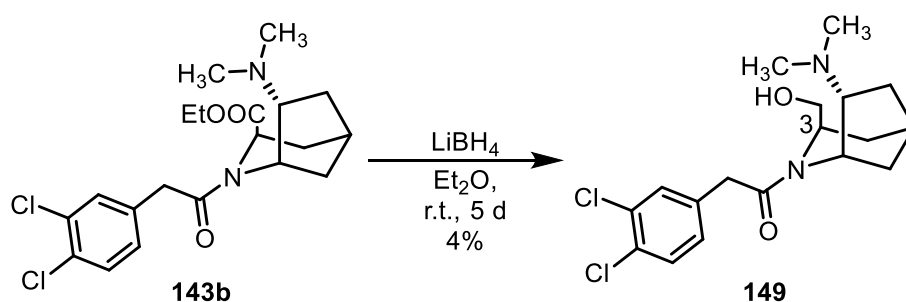
It was shown that the 2-azabicyclo[3.2.1]octanes **142a** and **143a** can easily epimerize in 3-position. Therefore, the reductive amination of bicyclic ketones **140** and **141** with $\text{HN}(\text{CH}_3)_2$ and $\text{NaBH}(\text{OAc})_3$ was performed using a 9:1 mixture of diastereomers **140** and **141**. (Scheme 75)



Scheme 75: Diastereoselective reductive amination of bicyclic ketones **140** and **141** yielding to dimethylamino derivatives **142b** and **143b**.

After stirring of the mixture of ketones **140** and **141** and $\text{HN}(\text{CH}_3)_2$ for 10 min to induce the formation of the iminium ion, $\text{NaBH}(\text{OAc})_3$ was added to obtain the bicyclic amines **142b** and **143b** in 4% and 60% yield, respectively, which represents a ratio of roughly 9:1. Therefore, an epimerization was not observed during the reductive amination of bicyclic ketones **140** and **141** with $\text{HN}(\text{CH}_3)_2$. The obtained bicyclic dimethylamines were separated by flash column chromatography. The ^1H NMR spectra show singlets at 2.20 ppm (**142b**) and 2.05 ppm and 2.06 ppm (**143b**), for the dimethylamino group. A new signal for 7-CH appears at 2.57 ppm (**142b**) and 2.36 – 2.45 ppm (**143b**). NOESY experiments showing the neighbourhood of 7-CH and 8- CH_{eq} confirm the *endo*-configuration of the dimethylamino moiety in 7-position of both diastereomers. (Figure S11 and Figure S12, Appendix)

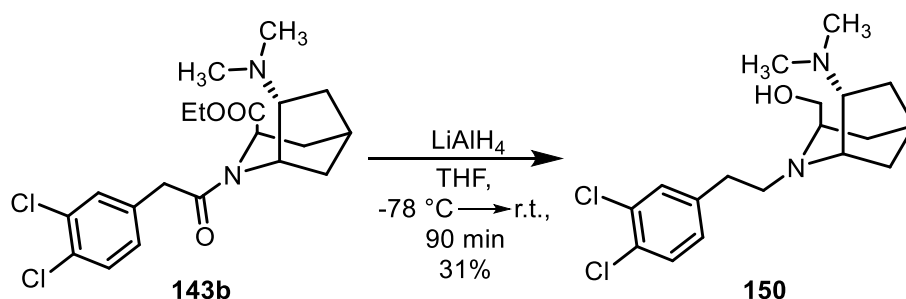
Finally, reduction of the ester to an alcohol was carried out to reduce the size of the substituent in 3-position and to increase the polarity of the KOR agonist. LiBH_4 is the preferred reducing agent to selectively transform esters into alcohols.¹³³ (Scheme 76)



Scheme 76: Selective reduction of ester **143b** with LiBH_4 .

Ester **143b** was treated with LiBH_4 and the mixture was stirred for 5 d leading to alcohol **149** in 4% yield. In the ^1H NMR spectrum of **149**, signals for the ethyl ester moiety cannot be observed anymore. Instead, two new signals at 3.66 ppm and at 3.72 –

3.79 ppm represent the newly formed CH_2OH group at C-3. Due to the low yield and the long reaction time, a stronger reducing agent was investigated. LiAlH_4 led to reduction of the ester group and simultaneously the amide moiety leading to bicyclic diamine in 31% yield. (Scheme 77)



Scheme 77: Reduction of ester **143b** with LiAlH_4 .

A missing $\text{C}=\text{O}$ band in the IR spectrum of **150** confirms the successful reduction of bicyclic amide **143b** to diamine **150**. Instead of the signals of the ester moiety two dd's at 3.19 ppm and 3.71 ppm represent the CH_2OH group at C-3 in the ^1H NMR spectrum of **150**. (Figure 46)

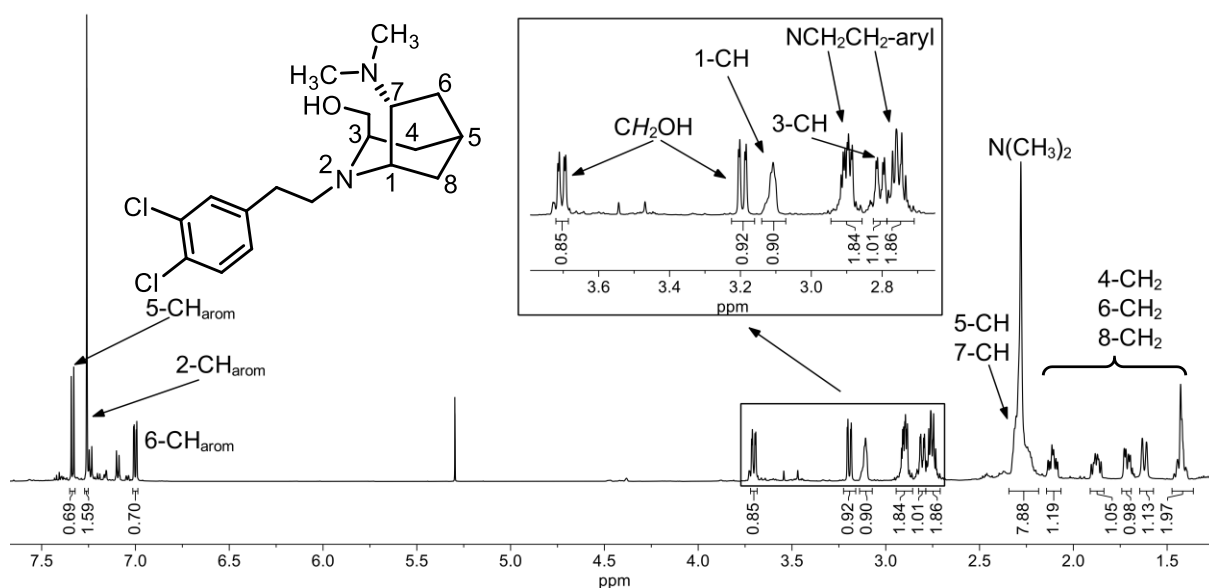


Figure 46: ^1H NMR spectrum (CDCl_3) of bicyclic diamine **150**.

Moreover, the protons of the ethylene moiety between the phenyl ring and N-1 cause two new signals at 2.72 – 2.77 ppm and 2.87 – 2.93 ppm. Due to the insufficient purity (HPLC, NMR) of **149** and **150**, their affinity towards KOR was not determined.

5. Pharmacological evaluation

The KOR affinity of the synthesized bicyclic amines was tested *in vitro* in receptor binding studies. In addition, their affinities towards MOR, DOR and the σ_1 - and σ_2 -receptor were determined to investigate the potential KOR selectivity.

5.1 Receptor binding studies

To determine the affinity of a test compound towards a receptor, a competitive receptor binding assay was pursued. In the assay, a ligand and a receptor form a reversible equilibrium with the receptor-ligand complex. A detailed description of the theory can be found in the dissertations of Dr. Donglin Gao, Dr. Denise Ilari, Dr. Daniele Aiello and Dr. Giovanni Tangherlini.

Since the IC_{50} value is highly dependent on the concentration of the receptor and the radioligand, the independent inhibition constant K_i is determined by the Cheng-Prusoff equation.¹³⁴

5.2 Assays

5.2.1 KOR binding assay

In the KOR binding assay, a preparation from guinea pig brain was used as source of the receptor and [3H]U-69,593 (**151**, Figure 47) served as the radioligand. Non-specific binding was determined with non-labeled U-69,593. To verify the *in vitro* assay the K_i values of reference compounds U-69,593 (**151**) U-50,488 (**12**) and naloxone were measured and compared with literature values. (Table 7)

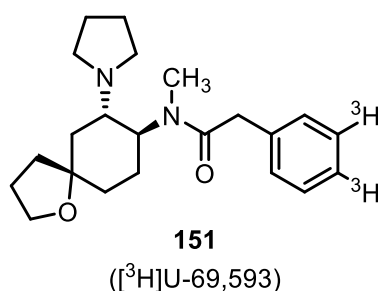


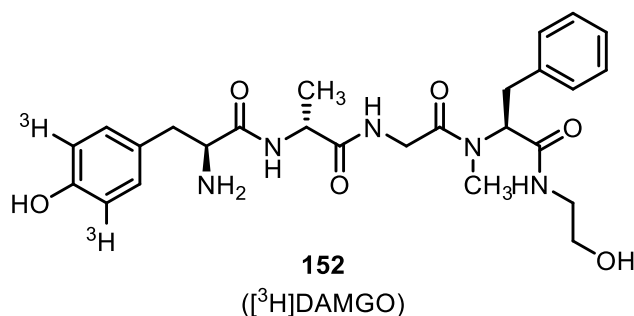
Figure 47: Radioligand in the KOR binding assay.

Table 7: Comparison of recorded and reported KOR affinities of reference compounds.

reference compound	$K_i \pm \text{SEM}$ [nM] (literature)	$K_i \pm \text{SEM}$ [nM] (experiment)
U-69,593 (151)	0.67 ± 0.04^{135}	0.88 ± 0.07
U-50,488 (12)	0.69 ± 0.04^{135}	0.34 ± 0.07
naloxone	4.9^{136}	6.9 ± 0.5

5.2.2 MOR binding assay

For the MOR assay, a preparation from guinea pig brain was used as source of the receptor and [³H]DAMGO (**152**, Figure 48) served as radioligand. An excess of non-labeled DAMGO was used for the determination of non-specific binding. The K_i values of reference compounds morphine and naloxone were determined and compared with literature values. (Table 8)

**Figure 48:** Radioligand in the MOR binding assay.**Table 8:** Comparison of recorded and reported MOR affinities of reference compounds.

reference compound	$K_i \pm \text{SEM}$ [nM] (literature)	$K_i \pm \text{SEM}$ [nM] (experiment)
morphine	1.8 ± 0.6^{137}	3.9 ± 0.07
naloxone	0.8^{138}	2.1 ± 0.5

5.2.3 DOR binding studies

In the DOR assay, a preparation from rat brain was used as source of the receptor and [³H]DPDPE (**153**, Figure 49) served as radioligand. Non-specific binding was

determined with an excess of non-labeled DPDPE. The K_i values of reference compounds morphine and naltrindole were determined and compared with literature values. (Table 9)

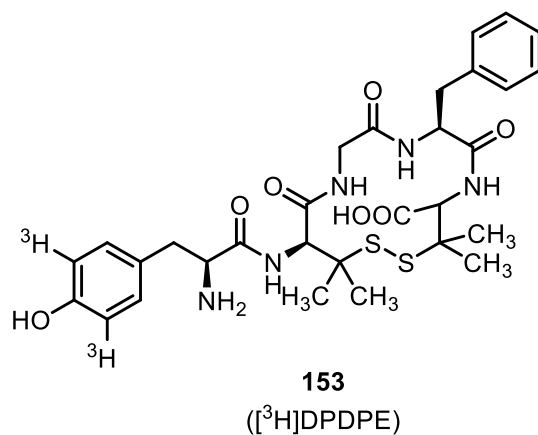


Figure 49: Radioligand in the DOR binding assay.

Table 9: Comparison of recorded and reported DOR affinities of reference compounds.

reference compound	$K_i \pm \text{SEM}$ [nM] (literature)	$K_i \pm \text{SEM}$ [nM] (experiment)
morphine	-	2.0 ± 0.3
naltrindole	0.15^{139}	2.4 ± 0.5

5.2.4 σ_1 binding assay

In the σ_1 assay, a preparation from pig brain was used as source of the receptor and [³H]-(+)-pentazocine ((+)-**11**, Figure 50) served as radioligand. Non-labeled (+)-pentazocine was used to determine non-specific binding. The K_i values of haloperidol and DTG were determined and compared with literature values. (Table 10)

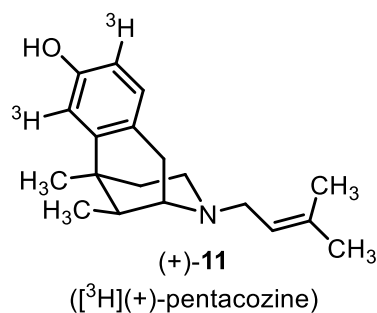


Figure 50: Radioligand in the σ_1 binding assay.

Table 10: Comparison of recorded and reported σ_1 affinities of reference compounds.

reference compound	$K_i \pm \text{SEM}$ [nM] (literature)	$K_i \pm \text{SEM}$ [nM] (experiment)
(+)-pentazocine ((+)- 11)	2.1 ± 0.1^{140}	5.4 ± 0.5
Haloperidol	1.8 ± 0.1^{141}	6.6 ± 0.9
DTG (154)	107 ± 21^{140}	71 ± 8

5.2.5 σ_2 binding assay

In the σ_2 assay, a preparation from guinea rat liver homogenates was used as source of the receptor and [³H]-DTG (**154**, Figure 51) served as radioligand. An excess of (+)-pentazocine was used to mask σ_1 receptors, since [³H]-DTG also shows high affinity towards σ_1 receptors. Non-specific binding was determined with unlabeled DTG. To verify the *in vitro* assay, the K_i values of reference compounds (+)-pentazocine, haloperidol and DTG were determined and compared with literature values. (Table 11)

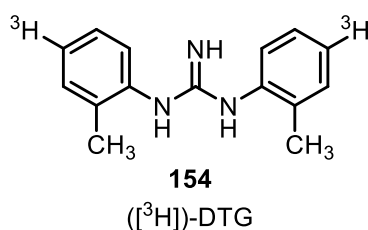


Figure 51: Radioligand in the σ_2 binding assay.

Table 11: Comparison of recorded and reported σ_2 affinities of reference compounds.

reference compound	$K_i \pm \text{SEM}$ [nM] (literature)	$K_i \pm \text{SEM}$ [nM] (experiment)
haloperidol	22 ± 8.5^{141}	125 ± 33
DTG (154)	40 ± 2.6^{142}	54 ± 8

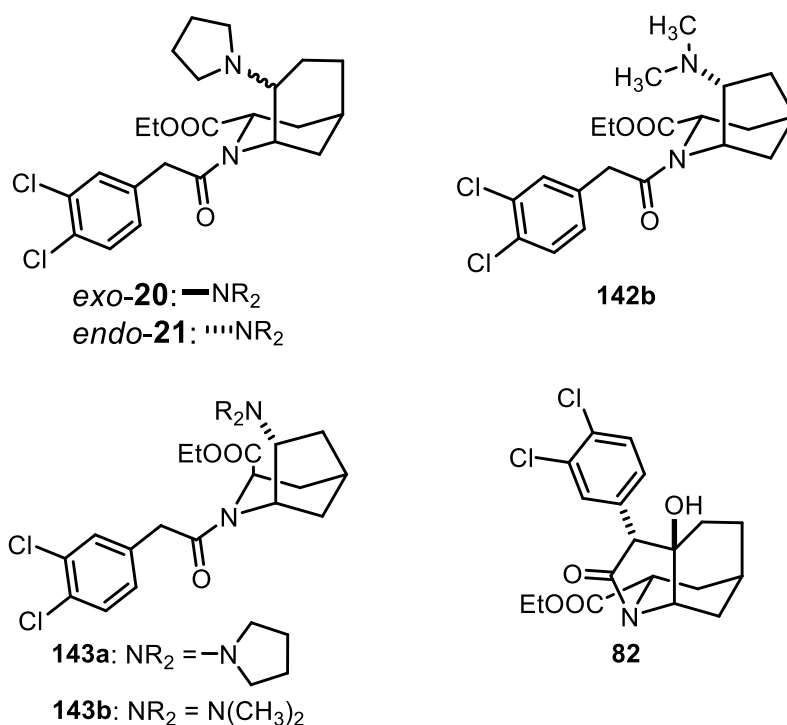
5.3 Receptor affinity

5.3.1 KOR affinity and selectivity of bicyclic compounds with an ester moiety in 3-position

In general, bicyclic amines with an additional ester moiety in 3-position show only moderate KOR affinity. *exo*-Configured pyrrolidine **exo-20** displays tenfold lower KOR affinity than the corresponding *endo*-configured pyrrolidine **endo-21**. Azabicyclo[3.3.1]nonane **endo-21** and the analog **142b** with a shorter C₂-bridge exhibit almost the same KOR affinity. However, changing the configuration of the ester moiety from *endo* in **142b** to *exo* in **143b** led to tenfold reduced KOR affinity. Whereas KOR affinity of **143b** is rather low, replacement of the dimethylamino moiety by a pyrrolidine ring **143a** results in fivefold increased KOR affinity ($K_i = 639$ nM). Tricyclic alcohol **82** differs from the other KOR agonists presented in this thesis by the absence of a basic N-atom, which is a key element for high affinity towards KOR. However, with a K_i value of 425 nM, alcohol **82** displays a moderate KOR affinity.

The *endo*-configured pyrrolidine **endo-21** ($K_i = 369$ nM) and the dimethylamine **endo-142b** ($K_i = 315$ nM) represent the most potent KOR agonists in this series. (Table 12)

Table 12: Receptor affinities of 2-azabicyclo[3.3.1]nonanes **20** and **21**, 2-azabicyclo[3.2.1]octanes **142b** and **143a,b** and tricyclic alcohol **82** with an additional ester moiety.



		$K_i \pm \text{SEM}$ [nM] (n = 3) ^{a)}				
compd	NR ₂	KOR	MOR	DOR	σ_1	σ_2
		[³ H] U-69,593	[³ H] DAMGO	[³ H] DPDPE	(+)- [³ H]pentazocine	[³ H] DTG
20		4100	0%	0%	0%	1200
21		369	0%	0%	205	5%
143a		639	0%	5%	0%	0%
142b		315	0%	11%	5%	0%
143b	$\text{N}(\text{CH}_3)_2$	3100	0%	0%	0%	0%
82	-	425	0%	0%	0%	0%

^{a)} A value in % reflects the inhibition of the radioligand binding at a test compound concentration of 1 μM . K_i values without SEM values represent the mean of two experiments (n = 2).

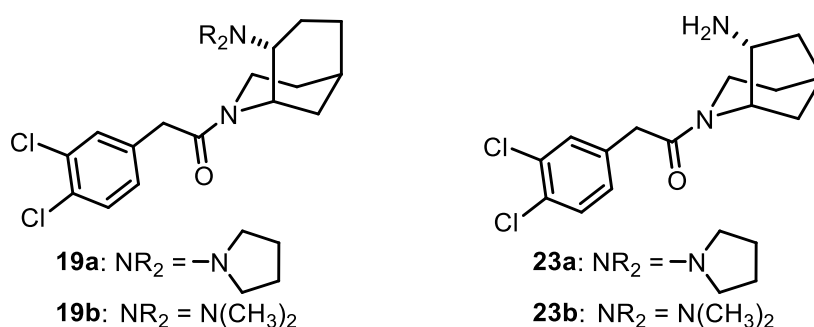
The bicyclic amines *exo*-**20**, *endo*-**21**, **142b** and **143a,b** and tricyclic alcohol **82** do not interact considerably with MOR and DOR indicating a high selectivity for KOR. Bicyclic amines **142b**, **143a** and **143b** with a C₂-bridge and tricyclic alcohol **82** show high selectivity over both σ_1 and σ_2 receptors. However, the pyrrolidines *exo*-**20** and

endo-**21** display σ_2 or σ_1 receptor affinity in the same range as their KOR affinity, respectively.

5.3.2 KOR affinity and selectivity of unsubstituted bicyclic compounds

The absence of an ester moiety increases remarkably the KOR affinity. (Table 13) In particular, unsubstituted racemic bicyclic amines **19a,b** and non-racemic bicyclic amines (ee ~50%) **23a,b** show K_i values in the low nanomolar range.

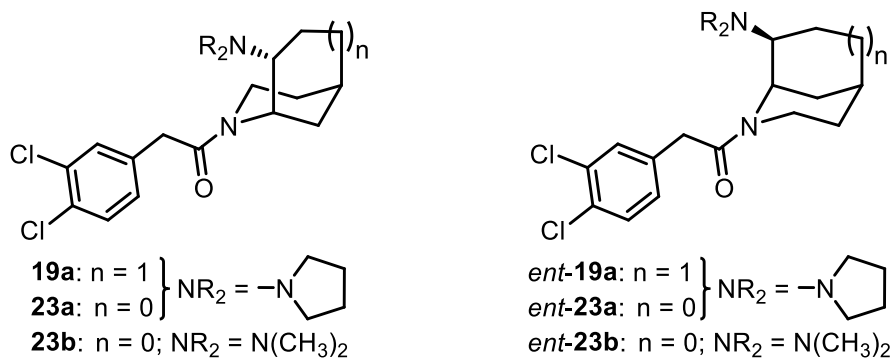
Table 13: Affinities of racemic 2-azabicyclo[3.3.1]nonanes **19a** and **19b** and non-racemic 2-azabicyclo[3.2.1]octanes **23a** and **23b** (ee ~50%).



compd.	NR ₂	ee [%]	$K_i \pm \text{SEM}$ [nM] (n = 3) ^{a)}				
			KOR	MOR	DOR	σ_1	σ_2
			[³ H] U-69,593	[³ H] DAMGO	[³ H] DPDPE	(+)- [³ H]pentazocine	[³ H] DTG
19a		0	26 ± 6	0%	2200	117	553
23a	-N(CH ₂) ₂ CH ₂	53.6	12 ± 2	8%	3200	7 ± 4	310
<i>ent</i> - 23a		52.8	53 ± 5	0%	1800	20 ± 4	243
19b		0	23 ± 4	0%	1300	170	608
23b	N(CH ₃) ₂	54.3	18 ± 2	10%	0%	76 ± 6	17%
<i>ent</i> - 23b		49.8	49 ± 18	5%	565	32 ± 10	366

^{a)} A value in % reflects the inhibition of the radioligand binding at a test compound concentration of 1 μ M. K_i values without SEM values represent the mean of two experiments (n = 2).

Due to the high KOR affinity of the racemic bicyclic amine **19a** and non-racemic bicyclic amines **23a** and **23b** (ee ~50%), the enantiomers were separated by preparative chiral HPLC. (Table 14) Racemic dimethylamine **19b** displays a high KOR affinity (K_i = 23 nM) as well, however, the racemate was not separated due to the low amounts of **19b** prepared from the precursor.

Table 14: Affinities of enantiomerically pure 2-azabicyclo[3.3.1]nonanes **19a** and 2-azabicyclo[3.2.1]octanes **23a** and **23b**.

compd.	NR ₂	config.	$K_i \pm \text{SEM}$ [nM] ($n = 3$) ^{a)}					e.r. ^{b)}
			KOR	MOR	DOR	σ_1	σ_2	
			[³ H] U-69,593	[³ H] DAMGO	[³ H] DPDPE	(+)- [³ H]pentazocine	[³ H] DTG	
19a		(1 <i>S</i> ,5 <i>R</i> ,8 <i>R</i>)	$18 \pm 3.5^{\text{c)}$	7%	0%	6.5 ± 4.3	154	6.8
ent-19a		(1 <i>R</i> ,5 <i>S</i> ,8 <i>S</i>)	123 ± 17	0%	0%	14 ± 1.9	487	
23a		(1 <i>S</i> ,5 <i>S</i> ,7 <i>R</i>)	$7.0 \pm 1.9^{\text{c)}$	0%	542	56 ± 10	534	250
ent-23a		(1 <i>R</i> ,5 <i>R</i> ,7 <i>S</i>)	1750	0%	0%	10 ± 2.5	171	
23b	N(CH ₃) ₂	(1 <i>S</i> ,5 <i>S</i> ,7 <i>R</i>)	$13 \pm 3.7^{\text{c)}$	1600	0%	292	811	41
ent-23b		(1 <i>R</i> ,5 <i>R</i> ,7 <i>S</i>)	531	0%	0%	17 ± 1.2	213	

^{a)} A value in % reflects the inhibition of the radioligand binding at a test compound concentration of 1 μM . K_i values without SEM values represent the mean of two experiments ($n = 2$) and K_i values with SEM values represent the mean of three experiments ($n = 3$). ^{b)} e.r. = eudismic ratio. The eudismic ratio refers to the KOR affinities. ^{c)} Independent sample t -test. For **19a** vs. **23a**, **19a** vs. **23b** and **23a** vs. **23b** $p > 0.05$.

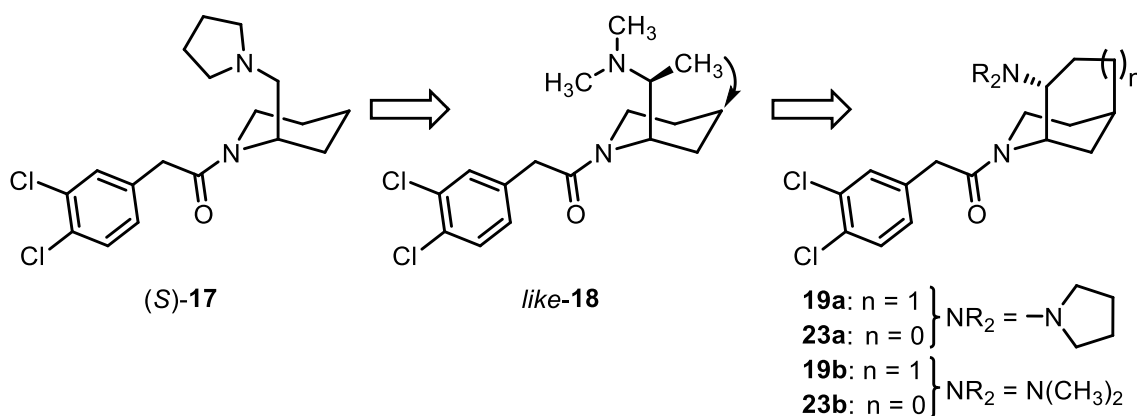
(1*S*)-Configured bicyclic amines **19a**, **23a** and **23b** are the eutomers, since they display higher KOR affinity ($K_i = 7 - 18$ nM) than their corresponding (1*R*)-enantiomers **ent-19a**, **ent-23a** and **ent-23b**. (Table 14) The difference between the KOR affinities of pyrrolidines **23a** and **ent-23a** is significantly larger (e.r. = 250) than the difference of **23b** enantiomers and **19a** enantiomers (e.r. = 41 and 6.8). These results fit to the reported observation of Vecchiotti *et al.*, who determined a higher KOR affinity for (S)-**17** ($K_i = 0.24$ nM), than for (R)-**17** ($K_i = 15.4$ nM).⁵³ (Scheme 78)

The KOR affinity of the three eutomers **19a**, **23a** and **23b** do not differ significantly ($p > 0.05$). Therefore, the reduction of the bridge size from three to two C-atoms had only a slight effect on the KOR affinity. Moreover, embedding the pharmacophoric basic N-atom into a pyrrolidino (**19a** and **23a**) or dimethylamino moiety (**23b**) did not affect the KOR affinity significantly.

All bicyclic amines (**19a**, **23a** and **23b**) display KOR selectivity over MOR, DOR and σ_2 receptors. Enantiomerically pure pyrrolidines **19**, *ent*-**19**, **23a** and *ent*-**23a** bind with high affinity towards the σ_1 receptor. In contrast, dimethylamines **23b** and *ent*-**23b** differ significantly in their σ_1 receptor affinity with a 17-fold decreased σ_1 receptor affinity for **23b**. Generally, the (1*S*,5*S*,7*R*)-configured 2-azabicyclo[3.2.1]octanamines **23a** and **23b** display a preference for KOR over the σ_1 receptor, while the (1*R*,5*R*,7*S*)-configured enantiomers *ent*-**23a** and *ent*-**23b** show an inversed selectivity profile. In particular, **23a** and **23b** show an eight- and 22-fold higher selectivity for KOR over the σ_1 receptor.

5.3.3 Discussion of the dihedral angle

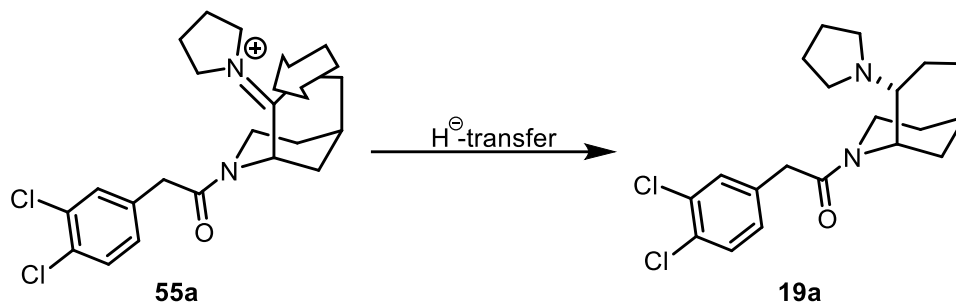
To investigate the bioactive conformation of flexible piperidine derivatives (*S*)-**17** and *like*-**18**, bridged piperidine derivatives **19a**, **19b**, **23a** and **23b** were synthesized, connecting the terminal methyl moiety of the side chain of piperidine derivative *like*-**18** with the 4-position of the piperidine ring. (Scheme 78)



Scheme 78: Bicyclic KOR agonists **19a**, **19b**, **23a** and **23b** deriving from piperidine-based KOR agonists (*S*)-**17** and *like*-**18**.

The essential *endo*-configuration of the bicyclic amines was achieved by a diastereoselective reduction of the iminium ion **55a** with sterically demanding

NaBH(OAc)₃ transferring the hydride from the backside. (Scheme 79) The relative configurations were determined by NOESY experiments.



Scheme 79: Transfer of hydride from the backside onto iminium ion **55a** leading to *endo*-configured bicyclic amine **19a**.

The KOR affinity of bicyclic ethylenediamines is highly dependent on the dihedral angle of the KOR pharmacophoric system (N-C-C-N) and consequently on the configuration of the bicyclic compounds. (Figure 52)

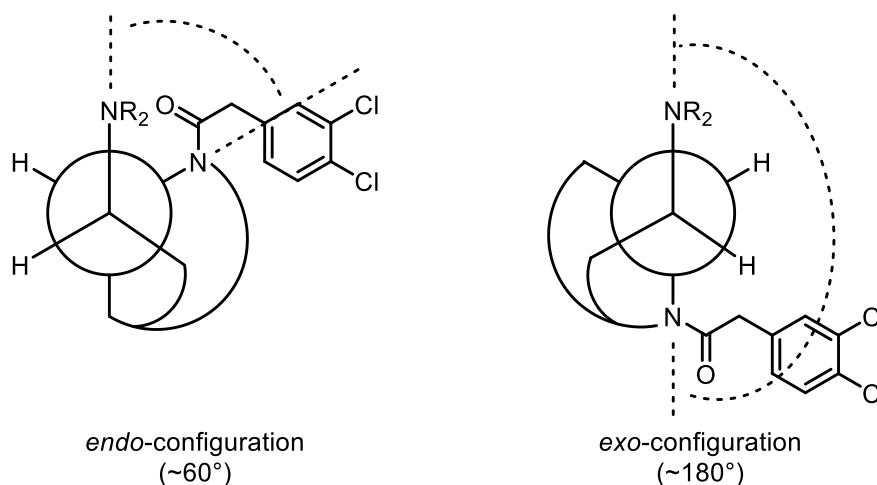


Figure 52: Dihedral angles of the KOR pharmacophoric system (N-C-C-N) for *endo*- and *exo*-configured bicyclic ethylenediamines.

The dihedral angles in this work were calculated with MOE¹⁴³ using energy-minimized structures. The minimization was done using the implemented MMFF94x force field. The dihedral angles of the *endo*-configured bicyclic amines **18a** (dh = 58.3°),⁵² (1*S*,5*R*,8*R*)-**19a** (dh = 68.2°) and (1*S*,5*S*,7*R*)-**23a** (dh = 41.9°) are significantly smaller than the dihedral angles of *exo*-configured bicyclic amines **16** (dh = 180°)⁵² and (1*S*,5*S*,7*S*)-**155** (dh = 137°)⁵⁴. (Figure 53)

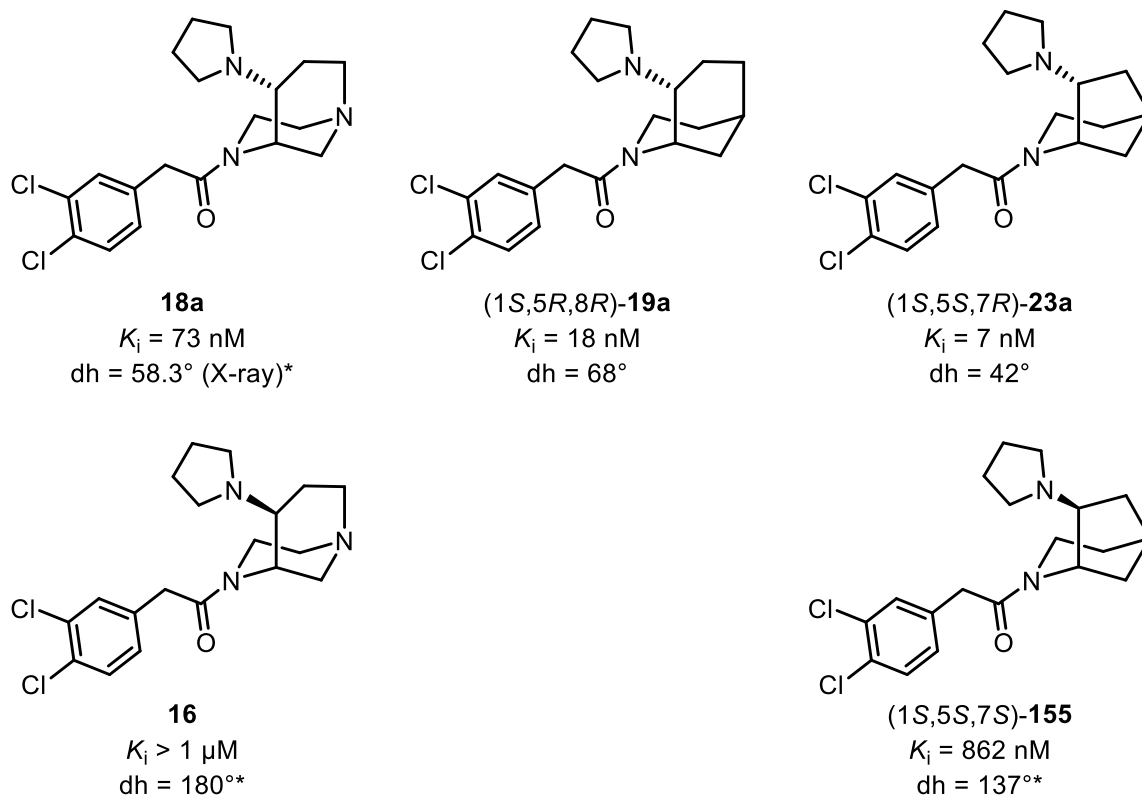


Figure 53: KOR affinity and dihedral angles (dh) of several 2,4-bridged KOR agonists with piperazine (**16** and **18a**) or piperidine substructure (**19a**, **23a** and **155**).

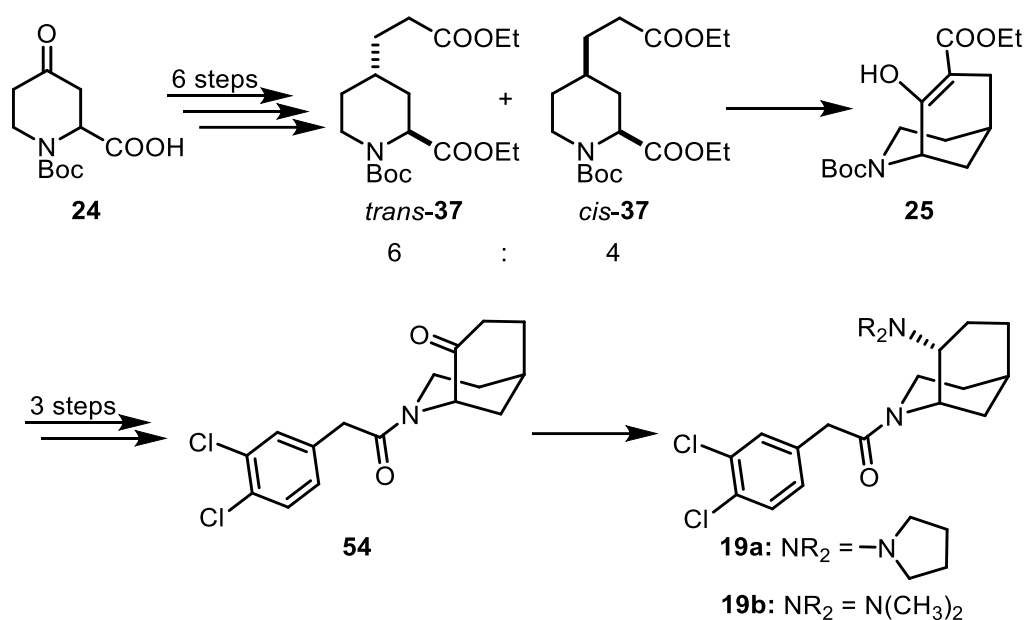
In the group of *endo*-configured bicyclic amines **18a**, **19a** and **23a**, a smaller dihedral angle (40 to 70°) contributes to an increased KOR affinity. Dihedral angles for the potential eutomers of racemic mixtures are marked with an asterisk (*).

Enantiomerically pure *endo*-configured, piperidines **19a** and **23a** show a higher KOR affinity than racemic bicyclic amine **18a**. According to the MOE calculations, the dihedral angle of 2-azabicyclo[3.3.1]nonane **19a** is larger, while the dihedral angle of 2-azabicyclo[3.2.1]octane **23a** is smaller than the dihedral angle of the bridged piperazine derivative **18a**. Obviously, small differences of the dihedral angle of *endo*-configured bicyclic amines are well tolerated by KOR. However, exchange of the N-atom of **18a** by a CH moiety has a stronger impact on KOR affinity. In particular, piperidine-based bicyclic amine **23a** binds with a 10-fold higher affinity at KOR than piperazine-based racemic bicyclic amine **18a**.

6. Summary

In this project, *endo*-configured bicyclic KOR agonists with a piperidine substructure were synthesized and pharmacologically evaluated. The dihedral angle between the tertiary amine and the amide moiety connected by a C₂-unit is crucial for high KOR affinity. Therefore, bicyclic compounds with different bridge lengths were prepared to obtain KOR agonists with various dihedral angles. Furthermore, substituents were introduced into the molecules to modify the polarity. Promising racemic test compounds were separated by chiral HPLC.

The first part of the project comprises the synthesis of 2-azabicyclo[3.3.1]nonanes **19a** and **19b**. (Scheme 80)

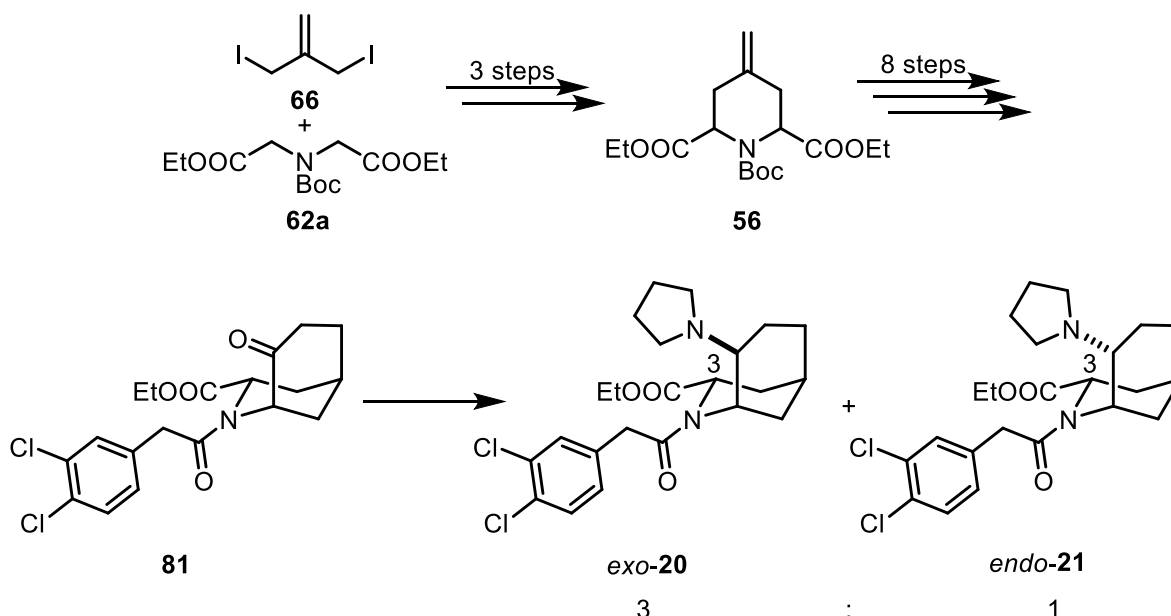


Scheme 80: Synthesis of 2-azabicyclo[3.3.1]nonanes **19a** and **19b**.

The synthesis started with the six-step transformation of racemic 4-oxopiperidine-2-carboxylic acid **24** into diesters **37**, which exists as a mixture of *trans*-**37** and *cis*-**37** in the ratio 6:4. The bicyclic ring system was established by a Dieckmann condensation. While *cis*-**37** could undergo the condensation reaction after a ring inversion accelerated by elevated temperature, *trans*-**37** was not able to cyclize directly due to geometrical restrictions. However, deprotonation in 2-position led to epimerization of *trans*-**37** into *cis*-**37**, which could further react to form the enol ester **25**. The enol ester **25** was converted into a ketone and the first KOR pharmacophoric element was introduced leading to dichlorophenylacetamide **54**. The final step was the reductive amination implementing the tertiary amine into the bicyclic system. After the formation of the iminium ion, the

reducing agent did attack from the less hindered backside to obtain the desired *endo*-configured amines **19a** and **19b**. The relative configuration was confirmed by a NOESY experiment. The enantiomers (1*R*,5*S*,8*S*)-**19a** and (1*S*,5*R*,8*R*)-**19a** were separated by chiral HPLC.

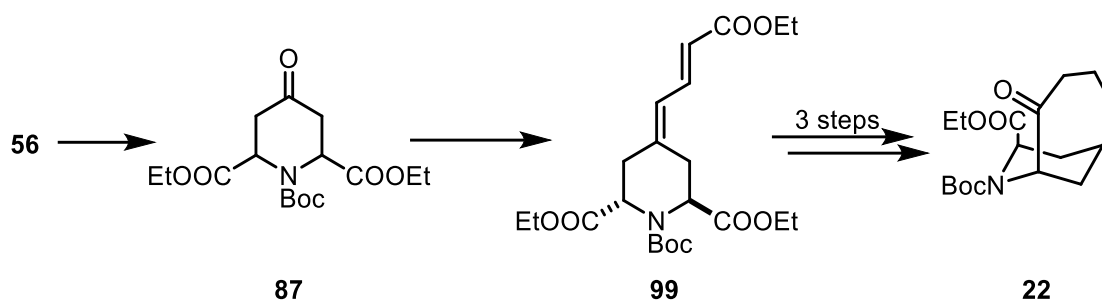
The synthesis of bicyclic derivatives **20** and **21** with an additional ester moiety in 3-position was performed as depicted in Scheme 81.



Scheme 81: Synthesis of bicyclic compounds **20** and **21** with an ester moiety in 3-position.

The synthesis started with the formation of 4-methylene piperidine **56** by double allylation of iminodiacetate **62a** with diiodide **66**. The following nine-step synthesis was performed in analogy to the synthesis of the unsubstituted analogs **19a** and **19b** resulting in the bicyclic amines **20** and **21**. In contrast to the selective formation of *endo*-configured KOR agonists **19a** and **19b**, the reductive amination of ketone **81** in the last step led to a 3:1 mixture of diastereomers *exo*-**20** and *endo*-**21**.

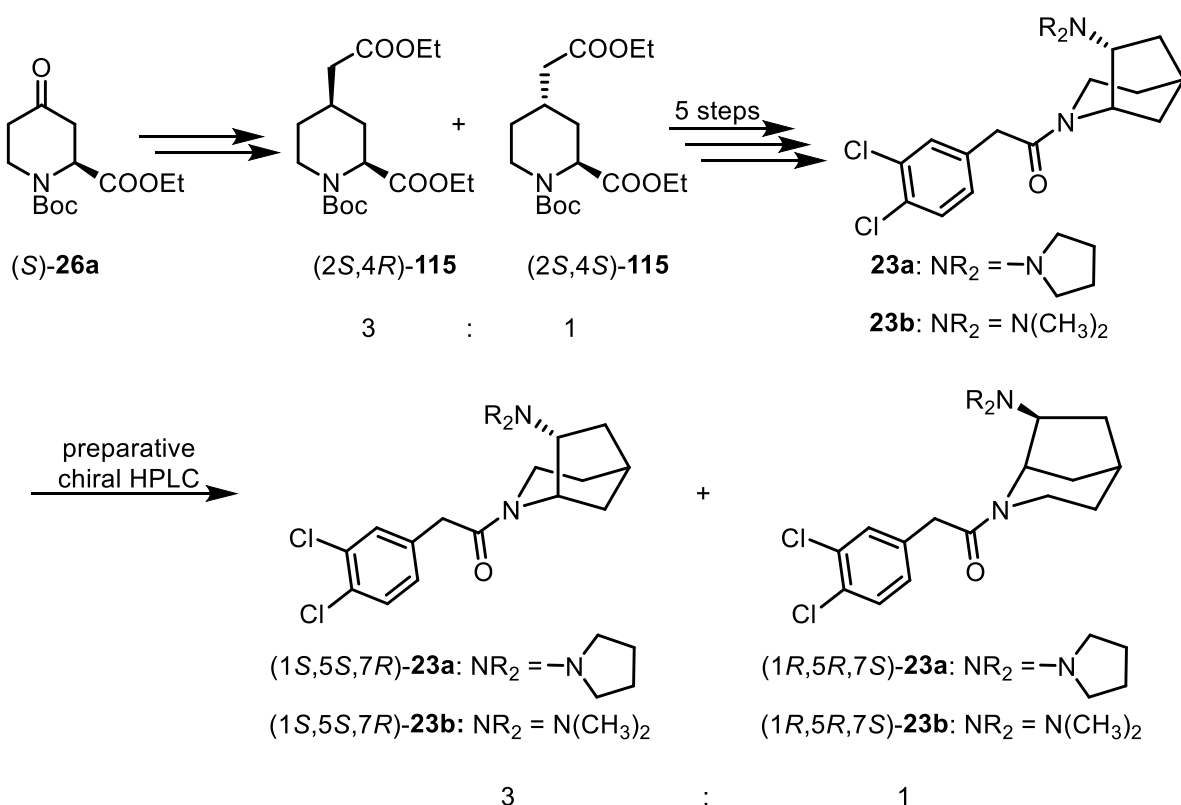
The third part of the project was devoted to the formation of butano bridged analog **22**. (Scheme 82)



Scheme 82: Synthesis of 7-azabicyclo[4.3.1]decane **22**.

Piperidinone **87** was obtained by Lemieux-Johnson oxidation of 4-methylenepiperidine **56**. The four-carbon homologation in 4-position of piperidinone **87** was performed by a Wittig reaction, leading to the diunsaturated ester **99**. The bicyclic ketone **22** was obtained in three steps comprising hydrogenation, Dieckmann condensation and deethoxycarbonylation. After the Dieckmann condensation the bicyclic β -keto ester was isolated in only low yields (<22%), which was explained by the high flexibility of the butanoate side chain. Therefore, the 7-azabicyclo[4.3.1]decane synthesis was not further investigated.

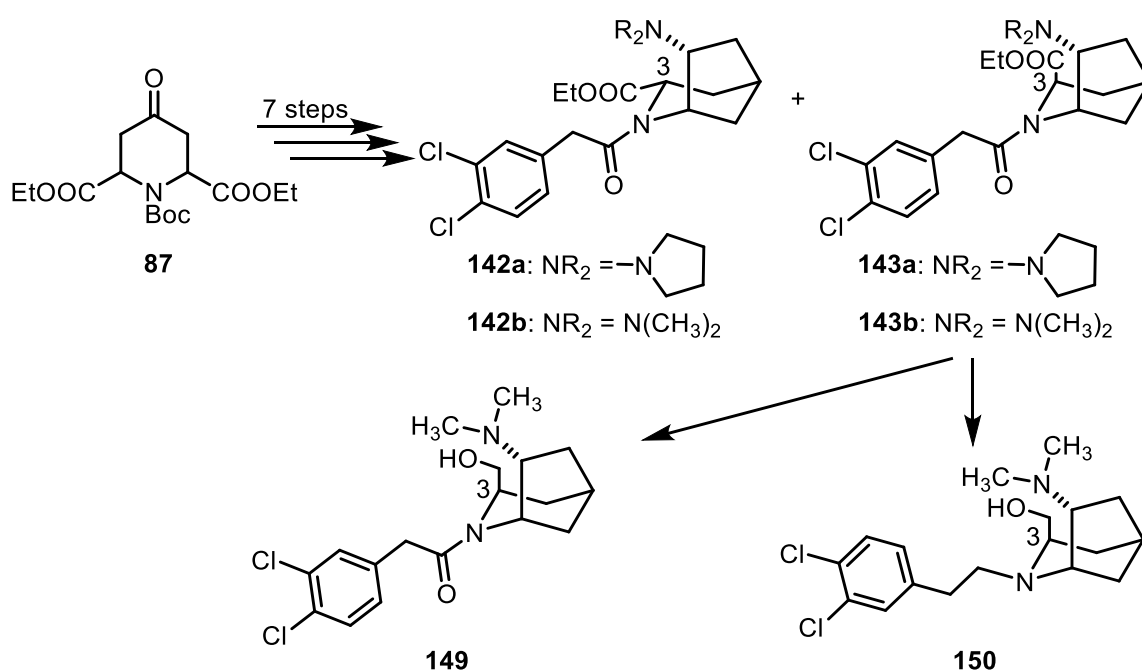
The fourth part of the thesis describes the chiral pool synthesis of unsubstituted bicyclic amines **23a** and **23b** with a reduced ring size. (Scheme 83)



Scheme 83: Synthesis of 2-azabicyclo[3.2.1]octanes **23a** and **23b**.

Enantiomerically pure piperidinone (*S*)-**26a** was converted into diesters **115** by a two-step synthesis comprising Wittig reaction and subsequent hydrogenation. During hydrogenation of the double bond diastereomers (*2S,4R*)-**115** and (*2S,4S*)-**115** were formed in a 3:1 ratio. Diesters **115** were transformed selectively into *endo*-configured 2-azabicyclo[3.2.1]octanamines **23a** and **23b**. Chiral HPLC analysis of **23a** and **23b** showed a 3:1 ratio of the enantiomers, which correlates with the ratio of diastereomers (*2S,4R*)-**115** and (*2S,4S*)-**115**. Due to epimerization of (*2S,4S*)-**115** into (*2S,4R*)-**115** during the Dieckmann condensation, the diastereomeric mixture of **115** provided a mixture of enantiomers with a ratio of 3:1. Therefore, the major enantiomers of the bicyclic amines **23a** and **23b**, derived from the major diastereomer of diester (*2S,4R*)-**115** are (*1S,5S,7R*)-configured. As a consequence, the minor enantiomers *ent*-**23a** and *ent*-**23b** are (*1R,5R,7S*)-configured. The results were confirmed by repeating the synthesis with the (*R*)-configured piperidinone (*R*)-**26a**. The diastereomeric ratio of diester (*2R,4S*)-**115** and (*2R,4R*)-**115** was 3:1 with opposite stereodescriptors compared to the obtained diesters generated from (*S*)-**26a**. Due to the high KOR affinity of the test compounds with *ee*-values of ~50%, the enantiomers were separated by preparative chiral HPLC.

The final chapter of the thesis deals with the synthesis of 2-azabicyclo[3.2.1]octanes **142a,b**, **143a,b**, **149** and **150** with additional substituents in 3-position. (Scheme 84)



Scheme 84: Synthesis of bicyclic derivatives with an ethano bridged piperidine scaffold and different substituents in 3-position.

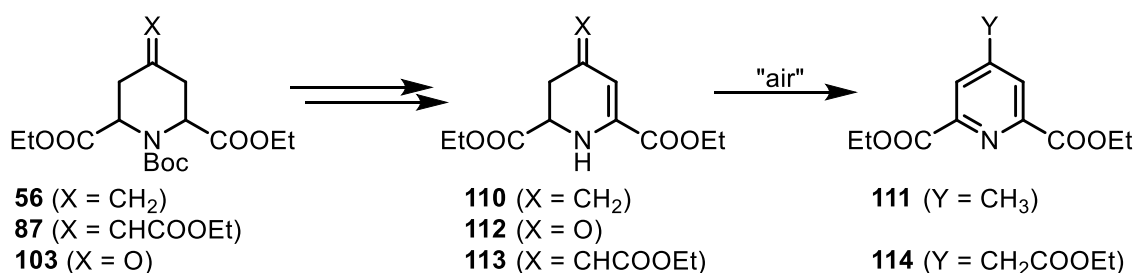
The seven-step synthesis of the *endo*-configured bicyclic amines **142a,b** and **143a,b** started with piperidinone **87** following the procedure developed for the unsubstituted 2-azabicyclo[3.2.1]octanes **23a,b**. Two diastereomers were obtained with an equatorially oriented ester (**142a,b**) and an axially oriented ester (**143a,b**). The ester moiety in 3-position of **143b** was reduced with LiBH_4 to obtain selectively the primary alcohol **149**. LiAlH_4 reduction of **143b** led to the fully reduced diamine **150**.

The affinity and selectivity of the synthesized KOR agonists were determined in competitive radioligand receptor binding studies.

endo-Configured bicyclic amines show higher KOR affinity than *exo*-configured analogs. An ester moiety in 3-position of the bicyclic amines is not tolerated - independent of its orientation. Thus, amines *endo*-**21**, **142b** and **143a,b** show low KOR affinity. Unsubstituted bicyclic amines **19a,b** and **23a,b** are well tolerated by KOR, displaying high KOR affinity with K_i values between 7-23 nM. The KOR affinity of *rac*-**19a** ($K_i = 26$ nM) is higher than the KOR affinity of the unsubstituted piperazine derivative *rac*-**15a**, ($K_i = 73$ nM) which served as lead compound.

Unsubstituted pyrrolidino and dimethylamino derivatives exhibit similar KOR affinity. The (1*S*,5*R*,8*R*)-configured 2-azabicyclo[3.3.1] nonane **19a** and (1*S*,5*S*,7*R*)-configured 2-azabicyclo[3.2.1]octanes **23a** and **23b** are the eutomers ($K_i = 7$ -18 nM) showing an eudismic ratio of 6.8, 41 and 250, respectively. All pyrrolidines and dimethylamines are highly selective over MOR, DOR and σ_2 receptors. Furthermore, bicyclic dimethylamine **23b** shows a 22-fold selectivity for KOR over σ_1 receptor.

In addition to bicyclic KOR agonists, oxygen-labile 1,2,3,4-tetrahydropyridine-2,6-dicarboxylates **110**, **112** and **113** were envisaged, which are structurally related to the natural product class of betalains. They were synthesized from intermediates **56**, **87** and **103**. (Scheme 85)



Scheme 85: Synthesis of oxygen-labile 1,2,3,4-tetrahydropyridine derivatives.

After removal of the Boc group of **56**, **87** and **103**, a double bond was introduced in 5,6-position with *in situ* formed *t*-BuOCl leading to 1,2,3,4-tetrahydropyridines **110**, **112** and **113**. The ¹H NMR spectra indicated the formation of compounds **110**, **112** and **113**, which show different sensitivity towards oxygen. Whereas 1,2,3,4-tetrahydropyridines **110** and **113** were slowly oxidized to pyridines **111** and **114**, ketone **112** was stable over a long period of time.

In conclusion, 12 bicyclic KOR agonists with an ethano or propano bridged piperidine scaffold and one tricyclic KOR agonist were synthesized by developing various synthetic procedures. This project showed the importance of the *endo*-configuration of bicyclic compounds for high KOR affinity. Furthermore, the eutomers of the unsubstituted bicyclic amines were identified as (1*S*,5*R*,8*R*)-**19a** ($K_i = 18$ nM), (1*S*,5*S*,7*R*)-**23a** ($K_i = 7$ nM) and (1*S*,5*S*,7*R*)-**23b** ($K_i = 13$ nM). KOR agonist (1*S*,5*S*,7*R*)-**23b** displays a high KOR affinity, while being selective over MOR, DOR, σ_1 and σ_2 receptors.

7. Experimental Part

7.1 General remarks

In this chapter, general methods and techniques, which are commonly used in our research group, are described and technical specifications of the analytical instruments are given.

7.1.1 General working techniques

Oxygen and moisture sensitive reactions were carried out under nitrogen, dried with silica gel with moisture indicator (orange gel, Merck) and in dry glassware (Schlenk flask or Schlenk tube). Reaction mixtures were stirred with magnetic stirrer MR 3001 K (Heidolph) or RCT CL (IKA).

Temperatures were controlled with dry ice/acetone (-78 °C), ice/water (0 °C), Cryostat (Julabo FT 901 or Huber TC100E-F), magnetic stirrer MR 3001 K (Heidolph) or RCT CL (IKA®), together with temperature controller EKT HeiCon (Heidolph) or VT-5 (VWR) and PEG or silicone bath.

The intermediates **24**, **58**, **63**, **65**, **98**, (*S*)-**26a** and (*R*)-**26a** are commercially available. Chemical structures were generated by ChemDraw (v16.0.0.106).

7.1.2 Solvents

All solvents were of analytical grade quality. Demineralized water was used. Water free solvents were freshly distilled under N₂ atmosphere prior to use or dried with molecular sieves.

CH ₃ CN:	dried with molecular sieves (3 Å)
CH ₂ Cl ₂ :	distilled from calcium hydride
DMF:	dried with molecular sieves (4 Å)
Ethanol abs.:	dried with molecular sieves (3 Å)
Ethyl acetate:	dried with molecular sieves (4 Å)
Methanol:	distilled from magnesium methanolate
Pyridine:	dried with molecular sieves (3 Å)
THF:	distilled from sodium/benzophenone

Toluene: dried with molecular sieves (4 Å)

HPLC solvents were of gradient grade quality and bidistilled water was used. All HPLC solvents were degassed by sonification prior to use.

7.1.3 Thin layer chromatography

Thin layer chromatography was conducted with TLC silica gel 60 F₂₅₄ on aluminum sheets (Merck) as stationary phase in a saturated chamber at ambient temperature. Spots were visualized with UV light (254 nm or 365 nm). Compositions of the mobile phase and retention factor (R_f) of the compounds are given in the description of the synthetic procedures. As the retention factor (R_f) values strongly depend on the exact ratio of components of the eluent and some of these are highly volatile, the given retention factor values represent just approximate values.

7.1.4 Flash column chromatography

Flash column chromatography was performed with silica gel 60 (40 - 63 µm, Macherey-Nagel) as stationary phase. Pressure was applied with compressed air. In the description of the synthetic procedures diameter of the column (\varnothing), length of the stationary phase (h), fraction size (V) and eluent are given in brackets.

7.1.5 Melting points

Melting points were determined with melting point system MP50 (Mettler Toledo) using an open capillary. The values are uncorrected.

7.1.6 HPLC

HPLC methods A - G were used to determine the (enantiomeric) purity of the synthesized compounds or to separate the enantiomers from each other. All HPLC methods were carried out at room temperature.

7.1.6.1 Method A (Chromni)

Equipment: Pump: LPG-3400SD, degasser: DG-1210, autosampler: ACC-3000T, UV detector: VWD-3400RS, interface: DIONEX UltiMate 3000, data acquisition: Chromeleon 7 (Thermo Fisher Scientific).

Column: LiChropher® 60 RP-select B (5 µm), LiChroCART® 250-4 mm cartridge

Guard column:	LiChropher® 60 RP-select B (5 µm), LiChroCART® 4-4 mm cartridge (No.: 1.50963.0001), manu-CART® NT cartridge holder
Solvent A:	demineralized water + 0.05% (V/V) trifluoroacetic acid
Solvent B:	acetonitrile with 0.05% (V/V) trifluoroacetic acid
Gradient elution (% A):	0 - 4 min: 90%; 4 - 29 min: gradient from 90% to 0%; 29 - 31 min: 0%; 31 - 31.5 min: gradient from 0% to 90%; 31.5 - 40 min: 90%.
Flow rate:	1.0 mL/min
Injection volume:	5.0 µL; method: cut lead and rear
Detection wavelength:	210 nm
Stop time:	30.0 min
Calculation:	manual integration, calculation method: area %, use of blank subtraction from the same series

7.1.6.2 Method B (Chromni)

Equipment: Pump: L-7100, degasser: L-7614, autosampler: L-7200, UV detector: L-7400, interface: D-7000, data transfer: D-line, data acquisition: HSM-Software (all from LaChrom, Merck Hitachi).

Column:	Phenomenex Gemini C18 110 Å, 250x4.6 mm; 4x3 security guard
Solvent A:	demineralized water + 0.05% (V/V) ammonium hydroxide
Solvent B:	acetonitrile with 0.05% (V/V) ammonium hydroxide
Gradient elution (% A):	0 - 4 min: 90%; 4 - 29 min: gradient from 90% to 0%; 29 - 31 min: 0%; 31 - 31.5 min: gradient from 0% to 90%; 31.5 - 40 min: 90%.
Flow rate:	1.0 mL/min
Injection volume:	5.0 µL; method: cut lead and rear
Detection wavelength:	210 nm
Stop time:	30.0 min

Calculation: manual integration, calculation method: area %, use of blank subtraction from the same series

7.1.6.3 Method C (chiral HPLC to determine the enantiomeric purity)

Equipment: DAD detector: L-7455; interface D-7000, Rheodyne 7725i; pump: L-6200A; data acquisition: HSM-software.

Column: Daicel CHIRALPAK® IA, 5 µm, 250 mm / 4.6 mm

Guard column: Daicel CHIRALPAK® IA, 5 µm, 10 mm / 4 mm

Solvent: *i*-hexane / EtOH = 9:1 + 0.1% diethyl amine + 0.1% formic acid, isocratic

Flow rate: 1.0 mL/min

Injection volume: 5.0 µL

Detection wavelength: 275 nm

Stop time: 120.0 min

7.1.6.4 Method D (chiral HPLC to determine the enantiomeric purity)

Equipment: DAD detector: L-7455; interface D-7000, Rheodyne 7725i; pump: L-6200A; data acquisition: HSM-software.

Column: Daicel CHIRALPAK® IA, 5 µm, 250 mm / 4.6 mm

Guard column: Daicel CHIRALPAK® IA, 5 µm, 10 mm / 4 mm

Solvent: *i*-hexane / *i*-propanol = 95:5 + 0.1% diethyl amine, isocratic

Flow rate: 1.0 mL/min

Injection volume: 5.0 µL

Detection wavelength: 275 nm

Stop time: 120.0 min

7.1.6.5 Method E (preparative chiral HPLC)

Equipment: UV detector: L-7400; interface D-7000, autosampler: L-7200; pump: L-7150A; data acquisition: HSM-software

Column: Daicel CHIRALPAK® IA, 5 µm, 250 mm / 20 mm

Guard column:	Daicel CHIRALPAK® IA, 5 µm, 10 mm / 20 mm
Solvent:	<i>i</i> -hexane / EtOH = 9:1 + 0.1% diethyl amine + 0.1% formic acid, isocratic
Flow rate:	0 - 1 min: 5.0 to 10.0 mL/min; 1 - 150 min: 10.0 mL/min
Injection volume:	400.0 µL
Detection wavelength:	275 nm
Stop time:	120.0 min

7.1.6.6 Method F (preparative chiral HPLC)

Equipment: UV detector: L-7400; interface D-7000, autosampler: L-7200; pump: L-7150A; data acquisition: HSM-software

Column:	Daicel CHIRALPAK® IA, 5 µm, 250 mm / 20 mm
Guard column:	Daicel CHIRALPAK® IA, 5 µm, 10 mm / 20 mm
Solvent:	<i>i</i> -hexane / <i>i</i> -propanol = 95:5 + 0.1% diethyl amine, isocratic
Flow rate:	0 - 2 min: 5.0 mL/min; 2 - 8 min: 5.0 to 10.0 mL/min; 8 - 150 min: 10.0 mL/min
Injection volume:	400.0 µL
Detection wavelength:	275 nm
Stop time:	120.0 min

7.1.6.7 Method G (preparative chiral HPLC)

Equipment: UV detector: L-7400; interface D-7000, autosampler: L-7200; pump: L-7150A; data acquisition: HSM-software

Column:	Daicel CHIRALPAK® IA, 5 µm, 250 mm / 20 mm
Guard column:	Daicel CHIRALPAK® IA, 5 µm, 10 mm / 20 mm
Solvent:	<i>i</i> -hexane / EtOH = 9:1 + 0.1% diethyl amine, isocratic
Flow rate:	0 - 2 min: 5.0 mL/min; 2 - 5 min: 5 to 8 mL/min; 5 - 150 min: 8.0 mL/min
Injection volume:	400.0 µL
Detection wavelength:	275 nm

Stop time: 120.0 min

7.1.7 NMR spectroscopy

NMR spectra were recorded on Agilent DD2 400 MHz and 600 MHz spectrometers. The frequencies are given in the descriptions of the synthetic procedures. MestReNova software (version 10.0.0 - 14381, © 2014 by Mestrelab Research S.L.) was used for analyzing NMR spectra. Abbreviations for the multiplicities of the signal: s = singlet, d = doublet, t = triplet, q = quartet, quint = quintet, sext = sextet, sept = septet, m = multiplet, dd = doublet of doublet, etc. The multiplicities are reported as observed in the spectra. Chemical shifts (δ) are reported in parts per million (ppm) against the reference substance tetramethylsilane (TMS) and calculated using the solvent residual peak of the undeuterated solvent.

^1H NMR spectroscopy (NMR frequency: 400 MHz and 600 MHz)

$$\delta (\text{TMS}) = \delta (\text{CDCl}_3) - 7.26$$

$$\delta (\text{TMS}) = \delta (\text{DMSO-}d_6) - 2.54$$

^{13}C NMR spectroscopy (NMR frequency: 101 MHz and 150 MHz)

$$\delta (\text{TMS}) = \delta (\text{CDCl}_3) - 77.16 \text{ ppm}$$

$$\delta (\text{TMS}) = \delta (\text{DMSO-}d_6) - 39.52 \text{ ppm}$$

If necessary, ^1H and ^{13}C NMR assignments were supported by the following two-dimensional NMR spectroscopy techniques:

COSY (^1H , ^1H correlation spectroscopy)

gHSQC (gradient heteronuclear single quantum coherence)

gHMBC (gradient heteronuclear multiple bond correlation)

7.1.8 IR spectroscopy

IR spectra were recorded on a FT/IR IRAffinity-1 IR spectrometer (Shimadzu) using ATR technique. All samples were applied to the device without solvent and were directly measured. Absorption bands are characterized by their wave numbers $\tilde{\nu}$ [cm^{-1}].

7.1.9 Mass spectrometry

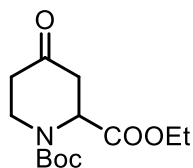
All samples were measured in the positive ion mode, so all specified molecules, fragments or adducts represent positively charged ions.

Exact mass spectra of synthesized compounds were recorded as follows:

Exact Mass (APCI): Atmospheric pressure chemical ionization (APCI) mass spectra were recorded with a MicroTOFQII mass spectrometer (Bruker Daltonics). Deviations of the found exact masses from the calculated exact masses were 5 mDa or less, unless otherwise stated. The data were analyzed with DataAnalysis (Bruker).

7.2 Synthetic procedures

1-*tert*-Butyl 2-ethyl 4-oxopiperidine-1,2-dicarboxylate (**26**)



At 0 °C, EDC · HCl (5.52 g, 28.8 mmol, 1.75 eq) was added in portions to a solution of 1-(*tert*-butoxycarbonyl)-4-oxopiperidine-2-carboxylic acid (**024**) (4.00 g, 16.4 mmol, 1.00 eq), 4-DMAP (0.20 g, 1.64 mmol, 0.10 eq) and EtOH abs. (38.4 mL, 658 mmol, 40.0 eq) in CH₂Cl₂ (40 mL). The mixture was stirred at room temperature for 16 h. Then, it was concentrated *in vacuo*, the residue was diluted with H₂O (30 mL) and the mixture was extracted with EtOAc (3 × 30 mL). The combined organic layers were dried (Na₂SO₄), filtered and concentrated *in vacuo*. The residue was purified by flash column chromatography (50 g cartridge, cHex/EtOAc 9:1 → 7:3). Colorless oil, yield 3.54 g (79%).

Chemical Formula: C₁₃H₂₁NO₅ (271.3 g/mol).

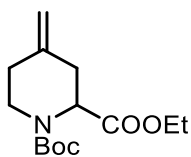
TLC: *R*_f = 0.39 (cHex/EtOAc 8:2).

¹H NMR (600 MHz, CDCl₃): δ (ppm) = 1.25 (t, *J* = 7.2 Hz, 3H, OCH₂CH₃), 1.44 (s, 9 × 0.55H, C(CH₃)₃), 1.47 (s, 9 × 0.45H, C(CH₃)₃^{*}), 2.37 – 2.61 (m, 2H, 5-CH₂), 2.66 – 2.91 (m, 2H, 3-CH₂), 3.61 (brs, 0.45H, 6-CH₂^{*}), 3.67 (brs, 0.55H, 6-CH₂), 4.02 (t, *J* = 5.8 Hz, 0.55H, 6-CH₂), 4.04 (t, *J* = 5.8 Hz, 0.45H, 6-CH₂^{*}), 4.17 (q, *J* = 7.2 Hz, 2H, OCH₂CH₃), 4.81 (s, 0.55H, 2-CH), 5.08 (s, 0.45H, 2-CH^{*}). Ratio of rotamers is 55:45. The signals for the minor rotamer are marked with an asterisk (*).

¹³C NMR (151 MHz, CDCl₃): δ (ppm) = 14.2 (1C, OCH₂CH₃), 28.4 (3C, C(CH₃)₃), 39.4 (0.55C, C-6), 39.8 (1C, C-5), 40.6 (0.45C, C-6^{*}), 41.1 (0.55C, C-3), 41.4 (0.45C, C-3^{*}), 54.1 (0.45C, C-2^{*}), 54.9 (0.55C, C-2), 61.8 (1C, OCH₂CH₃), 81.3 (1C, C(CH₃)₃), 154.5 (0.55C, N(C=O)O), 155.0 (0.45C, N(C=O)O^{*}), 171.1 (0.45C, O=COEt^{*}), 171.4 (0.55C, O=COEt), 206.1 (1C, C-4). Ratio of rotamers is 55:45. The signals for the minor rotamer are marked with an asterisk (*).

IR (neat): $\tilde{\nu}$ (cm⁻¹) = 2978 (C-H_{alip}), 1732 (C=O_{ester, ketone}), 1694 (C=O_{carbamate}), 1161, 1022 (C-N, C-O).

Exact mass (APCI): *m/z* = 272.1470 (calcd. 272.1492 for C₁₄H₂₄NO₄ [M+H]⁺).

1-tert-Butyl 2-ethyl 4-methylenepiperidine-1,2-dicarboxylate (30)

At 0 °C, THF (35 mL) was added to a mixture of methyltriphenylphosphonium bromide (6.3 g, 17.7 mmol, 1.6 eq) and KO^tBu (2.0 g, 17.7 mmol, 1.6 eq) under N₂ atmosphere and the mixture was stirred at room temperature for 45 min. Then at 0 °C, a solution of **26** (3.0 g, 11.1 mmol, 1.0 eq) in dry THF (6 mL) was added and the mixture was stirred for 3 h at room temperature. Afterwards, H₂O (40 mL) was added and the mixture was extracted with EtOAc (3 × 30 mL). The combined organic layers were dried (Na₂SO₄), filtered and concentrated *in vacuo*. The residue was purified by flash column chromatography (50 g cartridge, cHex/EtOAc 95:5 → 85:15). Colorless oil, yield 2.0 g (67%).

Chemical Formula: C₁₄H₂₃NO₄ (269.3 g/mol).

TLC: R_f = 0.63 (cHex/EtOAc 8:2).

¹H NMR (600 MHz, CDCl₃): δ (ppm) = 1.24 (t, *J* = 7.1 Hz, 3H, OCH₂CH₃), 1.44 (s, 9 × 0.5H, C(CH₃)₃), 1.46 (s, 9 × 0.5H, C(CH₃)₃), 2.12 – 2.27 (m, 2H, 5-CH₂), 2.37 – 2.47 (m, 1H, 3-CH₂), 2.70 – 2.81 (m, 1H, 3-CH₂), 2.94 – 3.02 (m, 0.5H, 6-CH₂), 3.03 – 3.10 (m, 0.5H, 6-CH₂), 3.98 – 4.05 (m, 0.5H, 6-CH₂), 4.07 – 4.23 (m, 2.5H, 6-CH₂, OCH₂CH₃), 4.74 – 4.82 (m, 2.5H, 2-CH, C=CH₂), 4.96 – 5.02 (m, 0.5H, 2-CH). Ratio of rotamers is 1:1.

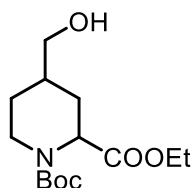
¹³C NMR (151 MHz, CDCl₃): δ (ppm) = 14.4 (1C, OCH₂CH₃), 28.5 (3C, C(CH₃)₃), 33.2 (0.5C, C-5), 33.6 (0.5C, C-5), 35.5 (0.5C, C-3), 35.6 (0.5C, C-3), 42.4 (0.5C, C-6), 43.4 (0.5C, C-6), 55.3 (0.5C, C-2), 56.4 (0.5C, C-2), 61.1 (1C, OCH₂CH₃), 80.4 (1C, C(CH₃)₃), 111.0 (1C, C=CH₂), 141.8 (0.5C, C-4), 142.0 (0.5C, C-4), 155.4 (0.5C, N(C=O)O), 155.8 (0.5C, N(C=O)O), 171.0 (0.5C, O=COEt), 171.2 (0.5C, O=COEt). Ratio of rotamers is 1:1.

Purity (HPLC, method A): 97.9% (*t_R* = 21.4 min).

IR (neat): $\tilde{\nu}$ (cm⁻¹) = 2978 (C-H_{alip}), 1740 (C=O_{ester}), 1694 (C=O_{carbamate}), 1655 (C=C), 1157, 1030 (C-N, C-O).

Exact mass (APCI): *m/z* = 270.1675 (calcd. 270.1700 for C₁₄H₂₄NO₄ [M+H]⁺).

1-tert-Butyl 2-ethyl *cis*- and *trans*-4-(hydroxymethyl)piperidine-1,2-dicarboxylate (31)



9-BBN (0.5 M in THF, 19.2 mL, 9.62 mmol, 1.3 eq) was added dropwise to a solution of **30** (1.99 g, 7.40 mmol, 1.0 eq) in dry THF (10 mL) and the mixture was stirred at 50 °C for 16 h. Then, at 0 °C, NaOH (2 M in H₂O, 5.55 mL, 11.1 mmol, 1.5 eq) and H₂O₂ (30%, 8.40 mL, 74.0 mmol, 10.0 eq) were added slowly and the mixture was stirred at room temperature for 2 h. The layers were separated, and the aqueous layer was extracted with EtOAc (3 × 25 mL). The combined organic layers were dried (Na₂SO₄), filtered and concentrated *in vacuo*. The residue was purified by flash column chromatography (50 g cartridge, cHex/EtOAc 7:3 → 1:1). Colorless oil, yield 1.67 g (78%).

Chemical Formula: C₁₄H₂₅NO₅ (287.4 g/mol).

TLC: *R*_f = 0.35 (cHex/EtOAc 1:1).

¹H NMR (600 MHz, CDCl₃): δ (ppm) = 0.93 – 1.04 (m, 0.6H, 3/5-CH₂), 1.14 – 1.22 (m, 3H, OCH₂CH₃), 1.22 – 1.32 (m, 1.2H, 3/5-CH₂, 4-CH), 1.33 – 1.43 (m, 9.4H, C(CH₃)₃, 3/5-CH₂*), 1.56 – 1.74 (m, 0.6 + 3 × 0.4H, 3/5-CH₂, 3-CH₂*, 4-CH*, 5-CH₂*), 1.92 (ddd, *J* = 13.4 / 6.0 / 4.8 Hz, 0.4H, 3/5-CH₂*), 2.08 – 2.15 (m, 0.6H, 3/5-CH₂), 2.79 (td, *J* = 13.2 / 3.2 Hz, 0.3H, 6-CH₂), 2.93 (td, *J* = 13.2 / 3.2 Hz, 0.3H, 6-CH₂), 3.12 – 3.25 (m, 0.6 + 3 × 0.4H, CH₂OH, 6-CH₂*), 3.27 (ddd, *J* = 10.8 / 7.0 / 5.2 Hz, 0.6H, CH₂OH), 3.36 – 3.50 (m, 0.4H, 6-CH₂*), 3.82 – 3.91 (m, 0.6H, 6-CH₂), 4.05 – 4.18 (m, 2.4H, OCH₂CH₃, 2-CH*), 4.50 – 4.54 (m, 1H, CH₂OH), 4.63 – 4.66 (m, 0.3H, 2-CH), 4.72 – 4.75 (m, 0.3H, 2-CH). Ratio of *cis*-**31** : *trans*-**31** is 6:4. The signals for the minor diastereomer *trans*-**31** are marked with an asterisk (*). Ratio of rotamers of *cis*-**31** is 1:1.

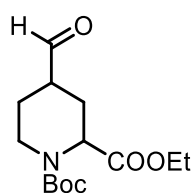
¹³C NMR (151 MHz, CDCl₃): δ (ppm) = 14.0 (0.4C, OCH₂CH₃*), 14.08 (0.3C, OCH₂CH₃), 14.10 (0.3C, OCH₂CH₃), 25.2 (0.4C, C-3/5*), 27.4 (0.3C, C-3/5), 27.6 (0.3C, C-3/5), 27.88 (0.9C, C(CH₃)₃), 27.90 (0.9C, C(CH₃)₃), 28.0 (1.2C, C(CH₃)₃*), 28.1 (0.4C, C-3/5*), 29.5 (0.6C, C-3/5), 33.7 (0.4C, C-4*), 34.8 (0.3C, C-4), 34.9 (0.3C, C-4), 40.6 (0.3C, C-6), 41.3 (0.3C, C-6), 53.2 (0.3C, C-2), 54.30 (0.3C, C-2), 54.34 (0.4C, C-2*), 60.3 (0.4C, OCH₂CH₃*), 60.59 (0.3C, OCH₂CH₃), 60.63 (0.3C, OCH₂CH₃), 63.2 (0.4C, CH₂OH), 65.43 (0.3C, CH₂OH), 65.45 (0.3C, CH₂OH), 79.1,

79.2 (1C, C(CH₃)₃, C(CH₃)₃*), 154.7 (0.3C, N(C=O)O), 155.1 (0.3C, N(C=O)O), 171.4 (0.3C, O=COEt), 171.5 (0.3C, O=COEt), 172 (0.4C, O=COEt*).). Ratio of *cis*-**31** : *trans*-**31** is 6:4. The signals for the minor diastereomer *trans*-**31** are marked with an asterisk (*). Ratio of rotamers of *cis*-**31** is 1:1. The signals for C-6* and N(C=O)O* are not seen in the spectrum.

IR (neat): $\tilde{\nu}$ (cm⁻¹) = 3463 (OH), 2974, 2928 (C-H_{alip}), 1736 (C=O_{ester}), 1694 (C=O_{carbamate}), 1157, 1030 (C-N, C-O).

Exact mass (APCI): m/z = 288.1798 (calcd. 288.1805 for C₁₄H₂₆NO₅ [M+H]⁺).

1-*tert*-Butyl 2-ethyl *cis*- and *trans*-4-formylpiperidine-1,2-dicarboxylate (**32**)



DMP (3.54 g, 8.35 mmol, 1.5 eq) was added to a solution of **31** (1.60 g, 5.57 mmol, 1.0 eq) in dry CH₂Cl₂ (20 mL) and the mixture was stirred at room temperature for 4 h. Then, the mixture was washed with NaOH (2 M in H₂O, 2 × 20 mL), Na₂SO₃ (2 × 20 mL) and brine (20 mL). The organic layer was dried (Na₂SO₄), filtered and concentrated *in vacuo*. The residue was purified by flash column chromatography (50 g cartridge, cHex/EtOAc 9:1 → 7:3). Colorless oil, yield 0.89 g (56%).

Chemical Formula: C₁₄H₂₃NO₅ (285.3 g/mol).

TLC: R_f = 0.41 (cHex/EtOAc 7:3).

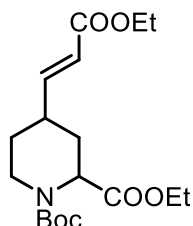
¹H NMR (600 MHz, CDCl₃): δ (ppm) = 1.23 – 1.30 (m, 3H, OCH₂CH₃, OCH₂CH₃*), 1.38 (td, J = 13.0 / 4.9 Hz, 0.6H, 5-CH₂), 1.44 (s, 9 × 0.6H, C(CH₃)₃), 1.47 (s, 9 × 0.4H, C(CH₃)₃*), 1.58 – 1.78 (m, 1H, 3-CH₂, 3/5-CH₂*), 1.92 (d, J = 13.0 Hz, 0.3H, 5-CH₂), 2.00 (d, J = 13.2 Hz, 0.3H, 5-CH₂), 2.09 (dt, J = 14.3 / 6.7 Hz, 0.4H, 3/5-CH₂*), 2.11 – 2.18 (m, 0.4H, 5-CH₂*), 2.23 – 2.38 (m, 0.6H, 4-CH), 2.42 – 2.59 (m, 1H, 3-CH₂, 4-CH*), 2.65 (d, J = 14.3 Hz, 0.4H, 3/5-CH₂*), 2.87 – 2.97 (m, 0.3H, 6-CH₂), 2.99 – 3.08 (m, 0.3H, 6-CH₂), 3.57 – 3.73 (m, 0.4H, 6-CH₂*), 3.78 – 3.93 (m, 0.4H, 6-CH₂*), 4.01 – 4.09 (m, 0.3H, 6-CH₂), 4.10 – 4.27 (m, 2.3H, 6-CH₂, OCH₂CH₃, OCH₂CH₃*), 4.57 – 4.77 (m, 0.4H, 2-CH*), 4.85 (d, J = 5.0 Hz, 0.3H, 2-CH), 5.04 (d, J = 5.0 Hz, 0.3H, 2-CH), 9.64 (s, 0.6H, CHO), 9.68 (s, 0.4H, CHO*). Ratio of *cis*-**32** : *trans*-**32** is 6:4. The signals for the minor diastereomer *trans*-**32** are marked with an asterisk (*). Ratio of rotamers of *cis*-**32** is 1:1.

^{13}C NMR (151 MHz, CDCl_3): δ (ppm) = 14.2, 14.4, 14.5 (1C, OCH_2CH_3 , $\text{OCH}_2\text{CH}_3^*$), 23.0 (0.4C, C-3/5*), 24.8 (0.3C, C-5), 24.9 (0.3C, C-5), 25.1 (0.4C, C-3/5*), 26.3 (0.3C, C-3), 26.4 (0.3C, C-3), 28.4, 28.45, 28.47 (3C, $\text{C}(\text{CH}_3)_3$, $\text{C}(\text{CH}_3)_3^*$), 40.2 (0.3C, C-6), 41.1 (0.3C, C-6), 43.8 (0.4C, C-4*), 45.0 (0.3C, C-4), 45.2 (0.3C, C-4), 53.0 (0.3C, C-2), 54.0 (0.3C, C-2), 61.5, 61.6, 61.9 (1C, OCH_2CH_3 , $\text{OCH}_2\text{CH}_3^*$), 80.5, 80.6, 80.7 (1C, $\text{C}(\text{CH}_3)_3$, $\text{C}(\text{CH}_3)_3^*$), 171.3 (0.3C, $\text{O}=\text{COEt}$), 171.5 (0.3C, $\text{O}=\text{COEt}$), 202.3 (0.6C, CHO), 202.6 (0.4C, CHO^*). Ratio of *cis*-**32** : *trans*-**32** is 6:4. The signals for the minor diastereomer *trans*-**32** are marked with an asterisk (*). Ratio of rotamers of *cis*-**32** is 1:1. Signals for C-2*, C-6*, $\text{N}(\text{C}=\text{O})\text{O}$, $\text{N}(\text{C}=\text{O})\text{O}^*$ and $\text{O}=\text{COEt}^*$ are not seen in the spectrum.

IR (neat): $\tilde{\nu}$ (cm^{-1}) = 2974 (C-H_{alip}), 1728 (C=O_{ester, aldehyde}), 1694 (C=O_{carbamate}), 1157, 1026 (C-N, C-O).

Exact mass (APCI): m/z = 286.1688 (calcd. 286.1649 for $\text{C}_{14}\text{H}_{24}\text{NO}_5$ [$\text{M}+\text{H}$]⁺).

1-*tert*-Butyl 2-ethyl *cis*- and *trans*-4-[(*E*)-2-(ethoxycarbonyl)vinyl]piperidine-1,2-dicarboxylate (**34**)



4-(Ethoxycarbonylmethylene)triphenylphosphorane (**33**) (1.64 g, 4.70 mmol, 1.5 eq) was added to a solution of **32** (0.89 g, 3.13 mmol, 1.0 eq) in dry CH_2Cl_2 (10 mL) and the mixture was stirred at reflux for 4 h. Then, it was concentrated *in vacuo* and the residue was purified by flash column chromatography (50 g cartridge, cHex/EtOAc 9:1 \rightarrow 8:2). Colorless oil, yield 0.74 g (67%).

Chemical Formula: $\text{C}_{18}\text{H}_{29}\text{NO}_6$ (355.4 g/mol).

TLC: R_{f1} = 0.37, R_{f2} = 0.32 (cHex/EtOAc 8:2).

^1H NMR (600 MHz, CDCl_3): δ (ppm) = 1.24 – 1.30 (m, 6H, 2 \times OCH_2CH_3), 1.31 – 1.36 (m, 0.6H, 5- CH_2), 1.44 (s, 9 \times 0.6H, $\text{C}(\text{CH}_3)_3$), 1.47 (s, 9 \times 0.4H, $\text{C}(\text{CH}_3)_3^*$), 1.50 – 1.57 (m, 0.6H, 3- CH_2), 1.66 – 1.73 (m, 0.7H, 5- CH_2^* , 5- CH_2), 1.74 – 1.79 (m, 0.3H, 5- CH_2), 1.80 – 1.87 (m, 0.4H, 5- CH_2^*), 2.07 – 2.22 (m, 1.4H, 3- CH_2^* , 4- CH), 2.25 – 2.36 (m, 0.6H, 3- CH_2), 2.56 – 2.61 (m, 0.4H, 4- CH^*), 2.92 (td, J = 13.3 / 2.9 Hz, 0.3H, 6- CH_2), 3.04 (td, J = 13.3 / 2.9 Hz, 0.3H, 6- CH_2), 3.31 – 3.42 (m, 0.4H, 6- CH_2^*), 3.65 – 3.79 (m,

0.4H, 6-CH₂*), 3.97 – 4.03 (m, 0.3H, 6-CH₂), 4.09 – 4.24 (m, 4.3H, 6-CH₂, 2 × OCH₂CH₃), 4.43 – 4.51 (m, 0.4H, 2-CH*), 4.79 (d, *J* = 5.4 Hz, 0.3H, 2-CH), 4.97 (d, *J* = 5.4 Hz, 0.3H, 2-CH), 5.78 – 5.85 (m, 1H, CH=CHCOOEt, CH=CHCOOEt*), 6.85 (dd, *J* = 15.8 / 6.6 Hz, 0.6H, CH=CHCOOEt), 6.90 (dd, *J* = 15.9 / 6.5 Hz, 0.4H, CH=CHCOOEt*). Ratio of diastereomers is 6:4 (*cis*-**34**/*trans*-**34**). The signals for the minor diastereomer (*trans*) are marked with an asterisk (*). Ratio of rotamers of *cis*-**34** is 1:1.

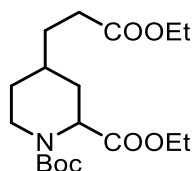
¹³C NMR (151 MHz, CDCl₃): δ (ppm) = 14.2, 14.4, 14.5 (2C, 2 × OCH₂CH₃), 28.0 (0.4C, C-5*), 28.4 (3 × 0.6C, C(CH₃)₃), 28.5 (3 × 0.4C, C(CH₃)₃*), 30.0 (0.3, C-5), 30.2 (0.3C, C-5), 31.0 (0.4C, C-3*), 31.6 (0.3C, C-3), 31.7 (0.3C, C-3), 33.6 (0.4C, C-4*), 35.1 (0.3C, C-4), 35.3 (0.3C, C-4), 40.6 (0.3C, C-6), 41.5 (0.3C, C-6), 53.4 (0.3C, C-2), 54.6 (0.3C, C-2), 60.5 (0.4C, OCH₂CH₃*), 60.6 (0.6C, OCH₂CH₃), 61.3, 61.37, 61.39 (1C, OCH₂CH₃), 80.45 (0.6C, C(CH₃)₃), 80.48 (0.4C, C(CH₃)₃*), 120.6 (0.3C, CH=CHCOOEt), 120.7 (0.3C, CH=CHCOOEt), 121.7 (0.4C, CH=CHCOOEt*), 149.7 (0.4C, CH=CHCOOEt*), 151.1 (0.3C, CH=CHCOOEt), 151.2 (0.3C, CH=CHCOOEt), 154.1 (0.4C, N(C=O)O*), 155.4 (0.3C, N(C=O)O), 155.8 (0.3C, N(C=O)O), 166.4 (0.4C, O=COEt*), 166.7 (0.6C, O=COEt), 171.5 (0.3C, O=COEt), 171.7 (0.3C, O=COEt), 172.3 (0.4C, O=COEt*). Ratio of *cis*-**34** : *trans*-**34** is 6:4. The signals for the minor diastereomer *trans*-**34** are marked with an asterisk (*). Ratio of rotamers of *cis*-**34** is 1:1. Signals for C-2* and C-6* are not seen in the spectrum.

Purity (HPLC, method A): 98.9% (*t*_{R1} = 21.4 min, *t*_{R2} = 22.0 min).

IR (neat): $\tilde{\nu}$ (cm⁻¹) = 2978 (C-H_{alip}), 1697, (C=O_{ester, carbamate}), 1651 (C=C), 1157, 1030 (C-N, C-O).

Exact mass (APCI): *m/z* = 356.2088 (calcd. 356.2068 for C₁₈H₃₀NO₆ [M+H]⁺).

1-*tert*-Butyl 2-ethyl *cis*- and *trans*-4-(2-ethoxycarbonyl)ethyl)piperidine-1,2-dicarboxylate (**37**)



Pd(OH)₂ (73 mg) was added to a solution of **34** (0.73 g, 2.05 mmol, 1 eq) in EtOH abs. (7 mL) and the mixture was stirred at room temperature for 16 h under H₂ (5 bar). Then, the mixture was filtered over Celite[®] and the filtrate was concentrated *in vacuo*. Colorless oil, yield 0.72 g (99%).

Chemical Formula: C₁₈H₃₁NO₆ (357.4 g/mol).

TLC: $R_f = 0.39$ (cHex/EtOAc 8:2).

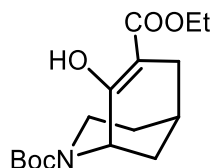
¹H NMR (600 MHz, DMSO-*d*₆): δ (ppm) = 0.93 – 1.03 (m, 0.6H, 5-CH₂), 1.13 – 1.21 (m, 6.6H, 4-CH, 2 × OCH₂CH₃, 2 × OCH₂CH₃*), 1.23 – 1.41 (m, 10H, 3-CH₂, 5-CH₂*, C(CH₃)₃, C(CH₃)₃*), 1.41 – 1.50 (m, 2H, CH₂CH₂COOEt, CH₂CH₂COOEt*), 1.57 – 1.68 (m, 1.4H, 4-CH*, 5-CH₂, 5-CH₂*), 1.69 – 1.74 (m, 0.4H, 3-CH₂*), 1.90 (ddd, $J = 13.8 / 6.3 / 4.7$ Hz, 0.4H, 3-CH₂*), 2.03 – 2.12 (m, 0.6H, 3-CH₂), 2.24 – 2.31 (m, 2H, CH₂CH₂COOEt, CH₂CH₂COOEt*), 2.75 (td, $J = 13.1 / 3.1$ Hz, 0.3H, 6-CH_{ax}), 2.90 (td, $J = 13.1 / 3.1$ Hz, 0.3H, 6-CH_{ax}), 3.10 – 3.28 (m, 0.4H, 6-CH_{eq}*), 3.39 – 3.53 (m, 0.4H, 6-CH_{ax}*), 3.80 – 3.88 (m, 0.6H, 6-CH_{eq}), 4.01 – 4.05 (m, 2H, OCH₂CH₃, OCH₂CH₃*), 4.06 – 4.16 (m, 2H, OCH₂CH₃, OCH₂CH₃*), 4.23 (t, $J = 6.2$ Hz, 0.4H, 2-CH*), 4.63 (dd, $J = 5.8$ Hz, 0.3H, 2-CH), 4.72 (dd, $J = 5.8$ Hz, 0.3H, 2-CH). Ratio of *trans*-**37** : *cis*-**37** is 6:4. The signals for the minor diastereomer *cis*-**37** are marked with an asterisk (*). Ratio of rotamers of *trans*-**37** is 1:1.

¹³C NMR (151 MHz, DMSO-*d*₆): δ (ppm) = 14.0, 14.06, 14.09, 14.13 (2C, 2 × OCH₂CH₃, 2 × OCH₂CH₃*), 27.7 (0.4C, CH₂CH₂COOEt*), 27.87 (3 × 0.3C, C(CH₃)₃), 27.90 (3 × 0.3C, C(CH₃)₃), 28.0 (3 × 0.4C, C(CH₃)₃*), 28.3 (0.4C, C-5*), 30.1 (0.4C, C-3*), 30.16 (0.4C, C-4*), 30.23 (0.3C, C-5), 30.5 (0.3C, C-5), 30.66 (0.3C, CH₂CH₂COOEt), 30.68 (0.3C, CH₂CH₂COOEt), 30.74 (0.6C, CH₂CH₂COOEt), 31.2 (0.3C, C-4), 31.3 (0.3C, C-4), 31.4 (0.4C, CH₂CH₂COOEt*), 32.28 (0.3C, C-3), 32.30 (0.3C, C-3), 40.1 (0.4C, C-6*), 40.7 (0.3C, C-6), 41.5 (0.3C, C-6), 53.4 (0.3C, C-2), 54.5 (0.3C, C-2), 59.73 (0.6C, OCH₂CH₃), 59.74 (0.4C, OCH₂CH₃*), 60.5 (0.4C, OCH₂CH₃*), 60.59 (0.3C, OCH₂CH₃), 60.64 (0.3C, OCH₂CH₃), 79.1 (0.3C, C(CH₃)₃), 79.25 (0.4C, C(CH₃)₃*), 79.28 (0.3C, C(CH₃)₃), 154.6 (0.3C, N(C=O)O), 155.0 (0.3C, N(C=O)O), 171.1 (0.3C, O=COEt), 171.3 (0.3C, O=COEt), 172.1 (0.4C, O=COEt*), 172.75 (0.4C, O=COEt*), 172.77 (0.6C, O=COEt). Ratio of *trans*-**37** : *cis*-**37** is 6:4. The signals for the minor diastereomer *cis*-**37** are marked with an asterisk (*). Ratio of rotamers of *trans*-**37** is 1:1. Signals for C-2* and N(C=O)O* are not seen in the spectrum.

IR (neat): $\tilde{\nu}$ (cm⁻¹) = 2978 (C-H_{alip}), 1732 (C=O_{ester}), 1694 (C=O_{carbamate}), 1157, 1096, 1026 (C-N, C-O).

Exact mass (APCI): $m/z = 358.2255$ (calcd. 358.2224 for C₁₈H₃₂NO₆ [M+H]⁺).

2-tert-Butyl 7-ethyl (1*RS*,5*SR*)-8-hydroxy-2-azabicyclo[3.3.1]non-7-ene-2,7-dicarboxylate (25)



NaHMDS (1 M in THF, 3.92 mL, 3.92 mmol, 2 eq) was added to a refluxing solution of **37** (0.70 g, 1.96 mmol, 1 eq) in dry THF (100 mL) and the mixture was heated to reflux for 2 h. Then, the mixture was poured into a half-sat. NH₄Cl (100 mL). The mixture was extracted with EtOAc (3 × 50 mL), the combined organic layers were dried (Na₂SO₄), filtered and concentrated *in vacuo*. The residue was purified by flash column chromatography (50 g cartridge, cHex/EtOAc 9:1 → 8:2). Colorless solid, mp 69 - 70 °C, yield 0.35 g (58%).

Chemical Formula: C₁₆H₂₅NO₅ (311.4 g/mol).

TLC: *R*_f = 0.77 (cHex/EtOAc 8:2).

¹H NMR (600 MHz, CDCl₃): δ (ppm) = 1.31 (t, *J* = 7.1 Hz, 3H, OCH₂CH₃), 1.46 (s, 9 × 0.4H, C(CH₃)₃*), 1.48 (s, 9 × 0.6H, C(CH₃)₃), 1.50 – 1.56 (m, 1H, 4-CH₂), 1.69 – 1.80 (m, 2H, 4-CH₂, 9-CH₂), 1.83 (dm, *J* = 12.7 Hz, 1H, 9-CH₂), 2.16 – 2.23 (m, 2H, 5-CH, 6-CH₂), 2.45 – 2.54 (m, 1H, 6-CH₂), 2.88 (t, *J* = 13.6 Hz, 0.6H, 3-CH₂), 2.98 (t, *J* = 12.5 Hz, 0.4H, 3-CH₂*), 3.77 – 3.84 (m, 0.4H, 3-CH₂*), 3.88 (dd, *J* = 13.0 / 5.4 Hz, 0.6H, 3-CH₂), 4.20 – 4.26 (m, 2H, OCH₂CH₃), 4.66 (s, 0.6H, 1-CH), 4.85 (s, 0.4H, 1-CH*), 11.70 (s, 1H, 8-COH). Ratio of rotamers is 6:4. The signals for the minor rotamer are marked with an asterisk (*).

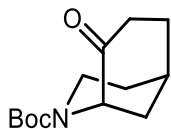
¹³C NMR (151 MHz, CDCl₃): δ (ppm) = 14.4 (1C, OCH₂CH₃), 24.6 (0.6C, C-5), 24.7 (0.4C, C-5*), 28.1 (0.6C, C-6), 28.2 (0.4C, C-6*), 28.6 (3C, C(CH₃)₃), 30.4 (0.4C, C-9*), 30.6 (0.6C, C-9), 31.9 (0.6C, C-4), 32.2 (0.4C, C-4*), 37.3 (0.6C, C-3), 38.5 (0.4C, C-3*), 48.2 (0.4C, C-1*), 49.6 (0.6C, C-1), 60.7 (1C, OCH₂CH₃), 80.0 (0.4C, C(CH₃)₃*), 80.1 (0.6C, C(CH₃)₃), 99.7 (0.6C, C-7), 99.8 (0.4C, C-7*), 155.2 (0.4C, N(C=O)O*), 155.4 (0.6C, N(C=O)O), 166.7 (0.6C, C-8), 167.1 (0.4C, C-8*), 172.0 (1C, O=COEt). Ratio of rotamers is 5:4. The signals for the minor rotamer are marked with an asterisk (*).

Purity (HPLC, method A): 82.4% (*t*_R = 22.7 min).

IR (neat): $\tilde{\nu}$ (cm⁻¹) = 2978, 2928 (C-H_{alip}), 1694 (C=O_{carbamate}), 1659 (C=O_{ester}), 1620 (C=C), 1273, 1207, 1165, 1053 (C-N, C-O).

Exact mass (APCI): $m/z = 312.1787$ (calcd. 312.1805 for $C_{16}H_{26}NO_5$ $[M+H]^+$).

tert-Butyl (1RS,5SR)-8-oxo-2-azabicyclo[3.3.1]nonane-2-carboxylate (51)



LiCl (204 mg, 4.82 mmol, 5 eq) and H₂O (4 drops) were added to a solution of **25** (300 mg, 0.96 mmol, 1 eq) in DMSO (4 mL) and the mixture was stirred at reflux in a preheated oil bath for 90 min. Then, it was added to H₂O (40 mL) and extracted with EtOAc (3 × 20 mL). The combined organic layers were dried (Na₂SO₄), filtered and concentrated *in vacuo*. The residue was purified by flash column chromatography (25 g cartridge, cHex/EtOAc 9:1 → 75:25) was done. Colorless solid, mp 68 - 69 °C, yield 160 mg (70%).

Chemical Formula: C₁₃H₂₁NO₃ (239.3 g/mol).

TLC: $R_f = 0.25$ (cHex/EtOAc 8:2).

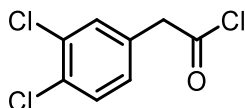
¹H NMR (600 MHz, CDCl₃): δ (ppm) = 1.42 (s, 9H, C(CH₃)₃), 1.73 – 1.85 (m, 2H, 4-CH₂, 9-CH₂), 1.86 – 1.91 (m, 1H, 6-CH₂), 1.92 – 1.98 (m, 1H, 6-CH₂), 2.02 – 2.13 (m, 1H, 4/9-CH₂), 2.16 – 2.34 (m, 3H, 5-CH, 4/9-CH₂, 7-CH₂), 2.64 – 2.87 (m, 1H, 7-CH₂), 2.33 – 2.54 (m, 1H, 3-CH₂), 2.55 – 2.85 (m, 1H, 3-CH₂), 4.03 – 4.37 (m, 1H, 1-CH).

¹³C NMR (151 MHz, CDCl₃): δ (ppm) = 23.8 (1C, C-5), 28.4 (3C, C(CH₃)₃), 29.0 (1C, C-4/9), 32.2 (1C, C-4/9), 33.4 (1C, C-6), 35.4 (1C, C-7), 37.3 (1C, C-3), 60.2 (1C, C-1), 80.7 (1C, C(CH₃)₃), 155.3 (1C, N(C=O)O), 210.5 (1C, C-8).

IR (neat): $\tilde{\nu}$ (cm⁻¹) = 2978 (C-H_{alip}), 1721 (C=O_{ketone}), 1686 (C=O_{carbamate}), 1153, 1115 (C-N, C-O).

Exact mass (APCI): $m/z = 240.1598$ (calcd. 240.1594 for C₁₃H₂₂NO₃ $[M+H]^+$).

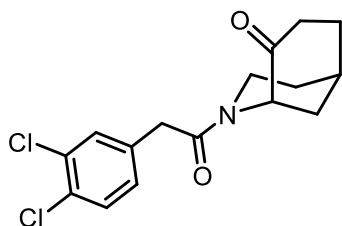
2-(3,4-Dichlorophenyl)acetyl chloride (53)



An excess of SOCl₂ (7.5 mL, 103 mmol, 1.7 eq) was added to 2-(3,4-dichlorophenyl)acetic acid (12.5 g, 61 mmol, 1.0 eq) and the mixture was heated at 60 °C for 1 h. Then, excess of SOCl₂ was removed *in vacuo*. Pale yellow solid, mp 32 - 33 °C, yield 13.5 g (99%).

Chemical Formula: C₈H₅Cl₃O (223.5 g/mol).

(1*RS*,5*SR*)-2-[2-(3,4-Dichlorophenyl)acetyl]-2-azabicyclo[3.3.1]nonan-8-one (54)



TFA (0.16 mL, 2.09 mmol, 5 eq) was added to a solution of **51** (100 mg, 0.42 mmol, 1 eq) in CH₂Cl₂ (4 mL) and the mixture was stirred at room temperature for 16 h. Then at 0 °C, NaOH (2 M in H₂O, 1.9 mL, 3.76 mmol, 9 eq) and a solution of **53** (187 mg, 0.84 mmol, 2 eq) in CH₂Cl₂ (2 mL) were added and the mixture was stirred at room temperature for 16 h. After extraction with CH₂Cl₂ (3 × 5 mL), the combined organic layers were dried (Na₂SO₄), filtered and concentrated *in vacuo*. The residue was purified by flash column chromatography (25 g cartridge, cHex/EtOAc 7:3 → 4:6). Colorless solid, mp 114 - 116 °C, yield 97 mg, (71%).

Chemical Formula: C₁₆H₁₇Cl₂NO₂ (398.3 g/mol).

TLC: R_f = 0.23 (cHex/EtOAc 1:1).

¹H NMR (600 MHz, CDCl₃): δ (ppm) = 1.59 – 1.71 (m, 0.35H, 4-CH₂*), 1.75 – 1.81 (m, 0.35H, 6-CH₂*), 1.82 – 1.88 (m, 0.65H, 4-CH₂), 1.91 – 2.01 (m, 2.0H, 4-CH₂*, 6-CH₂, 9-CH₂, 9-CH₂*), 2.02 – 2.16 (m, 3 × 0.65 + 2 × 0.35 H, 4-CH₂, 6-CH₂, 6-CH₂*, 9-CH₂, 9-CH₂*), 2.22 – 2.31 (m, 1H, 5-CH_{eq}, 5-CH_{eq}), 2.36 (ddd, *J* = 14.9 / 7.1 / 4.6 Hz, 0.35H, 7-CH₂*), 2.53 (ddd, *J* = 16.3 / 7.0 / 2.6 Hz, 0.65H, 7-CH₂), 2.53 (ddd, *J* = 14.9 / 9.8 / 7.5 Hz, 0.35H, 7-CH₂*) 2.65 (ddd, *J* = 16.3 / 11.1 / 8.2 Hz, 0.65H, 7-CH₂), 3.40 – 3.50 (m, 1H, 3-CH₂, 3-CH₂*), 3.50 – 3.56 (m, 0.35H, 3-CH₂*), 3.64 (d, *J* = 15.7 Hz, 0.65H, CH₂-aryl), 3.69 (s, 0.7H, CH₂-aryl*), 3.70 (d, *J* = 15.7 Hz, 0.65H, CH₂-aryl), 4.00 (ddd, *J* = 14.5 / 7.1 / 4.9 Hz, 0.65H, 3-CH₂), 4.20 – 4.23 (m, 0.65H, 1-CH_{eq}), 4.66 – 4.70 (m, 0.35H, 1-CH_{eq}*), 7.07 (dd, *J* = 8.3 / 1.9 Hz, 0.65H, 6-CH_{arom}), 7.10 (dd, *J* = 8.3 / 1.7 Hz, 0.35H, 6-CH_{arom}*), 7.34 – 7.36 (m, 1H, 2-CH_{arom}), 7.37 (d, *J* = 8.3 Hz, 0.65H, 5-CH_{arom}), 7.39 (d, *J* = 8.3 Hz, 0.35H, 5-CH_{arom}*). Ratio of rotamers is 65:35. The signals for the minor rotamer are marked with an asterisk (*).

¹³C NMR (151 MHz, CDCl₃): δ (ppm) = 23.7 (1C, C-5), 28.9 (0.65C, C-4), 30.1 (0.65C, C-6), 30.4 (0.35C, C-4*), 30.8 (0.35C, C-6*), 31.3 (0.35C, C-9*), 32.4 (0.65C, C-9), 35.9 (0.35C, C-7*), 37.2 (0.65C, C-7), 37.9 (0.65C, C-3), 39.8 (0.65C, CH₂-aryl), 40.3

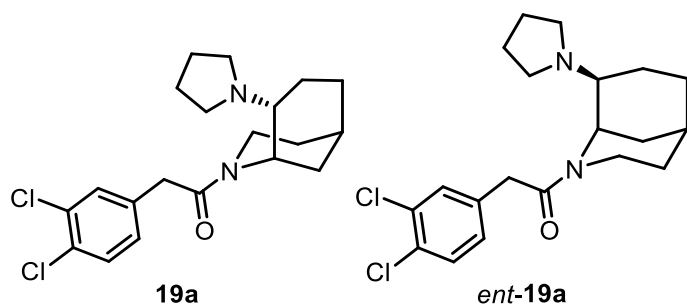
(0.35C, CH₂-aryl*), 40.7 (0.35C, C-3*), 57.9 (0.35C, C-1*), 59.7 (0.65C, C-1), 128.3 (0.35C, C-6_{arom}*), 128.9 (0.65C, C-6_{arom}), 130.5 (0.65C, C-5_{arom}), 130.8 (0.35C, C-5_{arom}*), 130.9 (0.35C, C-2_{arom}*), 131.2 (0.65C, C-3/4_{arom}), 131.3 (0.35C, C-3/4_{arom}*), 131.4 (0.65C, C-2_{arom}), 132.6 (0.65C, C-3/4_{arom}), 132.8 (0.35C, C-3/4_{arom}*), 134.8 (0.35C, C-1_{arom}*), 135.1 (0.65C, C-1_{arom}), 169.5 (0.35C, N(C=O)*), 171.1 (0.65C, N(C=O)), 208.7 (0.65C, C-8), 210.0 (0.35C, C-8*). Ratio of rotamers is 65:35. The signals for the minor rotamer are marked with an asterisk (*).

Purity (HPLC, method A): 97.8% (*t_R* = 19.2 min).

IR (neat): $\tilde{\nu}$ (cm⁻¹) = 2932 (C-H_{alip}), 1717 (C=O_{ketone}), 1639 (C=O_{amide}), 1246, 1030 (C-N, C-O).

Exact mass (APCI): *m/z* = 326.0718 (calcd. 326.0709 for C₁₆H₁₈³⁵Cl₂NO₂ [M+H]⁺).

2-(3,4-Dichlorophenyl)-1-((1*S*,5*R*,8*R*)-8-(pyrrolidin-1-yl)-2-azabicyclo[3.3.1]nonan-2-yl)ethan-1-one (19a) and 2-(3,4-dichlorophenyl)-1-((1*R*,5*S*,8*S*)-8-(pyrrolidin-1-yl)-2-azabicyclo[3.3.1]nonan-2-yl)ethan-1-one (*ent*-19a)



Pyrrolidine (57 μ L, 0.69 mmol, 5 eq) and AcOH (12 μ L, 0.21 mmol, 1.5 eq) were added to a solution of **54** (45 mg, 0.14 mmol, 1 eq) in CH₂Cl₂ (3 mL) and the mixture was stirred at room temperature for 30 min. Then, NaBH(OAc)₃ (58 mg, 0.28 mmol, 2 eq) was added and the mixture was stirred for 16 h. After addition of NaHCO₃ (5 mL), the mixture was extracted with CH₂Cl₂ (3 \times 5 mL). The combined organic layers were dried (Na₂SO₄), filtered and concentrated *in vacuo*. The residue was purified by flash column chromatography (ϕ = 1.5 cm, *h* = 9 cm, CH₂Cl₂/NH₃ (7 M in CH₃OH)/CH₃OH 98:2:0 \rightarrow 92:2:6, *V* = 12 mL). Colorless oil, yield 40 mg (75%). The two enantiomers were separated by chiral, preparative HPLC (HPLC method G) with six separations. (1*S*,5*R*,7*R*)-**19a** fraction: 38 - 45 min, (1*R*,5*S*,7*S*)-**19a** fraction: 54 - 62 min. The solvents were removed *in vacuo*.

Chemical Formula: C₂₀H₂₆Cl₂N₂O (381.3 g/mol).

TLC: $R_f = 0.20$ ($\text{CH}_2\text{Cl}_2/\text{CH}_3\text{OH}/\text{NH}_4\text{OH}$ 95:4:1).

^1H NMR (600 MHz, $\text{DMSO-}d_6$): δ (ppm) = 1.51 – 1.64 (m, $7 \times 0.85 + 4 \times 0.15\text{H}$, 4- CH_2 , 9- CH_2 , 9- CH_2^* , $\text{N}(\text{CH}_2\text{CH}_2)_2$, $\text{N}(\text{CH}_2\text{CH}_2)_2^*$), 1.65 – 1.85 (m, $5 \times 0.85 + 8 \times 0.15\text{H}$, 4- CH_2 , 4- CH_2^* , 6- CH_2 , 6- CH_2^* , 7- CH_2 , 7- CH_2^* , $\text{N}(\text{CH}_2\text{CH}_2)_2^*$), 1.86 – 1.90 (m, 1H, 5- CH , 5- CH^*), 2.10 – 2.19 (m, 0.85H, 8- CH), 2.31 – 2.41 (m, 2×0.85 H, $\text{N}(\text{CH}_2\text{CH}_2)_2$), 2.45 – 2.52 (m, $2 \times 0.15\text{C}$, $\text{N}(\text{CH}_2\text{CH}_2)_2^*$), 2.57 – 2.70 (m, $2 \times 0.85 + 3 \times 0.15\text{H}$, 8- CH^* , $\text{N}(\text{CH}_2\text{CH}_2)_2$, $\text{N}(\text{CH}_2\text{CH}_2)_2^*$), 3.06 – 3.16 (m, 0.15H, 3- CH_2^*), 3.38 (td, $J = 13.4 / 5.1$ Hz, 0.85H, 3- CH_2), 3.59 – 3.68 (m, $2 \times 0.85\text{H}$, 3- CH_2 , CH_2 -aryl), 3.73 (d, $J = 15.9$ Hz, 0.15H, CH_2 -aryl*), 3.88 (d, $J = 15.9$ Hz, 0.15H, CH_2 -aryl*), 3.90 (d, $J = 16.1$ Hz, 0.85H, CH_2 -aryl), 4.13 – 4.23 (m, $2 \times 0.15\text{H}$, 1- CH^* , 3- CH_2^*), 4.81 – 4.86 (m, 0.85H, 1- CH), 7.16 (dd, $J = 8.2 / 2.0$ Hz, 0.15H, 6- $\text{CH}_{\text{arom}}^*$), 7.26 (dd, $J = 8.3 / 2.1$ Hz, 0.85H, 6- CH_{arom}), 7.43 (d, $J = 2.0$ Hz, 0.15H, 2- $\text{CH}_{\text{arom}}^*$), 7.51 – 7.56 (m, $2 \times 0.85 + 0.15\text{H}$, 2- CH_{arom} , 5- CH_{arom} , 5- $\text{CH}_{\text{arom}}^*$). Ratio of rotamers is 85:15. The signals for the minor rotamer are marked with an asterisk (*). The signal for $\text{N}(\text{CH}_2\text{CH}_2)_2^*$ is overlapping with the $\text{DMSO-}d_6$ signal.

^{13}C NMR (151 MHz, $\text{DMSO-}d_6$): δ (ppm) = 22.7 (1.7C, $\text{N}(\text{CH}_2\text{CH}_2)_2$), 22.9 (0.15C, $\text{N}(\text{CH}_2\text{CH}_2)_2^*$), 24.4 (0.15C, C-4/6/7*), 24.7 (0.85C, C-5), 24.8 (0.15C, C-5*), 28.0 (0.85C, C-7), 29.0 (0.15C, C-4/6/7*), 29.1 (0.85C, C-6), 29.4 (0.15C, C-4/6/7*), 29.9 (0.85C, C-4), 32.4 (0.85C, C-9), 33.5 (0.15C, C-9*), 38.0 (0.15C, CH_2 -aryl*), 43.3 (0.85C, C-3), 44.9 (0.85C, C-1), 50.4 (0.3C, $\text{N}(\text{CH}_2\text{CH}_2)_2$), 51.6 (0.15C, C-1*), 51.7 (1.7C, $\text{N}(\text{CH}_2\text{CH}_2)_2$), 63.3 (0.15C, C-8*), 65.2 (0.85C, C-8), 128.7 (0.15C, C-3/4 $_{\text{arom}}^*$), 128.8 (0.85C, C-3/4 $_{\text{arom}}$), 129.3 (0.85C, C-6 $_{\text{arom}}$), 129.95 (0.15C, C-6 $_{\text{arom}}^*$), 130.04 (0.85C, C-3/4 $_{\text{arom}}$), 130.2 (0.85C, C-5 $_{\text{arom}}$), 130.4 (0.15C, C-3/4 $_{\text{arom}}^*$), 130.69 (0.85C, C-2 $_{\text{arom}}$), 130.72 (0.15C, C-5 $_{\text{arom}}^*$), 131.5 (0.15C, C-2 $_{\text{arom}}^*$), 137.6 (0.85C, C-1 $_{\text{arom}}$), 138.1 (0.15C, C-1*), 168.6 (0.85C, $\text{N}(\text{C}=\text{O})$), 169.6 (0.15C, $\text{N}(\text{C}=\text{O})^*$). Ratio of rotamers is 85:15. The signals for the minor rotamer are marked with an asterisk (*). The signals for C-3* and CH_2 -aryl are overlapping with the $\text{DMSO-}d_6$ signal.

Purity (HPLC, method A): 99.5% ($t_R = 17.7$ min).

IR (neat): $\tilde{\nu}$ (cm^{-1}) = 2924 (C- H_{alip}), 1628 (C=O $_{\text{amide}}$), 1130, 1030 (C-N, C-O).

Exact mass (APCI): $m/z = 381.1464$ (calcd. 381.1495 for $\text{C}_{20}\text{H}_{27}^{35}\text{Cl}_2\text{N}_2\text{O}$ $[\text{M}+\text{H}]^+$).

Enantiomerically pure (1*S*,5*R*,7*R*)-**19a**:

Purity (HPLC, method A): 91.4% ($t_R = 18.1$ min).

Enantiomeric excess (chiral HPLC, method C): 99.9% ($t_R = 44.3$ min).

Enantiomeric excess (chiral HPLC, method D): 99.9% ($t_R = 15.4$ min).

Exact mass (APCI): $m/z = 381.1463$ (calcd. 381.1495 for $C_{20}H_{27}^{35}Cl_2N_2O$ $[M+H]^+$).

Specific rotation: $[\alpha]_{20}^D = -23.8$ ($c = 0.12$; CH_3CN).

Enantiomerically pure (1*R*,5*S*,7*S*)-**19a**:

Purity (HPLC, method A): 93.3% ($t_R = 18.2$ min).

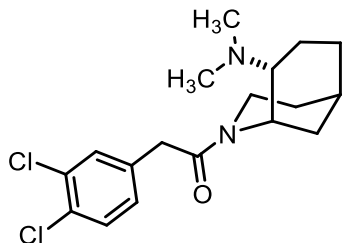
Enantiomeric excess (chiral HPLC, method C): 99.9% ($t_R = 38.6$ min).

Enantiomeric excess (chiral HPLC, method D): 99.9% ($t_R = 19.3$ min).

Exact mass (APCI): $m/z = 381.1438$ (calcd. 381.1495 for $C_{20}H_{27}^{35}Cl_2N_2O$ $[M+H]^+$).

Specific rotation: $[\alpha]_{20}^D = +22.6$ ($c = 0.12$; CH_3CN).

2-(3,4-Dichlorophenyl)-1-((1*RS*,5*SR*,8*SR*)-8-(dimethylamino)-2-azabicyclo[3.3.1]nonan-2-yl)ethan-1-one (19b)



$HN(CH_3)_2$ (2 M in THF, 0.3 mL, 0.61 mmol, 10 eq) and AcOH (12 μ L, 0.12 mmol, 2 eq) were added to a solution of **54** (20 mg, 0.06 mmol, 1 eq) in 1,2-dichloroethane (1 mL) and the mixture was stirred at room temperature for 30 min. Then, $NaBH(OAc)_3$ (26 mg, 0.12 mmol, 2 eq) was added and the mixture was stirred for 16 h. After addition of $NaHCO_3$ (5 mL), the mixture was extracted with CH_2Cl_2 (3×5 mL). The combined organic layers were dried (Na_2SO_4), filtered and concentrated *in vacuo*. The residue was purified by flash column chromatography ($\phi = 1.5$ cm, $h = 8$ cm, CH_2Cl_2/NH_3 (7 M in CH_3OH)/ CH_3OH 98:2:0 \rightarrow 95:2:3, $V = 12$ mL). Colorless oil, yield 6 mg (28%).

Chemical Formula: $C_{18}H_{24}Cl_2N_2O$ (355.3 g/mol).

TLC: $R_f = 0.21$ ($CH_2Cl_2/CH_3OH/NH_4OH$ 95:4:1).

1H NMR (600 MHz, $DMSO-d_6$): δ (ppm) = 1.53 – 1.59 (m, $3 \times 0.7H$, 4- CH_2 , 9- CH_2), 1.60 – 1.65 (m, $2 \times 0.3H$, 9- CH_2^*), 1.66 – 1.77 (m, $3 \times 0.7 + 5 \times 0.3H$, 4- CH_2 , 4- CH_2^* , 6- CH_2 , 6- CH_2^* , 7- CH_2 , 7- CH_2^*), 1.78 – 1.84 (m, 1.7H, 6- CH_2 , 7- CH_2 , 7- CH_2^*), 1.84 – 1.89 (m, 1H, 5- CH_{eq} , 5- CH_{eq}^*), 2.08 – 2.13 (m, 0.7H, 8- CH), 2.19 (s, $6 \times 0.7H$, $N(CH_3)_2$), 2.21 (s, $6 \times 0.3H$, $N(CH_3)_2^*$), 2.51 – 2.56 (m, 0.3H, 8- CH^*), 3.05 – 3.12 (m, 0.3H, 3- CH_{ax}^*), 3.41 (td, $J = 13.5 / 5.2$ Hz, 0.7H, 3- CH_{ax}), 3.64 (dd, $J = 14.0 / 7.6$ Hz, 0.7H,

3- CH_{eq}), 3.70 (d, $J = 16.0$ Hz, 0.7H, CH_2 -aryl), 3.80 (d, $J = 16.0$ Hz, 0.7H, CH_2 -aryl), 3.85 (d, $J = 15.9$ Hz, 0.3H, CH_2 -aryl*), 3.89 (d, $J = 15.9$ Hz, 0.3H, CH_2 -aryl*), 4.13 (dd, $J = 14.6 / 8.3$ Hz, 0.3H, 3- CH_{eq} *), 4.17 – 4.20 (m, 0.3H, 1- CH_{eq} *), 4.88 – 4.92 (m, 0.7H, 1- CH_{eq}), 7.16 (dd, $J = 8.2 / 2.0$ Hz, 0.3H, 6- CH_{arom} *), 7.24 (dd, $J = 8.2 / 2.0$ Hz, 0.7H, 6- CH_{arom}), 7.43 (d, $J = 2.0$ Hz, 0.3H, 2- CH_{arom} *), 7.52 – 7.56 (m, 1.7H, 2- CH_{arom} , 5- CH_{arom} , 5- CH_{arom} *). Ratio of rotamers is 7:3. The signals for the minor rotamer are marked with an asterisk (*).

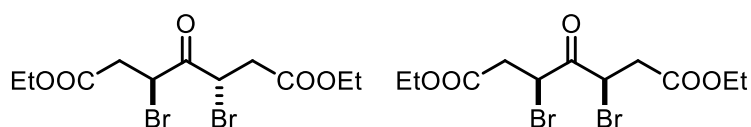
^{13}C NMR (151 MHz, DMSO- d_6): δ (ppm) = 21.7 (0.3C, C-7*), 24.5 (0.7C, C-5), 24.8 (0.3C, C-5*), 26.8 (0.7C, C-7), 28.8 (0.3C, C-4*), 29.37 (0.7C, C-6), 29.42 (0.3C, C-6*), 29.9 (0.7C, C-4), 32.7 (0.7C, C-9), 33.9 (0.3C, C-9*), 38.3 (0.3C, CH_2 -aryl*), 42.5 (0.6C, $N(CH_3)_2$ *), 43.0 (1.4C, $N(CH_3)_2$), 43.1 (0.7C, C-3), 43.4 (0.7C, C-1), 51.9 (0.3C, C-1*), 64.9 (0.3C, C-8*), 65.4 (0.7C, C-8), 128.7 (0.3C, C3/4 $_{arom}$ *), 128.8 (0.7C, C-3/4 $_{arom}$), 129.5 (0.7C, C-6 $_{arom}$), 129.99 (0.3C, C-5/6 $_{arom}$ *), 130.01 (0.3C, C-5/6 $_{arom}$ *), 130.2 (0.7C, C-5 $_{arom}$), 130.4 (0.3C, C-3/4 $_{arom}$ *), 130.6 (0.7C, C-3/4 $_{arom}$), 130.9 (0.7C, C-2 $_{arom}$), 131.5 (0.3C, C-2 $_{arom}$ *), 137.5 (0.7C, C-1 $_{arom}$), 138.1 (0.3C, C-1 $_{arom}$ *), 168.5 (0.7C, $N(C=O)$), 169.9 (0.3C, $N(C=O)$ *). Ratio of rotamers is 7:3. The signals for the minor rotamer are marked with an asterisk (*). The signals for C-3* and CH_2 -aryl are overlapping with the DMSO- d_6 signal.

Purity (HPLC, method A): 95.5% ($t_R = 17.2$ min).

IR (neat): $\tilde{\nu}$ (cm^{-1}) = 2924 (C- H_{alip}), 1628 (C=O $_{amide}$), 1130, 1030 (C-N, C-O).

Exact mass (APCI): $m/z = 355.1304$ (calcd. 355.1338 for $C_{18}H_{25}^{35}Cl_2N_2O$ [$M+H$] $^+$).

Diethyl (3*RS*,5*RS*)- and meso-3,5-dibromo-4-oxopimelate (59)¹⁴⁴



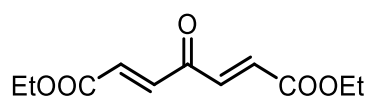
At 0 °C, a solution of Br_2 (4.8 mL, 93.2 mmol, 2 eq) in CH_2Cl_2 (20 mL) was added dropwise to a solution of diethyl 4-oxopimelate (10.0 mL, 46.6 mmol, 1 eq) in CH_2Cl_2 (60 mL) and the mixture was stirred at room temperature for 4 h. Then, the solution was washed with $NaHCO_3$ (40 mL), dried (Na_2SO_4), filtered and concentrated *in vacuo*. Yellow oil, yield 18.2 g (100%).

Chemical formula: $C_{11}H_{16}Br_2O_5$ (388.1 g/mol).

$^1\text{H NMR}$ (600 MHz, DMSO- d_6): δ (ppm) = 1.26 (t, $J = 7.1$ Hz, $6 \times 0.2\text{H}$, $2 \times \text{OCH}_2\text{CH}_3^*$), 1.27 (t, $J = 7.1$ Hz, $6 \times 0.8\text{H}$, $2 \times \text{OCH}_2\text{CH}_3$), 3.00 (dd, $J = 17.1 / 6.7$ Hz, 1.6H, $2 \times \text{CH}_2\text{COOEt}$), 3.01 (dd, $J = 17.3 / 6.8$ Hz, 0.4H, $2 \times \text{CH}_2\text{COOEt}^*$), 3.25 (dd, $J = 17.1 / 7.7$ Hz, 1.6H, $2 \times \text{CH}_2\text{COOEt}$), 3.30 (dd, $J = 17.3 / 7.7$ Hz, 0.4H, $2 \times \text{CH}_2\text{COOEt}^*$), 4.16 (q, $J = 7.1$ Hz, $4 \times 0.2\text{H}$, $2 \times \text{OCH}_2\text{CH}_3^*$), 4.18 (q, $J = 7.1$ Hz, $4 \times 0.8\text{H}$, $2 \times \text{OCH}_2\text{CH}_3$), 4.99 (dd, $J = 7.7 / 6.8$ Hz, 0.4H, $2 \times \text{CHBr}^*$), 5.33 (dd, $J = 7.7 / 6.7$ Hz, 1.6H, $2 \times \text{CHBr}$). Ratio of diastereomers is 8:2. The signals for the minor diastereomer are marked with an asterisk (*).

$^{13}\text{C NMR}$ (151 MHz, DMSO- d_6): δ (ppm) = 14.08 (0.4C, $\text{OCH}_2\text{CH}_3^*$), 14.11 (1.6C, OCH_2CH_3), 38.2 (1.6C, CH_2COOEt), 39.8 (0.4C, $\text{CH}_2\text{COOEt}^*$), 41.5 (1.6C, CHBr), 42.5 (0.4C, CHBr^*), 61.3 (1.6C, OCH_2CH_3), 61.4 (0.4C, $\text{OCH}_2\text{CH}_3^*$), 169.3 (1.6C, $\text{O}=\text{COEt}$), 169.8 (0.4C, $\text{O}=\text{COEt}^*$), 194.3 (0.8C, $\text{C}=\text{O}$), 197.6 (0.2C, $\text{C}=\text{O}^*$). Ratio of diastereomers is 8:2. The signals for the minor diastereomer are marked with an asterisk (*).

Diethyl (2*E*,5*E*)-4-oxohepta-2,5-dienedioate (**60**)¹⁴⁴

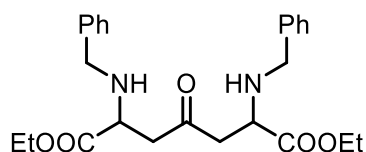


At 0 °C, NEt_3 (13.3 mL, 96.2 mmol, 2.05 eq) was added to a solution of **59** (18.2 g, 46.9 mmol, 1 eq) in CH_2Cl_2 (100 mL) and the mixture was stirred at room temperature for 30 min. Then, H_2O (80 mL) was added, the organic layer was separated and dried (Na_2SO_4), filtered and concentrated *in vacuo*. The residue was purified by flash column chromatography ($\varnothing = 8$ cm, $h = 15$ cm, cHex/EtOAc 1:0 \rightarrow 8:2, $V = 80$ mL). Yellow solid, mp 46 - 47 °C (lit.¹⁴⁴ 49 - 50 °C), 8.85 g (84%).

Chemical formula: $\text{C}_{11}\text{H}_{14}\text{O}_5$ (226.2 g/mol).

$^1\text{H NMR}$ (600 MHz, DMSO- d_6): δ (ppm) = 1.33 (t, $J = 7.2$ Hz, 6H, $2 \times \text{OCH}_2\text{CH}_3$), 4.28 (q, $J = 7.2$ Hz, 4H, $2 \times \text{OCH}_2\text{CH}_3$), 6.80 (d, $J = 15.9$ Hz, 2H, $2 \times \text{CH}=\text{CHCOOEt}$), 7.31 (d, $J = 15.9$ Hz, 2H, $2 \times \text{CH}=\text{CHCOOEt}$).

$^{13}\text{C NMR}$ (151 MHz, DMSO- d_6): δ (ppm) = 14.2 (2C, $2 \times \text{OCH}_2\text{CH}_3$), 61.8 (2C, $2 \times \text{OCH}_2\text{CH}_3$), 133.3 (2C, $2 \times \text{CH}=\text{CHCOOEt}$), 137.6 (2C, $2 \times \text{CH}=\text{CHCOOEt}$), 165.2 (2C, $2 \times \text{O}=\text{COEt}$), 188.4 (1C, $\text{C}=\text{O}$).

Diethyl 2,6-bis(benzylamino)-4-oxoheptanedioate (61)

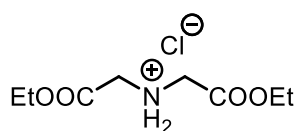
A solution of benzylamine (0.5 mL, 4.5 mmol, 1 eq) in THF (5 mL) was added dropwise to a solution of **60** (1.0 g, 4.5 mmol, 1 eq) in THF (15 mL) and the mixture was stirred at room temperature for 64 h. Then, the mixture was concentrated *in vacuo* and the residue was purified by flash column chromatography ($\varnothing = 4$ cm, $h = 16$ cm, cHex/EtOAc 9:1 \rightarrow 8:2, $V = 30$ mL). Yellow oil, yield 0.45 g (45%).

Chemical formula: C₂₅H₃₂N₂O₅ (440.5 g/mol).

¹H NMR (600 MHz, DMSO-*d*₆): δ (ppm) = 1.26 (t, $J = 7.1$ Hz, 6H, 2 \times OCH₂CH₃), 1.97 (brs, 2H, 2 \times NH), 2.71 – 2.88 (m, 4H, 2 \times NCHCH₂), 3.64 – 3.71 (m, 4H, 2 \times NCHCH₂, 2 \times CH₂-Ph), 3.85 (d, $J = 12.9$ Hz, 2H, 2 \times CH₂-Ph), 4.18 (q, $J = 7.1$ Hz, 4H, 2 \times OCH₂CH₃), 7.19 – 7.45 (m, 10H, 2 \times 2-CH_{arom}, 2 \times 3-CH_{arom}, 2 \times 4-CH_{arom}, 2 \times 5-CH_{arom}, 2 \times 6-CH_{arom}).

¹³C NMR (151 MHz, DMSO-*d*₆): δ (ppm) = 14.4 (2C, 2 \times OCH₂CH₃), 46.4 (2C, 2 \times NCHCH₂), 52.3 (2C, 2 \times CH₂-Ph), 56.6 (2C, 2 \times NCHCH₂), 61.2 (2C, 2 \times OCH₂CH₃), 127.3 (2C, 2 \times C-4_{arom}), 128.4 (4C, 2 \times C-2/3_{arom}, 2 \times C-5/6_{arom}), 128.5 (4C, 2 \times C-2/3_{arom}, 2 \times C-5/6_{arom}), 139.8 (2C, 2 \times C-1_{arom}), 174.0 (2C, 2 \times O=COEt), 205.7 (1C, C=O).

Exact mass (APCI): $m/z = 441.2484$ (calcd. 441.2384 for C₂₅H₃₃N₂O₅ [M-H]⁺).

Diethyl 2,2'-iminodiacetate·HCl (64)

At 0 °C, SOCl₂ (20.0 mL, 275 mmol, 1.5 eq) was added dropwise to a suspension of iminodiacetic acid (**63**) (24.4 g, 184 mmol, 1.0 eq) in EtOH abs. (200 mL). Afterwards, the reaction mixture was heated to reflux for 16 h. The solution was cooled down to room temperature and concentrated *in vacuo*. Colorless solid, mp 88 – 89 °C, yield 40.6 g (98%).

Chemical formula: C₈H₁₆ClNO₄ (225.7 g/mol).

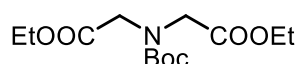
^1H NMR (600 MHz, DMSO- d_6): δ (ppm) = 1.24 (t, J = 7.1 Hz, 6H, 2 \times OCH₂CH₃), 3.70 (brs, 2H, NH₂⁺), 3.99 (s, 4H, 2 \times CH₂), 4.21 (q, J = 7.1 Hz, 4H, 2 \times OCH₂CH₃).

^{13}C NMR (151 MHz, DMSO- d_6): δ (ppm) = 13.9 (2C, 2 \times OCH₂CH₃), 46.4 (2C, 2 \times CH₂), 61.8 (2C, 2 \times OCH₂CH₃), 166.4 (2C, 2 \times O=COEt).

IR (neat): $\tilde{\nu}$ (cm⁻¹) = 2936 (C-H_{aliph}), 1736 (C=O_{ester}), 1204, 1076, 1015 (C-N, C-O).

Exact mass (APCI): m/z = 190.1073 (calcd. 190.1074 for C₈H₁₆NO₄ [M-Cl]⁺).

Diethyl 2,2'-[N-(*tert*-butoxycarbonyl)imino]diacetate (**62a**)



NaHCO₃ (22.8 g, 271 mmol, 3.0 eq) was added to a solution of **64** (20.4 g, 90.4 mmol, 1.0 eq) in THF (80 mL) and H₂O (20 mL). The reaction mixture was stirred for 30 min at room temperature. After the addition of Boc₂O (19.3 mL, 90.4 mmol, 1.0 eq), the mixture was stirred at room temperature for 16 h. Then, it was extracted with EtOAc (3 \times 50 mL), the combined organic layers were dried (Na₂SO₄), filtered and concentrated *in vacuo*. The residue was purified by flash column chromatography (\varnothing = 8 cm, h = 16 cm, cHex/EtOAc 8:2, V = 80 mL). Colorless oil, yield 19.9 g (76%).

Chemical formula: C₁₃H₂₃NO₆ (289.3 g/mol).

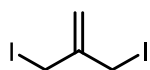
TLC: R_f = 0.36 (cHex/EtOAc 8:2).

^1H NMR (400 MHz, DMSO- d_6): δ (ppm) = 1.19 (t, J = 7.1 Hz, 3H, OCH₂CH₃), 1.20 (t, J = 7.1 Hz, 3H, OCH₂CH₃), 1.35 (s, 9H, C(CH₃)₃), 3.98 (s, 2H, NCH₂), 4.01 (s, 2H, NCH₂), 4.10 (q, J = 7.1 Hz, 2H, OCH₂CH₃), 4.12 (q, J = 7.1 Hz, 2H, OCH₂CH₃). Ratio of rotamers is 1:1.

^{13}C NMR (151 MHz, DMSO- d_6): δ (ppm) = 14.0 (1C, OCH₂CH₃), 14.1 (1C, OCH₂CH₃), 27.7 (3C, C(CH₃)₃), 49.2 (1C, CH₂), 49.7 (1C, CH₂), 60.4 (2C, OCH₂CH₃), 79.9 (1C, C(CH₃)₃), 154.6 (1C, N(C=O)O), 169.45 (1C, O=COEt), 169.53 (1C, O=COEt). Ratio of rotamers is 1:1.

IR (neat): $\tilde{\nu}$ (cm⁻¹) = 2978 (C-H_{aliph}), 1747 (C=O_{ester}), 1700 (C=O_{carbamate}), 1185, 1159, 1026 (C-N, C-O).

Exact mass (APCI): m/z = 290.1587 (calcd. 290.1598 for C₁₃H₂₄NO₆ [M+H]⁺).

3-Iodo-2-(iodomethyl)prop-1-ene (66)¹⁰⁴

NaI (17.8 g, 119 mmol, 2.5 eq) was added to a solution of 3-chloro-2-(chloromethyl)prop-1-ene (**65**) (5.50 mL, 47.5 mmol, 1.0 eq) in acetone (100 mL) and the mixture was stirred at reflux for 16 h. The suspension was cooled to room temperature and concentrated *in vacuo*. The residue was dissolved in H₂O (75 mL) and cHex (75 mL). After separation of the two layers, the organic layer was washed with Na₂SO₃ (2 × 50 mL) and H₂O (50 mL), dried (Na₂SO₄), filtered and concentrated *in vacuo*. Light green solid, mp 28 – 29 °C, yield 14.5 g (99%).

Chemical formula: C₄H₆I₂ (307.9 g/mol).

¹H NMR (600 MHz, CD₃OD): δ (ppm) = 4.21 (s, 4H, 2 × CH₂I), 5.40 (s, 2H, R₂C=CH₂).

¹³C NMR (151 MHz, CD₃OD): δ (ppm) = 6.6 (2C, 2 × CH₂I), 116.4 (1C, R₂C=CH₂), 146.0 (1C, R₂C=CH₂).

Exact mass (APCI): *m/z* = 308.8637 (calcd. 308.8632 for C₄H₇I₂ [M+H]⁺).

1-tert-Butyl 2,6-diethyl cis- and trans-4-methylenepiperidine-1,2,6-tricarboxylate (56)⁶⁰

At -78 °C, *n*-BuLi (1.6 M in *n*-hexane, 74.4 mL, 119 mmol, 2.1 eq) was added dropwise to a solution of *i*-Pr₂NH (16.7 mL, 119 mmol, 2.1 eq) in dry THF (170 mL). After the mixture was stirred for 1 h, a solution of **62a** (16.4 g, 56.7 mmol, 1.0 eq) in dry THF (15 mL) was added and the mixture was stirred for 1 h at -78 °C. Then, a solution of **66** (22.1 g, 68.1 mmol, 1.2 eq) in dry THF (15 mL) was added, the reaction mixture was stirred for 30 min at -78 °C and warmed up to room temperature over 16 h. At 0 °C, H₂O (150 mL) was added and the mixture was extracted with EtOAc (3 × 80 mL). The combined organic layers were dried (Na₂SO₄), filtered and concentrated *in vacuo*. The residue was purified twice by flash column chromatography (1. ø = 8 cm, *h* = 25 cm, cHex/EtOAc 9:1 → 8:2, *V* = 80 mL, 2. ø = 8 cm, *h* = 25 cm, cHex/EtOAc 9:1 → 8:2, *V* = 80 mL). Yellow oil, yield 14.8 g (77%).

Chemical fomula: C₁₇H₂₇NO₆ (341.4 g/mol).

TLC: R_f = 0.26 (cHex/EtOAc 8:2).

¹H NMR (600 MHz, CDCl₃): δ (ppm) = 1.25 (t, *J* = 7.1 Hz, 3H, OCH₂CH₃), 1.26 (t, *J* = 7.1 Hz, 3H, OCH₂CH₃), 1.42 (s, 9 × 0.9H, C(CH₃)₃), 1.47 (s, 9 × 0.1H, C(CH₃)₃*), 2.43 – 2.51 (m, 2 × 0.1H, 3/5-CH₂*), 2.65 (dd, *J* = 15.9 / 2.7 Hz, 1H, 3/5-CH₂), 2.74 (dd, *J* = 16.0 / 3.6 Hz, 1H, 3/5-CH₂), 2.79 – 2.87 (m, 2 × 0.9H, 3/5-CH₂), 4.09 – 4.24 (m, 4H, 2 × OCH₂CH₃), 4.60 (dd, *J* = 3.5 / 3.0 Hz, 1H, 2/6-CH), 4.69 (dd, *J* = 6.2 / 4.1 Hz, 1H, 2/6-CH), 4.83 (s, 2 × 0.9H, R₂C=CH₂), 4.92 (s, 2 × 0.1H, R₂C=CH₂*). Ratio of isomers is 9:1 (*trans*:*cis*). Signals for the *cis* diastereomer are marked with an asterisk (*).

¹³C NMR (151 MHz, CDCl₃): δ (ppm) = 14.3 (1C, OCH₂CH₃), 14.5 (1C, OCH₂CH₃), 28.3 (3 × 0.9C, C(CH₃)₃), 28.4 (3 × 0.1C, C(CH₃)₃*), 33.25 (0.9C, C-3/5), 33.34 (0.9C, C-3/5), 33.6 (2 × 0.1C, C-3*, C-5*), 54.6 (1C, C-2/6), 55.7 (1C, C-2/6), 61.0 (2 × 0.1C, OCH₂CH₃*), 61.2 (0.9C, OCH₂CH₃), 61.3 (0.9C, OCH₂CH₃), 81.17 (0.9C, C(CH₃)₃), 81.21 (0.1C, C(CH₃)₃*), 112.3 (0.9C, R₂C=CH₂), 112.7 (0.1C, R₂C=CH₂*), 137.5 (0.9C, R₂C=CH₂), 138.1 (0.1C, R₂C=CH₂*), 155.2 (0.1C, N(C=O)O*), 155.5 (0.9C, N(C=O)O), 171.3 (2 × 0.1C, O=COEt*), 172.8 (2 × 0.9C, O=COEt). Ratio of isomers is 9:1 (*trans*:*cis*). Signals for the *cis* diastereomer are marked with an asterisk (*).

Purity (HPLC, method A): 94.4% (*t_R* = 21.5 min).

IR (neat): $\tilde{\nu}$ (cm⁻¹) = 2978 (CH_{aliph}), 1740 (C=O_{ester}), 1701 (C=O_{carbamate}), 1655 (C=C), 1180, 1165, 1022 (C-N, C-O).

Exact mass (APCI): *m/z* = 342.1913 (calcd. 342.1911 for C₁₇H₂₈NO₆ [M+H]⁺).

Diethyl *cis*-4-methylenepiperidine-2,6-dicarboxylate (69) and Diethyl *trans*-4-methylenepiperidine-2,6-dicarboxylate (70)



CF₃COOH (6.5 mL, 87.9 mmol, 30 eq) was added to a solution of **56** (1.0 g, 2.9 mmol, 1.0 eq) in dry CH₂Cl₂ (50 mL) and the mixture was stirred at room temperature for 16 h. The next day, Na₂CO₃ was added, the layers were separated and the aqueous layer was extracted with CH₂Cl₂ (2 × 40 mL). The combined organic layers were dried (Na₂SO₄), filtered and concentrated *in vacuo*. The diastereomers were separated twice

by flash column chromatography (1. 50 g cartridge, cHex/EtOAc 8:2 → 6:4; 2. 25 g cartridge, cHex/EtOAc 8:2).

Chemical Formula: C₁₂H₁₉NO₄ (241.3 g/mol).

cis-**69**:

Yellow oil, yield 79 mg (11%).

TLC: R_f = 0.31 (cHex/EtOAc 1:1).

¹H NMR (600 MHz CDCl₃) δ = 1.29 (t, J = 7.1 Hz, 6H, 2 × OCH₂CH₃), 2.10 – 2.17 (m, 2H, 3-CH_{ax}, 5-CH_{ax}), 2.62 (dd, J = 13.5 / 2.7 Hz, 2H, 3-CH_{eq}, 5-CH_{eq}), 3.37 (dd, J = 11.8 / 3.0 Hz, 2H, 2-CH_{ax}, 6-CH_{ax}), 4.22 (dq, J = 7.1 / 1.4 Hz, 4H, 2 × OCH₂CH₃), 4.87 (t, J = 1.7 Hz, 2H, R₂C=CH₂). NH signal is missing.

¹³C NMR (151 MHz, CDCl₃) δ = 14.3 (2C, 2 × OCH₂CH₃), 37.7 (2C, C-3, C-5), 58.9 (2C, C-2, C-6), 61.4 (2C, 2 × OCH₂CH₃), 111.4 (1C, R₂C=CH₂), 142.5 (1C, C-4), 171.9 (2C, 2 × O=COEt).

IR (neat): $\tilde{\nu}$ (cm⁻¹) = 2982 (C-H_{aliph}), 1732 (C=O_{ester}), 1651 (C=C), 1180, 1026 (C-N, C-O).

Exact mass (APCI): m/z = 242.1360 (calcd. 242.1387 for C₁₂H₂₀NO₄ [M+H]⁺).

trans-**70**:

Yellow oil, yield 623 mg (89%).

TLC: R_f = 0.20 (cHex/EtOAc 1:1).

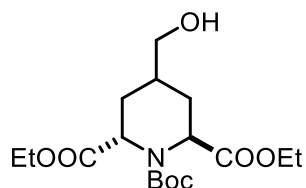
¹H NMR (600 MHz, CDCl₃): δ (ppm) = 1.29 (t, J = 7.1 Hz, 6H, 2 × OCH₂CH₃), 2.46 (dd, J = 13.2 / 7.0 Hz, 2H, 3-CH₂, 5-CH₂), 2.56 (dd, J = 13.2 / 5.0 Hz, 2H, 3-CH₂, 5-CH₂), 3.84 (dd, J = 7.0 / 5.0 Hz, 2H, 2-CH, 6-CH), 4.14 – 4.24 (m, 4H, 2 × OCH₂CH₃), 4.87 (s, 2H, R₂C=CH₂). NH signal is missing.

¹³C NMR (151 MHz, CDCl₃): δ (ppm) = 14.4 (2C, 2 × OCH₂CH₃), 36.3 (2C, C-3, C-5), 56.1 (2C, C-2, C-6), 61.2 (2C, 2 × OCH₂CH₃), 111.7 (1C, R₂C=CH₂), 141.3 (1C, C-4), 172.7 (2C, 2 × O=COEt).

IR (neat): $\tilde{\nu}$ (cm⁻¹) = 3356 (N-H), 2978 (C-H_{alip}), 1728 (C=O_{ester}), 1655 (C=C), 1200, 1165, 1026 (C-N, C-O).

Exact mass (APCI): m/z = 242.1373 (calcd. 242.1387 for C₁₂H₂₀NO₄ [M+H]⁺).

1-tert-Butyl trans-2,6-diethyl 4-(hydroxymethyl)piperidine-1,2,6-tricarboxylate (71)



9-BBN (0.5 M in THF, 24.0 mL, 12.0 mmol, 1.5 eq) was added dropwise to a solution of **56** (2.75 g, 8.0 mmol, 1.0 eq) in dry THF (55 mL) and the mixture was stirred at 50 °C for 16 h. Then at 0 °C, NaOH (2 M in H₂O, 8.0 mL, 16.0 mmol, 2 eq) and H₂O₂ (30% in H₂O, 9.1 mL, 80.4 mmol, 10.0 eq) were added slowly and the mixture was stirred at room temperature for 2 h. The layers were separated, and the aqueous layer was extracted with EtOAc (3 × 25 mL). The combined organic layers were dried (Na₂SO₄), filtered and concentrated *in vacuo*. The residue was purified by flash column chromatography (100 g cartridge, cHex/EtOAc 7:3 → 1:1). Colorless oil, yield 2.0 g (70%).

Chemical Formula: C₁₇H₂₉NO₇ (359.4 g/mol).

TLC: *R*_F = 0.27 (cHex/EtOAc 1:1).

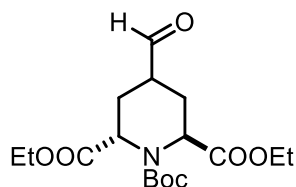
¹H NMR (600 MHz, DMSO-*d*₆): δ (ppm) = 1.12 – 1.29 (m, 7H, 2 × OCH₂CH₃, 3/5-CH₂), 1.37 (s, 9H, C(CH₃)₃), 1.35 – 1.41 (m, 1H, 4-CH), 1.42 – 1.51 (m, 1H, 3/5-CH₂), 1.91 – 2.11 (m, 2H, 3-CH₂, 5-CH₂), 3.17 – 3.23 (m, 2H, RCH₂OH), 3.95 (dd, *J* = 11.0 / 5.0 Hz, 0.83H, 2/6-CH), 3.98 – 4.21 (m, 4.17H, 2 × OCH₂CH₃, 2/6-CH*), 4.54 – 4.66 (m, 2H, 2/6-CH, RCH₂OH). Ratio of rotamers is 83:17. The signals for the minor rotamer are marked with an asterisk (*).

¹³C NMR (151 MHz, DMSO-*d*₆): δ (ppm) = 13.9 (0.17C, OCH₂CH₃*), 14.0 (0.83C, OCH₂CH₃), 14.1 (0.17C, OCH₂CH₃*), 14.2 (0.83C, OCH₂CH₃), 27.6 (3C, C(CH₃)₃), 28.5 (0.17C, C-3/5*), 28.7 (0.83C, C-3/5), 30.2 (0.17C, C-3/5*), 30.5 (0.83C, C-3/5), 32.0 (0.17C, C-4*), 32.1 (0.83C, C-4), 55.0 (0.17C, C-2/6*), 55.2 (1C, C-2/6), 55.5 (0.83C, C-2/6), 60.0 (0.83C, OCH₂CH₃), 60.2 (0.17C, OCH₂CH₃*), 60.7 (0.17C, OCH₂CH₃*), 60.9 (0.83C, OCH₂CH₃), 64.6 (0.17C, C(CH₃)₃*), 64.7 (0.83C, C(CH₃)₃), 64.6 (0.17C, R₂CH₂OH*), 64.7 (0.83, R₂CH₂OH), 155.59 (0.17C, N(C=O)O*), 155.65 (0.83C, N(C=O)O), 172.1 (0.83C, O=COEt), 172.3 (0.17C, O=COEt*), 172.5 (0.83C, O=COEt), 172.7 (0.17C, O=COEt*). Ratio of rotamers is 83:17. The signals for the minor rotamer are marked with an asterisk (*).

IR (neat): $\tilde{\nu}$ (cm⁻¹) = 3490 (O-H), 2981, 2935 (C-H_{aliph}), 1736 (C=O_{ester}), 1703 (C=O_{carbamate}), 1185, 1163, 1026 (C-N, C-O).

Exact mass (APCI): m/z = 360.2052 (calcd. 360.2017 for C₁₇H₃₀NO₇ [M+H]⁺).

1-*tert*-Butyl *trans*-2,6-diethyl 4-formylpiperidine-1,2,6-tricarboxylate (**72**)



Dess-Martin Periodinane (2.9 g, 6.7 mmol, 1.2 eq) was added to a solution of **71** (2.0 g, 5.6 mmol, 1.0 eq) in dry CH₂Cl₂ (100 mL) and the mixture was stirred at room temperature for 3 h. Afterwards, NaOH (2 M in H₂O, 15 mL) was added and the mixture was stirred at room temperature for 1 h. The mixture was extracted with CH₂Cl₂ (2 × 50 mL), the combined organic layers were dried (Na₂SO₄), filtered and concentrated *in vacuo*. The residue was purified by flash column chromatography (\varnothing = 4 cm, h = 17 cm, cHex/EtOAc 8:2 → 7:3, V = 80 mL). Colorless oil, yield 1.21 g (60%).

Chemical Formula: C₁₇H₂₇NO₇ (357.4 g/mol).

TLC: R_f = 0.25 (cHex/EtOAc 7:3).

¹H NMR (600 MHz, CDCl₃): δ (ppm) = 1.23 – 1.32 (m, 6H, 2 × OCH₂CH₃), 1.42 (s, 9H, C(CH₃)₃), 1.95 – 2.05 (m, 0.6H, 3/5-CH₂), 2.06 – 2.14 (m, 1H, 3/5-CH₂), 2.15 – 2.23 (m, 0.4H, 3/5-CH₂*), 2.26 – 2.53 (m, 3H, 3-CH₂, 4-CH, 5-CH₂), 4.10 – 4.28 (m, 4H, OCH₂CH₃), 4.42 (t, J = 5.7 Hz, 0.4H, 2/6-CH*), 4.45 (t, J = 6.1 Hz, 0.6H, 2/6-CH), 4.70 (d, J = 4.3 Hz, 0.6H, 2/6-CH), 4.80 – 4.85 (m, 0.4H, 2/6-CH), 9.60 (s, 0.4H, CHO*), 9.61 (s, 0.6H, CHO). Ratio of rotamers is 6:4. The signals for the minor rotamer are marked with an asterisk (*).

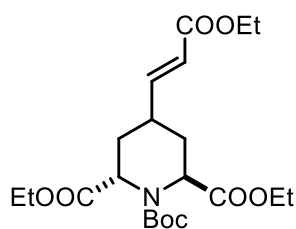
¹³C NMR (151 MHz, CDCl₃): δ (ppm) = 14.19 (0.6C, OCH₂CH₃), 14.23 (0.4C, OCH₂CH₃*), 14.3 (0.4C, OCH₂CH₃*), 14.5 (0.6C, OCH₂CH₃), 24.6 (0.4C, C-3/5*), 24.8 (0.6C, C-3/5), 25.0 (0.4C, C-3/5*), 25.7 (0.6C, C-3/5), 28.3 (3C, C(CH₃)₃), 41.0 (0.4C, C-4*), 41.3 (0.6C, C-4), 53.5 (0.4C, C-2*), 53.7 (0.6C, C-6), 54.1 (0.4C, C-6*), 54.6 (0.6C, C-2), 61.5 (0.8C, 2 × OCH₂CH₃*), 61.6 (1.2C, 2 × OCH₂CH₃), 81.5 (0.6C, C(CH₃)₃), 81.7 (0.4C, C(CH₃)₃*), 155.5 (0.4C, N(C=O)O*), 155.6 (0.6C, N(C=O)O), 172.48 (0.4C, O=COEt*), 172.50 (0.6C, O=COEt), 172.6 (0.6C, O=COEt), 172.8 (0.4C,

O=COEt*), 201.2 (1C, CHO). Ratio of rotamers is 6:4. The signals for the minor rotamer are marked with an asterisk (*).

IR (neat): $\tilde{\nu}$ (cm⁻¹) = 2977 (C-H_{aliph}), 1733 (C=O_{ester, aldehyde}), 1700 (C=O_{carbamate}), 1186, 1162, 1026 (C-N, C-O).

Exact mass (APCI): m/z = 358.1870 (calcd. 358.1860 for C₁₇H₂₈NO₇ [M+H]⁺).

1-tert-Butyl trans-2,6-diethyl 4-[(E)-2-(ethoxycarbonyl)vinyl]piperidine-1,2,6-tricarboxylate (73)



4-(Ethoxycarbonylmethylene)triphenylphosphorane (**33**) (1.53 g, 4.40 mmol, 1.3 eq) was added to a solution of **72** (1.21 g, 3.39 mmol, 1.0 eq) in dry CH₂Cl₂ (50 mL) and the mixture was stirred at 40 °C for 3 h. After the mixture was concentrated *in vacuo*, the residue was purified by flash column chromatography (100 g cartridge, cHex/EtOAc 8:2 → 7:3). Colorless oil, yield 1.04 g (71%).

Chemical Formula: C₂₁H₃₃NO₈ (427.5 g/mol).

TLC: R_f = 0.31 (cHex/EtOAc 8:2).

¹H NMR (600 MHz, CDCl₃): δ (ppm) = 1.23 - 1.31 (m, 9H, 3 × OCH₂CH₃), 1.41 (s, 9H, C(CH₃)₃), 1.54 - 1.62 (m, 1H, 5-CH₂, 5-CH₂*), 1.80 (ddd, J = 13.6 / 12.6 / 6.1 Hz, 1H, 3-CH₂), 2.11 - 2.30 (m, 3H, 3-CH₂, 4-CH, 5-CH₂), 4.09 - 4.32 (m, 7H, 6-CH₂, 6-CH₂*, 3 × OCH₂CH₃), 4.72 (d, J = 5.2 Hz, 0.6H, 2-CH), 4.83 (d, J = 3.6 Hz, 0.4H, 2-CH*), 5.80 (dd, J = 15.8 / 1.2 Hz, 1H, R₂CH=CHCOOEt), 6.80 (dd, J = 15.8 / 6.6 Hz, 1H, R₂CH=CHCOOEt). Ratio of rotamers is 6:4. The signals for the minor rotamer are marked with an asterisk (*).

¹³C NMR (151 MHz, CDCl₃): δ (ppm) = 14.2 (1C, OCH₂CH₃), 14.4 (1C, OCH₂CH₃), 14.5 (1C, OCH₂CH₃), 28.2 (3C, C(CH₃)₃), 30.8 (0.4C, C-3*), 31.0 (0.6C, C-3), 32.4 (0.4C, C-4*), 32.4 (0.6C, C-4), 32.7 (0.4C, C-5*), 32.8 (0.6C, C-5), 55.3 (0.4C, C-2*), 55.4 (0.6C, C-6), 55.5 (0.4C, C-6*), 55.9 (0.6C, C-2), 60.6 (1C, OCH₂CH₃), 61.2 (1C, OCH₂CH₃), 61.6 (1C, OCH₂CH₃), 81.5 (0.6C, C(CH₃)₃), 82.0 (0.4C, C(CH₃)₃*), 121.3 (1C, CH=CHCOOEt), 149.7 (1C, CH=CHCOOEt), 156.2 (1C, N(C=O)O), 166.3 (1C, O=COEt), 172.5 (0.4C, O=COEt*), 172.6 (0.6C, O=COEt),

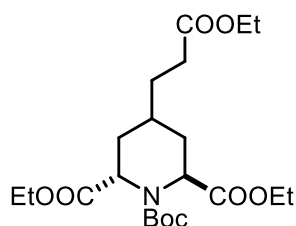
172.6 (0.6C, O=COEt), 172.9 (0.4C, O=COEt*). Ratio of rotamers is 6:4. The signals for the minor rotamer are marked with an asterisk (*).

Purity (HPLC, method A): 88.1% (t_R = 22.1 min).

IR (neat): $\tilde{\nu}$ (cm^{-1}) = 2980 (C-H_{aliph}), 1737 (C=O_{ester}), 1706 (C=O_{carbamate}), 1654 (C=C), 1180, 1160, 1029 (C-N, C-O).

Exact mass (APCI): m/z = 428.2283 (calcd. 428.2279 for C₂₁H₃₄NO₈ [M+H]⁺).

1-tert-Butyl trans-2,6-diethyl 4-(3-ethoxy-3-oxopropyl)piperidine-1,2,6-tricarboxylate (74)



Pd(OH)₂ (118 mg) was added to a solution of α,β -unsaturated ester **73** (2.36 g, 5.52 mmol, 1.0 eq) in EtOH abs. (20 mL) and the suspension was stirred at room temperature for 16 h under H₂ (5 bar). The mixture was filtered over Celite[®] and the filtrate was concentrated *in vacuo*. Colorless oil, yield 2.33 g (98%).

Chemical Formula: C₂₁H₃₅NO₈ (429.5 g/mol).

TLC: R_f = 0.34 (cHex/EtOAc 7:3).

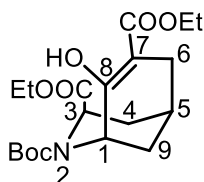
¹H NMR (600 MHz, CDCl₃): δ (ppm) = 1.21 - 1.32 (m, 9H, 3 × OCH₂CH₃), 1.32 - 1.44 (m, 11H, C(CH₃)₃, 3/5-CH₂, 4-CH), 1.47 - 1.69 (m, 3H, 3/5-CH₂, CH₂CH₂COOEt), 2.00 - 2.23 (m, 2H, 3-CH₂, 5-CH₂), 2.25 - 2.32 (m, 2H, CH₂CH₂COOEt), 4.05 - 4.32 (m, 7H, 3 × OCH₂CH₃, 2/6-CH, 2/6-CH_a*), 4.67 (d, J = 4.9 Hz, 0.6H, 2/6-CH), 4.74 - 4.83 (m, 0.4H, 2/6-CH*). Ratio of rotamers is 6:4. The signals for the minor rotamer are marked with an asterisk (*).

¹³C NMR (600 MHz, CDCl₃): δ (ppm) = 14.3 (1C, OCH₂CH₃), 14.4 (1C, OCH₂CH₃), 14.5* (1C, OCH₂CH₃), 28.2 (3C, C(CH₃)₃), 29.4 (1C, C-4), 31.1 (1C, CH₂CH₂COOEt), 31.6 (1C, CH₂CH₂COOEt), 32.2 (1C, C-3/5), 34.0 (1C, C-3/5), 56.0* (1C, C-2/6), 56.4* (1C, C-2/6), 60.6 (1C, OCH₂CH₃), 61.1* (1C, OCH₂CH₃), 61.4* (1C, OCH₂CH₃), 81.2* (1C, C(CH₃)₃), 156.4* (1C, N(C=O)O), 172.9* (1C, O=COEt), 173.1* (1C, O=COEt), 173.2 (1C, O=COEt). Several signals show broadened singlets which are caused by rotamers. The signals are marked with an asterisk (*).

IR (neat): $\tilde{\nu}$ (cm⁻¹) = 2978, 2932 (C-H_{aliph}), 1736 (C=O_{ester}), 1705 (C=O_{carbamate}), 1180, 1161, 1096, 1026 (C-N, C-O).

Exact mass (APCI): m/z = 430.2410 (calcd. 430.2435 for C₂₁H₃₆NO₈ [M+H]⁺).

2-tert-Butyl 3,7-diethyl (1*RS*,3*RS*,5*RS*)-8-hydroxy-2-azabicyclo[3.3.1]non-7-ene-2,3,7-tricarboxylate (75)



NaHMDS (1.9 M in THF, 7.13 mL, 13.5 mmol, 2.5 eq) was added to a refluxing solution of **74** (2.33 g, 5.42 mmol, 1.0 eq) in THF (270 mL) under N₂ and the mixture was heated to reflux for 2 h. Then, the mixture was poured into a half-sat. NH₄Cl solution (250 mL). The mixture was extracted with EtOAc (3 × 100 mL), the combined organic layers were dried (Na₂SO₄), filtered and concentrated *in vacuo*. The residue was purified by flash column chromatography (100 g cartridge, cHex/EtOAc 9:1). Colorless solid, mp 87 - 88 °C, yield 1.38 g (66%).

Chemical Formula: C₁₉H₂₉NO₇ (383.4 g/mol).

TLC: R_f = 0.46 (cHex/EtOAc 8:2).

¹H NMR (600 MHz, CDCl₃): δ (ppm) = 1.19 (t, J = 7.1 Hz, 1.5H, OCH₂CH₃), 2.21 (t, J = 7.1 Hz, 1.5H, OCH₂CH₃), 1.28 (t, J = 7.1 Hz, 3.0H, OCH₂CH₃), 1.46 (s, 4.5H, C(CH₃)₃), 1.52 (s, 4.5H, C(CH₃)₃), 1.68 – 1.79 (m, 2H, 9-CH₂), 1.88 – 1.97 (m, 1H, 4-CH₂), 2.24 (bs, 1H, 5-CH), 2.27 (dd, J = 16.9 / 12.8 Hz, 1H, 6-CH₂), 2.39 (dt, J = 16.9 / 7.0 Hz, 1H, 6-CH₂), 2.47 (t, J = 13.7 Hz, 1H, 4-CH₂), 3.79 (dq, J = 10.7 / 7.2 Hz, 0.5H, OCH₂CH₃), 3.83 (dq, J = 10.7 / 7.2 Hz, 0.5H, OCH₂CH₃), 4.02 (dq, J = 10.7 / 7.2 Hz, 0.5H, OCH₂CH₃), 4.08 (dq, J = 10.7 / 7.2 Hz, 0.5H, OCH₂CH₃), 4.18 (q, J = 7.2 Hz, 2H, OCH₂CH₃), 4.65 (d, J = 7.9 Hz, 0.5H, 3-CH), 4.72 (t, J = 3.2 Hz, 0.5H, 1-CH), 4.80 (d, J = 7.9 Hz, 0.5H, 3-CH), 4.90 (t, J = 3.0 Hz, 0.5H, 1-CH), 11.68 (s, 0.5H, 8-COH), 11.69 (s, 0.5H, 8-COH). Ratio of rotamers is 1:1.

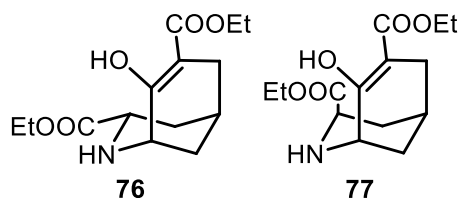
¹³C NMR (151 MHz, CDCl₃): δ (ppm) = 14.0 (0.5C, OCH₂CH₃), 14.2 (0.5C, OCH₂CH₃), 14.35 (0.5C, OCH₂CH₃), 14.37 (0.5C, OCH₂CH₃), 23.95 (0.5C, C-5), 24.00 (0.5C, C-5), 27.67 (0.5C, C-6), 27.73 (0.5C, C-6), 28.3 (1.5C, C(CH₃)₃), 28.5 (1.5C, C(CH₃)₃), 29.9 (0.5C, C-9), 30.2 (0.5C, C-9), 30.3 (0.5C, C-4), 30.5 (0.5C, C-4), 46.6 (0.5C, C-1), 48.3 (0.5C, C-1), 50.4 (0.5C, C-3), 51.6 (0.5C, C-3), 60.7 (1C, OCH₂CH₃), 61.32 (0.5C,

OCH₂CH₃), 61.34 (0.5C, OCH₂CH₃), 80.6 (0.5C, C(CH₃)₃), 80.8 (0.5C, C(CH₃)₃), 98.8 (0.5C, C-8), 98.8 (0.5C, C-8), 155.0 (0.5C, N(C=O)O), 155.2 (0.5C, N(C=O)O), 167.1 (0.5C, C-7), 167.4 (0.5C, C-7), 171.9 (0.5C, O=COEt), 172.09 (0.5C, O=COEt), 172.12 (0.5C, O=COEt), 172.3 (0.5C, O=COEt). Ratio of rotamers is 1:1.

IR (neat): $\tilde{\nu}$ (cm⁻¹) = 2977, 2931 (C-H_{aliph}), 1695 (C=O_{ester, carbamate}), 1662 (C=O_{unsat. ester}), 1621 (C=C), 1203, 1170, 1065, 1031 (C-N, C-O).

Exact mass (APCI): m/z = 384.2041 (calcd. 384.2017 for C₁₉H₃₀NO₇ [M+H]⁺).

Diethyl (1*RS*,3*RS*,5*RS*)-8-hydroxy-2-azabicyclo[3.3.1]non-7-ene-3,7-dicarboxylate (76) and Diethyl (1*RS*,3*SR*,5*RS*)-8-hydroxy-2-azabicyclo[3.3.1]non-7-ene-3,7-dicarboxylate (77)



TFA (3.71 mL, 48.2 mmol, 10 eq) was added to a solution of **75** (1.85 g, 4.82 mmol, 1.0 eq) in dry CH₂Cl₂ (20 mL) and the mixture was stirred at room temperature for 16 h. Then, NaHCO₃ was added, the mixture was extracted with CH₂Cl₂ (3 × 20 mL), the combined organic layers were dried (Na₂SO₄), filtered and concentrated *in vacuo*. The residue was purified twice by flash column chromatography (1. 50 g cartridge, cHex/EtOAc 8:2 → 7:3; 2. 25 g cartridge, cHex/EtOAc 8:2 → 7:3). At first **76**, then **77** was eluted.

Chemical Formula: C₁₄H₂₁NO₅ (283.3 g/mol).

76: Colorless oil, yield 253 mg (19%).

TLC: R_f = 0.30 (cHex/EtOAc 7:3).

¹H NMR (600 MHz, CDCl₃): δ (ppm) = 1.26 (t, J = 7.1 Hz, 3H, OCH₂CH₃), 1.33 (t, J = 7.1 Hz, 3H, OCH₂CH₃), 1.72 (dtd, J = 12.7 / 3.2 / 2.1 Hz, 1H, 9-CH_{eq}), 1.78 (mdd, J = 4.2 / 1.1 Hz, 1H, 4-CH_{ax}), 1.90 (dm, J = 13.2 Hz, 1H, 4-CH_{eq}), 1.98 (dt, J = 12.6 / 2.5 Hz, 1H, 9-CH_{ax}), 2.22 (dt, J = 16.9 / 1.2 Hz, 1H, 6-CH₂), 2.28 (s, 1H, 5-CH), 2.50 (ddd, J = 17.0 / 6.7 / 1.4 Hz, 1H, 6-CH₂), 3.55 (t, J = 3.5 Hz, 1H, 1-CH), 3.62 (dd, J = 12.5 / 3.8 Hz, 1H, 3-CH_{ax}), 4.13 – 4.20 (m, 2H, OCH₂CH₃), 4.21 – 4.27 (m, 2H, OCH₂CH₃), 11.88 (s, 1H, 8-COH).

¹³C NMR (151 MHz, CDCl₃): δ (ppm) = 14.3 (1C, OCH₂CH₃), 14.4 (1C, OCH₂CH₃), 25.4 (1C, C-5), 28.6 (1C, C-6), 30.0 (1C, C-9), 35.4 (1C, C-4), 50.5 (1C, C-1), 51.5 (1C, C-3), 60.7 (1C, OCH₂CH₃), 61.1 (1C, OCH₂CH₃), 99.0 (1C, C-7), 167.7 (1C, C-8), 172.0 (1C, O=COEt), 173.3 (1C, O=COEt).

Purity (HPLC, method A): 95.5% (t_R = 13.3 min).

IR (neat): $\tilde{\nu}$ (cm⁻¹) = 2936 (C-H_{alip}), 1736 (C=O_{ester}), 1655 (C=O_{unsat. ester}), 1612 (C=C), 1261, 1200, 1026 (C-N, C-O).

Exact mass (APCI): m/z = 284.1490 (calcd. 284.1492 for C₁₄H₂₂NO₅ [M+H]⁺).

77: Colorless solid, mp 48 - 49 °C, yield 850 mg (62%).

TLC: R_f = 0.17 (cHex/EtOAc 7:3).

¹H NMR (600 MHz, CDCl₃): δ (ppm) = 1.23 (t, J = 7.2 Hz, 3H, OCH₂CH₃), 1.29 (t, J = 7.1 Hz, 3H, OCH₂CH₃), 1.68 (dm, J = 12.5 Hz, 1H, 9-CH₂), 1.93 (dt, J = 12.5 / 3.1 Hz, 1H, 9-CH₂), 2.04 (dddd, J = 14.0 / 7.5 / 4.9 / 0.8 Hz, 1H, 4-CH_{ax}), 2.16 – 2.23 (m, 1H, 5-CH), 2.29 (d, J = 16.6 Hz, 1H, 6-CH₂), 2.36 (dd, J = 16.6 / 6.4 Hz, 1H, 6-CH₂), 2.39 (dm, J = 14.0 Hz, 1H, 4-CH_{eq}), 2.50 (brs, 1H, NH), 3.37 (t, J = 3.1 Hz, 1H, 1-CH), 3.53 (d, J = 7.5 Hz, 1H, 3-CH_{eq}), 3.91 (dq, J = 10.8 / 7.1 Hz, 1H, OCH₂CH₃), 4.01 (dq, J = 10.8 / 7.1 Hz, 1H, OCH₂CH₃), 4.14 – 4.22 (m, 2H, OCH₂CH₃), 11.80 (s, 1H, 8-COH).

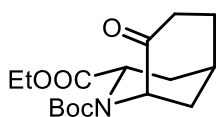
¹³C NMR (151 MHz, CDCl₃): δ (ppm) = 14.1 (1C, OCH₂CH₃), 14.4 (1C, OCH₂CH₃), 24.4 (1C, C-5), 28.2 (1C, C-6), 30.0 (1C, C-9), 30.2 (1C, C-4), 49.2 (1C, C-1), 52.1 (1C, C-3), 60.6 (1C, OCH₂CH₃), 61.1 (1C, OCH₂CH₃), 98.3 (1C, C-7), 169.5 (1C, C-8), 172.2 (1C, O=COEt), 174.2 (1C, O=COEt).

Purity (HPLC, method A): 99.6% (t_R = 13.1 min).

IR (neat): $\tilde{\nu}$ (cm⁻¹) = 3368 (N-H, O-H), 2928, 2909 (C-H_{alip}), 1724 (C=O_{ester}), 1651 (C=O_{unsat. ester}), 1609 (C=C), 1261, 1200, 1026 (C-N, C-O).

Exact mass (APCI): m/z = 284.1491 (calcd. 284.1492 for C₁₄H₂₂NO₅ [M+H]⁺).

2-tert-Butyl 3-ethyl (1RS,3RS,5RS)-8-oxo-2-azabicyclo[3.3.1]nonane-2,3-dicarboxylate (78)



LiCl (166 mg, 3.91 mmol 5.0 eq) and H₂O (3 drops) were added to a solution of **75** (300 mg, 0.78 mmol, 1.0 eq) in DMSO (3 mL). The mixture was stirred at 160 °C for 2 h. Then, it was added to H₂O (30 mL), the mixture was extracted with EtOAc

(3 × 20 mL), the combined organic layers were dried (Na₂SO₄), filtered and concentrated *in vacuo*. The residue was purified by flash column chromatography (25 g cartridge, cHex/EtOAc 9:1 → 8:1). Colorless solid, mp 69 - 70 °C, yield 28 mg (12%).

Chemical Formula: C₁₆H₂₅NO₅ (311.4 g/mol).

TLC: R_f = 0.39 (cHex/EtOAc 7:3).

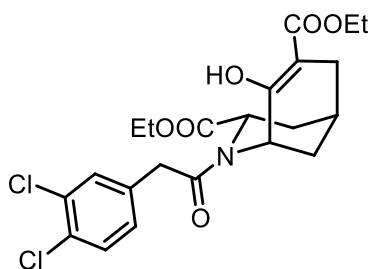
¹H NMR (600 MHz, CDCl₃): δ (ppm) = 1.28 (t, *J* = 7.0 Hz, 3H, OCH₂CH₃), 1.42 (s, 9H, C(CH₃)₃), 1.74 (d, *J* = 14.6 Hz, 1H, 9-CH₂), 1.84 – 1.89 (m, 2H, 6-CH₂), 2.08 – 2.20 (m, 3H, 9-CH₂, 4-CH₂, 7-CH₂), 2.20 – 2.26 (m, 1H, 5-CH), 2.70 – 2.80 (m, 1H, 4-CH₂), 2.91 (dt, *J* = 12.9 / 10.5 Hz, 1H, 7-CH₂), 4.09 (s, 1H, 1-CH), 4.16 – 4.25 (m, 2H, OCH₂CH₃), 4.85 (d, *J* = 8.5 Hz, 1H, 3-CH_{ax}).

¹³C NMR (151 MHz, CDCl₃): δ (ppm) = 14.3 (1C, OCH₂CH₃), 23.1 (1C, C-5), 28.3 (3C, C(CH₃)₃), 30.6 (1C, C-4), 31.9 (1C, C-9), 33.9 (1C, C-7), 35.1 (1C, C-6), 50.5 (1C, C-3), 60.5 (1C, C-1), 61.8 (1C, OCH₂CH₃), 81.6 (1C, C(CH₃)₃), 155.6 (1C, N(C=O)O), 173.8 (1C, O=COEt), 210.6 (1C, C-8).

IR (neat): $\tilde{\nu}$ (cm⁻¹) = 2974, 2936 (C-H_{alip}), 1701 (C=O_{ester, ketone, carbamate}), 1227, 1169, 1084 (C-N, C-O).

Exact mass (APCI): *m/z* = 312.1800 (calcd. 312.1805 for C₁₆H₂₆NO₅ [M+H]⁺).

Diethyl (1*RS*,3*RS*,5*RS*)-2-[2-(3,4-dichlorophenyl)acetyl]-8-hydroxy-2-azabicyclo[3.3.1]non-7-ene-3,7-dicarboxylate (79)



At 0 °C, a solution of **53** (300 mg, 1.34 mmol, 1.5 eq) in dry CH₂Cl₂ (2 mL) was added to a mixture of **76** (253 mg, 0.89 mmol, 1.0 eq) and DIPEA (0.25 mL, 1.34 mmol, 1.5 eq) in dry CH₂Cl₂ (3 mL). The mixture was stirred at room temperature for 2 h, then it was washed with NaHCO₃ (5 mL) and brine (5 mL). The organic layer was dried (Na₂SO₄), filtered and concentrated *in vacuo*. The residue was purified by flash column chromatography (25 g cartridge, cHex/EtOAc 85:15 → 75:25). Colorless solid, mp 96 - 97 °C, yield 330 mg (79%).

Chemical Formula: C₂₂H₂₅Cl₂NO₆ (470.3 g/mol).

TLC: $R_f = 0.53$ (cHex/EtOAc 7:3).

¹H NMR (600 MHz, CDCl₃): δ (ppm) = 1.25 (t, $J = 7.2$ Hz, 3H, OCH₂CH₃), 1.32 (t, $J = 7.1$ Hz, 3H, OCH₂CH₃), 1.74 (dm, $J = 13.3$ Hz, 1H, 9-CH₂), 1.86 (dddd, $J = 14.3 / 6.0 / 3.6 / 1.5$ Hz, 1H, 4-CH), 2.03 (dt, $J = 13.3 / 2.8$ Hz, 1H, 9-CH₂), 2.17 (ddd, $J = 14.3 / 8.7 / 6.9$ Hz, 1H, 4-CH_{ax}), 2.24 (d, $J = 16.9$ Hz, 1H, 6-CH₂), 2.32 (bs, 1H, 5-CH_{eq}), 2.42 (dd, $J = 16.9 / 5.7$ Hz, 1H, 6-CH₂), 4.01 (d, $J = 16.3$ Hz, 1H, CH₂-aryl), 4.05 (d, $J = 16.3$ Hz, 1H, CH₂-aryl), 4.14 (dd, $J = 8.7 / 6.0$ Hz, 1H, 3-CH_{ax}), 4.18 (q, $J = 7.1$ Hz, 2H, OCH₂CH₃), 4.21 – 4.27 (m, 2H, OCH₂CH₃), 4.40 (t, $J = 3.2$ Hz, 1H, 1-CH_{eq}), 7.15 (dd, $J = 8.2 / 2.0$ Hz, 1H, 6-CH_{arom}), 7.38 (d, $J = 8.2$ Hz, 1H, 5-CH_{arom}), 7.40 (d, $J = 2.0$ Hz, 1H, 2-CH_{arom}), 12.01 (s, 1H, 8-COH).

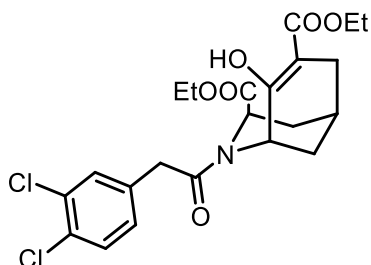
¹³C NMR (151 MHz, CDCl₃): δ (ppm) = 14.3 (1C, OCH₂CH₃), 14.4 (1C, OCH₂CH₃), 22.9 (1C, C-5), 28.3 (1C, C-9), 29.0 (1C, C-6), 32.8 (1C, C-4), 39.7 (1C, CH₂-aryl), 50.4 (1C, C-1), 52.4 (1C, C-3), 61.2 (1C, OCH₂CH₃), 61.3 (1C, OCH₂CH₃), 98.5 (1C, C-7), 129.0 (1C, C-6_{arom}), 130.5 (1C, C-5_{arom}), 131.0 (1C, C-3/4_{arom}), 131.5 (1C, C-2_{arom}), 132.5 (1C, C-3/4_{arom}), 135.6 (1C, C-1_{arom}), 166.6 (1C, C-8), 172.2 (1C, O=COEt), 172.6 (1C, O=COEt), 173.0 (1C, N(C=O)).

Purity (HPLC, method A): 89.2% ($t_R = 23.9$ min).

IR (neat): $\tilde{\nu}$ (cm⁻¹) = 2978, 2928 (C-H_{alip}), 1744 (C=O_{ester}), 1651 (C=O_{amide}), 1616 (C=C), 1261, 1196, 1169, 1030 (C-N, C-O).

Exact mass (APCI): $m/z = 470.1154$ (calcd. 470.1132 for C₂₂H₂₆³⁵Cl₂NO₆ [M+H]⁺).

Diethyl (1*RS*,3*SR*,5*RS*)-2-[2-(3,4-dichlorophenyl)acetyl]-8-hydroxy-2-azabicyclo[3.3.1]non-7-ene-3,7-dicarboxylate (80)



At 0 °C, a solution of **53** (1.0 g, 4.5 mmol, 1.5 eq) in dry CH₂Cl₂ (5 mL) was added to a mixture of **77** (850 mg, 3.0 mmol, 1.0 eq) and DIPEA (0.8 mL, 4.5 mmol, 1.5 eq) in dry CH₂Cl₂ (10 mL). The mixture was stirred at room temperature for 2 h, then it was washed with NaHCO₃ (15 mL) and brine (15 mL). The organic layer was dried (Na₂SO₄), filtered and concentrated *in vacuo*. The residue was purified by flash column

chromatography (50 g cartridge, cHex/EtOAc 85:15 → 65:35). Colorless solid, mp 111 - 112 °C, yield 1.33 g (94%).

Chemical Formula: C₂₂H₂₅Cl₂NO₆ (470.3 g/mol).

TLC: R_f = 0.40 (cHex/EtOAc 7:3).

¹H NMR (600 MHz, CDCl₃): δ (ppm) = 1.18 (t, *J* = 7.1 Hz, 3 × 0.75H, OCH₂CH₃), 1.22 (t, *J* = 7.1 Hz, 3 × 0.25H, OCH₂CH₃*), 1.29 (t, *J* = 7.1 Hz, 3H, OCH₂CH₃), 1.66 (dt, *J* = 12.9 / 2.9 Hz, 0.75H, 9-CH₂), 1.71 (dt, *J* = 13.0 / 3.0 Hz, 0.25H, 9-CH₂*), 1.74 – 1.82 (m, 1.25H, 9-CH₂, 9-CH₂*, 4-CH₂*), 1.91 (ddd, *J* = 14.1 / 8.4 / 4.8 Hz, 0.75H, 4-CH₂), 2.25 – 2.30 (m, 1H, 5-CH_{eq}, 5-CH_{eq}*), 2.32 (d, *J* = 17.0 Hz, 0.75H, 6-CH₂), 2.34 (d, *J* = 16.8 Hz, 0.25H, 6-CH₂*), 2.39 – 2.45 (m, 1H, 6-CH₂, 6-CH₂*), 2.50 – 2.56 (m, 1H, 4-CH₂, 4-CH₂*), 3.62 (d, *J* = 15.8 Hz, 0.25H, CH₂-aryl*), 3.74 (d, *J* = 15.8 Hz, 0.25H, CH₂-aryl*), 3.84 (dq, *J* = 10.8 / 7.2 Hz, 0.75H, OCH₂CH₃), 3.86 (d, *J* = 15.8 Hz, 0.75H, CH₂-aryl), 3.92 (dq, *J* = 10.7 / 7.1 Hz, 0.25H, OCH₂CH₃*), 4.01 (dq, *J* = 10.7 / 7.2 Hz, 0.75H, OCH₂CH₃), 4.02 (d, *J* = 15.8 Hz, 0.75H, CH₂-aryl), 4.08 (dq, *J* = 10.7 / 7.1 Hz, 0.25H, OCH₂CH₃*), 4.19 (q, *J* = 7.1 Hz, 0.5H, OCH₂CH₃*), 4.20 (q, *J* = 7.1 Hz, 1.5H, OCH₂CH₃), 4.38 – 4.41 (m, 1H, 1-CH_{eq}, 3-CH_{eq}*), 5.28 (d, *J* = 7.9 Hz, 0.75H, 3-CH_{eq}), 5.45 (t, *J* = 3.0 Hz, 0.25H, 1-CH_{eq}*), 7.09 (dd, *J* = 8.3 / 2.1 Hz, 0.25H, 6-CH_{arom}*), 7.14 (dd, *J* = 8.2 / 2.1 Hz, 0.75H, 6-CH_{arom}), 7.34 (dd, *J* = 2.1 Hz, 0.25H, 2-CH_{arom}*), 7.38 (d, *J* = 8.3 Hz, 0.25H, 5-CH_{arom}*), 7.39 (d, *J* = 8.4 Hz, 0.75H, 5-CH_{arom}), 7.40 (d, *J* = 2.1 Hz, 0.75H, 2-CH_{arom}), 11.63 (s, 0.25H, 8-OH*), 11.77 (s, 0.75H, 8-OH). Ratio of rotamers is 3:1. The signals for the minor rotamer are marked with an asterisk (*).

¹³C NMR (151 MHz, CDCl₃): δ (ppm) = 14.0 (0.75C, OCH₂CH₃), 14.1 (0.25C, OCH₂CH₃*), 14.3 (0.75C, OCH₂CH₃), 14.3 (0.25C, OCH₂CH₃*), 23.8 (0.75C, C-5), 24.0 (0.25C, C-5*), 27.5 (0.75C, C-6), 27.8 (0.25C, C-6*), 29.8 (0.25C, C-9*), 30.2 (0.75C, C-4), 30.5 (0.75C, C-9), 30.7 (0.25C, C-4*), 39.6 (0.75C, CH₂-aryl), 40.0 (0.25C, CH₂-aryl*), 45.3 (0.25C, C-1*), 49.1 (0.75C, C-3), 50.3 (0.75C, C-1), 53.5 (0.25C, C-3*), 60.9 (0.25C, OCH₂CH₃*), 61.0 (0.75C, OCH₂CH₃), 61.6 (0.75C, OCH₂CH₃), 62.1 (0.25C, OCH₂CH₃*), 99.7 (0.75C, C-7), 100.1 (0.25C, C-7*), 128.6 (0.25C, C-6_{arom}*), 128.9 (0.75C, C-6_{arom}), 130.5 (0.75C, C-5_{arom}), 130.6 (0.25C, C-5_{arom}*), 131.1 (1C, C-3/4_{arom}, C-2_{arom}*), 131.2 (0.25C, C-3/4_{arom}*), 131.3 (0.75C, C-2_{arom}), 132.6 (0.75C, C-3/4_{arom}), 132.7 (0.25C, C-3/4_{arom}*), 135.2 (0.25C, C-1_{arom}*), 135.5 (0.75C, C-1_{arom}), 165.2 (0.75C, C-8), 166.3 (0.25C, C-8*), 170.0 (0.25C, N(C=O)*), 170.2 (0.75C, N(C=O)), 170.6 (0.25C, O=COEt*), 170.9 (0.75C, O=COEt), 171.8 (0.25C, O=COEt*),

171.9 (0.75C, O=COEt). Ratio of rotamers is 3:1. The signals for the minor rotamer are marked with an asterisk (*).

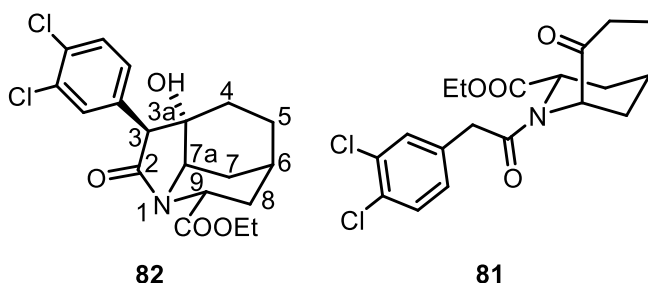
Purity (HPLC, method A): 95.7% (t_R = 23.1 min).

IR (neat): $\tilde{\nu}$ (cm^{-1}) = 2982, 2928 (C-H_{alip}), 1728 (C=O_{ester}), 1655 (C=O_{amide}), 1258, 1204, 1030 (C-N, C-O).

Exact mass (APCI): m/z = 470.1110 (calcd. 470.1132 for C₂₂H₂₆³⁵Cl₂NO₆ [M+H]⁺).

Ethyl (3RS,3aRS,6SR,7aSR,9SR)-3-(3,4-dichlorophenyl)-3a-hydroxy-2-oxooctahydro-1,6-ethanoindole-9-carboxylate (82) and

Ethyl (1RS,3RS,5RS)-2-[2-(3,4-dichlorophenyl)acetyl]-8-oxo-2-azabicyclo[3.3.1]nonane-3-carboxylate (81)



LiCl (56 mg, 1.3 mmol, 5 eq) and H₂O (1 drop) were added to a solution of **79** (125 mg, 0.27 mmol, 1 eq) in DMSO (1.5 mL). The mixture was stirred at 160 °C for 1.5 h. Then, it was added to H₂O (15 mL) and the mixture was extracted with EtOAc (3 × 10 mL). The combined organic layers were dried (Na₂SO₄), filtered and concentrated *in vacuo*. The residue was purified by flash column chromatography (25 g cartridge, cHex/EtOAc 8:2 → 6:4). At first **82**, then **81** was eluted.

82: Colorless solid, mp 145 - 146 °C, yield 17 mg (10%).

Chemical Formula: C₁₉H₂₁Cl₂NO₄ (398.3 g/mol).

TLC: R_f = 0.29 (cHex/EtOAc 7:3).

¹H NMR (600 MHz, CDCl₃): δ (ppm) = 1.18 – 1.21 (m, 2H, 4-CH₂, 5-CH₂), 1.31 (t, J = 7.2 Hz, 3H, OCH₂CH₃), 1.50 – 1.55 (m, 1H, 4-CH₂), 1.66 (ddd, J = 14.5 / 4.9 / 2.0 Hz, 1H, 7-CH₂), 1.80 – 1.87 (m, 2H, 5-CH₂, 3a-OH), 1.93 (dd, J = 14.4 / 4.4 Hz, 1H, 7-CH₂), 2.08 – 2.19 (m, 2H, 8-CH₂, 6-CH), 2.34 (ddd, J = 14.3 / 7.5 / 1.9 Hz, 1H, 8-CH₂), 3.98 (s, 1H, 3-CH), 4.03 (dt, J = 5.0 / 1.2 Hz, 1H, 7a-CH), 4.22 (dq, J = 10.8 / 7.1 Hz, 1H, OCH₂CH₃), 4.24 (dq, J = 10.8 / 7.1 Hz, 1H, OCH₂CH₃), 5.09 (dd, J = 10.9 / 1.9 Hz, 1H, 9-CH_{ax}), 7.24 (dd, J = 8.3 / 2.1 Hz, 1H, 6-CH_{arom}), 7.44 (d, J = 8.3 Hz, 1H, 5-CH_{arom}), 7.50 (d, J = 2.1 Hz, 1H, 2-CH_{arom}).

^{13}C NMR (151 MHz, CDCl_3): δ (ppm) = 14.4 (1C, OCH_2CH_3), 22.0 (1C, C-7), 22.2 (1C, C-6), 26.3 (1C, C-5), 28.7 (1C, C-4), 33.6 (1C, C-8), 47.4 (1C, C-9), 58.1 (1C, C-3), 58.6 (1C, C-7a), 61.8 (1C, OCH_2CH_3), 79.8 (1C, C-3a), 129.5 (1C, C-6_{arom}), 130.4 (1C, C-5_{arom}), 131.9 (1C, C-3/4_{arom}), 132.0 (1C, C-2_{arom}), 132.6 (1C, C-3/4_{arom}), 133.5 (1C, C-1_{arom}), 172.9 (1C, $\text{O}=\text{COEt}$), 172.9 (1C, $\text{N}(\text{C}=\text{O})$).

Purity (HPLC, method A): 96.6% ($t_{\text{R}} = 19.6$ min).

IR (neat): $\tilde{\nu}$ (cm^{-1}) = 3391 (O-H), 2928 (C-H_{alip}), 1736 (C=O_{ester}), 1674 (C=O_{amide}), 1196, 1088, 1030 (C-N, C-O).

Exact mass (APCI): $m/z = 398.0955$ (calcd. 398.0920 for $\text{C}_{19}\text{H}_{22}^{35}\text{Cl}_2\text{NO}_4$ [$\text{M}+\text{H}$]⁺).

81: Colorless solid, mp 107 - 108 °C, yield 81 mg (75%).

Chemical Formula: $\text{C}_{19}\text{H}_{21}\text{Cl}_2\text{NO}_4$ (398.3 g/mol).

TLC: $R_{\text{f}} = 0.24$ (cHex/EtOAc 7:3)

^1H NMR (600 MHz, CDCl_3): δ (ppm) = 1.23 (t, $J = 7.2$ Hz, 3H, OCH_2CH_3), 1.84 (dm, $J = 14.6$ Hz, 1H, 9- CH_2), 1.88 – 1.96 (m, 2H, 6- CH_2), 2.16 (ddm, $J = 15.2 / 9.1$ Hz, 1H, 4- CH_2), 2.25 (dm, $J = 14.6$ Hz, 1H, 9- CH_2), 2.28 – 2.37 (m, 2H, 5- CH , 7- CH_2) 2.68 (ddd, $J = 15.2 / 10.0 / 3.5$ Hz, 1H, 4- CH_2), 2.85 (ddd, $J = 14.5 / 12.4 / 8.3$ Hz, 1H, 7- CH_2), 3.56 (d, $J = 15.7$ Hz, 1H, CH_2 -aryl), 3.71 (d, $J = 15.7$ Hz, 1H, CH_2 -aryl), 4.18 – 4.21 (m, 2H, OCH_2CH_3), 4.21 – 4.23 (m, 1H, 1- CH), 5.05 (dd, $J = 9.1 / 3.5$ Hz, 1H, 3- CH_{ax}), 7.10 (dd, $J = 8.2 / 2.1$ Hz, 1H, 6- CH_{arom}), 7.35 (d, $J = 8.2$ Hz, 1H, 5- CH_{arom}), 7.37 (d, $J = 2.1$ Hz, 1H, 2- CH_{arom}).

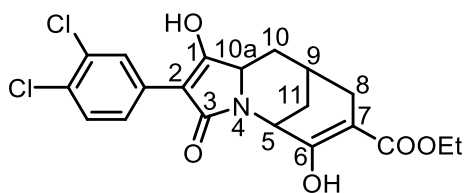
^{13}C NMR (151 MHz, CDCl_3): δ (ppm) = 14.2 (1C, OCH_2CH_3), 22.6 (1C, C-5), 29.6 (1C, C-4), 31.6 (1C, C-9), 33.7 (1C, C-6), 34.4 (1C, C-7), 39.5 (1C, CH_2 -aryl), 50.5 (1C, C-3), 60.3 (1C, C-1), 61.9 (1C, OCH_2CH_3), 129.0 (1C, C-6_{arom}), 130.5 (1C, C-5_{arom}), 131.2 (1C, C-3/4_{arom}), 131.4 (1C, C-2_{arom}), 132.5 (1C, C-3/4_{arom}), 134.3 (1C, C-1_{arom}), 172.2 (1C, $\text{N}(\text{C}=\text{O})$), 172.9 (1C, $\text{O}=\text{COEt}$), 209.5 (1C, C-8).

Purity (HPLC, method A): 95.8% ($t_{\text{R}} = 20.4$ min).

IR (neat): $\tilde{\nu}$ (cm^{-1}) = 2947 (C-H_{alip}), 1732 (C=O_{ester}), 1713 (C=O_{ketone}), 1651 (C=O_{amide}), 1200, 1026 (C-N, C-O).

Exact mass (APCI): $m/z = 398.0923$ (calcd. 398.0920 for $\text{C}_{19}\text{H}_{22}^{35}\text{Cl}_2\text{NO}_4$ [$\text{M}+\text{H}$]⁺).

Ethyl (5*RS*,9*SR*,10*aSR*)-2-(3,4-dichlorophenyl)-1,6-dihydroxy-3-oxo-3,5,8,9,10,10*a*-hexahydro-5,9-methanopyrrolo[1,2-*a*]azocine-7-carboxylate (84)



NaHMDS (1 M in THF, 1.2 mL, 1.2 mmol, 2 eq) was added to a solution of **80** (275 mg, 0.6 mmol, 1 eq) in dry THF (4 mL). The solution was stirred at room temperature for 16 h. Then, NH₄Cl (10 mL) was added, and the mixture was extracted with EtOAc (3 × 10 mL). The combined organic layers were dried (Na₂SO₄), filtered and concentrated *in vacuo*. The residue was purified by flash column chromatography (25 g cartridge, cHex/EtOAc 1:1 → 0:1). Colorless solid, mp 230 °C (decomp.), yield 180 mg (73%).

Chemical Formula: C₂₀H₁₉Cl₂NO₅ (424.3 g/mol).

TLC: *R*_f = 0.14 (cHex/EtOAc 1:1).

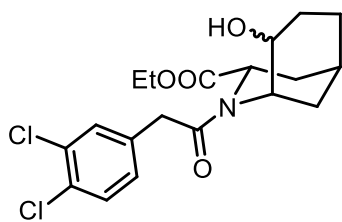
¹H NMR (600 MHz, CDCl₃): δ (ppm) = 0.99 (td, *J* = 13.3 / 5.5 Hz, 1H, 10-CH₂), 1.15 (t, *J* = 7.1 Hz, 3H, OCH₂CH₃), 1.60 – 1.67 (m, 1H, 11-CH₂), 2.08 (d, *J* = 15.8 Hz, 1H, 8-CH₂), 2.13 – 2.19 (m, 1H, 11-CH₂), 2.28 (dd, *J* = 15.8 / 4.6 Hz, 1H, 8-CH₂), 2.41 – 2.47 (m, 1H, 9-CH), 2.74 (ddd, *J* = 13.4 / 10.8 / 4.2 Hz, 1H, 10-CH₂), 4.00 (q, *J* = 7.1 Hz, 2H, OCH₂CH₃), 4.26 (dd, *J* = 13.1 / 4.3 Hz, 1H, 10a-CH), 4.40 – 4.43 (m, 1H, 5-CH), 6.52 (brs, 1H, OH), 7.58 (d, *J* = 8.6 Hz, 1H, 5-CH_{arom}), 7.99 (dd, *J* = 8.6 / 2.0 Hz, 1H, 6-CH_{arom}), 8.28 (d, *J* = 2.0 Hz, 1H, 2-CH_{arom}), 12.26 (brs, 1H, OH).

¹³C NMR (151 MHz, CDCl₃): δ (ppm) = 14.5 (1C, OCH₂CH₃), 22.1 (1C, C-9), 25.9 (1C, C-11), 29.6 (1C, C-10), 32.2 (1C, C-8) 47.3 (1C, C-5), 52.8 (1C, C-10a), 58.4 (1C, OCH₂CH₃), 86.3 (1C, C-7), 101.3 (1C, C-2), 126.6 (1C, C-6_{arom}), 127.58 (1C, C-2_{arom}), 127.72 (1C, C-3/4_{arom}), 130.1 (1C, C-5_{arom}), 130.5 (1C, C-3/4_{arom}), 132.8 (1C, C-1_{arom}), 157.6 (1C, C-6), 170.0 (1C, O=COEt), 170.6 (1C, N(C=O)), 172.4 (1C, C-1).

Purity (HPLC, method 2): 96.3% (*t*_R = 14.2 min).

IR (neat): $\tilde{\nu}$ (cm⁻¹) = 3456, 3105 (O-H), 2982 (C-H_{alip}), 1674 (C=O_{ester, amide}), 1616 (C=C), 1265, 1207 (C-N, C-O).

Ethyl (1*RS*,3*RS*,5*RS*8*RS*)- and (1*RS*,3*RS*,5*RS*8*SR*)-2-(2-(3,4-dichlorophenyl)acetyl)-8-hydroxy-2-azabicyclo[3.3.1]nonane-3-carboxylate (86)



Pyrrolidine (15 μ L, 0.18 mmol, 1.1 eq) and AcOH (1 drop) were added to a solution of **81** (66 mg, 0.17 mmol, 1.0 eq) in dry THF (2 mL). After 30 min, NaBH(OAc)₃ (52 mg, 0.25 mmol, 1.5 eq) was added and the mixture was stirred at room temperature for 16 h. Then, NaHCO₃ (5 mL) was added and the mixture was extracted with EtOAc (3 \times 5 mL). The combined organic layers were dried (Na₂SO₄), filtered and concentrated *in vacuo*. The residue was purified by flash column chromatography (25 g cartridge, cHex/EtOAc 6:4 \rightarrow 4:6). Colorless oil, yield 15 mg (22%).

Chemical Formula: C₁₉H₂₃Cl₂NO₄ (400.3 g/mol).

TLC: R_f = 0.28 (cHex/EtOAc 1:1).

¹H NMR (600 MHz, CDCl₃): δ (ppm) = 1.24 (t, J = 7.2 Hz, 1.2H, OCH₂CH₃^{*}), 1.30 (t, J = 7.1 Hz, 1.8H, OCH₂CH₃), 1.39 – 1.50 (m, 3 \times 0.6 + 0.4H, 6-CH₂, 6/7-CH₂^{*}, 9-CH₂), 1.52 - 1.66 (m, 0.6 + 3 \times 0.4H, 6-CH₂^{*}, 7-CH₂, 7-CH₂^{*}, 9-CH₂^{*}), 1.67 – 1.84 (m, 3 \times 0.6 + 0.4H, 4-CH₂, 6/7-CH₂^{*}, 7-CH₂, 9-CH₂), 1.90 (dm, J = 13.5 Hz, 0.4H, 9-CH₂^{*}), 1.93 – 1.99 (m, 0.4H, 4-CH₂^{*}), 1.99 – 2.06 (m, 0.8H, 4-CH₂^{*}, 5-CH^{*}), 2.07 – 2.12 (m, 0.6H, 5-CH), 2.52 (d, J = 5.2 Hz, 0.4H, OH^{*}), 2.70 (dd, J = 15.2 / 11.3 Hz, 0.6H, 4-CH₂), 3.58 (d, J = 16.0 Hz, 0.6H, CH₂-aryl), 3.64 (d, J = 16.0 Hz, 0.6H, CH₂-aryl), 3.70 – 3.76 (m, 1H, 8-CH, 8-CH^{*}), 3.92 (d, J = 16.3 Hz, 0.4H, CH₂-aryl^{*}), 4.04 (d, J = 16.3 Hz, 0.4H, CH₂-aryl^{*}), 4.12 – 4.19 (m, 3 \times 0.4H, 1-CH^{*}, OCH₂CH₃^{*}), 4.24 (q, J = 7.1 Hz, 1.2H, OCH₂CH₃), 4.35 (d, J = 8.2 Hz, 0.6H, 3-CH_{ax}), 4.42 (dd, J = 9.4 / 8.2 Hz, 0.4H, 3-CH_{ax}^{*}), 4.73 (bs, 0.6H, 1-CH), 4.91 (d, J = 1.8 Hz, 0.6H, OH), 7.09 (dd, J = 8.2 / 2.1 Hz, 0.6H, 6-CH_{arom}), 7.14 (dd, J = 8.3 / 2.0 Hz, 0.4H, 6-CH_{arom}^{*}), 7.32 (d, J = 2.1 Hz, 0.6H, 5-CH_{arom}), 7.35 (d, J = 8.3 Hz, 0.4H, 2-CH_{arom}^{*}), 7.38 – 7.41 (m, 1H, 2-CH_{arom}, 5-CH_{arom}^{*}). Ratio of diastereomers is 6:4. The signals for the minor diastereomer are marked with an asterisk (*).

¹³C NMR (151 MHz, CDCl₃): δ (ppm) = 16.79 (0.4C, OCH₂CH₃^{*}), 16.81 (0.6C, OCH₂CH₃), 24.4 (0.6C, C-5), 26.4 (0.4C, C-5^{*}), 27.9 (0.6C, C-7), 30.4 (0.6C, C-9), 31.9 (0.6C, C-4), 32.0 (0.4C, C-6/7^{*}), 32.1 (0.4C, C-6/7^{*}), 32.9 (0.4C, C-9^{*}), 33.6 (0.6C, C-6), 34.4 (0.4C, C-4^{*}), 42.6 (0.4C, CH₂-aryl^{*}), 43.1 (0.6C, CH₂-aryl), 55.8 (0.4C, C-1^{*}), 56.0 (0.6C, C-1), 56.7 (0.6C, C-3), 57.5 (0.4C, C-3^{*}), 63.6 (0.4C, OCH₂CH₃^{*}), 65.1

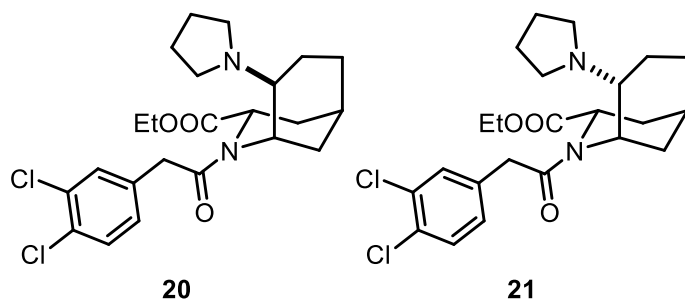
(0.6C, OCH₂CH₃), 75.6 (0.4C, 8-CH*), 77.2 (0.6C, 8-CH), 131.2 (0.6C, C-6_{arom}), 131.5 (0.4C, C-6_{arom}*), 132.8 (0.6C, C-5_{arom}), 133.1 (0.4C, C-3/4_{arom}*), 133.2 (0.4C, C-5_{arom}*), 133.8 (0.6C, C-2_{arom}), 133.9 (0.4C, C-2_{arom}*), 134.0 (0.6C, C-3/4_{arom}), 134.8 (0.4C, C-3/4_{arom}*), 135.3 (0.6C, C-3/4_{arom}), 137.1 (0.6C, C-1_{arom}), 138.7 (0.4C, C-1_{arom}*), 175.5 (0.6C, O=COEt), 176.1, (0.4C, O=COEt*) 176.5 (0.4C, N(C=O)*), 178.7 (0.6C, N(C=O)). Ratio of diastereomers is 6:4. The signals for the minor diastereomer are marked with an asterisk (*).

Purity (HPLC, method A): 99.4% (*t_R* = 19.6 min).

IR (neat): $\tilde{\nu}$ (cm⁻¹) = 3472 (O-H), 2932 (C-H_{alip}), 1728 (C=O_{ester}), 1636 (C=O_{amide}), 1258, 1231, 1084, 1042 (C-N, C-O).

Exact mass (APCI): *m/z* = 400.1094 (calcd. 400.1077 for C₁₉H₂₄³⁵Cl₂NO₄ [M+H]⁺).

Ethyl (1*RS*,3*RS*,5*RS*,8*RS*)-2-(2-(3,4-dichlorophenyl)acetyl)-8-(pyrrolidin-1-yl)-2-azabicyclo[3.3.1]nonane-3-carboxylate (20) and Ethyl (1*RS*,3*RS*,5*RS*,8*SR*)-2-(2-(3,4-dichlorophenyl)acetyl)-8-(pyrrolidin-1-yl)-2-azabicyclo[3.3.1]nonane-3-carboxylate (21)



Pyrrolidine (52 μ L, 0.63 mmol, 5.0 eq) and AcOH (9 μ L, 0.13 mmol, 1 eq) were added to a solution of **81** (50 mg, 0.13 mmol, 1 eq) in dry CH₂Cl₂ (3 mL) and the mixture was stirred at room temperature for 16 h. Then, NaBH(OAc)₃ (40 mg, 0.19 mmol, 1.5 eq) was added and the mixture was stirred at room temperature for 16 h. Then, NaHCO₃ (8 mL) was added and the mixture was extracted with CH₂Cl₂ (3 \times 8 mL). The combined organic layers were dried (Na₂SO₄), filtered and concentrated *in vacuo*. The residue was purified by flash column chromatography (1. ϕ = 3 cm, *h* = 13 cm, CH₂Cl₂/CH₃OH/NH₄OH 96:3:1 \rightarrow 94:5:1, *V* = 12 mL, 2. ϕ = 2 cm, *h* = 10 cm, CH₂Cl₂/CH₃OH/NH₄OH 97.5:2:0.5 \rightarrow 95:4:1, *V* = 12 mL). At first **20**, then **21** was eluted.

20: Yellow oil, 17 mg, (29%).

Chemical Formula: C₂₃H₃₀Cl₂N₂O₃ (453.4 g/mol).

TLC: *R_f* = 0.41 (CH₂Cl₂/CH₃OH/NH₄OH 96:3:1).

¹H NMR (600 MHz, CDCl₃): δ (ppm) = 1.05 – 1.14 (m, 0.3H, 6/9-CH₂*), 1.23 (t, J = 7.1 Hz, 2.1H, OCH₂CH₃), 1.28 (t, J = 7.1 Hz, 0.9H, OCH₂CH₃*), 1.29 – 1.33 (m, 1H, 6-CH₂, 6/9-CH₂*), 1.55 – 1.59 (m, 0.7H, 9-CH₂), 1.60 – 1.65 (m, 0.6H, 7-CH₂*), 1.66 – 1.69 (m, 0.7H, 7-CH₂), 1.70 – 1.82 (m, 5H, 7-CH₂, 6/9-CH₂*, N(CH₂CH₂)₂, N(CH₂CH₂)₂*), 1.85 – 1.92 (m, 1H, 4-CH₂*, 6-CH₂), 2.03 – 2.10 (m, 1.7H, 4-CH₂, 5-CH, 5-CH*), 2.15 – 2.21 (m, 1H, 4-CH₂, 6/9-CH₂*), 2.21 – 2.26 (m, 0.7H, 9-CH₂), 2.31 – 2.34 (m, 0.7H, 8-CH), 2.50 – 2.76 (m, 4.6H, 4-CH₂*, 8-CH*, N(CH₂CH₂)₂), 3.55 (d, J = 15.8 Hz, 0.3H, CH₂-aryl*), 3.59 (d, J = 15.8 Hz, 0.3H, CH₂-aryl*), 3.67 (d, J = 15.8 Hz, 0.7H, CH₂-aryl), 3.84 (d, J = 15.8 Hz, 0.7H, CH₂-aryl), 4.08 (bs, 0.7H, 1-CH), 4.12 – 4.24 (m, 2H, OCH₂CH₃, OCH₂CH₃*), 4.38 – 4.44 (m, 0.6H, 1-CH*, 3-CH_{ax}*), 4.74 (dd, J = 9.4 / 6.4 Hz, 0.7H, 3-CH_{ax}), 7.06 (d, J = 7.9 Hz, 0.3H, 6-CH_{arom}*), 7.13 (dd, J = 8.3 / 2.1 Hz, 0.7H, 6-CH_{arom}), 7.30 (bs, 0.3H, 2-CH_{arom}*), 7.36 – 7.41 (m, 1.7H, 2-CH_{arom}, 5-CH_{arom}, 5-CH_{arom}*). Ratio of rotamers is 7:3. The signals for the minor rotamer are marked with an asterisk (*).

¹³C NMR (151 MHz, CDCl₃): δ (ppm) = 16.76 (0.7C, OCH₂CH₃), 16.79 (0.3C, OCH₂CH₃*), 23.8 (0.3C, C-7*), 25.27 (0.7C, C-7), 25.34 (0.3C, C-6/9*), 26.1 (2.1C, C-5, N(CH₂CH₂)₂), 26.2 (0.6C, N(CH₂CH₂)₂*), 27.1 (0.7C, C-9), 29.3 (0.7C, C-6), 30.2 (0.3C, C-6/9*), 32.3 (0.3C, C-4*), 33.4 (0.7C, C-4), 41.7 (0.7C, CH₂-aryl), 43.1 (0.3C, CH₂-aryl*), 53.2 (0.3C, C-1/3*), 53.7 (0.7C, C-1), 54.38 (1.4C, N(CH₂CH₂)₂), 54.44 (0.6C, N(CH₂CH₂)₂*), 55.7 (0.7C, C-3), 56.8 (0.3C, C-1/3*), 63.1 (0.3C, C-8*), 63.7 (0.7C, OCH₂CH₃), 64.8 (0.3C, OCH₂CH₃*), 67.6 (0.7C, C-8), 131.2 (0.7C, C-6_{arom}), 131.4 (0.3C, C-6_{arom}*), 133.0 (0.7C, C-5_{arom}), 133.1 (0.3C, C-3/4_{arom}*), 133.5 (0.3C, C-5_{arom}*), 133.7 (0.7C, C-2_{arom}), 133.8 (0.3C, C-2_{arom}*), 135.0 (0.7C, C-3/4_{arom}), 135.1 (0.3C, C-3/4_{arom}*), 137.8 (0.3C, C-1_{arom}*), 138.0 (0.7C, C-1_{arom}), 173.9 (0.3C, N(C=O)*), 174.3 (0.7C, N(C=O)), 176.1 (0.3C, O=COEt*), 176.4 (0.7C, O=COEt). Ratio of rotamers is 7:3. The signals for the minor rotamer are marked with an asterisk (*). The signals for C-5* and C-3/4_{arom} are not seen in the spectrum.

Purity (HPLC, method A): 95.1% (t_R = 19.1 min).

IR (neat): $\tilde{\nu}$ (cm⁻¹) = 2959 (C-H_{alip}), 1732 (C=O_{ester}), 1643 (C=O_{amide}), 1192, 1096, 1030 (C-N, C-O).

Exact mass (APCI): m/z = 453.1675 (calcd. 453.1706 for C₂₃H₃₁³⁵Cl₂N₂O₃ [M+H]⁺).

21: Yellow oil, 6 mg (10%).

Chemical Formula: C₂₃H₃₀Cl₂N₂O₃ (453.4 g/mol).

TLC: R_f = 0.23 (CH₂Cl₂/CH₃OH/NH₄OH).

¹H NMR (600 MHz, CDCl₃): δ (ppm) = 1.22 (t, J = 7.1 Hz, 3H, OCH₂CH₃), 1.57 – 1.70 (m, 7H, N(CH₂CH₂)₂, 6-CH₂, 7-CH₂, 9-CH₂), 1.74 – 1.82 (m, 2H, 6-CH₂, 7-CH₂), 1.88 (dm, J = 13.2 Hz, 1H, 9-CH₂), 1.95 (ddd, J = 13.6 / 10.0 / 6.0 Hz, 1H, 4-CH₂), 2.01 – 2.05 (m, 1H, 5-CH), 2.07 (ddt, J = 13.6 / 8.0 / 2.1 Hz, 1H, 4-CH₂), 2.46 – 2.54 (m, 2H, N(CH₂CH₂)₂), 2.57 – 2.63 (m, 1H, 8-CH), 2.65 – 2.75 (m, 2H, N(CH₂CH₂)₂), 3.85 (d, J = 16.2 Hz, 1H, CH₂-aryl), 4.05 (d, J = 16.2 Hz, 1H, CH₂-aryl), 4.08 (brs, 1H, 1-CH), 4.14 (q, J = 7.2 Hz, 2H, OCH₂CH₃), 4.45 (dd, J = 10.2 / 8.0 Hz, 1H, 3-CH_{ax}), 7.14 (dd, J = 8.3 / 1.9 Hz, 1H, 6-CH_{arom}), 7.36 (d, J = 8.3 Hz, 1H, 5-CH_{arom}), 7.37 (d, J = 1.9 Hz, 1H, 2-CH_{arom}).

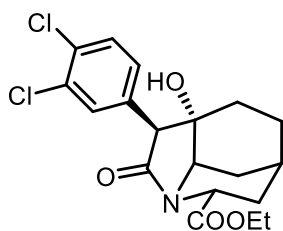
¹³C NMR (151 MHz, CDCl₃): δ (ppm) = 14.3 (1C, OCH₂CH₃), 23.2 (1C, C-6/7), 23.4 (2C, N(CH₂CH₂)₂), 24.7 (1C, C-5), 30.7 (1C, C-6/7), 32.0 (1C, C-9), 32.5 (1C, C-4), 39.6 (1C, CH₂-aryl), 51.2 (2C, N(CH₂CH₂)₂), 53.3 (1C, C-1), 55.7 (1C, C-3), 61.0 (1C, OCH₂CH₃), 65.8 (1C, C-8), 128.8 (1C, C-6_{arom}), 130.3 (1C, C-5_{arom}), 130.5 (1C, C-3/4_{arom}), 131.2 (1C, C-2_{arom}), 132.2 (1C, C-3/4_{arom}), 136.7 (1C, C-1_{arom}), 173.7 (1C, N(C=O)O), 173.9 (1C, O=COEt).

Purity (HPLC, method A): 96.7% (t_R = 20.3 min).

IR (neat): $\tilde{\nu}$ (cm⁻¹) = 2928 (C-H_{alip}), 1732 (C=O_{ester}), 1639 (C=O_{amide}), 1188, 1130, 1030 (C-N, C-O).

Exact mass (APCI): m/z = 453.1683 (calcd. 453.1706 for C₂₃H₃₁³⁵Cl₂N₂O₃ [M+H]⁺).

Ethyl (3RS,3aRS,6SR,7aSR,9SR)-3-(3,4-dichlorophenyl)-3a-hydroxy-2-oxooctahydro-1,6-ethanoindole-9-carboxylate (82)

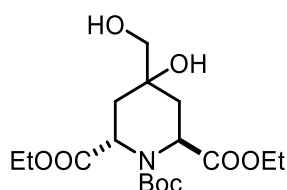


Pyrrolidine (150 μ L, 1.83 mmol, 10 eq) and AcOH (10.5 μ L, 0.18 mmol, 1 eq) were added to a solution of **81** (73 mg, 0.18 mmol, 1 eq) in dry THF (2 mL). The mixture was stirred at room temperature for 16 h. Then, NaBH(OAc)₃ (78 mg, 0.37 mmol, 2 eq) was added and the mixture was stirred for additional 24 h. NaHCO₃ (5 mL) was added and the mixture was extracted with EtOAc (3 \times 5 mL), the combined organic layers were dried (Na₂SO₄), filtered and concentrated *in vacuo*. The residue was purified by flash column chromatography (ϕ = 3 cm, h = 12 cm, CH₂Cl₂/NH₃(7 M in CH₃OH)/CH₃OH 98:2:0 \rightarrow 97:3:1, V = 12 mL). Colorless solid, mp 145 - 146 $^{\circ}$ C, yield 60 mg (82%).

Chemical Formula: C₁₉H₂₁Cl₂NO₄ (398.3 g/mol).

Analytical data: see 82.

1-tert-Butyl 2,6-diethyl trans-4-hydroxy-4-(hydroxymethyl)piperidine-1,2,6-tricarboxylate (89)



Method A:

56 (5.60 g, 16.3 mmol, 1.0 eq) was added to a solution of AD-mix α (28.5 g) in *t*-BuOH (125 mL) and H₂O (125 mL) and the mixture was stirred at room temperature for 16 h. Then, Na₂SO₃ (50 mL) was added and the mixture was stirred vigorously for 1 h at room temperature. After extraction with EtOAc (3 \times 50 mL), the combined organic layers were dried (Na₂SO₄), filtered and concentrated *in vacuo*. The residue was purified by flash column chromatography (\varnothing = 4 cm, *h* = 20 cm, cHex/EtOAc 2:8, *V* = 24 mL). Colorless oil, yield 3.85 g (63%).

Method B:

KMnO₄ (2.80 g, 17.7 mmol, 1.2 eq) was added to a solution of **56** (5.00 g, 14.7 mmol, 1.0 eq) in *t*-BuOH (20 mL) and H₂O (100 mL) and the mixture was irradiated with ultrasound for 10 min. Then, Na₂SO₃ (40 mL) was added to the mixture, the suspension was filtered over Celite[®] and the filtrate was extracted with CH₂Cl₂ (3 \times 50 mL). The combined organic layers were dried (Na₂SO₄), filtered and concentrated *in vacuo*. The residue was purified by flash column chromatography (\varnothing = 4 cm, *h* = 18 cm, cHex/EtOAc 3:7, *V* = 80 mL). Colorless oil, yield 2.80 g (51%).

Chemical formula: C₁₇H₂₉NO₈ (375.4 g/mol).

TLC: *R*_f = 0.49 (EtOAc).

¹H NMR (600 MHz, DMSO-*d*₆): δ (ppm) = 1.15 – 1.22 (m, 6H, 2 \times OCH₂CH₃), 1.32 (s, 9 \times 0.67H, C(CH₃)₃), 1.34 (s, 9 \times 0.33H, C(CH₃)₃^{*}), 1.61 (dd, *J* = 13.3 / 11.9 Hz, 0.67H, 3/5-CH₂), 1.66 (dd, *J* = 13.6 / 10.6 Hz, 0.33H, 3/5-CH₂^{*}), 1.70 (ddd, *J* = 13.3 / 4.4 / 2.3 Hz, 0.67H, 3/5-CH₂), 1.73 (ddd, *J* = 13.6 / 5.0 / 2.0 Hz, 0.33H, 3/5-CH₂^{*}), 1.83 –

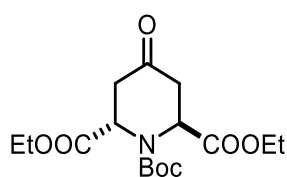
1.89 (m, 1H, 3/5-CH₂), 1.93 – 2.00 (m, 1H, 3/5-CH₂), 3.12 – 3.19 (m, 2H, CH₂OH), 3.93 – 4.19 (m, 5H, 2/6-CH, 2 × OCH₂CH₃), 4.41 (s, 1H, R₃COH), 4.46 (dd, *J* = 6.9 / 2.0 Hz, 0.67H, 2/6-CH), 4.54 (dd, *J* = 6.6 / 2.4 Hz, 0.33H, 2/6-CH*), 4.73 (t, *J* = 5.8 Hz, 1H, CH₂OH). Ratio of rotamers is 67:33. Signals for the minor rotamer are marked with an asterisk (*).

¹³C NMR (151 MHz, DMSO-*d*₆): δ (ppm) = 13.96 (0.33C, OCH₂CH₃*), 14.00 (0.67C, OCH₂CH₃), 14.05 (0.67C, OCH₂CH₃), 14.09 (0.33C, OCH₂CH₃*), 27.66 (3 × 0.33C, C(CH₃)₃*), 27.67 (3 × 0.67H, C(CH₃)₃), 33.3 (0.67C, 3/5-CH₂), 33.4 (0.33C, 3/5-CH₂*), 35.5 (0.67C, 3/5-CH₂), 35.6 (0.33C, 3/5-CH₂*), 52.5 (0.67C, 2/6-CH), 52.80, (0.33C, 2/6-CH*), 52.82 (0.33C, 2/6-CH*), 53.2 (0.67C, 2/6-CH), 59.8 (0.67C, OCH₂CH₃), 60.2 (0.33C, OCH₂CH₃*), 60.26 (0.33C, OCH₂CH₃*), 60.31 (0.67C, OCH₂CH₃), 67.6, (0.67C, R₃COH), 67.8 (0.33C, R₃COH*), 68.9 (0.33C, CH₂OH*), 69.0 (0.67C, CH₂OH), 79.8 (0.67C, C(CH₃)₃), 80.4 (0.33C, C(CH₃)₃*), 155.7 (0.33C, N(C=O)O*), 155.9 (0.67C, N(C=O)O), 171.9 (0.33C, O=COEt*), 172.2 (0.67C, O=COEt), 172.4 (0.67C, O=COEt), 172.9 (0.33C, O=COEt*). Ratio of rotamers is 67:33. Signals for the minor rotamer are marked with an asterisk (*).

IR (neat): $\tilde{\nu}$ (cm⁻¹) = 3460 (OH), 2978 (CH_{aliph}), 1736 (C=O_{ester}), 1705 (C=O_{carbamate}), 1184, 1161, 1119, 1030 (C-N, C-O).

Exact mass (APCI): *m/z* = 376.1991 (calcd. 376.1966 for C₁₇H₃₀NO₈ [M+H]⁺).

1-*tert*-Butyl 2,6-diethyl *trans*-4-oxopiperidine-1,2,6-tricarboxylate (**87**)



Method A:

NaIO₄ (4.40 g, 20.6 mmol, 2.0 eq) was added to a solution of **89** (3.85 g, 10.3 mmol, 1.0 eq) in EtOH (50 mL) and H₂O (75 mL) and the suspension was stirred at room temperature for 16 h. Then, the mixture was filtered and extracted with EtOAc (3 × 50 mL). The combined organic layers were dried (Na₂SO₄), filtered and concentrated *in vacuo*. The residue was purified by flash column chromatography (∅ = 3 cm, *h* = 15 cm, cHex/EtOAc 8:2, *V* = 12 mL). Colorless solid, mp 49 - 50 °C, yield 2.24 g (63%).

Method B:

OsO₄ (0.05 M in H₂SO₄, 3.60 mL, 0.18 mmol, 0.01 eq), pyridine (0.70 mL, 9.10 mmol, 0.5 eq) and NaIO₄ (15.6 g, 72.8 mmol, 4.0 eq) were added to a solution of **56** (6.20 g, 18.2 mmol, 1.0 eq) in *t*-BuOH (80 mL) and H₂O (120 mL) and the suspension was stirred at room temperature for 48 h. Then, the mixture was filtered and Na₂SO₃ (50 mL) and EtOAc (50 mL) were added to the solution. The aqueous layer was extracted with EtOAc (3 × 50 mL) and the combined organic layers were dried (Na₂SO₄), filtered and concentrated *in vacuo*. The residue was purified by flash column chromatography (\varnothing = 8 cm, *h* = 16 cm, cHex/EtOAc 9:1 → 8:2, *V* = 80 mL). Colorless solid, mp 49 - 50 °C, yield 4.55 g (73%).

Chemical formula: C₁₆H₂₅NO₇ (343.4 g/mol).

TLC: *R*_f = 0.33 (cHex/EtOAc 8:2).

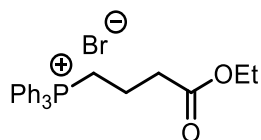
¹H NMR (600 MHz, CDCl₃): δ (ppm) = 1.25 (t, *J* = 7.1 Hz, 3H, OCH₂CH₃), 1.27 (t, *J* = 7.1 Hz, 3H, OCH₂CH₃), 1.45 (s, 9H, C(CH₃)₃), 2.72 (dd, *J* = 18.0 / 1.4 Hz, 1H, 3/5-CH_{eq}), 2.86 (dd, *J* = 18.0 / 1.4 Hz, 1H, 3/5-CH_{eq}), 3.01 – 3.08 (m, 2H, 3-CH_{ax}, 5-CH_{ax}), 4.12 – 4.26 (m, 4H, 2 × OCH₂CH₃), 4.83 (d, *J* = 7.8 Hz, 1H, 2/6-CH), 5.06 (d, *J* = 7.8 Hz, 1H, 2/6-CH).

¹³C NMR (151 MHz, CDCl₃): δ (ppm) = 14.2 (1C, OCH₂CH₃), 14.3 (1C, OCH₂CH₃), 28.3 (3C, C(CH₃)₃), 40.6 (1C, C-3/5), 41.0 (1C, C-3/5), 53.0 (1C, C-2/6), 54.2 (1C, C-2/6), 61.9 (1C, OCH₂CH₃), 62.1 (1C, OCH₂CH₃), 81.9 (1C, C(CH₃)₃), 154.5 (1C, N(C=O)O), 172.3 (1C, O=COEt), 172.4 (1C, O=COEt), 203.8 (1C, C-4).

IR (neat): $\tilde{\nu}$ (cm⁻¹) = 2978 (CH_{aliph}), 1736 (C=O_{ester}), 1701 (C=O_{ketone, carbamate}), 1188, 1115, 1026 (C-N, C-O).

Exact mass (APCI): *m/z* = 344.1690 (calcd. 344.1704 for C₁₆H₂₆NO₇ [M+H]⁺).

3-(Ethoxycarbonyl)propyltriphenylphosphonium bromide (**94**)¹²²



PPh₃ (11.0 g, 41.9 mmol, 1 eq) was added to ethyl 4-bromobutyrate (6.00 mL, 41.9 mmol, 1 eq) and the mixture was stirred at 110 °C for 16 h. The solid was collected, washed with Et₂O (3 × 30 mL) and dried *in vacuo*. Colorless solid, mp 167 - 168 °C (lit.¹²² 171 - 173 °C), yield 9.83 g (51%).

Chemical Formula: C₂₄H₂₆BrO₂P (457.3 g/mol).

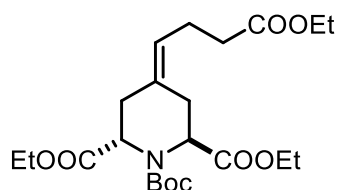
¹H NMR (600 MHz, DMSO-*d*₆): δ (ppm) = 1.17 (t, *J* = 7.2 Hz, 3H, OCH₂CH₃), 1.72 – 1.79 (m, 2H, CH₂CH₂CH₂), 2.55 (t, *J* = 7.0 Hz, 2H, CH₂COOEt), 3.55 – 3.62 (m, 2H, R₃P⁺CH₂), 4.06 (q, *J* = 7.2 Hz, 2H, OCH₂CH₃), 7.75 – 7.80 (m, 6H, 3-CH_{arom}, 5-CH_{arom}), 7.80 – 7.85 (m, 6H, 2-CH_{arom}, 6-CH_{arom}), 7.89 – 7.93 (m, 3H, 4-CH_{arom}).

¹³C NMR (151 MHz, DMSO-*d*₆): δ (ppm) = 14.1 (1C, OCH₂CH₃), 17.7 (d, *J* = 3.1 Hz, 1C, CH₂CH₂CH₂), 19.8 (d, *J* = 51.5 Hz, 1C, R₃P⁺CH₂), 33.5 (d, *J* = 18.4 Hz, 1C, CH₂COOEt), 60.2 (1C, OCH₂CH₃), 118.3 (d, *J* = 85.9 Hz, 3C, C-1_{arom}), 130.3 (d, *J* = 12.7 Hz, 6C, C-2_{arom}, C-6_{arom}), 133.6 (d, *J* = 10.1 Hz, 6C, C-3_{arom}, C-5_{arom}), 135.0 (d, *J* = 3.1 Hz, 3C, C-4_{arom}), 171.8 (1C, O=COEt).

IR (neat): $\tilde{\nu}$ (cm⁻¹) = 3043 (C-H_{arom}), 2892 (C-H_{aliph}), 1719 (C=O_{ester}), 1112 (C-O).

Exact mass (APCI): *m/z* = 377.1661 (calcd. 377.1664 for C₂₄H₂₆O₂P [M+H]⁺).

1-*tert*-Butyl *trans*-2,6-diethyl 4-(3-ethoxycarbonyl)propylidenepiperidine-1,2,6-tricarboxylate (95)



At 0 °C, KO^tBu (0.23 g, 2.04 mmol, 1.4 eq) was added to a suspension of **94** (1.0 g, 2.18 mmol, 1.5 eq) in dry THF (15 mL) and the mixture was stirred for 30 min. Afterwards, a solution of **87** (0.5 g, 1.46 mmol, 1.0 eq) in dry THF (3 mL) was added and the mixture was stirred at room temperature for 4 h. Then, the mixture was poured into half-sat. NH₄Cl (30 mL) and the mixture was extracted with EtOAc (3 × 20 mL). The combined organic layers were dried (Na₂SO₄), filtered and concentrated *in vacuo*. The residue was purified by flash column chromatography (25 g cartridge, CH₂Cl₂/EtOAc 98:2 → 95:5). Colorless oil, yield 48 mg (7%).

Chemical Formula: C₂₂H₃₅NO₈ (441.5 g/mol).

TLC: R_f = 0.49 (cHex/EtOAc 7:3).

¹H NMR (600 MHz, CDCl₃): δ (ppm) = 1.20 – 1.29 (m, 9H, OCH₂CH₃), 1.42 (s, 9H, C(CH₃)₃), 2.21 – 2.32 (m, 4H, R₂C=CHCH₂CH₂), 2.49 (dd, *J* = 15.6 / 2.7 Hz, 0.55H, 3/5-CH₂), 2.59 (dd, *J* = 15.5 / 3.6 Hz, 0.45H, 3/5-CH₂^{*}), 2.66 – 2.83 (m, 2H, 3-CH₂, 3-CH₂^{*}, 5-CH₂, 5-CH₂^{*}), 2.84 – 2.96 (m, 1H, 3/5-CH₂, 3/5-CH₂^{*}), 4.07 – 4.24 (m, 6H, OCH₂CH₃), 4.55 (dd, *J* = 6.3 / 2.8 Hz, 0.55H, 2/6-CH), 4.62 – 4.67 (m, 0.9H, 2-CH^{*},

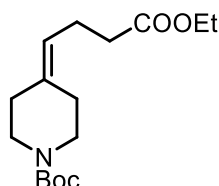
6-CH^{*}), 4.80 (dd, $J = 6.9 / 3.0$ Hz, 0.55H, 2/6-CH), 5.18 – 5.23 (m, 1H, R₂C=CHCH₂CH₂). Ratio of rotamers is 55:45. The signals for the minor rotamer are marked with an asterisk (*).

¹³C NMR (151 MHz, CDCl₃): δ (ppm) = 14.3, 14.37, 14.42, 14.5 (3C, 3 × OCH₂CH₃, 3 × OCH₂CH₃^{*}), 20.08 (0.55C, R₂C=CHCH₂CH₂), 20.14 (0.45C, R₂C=CHCH₂CH₂^{*}), 28.2, 28.31, 28.34, 28.4 (4C, C-3/5, C(CH₃)₃), 34.0, 34.1, 34.2 (2C, C-3/5, R₂C=CHCH₂CH₂), 53.3 (0.55C, C-2/6), 54.7 (0.45C, C-2/6^{*}), 55.1 (0.45C, C-2/6^{*}), 56.1 (0.55C, C-2/6), 60.5 (1C, OCH₂CH₃), 61.1 (0.55C, OCH₂CH₃), 61.2 (0.45C, OCH₂CH₃^{*}), 61.4 (0.45C, OCH₂CH₃^{*}), 61.5 (0.55C, OCH₂CH₃), 81.1 (1C, C(CH₃)₃), 125.3 (1C, R₂C=CHCH₂CH₂), 128.86 (0.55C, C-4), 128.91 (0.45C, C-4^{*}), 155.3 (1C, N(C=O)O), 172.6 (0.9C, 2 × O=COEt^{*}), 172.7 (1.1C, 2 × O=COEt), 173.0 (0.45C, O=COEt^{*}), 173.1 (0.55C, O=COEt). Ratio of rotamers is 55:45. The signals for the minor rotamer are marked with an asterisk (*).

IR (neat): $\tilde{\nu}$ (cm⁻¹) = 2978 (C-H_{aliph}), 1736 (C=O_{ester}), 1701 (C=O_{carbamate}), 1177, 1165, 1026 (C-N, C-O).

Exact mass (APCI): $m/z = 442.2438$ (calcd. 442.2435 for C₂₂H₃₆NO₈ [M+H]⁺).

***tert*-Butyl 4-(3-ethoxycarbonyl)propylidenepiperidine-1-carboxylate (97)**



At 0 °C, KO^tBu (0.40 g, 3.50 mmol, 1.4 eq) was added to a suspension of **94** (1.73 g, 3.75 mmol, 1.5 eq) in dry THF (10 mL) and the mixture was stirred for 30 min. Afterwards, a solution of *tert*-butyl 4-oxo-1-piperidinecarboxylate (0.50 g, 2.50 mmol, 1.0 eq) in dry THF (3 mL) was added and the mixture was stirred at room temperature for 1 h. Then, the mixture was poured into half-sat. NH₄Cl (30 mL) and the mixture was extracted with EtOAc (3 × 20 mL). The combined organic layers were dried (Na₂SO₄), filtered and concentrated *in vacuo*. The residue was purified by flash column chromatography (50 g cartridge, cHex/EtOAc 95:5 → 9:1). Colorless oil (0.45 mg, 60%).

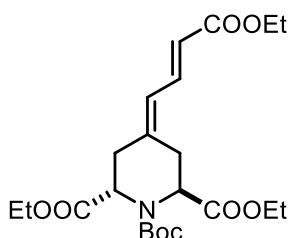
Chemical Formula: C₁₆H₂₇NO₄ (297.4 g/mol).

TLC: R_f = 0.44 (cHex/EtOAc 8:2).

¹H NMR (600 MHz, CDCl₃): δ (ppm) = 1.25 (t, J = 7.1 Hz, 3H, OCH₂CH₃), 1.46 (s, 9H, C(CH₃)₃), 2.09 – 2.14 (t, J = 5.7 Hz, 2H, 3/5-CH₂), 2.19 – 2.23 (t, J = 5.8 Hz, 2H, 3/5-CH₂), 2.30 – 2.36 (m, 4H, CH₂CH₂COOEt), 3.32 – 3.41 (m, 4H, 2-CH₂, 6-CH₂), 4.12 (q, J = 7.1 Hz, 2H, OCH₂CH₃), 5.16 – 5.21 (m, 1H, R₂C=CHR').

¹³C NMR (151 MHz, CDCl₃): δ (ppm) = 14.4 (1C, OCH₂CH₃), 22.9 (1C, CH₂CH₂COOEt), 28.5 (2C, C-3/5), 28.6 (3C, C(CH₃)₃), 34.5 (1C, CH₂CH₂COOEt), 36.0 (2C, C-3/5), 60.5 (1C, OCH₂CH₃), 79.6 (1C, C(CH₃)₃), 122.0 (1C, R₂C=CHR'), 136.7 (1C, R₂C=CHR'), 154.9 (1C, N(C=O)O), 173.3 (O=COEt). Signals for C-2 and C-6 are not seen in the spectrum.

1-tert-Butyl trans-2,6-diethyl 4-[(E)-3-(ethoxycarbonyl)prop-2-en-1-ylidene] piperidine-1,2,6-tricarboxylate (99)



At 0 °C, NaHMDS (1 M in THF, 0.22 mL, 0.22 mmol, 1.1 eq) was added dropwise to a solution of **87** (70 mg, 0.20 mmol, 1.0 eq) and triethyl-4-phosphonocrotonate (50 μ L, 0.22 mmol, 1.1 eq) in dry THF (2 mL) and the mixture was stirred at room temperature for 4 h. Then, H₂O (6 mL) was added and the mixture was extracted with EtOAc (3 \times 6 mL). The combined organic layers were dried (Na₂SO₄), filtered and concentrated *in vacuo*. The residue was purified by flash column chromatography (25 g cartridge, CH₂Cl₂/EtOAc 98:2 \rightarrow 95:5). Colorless oil, yield 74 mg (84%).

Chemical Formula: C₂₂H₃₃NO₈ (439.5 g/mol).

TLC: R_f = 0.42 (CH₂Cl₂/EtOAc 95:5).

¹H NMR (600 MHz, CDCl₃): δ (ppm) = 1.20 – 1.26 (m, 6H, OCH₂CH₃, OCH₂CH₃*) 1.29 (t, J = 7.1 Hz, 3H, OCH₂CH₃), 1.42 (s, 9 \times 0.53H, C(CH₃)₃), 1.43 (s, 9 \times 0.47H, C(CH₃)₃*), 2.66 (dd, J = 16.6 / 2.3 Hz, 0.53H, 3/5-CH₂), 2.78 (dd, J = 16.6 / 3.0 Hz, 0.47H, 3/5-CH₂*), 2.91 (dm, J = 17.3 Hz, 0.47H, 3/5-CH₂*), 2.94 – 3.03 (m, 2 \times 0.53 + 0.47H, 3-CH₂, 5-CH₂, 3/5-CH₂*), 3.19 (d, J = 17.3 Hz, 0.47H, 3/5-CH₂*), 3.24 (d, J = 17.7 Hz, 0.53H, 3/5-CH₂), 4.09 – 4.24 (m, 6H, OCH₂CH₃, OCH₂CH₃*), 4.62 (dd, J = 6.5 / 2.7 Hz, 0.53H, 2/6-CH), 4.71 (dd, J = 7.0 / 2.4 Hz, 0.47H, 2/6-CH*), 4.75 (dd, J = 6.4 / 3.3 Hz, 0.47H, 2/6-CH*), 4.88 (dd, J = 6.7 / 2.5 Hz, 0.53H, 2/6-CH), 5.78 (d,

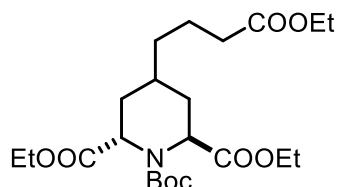
$J = 6.9$ Hz, 0.47H, $R_2C=CH-CH=CH^*$), 5.81 (d, $J = 6.9$ Hz, 0.53H, $R_2C=CH-CH=CH$), 5.98 – 6.05 (m, 1H, $R_2C=CH-CH=CH$, $R_2C=CH-CH=CH^*$), 7.38 (dd, $J = 11.6 / 4.0$ Hz, 0.47H, $R_2C=CH-CH=CH^*$), 7.41 (dd, $J = 11.6 / 4.0$ Hz, 0.53H, $R_2C=CH-CH=CH$). Ratio of rotamers is 53:47. The signals for the minor rotamer are marked with an asterisk (*). ^{13}C NMR (151 MHz, $CDCl_3$): δ (ppm) = 14.3 (0.53C, OCH_2CH_3), 14.3 (0.47C, OCH_2CH_3), 14.40 (0.47C, OCH_2CH_3), 14.44 (1C, OCH_2CH_3), 14.5 (0.53C, OCH_2CH_3), 28.3 (3C, $C(CH_3)_3$), 29.0 (0.47C, CH_2^*), 29.2 (0.53C, CH_2), 34.6 (0.53C, CH_2), 34.7 (0.47C, CH_2^*), 52.9 (0.53C, C-2/6), 54.1 (0.47C, C-2/6*), 54.3 (0.53C, C-2/6), 55.3 (0.47C, C-2/6), 60.5 (1C, OCH_2CH_3), 61.4 (0.53C, OCH_2CH_3), 61.5 (0.47C, $OCH_2CH_3^*$), 61.6 (0.47C, $OCH_2CH_3^*$), 61.7 (0.53C, OCH_2CH_3), 81.4 (1C, $C(CH_3)_3$), 121.29 (0.47C, $R_2C=CH-CH=CH^*$), 121.34 (0.53C, $R_2C=CH-CH=CH$), 124.9 (0.53C, $R_2C=CH-CH=CH$), 125.0 (0.47C, $R_2C=CH-CH=CH^*$), 138.6 (0.53C, $R_2C=CH-CH=CH$), 138.7 (0.47C, $R_2C=CH-CH=CH^*$), 140.26 (0.53C, $R_2C=CH-CH=CH$), 140.30 (0.47C, $R_2C=CH-CH=CH^*$), 154.99 (0.53C, $N(C=O)O$), 155.03 (0.47C, $N(C=O)O^*$), 167.2 (0.53C, $O=COEt$), 167.3 (0.47C, $O=COEt^*$), 172.4 (0.47C, $O=COEt^*$), 172.5 (0.53C, $O=COEt$), 172.59 (0.47C, $O=COEt^*$), 172.63 (0.53C, $O=COEt$). Ratio of rotamers is 53:47. The signals for the minor rotamer are marked with an asterisk (*).

Purity (HPLC, method A): 92.4 % ($t_R = 22.4$ min).

IR (neat): $\tilde{\nu}$ (cm^{-1}) = 2978 (C-H_{alip}), 1740 (C=O_{ester}), 1701 (C=O_{carbamate}), 1640, 1616 (C=C), 1184, 1157, 1026 (C-N, C-O).

Exact mass (APCI): $m/z = 440.2255$ (calcd. 440.2279 for $C_{22}H_{34}NO_8$ $[M+H]^+$).

1-tert-Butyl trans-2,6-diethyl 4-[(3-ethoxycarbonyl)propyl]piperidine-1,2,6-tricarboxylate (88)



Method A:

$Pd(OH)_2$ (5 mg) was added to a solution of **95** (48 mg, 0.11 mmol, 1.0 eq) in EtOH (3 mL) and the suspension was stirred at room temperature for 16 h under H_2 (5 bar). The suspension was filtered through Celite® and the filtrate was concentrated *in vacuo*. Colorless oil, yield 49 mg (100%).

Method B:

Pd/C (10 mg) was added to a solution of **99** (369 mg, 0.84 mmol, 1 eq) in EtOH (4 mL) and the suspension was stirred at room temperature for 16 h under H₂ (5 bar). The suspension was filtered through Celite[®] and the filtrate was concentrated *in vacuo*. Colorless oil, yield 355 mg (95%).

Chemical Formula: C₂₂H₃₇NO₈ (443.5 g/mol).

TLC: R_f = 0.42 (cHex/EtOAc 7:3).

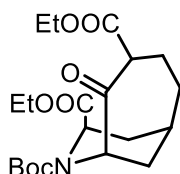
¹H NMR (600 MHz, CDCl₃): δ (ppm) = 1.20 – 1.30 (m, 11H, OCH₂CH₃, R₂CHCH₂CH₂CH₂), 1.31 – 1.37 (m, 2H, 3/5-CH₂, 4-CH), 1.40 (s, 9 × 0.6H, C(CH₃)₃), 1.41 (s, 9 × 0.4H, C(CH₃)₃*), 1.48 – 1.56 (m, 1H, 3/5-CH₂), 1.57 – 1.64 (m, 2H, R₂CHCH₂CH₂CH₂), 2.03 – 2.10 (m, 1H, 3/5-CH₂), 2.13 (d, J = 13.7 Hz, 0.6H, 3/5-CH₂), 2.19 (d, J = 13.4 Hz, 0.4H, 3/5-CH₂*), 2.25 (t, J = 7.4 Hz, 2H, R₂CHCH₂CH₂CH₂), 4.08 – 4.30 (m, 7H, OCH₂CH₃, 2/6-CH), 4.66 (d, J = 6.3 Hz, 0.6H, 2/6-CH), 4.78 (d, J = 4.3 Hz, 0.4H, 2/6-CH*). Ratio of rotamers is 60:40. The signals for the minor rotamer are marked with an asterisk (*).

¹³C NMR (151 MHz, CDCl₃): δ (ppm) = 14.3 (1C, OCH₂CH₃), 14.4 (1C, OCH₂CH₃), 14.5 (1C, OCH₂CH₃), 22.1 (1C, R₂CHCH₂CH₂CH₂), 28.2 (3C, C(CH₃)₃), 29.7 (1C, C-4), 32.2 (0.4C, C-3/5*), 32.4 (0.6C, C-3/5), 34.25 (1C, C-3/5), 34.32 (1C, R₂CHCH₂CH₂CH₂), 35.45 (0.4C, R₂CHCH₂CH₂CH₂*), 35.53 (0.6C, R₂CHCH₂CH₂CH₂), 55.98 (0.4C, C-2/6), 56.04 (0.6C, C-2/6), 56.1 (0.4C, C-2/6), 56.5 (0.6C, C-2/6), 60.5 (1C, OCH₂CH₃), 60.9 (0.4C, OCH₂CH₃*), 61.0 (0.6C, OCH₂CH₃), 61.30 (0.4C, OCH₂CH₃*), 61.33 (0.6C, OCH₂CH₃), 81.1 (0.6C, C(CH₃)₃), 81.7 (0.4C, C(CH₃)₃*), 156.5 (0.6C, N(C=O)O), 156.6 (0.4C N(C=O)O*), 172.8 (0.4C, O=COEt*), 173.0 (0.6C, O=COEt), 173.2 (0.6C, O=COEt), 173.5 (1C, O=COEt). Ratio of rotamers is 60:40. The signals for the minor rotamer are marked with an asterisk (*). A signal for O=COEt* is not seen in the spectrum.

IR (neat): $\tilde{\nu}$ (cm⁻¹) = 2978, 2936 (C-H_{aliph}), 1732 (C=O_{ester}), 1705 (C=O_{carbamate}), 1180, 1161, 1096, 1026 (C-N, C-O).

Exact mass (APCI): *m/z* = 444.2590 (calcd. 444.2592 for C₂₂H₃₈NO₈ [M+H]⁺).

7-(tert-Butyl) 4,8-diethyl (1RS,6RS,8SR)-5-oxo-7-azabicyclo[4.3.1]decane-4,7,8-tricarboxylate (100)



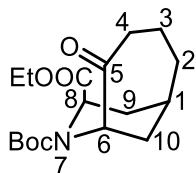
NaHMDS (1.0 M in THF, 1.13 mL, 1.13 mmol, 2 eq) was added to a refluxing solution of **88** (250 mg, 0.56 mmol, 1.0 eq) in dry THF (30 mL). The mixture was heated to reflux for 4 h. Then, the mixture was poured into half sat. NH_4Cl (30 mL) and extracted with EtOAc (3 \times 15 mL). The combined organic layers were dried (Na_2SO_4), filtered and concentrated *in vacuo*. The residue was purified by flash column chromatography (25 g cartridge, cHex/EtOAc 9:1 \rightarrow 8:2). Yellow oil, yield 48 mg (22%).

Chemical Formula: $\text{C}_{20}\text{H}_{31}\text{NO}_7$ (397.5 g/mol).

TLC: $R_f = 0.36$ (cHex/EtOAc 7:3).

IR (neat): $\tilde{\nu}$ (cm^{-1}) = 2978 (C-H_{alip}), 1740 (C=O_{ester}), 1701 (C=O_{carbamate, ketone}), 1184, 1111, 1038 (C-N, C-O).

7-tert-Butyl 8-ethyl (1*RS*,6*RS*,8*SR*)-5-oxo-7-azabicyclo[4.3.1]decane-7,8-dicarboxylate (22)



LiCl (26 mg, 0.60 mmol, 5.0 eq) and H_2O (1 drops) were added to a solution of **100** (48 mg, 0.12 mmol, 1.0 eq) in DMSO (1 mL) and the mixture was heated to 160 $^\circ\text{C}$ in a preheated oil bath for 4 h. The solution was poured into H_2O (10 mL) and the mixture was extracted with EtOAc (3 \times 5 mL). The combined organic layers were dried (Na_2SO_4), filtered and concentrated *in vacuo*. The residue was purified by flash column chromatography (25 g cartridge, cHex/EtOAc 9:1 \rightarrow 8:2). Colorless solid, mp 73 - 75 $^\circ\text{C}$, yield 11 mg (28%).

Chemical Formula: $\text{C}_{17}\text{H}_{27}\text{NO}_5$ (325.4 g/mol).

TLC: $R_f = 0.36$ (cHex/EtOAc 7:3).

^1H NMR (600 MHz, CDCl_3): δ (ppm) = 1.26 (t, $J = 7.2$ Hz, 3 \times 0.55H, OCH_2CH_3), 1.27 (t, $J = 7.2$ Hz, 3 \times 0.45H, $\text{OCH}_2\text{CH}_3^*$), 1.44 (s, 9H, $\text{C}(\text{CH}_3)_3$), 1.48 – 1.55 (m, 0.55H, 2- CH_2), 1.57 – 1.65 (m, 0.45H, 2- CH_2^*), 1.71 – 1.85 (m, 3 \times 0.55 + 4 \times 0.45H,

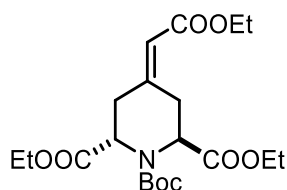
$2 \times 3\text{-CH}_2$, $2 \times 3\text{-CH}_2^*$, 2-CH_2 , 2-CH_2^* , 9-CH_2^* , 1.86 – 1.95 (m, $2 \times 0.55\text{H}$, 9-CH_2 , 10-CH_2), 2.02 (dd, $J = 15.0 / 2.8$ Hz, 0.45H , 10-CH_2^*), 2.10 (ddd, $J = 15.1 / 9.0 / 2.3$ Hz, 0.45H , 9-CH_2^*), 2.14 (dt, $J = 15.1 / 6.2$ Hz, 0.55H , 10-CH_2), 2.18 – 2.27 (m, 1H , 1-CH , 1-CH^*), 2.27 – 2.35 (m, 1H , 9-CH_2 , 10-CH_2^*), 2.47 (dm, $J = 12.6$ Hz, 0.45H , 4-CH_2^*), 2.55 (dt, $J = 14.5 / 4.7$ Hz, 0.55H , 4-CH_2), 2.62 (ddd, $J = 14.5 / 12.2 / 4.9$ Hz, 0.55H , 4-CH_2), 2.77 (td, $J = 12.6 / 4.4$ Hz, 0.45H , 4-CH_2^*), 4.13 – 4.24 (m, 2H , OCH_2CH_3 , $\text{OCH}_2\text{CH}_3^*$), 4.34 (dd, $J = 6.2 / 2.2$ Hz, 0.55H , 6-CH), 4.49 (dd, $J = 7.4 / 2.4$ Hz, 0.45H , 8-CH^*), 4.55 (t, $J = 3.9$ Hz, 0.45H , 6-CH^*), 4.73 (dd, $J = 8.6 / 2.2$ Hz, 0.55H , 8-CH). Ratio of rotamers is 55:45. The signals for the minor rotamer are marked with an asterisk (*).

^{13}C NMR (151 MHz, CDCl_3): δ (ppm) = 14.3 (0.55C , OCH_2CH_3), 14.5 (0.45C , $\text{OCH}_2\text{CH}_3^*$), 19.8 (0.55C , C-3), 21.6 (0.45C , C-3^*), 26.1 (0.55C , C-1), 26.4 (0.45C , C-9^*), 26.5 (0.45C , C-1^*), 27.0 (0.55C , C-9), 28.3 ($3 \times 0.55\text{C}$, $\text{C}(\text{CH}_3)_3$), 28.4 ($3 \times 0.45\text{C}$, $\text{C}(\text{CH}_3)_3^*$), 28.8 (0.45C , C-10^*), 28.9 (0.55C , C-10), 33.5 (0.45C , C-2^*), 33.9 (0.55C , C-2), 40.9 (0.55C , C-4), 41.1 (0.45C , C-4^*), 51.4 (0.55C , C-8), 52.9 (0.45C , C-8^*), 58.6 (0.45C , C-6^*), 61.1 (0.55C , C-6), 61.3 (0.45C , $\text{OCH}_2\text{CH}_3^*$), 61.5 (0.55C , OCH_2CH_3), 80.7 (0.45C , $\text{C}(\text{CH}_3)_3^*$), 81.3 (0.55C , $\text{C}(\text{CH}_3)_3$), 155.5 (0.45C , $\text{N}(\text{C}=\text{O})\text{O}^*$), 155.9 (0.55C , $\text{N}(\text{C}=\text{O})\text{O}$), 173.4 (0.45C , $\text{O}=\text{COEt}^*$), 173.4 (0.55C , $\text{O}=\text{COEt}$), 212.3 (0.55C , C-5), 212.5 (0.45C , C-5^*). Ratio of rotamers is 55:45. The signals for the minor rotamer are marked with an asterisk (*).

IR (neat): $\tilde{\nu}$ (cm^{-1}) = 2970 (C-H_{alip}), 1740 ($\text{C}=\text{O}_{\text{ester}}$), 1717 ($\text{C}=\text{O}_{\text{ketone}}$), 1694 ($\text{C}=\text{O}_{\text{carbamate}}$), 1184, 1111, 1096, 1037 (C-N , C-O).

Exact mass (APCI): $m/z = 326.1953$ (calcd. 326.1962 for $\text{C}_{17}\text{H}_{28}\text{NO}_5$ $[\text{M}+\text{H}]^+$).

1-tert-Butyl 2,6-diethyl trans-4-(ethoxycarbonylmethylene)piperidine-1,2,6-tricarboxylate (103)



4-(Ethoxycarbonylmethylene)triphenylphosphorane (7.60 g, 21.7 mmol, 1.75 eq) was added to a solution of **87** (4.30 g, 12.4 mmol, 1.0 eq) in toluene (50 mL) and the mixture was heated at reflux for 48 h. After concentrating the mixture *in vacuo*, the residue was

purified by flash column chromatography ($\varnothing = 6$ cm, $h = 17$ cm, cHex/EtOAc 9:1, $V = 80$ mL). Colorless oil, yield 3.9 g (75%).

Chemical formula: $C_{20}H_{31}NO_8$ (413.5 g/mol).

TLC: $R_f = 0.35$ (cHex/EtOAc 8:2).

1H NMR (600 MHz, DMSO- d_6): δ (ppm) = 1.11 – 1.22 (m, 9H, 3 \times OCH_2CH_3), 1.35 (s, 9 \times 0.54H, $C(CH_3)_3$), 1.36 (s, 9 \times 0.46H, $C(CH_3)_3^*$), 2.71 (dd, $J = 16.8 / 2.2$ Hz, 0.54H, 3/5- CH_2), 2.78 (dd, $J = 17.1 / 3.2$ Hz, 0.46H, 3/5- CH_2^*), 2.83 – 2.95 (m, 1.46H, 3/5- CH_2 , 3- CH_2^* , 5- CH_2^*), 3.01 (ddm, $J = 18.9 / 7.3$ Hz, 0.54H, 3/5- CH_2), 3.61 (dm, $J = 18.9$ Hz, 0.54H, 3/5- CH_2), 3.68 (dm, $J = 18.5$ Hz, 0.46H, 3/5- CH_2^*), 4.02 – 4.17 (m, 6H, 3 \times OCH_2CH_3), 4.57 (dd, $J = 6.7 / 2.3$ Hz, 0.54H, 2/6- CH), 4.62 (dd, $J = 6.4 / 3.1$ Hz, 0.46H, 2/6- CH^*), 4.67 (dd, $J = 7.2 / 1.9$ Hz, 0.46H, 2/6- CH^*), 4.75 (dd, $J = 7.3 / 2.3$ Hz, 0.54H, 2/6- CH), 5.80 (s, 0.54H, $R_2C=CH$), 5.81 (s, 0.46H, $R_2C=CH^*$). Ratio of rotamers is 54:46. Signals for the minor rotamer are marked with an asterisk (*).

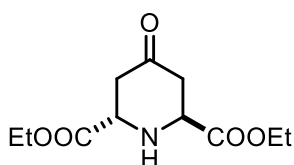
^{13}C NMR (151 MHz, DMSO- d_6): δ (ppm) = 13.9 (0.54C, OCH_2CH_3), 14.0 (0.46C, $OCH_2CH_3^*$), 14.0 (0.46C, $OCH_2CH_3^*$), 14.1 (0.54C, OCH_2CH_3), 14.11 (1C, OCH_2CH_3), 27.7 (s, 3C, $C(CH_3)_3$), 29.8 (0.46C, C-3/5*), 30.4 (0.54C, C-3/5), 33.8 (0.54C, C-3/5), 34.0 (0.46C, C-3/5*), 51.6 (0.54C, C-2/6), 53.0 (0.46C, C-2/6*), 53.1 (0.46C, C-2/6*), 54.1 (0.54C, C-2/6), 59.5 (1C, OCH_2CH_3), 60.8 (0.46C, $OCH_2CH_3^*$), 60.9 (54C, OCH_2CH_3), 61.0 (0.46C, $OCH_2CH_3^*$), 61.1 (0.54C, OCH_2CH_3), 80.3 (0.54C, $C(CH_3)_3$), 80.4 (0.46C, $C(CH_3)_3^*$), 116.9 (0.54C, $R_2C=CH_2$), 117.0 (0.46C, $R_2C=CH_2^*$), 151.4 (0.46C, $R_2C=CH_2^*$), 151.6 (0.54C, $R_2C=CH_2$), 154.0 (0.54C, $N(C=O)O$), 154.2 (0.46C, $N(C=O)O^*$), 165.0 (1C, $O=COEt$), 171.5 (0.46C, $O=COEt^*$), 171.7 (0.54C, $O=COEt$), 172.0 (0.54C, $O=COEt$), 172.2 (0.46C, $O=COEt^*$). Ratio of rotamers is 54:46. Signals for the minor rotamer are marked with an asterisk (*).

Purity (HPLC, method A): 98.9% ($t_R = 22.1$ min).

IR (neat): $\tilde{\nu}$ (cm^{-1}) = 2978 (C- H_{aliph}), 1744 (C=O_{ester}), 1701 (C=O_{carbamate}), 1651 (C=C), 1184, 1142, 1026 (C-N, C-O).

Exact mass (APCI): $m/z = 414.2144$ (calcd. 414.2122 for $C_{20}H_{32}NO_8$ $[M+H]^+$).

Diethyl *trans*-4-oxopiperidine-2,6-dicarboxylate (104)



TFA (3.60 mL, 47.0 mmol, 30 eq) was added to a solution of **87** (0.54 g, 1.57 mmol, 1 eq) in CH₂Cl₂ (15 mL) and the mixture was stirred at room temperature for 16 h. Then, the mixture was washed with NaHCO₃ (30 mL). The aqueous phase was extracted with CH₂Cl₂ (3 × 20 mL), the combined organic layers were dried (Na₂SO₄), filtered and concentrated *in vacuo*. Yellow oil, yield 0.27 g (71%).

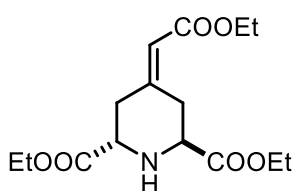
Chemical formula: C₁₁H₁₇NO₅ (243.3 g/mol).

TLC: *R*_f = 0.22 (cHex/EtOAc 1:1).

¹H NMR (600 MHz, CDCl₃): δ (ppm) = 1.28 (t, *J* = 7.1 Hz, 6H, 2 × OCH₂CH₃), 2.61 (ddd, *J* = 15.1 / 7.0 / 1.4 Hz, 2H, 3-CH_{ax}, 5-CH_{ax}), 2.71 (ddd, *J* = 15.0 / 5.5 / 1.3 Hz, 2H, 3-CH_{eq}, 5-CH_{eq}), 4.05 (dd, *J* = 7.0 / 5.5 Hz, 2H, 2-CH, 6-CH), 4.21 (q, *J* = 7.1 Hz, 4H, 2 × OCH₂CH₃). The signal for NH is not seen in the spectrum.

¹³C NMR (151 MHz, CDCl₃): δ (ppm) = 14.3 (2C, 2 × OCH₂CH₃), 42.7 (2C, C-3, C-5), 54.8 (2C, C-2, C-6), 61.8 (2C, 2 × OCH₂CH₃), 171.7 (2C, 2 × O=COEt), 204.7 (1C, C-4).

Diethyl *trans*-4-(2-ethoxy-2-oxoethylidene)piperidine-2,6-dicarboxylate (**105**)



TFA (2.10 mL, 28.4 mmol, 30 eq) was added to a solution of **103** (0.39 g, 0.95 mmol, 1 eq) in CH₂Cl₂ (10 mL) and the mixture was stirred at room temperature for 16 h. Then, the mixture was washed with NaHCO₃ (20 mL). The aqueous phase was extracted with CH₂Cl₂ (3 × 15 mL), the combined organic layers were dried (Na₂SO₄), filtered and concentrated *in vacuo*. Yellow oil, yield 0.27 g (90%).

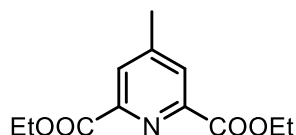
Chemical formula: C₁₅H₂₃NO₆ (313.4 g/mol).

TLC: *R*_f = 0.35 (cHex/EtOAc 1:1).

¹H NMR (600 MHz, CDCl₃): δ (ppm) = 1.25 (t, $J = 7.1$ Hz, 3H, OCH₂CH₃), 1.27 (t, $J = 7.1$ Hz, 3H, OCH₂CH₃), 1.28 (t, $J = 7.1$ Hz, 3H, OCH₂CH₃), 2.52 (dd, $J = 13.3 / 7.1$ Hz, 1H, 3/5-CH_{ax}), 2.61 (dd, $J = 13.3 / 5.0$ Hz, 1H, 3/5-CH_{eq}), 3.21 (dd, $J = 13.8, 6.9$ Hz, 1H, 3/5-CH_{ax}), 3.26 (dd, $J = 13.8 / 5.3$ Hz, 1H, 3/5-CH_{eq}), 3.86 (dd, $J = 6.9 / 5.3$ Hz, 1H, 2/6-CH), 3.92 (dd, $J = 7.1 / 5.0$ Hz, 1H, 2/6-CH), 4.12 – 4.24 (m, 6H, 3 × OCH₂CH₃), 5.75 (s, 1H, R₂C=CH).

¹³C NMR (151 MHz, CDCl₃): δ (ppm) = 14.3 (1C, OCH₂CH₃), 14.4 (2C, 2 × OCH₂CH₃), 31.2 (1C, C-3/5), 38.2 (1C, C-3/5), 55.6 (1C, C-2/6), 56.0 (1C, C-2/6), 60.0 (1C, OCH₂CH₃), 61.3 (1C, OCH₂CH₃), 61.4 (1C, OCH₂CH₃), 117.5 (1C, R₂C=CH), 153.4 (1C, R₂C=CH), 166.0 (1C, O=COEt), 172.2 (1C, O=COEt), 172.6 (1C, O=COEt).

Diethyl 4-methylpyridine-2,6-dicarboxylate (111)



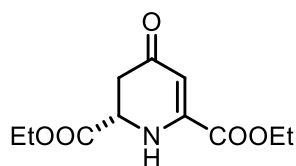
At 0 °C, NaOCl (0.75 M in H₂O, 3.90 mL, 2.90 mmol, 2 eq) was added to a solution of **70** (350 mg, 1.45 mmol, 1 eq) and AcOH (0.17 mL, 2.90 mmol, 2 eq) in *t*-BuOH (0.20 mL, 1.74 mmol, 1.2 eq) and methyl *t*-butyl methyl ether (8 mL) and the mixture was stirred for 1 h. Then, DIPEA (2.05 mL, 11.6 mmol, 8 eq) was added and the mixture was stirred at room temperature for 16 h. After the addition of H₂O (10 mL), the mixture was extracted with EtOAc (3 × 15 mL). The combined organic layers were dried (Na₂SO₄), filtered and concentrated *in vacuo*. The residue was purified by flash column chromatography (25 g cartridge, cHex/EtOAc 95:5 → 9:1). Yellow oil, yield 20 mg (6%).

Chemical formula: C₁₂H₁₅NO₄ (237.3 g/mol).

TLC: $R_f = 0.59$ (cHex/EtOAc 9:1).

¹H NMR (600 MHz, CDCl₃): δ (ppm) = 1.45 (t, $J = 7.2$ Hz, 6H, 2 × OCH₂CH₃), 2.51 (s, 3H, CH₃), 4.47 (q, $J =$ Hz, 4H, 2 × OCH₂CH₃), 8.10 (s, 2H, 3-CH_{arom}, 5-CH_{arom}).

¹³C NMR (151 MHz, CDCl₃): δ (ppm) = 14.4 (2C, 2 × OCH₂CH₃), 21.3 (1C, CH₃), 62.4 (2C, 2 × OCH₂CH₃), 128.8 (2C, C-3_{arom}, C-5_{arom}), 148.6 (2C, C-2_{arom}, C-6_{arom}), 150.2 (1C, C-4_{arom}), 165.1 (2C, 2 × O=COEt).

Diethyl (*RS*)-4-oxo-1,2,3,4-tetrahydropyridine-2,6-dicarboxylate (112)

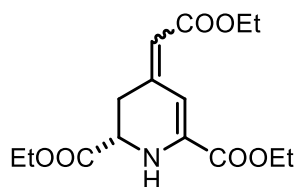
At 0 °C, NaOCl (0.75 M in H₂O, 1.70 mL, 1.28 mmol, 1.2 eq) was added to a solution of **104** (260 mg, 1.07 mmol, 1 eq) and AcOH (0.07 mL, 1.28 mmol, 1.2 eq) in *t*-BuOH (0.12 mL, 1.28 mmol, 1.2 eq) and methyl *t*-butyl methyl ether (10 mL) and the mixture was stirred for 1 h. Then, DIPEA (0.90 mL, 5.35 mmol, 5 eq) was added and the mixture was stirred at room temperature for 16 h. H₂O (15 mL) was added and the mixture was extracted with EtOAc (3 × 15 mL), dried (Na₂SO₄), filtered and concentrated *in vacuo*. The residue was purified by flash column chromatography (25 g cartridge, cHex/EtOAc 7:3 → 1:1). Colorless oil, yield 101 mg (39%).

Chemical formula: C₁₁H₁₅NO₅ (241.2 g/mol).

TLC: *R*_f = 0.40 (cHex/EtOAc 1:1).

¹H NMR (600 MHz, CDCl₃): δ (ppm) = 1.30 (t, *J* = 7.1 Hz, 3H, OCH₂CH₃), 1.35 (t, *J* = 7.1 Hz, 3H, OCH₂CH₃), 2.70 (dd, *J* = 16.5 / 12.3 Hz, 1H, 3-CH₂), 2.80 (dd, *J* = 16.5 / 5.8 Hz, 1H, 3-CH₂), 4.23 – 4.29 (m, 2H, OCH₂CH₃), 4.32 – 4.37 (m, 3H, 2-CH, OCH₂CH₃), 5.77 (s, 1H, 5-CH), 6.07 (s, 1H, NH).

¹³C NMR (151 MHz, CDCl₃): δ (ppm) = 14.1 (1C, OCH₂CH₃), 14.2 (1C, OCH₂CH₃), 38.2 (1C, C-3), 54.8 (1C, C-2), 62.4 (1C, OCH₂CH₃), 63.0 (1C, OCH₂CH₃), 102.2 (1C, C-5), 147.7 (1C, C-6), 162.9 (1C, O=COEt), 169.9 (1C, O=COEt), 192.5 (1C, C-4).

Diethyl (*E*- and (*Z*)-(*RS*)-4-(2-ethoxy-2-oxoethylidene)-1,2,3,4-tetrahydropyridine-2,6-dicarboxylate (113)

At 0 °C, NaOCl (0.75 M in H₂O, 2.20 mL, 1.65 mmol, 2 eq) was added to a solution of **105** (260 mg, 0.82 mmol, 1 eq) and AcOH (0.10 mL, 1.65 mmol, 2 eq) in *t*-BuOH (0.10 mL, 1.00 mmol, 1.2 eq) and methyl *t*-butyl ether (8 mL) and the mixture was stirred for 1 h. Then, DIPEA (1.15 mL, 6.61 mmol, 8 eq) was added and the mixture

was stirred at room temperature for 16 h. H₂O (10 mL) was added and the mixture was extracted with EtOAc (3 × 15 mL), dried (Na₂SO₄), filtered and concentrated *in vacuo*. The residue was purified by flash column chromatography (25 g cartridge, cHex/EtOAc 8:2 → 6:4). Yellow oil, yield 77 mg (30%).

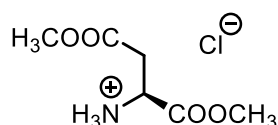
Chemical formula: C₁₅H₂₁NO₆ (311.3 g/mol).

TLC: R_f = 0.49 (cHex/EtOAc 7:3).

¹H NMR (600 MHz, CDCl₃): δ (ppm) = 1.24 – 1.32 (m, 6H, 2 × OCH₂CH₃, 2 × OCH₂CH₃*), 1.34 (t, *J* = 7.1 Hz, 3 × 0.55H, OCH₂CH₃), 1.35 (t, *J* = 7.1 Hz, 3 × 0.45H, OCH₂CH₃*), 2.76 (ddd, *J* = 15.5 / 9.6 / 1.5 Hz, 0.45H, 3-CH₂*), 2.83 (ddd, *J* = 15.5 / 5.0 / 1.2 Hz, 0.45H, 3-CH₂*), 3.10 (ddd, *J* = 17.0 / 10.2 / 2.0 Hz, 0.55H, 3-CH₂), 3.70 (ddd, *J* = 17.0 / 4.8 / 1.6 Hz, 0.55H, 3-CH₂), 4.00 (dd, *J* = 10.2 / 4.8 Hz, 0.55H, 2-CH), 4.06 (dd, *J* = 9.6 / 5.0 Hz, 0.45H, 2-CH*), 4.12 – 4.27 (m, 4H, 2 × OCH₂CH₃, 2 × OCH₂CH₃*), 4.30 (q, *J* = 7.1 Hz, 1.10H, OCH₂CH₃), 4.31 (q, *J* = 7.1 Hz, 0.9H, OCH₂CH₃*), 5.43 (s, 0.45H, 5-CH*), 5.66 (s, 0.55H, 5-CH), 6.08 (s, 0.55H, CHCOOEt), 7.37 (s, 0.45H, CHCOOEt*). Ratio of diastereomers is 55:45. The signals for the minor diastereomer are marked with an asterisk (*).

¹³C NMR (151 MHz, CDCl₃): δ (ppm) = 14.25, 14.28, 14.20, 14.31 (2C, 2 × OCH₂CH₃, 2 × OCH₂CH₃*), 14.50, 14.51 (1C, OCH₂CH₃, OCH₂CH₃*), 28.4 (0.55C, 3-C), 33.7 (0.45C, C-3*), 53.5 (0.55C, C-2), 55.8 (0.45C, C-2*), 59.82 (0.55, OCH₂CH₃), 59.84 (0.45C, OCH₂CH₃*), 61.8 (0.45C, OCH₂CH₃*), 61.9 (0.55C, OCH₂CH₃), 62.06 (0.55C, OCH₂CH₃), 62.13 (0.45C, OCH₂CH₃*), 102.4 (0.45C, CHCOOEt*), 107.1 (0.55C, CHCOOEt), 112.3 (0.45C, C-5*), 113.2 (0.55C, C-5), 137.9 (0.55C, C-6), 138.1 (0.45C, C-6*), 146.1 (0.45C, C-4*), 148.0 (0.55C, C-4), 163.2 (0.55C, O=COEt), 163.9 (0.45C, O=COEt*), 166.7 (0.45C, O=COEt*), 167.0 (0.55C, O=COEt), 170.8 (0.45C, O=COEt*), 171.2 (0.55C, O=COEt). Ratio of diastereomers is 55:45. The signals for the minor diastereomer are marked with an asterisk (*).

Dimethyl (S)-aspartate hydrochloride (125)¹⁴⁵



At 0 °C, SOCl₂ (3.8 mL, 53 mmol, 1.4 eq) was added dropwise to a suspension of (S)-aspartic acid (5.0 g, 38 mmol, 1 eq) in dry CH₃OH (30 mL) and the reaction mixture

was stirred at reflux for 16 h. Then, toluene (10 mL) and CH₂Cl₂ (10 mL) were added to the mixture and it was concentrated *in vacuo*. Colorless solid, mp 110 - 112 °C (lit.¹⁴⁵ 114 - 115 °C), yield 7.6 g (100%).

Chemical Formula: C₆H₁₂ClNO₄ (197.6 g/mol).

¹H NMR (600 MHz, CDCl₃) δ (ppm) = 3.13 – 3.42 (m, 2H, CH₂COOCH₃), 3.75 (s, 3H, OCH₃), 3.85 (s, 3H, OCH₃), 4.62 (brs, 1H, CHCOOCH₃), 8.67 (brs, 3H, NH₃⁺).

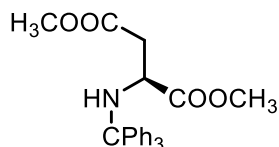
¹³C NMR (101 MHz, CDCl₃) δ (ppm) = 34.2 (1C, CH₂COOCH₃), 50.0 (1C, CHCOOCH₃), 53.1 (1C, OCH₃), 54.3 (1C, OCH₃), 168.9 (1C, CH₂COOCH₃), 170.7 (1C, CHCOOCH₃).

IR (neat): ν (cm⁻¹) = 2862 (C-H_{alip}), 1759, 1732 (C=O_{ester}), 1204, 1180, 1161, 1115 (C-N, C-O).

Exact mass (APCI): m/z = 162.0750 (calcd. 162.0761 for C₆H₁₂NO₄ [M-Cl]⁺).

Specific rotation: [α]_D²⁰ = +15.7 (c = 0.59, CH₃CN) (lit.⁶¹ [α]_D²⁴ = +22.0 (c = 1.0, CH₃OH)).

Dimethyl (S)-N-trityl aspartate (**121**)¹⁴⁶



NEt₃ (1.2 mL, 8.8 mmol, 2.0 eq) was added dropwise to a solution of **125** (1.0 g, 4.4 mmol, 1.0 eq) in CH₂Cl₂ (35 mL) and the mixture was stirred for 30 min at room temperature. Then at 0 °C, trityl chloride (1.5 g, 5.3 mmol, 1.2 eq) was added to the mixture and it was stirred at room temperature for 16 h. Then, the mixture was diluted with CH₂Cl₂ (5 mL) and washed with citric acid (2 M in H₂O, 35 mL), H₂O (35 mL) and brine (35 mL). The organic layer was dried (Na₂SO₄), filtered and concentrated *in vacuo*. The residue was purified by flash column chromatography (ø = 3 cm, h = 17 cm, cHex/EtOAc 8:2, V = 20 mL). Colorless oil, yield 9.6 g (62%).

Chemical Formula: C₂₅H₂₅NO₄ (403.5 g/mol).

TLC: R_f = 0.47 (cHex/EtOAc 8:2).

¹H NMR (600 MHz, CDCl₃) δ (ppm) = 2.51 (dd, J = 14.0 / 7.1 Hz, 1H, CH₂COOCH₃), 2.65 (dd, J = 14.0 / 5.4 Hz, 1H, CH₂COOCH₃), 2.93 (d, J = 10.0 Hz, 1H, NH-CPh₃), 3.26

(s, 3H, OCH₃), 3.68 (s, 3H, OCH₃), 3.70 (ddd, $J = 10.0 / 7.1 / 5.4$ Hz, 1H, CHCOOCH₃), 7.17 – 7.20 (m, 3H, 3 × 4-CH_{arom}), 7.24 – 7.28 (m, 6H, 3 × 3-CH_{arom}, 3 × 5-CH_{arom}), 7.45 – 7.52 (m, 6H, 3 × 2-CH_{arom}, 3 × 6-CH_{arom}).

¹³C NMR (151 MHz, CDCl₃) δ (ppm) = 40.4 (1C, CH₂COOCH₃), 51.9 (1C, OCH₃), 52.1 (1C, OCH₃), 53.8 (1C, CHCOOCH₃), 71.3 (1C, CPh₃), 126.7 (3C, 3 × C-4_{arom}), 128.0 (6C, 3 × C-3_{arom}, 3 × C-5_{arom}), 128.9 (6C, 3 × C-2_{arom}, 3 × C-6_{arom}) 145.8 (3C, 3 × C-1_{arom}), 171.2 (1C, CH₂COOCH₃), 174.1 (1C, CHCOOCH₃).

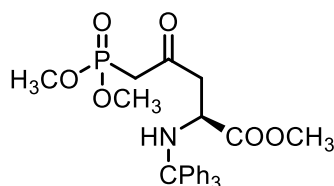
Purity (HPLC, method B): 98.2% ($t_R = 27.3$ min).

IR (neat): ν (cm⁻¹) = 3059 (C-H_{arom}), 2951 (C-H_{alip}), 1736 (C=O_{ester}), 1157, 1030 (C-N, C-O).

Exact mass (APCI): $m/z = 404.1808$ (calcd. 404.1856 for C₂₅H₂₆NO₄ [M+H]⁺).

Specific rotation: $[\alpha]_D^{20} = +15.5$ ($c = 0.93$, CH₃CN), (lit.⁶¹ $[\alpha]_D^{24} = +36.6$ ($c = 1.0$, CHCl₃)).

Methyl (S)-5-(dimethoxyphosphoryl)-4-oxo-2-(tritylamino)pentanoate (**122**)¹⁴⁶



At -78 °C, *n*-BuLi (2.5 M in hexane, 13.6 mL, 34 mmol, 2.3 eq) was added to a solution of dimethyl methylphosphonate (3.5 mL, 33 mmol, 2.2 eq) in dry THF (40 mL) and the mixture was stirred for 45 min. Then, the solution was transferred *via* cannula to a solution of **121** (6.1 g, 15 mmol, 1 eq) in dry THF (90 mL) at -78 °C and the mixture was stirred for 3 h. Then, NH₄Cl (2 mL) was added and the mixture was concentrated *in vacuo*. The residue was diluted in EtOAc (100 mL) and the solution was washed with H₂O (100 mL) and brine (100 mL). The organic layer was dried (Na₂SO₄), filtered and concentrated *in vacuo*. The residue was purified by flash column chromatography ($\varnothing = 6$ cm, $h = 15$ cm, cHex/EtOAc 2:8, $V = 80$ mL). Beige solid, mp 114 - 115 °C (lit.¹⁴⁶ 117 - 119 °C), yield 1.9 g (59%).

Chemical Formula: C₂₇H₃₀NO₆P (495.5 g/mol).

TLC: $R_f = 0.25$ (cHex/EtOAc 8:2).

¹H NMR (400 MHz, CDCl₃) δ (ppm) = 2.77 (dd, $J = 16.7 / 6.9$ Hz, 1H, 3-CH₂), 2.88 (dd, $J = 16.7 / 4.6$ Hz, 1H, 3-CH₂), 2.93 (d, $J = 9.5$ Hz, 1H, NHCPH₃), 3.02 (d, $J = 1.6$ Hz,

^1H , 5- CH_2), 3.08 (d, $J = 1.6$ Hz, 1H, 5- CH_2), 3.29 (s, 3H, OCH_3), 3.66 – 3.73 (m, 1H, 2- CH), 3.76 (s, 3H, OCH_3), 3.79 (s, 3H, OCH_3), 7.15 – 7.20 (m, 3H, 3 \times 4- CH_{arom}), 7.22 – 7.35 (m, 6H, 3 \times 3- CH_{arom} , 3 \times 5- CH_{arom}), 7.43 – 7.51 (m, 6H, 3 \times 2- CH_{arom} , 3 \times 6- CH_{arom}).

^{13}C NMR (101 MHz, CDCl_3) δ (ppm) = 42.0 (d, 1C, $J = 127.9$ Hz, C-5), 48.9 (1C, C-3), 52.2 (1C, OCH_3), 53.1 (1C, C-2), 53.2 (d, 1C, $J = 5.7$ Hz, POCH_3), 53.3 (d, 1C, $J = 5.7$ Hz, POCH_3), 71.4 (1C, CPh_3), 126.7 (3C, 3 \times C-4 $_{\text{arom}}$), 128.1 (6C, 3 \times C-3 $_{\text{arom}}$, 3 \times C-5 $_{\text{arom}}$), 128.9 (6C, 3 \times C-2 $_{\text{arom}}$, 3 \times C-6 $_{\text{arom}}$), 145.8 (3C, 3 \times C-1 $_{\text{arom}}$), 174.2 (1C, $\text{O}=\text{COEt}$), 199.4 (d, 1C, $J = 6.2$ Hz, C-4).

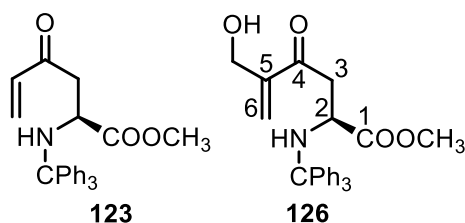
Purity (HPLC, method B): 95.7% ($t_{\text{R}} = 24.4$ min).

IR (neat): ν (cm^{-1}) = 3321 (N-H), 3055 (C- H_{arom}), 2951 (C- H_{alip}), 1717 (C=O $_{\text{ester}}$, ketone), 1265, 1034 (C-N, C-O).

Exact mass (APCI): $m/z = 496.1909$ (calcd. 496.1884 for $\text{C}_{27}\text{H}_{31}\text{NO}_6\text{P}$ [$\text{M}+\text{H}$] $^+$).

Specific rotation: $[\alpha]_{\text{D}}^{20} = +24.1$ ($c = 0.59$, CH_3CN), (lit.⁶¹ $[\alpha]_{\text{D}}^{24} = +31.1$ ($c = 1.0$, CHCl_3)).

Methyl (S)-4-oxo-2-(tritylamino)hex-5-enoate (123) and methyl (2S)-5-(hydroxymethyl)-4-oxo-2-(tritylamino)hex-5-enoate (126)



NaH (60%, 48 mg, 1.20 mmol, 1.2 eq) and formalin (37% in H_2O , 0.16 mL, 2.00 mmol, 2 eq) were added to a solution of **122** (500 mg, 1.00 mmol, 1 eq) in CH_3CN (12 mL) and the mixture was stirred at 40 °C for 16 h. Then, the mixture was concentrated *in vacuo*, the residue was diluted with EtOAc (20 mL) and the solution was washed with H_2O (20 mL) and brine (20 mL). The organic layer was dried (Na_2SO_4), filtered and concentrated *in vacuo*. The residue was purified by flash column chromatography (25 g cartridge, cHex/EtOAc 9:1 \rightarrow 4:6). At first **123**, then **126** was eluted.

123: Colorless solid, yield 134 mg (34%).

Chemical Formula: $\text{C}_{26}\text{H}_{25}\text{NO}_3$ (399.5 g/mol).

Analytical data: see **123**.

126: Colorless solid, mp 128 - 130 °C, yield 184 mg (43%).

Chemical Formula: C₂₇H₂₇NO₄ (429.5 g/mol).

TLC: R_f = 0.54 (cHex/EtOAc 1:1).

¹H NMR (600 MHz, DMSO-*d*₆): δ (ppm) = 2.76 (d, *J* = 6.6 Hz, 2H, 3-CH₂), 3.17 (d, *J* = 9.9 Hz, 1H, NHCPH₃), 3.21 (s, 3H, OCH₃), 3.50 (dt, *J* = 9.8 / 6.6 Hz, 1H, 2-CH), 4.03 (dt, *J* = 5.5 / 1.8 Hz, 2H, CH₂OH), 4.97 (t, *J* = 5.5 Hz, 1H, CH₂OH), 5.95 – 5.96 (m, 1H, C=CH₂), 6.03 – 6.04 (m, 1H, C=CH₂), 7.16 – 7.22 (m, 3H, 3 × 4-CH_{arom}), 7.25 – 7.30 (m, 6H, 3 × 3-CH_{arom}, 3 × 5-CH_{arom}), 7.37 – 7.44 (m, 6H, 3 × 2-CH_{arom}, 3 × 6-CH_{arom}).

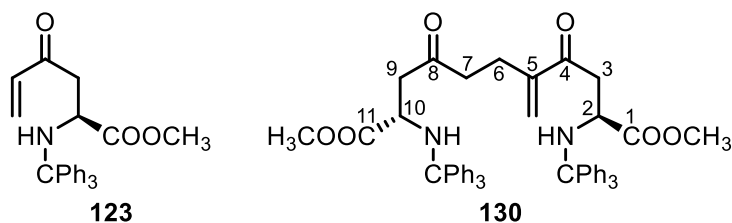
¹³C NMR (151 MHz, DMSO-*d*₆): δ (ppm) = 42.3 (1C, C-3), 51.3 (1C, OCH₃), 53.4 (1C, C-2), 58.9 (1C, CH₂OH), 70.7 (1C, CPh₃), 124.0 (C=CH₂), 126.4 (3C, 3 × C-4_{arom}), 127.8 (6C, 3 × C-3_{arom}, 3 × C-5_{arom}), 128.4 (6C, 3 × C-2_{arom}, 3 × C-6_{arom}), 145.7 (3C, 3 × C-1_{arom}), 147.9 (1C, C=CH₂), 173.5 (O=COCH₃), 198.9 (1C, C-4).

Purity (HPLC, method B): 99.6% (t_r = 24.9 min).

IR (neat): ν (cm⁻¹) = 3317 (O-H), 3055 (C-H_{arom}), 2947 (C-H_{alip}), 1736, (C=O_{ester}), 1678 (C=O_{ketone}), 1612, 1597 (C=C), 1200, 1169, 1030 (C-N, C-O).

Specific rotation: [α]_D²⁰ = +17.4 (c = 0.80, CH₃CN).

Methyl (S)-4-oxo-2-(tritylamino)hex-5-enoate (123) and dimethyl (2S,10S)-5-methylene-4,8-dioxo-2,10-bis(tritylamino)undecanedioate (130)



KOtBu (46 mg, 0.4 mmol, 1 eq) and *para*-formaldehyde (13 mg, 0.4 mmol, 1 eq) were added to a solution of **122** (0.2 g, 0.4 mmol, 1 eq) in CH₃CN (20 mL) and the mixture was stirred at 40 °C for 16 h. Then, it was concentrated *in vacuo*, the residue was dissolved in EtOAc, the solution was washed with H₂O (20 mL) and brine (20 mL). The organic layer was dried (Na₂SO₄), filtered and concentrated *in vacuo*. The residue was purified by flash column chromatography (25 g cartridge, cHex/EtOAc 9:1 → 8:2). At first **123**, then **130** was eluted.

123: Colorless oil, yield 18 mg (11%).

Chemical Formula: C₂₆H₂₅NO₃ (399.5 g/mol).

Analytical data: see **123**.

C57_2: Colorless solid, mp 132 - 135 °C, yield 30 mg (19%).

Chemical Formula: C₅₂H₅₀N₂O₆ (799.0 g/mol).

TLC: $R_f = 0.27$ (cHex/EtOAc 8:2).

¹H NMR (600 MHz, DMSO-*d*₆): δ (ppm) = 2.23 (t, $J = 7.4$ Hz, 2H, 6-CH₂), 2.31 – 2.43 (m, 3H, 7-CH₂, 9-CH₂), 2.46 (dd, $J = 16.2 / 7.3$ Hz, 1H, 9-CH₂), 2.70 (dd, $J = 15.8 / 5.5$ Hz, 1H, 3-CH₂), 2.74 (dd, $J = 15.8 / 8.0$ Hz, 1H, 3-CH₂), 3.14 – 3.18 (m, 2H, 2 × NH), 3.21 (s, 3H, OCH₃), 3.22 (s, 3H, OCH₃), 3.47 (ddd, $J = 9.7 / 7.3 / 5.2$ Hz, 1H, 10-CH), 3.50 (ddd, $J = 9.8 / 7.5 / 5.5$ Hz, 1H, 2-CH), 5.76 (s, 1H, C=CH₂), 5.94 (s, 1H, C=CH₂), 7.16 – 7.20 (m, 6H, 6 × 4-CH_{arom}), 7.24 – 7.28 (m, 12H, 6 × 3-CH_{arom}, 6 × 5-CH_{arom}), 7.37 – 7.41 (m, 12H, 6 × 2-CH_{arom}, 6 × 6-CH_{arom}).

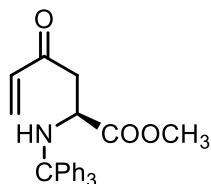
¹³C NMR (151 MHz, DMSO-*d*₆): δ (ppm) = 24.2 (1C, C-6), 41.1 (1C, C-7), 41.8 (1C, C-3), 46.2 (1C, C-9), 51.4 (1C, OCH₃), 51.4 (1C, OCH₃), 52.6 (1C, C-10), 53.5 (1C, C-2), 70.68 (1C, CPh₃), 70.69 (1C, CPh₃), 126.2 (1C, C=CH₂), 126.35 (3C, 3 × C-4_{arom}), 126.37 (3C, 3 × C-4_{arom}), 127.78 (6C, 3 × C-3_{arom}, 3 × C-5_{arom}), 127.79 (6C, 3 × C-3_{arom}, 3 × C-5_{arom}), 128.4 (12C, 6 × C-2_{arom}, 6 × C-6_{arom}), 145.70 (3C, 3 × C-1_{arom}), 145.72 (3C, 3 × C-1_{arom}), 146.5 (1C, C=CH₂), 173.5 (1C, C-1), 173.6 (1C, C-11), 199.1 (1C, C-4), 207.1 (1C, C-8).

Purity (HPLC, method B): 86.4% ($t_R = 31.2$ min).

IR (neat): ν (cm⁻¹) = 3055 (C-H_{arom}), 1732 (C=O_{ester}), 1674 (C=O_{ketone}), 1593 (C=C), 1238, 1042 (C-N, C-O).

Specific rotation: $[\alpha]_D^{20} = +26.1$ ($c = 0.46$, CH₃CN).

Methyl (S)-4-oxo-2-(tritylamino)hex-5-enoate (123)



Para-formaldehyde (43 mg, 1.4 mmol, 1 eq) was added to a mixture of **122** (0.7 g, 1.4 mmol, 1 eq) and K₂CO₃ (0.2 g, 1.4 mmol, 1 eq) in CH₃CN (150 mL) and the mixture was stirred at 40 °C for 16 h. Then, the mixture was concentrated *in vacuo*, diluted with EtOAc (20 mL) and washed with H₂O (20 mL) and brine (20 mL). The organic layer was dried (Na₂SO₄), filtered and concentrated *in vacuo*. The residue was purified by

flash column chromatography ($\varnothing = 3$ cm, $h = 18$ cm, cHex/Et₂O 8:2, $V = 12$ mL). Colorless oil, yield 0.34 g (61%).

Chemical Formula: C₂₆H₂₅NO₃ (399.5 g/mol).

TLC: $R_f = 0.33$ (cHex/EtOAc 8:2).

¹H NMR (600 MHz, DMSO-*d*₆): δ (ppm) = 2.61 (dd, $J = 15.9 / 5.3$ Hz, 1H, 3-CH₂), 2.70 (dd, $J = 15.9 / 7.5$ Hz, 1H, 3-CH₂), 3.18 (d, $J = 9.9$ Hz, 1H, NHCPH₃), 3.22 (s, 3H, OCH₃), 3.51 (ddd, $J = 9.8 / 7.4 / 5.3$ Hz, 1H, 2-CH), 5.93 (dd, $J = 10.6 / 1.0$ Hz, 1H, CH=CH₂), 6.13 (dd, $J = 17.7 / 1.0$ Hz, 1H, CH=CH₂), 6.25 (dd, $J = 17.7 / 10.6$ Hz, 1H, CH=CH₂), 7.17 – 7.21 (m, 3H, 3 × 4-CH_{arom}), 7.25 – 7.30 (m, 6H, 3 × 3-CH_{arom}, 3 × 5-CH_{arom}), 7.39 – 7.42 (m, 6H, 3 × 2-CH_{arom}, 3 × 6-CH_{arom}).

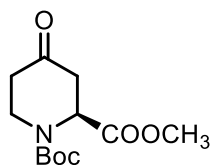
¹³C NMR (151 MHz, DMSO-*d*₆): δ (ppm) = 43.2 (1C, C-3), 51.4 (1C, OCH₃), 53.0 (1C, C-2), 70.7 (1C, NHCPH₃), 126.4 (3C, 3 × C-4_{arom}), 127.8 (6C, 3 × C-3_{arom}, 3 × C-5_{arom}), 128.4 (6C, 3 × C-2_{arom}, 3 × C-6_{arom}), 129.7 (1C, C-6), 136.5 (1C, C-5), 145.7 (3C, 3 × C-1_{arom}), 173.5 (1C, O=COEt), 198.3 (1C, C-4).

Purity (HPLC, method B): 98.8% ($t_R = 27.3$ min).

IR (neat): ν (cm⁻¹) = 3318 (N-H), 3055, 3021 (C-H_{arom}), 2924 (C-H_{alip}), 1736 (C=O_{ester}), 1678 (C=O_{ketone}), 1612, 1597 (C=C), 1200, 1169, 1030 (C-N, C-O).

Specific rotation: $[\alpha]_D^{20} = +21.6$ ($c = 0.62$, CH₂Cl₂).

1-*tert*-Butyl 2-methyl (*S*)-4-oxopiperidine-1,2-dicarboxylate ((*S*)-26b)



HCl (2 M in H₂O, 35 mL) was added to a solution of **123** (0.9 g, 2.2 mmol, 1 eq) in CH₃OH (120 mL) and the mixture was stirred at room temperature for 1 h. Then, Na₂CO₃ (25 mL) was added until pH 8 and the mixture was stirred at room temperature for 16 h. Then, Boc₂O (0.6 mL, 2.7 mmol, 1.2 eq) was added and the mixture was stirred at room temperature for 16 h. Then, brine (20 mL) was added and the mixture was extracted with EtOAc (3 × 20 mL). The combined organic layers were dried (Na₂SO₄), filtered and concentrated *in vacuo*. The residue was purified by flash column chromatography ($\varnothing = 3$ cm, $h = 15$ cm, cHex/Et₂O 6:4, $V = 12$ mL). Colorless oil, yield 0.18 g (32%).

Chemical Formula: C₁₂H₁₉NO₅ (257.3 g/mol).

TLC: $R_f = 0.17$ (cHex/EtOAc 8:2).

¹H NMR (600 MHz, CDCl₃) δ (ppm) = 1.46 (s, 4.5H, C(CH₃)₃), 1.49 (s, 4.5H, C(CH₃)₃), 2.42 – 2.62 (m, 2H, 5-CH₂), 2.71 – 2.89 (m, 2H, 3-CH₂), 3.55 – 3.71 (m, 1H, 6-CH₂), 3.74 (s, 3H, OCH₃), 4.02 – 4.10 (m, 1H, 6-CH₂), 4.85 (s, 0.5H, 2-CH), 5.13 (s, 0.5H, 2-CH). Ratio of rotamers is 1:1.

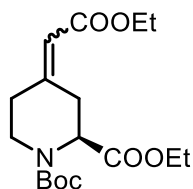
¹³C NMR (151 MHz, CDCl₃) δ (ppm) = 28.4 (3C, C(CH₃)₃), 39.5 (0.5C, C-6), 39.9 (1C, C-5), 40.7 (0.5C, C-6), 41.1 (0.5C, C-3), 41.4 (0.5C, C-3), 52.8 (1C, OCH₃), 54.1 (0.5C, C-2), 54.9 (0.5C, C-2). 81.4 (1C, C(CH₃)₃), 206.0 (1C, C-4). Ratio of rotamers is 1:1. Signals for N(C=O)O and O=COEt are not seen in the spectrum.

IR (neat): ν (cm⁻¹) = 2974 (C-H_{alip}), 1728 (C=O_{ester, ketone}), 1694 (C=O_{carbamate}), 1161, 1018 (C-N, C-O).

Exact mass (APCI): $m/z = 158.0860$ (calcd. 158.0812 for C₇H₁₂NO₃ [M-Boc+H]⁺).

Specific rotation: $[\alpha]_D^{20} = -19.8$ (c = 0.38, CH₃CN).

1-*tert*-Butyl 2-ethyl (*E*- and (*Z*)-(*S*)-4-(2-ethoxy-2-oxoethylidene)piperidine-1,2-dicarboxylate (**135**)



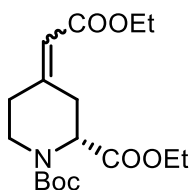
4-(Ethoxycarbonylmethylenetriphenylphosphorane (**33**) (5.00 g, 14.4 mmol, 2.0 eq) was added to a solution of 1-*tert*-Butyl 2-ethyl (*R*)-4-oxopiperidine-1,2-dicarboxylate ((*S*)-**26a**) (1.95 g, 7.19 mmol, 1.0 eq) in toluene (15 mL) and the mixture was stirred at reflux for 4 h. After concentrating the mixture *in vacuo*, the residue was purified by flash column chromatography (50 g cartridge, cHex/EtOAc 9:1 → 7:3). Colorless oil, yield 2.23 g (91%).

Purity (HPLC, method A): 99.8% ($t_R = 21.4$ min).

Exact mass (APCI): $m/z = 342.1950$ (calcd. 342.1911 for C₁₇H₂₇NO₆ [M+H]⁺).

Specific rotation: $[\alpha]_{20}^D = -17.8$ (c = 0.65; CH₃CN).

1-*tert*-Butyl 2-ethyl (*E*- and (*Z*)-(*R*)-4-(2-ethoxy-2-oxoethylidene)piperidine-1,2-dicarboxylate (*ent*-135)



As described for the synthesis of **135**, 1-*tert*-Butyl 2-ethyl (*S*)-4-oxopiperidine-1,2-dicarboxylate ((*R*)-**26a**) (1.40 g, 5.16 mmol, 1.0 eq) was reacted with 4-(ethoxycarbonylmethylenetriphenylphosphorane (**33**) (3.60 g, 10.3 mmol, 2.0 eq) in toluene (30 mL). Work-up was performed as described above. Purification was performed by flash column chromatography (50 g cartridge, cHex/EtOAc 9:1 → 7:3). Colorless oil, yield: 1.30 g (73%).

Purity (HPLC, method A): 99.8% ($t_R = 21.4$ min).

Exact mass (APCI): $m/z = 342.1928$ (calcd. 342.1911 for $C_{17}H_{27}NO_6$ [M+H]⁺).

Specific rotation: $[\alpha]_{20}^D = +7.8$ ($c = 0.62$; CH_3CN).

General analytical data for 135 and *ent*-135:

Chemical Formula: $C_{17}H_{27}NO_6$ (341.4 g/mol).

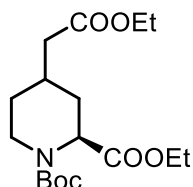
TLC: $R_f = 0.59$ (cHex/EtOAc 8:2).

¹H NMR (600 MHz, $CDCl_3$): δ (ppm) = 1.20 – 1.29 (m, 6H, 2 × OCH_2CH_3), 1.47 (s, 9H, $C(CH_3)_3$), 2.18 – 2.54 (m, 2H, CH_2), 2.56 – 2.68 (m, 0.5H, CH_2), 2.69 – 2.81 (m, 0.5H, CH_2), 3.13 – 3.34 (m, 1H, CH_2), 3.43 – 3.63 (m, 0.5H, CH_2), 3.91 – 4.07 (m, 1H, CH_2), 4.08 – 4.29 (m, 4.5 H, 2 × OCH_2CH_3 , CH_2) 4.64 – 4.85 (m, 0.5H, 2- CH), 4.90 – 5.06 (m, 0.5H, 2- CH), 5.70 – 5.77 (m, 1.0H, $R_2C=CH$). Ratio of isomers is 1:1 ((*E*)-**135** : (*Z*)-**135**).

¹³C NMR (151 MHz, $CDCl_3$): δ (ppm) = 14.27, 14.29, 14.40, 14.41 (2C, 2 × OCH_2CH_3), 28.5 (3C, $C(CH_3)_3$), 29.0, 30.2, 30.5 (1C, C-6), 34.9, 35.2, 36.8, 37.1 (1C, C-3/5), 40.4, 41.5, 42.0, 42.7 (1C, C-3/5), 54.5, 55.3, 55.4, 56.2 (1C, C-2), 59.97, 60.00 (1C, OCH_2CH_3), 61.3, 61.4 (1C, OCH_2CH_3), 80.7 (1C, $C(CH_3)_3$), 117.1 (1C, $R_2C=CH$), 154.0, 154.5 (1C, $N(C=O)O$), 165.6, 166.0 (1C, $O=COEt$), 170.9, 171.2 (1C, $O=COEt$). Ratio of isomers is 1:1 ((*E*)-**135** : (*Z*)-**135**). Ratio of rotamers is 1:1. The signal for C-4 is missing.

IR (neat): $\tilde{\nu}$ (cm⁻¹) = 2978 (CH_{aliph}), 1744 (C=O_{ester}), 1697 (C=O_{carbamate}), 1655 (C=C), 1250, 1157, 1138, 1111, 1034 (C-N, C-O).

1-*tert*-Butyl 2-ethyl (2*S*,4*R*)- and (2*S*,4*S*)-4-(2-ethoxy-2-oxoethyl)piperidine-1,2-dicarboxylate (115)

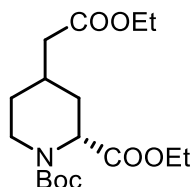


Pd/C (0.43 mg) was added to a solution of **135** (2.13 g, 6.24 mmol, 1.0 eq) in EtOH abs. (6 mL) and the suspension was stirred at room temperature for 16 h under H₂ (5 bar). Afterwards, the mixture was filtered over Celite[®] and the filtrate concentrated *in vacuo*. Colorless oil, yield 2.07 g (96%).

Exact mass (APCI): $m/z = 344.2129$ (calcd. 344.2068 for C₁₇H₃₀NO₆ [M+H]⁺).

Specific rotation: $[\alpha]_{20}^D = -21.5$ (c = 0.44; CH₃CN).

1-*tert*-Butyl 2-ethyl (2*R*,4*S*)- and (2*R*,4*R*)-4-(2-ethoxy-2-oxoethyl)piperidine-1,2-dicarboxylate (*ent*-115)



As described for the synthesis of **115**, *ent*-**135** (1.27 g, 3.72 mmol, 1.0 eq) was reduced with H₂ (1 bar) using Pd(OH)₂ (0.25 g) in EtOH (10 mL). Work-up was performed as described above. Colorless oil, yield 1.28 g (100%).

Exact mass (APCI): $m/z = 344.2083$ (calcd. 344.2068 for C₁₇H₃₀NO₆ [M+H]⁺).

Specific rotation: $[\alpha]_{20}^D = +14.7$ (c = 0.62; CH₃CN).

General analytical data for 115 and *ent*-115:

Chemical Formula: C₁₇H₂₉NO₆ (343.4 g/mol).

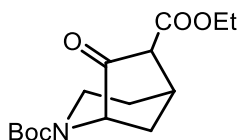
TLC: $R_f = 0.54$ (cHex/EtOAc 7:3).

¹H NMR (400 MHz, CDCl₃): δ (ppm) = 1.10 – 1.17 (m, 0.25H, 5-CH₂*), 1.20 – 1.30 (m, 6H, 2 × OCH₂CH₃), 1.35 – 1.50 (m, 10H, C(CH₃)₃, 5-CH₂, 3-CH₂*), 1.65 – 1.74 (m, 0.25H, 5-CH₂*), 1.76 – 1.84 (m, 1H, 4-CH_{ax}*, 5-CH₂), 1.85 – 1.94 (m, 0.75H, 3-CH₂), 2.03 (ddd, $J = 13.8 / 6.6 / 4.3$ Hz, 0.75H, 3-CH₂), 2.17 – 2.31 (m, 3H, 3-CH₂*, 4-CH_{ax}, CH₂COOEt, CH₂COOEt*), 2.92 (td, $J = 13.3 / 2.7$ Hz, 0.125H, 6-CH_{ax}*), 3.03 (td, $J = 13.3 / 2.7$ Hz, 0.125H, 6-CH_{ax}*), 3.33 (brs, 0.75H, 6-CH_{eq}), 3.63 (brs, 0.75H, 6-CH_{ax}), 3.94 (d, $J = 12.8$ Hz, 0.125H, 6-CH_{eq}*), 4.05 (d, $J = 12.3$ Hz, 0.125H, 6-CH_{eq}*), 4.08 – 4.25 (m, 4H, 2 × OCH₂CH₃), 4.37 (t, $J = 6.2$ Hz, 0.75H, 2-CH_{ax}), 4.73 (d, $J = 5.3$ Hz, 0.125H, 2-CH_{eq}*), 4.91 (d, $J = 5.3$ Hz, 0.125H, 2-CH_{eq}*). Ratio of diastereomers is 3:1 ((2*S*,4*R*)-**115**:(2*S*,4*S*)-**115**). The signals for the minor diastereomer (2*S*,4*S*)-**115** are marked with an asterisk (*). Ratio of rotamers is 1:1.

¹³C NMR (151 MHz, CDCl₃): δ (ppm) = 14.3 14.38 14.40 14.5 (2C, 2 × OCH₂CH₃), 28.3 (0.75, C-4), 28.5 (3 × 0.75C, C(CH₃)₃), 28.5 (3 × 0.25C, C(CH₃)₃*), 28.9 (0.75C, C-5), 29.8 (0.125C, C-4*), 29.9 (0.125C, C-4*), 31.1 (0.125C, C-5*), 31.1 (0.75C, C-3), 31.3 (0.125C, C-5*), 32.9 (0.125C, C-3*), 32.9 (0.125C, C-3*), 38.0 (0.74C, CHCH₂COOEt), 38.3 (0.75C, C-6), 41.0 (0.125C, C-6*), 41.2 (0.125C, CHCH₂COOEt*), 41.2 (0.125C, CHCH₂COOEt*), 41.8 (0.125C, C-6*), 53.9 (0.125C, C-2*), 54.1 (0.75C, C-2), 55.0 (0.125C, C-2*), 60.5 (0.25C, OCH₂CH₃*), 60.6 (0.75C, OCH₂CH₃), 61.2 (0.75C, OCH₂CH₃), 61.3 (0.125C, OCH₂CH₃*), 61.3 (0.125C, OCH₂CH₃*), 80.2 (0.25C, C(CH₃)₃*), 80.2 (0.75C, C(CH₃)₃), 171.6 (0.125C, O=COEt*), 171.8 (0.125C, O=COEt*), 172.1 (0.125C, O=COEt*), 172.1 (0.125C, O=COEt*), 172.3 (0.75C, O=COEt), 172.8 (0.75C, O=COEt). Ratio of diastereomers is 3:1 ((2*S*,4*R*)-**115**:(2*S*,4*S*)-**115**). The signals for the minor diastereomer (2*S*,4*S*)-**115** are marked with an asterisk (*). Ratio of rotamers is 1:1.

IR (neat): $\tilde{\nu}$ (cm⁻¹) = 2978 (C-H_{aliph}), 1732 (C=O_{ester}), 1697 (C=O_{carbamate}), 1259, 1092, 1030 (C-N, C-O).

2-tert-Butyl 6-ethyl (1*S*,5*R*)-7-oxo-2-azabicyclo[3.2.1]octane-2,6-dicarboxylate (136)



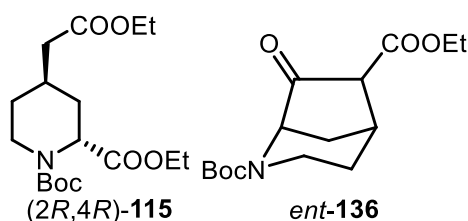
NaHMDS (1.0 M in THF, 11.7 mL, 11.7 mmol, 2.0 eq) was added to a refluxing solution of **115** (2.00 g, 5.82 mmol, 1.0 eq) in dry THF (300 mL) under N₂ and the mixture was

heated to reflux for 3 h. Then, the mixture was poured into a half-sat. NH_4Cl solution (150 mL). The mixture was extracted with EtOAc (3 × 75 mL), the combined organic layers were dried (Na_2SO_4), filtered and concentrated *in vacuo*. The residue was purified by flash column chromatography (50 g cartridge, cHex/EtOAc 9:1 → 7:3). Colorless oil, yield 1.56 g (90%).

Exact mass (APCI): $m/z = 298.1646$ (calcd. 298.1649 for $\text{C}_{15}\text{H}_{24}\text{NO}_5$ $[\text{M}+\text{H}]^+$).

Specific rotation: $[\alpha]_{20}^{\text{D}} = -114.5$ ($c = 0.60$; CH_3CN).

1-*tert*-Butyl 2-ethyl (2*R*,4*R*)-4-(2-ethoxy-2-oxoethyl)piperidine-1,2-dicarboxylate ((2*R*,4*R*)-115) and 2-*tert*-Butyl 6-ethyl (1*R*,5*S*)-7-oxo-2-azabicyclo[3.2.1]octane-2,6-dicarboxylate (*ent*-136)



As described for the synthesis of **136**, *ent*-**115** (2.00 g, 5.82 mmol, 1.0 eq) was reacted with NaHMDS (1.0 M in THF, 11.7 mL, 11.7 mmol, 2.0 eq) in dry THF (300 mL). Work-up was performed as described above. Purification was performed by flash column chromatography (50 g cartridge, cHex/EtOAc 9:1 → 7:3). At first (2*R*,4*R*)-**115**, then *ent*-**136** was eluted.

(2*R*,4*R*)-**115**: Colorless oil, yield 0.08 g (7%).

TLC: $R_f = 0.54$ (cHex/EtOAc 7:3).

$^1\text{H NMR}$ (600 MHz, CDCl_3): δ (ppm) = 1.09 – 1.19 (m, 1H, 5- CH_{ax}), 1.22 – 1.31 (m, 6H, 2 × OCH_2CH_3), 1.35 – 1.42 (m, 1H, 3- CH_{ax}), 1.43 (s, 4.5H, $\text{C}(\text{CH}_3)_3$), 1.46 (m, 4.5H, $\text{C}(\text{CH}_3)_3$), 1.69 (dm, $J = 13.0$ Hz, 0.5H, 5- CH_{eq}), 1.75 (dm, $J = 13.0$ Hz, 0.5H, 5- CH_{eq}), 1.77 – 1.84 (m, 1H, 4- CH_{ax}), 2.15 – 2.30 (m, 3H, 3- CH_{eq} , $\text{CHCH}_2\text{COOEt}$), 2.92 (td, $J = 13.3 / 3.0$ Hz, 0.5H, 6- CH_{ax}), 3.03 (td, $J = 13.3 / 3.1$ Hz, 0.5H, 6- CH_{ax}), 3.94 (d, $J = 13.3$ Hz, 0.5H, 6- CH_{eq}), 4.06 (d, $J = 13.3$ Hz, 0.5H, 6- CH_{eq}), 4.10 – 4.15 (m, 2H, OCH_2CH_3), 4.16 – 4.23 (m, 2H, OCH_2CH_3), 4.73 (d, $J = 5.3$ Hz, 0.5H, 2- CH_{eq}), 4.91 (d, $J = 5.3$ Hz, 0.5H, 2- CH_{eq}). Ratio of rotamers is 1:1.

$^{13}\text{C NMR}$ (151 MHz, CDCl_3): δ (ppm) = 14.36 (0.5C, OCH_2CH_3), 14.40 (1C, OCH_2CH_3), 14.5 (0.5C, OCH_2CH_3), 28.4 (1.5C, $\text{C}(\text{CH}_3)_3$), 28.5 (1.5C, $\text{C}(\text{CH}_3)_3$), 29.7 (0.5C, C-4),

29.9 (0.5C, C-4), 31.0 (0.5C, C-5), 31.3 (0.5C, C-5), 32.9 (0.5C, C-3), 32.9 (0.5C, C-3), 41.0 (0.5C, C-6), 41.2 (0.5C, CHCH₂COOEt), 41.2 (0.5C, CHCH₂COOEt), 41.8 (0.5C, C-6), 53.9 (0.5C, C-2), 54.9 (0.5C, C-2), 60.5 (1C, OCH₂CH₃), 61.27 (0.5C, OCH₂CH₃), 61.29 (0.5C, OCH₂CH₃), 80.2 (1C, C(CH₃)₃), 155.5 (0.5C, N(C=O)O), 156.0 (0.5C, N(C=O)O), 171.6 (0.5C, O=COEt), 171.8 (0.5C, O=COEt), 172.1 (0.5C, O=COEt), 172.1 (0.5C, O=COEt). Ratio of rotamers is 1:1.

IR (neat): $\tilde{\nu}$ (cm⁻¹) = 2971 (C-H_{aliph}), 1732 (C=O_{ester}), 1694 (C=O_{carbamate}), 1157, 1030 (C-N, C-O).

Exact mass (APCI): m/z = 344.2077 (calcd. 344.2068 for C₁₇H₃₀NO₆ [M+H]⁺).

Specific rotation: $[\alpha]_{20}^D$ = -9.6 (c = 0.64; CH₃CN).

ent-136: Yellow oil, yield 0.55 g (55%).

Exact mass (APCI): m/z = 298.1618 (calcd. 298.1649 for C₁₅H₂₄NO₅ [M+H]⁺).

Specific rotation: $[\alpha]_{20}^D$ = +106.2 (c = 0.61; CH₃CN).

General analytical data for 136 and *ent*-136:

Chemical Formula: C₁₅H₂₃NO₅ (297.4 g/mol).

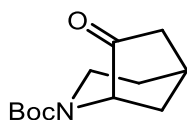
TLC: R_f = 0.44 (cHex/EtOAc 7:3).

¹H NMR (600 MHz, CDCl₃): δ (ppm) = 1.23 – 1.32 (m, 3H, OCHCH₃), 1.45 (s, 9H, C(CH₃)₃), 1.64 – 1.76 (m, 1H, 4/8-CH₂), 1.79 – 1.88 (m, 1H, 4/8-CH₂), 1.90 – 2.03 (m, 1H, 4/8-CH₂), 2.20 – 2.31 (m, 1H, 4/8-CH₂), 2.83 – 3.05 (m, 2.5H, 3-CH₂, 5-CH, 6-CH), 3.12 – 3.31 (m, 0.5H, 6-CH), 3.75 – 4.01 (m, 1H, 3-CH₂), 4.07 – 4.29 (m, 2H, OCH₂CH₃), 4.35 – 4.68 (m, 1H, 1-CH).

¹³C NMR (151 MHz, CDCl₃): δ (ppm) = 14.3 (1C, OCH₂CH₃), 28.5 (3C, C(CH₃)₃), 29.8 (1C, C-4/8), 34.7 (1C, C-4/8), 35.4 (1C, C-4), 57.2 (1C, C-6), 61.9 (1C, OCH₂CH₃), 80.8 (1C, C(CH₃)₃), 154.3 (1C, N(C=O)O), 167.9 (1C, O=COEt). The signals for C-1 and C-7 are missing.

IR (neat): $\tilde{\nu}$ (cm⁻¹) = 2974, 2936 (C-H_{aliph}), 1763 (C=O_{ester}), 1724 (C=O_{ketone}), 1690 (C=O_{carbamate}), 1161, 1057, 1030 (C-N, C-O).

tert-Butyl (1*S*,5*R*)-7-oxo-2-azabicyclo[3.2.1]octane-2-carboxylate (137)

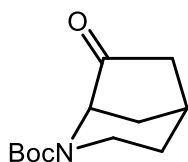


LiCl (1.07 g, 25.2 mmol, 5.0 eq) and H₂O (10 drops) were added to a solution of **136** (1.50 g, 5.04 mmol, 1.0 eq) in DMSO (10 mL) and the mixture was stirred at 160 °C for 2 h. After adding the solution to H₂O (100 mL), it was extracted with EtOAc (3 × 50 mL), the combined organic layers were dried (Na₂SO₄), filtered and concentrated *in vacuo*. The residue was purified by a flash column chromatography (50 g cartridge, cHex/EtOAc 9:1 → 7:3). Colorless solid, mp 107 - 110 °C, yield 0.81 g (72%).

Exact mass (APCI): $m/z = 226.1432$ (calcd. 226.1438 for C₁₂H₂₀NO₃ [M+H]⁺).

Specific rotation: $[\alpha]_{20}^D = -147.1$ (c = 0.56; CH₃OH).

***tert*-Butyl (1*R*,5*S*)-7-oxo-2-azabicyclo[3.2.1]octane-2-carboxylate (*ent*-**137**)**



As described for the synthesis of **137**, *ent*-**136** (166 mg, 0.56 mmol, 1.0 eq) was reacted with LiCl (118 mg, 2.79 mmol, 5.0 eq) in DMSO (2 mL) and H₂O (2 drops). Work-up was performed as described above. Purification was performed by flash column chromatography (25 g cartridge, cHex/EtOAc 9:1 → 8:2). Colorless solid, mp 107 - 110 °C, yield 93 mg (74%).

Exact mass (APCI): $m/z = 226.1444$ (calcd. 226.1438 for C₁₂H₂₀NO₃ [M+H]⁺).

Specific rotation: $[\alpha]_{20}^D = +120.4$ (c = 0.63; CH₃OH).

General analytical data for **137 and *ent*-**137**:**

Chemical Formula: C₁₂H₁₉NO₃ (225.3 g/mol).

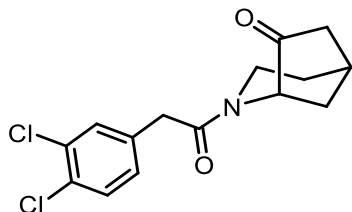
TLC: $R_f = 0.43$ (cHex/EtOAc 7:3).

¹H NMR (400 MHz, CDCl₃): δ (ppm) = 1.44 (s, 9H, C(CH₃)₃), 1.61 (d, $J = 9.9$ Hz, 1H, 4-CH₂), 1.85 (s, 2H, 6-CH₂), 1.87 – 1.97 (m, 1H, 4-CH₂), 2.07 (d, $J = 18.8$ Hz, 1H, 8-CH₂), 2.30 (dd, $J = 18.8 / 6.6$ Hz, 1H, 8-CH₂), 2.67 – 2.74 (m, 1H, 5-CH), 2.86 – 3.00 (m, 1H, 3-CH₂), 3.80 – 4.06 (m, 1H, 3-CH₂), 4.21 – 4.51 (m, 1H, 1-CH).

¹³C NMR (151 MHz, CDCl₃): δ (ppm) = 28.5 (3C, C(CH₃)₃), 29.9 (1C, C-4), 30.9 (1C, C-5), 36.4 (1C, C-6), 42.0 (1C, C-8), 80.5 (1C, C(CH₃)₃), 154.4 (1C, N(C=O)O), 214.5 (1C, C-7). Signals for C-1 and C-3 are missing.

IR (neat): $\tilde{\nu}$ (cm⁻¹) = 2974, 2866 (C-H_{aliph}), 1744 (C=O_{ketone}), 1678 (C=O_{carbamate}), 1150, 1111, 1049 (C-N, C-O).

(1*S*,5*R*)-2-[2-(3,4-dichlorophenyl)acetyl]-2-azabicyclo[3.2.1]octan-7-one (139)



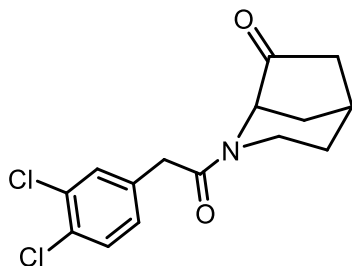
A suspension of **137** (0.30 g, 1.33 mmol, 1.0 eq) in EtOH (3 mL) and H₂O (12 mL) was stirred at 100 °C for 40 h. Afterwards at 0 °C, NaOH (60 mg, 1.49 mmol, 3.0 eq) and a solution of **53** (0.75 mg, 3.36 mmol, 2.5 eq) in THF (5 mL) were added and the mixture was stirred at room temperature for 2 h. Then, it was extracted with EtOAc (3 × 20 mL), the combined organic layers were dried (Na₂SO₄), filtered and concentrated *in vacuo*. The residue was purified by flash column chromatography (25 g cartridge, cHex/EtOAc 7:3 → 4:6). Colorless solid, 152 - 154 °C, yield 0.21 g (52%).

Purity (HPLC, method A): 87.4% (*t_R* = 18.8 min).

Exact mass (APCI): *m/z* = 312.0571 (calcd. 312.0553 for C₁₅H₁₆³⁵Cl₂NO₂ [M+H]⁺).

Specific rotation: $[\alpha]_{20}^D = -97.9$ (c = 0.60; CH₃OH).

(1*R*,5*S*)-2-[2-(3,4-dichlorophenyl)acetyl]-2-azabicyclo[3.2.1]octan-7-one (ent-139)



As described for the synthesis of **139**, *ent*-**137** (112 mg, 0.50 mmol, 1.0 eq) was stirred in EtOH (1 mL) and H₂O (4 mL) at 100 °C for 16 h and reacted then with **53** (333 mg, 1.49 mmol, 3.0 eq). Work-up was performed as described above. Purification was performed by flash column chromatography (25 g cartridge, cHex/EtOAc 6:4 → 1:1). Colorless solid, mp 152 - 154 °C, yield 117 mg (75%).

Purity (HPLC, method A): 86.2% (*t_R* = 18.9 min).

Exact mass (APCI): $m/z = 312.0540$ (calcd. 312.0553 for $C_{15}H_{16}^{35}Cl_2NO_2 [M+H]^+$).

Specific rotation: $[\alpha]_{20}^D = +96.2$ ($c = 0.47$; CH_3OH).

General analytical data for 139 and *ent*-139:

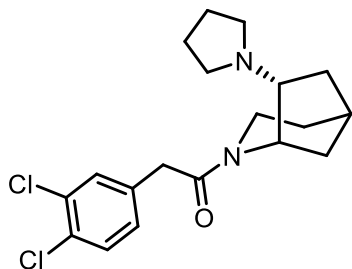
Chemical Formula: $C_{15}H_{15}Cl_2NO_2$ (312.2 g/mol).

TLC: $R_f = 0.28$ (cHex/EtOAc 4:6).

1H NMR (600 MHz, $CDCl_3$): δ (ppm) = 1.63 (dm, $J = 13.3$ Hz, 0.45H, 4/8- CH_2^*), 1.73 (dm, $J = 13.5$ Hz, 0.55H, 4/8- CH_2), 1.76 – 2.00 (m, 3H, 4- CH_2 , 8- CH_2), 2.12 (ddd, $J = 18.8 / 3.7$ Hz, 0.45H, 6- CH_2^*), 2.19 (dd, $J = 19.1 / 3.5$ Hz, 0.55H, 6- CH_2), 2.37 (dm, $J = 18.9$ Hz, 1H, 6- CH_2), 2.78 (s, 1H, 5- CH_{eq}), 2.92 (ddd, $J = 14.5 / 12.1 / 5.4$ Hz, 0.55H, 3- CH_{ax}), 3.19 (dd, $J = 13.3 / 4.8$ Hz, 0.45H, 3- CH_{ax}^*), 3.58 – 3.79 (m, 2.45H, CH_2 -aryl, 3- CH_{eq}^*), 4.04 (d, $J = 4.5$ Hz, 0.55H, 1- CH_{eq}), 4.37 (dd, $J = 14.5 / 6.9$ Hz, 0.55H, 3- CH_{eq}), 4.96 (d, $J = 4.3$ Hz, 0.45H, 1- CH_{eq}^*), 7.04 – 7.10 (m, 1H, 6- CH_{arom}), 7.32 (d, $J = 2.0$ Hz, 0.45H, 2- CH_{arom}^*), 7.35 (d, $J = 2.0$ Hz, 0.55H, 2- CH_{arom}), 7.37 – 7.43 (m, 1H, 5- CH_{arom}). Ratio of rotamers is 55:45. The signals for the minor rotamer are marked with an asterisk (*).

^{13}C NMR (151 MHz, $CDCl_3$): δ (ppm) = 29.6 (0.55C, C-4/8), 30.5 (0.45C, C-4/8*), 30.9 (0.55C, C-5), 31.1 (0.45C, C-5*), 36.3 (0.55C, C-4/8), 36.5 (0.45C, C-4/8*), 37.2 (0.55C, C-3), 39.8 (0.55C, CH_2 -aryl), 39.9 (0.45C, CH_2 -aryl*), 41.3 (0.45C, C-3*), 42.0 (0.55C, C-6), 42.6 (0.45C, C-6*), 56.1 (0.45C, C-1*), 60.0 (0.55C, C-1), 128.2 (0.45C, C-6 $_{arom}^*$), 128.7 (0.55C, C-6 $_{arom}$), 130.6 (0.55C, C-2/5 $_{arom}$), 130.6 (0.45C, C-2/5 $_{arom}^*$), 130.8 (0.45C, C-2/5 $_{arom}^*$), 131.3 (0.55C, C-2/5 $_{arom}$), 132.7 (0.55C, C-3/4 $_{arom}$), 132.8 (0.45C, C-3/4 $_{arom}^*$), 132.8 (0.45C, C-3/4 $_{arom}^*$), 133.7 (0.55C, C-3/4 $_{arom}$), 134.8 (0.45C, C-1 $_{arom}^*$), 135.1 (0.55C, C-1 $_{arom}$), 168.1 (0.55C, N(C=O)), 169.0 (0.45C, N(C=O)*), 214.1 (0.55C, C-7), 215.6 (0.45C, C-7*). Ratio of rotamers is 55:45. The signals for the minor rotamer are marked with an asterisk (*).

IR (neat): $\tilde{\nu}$ (cm^{-1}) = 2947 (C-H $_{alip}$), 1748 (C=O $_{ketone}$), 1632 (C=O $_{amide}$), 1151, 1126, 1065 (C-N, C-O).

2-(3,4-dichlorophenyl)-1-[(1*S*,5*S*,7*R*)-7-(pyrrolidin-1-yl)-2-azabicyclo[3.2.1]octan-2-yl]ethan-1-one (23a)

Pyrrolidine (0.26 mL, 3.20 mmol, 10 eq) and AcOH (18 μ L, 0.32 mmol, 1 eq) were added to a solution of **139** (110 mg, 0.32 mmol, 1 eq) in dry THF (2 mL) and the mixture was stirred for 16 h. Then, NaBH(OAc)₃ (136 mg, 0.64 mmol, 2 eq) was added and the mixture was stirred at room temperature for 2 h. Afterwards, NaHCO₃ (10 mL) was added, the mixture was extracted with CH₂Cl₂ (3 \times 7 mL), the combined organic layers were dried (Na₂SO₄), filtered and concentrated *in vacuo*. The residue was purified by a flash column chromatography (ϕ = 3 cm, h = 12 cm, CH₂Cl₂/NH₃ (7 M in CH₃OH)/CH₃OH 99:1:0 \rightarrow 96:2:2, V = 12 mL). Colorless solid, mp 80 - 81 $^{\circ}$ C, yield 86 mg (73%). The two enantiomers were separated by chiral, preparative HPLC (HPLC method E) with five separations. (1*R*,5*R*,7*S*)-**23a** fraction: 45 - 48 min, (1*S*,5*S*,7*R*)-**23a** fraction: 53 - 59 min. The solvents were removed *in vacuo*.

(1*S*,5*S*,7*R*)-23a:

Purity (HPLC, method A): 99.1% (t_R = 17.1 min).

Enantiomeric excess (chiral HPLC, method C): 53.6% (t_R = 28.6 min).

Exact mass (APCI): m/z = 367.1329 (calcd. 367.1338 for C₁₉H₂₅³⁵Cl₂N₂O [M+H]⁺).

Specific rotation: $[\alpha]_{20}^D$ = -40.3 (c = 0.36; CH₃OH).

Enantiomerically pure (1*S*,5*S*,7*R*)-23a:

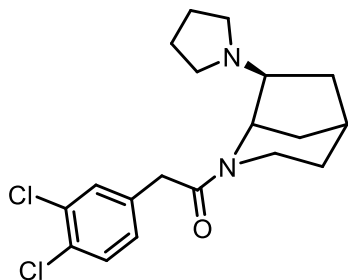
Purity (HPLC, method A): 95.1% (t_R = 17.1 min).

Enantiomeric excess (chiral HPLC, method C): 99.9% (t_R = 21.8 min).

Exact mass (APCI): m/z = 367.1317 (calcd. 367.1338 for C₁₉H₂₅³⁵Cl₂N₂O [M+H]⁺).

Specific rotation: $[\alpha]_{20}^D$ = -70.4 (c = 0.17; CH₃OH).

2-(3,4-dichlorophenyl)-1-[(1*R*,5*R*,7*S*)-7-(pyrrolidin-1-yl)-2-azabicyclo[3.2.1]octan-2-yl]ethan-1-one (*ent*-23a**)**



As described for the synthesis of **23a**, *ent*-**139** (50 mg, 0.16 mmol, 1.0 eq) was reacted with pyrrolidine (17 μ L, 0.21 mmol, 1.3 eq) and AcOH (1 drop) in dry THF (3 mL). After 15 min, NaBH(OAc)₃ (70 mg, 0.32 mmol, 2.0 eq) was added. Work-up was performed as described above. Purification was performed by flash column chromatography ($\varnothing = 1$ cm, $h = 14$ cm, CH₂Cl₂/CH₃OH/NH₄OH 96:3:1 \rightarrow 94:5:1, $V = 12$ mL). Colorless solid, mp 84 - 85 $^{\circ}$ C, yield 30 mg (51%).

(1*R*,5*R*,7*S*)-23a:

Purity (HPLC, method A): 97.2% ($t_R = 17.2$ min).

Enantiomeric excess (chiral HPLC, method C): 52.8% ($t_R = 24.1$ min).

Exact mass (APCI): $m/z = 367.1314$ (calcd. 367.1338 for C₁₉H₂₅³⁵Cl₂N₂O [M+H]⁺).

Specific rotation: $[\alpha]_{20}^D = +38.6$ ($c = 0.36$; CH₃OH).

Enantiomerically pure (1*R*,5*R*,7*S*)-23a:

Purity (HPLC, method A): 95.7% ($t_R = 17.1$ min).

Enantiomeric excess (chiral HPLC, method C): 96.3% ($t_R = 19.2$ min).

Exact mass (APCI): $m/z = 367.1307$ (calcd. 367.1338 for C₁₉H₂₅³⁵Cl₂N₂O [M+H]⁺).

Specific rotation: $[\alpha]_{20}^D = +65.9$ ($c = 0.13$; CH₃OH).

General analytical data for 23a and *ent*-23a:

Chemical Formula: C₁₉H₂₄Cl₂N₂O (367.3 g/mol).

TLC: $R_f = 0.32$ (CH₂Cl₂/CH₃OH 95:5).

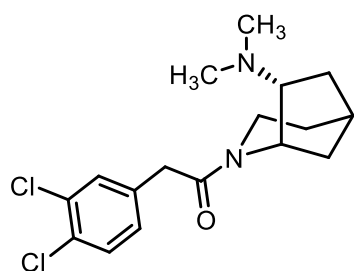
¹H NMR (600 MHz, CDCl₃): δ (ppm) = 1.22 – 1.26 (m, 0.2H, 8-CH₂*), 1.32 – 1.40 (m, 1H, 4-CH₂, 4-CH₂*), 1.41 – 1.47 (m, 1.6H, 6-CH₂, 8-CH₂), 1.50 – 1.57 (m, 1.2H, 4-CH₂, 4-CH₂*, 6-CH₂*), 1.58 – 1.61 (m, 0.2H, 8-CH₂*), 1.62 – 1.74 (m, 5 \times 0.8 + 4 \times 0.2H, 8-CH₂, N(CH₂CH₂)₂, N(CH₂CH₂)₂*), 1.98 – 2.13 (m, 1H, 6-CH₂, 6-CH₂*), 2.28 – 2.51

(m, 5H, 5-CH, N(CH₂CH₂)₂), 5-CH*, N(CH₂CH₂)₂*), 2.52 – 2.57 (m, 0.8H, 7-CH), 2.58 – 2.62 (m, 0.2H, 7-CH*), 3.43 (td, *J* = 13.3 / 5.0 Hz, 0.2H, 3-CH₂*), 3.54 (dd, *J* = 12.9 / 6.0 Hz, 0.8H, 3-CH₂), 3.62 – 3.69 (m, 0.8 + 2 × 0.2H, CH₂-aryl, CH₂-aryl*), 3.70 – 3.77 (m, 1.6H, 3-CH₂, CH₂-aryl), 4.02 (t, *J* = 4.2 Hz, 0.2H, 1-CH*), 4.46 (dd, *J* = 13.3 / 6.2 Hz, 0.2H, 3-CH₂*), 4.98 (brs, 0.8H, 1-CH), 7.10 (d, *J* = 8.3 Hz, 0.8H, 6-CH_{arom}), 7.12 (dd, *J* = 8.3 / 2.0 Hz, 0.2H, 6-CH_{arom}*), 7.34 (brs, 0.8H, 2-CH_{arom}), 7.36 (d, *J* = 8.2 Hz, 0.8H, 5-CH_{arom}), 7.37 – 7.39 (m, 0.4H, 2-CH_{arom}*, 5-CH_{arom}). Ratio of rotamers is 8:2. The signals for the minor rotamer are marked with an asterisk (*).

¹³C NMR (151 MHz, CDCl₃): δ (ppm) = 23.6 (1.6C, N(CH₂CH₂)₂), 23.7 (0.4C, N(CH₂CH₂)₂*), 31.4 (0.2C, C-4*), 32.0 (0.8C, C-4), 33.6 (0.8C, C-5), 33.91 (0.2C, C-5*), 33.93 (0.8C, C-6), 34.5 (0.2C, C-6*), 37.6 (0.8C, C-8), 37.8 (0.2C, C-3*), 38.4 (0.2C, C-8*), 40.0 (0.2C, CH₂-aryl*), 40.5 (0.8C, CH₂-aryl), 42.3 (0.8C, C-3), 53.5 (0.8C, C-1), 54.1 (0.4C, N(CH₂CH₂)₂*), 54.5 (1.6C, N(CH₂CH₂)₂), 58.7 (0.2C, C-1*), 68.5 (0.8C, C-7), 68.8 (0.2C, C-7*), 128.3 (0.8C, C-6_{arom}), 128.7 (0.2C, C-6_{arom}*), 130.49 (0.2C, C-5_{arom}*), 130.51 (0.8C, C-5_{arom}), 130.75 (0.8C, C-2_{arom}), 130.78 (0.2C, C-2_{arom}*), 130.9 (0.2C, C-3/4_{arom}*), 131.2 (0.8C, C3/4_{arom}), 132.56 (0.2C, C-3/4_{arom}*), 132.59 (0.8C, C-3/4_{arom}), 135.97 (0.2C, C-1_{arom}*), 136.02 (0.8C, C-1_{arom}), 167.8 (0.2C, N(C=O)*), 168.0 (0.8C, N(C=O)). Ratio of rotamers is 8:2. The signals for the minor rotamer are marked with an asterisk (*).

IR (neat): $\tilde{\nu}$ (cm⁻¹) = 2947 (C-H_{alip}), 1628 (C=O_{amide}), 1126, 1030 (C-N, C-O).

2-(3,4-dichlorophenyl)-1-[(1*S*,5*S*,7*R*)-7-(dimethylamino)-2-azabicyclo[3.2.1]octan-2-yl]ethan-1-one (23b)



HN(CH₃)₂ (2 M in THF, 1.12 mL, 2.24 mmol, 10 eq) and AcOH (13 μL, 0.22 mmol, 1 eq) were added to a solution of **139** (70 mg, 0.22 mmol, 1 eq) in dry THF (2 mL). After the mixture was stirred for 2 h at room temperature, NaBH(OAc)₃ (95 mg, 0.45 mmol, 2 eq) was added and the mixture was stirred at room temperature overnight. Afterwards, NaHCO₃ (10 mL) was added, the mixture was extracted with EtOAc (3 × 7 mL), the combined organic layers were dried (Na₂SO₄), filtered and concentrated *in vacuo*. The

residue was purified by a flash column chromatography (10 g cartridge, CH₂Cl₂/CH₃OH 98:2 → 95:5). Yellow oil, yield 51 mg (68%). The two enantiomers were separated by chiral, preparative HPLC (HPLC method F) with four separations. (1*S*,5*S*,7*R*)-**23b** fraction: 34 - 39 min, (1*R*,5*R*,7*S*)-**23b** fraction: 45 - 54 min. The solvents were removed *in vacuo*.

(1*S*,5*S*,7*R*)-**23b**:

Purity (HPLC, method A): 99.2% (*t_R* = 16.2 min).

Enantiomeric excess (chiral HPLC, method D): 54.3% (*t_R* = 12.5 min).

Exact mass (APCI): *m/z* = 341.1211 (calcd. 341.1182 for C₁₇H₂₃³⁵Cl₂N₂O [M+H]⁺).

Specific rotation: $[\alpha]_{20}^D = -37.9$ (*c* = 0.36; CH₃OH).

Enantiomerically pure (1*S*,5*S*,7*R*)-**23b**:

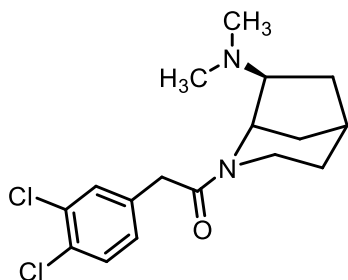
Purity (HPLC, method A): 98.0% (*t_R* = 16.3 min).

Enantiomeric excess (chiral HPLC, method D): 99.9% (*t_R* = 12.3 min).

Exact mass (APCI): *m/z* = 341.1168 (calcd. 341.1182 for C₁₇H₂₃³⁵Cl₂N₂O [M+H]⁺).

Specific rotation: $[\alpha]_{20}^D = -73.8$ (*c* = 0.31; CH₃OH).

2-(3,4-dichlorophenyl)-1-[(1*R*,5*R*,7*S*)-7-(dimethylamino)-2-azabicyclo[3.2.1]octan-2-yl]ethan-1-one (*ent*-23b**)**



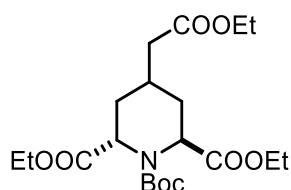
As described for the synthesis of **23b**, *ent*-**139** (74 mg, 0.24 mmol, 1.0 eq) was reacted with HN(CH₃)₂ (2 M in THF, 1.2 mL, 2.37 mmol, 10.0 eq) and AcOH (14 μL, 0.24 mmol, 1.0 eq) in dry THF (3 mL). After 16 h, NaBH(OAc)₃ (100 mg, 0.47 mmol, 2.0 eq) was added. Work-up was performed as described above. Purification was performed by flash column chromatography (10 g cartridge, CH₂Cl₂/CH₃OH 98:2 → 95:5). Yellow oil, yield 62 mg (76%).

(1*R*,5*R*,7*S*)-23b:**Purity** (HPLC, method A): 98.6% ($t_R = 16.4$ min).**Enantiomeric excess** (chiral HPLC, method D): 49.8 ($t_R = 16.2$ min).**Exact mass** (APCI): $m/z = 341.1182$ (calcd. 341.1182 for $C_{17}H_{23}^{35}Cl_2N_2O$ $[M+H]^+$).**Specific rotation:** $[\alpha]_{20}^D = +37.6$ ($c = 0.36$; CH_3OH).**Enantiomerically pure (1*R*,5*R*,7*S*)-23b:****Purity** (HPLC, method A): 95.1% ($t_R = 16.4$ min).**Enantiomeric excess** (chiral HPLC, method D): 98.8% ($t_R = 16.5$ min).**Exact mass** (APCI): $m/z = 341.1152$ (calcd. 341.1182 for $C_{17}H_{23}^{35}Cl_2N_2O$ $[M+H]^+$).**Specific rotation:** $[\alpha]_{20}^D = +74.3$ ($c = 0.26$; CH_3OH).**General analytical data for 23b and ent-23b:****Chemical Formula:** $C_{17}H_{22}Cl_2N_2O$ (341.3 g/mol).**TLC:** $R_f = 0.38$ (CH_2Cl_2/CH_3OH 95:5). **1H NMR** (600 MHz, $CDCl_3$): δ (ppm) = 1.23 – 1.27 (m, 0.14H, 8- CH_2^*), 1.33 – 1.43 (m, 1.86H, 4- CH_2 , 6- CH_2^*), 1.45 (d, $J = 12.1$ Hz, 0.86H, 8- CH_2), 1.47 – 1.54 (m, 1.0H, 4- CH_2 , 6- CH_2^*), 1.56 (ddm, $J = 13.0 / 6.3$ Hz, 0.14H, 4- CH_2^*), 1.60 – 1.64 (m, 0.14H, 8- CH_2^*), 1.66 – 1.72 (m, 0.86H, 8- CH_2), 1.99 – 2.09 (m, 1.0H, 6- CH_2), 2.17 (s, 0.84H, $N(CH_3)_2^*$) 2.19 (s, 5.16H, $N(CH_3)_2$), 2.36 – 2.46 (m, 2H, 5- CH , 7- CH), 3.37 (td, $J = 13.2 / 4.9$ Hz, 0.14H, 3- CH_2^*), 3.55 (dd, $J = 13.2 / 6.2$ Hz, 0.86H, 3- CH_2), 3.64 – 3.74 (m, 2.86H, CH_2 -aryl, 3- CH_2), 4.02 (t, $J = 4.1$ Hz, 0.14H, 1- CH^*), 4.50 (dd, $J = 13.7 / 6.2$ Hz, 0.14H, 3- CH_2), 4.97 – 5.02 (m, 0.86H, 1- CH), 7.08 (d, $J = 8.3$ Hz, 0.86H, 6- CH_{arom}), 7.12 (dd, $J = 8.3 / 2.1$ Hz, 0.14H, 6- CH_{arom}^*), 7.35 – 7.40 (m, 2H, 2- CH_{arom} , 5- CH_{arom}). Ratio of rotamers is 86:14. The signals for the minor rotamer are marked with an asterisk (*). **^{13}C NMR** (151 MHz, $CDCl_3$): δ (ppm) = 31.5 (0.14C, C-4*), 32.1 (0.86C, C-4), 33.5 (0.86C, C-5), 33.75 (0.86C, C-6), 33.81 (0.14C, C-5*), 34.3 (0.14C, C-6*), 37.6 (0.14C, C-3*), 37.8 (0.86C, C-8), 38.7 (0.14C, C-8*), 39.9 (0.14C, CH_2 -aryl*), 40.4 (0.86C, CH_2 -aryl), 41.9 (0.86C, C-3), 45.7 (0.28C, $N(CH_3)_2^*$), 45.9 (1.72C, $N(CH_3)_2$), 52.6 (0.86C, C-1), 57.7 (0.14C, C-1*), 70.3 (1C, C-7), 178.4 (0.86C, C-6 $_{arom}$), 178.7 (0.14C, C-6 $_{arom}^*$), 130.48 (0.86C, C-5 $_{arom}$), 130.51 (0.14C, C-5 $_{arom}^*$), 130.79 (0.14C, C-2 $_{arom}^*$), 130.81 (0.86C, C-2 $_{arom}$), 131.0 (0.14, C $_{arom}$ -Cl*), 131.2 (0.86C, C $_{arom}$ -Cl), 132.56 (0.14C, C $_{arom}$ -Cl*), 132.61 (0.86C, C $_{arom}$ -Cl), 135.8 (0.14C, C-1 $_{arom}^*$), 135.9 (0.86C,

C-1_{arom}), 167.9 (0.14C, N(C=O)*), 168.0 (0.86C, N(C=O)). Ratio of rotamers is 86:14. The signals for the minor rotamer are marked with an asterisk (*).

IR (neat): $\tilde{\nu}$ (cm⁻¹) = 2947 (C-H_{alip}), 1628 (C=O_{amide}), 1165, 1134, 1030 (C-N, C-O).

1-tert-Butyl 2,6-diethyl trans-4-(2-ethoxy-2-oxoethyl)piperidine-1,2,6-tricarboxylate (144)



Pd/C (0.2 g) was added to a solution of **103** (3.9 g, 9.5 mmol, 1.0 eq) in EtOH abs. (40 mL) and the mixture was stirred under H₂ (1 bar) at room temperature for 16 h. Then, the mixture was filtered over Celite[®] and the filtrate was concentrated *in vacuo*. Colorless solid, mp 57 - 58 °C, yield 3.6 g (92%).

Chemical Formula: C₂₀H₃₃NO₈ (415.5 g/mol).

TLC: R_f = 0.48 (cHex/EtOAc 7:3).

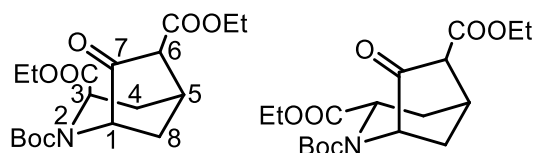
¹H NMR (600 MHz, DMSO-d₆): δ (ppm) = 1.13 – 1.28 (m, 10H, 3 × OCH₂CH₃, 3/5-CH₂), 1.32 (s, 9H, C(CH₃)₃), 1.48 – 1.59 (m, 1H, 3/5-CH₂), 1.62 – 1.73 (m, 1H, 4-CH), 1.94 – 2.01 (m, 2H, 3-CH₂, 5-CH₂), 2.23 (dd, *J* = 16.0 / 7.2 Hz, 1H, R₂CH₂COOEt), 2.29 (dd, *J* = 16.0 / 6.6 Hz, 1H, R₂CH₂COOEt), 3.92 (dd, *J* = 11.5 / 4.7 Hz, 0.6H, 2/6-CH), 3.98 – 4.23 (m, 6.4H, 3 × OCH₂CH₃, 2/6-CH*), 4.56 (d, *J* = 6.0 Hz, 0.6H, 2/6-CH), 4.60 (d, *J* = 5.7 Hz, 0.4H, 2/6-CH*). Ratio of rotamers is 6:4. The signals for the minor rotamer are marked with an asterisk (*).

¹³C NMR (151 MHz, DMSO-d₆): δ (ppm) = 14.0 (1C, OCH₂CH₃), 14.1 (1C, OCH₂CH₃), 14.2 (1C, OCH₂CH₃), 26.6 (1C, C-4), 27.7 (3C, C(CH₃)₃), 31.1 (1C, C-3/5), 33.2 (1C, C-3/5), 39.1 (1C, R₂CH₂COOEt), 55.3 (0.4C, C-2/6*), 55.6 (0.4C, C-2/6*), 55.62 (0.6, C-2/6), 55.7 (0.6C, C-2/6), 60.0 (1C, OCH₂CH₃), 60.1 (0.6C, OCH₂CH₃), 60.6 (0.4C, OCH₂CH₃*), 60.9 (0.4C, OCH₂CH₃*), 61.0 (0.6C, OCH₂CH₃), 80.4 (0.6C, C(CH₃)₃), 81.0 (0.4C, C(CH₃)₃*), 155.8 (1.0C, N(C=O)O), 171.4 (1.0C, O=COEt) 171.8 (0.6C, O=COEt) 172.1 (0.4C, O=COEt*) 172.40 (0.6C, O=COEt) 172.44 (0.4C, O=COEt*). Ratio of rotamers is 6:4. The signals for the minor rotamer are marked with an asterisk (*).

IR (neat): $\tilde{\nu}$ (cm⁻¹) = 2978 (C-H_{aliph}), 1732 (C=O_{ester}), 1705 (C=O_{carbamate}), 1157, 1096, 1030 (C-N, C-O).

Exact mass (APCI): m/z = 416.2289 (calcd. 416.2279 for C₂₀H₃₄NO₈ [M+H]⁺).

2-tert-Butyl 3,6-diethyl (1RS,3RS,5RS)- and (1RS,3SR,5RS)-7-oxo-2-azabicyclo[3.2.1]octane-2,3,6-tricarboxylate (145)



NaHMDS (1.9 M in THF, 4.4 mL, 8.4 mmol, 2.0 eq) was added to a refluxing solution of **144** in dry THF (210 mL) under N₂ and the mixture was heated to reflux for 2 h. Then, the mixture was poured into a half-sat. NH₄Cl solution (150 mL). The mixture was extracted with EtOAc (3 × 75 mL), the combined organic layers were dried (Na₂SO₄), filtered and concentrated *in vacuo*. The residue was purified by flash column chromatography (100 g cartridge, cHex/EtOAc 8:2). Colorless solid, mp 44 - 45 °C, yield 1.24 g (80%).

Chemical Formula: C₁₈H₂₇NO₇ (369.4 g/mol).

TLC: R_f = 0.37 (cHex/EtOAc 7:3).

¹H NMR (400 MHz, CDCl₃): δ = 1.20 – 3.21 (m, 6H, 2 × OCH₂CH₃), 1.39, 1.41, 1.43, 1.47, 1.48, 1.49 (s, 9H, C(CH₃)₃), 1.54 (dd, J = 10.8 / 3.8 Hz, 0.16H, 4/8-CH₂), 1.74 (dm, J = 12.9 Hz, 0.80H, 4/8-CH₂), 1.76 – 1.93 (m, 0.22H, 4/8-CH₂), 1.96 – 2.01 (m, 0.12H, 4/8-CH₂), 2.04 (dm, J = 10.8 Hz, 0.08H, 4/8-CH₂), 2.10 (dd, J = 13.4 / 2.1 Hz, 0.08H, 4/8-CH₂), 2.11 (dddd, J = 13.6 / 8.2 / 5.0 / 2.2 Hz, 0.08H, 4/8-CH₂), 2.18 – 2.28 (m, 1.30H, 4/8-CH₂), 2.29 – 2.36 (m, 1.16H, 4/8-CH₂), 2.87 (d, J = 3.3 Hz, 0.32H, 6-CH), 2.89 – 2.99 (m, 1.50H, 5-CH, 6-CH), 3.10 (d, J = 2.7 Hz, 0.14H, 6-CH), 3.14 (d, J = 6.0 Hz, 0.02H, 5-CH, 6-CH), 3.18 (d, J = 5.7 Hz, 0.02H, 5-CH, 6-CH), 3.95 – 4.26 (m, 4H, 2 × OCH₂CH₃), 4.55 (d, J = 4.7 Hz, 0.46H, 1/3-CH), 4.59 (d, J = 9.7 Hz, 0.46H, 1/3-CH), 4.68 (dd, J = 6.8 / 4.2 Hz, 0.46H, 1/3-CH), 4.72 – 4.76 (m, 0.46H, 1/3-CH), 4.80 (d, J = 4.8 Hz, 0.08H, 1/3-CH), 4.98 (d, J = 4.5 Hz, 0.08H, 1/3-CH). Mixture of diastereomers, tautomers and rotamers.

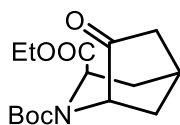
¹³C NMR δ = 14.0, 14.1, 14.25, 14.27, 14.34, 14.35, 14.49, 14.50 (2C, 2 × OCH₂CH₃), 28.2, 28.27, 28.30, 28.38, 28.43, 28.5 (3C, C(CH₃)₃), 30.1, 30.2, 31.1, 31.3 (1C, C-4/8)

33.5, 33.7, 40.0, 40.1 (1C, C-4/8), 34.25, 34.34, 34.6 (1C, C-5), 51.7, 51.9, 52.6, 52.9 (1C, C-1/3), 55.66, 55.72, 57.2 (1C, C-6), 56.3, 57.1, 57.8 (1C, C-1/3), 60.3, 60.4, 60.5, 60.7, 61.51, 61.53, 61.6, 61.83, 61.85, 61.9, 61.96, 61.98 (2C, 2 × OCH₂CH₃), 80.7, 80.8, 81.4, 81.7 (1C, C(CH₃)₃), 168.06, 168.12 (1C, N(C=O)O), 172.6, 172.9, 173.1, 173.3 (2C, 2 × O=COEt), 205.1, 205.3 (1C, C-7). Mixture of diastereomers, tautomers and rotamers.

IR (neat): $\tilde{\nu}$ (cm⁻¹) = 2970 (C-H_{aliph}), 1759, 1740 (C=O_{ester}), 1721 (C=O_{ketone}), 1705 (C=O_{carbamate}), 1196, 1153 (C-N, C-O).

Exact mass (APCI): m/z = 370.1889 (calcd. 370.1860 for C₁₈H₂₈NO₇ [M+H]⁺).

2-tert-Butyl 3-ethyl (1RS,3SR,5RS)-7-oxo-2-azabicyclo[3.2.1]octane-2,3-dicarboxylate (146)



Method 1:

LiCl (115 mg, 2.70 mmol, 5.0 eq) and H₂O (2 drops) were added to a solution of **145** (200 mg, 0.54 mmol, 1.0 eq) in DMSO (2 mL) and the mixture was stirred in a preheated oil bath at 160 °C for 1.5 h. After pouring the solution into H₂O (20 mL), the mixture was extracted with EtOAc (3 × 15 mL) and the combined organic layers were dried (Na₂SO₄), filtered and concentrated *in vacuo*. The residue was purified by flash column chromatography (25 g cartridge, cHex/EtOAc 9:1 → 8:2). Colorless oil, yield 96 mg (60%).

Method 2:

A solution of **145** (1.84 g, 5.0 mmol, 1.0 eq) in EtOH (15 mL) and H₂O (3 mL) was heated to reflux for 40 h. The solution was concentrated *in vacuo* and the residue was purified twice by flash column chromatography (1. 25 g cartridge, cHex/EtOAc 7:3 → 4:6; 2. 25 g cartridge, 9:1 → 7:3). Colorless oil, yield 1.39 g (94%).

Chemical Formula: C₁₅H₂₃NO₅ (297.4 g/mol).

TLC: R_f = 0.38 (cHex/EtOAc 7:3).

¹H NMR (600 MHz, CDCl₃): δ (ppm) = 1.19 – 1.29 (m, 3H, OCH₂CH₃), 1.42 (s, 4.5H, C(CH₃)₃), 1.49 (s, 4.5H, C(CH₃)₃), 1.74 – 1.82 (m, 1.5H, 8-CH₂), 1.83 – 1.87 (m, 0.5H,

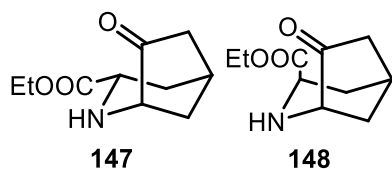
8-CH₂), 1.90 (dd, $J = 19.2 / 3.7$ Hz, 0.5H, 6-CH₂), 1.94 (dd, $J = 19.3 / 3.4$ Hz, 0.5H, 6-CH₂), 2.15 – 2.22 (m, 1H, 6-CH₂), 2.23 – 2.35 (m, 2H, 4-CH₂), 2.67 – 2.73 (m, 1H, 5-CH), 4.04 – 4.20 (m, 2H, OCH₂CH₃), 4.40 (d, $J = 4.2$ Hz, 0.5H, 1-CH), 4.59 – 4.62 (m, 1H, 1-CH, 3-CH_{eq}), 4.72 (d, $J = 9.4$ Hz, 0.5H, 3-CH_{eq}). Ratio of rotamers is 1:1.

¹³C NMR (151 MHz, CDCl₃): δ (ppm) = 14.0 (0.5C, OCH₂CH₃), 14.1 (0.5C, OCH₂CH₃), 28.3 (1.5C, C(CH₃)₃), 28.4 (1.5C, C(CH₃)₃), 30.1 (0.5C, C-5), 30.1 (0.5C, C-5), 31.2 (0.5C, C-4), 31.5 (0.5C, C-4), 35.1 (0.5C, C-8), 35.3 (0.5C, C-8), 40.4 (0.5C, C-6), 40.5 (0.5C, C-6), 51.8 (0.5C, C-3), 52.7 (0.5C, C-3), 55.8 (0.5C, C-1), 57.4 (0.5C, C-1), 61.8 (0.5C, OCH₂CH₃), 61.8 (0.5C, OCH₂CH₃), 81.1 (0.5C, C(CH₃)₃), 81.3 (0.5C, C(CH₃)₃), 154.2 (0.5C, N(C=O)O), 154.5 (0.5C, N(C=O)O), 172.8 (0.5C, O=COEt), 173.2 (0.5C, O=COEt), 212.7 (0.5C, C-7), 212.8 (0.5C, C-7). Ratio of rotamers is 1:1.

IR (neat): $\tilde{\nu}$ (cm⁻¹) = 2974 (C-H_{aliph}), 1755 (C=O_{ester}), 1728 (C=O_{ketone}) 1694 (C=O_{carbamate}), 1188, 1157, 1107, 1069, 1026 (C-N, C-O).

Exact mass (APCI): $m/z = 298.1632$ (calcd. 298.1649 for C₁₅H₂₄NO₅ [M+H]⁺).

Ethyl (1*RS*,3*RS*,5*RS*)-7-oxo-2-azabicyclo[3.2.1]octane-3-carboxylate (147) and Ethyl (1*RS*,3*SR*,5*RS*)-7-oxo-2-azabicyclo[3.2.1]octane-3-carboxylate (148)



TFA (1.42 mL, 18.5 mmol, 5 eq) was added to a solution of **146** (1.10 g, 3.69 mmol, 1 eq) in CH₂Cl₂ (25 mL) and the mixture was stirred at room temperature for 16 h. Then, the mixture was washed with NaHCO₃ (30 mL) and the aqueous phase was extracted with CH₂Cl₂ (3 × 20 mL). The combined organic layers were dried (Na₂SO₄), filtered and concentrated *in vacuo*. Colorless oil, yield 0.58 g (80%). The diastereomers were not separated by flash column chromatography. According to the ¹H NMR spectrum a mix of diastereomers in the ratio 1:9 (**147/148**) was obtained.

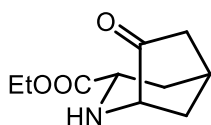
Chemical Formula: C₁₀H₁₅NO₃ (197.2 g/mol).

147:

Analytical data: see **147**.

148:

Analytical data: see **148**.

Ethyl (1*RS*,3*RS*,5*RS*)-7-oxo-2-azabicyclo[3.2.1]octane-3-carboxylate (147)

H₂O (5 mL) was added to a solution of **145** (186 mg, 0.50 mmol, 1.0 eq) in EtOH (1 mL) and the mixture was heated to reflux for 16 h. Afterwards, NaHCO₃ (10 ml) was added and the mixture was extracted with CH₂Cl₂ (3 × 15 mL). The combined organic layers were dried (Na₂SO₄), filtered and concentrated *in vacuo*. The residue was purified by flash column chromatography (10 g cartridge, cHex/EtOAc 3:7 → 1:9) Yellow oil, yield 32 mg, (32%).

Chemical Formula: C₁₀H₁₅NO₃ (197.2 g/mol).

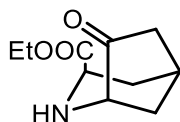
TLC: *R*_f = 0.36 (EtOAc).

¹H NMR (600 MHz, CDCl₃): δ (ppm) = 1.25 (t, *J* = 7.1 Hz, 3H, OCH₂CH₃), 1.81 – 1.86 (m, *J* = 12.2 / 4.8 / 2.3 Hz, 1H, 8-CH_{ax}), 1.90 – 1.96 m, 2H, 4-CH_{eq}, 8-CH_{eq}), 1.99 – 2.04 (m, 2H, 4-CH_{ax}, 6-CH₂), 2.34 (dd, *J* = 18.7 / 6.9 Hz, 1H, 6-CH₂), 2.69 – 2.73 (m, 1H, 5-CH), 3.21 (d, *J* = 4.6 Hz, 1H, 1-CH), 3.66 (dd, *J* = 11.9 / 4.9 Hz, 1H, 3-CH_{ax}), 4.12 – 4.23 (m, 2H, OCH₂CH₃). A signal for NH is not seen in the spectrum.

¹³C NMR (151 MHz, CDCl₃): δ (ppm) = 14.3 (1C, OCH₂CH₃), 30.9 (1C, C-5), 33.0 (1C, C-4), 36.3 (1C, C-8), 42.6 (1C, C-6), 52.0 (1C, C-3), 59.3 (1C, C-1), 61.3 (1C, OCH₂CH₃), 172.7 (1C, O=COEt), 219.6 (1C, C-7).

IR (neat): $\tilde{\nu}$ (cm⁻¹) = 3325 (N-H), 2951 (C-H_{aliph}), 1736 (C=O_{ester, ketone}), 1184, 1084, 1026 (C-N, C-O).

Exact mass (APCI): *m/z* = 198.1134 (calcd. 198.1125 for C₁₀H₁₆NO₃ [M+H]⁺).

Ethyl (1*RS*,3*SR*,5*RS*)-7-oxo-2-azabicyclo[3.2.1]octane-3-carboxylate (148)

HCl (1 M in H₂O, 9 mL) was added to a solution of **145** (850 mg, 2.30 mmol, 1.0 eq) in EtOH (19 mL) and the mixture was heated to reflux for 1.5 h. Afterwards, NaHCO₃ (20 mL) was added and the mixture was extracted with CH₂Cl₂ (3 × 15 mL). The combined organic layers were dried (Na₂SO₄), filtered and concentrated *in vacuo*. The residue was purified by flash column chromatography (10 g cartridge, cHex/EtOAc 3:7 → 1:9). Colorless oil, yield 111 mg, (24%).

Chemical Formula: C₁₀H₁₅NO₃ (197.2 g/mol).

TLC: *R*_f = 0.23 (EtOAc).

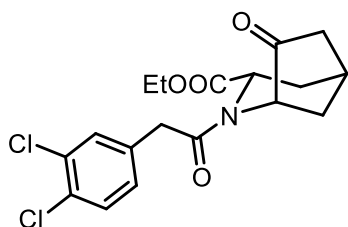
¹H NMR (600 MHz, CDCl₃): δ (ppm) = 1.27 (t, *J* = 7.1 Hz, 3H, OCH₂CH₃), 1.79 (dm, *J* = 12.1 Hz, 1H, 8-CH_{eq}), 1.89 (ddm, *J* = 12.1 / 3.8 Hz, 1H, 8-CH_{ax}), 1.94 (dd, *J* = 19.0 / 3.8 Hz, 1H, 6-CH₂), 2.15 (dd, *J* = 19.0 / 7.0 Hz, 1H, 6-CH₂), 2.31 (dddd, *J* = 14.0 / 8.4 / 3.1 / 1.6 Hz, 1H, 4-CH_{ax}), 2.44 (dm, *J* = 14.0 Hz, 1H, 4-CH_{eq}), 2.63 – 2.67 (m, 1H, 5-CH), 3.10 (d, *J* = 4.7 Hz, 1H, 1-CH), 3.75 (dd, *J* = 8.4 / 1.1 Hz, 1H, 3-CH_{eq}), 4.12 – 4.23 (m, 2H, OCH₂CH₃). A signal for NH is not seen in the spectrum.

¹³C NMR (151 MHz, CDCl₃): δ (ppm) = 14.2 (1C, OCH₂CH₃), 30.5 (1C, C-5), 31.0 (1C, C-4), 35.5 (1C, C-8), 41.1 (1C, C-6), 52.5 (1C, C-3), 58.4 (1C, C-1), 61.8 (1C, OCH₂CH₃), 174.4 (1C, O=COEt), 218.7 (1C, C-7).

IR (neat): $\tilde{\nu}$ (cm⁻¹) = 3341 (N-H), 2955 (C-H_{aliph}), 1724 (C=O_{ester, ketone}), 1200, 1099, 1072, 1022 (C-N, C-O).

Exact mass (APCI): *m/z* = 198.1138 (calcd. 198.1125 for C₁₀H₁₆NO₃ [M+H]⁺).

Ethyl (1*RS*,3*RS*,5*RS*)-2-[2-(3,4-dichlorophenyl)acetyl]-7-oxo-2-azabicyclo[3.2.1]octane-3-carboxylate (140)



At 0 °C, a solution of **53** (162 mg, 0.72 mmol, 2.6 eq) in CH₂Cl₂ (3 mL) was added to a solution of **147** (55 mg, 0.28 mmol, 1.0 eq) and DIPEA (0.15 mL, 0.84 mmol, 3.0 eq) in CH₂Cl₂ (4 mL). The mixture was stirred at room temperature for 2 h. Then, NaHCO₃ was added and the mixture was extracted with CH₂Cl₂ (3 × 5 mL), the combined organic layers were dried (Na₂SO₄), filtered and concentrated *in vacuo*. The residue was purified by flash column chromatography (10 g cartridge, cHex/EtOAc 6:4 → 1:1). Colorless oil, yield 70 mg, (65%).

Chemical Formula: C₁₈H₁₉Cl₂NO₄ (384.3 g/mol).

TLC: *R*_f = 0.36 (cHex/EtOAc 1:1).

¹H NMR (600 MHz, CDCl₃): δ (ppm) = 1.26 (t, *J* = 7.1 Hz, 3H, OCH₂CH₃), 1.89 (dm, *J* = 13.4 Hz, 1H, 8-CH_{ax}), 2.11 (dd, *J* = 13.3 / 3.5 Hz, 1H, 8-CH_{eq}), 2.15 – 2.25 (m, 2H, 4-CH₂, 6-CH₂), 2.33 – 2.44 (m, 2H, 4-CH₂, 6-CH₂), 2.78 (bs, 1H, 5-CH), 3.87 (d,

$J = 16.1$ Hz, 1H, $\text{CH}_2\text{-aryl}$), 3.96 (d, $J = 16.1$ Hz, 1H, $\text{CH}_2\text{-aryl}$), 4.12 (d, $J = 4.6$ Hz, 1H, 1-CH), 4.20 (q, $J = 7.1$ Hz, 2H, OCH_2CH_3), 4.58 (dd, $J = 9.4 / 5.8$ Hz, 1H, 3- CH_{ax}), 7.13 (dd, $J = 8.2 / 2.1$ Hz, 1H, 6- CH_{arom}), 7.37 – 7.41 (m, 2H, 2- CH_{arom} , 5- CH_{arom}).

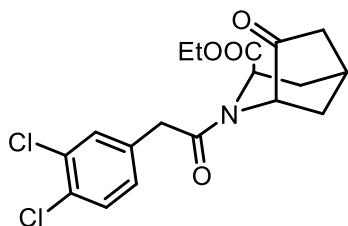
^{13}C NMR (151 MHz, CDCl_3): δ (ppm) = 14.3 (1C, OCH_2CH_3), 28.4 (1C, C-5), 31.8 (1C, C-8), 33.1 (1C, C-4), 39.8 (1C, $\text{CH}_2\text{-aryl}$), 42.6 (1C, C-6), 50.5 (1C, C-3), 58.1 (1C, C-1), 61.7 (1C, OCH_2CH_3), 128.9 (1C, C-6 $_{\text{arom}}$), 130.6 (1C, C-5 $_{\text{arom}}$), 131.2 (1C, C-3/4 $_{\text{arom}}$), 131.4 (1C, C-2 $_{\text{arom}}$), 132.6 (1C, C-3/4 $_{\text{arom}}$), 134.7 (1C, C-1 $_{\text{arom}}$), 171.7 (1C, N(C=O)), 172.7 (1C, O=COEt), 212.3 (1C, C-7).

Purity (HPLC, method A): 93.6% ($t_{\text{R}} = 20.2$ min).

IR (neat): $\tilde{\nu}$ (cm^{-1}) = 2978 (C-H $_{\text{aliph}}$), 1740 (C=O $_{\text{ester, ketone}}$), 1651 (C=O $_{\text{amide}}$), 1188, 1030 (C-N, C-O).

Exact mass (APCI): $m/z = 384.0747$ (calcd. 384.0764 for $\text{C}_{18}\text{H}_{20}^{35}\text{Cl}_2\text{NO}_4$ [M+H] $^+$).

Ethyl (1*RS*,3*SR*,5*RS*)-2-[2-(3,4-dichlorophenyl)acetyl]-7-oxo-2-azabicyclo[3.2.1]octane-3-carboxylate (141)



At 0 °C, a solution of acid chloride **53** (33 mg, 0.15 mmol, 1.2 eq) in CH_2Cl_2 (1 mL) was added to a solution of secondary amine **148** (24 mg, 0.12 mmol, 1.0 eq) and DIPEA (60 μL , 0.37 mmol, 3.0 eq) in CH_2Cl_2 (2 mL). The mixture was stirred at room temperature for 2 h. Then, NaHCO_3 was added and the mixture was extracted with CH_2Cl_2 (3 \times 5 mL), the combined organic layers were dried (Na_2SO_4), filtered and concentrated *in vacuo*. The residue was purified by flash column chromatography ($\phi = 1.5$ cm, $h = 8$ cm, cHex/EtOAc 7:3, $V = 12$ mL). Colorless oil, yield 31 mg, (67%).

Chemical Formula: $\text{C}_{18}\text{H}_{19}\text{Cl}_2\text{NO}_4$ (384.3 g/mol).

TLC: $R_{\text{f}} = 0.27$ (cHex/EtOAc 1:1).

^1H NMR (600 MHz, CDCl_3): δ (ppm) = 1.22 (t, $J = 7.2$ Hz, 3 \times 0.85H, OCH_2CH_3), 1.27 (t, $J = 7.2$ Hz, 3 \times 0.15H, $\text{OCH}_2\text{CH}_3^*$), 1.75 (dd, $J = 12.7 / 3.6$ Hz, 1H, 8- CH_2), 1.88 (dm, $J = 12.6$ Hz, 0.85H, 8- CH_2), 1.90 – 1.93 (m, 0.15H, 8- CH_2^*), 2.04 (dd, $J = 19.5 / 3.7$ Hz, 1H, 6- CH_2 , 6- CH_2^*), 2.14 – 2.19 (m, 0.15H, 4- CH_2^*), 2.22 – 2.36 (m, 3 \times 0.85 + 0.15H, 4- CH_2 , 4- CH_2^* , 6- CH_2), 2.51 (dm, $J = 14.1$ Hz, 0.15H, , 4- CH_2^*),

2.74 – 2.80 (m, 1H, 5-CH, 5-CH^{*}), 3.54 (d, $J = 15.7$ Hz, 0.15H, CH₂-aryl^{*}), 3.62 (d, $J = 15.7$ Hz, 0.15H, CH₂-aryl^{*}), 3.79 (d, $J = 15.9$ Hz, 0.85H, CH₂-aryl), 3.87 (d, $J = 15.9$ Hz, 0.85H, CH₂-aryl), 4.08 – 4.19 (m, 2.85H, 1-CH, OCH₂CH₃, OCH₂CH₃^{*}), 4.53 (d, $J = 8.8$ Hz, 0.15H, 3-CH_{eq}^{*}), 5.02 (dd, $J = 9.0 / 2.0$ Hz, 0.85H, 3-CH_{eq}), 5.11 (d, $J = 4.6$ Hz, 0.15H, 1-CH), 7.06 (dd, $J = 8.2 / 1.9$ Hz, 0.15H, 6-CH_{arom}^{*}), 7.10 (dd, $J = 8.2 / 1.9$ Hz, 0.85H, 6-CH_{arom}), 7.31 (d, $J = 1.9$ Hz, 0.15H, 2-CH_{arom}^{*}), 7.36 (d, $J = 1.9$ Hz, 0.85H, 2-CH_{arom}), 7.39 (d, $J = 8.2$ Hz, 0.15H, 5-CH_{arom}^{*}), 7.40 (d, $J = 8.2$ Hz, 0.85H, 5-CH_{arom}). Ratio of rotamers is 85:15. The signals for the minor rotamer are marked with an asterisk (*).

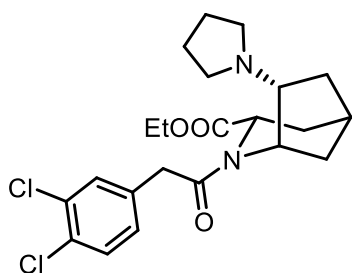
¹³C NMR (151 MHz, CDCl₃): δ (ppm) = 13.9 (0.15C, OCH₂CH₃^{*}), 14.0 (0.85C, OCH₂CH₃), 30.1 (0.85C, C-5), 30.6 (0.15C, C-5^{*}), 31.2 (0.85C, C-4), 31.3 (0.15C, C-4^{*}), 35.3 (0.85C, C-8), 35.8 (0.15C, C-8^{*}), 39.4 (0.15C, CH₂-aryl^{*}), 39.8 (0.85C, CH₂-aryl), 40.4 (0.85C, C-6), 41.4 (0.15C, C-6^{*}), 51.0 (0.85C, C-3), 54.2 (0.15C, C-3^{*}), 54.7 (0.15C, C-1^{*}), 59.2 (0.85C, C-1), 62.0 (0.85C, OCH₂CH₃), 63.0 (0.15C, OCH₂CH₃^{*}), 128.6 (0.15C, C-6_{arom}^{*}), 128.8 (0.85C, C-6_{arom}), 130.6 (0.85C, C-5_{arom}), 130.7 (0.15C, C-5_{arom}^{*}), 131.1 (0.15C, C-2_{arom}^{*}), 131.26 (0.85C, C-2_{arom}), 131.31 (0.85C, C-1_{arom}), 131.4 (0.15C, C-1_{arom}^{*}), 132.7 (0.85C, C-3/4_{arom}), 132.8 (0.15C, C-3/4_{arom}^{*}), 134.6 (0.15C, C-3/4_{arom}^{*}), 134.7 (0.85C, C-3/4_{arom}), 169.3 (0.15C, N(C=O)^{*}), 170.0 (0.85C, N(C=O)), 171.2 (0.15C, O=COEt^{*}), 172.0 (0.85C, O=COEt), 211.2 (0.85C, C-7) 212.9 (0.15C, C-7^{*}). Ratio of rotamers is 85:15. The signals for the minor rotamer are marked with an asterisk (*).

Purity (HPLC, method A): 92.8% ($t_R = 19.9$ min).

IR (neat): $\tilde{\nu}$ (cm⁻¹) = 2978, 2954 (C-H_{aliph}), 1755 (C=O_{ester}), 1732 (C=O_{ketone}), 1647 (C=O_{amide}), 1196, 1064, 1029 (C-N, C-O).

Exact mass (APCI): $m/z = 384.0747$ (calcd. 384.0764 for C₁₈H₂₀³⁵Cl₂NO₄ [M+H]⁺).

Ethyl (1*RS*,3*RS*,5*RS*,7*SR*)-2-[2-(3,4-dichlorophenyl)acetyl]-7-(pyrrolidin-1-yl)-2-azabicyclo[3.2.1] octane-3-carboxylate (142a)



Pyrrolidine (51 μ L, 0.62 mmol, 1.1 eq), NaBH(OAc)₃ (180 mg, 0.84 mmol, 1.5 eq) and AcOH (2 drops) were added to a solution of ketone **140** (202 mg, 0.56 mmol, 1.0 eq) in THF (3 mL). The mixture was stirred at room temperature for 16 h. After addition of NaHCO₃ (7 mL), the mixture was extracted with CH₂Cl₂ (3 \times 5 mL), the combined organic layers were dried (Na₂SO₄), filtered and concentrated *in vacuo*. The residue was purified by flash column chromatography (ϕ = 1.5 cm, *h* = 10 cm, CH₂Cl₂/NH₃ (7 M in CH₃OH)/ CH₃OH 96:3:1, *V* = 12 mL). Colorless solid, mp 115 - 116 °C, yield 51 mg (21%).

Chemical Formula: C₂₂H₂₈Cl₂N₂O₃ (439.4 g/mol).

TLC: *R*_f = 0.58 (CH₂Cl₂/CH₃OH/NH₄OH 94/5/1).

¹H-NMR (600 MHz, CDCl₃): δ (ppm) = 1.23 (t, *J* = 7.1 Hz, 3H, OCH₂CH₃), 1.45 – 1.51 (m, 2H, 6-CH₂, 8-CH₂), 1.58 – 1.63 (m, 1H, 8-CH₂), 1.63 – 1.73 (m, 4H, N(CH₂CH₂)₂), 1.74 – 1.79 (m, 1H, 4-CH₂), 1.84 – 1.90 (m, 1H, 4-CH₂), 1.99 – 2.06 (m, 1H, 6-CH₂), 2.39 (bs, 1H, 5-CH), 2.44 – 2.49 (m, 2H, N(CH₂CH₂)₂), 2.50 – 2.55 (m, 2H, N(CH₂CH₂)₂), 2.74 (ddd, *J* = 10.7 / 6.0 / 4.7 Hz, 1H, 7-CH), 3.70 (d, *J* = 15.9 Hz, 1H, CH₂-aryl), 3.84 (d, *J* = 15.9 Hz, 1H, CH₂-aryl), 4.07 (t, *J* = 4.3 Hz, 1H, 1-CH_{eq}), 4.13 – 4.21 (m, 2H, OCH₂CH₃), 4.32 (dd, *J* = 11.0 / 6.6 Hz, 1H, 3-CH_{ax}), 7.17 (dd, *J* = 8.3 / 2.1 Hz, 1H, 6-CH_{arom}), 7.38 (d, *J* = 8.3 Hz, 1H, 5-CH_{arom}), 7.41 (d, *J* = 2.1 Hz, 1H, 2-CH_{arom}).

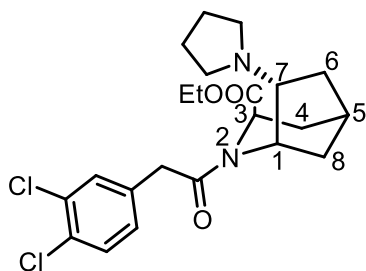
¹³C-NMR (151 MHz, CDCl₃): δ (ppm) = 16.7 (1C, OCH₂CH₃), 26.3 (2C, N(CH₂CH₂)₂), 34.9 (1C, C-5), 35.0 (1C, C-6), 38.2 (1C, C-4), 38.3 (1C, C-8), 42.7 (1C, CH₂-aryl), 56.3 (2C, N(CH₂CH₂)₂), 56.4 (1C, C-3), 61.4 (1C, C-1), 63.4 (1C, OCH₂CH₃), 71.6 (1C, C-7), 131.2 (1C, C-6_{arom}), 133.0 (1C, C-5_{arom}), 133.4 (1C, C-3/4_{arom}), 133.6 (1C, C-2_{arom}), 134.9 (1C, C-3/4_{arom}), 138.4 (1C, C-1_{arom}), 173.3 (1C, N(C=O)), 175.6 (1C, O=COEt).

Purity (HPLC, method A): 78.0% (*t*_R = 18.7 min).

IR (neat): $\tilde{\nu}$ (cm⁻¹) = 2936 (C-H_{alip}), 1717 (C=O_{ester}), 1632 (C=O_{amide}), 1265, 1030 (C-N, C-O).

Exact mass (APCI): *m/z* = 439.1530 (calcd. 439.1550 for C₂₂H₂₉³⁵Cl₂N₂O₃ [M+H]⁺).

Ethyl (1*RS*,3*SR*,5*RS*,7*SR*)-2-[2-(3,4-dichlorophenyl)acetyl]-7-(pyrrolidin-1-yl)-2-azabicyclo[3.2.1] octane-3-carboxylate (143a)



Pyrrolidine (40 μ L, 0.48 mmol, 1.2 eq), $\text{NaBH}(\text{OAc})_3$ (170 mg, 0.80 mmol, 2.0 eq) and AcOH (5 drops) were added to a solution of ketone **141** (153 mg, 0.40 mmol, 1.0 eq) in THF (10 mL). The mixture was stirred at room temperature for 16 h. After addition of NaHCO_3 (15 mL), the mixture was extracted with CH_2Cl_2 (3 \times 10 mL), the combined organic layers were dried (Na_2SO_4), filtered and concentrated *in vacuo*. The residue was purified by flash column chromatography ($\varnothing = 2$ cm, $h = 13$ cm, $\text{CH}_2\text{Cl}_2/\text{CH}_3\text{OH}/\text{NH}_4\text{OH}$ 96:3:1, $V = 12$ mL). Colorless solid, mp 110 - 111 $^\circ\text{C}$, yield 131 mg (75%).

Chemical Formula: $\text{C}_{22}\text{H}_{28}\text{Cl}_2\text{N}_2\text{O}_3$ (439.4 g/mol).

TLC: $R_f = 0.32$ ($\text{CH}_2\text{Cl}_2/\text{CH}_3\text{OH}/\text{NH}_4\text{OH}$ 94:5:1).

^1H NMR (600 MHz, CDCl_3): δ (ppm) = 1.17 – 1.37 (m, 4H, OCH_2CH_3 , 8- CH_2), 1.55 (mdd, $J = 8.5 / 2.3$ Hz, 1H, 4- CH_{ax}), 1.59 – 1.69 (m, 5H, $\text{N}(\text{CH}_2\text{CH}_2)_2$, 8- CH_2), 1.77 – 1.88 (m, 2H, 6- CH_2), 2.17 – 2.53 (m, 6H, $\text{N}(\text{CH}_2\text{CH}_2)_2$, 4- CH_{eq} , 5- CH), 2.53 – 2.59 (m, 1H, 7- CH), 3.70 – 3.82 (m, 3 \times 0.25H, CH_2 -aryl*, $\text{OCH}_2\text{CH}_3^*$), 3.83 – 3.97 (m, 3 \times 0.75H, CH_2 -aryl, OCH_2CH_3), 4.08 – 4.12 (m, 0.25H, 1- CH^*), 4.15 – 4.23 (m, 0.25H, $\text{OCH}_2\text{CH}_3^*$), 4.25 – 4.31 (m, 0.75H, OCH_2CH_3), 4.38 (d, $J = 8.5$ Hz, 0.75H, 3- CH_{eq}), 5.10 – 5.15 (m, 0.75H, 1- CH), 5.44 (d, $J = 7.5$ Hz, 0.25H, 3- CH_{eq}^*), 7.08 (dd, $J = 8.2 / 1.9$ Hz, 0.75H, 6- CH_{arom}), 7.14 (d, $J = 8.2$ Hz, 0.25H, 6- $\text{CH}_{\text{arom}}^*$), 7.34 (d, $J = 1.9$ Hz, 0.75H, 2- CH_{arom}), 7.37 – 7.42 (m, 1.25H, 2- $\text{CH}_{\text{arom}}^*$, 5- CH_{arom} , 5- $\text{CH}_{\text{arom}}^*$). Ratio of rotamers is 75:25. The signals for the minor rotamer are marked with an asterisk (*).

^{13}C NMR (151 MHz, CDCl_3): δ (ppm) = 14.2 (0.25C, $\text{OCH}_2\text{CH}_3^*$), 14.3 (0.75C, OCH_2CH_3), 23.77 (1.50C, $\text{N}(\text{CH}_2\text{CH}_2)_2$), 23.81 (0.50C, $\text{N}(\text{CH}_2\text{CH}_2)_2^*$), 29.3 (0.75C, C-4), 30.1 (0.25C, C-4*), 32.5 (0.75C, C-6), 32.8 (0.25C, C-6*), 33.1 (0.75C, C-5), 37.4 (0.75C, C-8), 38.0 (0.25C, C-8*), 40.0 (0.75C, CH_2 -aryl), 40.1 (0.25C, CH_2 -aryl*), 48.9 (0.25C, C-3*), 53.4 (0.5C, $\text{N}(\text{CH}_2\text{CH}_2)_2^*$), 53.50 (1.5C, $\text{N}(\text{CH}_2\text{CH}_2)_2$), 53.53 (0.75C, C-1/3), 53.6 (0.75C, C-1/3), 58.7 (0.25C, C-1*), 60.9 (0.25C, $\text{OCH}_2\text{CH}_3^*$), 61.4 (0.75C,

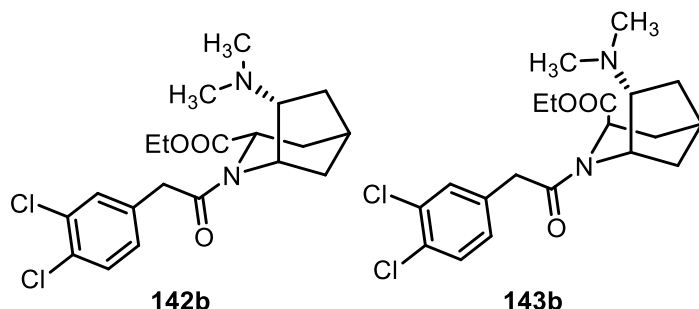
OCH₂CH₃), 67.9 (0.75C, C-7), 68.6 (0.25C, C-7*), 128.5 (0.75C, C-6_{arom}), 128.7 (0.25C, C-6_{arom}*), 130.6 (0.75C, C-5_{arom}), 130.99 (0.75C, C3/4_{arom}), 131.03 (0.75C, CH_{arom}-2), 131.1 (0.25C, C3/4_{arom}*), 131.2 (0.25, C-2_{arom}*), 132.6 (0.75C, C3/4_{arom}), 132.7 (0.25C, C3/4_{arom}*), 135.5 (0.25C, C-1_{arom}*), 136.1 (0.75C, C-1_{arom}), 168.9 (0.25C, N(C=O)*), 170.4 (0.75C, N(C=O)), 170.5 (0.75C, O=COEt), 171.6 (0.25C, O=COEt*). Ratio of rotamers is 75:25. The signals for the minor rotamer are marked with an asterisk (*). The signals for C-5* and C-5_{arom}* are not seen in the spectrum.

Purity (HPLC, method A): 96.2% (*t_R* = 19.9 min).

IR (neat): $\tilde{\nu}$ (cm⁻¹) = 2951, 2936 (C-H_{alip}), 1732 (C=O_{ester}), 1616 (C=O_{amide}), 1196, 1030 (C-N, C-O).

Exact mass (APCI): *m/z* = 439.1530 (calcd. 439.1550 for C₂₂H₂₉³⁵Cl₂N₂O₃ [M+H]⁺).

Ethyl (1*RS*,3*RS*,5*RS*,7*SR*)-2-(2-(3,4-dichlorophenyl)acetyl)-7-(dimethylamino)-2-azabicyclo[3.2.1]octane-3-carboxylate (142b) and ethyl (1*RS*,3*SR*,5*RS*,7*SR*)-2-(2-(3,4-dichlorophenyl)acetyl)-7-(dimethylamino)-2-azabicyclo[3.2.1]octane-3-carboxylate (143b)



HN(CH₃)₂ (2 M in THF, 4.6 mL, 9.1 mmol, 10 eq) and AcOH (53 μ L, 0.9 mmol, 1 eq) were added to a mixture of diastereomeric esters **141** and **140** (350 mg, 0.9 mmol, 1 eq) in THF (8 mL). After 10 min, NaBH(OAc)₃ (387 mg, 1.8 mmol, 2 eq) was added and the mixture was stirred at room temperature for 16 h. Then, NaHCO₃ (10 mL) was added and the mixture was extracted with EtOAc (3 \times 10 mL), the combined organic layers were dried (Na₂SO₄), filtered and concentrated *in vacuo*. The residue was purified by flash column chromatography (1. ϕ = 3 cm, *h* = 20 cm, CH₂Cl₂/CH₃OH/NH₃ (7 M in CH₃OH) 99:0:1 \rightarrow 96:2:2, *V* = 12 mL, 2. ϕ = 4 cm, *h* = 10 cm, CH₂Cl₂/CH₃OH/NH₃ (7 M in CH₃OH) 99:0:1 \rightarrow 97:1:2, *V* = 12 mL). At first **142b**, then **143b** was eluted.

Chemical Formula: C₂₀H₂₆Cl₂N₂O₃ (413.3 g/mol).

142b: Colorless solid, mp 98 - 99 °C, yield 14 mg (4%).

TLC: $R_f = 0.42$ (CH₂Cl₂/CH₃OH/NH₄OH 95:4:1).

¹H-NMR (600 MHz, CDCl₃): δ (ppm) = 1.23 (t, $J = 7.1$ Hz, 3H, OCH₂CH₃), 1.45 (ddd, $J = 13.3 / 6.5 / 1.7$ Hz, 1H, 6-CH₂), 1.51 (d, $J = 12.1$ Hz, 1H, 8-CH₂), 1.61 (dm, $J = 12.1$ Hz, 1H, 8-CH₂), 1.75 – 1.83 (m, 1H, 4-CH₂), 1.85 – 1.90 (m, 1H, 4-CH₂), 1.99 (ddd, $J = 13.3 / 11.2 / 7.2$ Hz, 1H, 6-CH₂), 2.20 (s, 6H, N(CH₃)₂), 2.38 – 2.42 (m, 1H, 5-CH), 2.57 (ddd, $J = 10.8 / 6.4 / 4.6$ Hz, 1H, 7-CH), 3.73 (d, $J = 15.8$ Hz, 1H, CH₂-aryl), 3.84 (d, $J = 15.8$ Hz, 1H, CH₂-aryl), 4.12 (t, $J = 4.1$ Hz, 1H, 1-CH), 4.16 (qd, $J = 7.1 / 1.1$ Hz, 2H, OCH₂CH₃), 4.31 (dd, $J = 10.7 / 6.6$ Hz, 1H, 3-CH_{ax}), 7.17 (dd, $J = 8.2 / 2.1$ Hz, 1H, 6-CH_{arom}), 7.37 (d, $J = 8.2$ Hz, 1H, 5-CH_{arom}), 7.42 (d, $J = 2.1$ Hz, 1H, 2-CH_{arom}).

¹³C-NMR (151 MHz, CDCl₃): δ (ppm) = 14.2 (1C, OCH₂CH₃), 31.4 (1C, C-6), 32.2 (1C, C-5), 35.7 (1C, C-4), 35.8 (1C, C-8), 40.1 (1C, CH₂-aryl), 45.5 (2C, N(CH₃)₂), 53.7 (1C, C-3), 58.1 (1C, C-1), 60.9 (1C, OCH₂CH₃), 70.6 (1C, C-7), 128.7 (1C, C-6_{arom}), 130.5 (1C, C-5_{arom}), 130.9 (1C, C3/4_{arom}), 131.1 (1C, C-2_{arom}), 132.4 (1C, C-3/4_{arom}), 135.8 (1C, C-1_{arom}), 171.0 (1C, N(C=O)), 172.9 (1C, O=COEt).

Purity (HPLC, method A): 94.5% ($t_R = 18.1$ min).

IR (neat): $\tilde{\nu}$ (cm⁻¹) = 2936 (C-H_{alip}), 1728 (C=O_{ester}), 1629 (C=O_{amide}), 1265, 1234, 1030 (C-N, C-O).

Exact mass (APCI): $m/z = 413.1372$ (calcd. 413.1393 for C₂₀H₂₇³⁵Cl₂N₂O₃ [M+H]⁺).

143b: Colorless solid, mp 148 - 150 °C, yield 229 mg (61%).

TLC: $R_f = 0.54$ (CH₂Cl₂/CH₃OH/NH₄OH 95:4:1).

¹H-NMR (600 MHz, CDCl₃): δ (ppm) = 1.19 – 1.23 (m, 0.17H, 8-CH₂^{*}), 1.25 (t, $J = 7.1$ Hz, 3 × 0.17H, OCH₂CH₃^{*}), 1.32 (t, $J = 7.1$ Hz, 3 × 0.83H, OCH₂CH₃), 1.34 – 1.38 (m, 0.83H, 8-CH₂), 1.50 – 1.55 (m, 0.83H, 4-CH₂), 1.56 – 1.68 (m, 1.17H, 4-CH₂^{*}, 8-CH₂, 8-CH₂^{*}), 1.73 – 1.86 (m, 2H, 6-CH₂, 6-CH₂^{*}), 2.05 (s, 6 × 0.17H, N(CH₃)₂^{*}), 2.06 (s, 6 × 0.83H, N(CH₃)₂), 2.31 – 2.36 (m, 1H, 5-CH, 5-CH^{*}), 2.36 – 2.45 (m, 2H, 4-CH₂, 4-CH₂^{*}, 7-CH, 7-CH^{*}), 3.73 (d, $J = 15.4$ Hz, 0.17H, CH₂-aryl^{*}), 3.80 (d, $J = 15.4$ Hz, 0.17H, CH₂-aryl^{*}), 3.82 – 3.87 (m, 1H, CH₂-aryl, OCH₂CH₂^{*}), 3.89 – 3.95 (m, 1.66H, CH₂-aryl, OCH₂CH₃), 4.11 – 4.17 (m, 0.34H, 1-CH^{*}, OCH₂CH₃^{*}), 4.26 (dq, $J = 10.7 / 7.1$ Hz, 0.83H, OCH₂CH₃), 4.37 (d, $J = 8.5$ Hz, 0.83H, 3-CH_{eq}), 5.10 – 5.15 (m, 0.83H, 1-CH), 5.45 (d, $J = 8.9$ Hz, 0.17H, 3-CH_{eq}^{*}), 7.08 (dd, $J = 8.2 / 2.0$ Hz, 0.83H, 6-CH_{arom}), 7.14 (dd, $J = 8.2 / 1.7$ Hz, 0.17H, 6-CH_{arom}^{*}), 7.34 (d, $J = 2.0$ Hz, 0.83H,

2- CH_{arom}), 7.37 – 7.41 (m, 1.17H, 2- CH_{arom} *, 5- CH_{arom} , 5- CH_{arom} *). Ratio of rotamers is 83:17. The signals for the minor rotamer are marked with an asterisk (*).

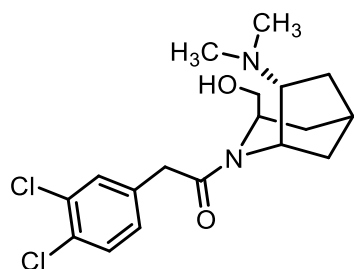
$^{13}\text{C-NMR}$ (151 MHz, CDCl_3): δ (ppm) = 16.7 (0.17C, $\text{OCH}_2\text{CH}_3^*$), 16.8 (0.83C, OCH_2CH_3), 31.8 (0.17C, C-4*), 32.4 (0.83C, C-4), 34.7 (0.83C, C-6), 35.1 (0.17C, C-6*), 35.6 (0.83C, C-5), 35.7 (0.17C, C-5*), 40.1 (0.83C, C-8), 40.7 (0.17C, C-8*), 42.4 (0.17C, $\text{CH}_2\text{-aryl}^*$), 42.5 (0.83C, $\text{CH}_2\text{-aryl}$), 47.6 ($2 \times 0.17\text{C}$, $\text{N}(\text{CH}_3)_2^*$), 47.7 ($2 \times 0.83\text{C}$, $\text{N}(\text{CH}_3)_2$), 51.5 (0.17C, C-3*), 55.2 (0.83C, C-1), 55.9 (0.83C, C-3), 60.3 (0.17C, C-1*), 63.4 (0.17C, $\text{OCH}_2\text{CH}_3^*$), 63.9 (0.83C, OCH_2CH_3), 71.2 (0.83C, C-7), 71.8 (0.17C, C-7*), 131.0 (0.83C, C-6 $_{\text{arom}}$), 131.2 (0.17C, C-6 $_{\text{arom}}$ *), 133.07 (0.17C, C-5 $_{\text{arom}}$ *), 133.10 (0.83C, C-5 $_{\text{arom}}$), 133.53 (0.83C, C-2 $_{\text{arom}}$), 133.54 (0.17C, C-2 $_{\text{arom}}$ *), 133.7 (0.83C, C-3/4 $_{\text{arom}}$), 135.2 (0.83C, C-3/4 $_{\text{arom}}$), 137.9 (0.17C, C-1 $_{\text{arom}}$ *), 138.5 (0.83C, C-1 $_{\text{arom}}$), 171.4 (0.17C, $\text{N}(\text{C}=\text{O})^*$), 172.8 (0.83C, $\text{N}(\text{C}=\text{O})$), 173.1 (0.83C, $\text{O}=\text{COEt}$), 174.2 (0.17C, $\text{O}=\text{COEt}^*$). Ratio of rotamers is 83:17. The signals for the minor rotamer are marked with an asterisk (*). The signals for C-3* and C-4* are not seen in the spectrum.

Purity (HPLC, method A): 95.6% (t_{R} = 18.9 min).

IR (neat): $\tilde{\nu}$ (cm^{-1}) = 2947 (C-H $_{\text{alip}}$), 1732 (C=O $_{\text{ester}}$), 1616 (C=O $_{\text{amide}}$), 1200, 1026 (C-N, C-O).

Exact mass (APCI): m/z = 413.1408 (calcd. 413.1393 for $\text{C}_{20}\text{H}_{27}^{35}\text{Cl}_2\text{N}_2\text{O}_3$ [$\text{M}+\text{H}$] $^+$).

2-(3,4-Dichlorophenyl)-1-((1*RS*,3*SR*,5*RS*,7*SR*)-7-(dimethylamino)-3-(hydroxy methyl)-2-azabicyclo[3.2.1]octan-2-yl)ethan-1-one (149)



LiBH_4 (2 M in THF, 1.1 mL, 2.2 mmol, 2 eq) was added to a solution of **143b** (0.47 g, 1.1 mmol, 1 eq) in Et_2O (25 mL) and the mixture was stirred at room temperature for 5 d. Then, NH_4Cl (15 mL) was added and the mixture was extracted with EtOAc (3×20 mL). The combined organic layers were dried (Na_2SO_4), filtered and concentrated *in vacuo*. The residue was purified by flash column chromatography ($\varnothing = 4$ cm, $h = 12$ cm, $\text{CH}_2\text{Cl}_2/\text{NH}_3$ (7 M in CH_3OH)/ CH_3OH 99:1:0 \rightarrow 95:2:3, $V = 20$ mL). Colorless oil, yield 15 mg (4 %).

Chemical Formula: C₁₈H₂₄Cl₂N₂O₂ (371.3 g/mol).

TLC: *R_f* = 0.37 (CH₂Cl₂/CH₃OH/NH₄OH 95:4:1).

¹H NMR (400 MHz, DMSO-*d*₆): δ (ppm) = 1.39 (d, *J* = 12.2 Hz, 1H, 8-CH₂), 1.52 (d, *J* = 14.2 Hz, 1H, 4-CH₂), 1.70 (dm, *J* = 12.2 Hz, 1H, 8-CH₂), 1.78 – 1.97 (m, 2H, 4-CH₂, 6-CH₂), 1.98 – 2.07 (m, 1H, 6-CH₂), 2.22 – 2.45 (m, 8H, 5-CH, N(CH₃)₂, CH₂OH), 2.48 – 2.61 (m, 1H, 7-CH), 3.66 (dd, *J* = 12.0 / 8.0 Hz, 1H, CH₂OH), 3.70 (d, *J* = 15.7 Hz, 1H, CH₂-aryl), 3.72 – 3.79 (m, 1H, CH₂OH), 3.85 (d, *J* = 15.7 Hz, 1H, CH₂-aryl), 4.02 – 4.09 (m, 1H, 3-CH_{eq}), 5.33 (t, *J* = 4.3 Hz, 1H, 1-CH), 7.10 (dd, *J* = 8.2 / 2.1 Hz, 1H, 6-CH_{arom}), 7.34 (d, *J* = 2.1 Hz, 1H, 2-CH_{arom}), 7.37 (d, *J* = 8.2 Hz, 1H, 5-CH_{arom}).

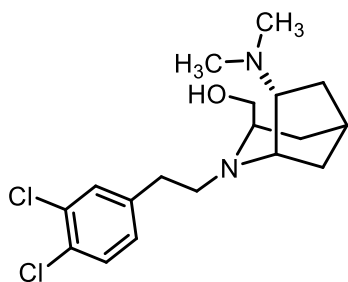
¹³C NMR (101 MHz, DMSO-*d*₆): δ (ppm) = 32.4 (1C, C-6), 32.7 (1C, C-4), 32.9 (1C, C-5), 36.7 (1C, C-8), 40.3 (1C, CH₂-aryl), 45.1 (2C, N(CH₃)₂), 50.0 (1C, C-3), 51.3 (1C, C-1), 64.3 (1C, CH₂OH), 69.9 (1C, C-7), 128.7 (1C, C-6_{arom}), 130.3 (1C, C-5_{arom}), 131.1 (1C, C-2_{arom}). The signals for C-1_{arom}, C-3_{arom}, C-4_{arom} and N(C=O) are not seen in the spectrum.

Purity (HPLC, method A): 70.4% (*t_R* = 16.6 min).

IR (neat): $\tilde{\nu}$ (cm⁻¹) = 3298 (O-H), 2943 (C-H_{alip}), 1628 (C=O_{amide}), 1030 (C-N, C-O).

Exact mass (APCI): *m/z* = 371.1275 (calcd. 371.1288 for C₁₈H₂₅³⁵Cl₂N₂O₂ [M+H]⁺).

{{(1*RS*,3*SR*,5*RS*,7*SR*)-2-(3,4-Dichlorophenethyl)-7-(dimethylamino)-2-azabicyclo[3.2.1]octan-3-yl}methanol (150)



At -78 °C, LiAlH₄ (1 M in THF, 1.0 mL, 1.0 mmol, 4 eq) was added to a solution of **143b** (0.1 g, 0.25 mmol, 1 eq) in dry THF (5 mL) and the mixture was stirred first at -78 °C for 1 h and then at 0 °C for 90 min. Then, H₂O (7 mL) and potassium sodium tartrate solution (3 mL) were added, and the mixture was extracted with EtOAc (3 × 10 mL). The combined organic layers were dried (Na₂SO₄), filtered and concentrated *in vacuo*. The residue was purified by flash column chromatography (ø = 4 cm, *h* = 8 cm, CH₂Cl₂/NH₃ (7 M in CH₃OH)/CH₃OH 99:2:0 → 90:8:2, *V* = 12 mL). Yellow oil, yield 27 mg, (31%).

Chemical Formula: $C_{18}H_{26}Cl_2N_2O$ (357.3 g/mol).

TLC: $R_f = 0.23$ ($CH_2Cl_2/CH_3OH/NH_4OH$ 90:9:1).

1H NMR (600 MHz, $CDCl_3$): δ (ppm) = 1.39 – 1.47 (m, 2H, 8- CH_2), 1.62 (d, $J = 13.3$ Hz, 1H, 4- CH_2), 1.72 (dd, $J = 13.3 / 5.4$ Hz, 1H, 6- CH_2), 1.84 – 1.91 (m, 1H, 6- CH_2), 2.09 – 2.16 (m, 1H, 4- CH_2), 2.20 – 2.35 (m, 8H, 5- CH , 7- CH , $N(CH_3)_2$), 2.72 – 2.77 (m, 2H, NCH_2CH_2 -aryl), 2.78 – 2.83 (m, 1H, 3- CH_{eq}), 2.87 – 2.93 (m, 2H, NCH_2CH -aryl), 3.09 – 3.14 (m, 1H, 1- CH), 3.19 (dd, $J = 10.7 / 2.2$ Hz, 1H, CH_2OH), 3.71 (dd, $J = 10.7 / 2.6$ Hz, 1H, CH_2OH), 7.00 (dd, $J = 8.2 / 2.0$ Hz, 1H, 6- CH_{arom}), 7.34 (d, $J = 8.2$ Hz, 1H, 5- CH_{arom}). The signal for CH_2OH is not seen in the spectrum. The signal for 2- CH_{arom} is overlapping with the $CDCl_3$ signal.

^{13}C NMR (151 MHz, $CDCl_3$): δ (ppm) = 32.5 (1C, C-5), 33.35 (1C, C-8), 33.38 (1C, C-4), 33.6 (1C, NCH_2CH_2 -aryl), 34.6 (1C, C-6), 44.3 (2C, $N(CH_3)_2$), 53.3 (1C, C-3), 60.67 (1C, NCH_2CH_2 -aryl), 60.71 (1C, C-1), 68.0 (1C, CH_2OH), 70.2 (1C, C-7), 128.3 (1C, C-6 $_{arom}$), 130.1 (1C, C-3/4 $_{arom}$), 130.5 (1C, C-5 $_{arom}$), 130.7 (1C, C-2 $_{arom}$), 132.4 (1C, C-3/4 $_{arom}$), 140.6 (1C, C-1 $_{arom}$).

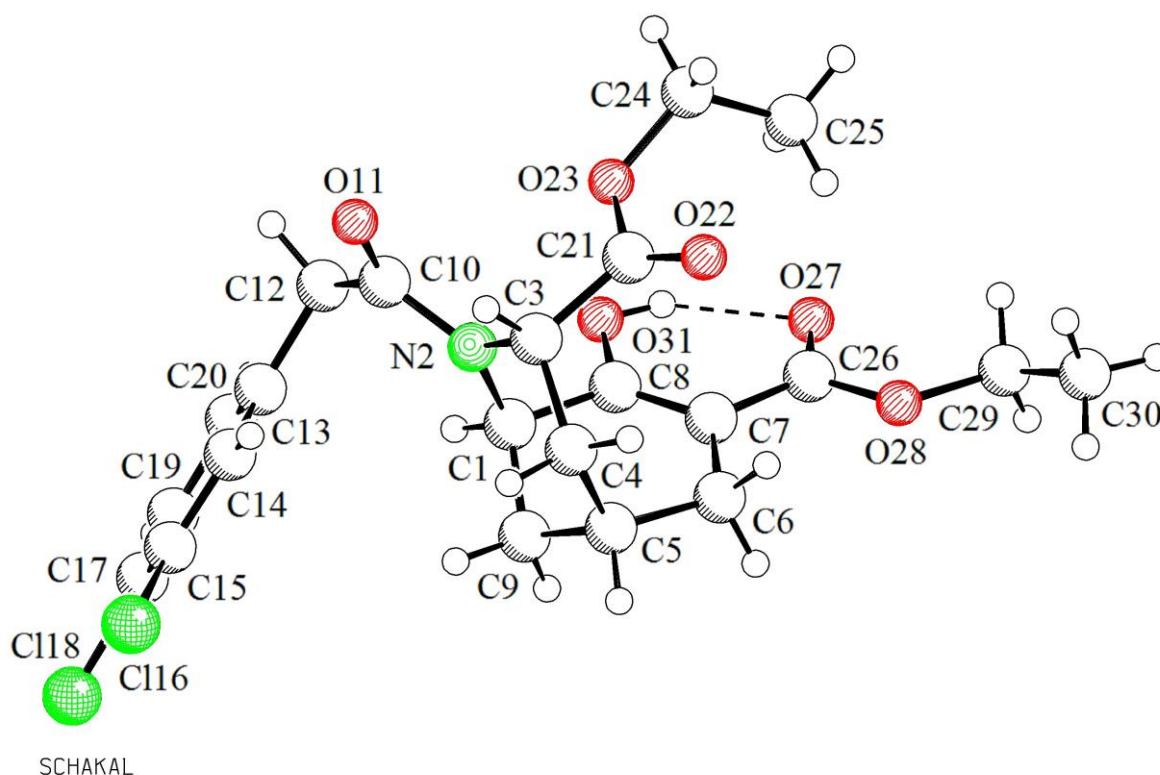
IR (neat): $\tilde{\nu}$ (cm^{-1}) = 3101 (O-H), 2932 (C-H $_{alip}$), 1130, 1030 (C-N, C-O).

Exact mass (APCI): $m/z = 357.1444$ (calcd. 357.1495 for $C_{18}H_{27}^{35}Cl_2N_2O$ $[M+H]^+$).

7.3 Crystallography section

In the attempt to obtain a single crystal of compounds **80**, **82**, **84**, **144** and **143a** the vapour diffusion method of crystallization was selected. Only clean and dust-free glassware was employed for the experiment. The solvent (inner solvent) used was EtOAc and the anti-solvent (outer solvent) was cHex. Therefore, the compound (5 – 12 mg) was dissolved in EtOAc (0.7 mL) in an HPLC vial, which was placed into a larger vial containing cHex (2 mL). The outer container was sealed and, after 2 – 7 d, a colorless single crystal could be observed. The whole crystallization phase took place at room temperature (isothermal method) and the two-vials system was never moved. The relative large amount of substance was responsible for the big dimension of the crystals, which was, therefore, cut down by the expert for the analysis.

7.3.1 X-ray crystal structure of enol ester **80**



A colorless prism-like specimen of $C_{22}H_{25}Cl_2NO_6$, approximate dimensions 0.127 mm x 0.141 mm x 0.217 mm, was used for the X-ray crystallographic analysis. The X-ray intensity data were measured on a Bruker D8 Venture PHOTON III Diffractometer system equipped with a micro focus tube Cu Ims ($CuK\alpha$, $\lambda = 1.54178 \text{ \AA}$) and a MX mirror monochromator.

A total of 1202 frames were collected. The total exposure time was 16.25 hours. The frames were integrated with the Bruker SAINT software package using a wide-frame algorithm. The integration of the data using a triclinic unit cell yielded a total of 15124 reflections to a maximum θ angle of 66.71° (0.84 \AA resolution), of which 3585 were independent (average redundancy 4.219, completeness = 95.2%, $R_{\text{int}} = 3.18\%$, $R_{\text{sig}} = 2.96\%$) and 3493 (97.43%) were greater than $2\sigma(F^2)$. The final cell constants of $a = 8.0455(3) \text{ \AA}$, $b = 10.8027(4) \text{ \AA}$, $c = 12.4892(5) \text{ \AA}$, $\alpha = 100.9000(10)^\circ$, $\beta = 91.7250(10)^\circ$, $\gamma = 93.5580(10)^\circ$, volume = $1062.87(7) \text{ \AA}^3$, are based upon the refinement of the XYZ-centroids of 9869 reflections above $20 \sigma(I)$ with $11.02^\circ < 2\theta < 133.4^\circ$. Data were corrected for absorption effects using the Multi-Scan method (SADABS). The ratio of minimum to maximum apparent transmission was 0.885. The calculated minimum and maximum transmission coefficients (based on crystal size) are 0.5530 and 0.6940.

The structure was solved and refined using the Bruker SHELXTL Software Package, using the space group P -1, with $Z = 2$ for the formula unit, $\text{C}_{22}\text{H}_{25}\text{Cl}_2\text{NO}_6$. The final anisotropic full-matrix least-squares refinement on F^2 with 306 variables converged at $R_1 = 3.06\%$, for the observed data and $wR_2 = 7.77\%$ for all data. The goodness-of-fit was 1.041. The largest peak in the final difference electron density synthesis was $0.232 \text{ e}/\text{\AA}^3$ and the largest hole was $-0.229 \text{ e}/\text{\AA}^3$ with an RMS deviation of $0.040 \text{ e}/\text{\AA}^3$. On the basis of the final model, the calculated density was $1.470 \text{ g}/\text{cm}^3$ and $F(000)$, 492 e^- .

Table 15: Sample and crystal data for **80**.

Identification code	dan9905	
Chemical formula	$\text{C}_{22}\text{H}_{25}\text{Cl}_2\text{NO}$	
Formula weight	470.33 g/mol	
Temperature	100(2) K	
Wavelength	1.54178 \AA	
Crystal size	0.127 x 0.141 x 0.217 mm	
Crystal habit	colorless prism	
Crystal system	triclinic	
Space group	P -1	
Unit cell dimensions	$a = 8.0455(3) \text{ \AA}$	$\alpha = 100.9000(10)^\circ$

	$b = 10.8027(4) \text{ \AA}$	$\beta = 91.7250(10)^\circ$
	$c = 12.4892(5) \text{ \AA}$	$\gamma = 93.5580(10)^\circ$
Volume	1062.87(7) \AA^3	
Z	2	
Density (calculated)	1.470 g/cm^3	
Absorption coefficient	3.099 mm^{-1}	
F(000)	492	

Table 16: Data collection and structure refinement for **80**.

Diffractometer	Bruker D8 Venture PHOTON III Diffractometer
Radiation source	micro focus tube Cu Ims ($\text{CuK}\alpha$, $\lambda = 1.54178 \text{ \AA}$)
Theta range for data collection	5.51 to 66.71°
Index ranges	$-9 \leq h \leq 9$, $-12 \leq k \leq 12$, $-14 \leq l \leq 14$
Reflections collected	15124
Independent reflections	3585 [$R(\text{int}) = 0.0318$]
Coverage of independent reflections	95.2%
Absorption correction	Multi-Scan
Max. and min. transmission	0.6940 and 0.5530
Structure solution technique	direct methods
Structure solution program	SHELXT 2014/5 (Sheldrick, 2014)
Refinement method	Full-matrix least-squares on F^2
Refinement program	SHELXL-2018/3 (Sheldrick, 2018)
Function minimized	$\sum w(F_o^2 - F_c^2)^2$
Data / restraints / parameters	3585 / 45 / 306
Goodness-of-fit on F^2	1.041

D/smax	0.001
Final R indices	3493 data; $I > 2\sigma(I)$ R1 = 0.0306, wR2 = 0.0772
	all data R1 = 0.0312, wR2 = 0.0777
Weighting scheme	$w = 1/[\sigma^2(F_o^2) + (0.0307P)^2 + 0.5760P]$ where $P = (F_o^2 + 2F_c^2)/3$
Largest diff. peak and hole	0.232 and -0.229 eÅ ⁻³
R.M.S. deviation from mean	0.040 eÅ ⁻³

Table 17: Bond lengths (Å) for **80**.

N2-C10	1.3650(18)	N2-C3	1.4624(17)
N2-C1	1.4754(17)	C1-C8	1.509(2)
C1-C9	1.5299(19)	C1-H1	1.0
C3-C21	1.5269(19)	C3-C4	1.5351(18)
C3-H3	1.0	C4-C5	1.5324(19)
C4-H4A	0.99	C4-H4B	0.99
C5-C9	1.525(2)	C5-C6	1.5417(19)
C5-H5	1.0	C6-C7	1.5152(19)
C6-H6A	0.99	C6-H6B	0.99
C7-C8	1.351(2)	C7-C26	1.463(2)
C8-O31	1.3464(17)	C9-H9A	0.99
C9-H9B	0.99	C10-O11	1.2257(18)
C10-C12	1.519(2)	C12-C13	1.5140(19)
C12-H12A	0.99	C12-H12B	0.99
C13-C14	1.391(2)	C13-C20	1.396(2)
C14-C15	1.386(2)	C14-H14	0.95
C15-C17	1.391(2)	C15-Cl16	1.7310(14)
C17-C19	1.385(2)	C17-Cl18	1.7329(14)
C19-C20	1.385(2)	C19-H19	0.95
C20-H20	0.95	C21-O22	1.2061(17)
C21-O23	1.3386(17)	C24-O23	1.4580(17)
C24-C25	1.505(2)	C24-H24A	0.99
C24-H24B	0.99	C25-H25A	0.98
C25-H25B	0.98	C25-H25C	0.98

C26-O27	1.2286(19)	C26-O28	1.3396(19)
O28-C29	1.451(7)	O28-C29A	1.488(10)
C29-C30	1.487(8)	C29-H29A	0.99
C29-H29B	0.99	C30-H30A	0.98
C30-H30B	0.98	C30-H30C	0.98
C29A-C30A	1.496(11)	C29A-H29C	0.99
C29A-H29D	0.99	C30A-H30D	0.98
C30A-H30E	0.98	C30A-H30F	0.98
O31-H31	0.82(3)		

Table 18: Bond angles (°) for **80**.

C10-N2-C3	118.16(11)	C10-N2-C1	124.73(11)
C3-N2-C1	117.08(10)	N2-C1-C8	110.32(11)
N2-C1-C9	110.27(11)	C8-C1-C9	109.75(11)
N2-C1-H1	108.8	C8-C1-H1	108.8
C9-C1-H1	108.8	N2-C3-C21	113.59(11)
N2-C3-C4	112.11(11)	C21-C3-C4	113.75(11)
N2-C3-H3	105.5	C21-C3-H3	105.5
C4-C3-H3	105.5	C5-C4-C3	114.75(11)
C5-C4-H4A	108.6	C3-C4-H4A	108.6
C5-C4-H4B	108.6	C3-C4-H4B	108.6
H4A-C4-H4B	107.6	C9-C5-C4	108.26(11)
C9-C5-C6	109.60(11)	C4-C5-C6	114.49(12)
C9-C5-H5	108.1	C4-C5-H5	108.1
C6-C5-H5	108.1	C7-C6-C5	114.64(11)
C7-C6-H6A	108.6	C5-C6-H6A	108.6
C7-C6-H6B	108.6	C5-C6-H6B	108.6
H6A-C6-H6B	107.6	C8-C7-C26	117.94(13)
C8-C7-C6	122.14(13)	C26-C7-C6	119.90(12)
O31-C8-C7	125.82(13)	O31-C8-C1	112.55(12)
C7-C8-C1	121.62(12)	C5-C9-C1	108.06(11)
C5-C9-H9A	110.1	C1-C9-H9A	110.1
C5-C9-H9B	110.1	C1-C9-H9B	110.1
H9A-C9-H9B	108.4	O11-C10-N2	121.66(13)
O11-C10-C12	120.53(12)	N2-C10-C12	117.80(12)

C13-C12-C10	114.25(11)	C13-C12-H12A	108.7
C10-C12-H12A	108.7	C13-C12-H12B	108.7
C10-C12-H12B	108.7	H12A-C12-H12B	107.6
C14-C13-C20	118.67(13)	C14-C13-C12	121.41(13)
C20-C13-C12	119.91(13)	C15-C14-C13	120.42(13)
C15-C14-H14	119.8	C13-C14-H14	119.8
C14-C15-C17	120.44(12)	C14-C15-C16	118.73(11)
C17-C15-C16	120.83(11)	C19-C17-C15	119.47(13)
C19-C17-C18	119.29(11)	C15-C17-C18	121.24(11)
C20-C19-C17	120.08(13)	C20-C19-H19	120.0
C17-C19-H19	120.0	C19-C20-C13	120.89(13)
C19-C20-H20	119.6	C13-C20-H20	119.6
O22-C21-O23	123.92(13)	O22-C21-C3	122.95(12)
O23-C21-C3	112.85(11)	O23-C24-C25	112.02(12)
O23-C24-H24A	109.2	C25-C24-H24A	109.2
O23-C24-H24B	109.2	C25-C24-H24B	109.2
H24A-C24-H24B	107.9	C24-C25-H25A	109.5
C24-C25-H25B	109.5	H25A-C25-H25B	109.5
C24-C25-H25C	109.5	H25A-C25-H25C	109.5
H25B-C25-H25C	109.5	O27-C26-O28	122.28(13)
O27-C26-C7	124.86(14)	O28-C26-C7	112.85(12)
C21-O23-C24	115.51(11)	C26-O28-C29	120.7(4)
C26-O28-C29A	110.4(5)	O28-C29-C30	110.2(6)
O28-C29-H29A	109.6	C30-C29-H29A	109.6
O28-C29-H29B	109.6	C30-C29-H29B	109.6
H29A-C29-H29B	108.1	C29-C30-H30A	109.5
C29-C30-H30B	109.5	H30A-C30-H30B	109.5
C29-C30-H30C	109.5	H30A-C30-H30C	109.5
H30B-C30-H30C	109.5	O28-C29A-C30A	103.4(8)
O28-C29A-H29C	111.1	C30A-C29A-H29C	111.1
O28-C29A-H29D	111.1	C30A-C29A-H29D	111.1
H29C-C29A-H29D	109.0	C29A-C30A-H30D	109.5
C29A-C30A-H30E	109.5	H30D-C30A-H30E	109.5
C29A-C30A-H30F	109.5	H30D-C30A-H30F	109.5
H30E-C30A-H30F	109.5	C8-O31-H31	104.9(16)

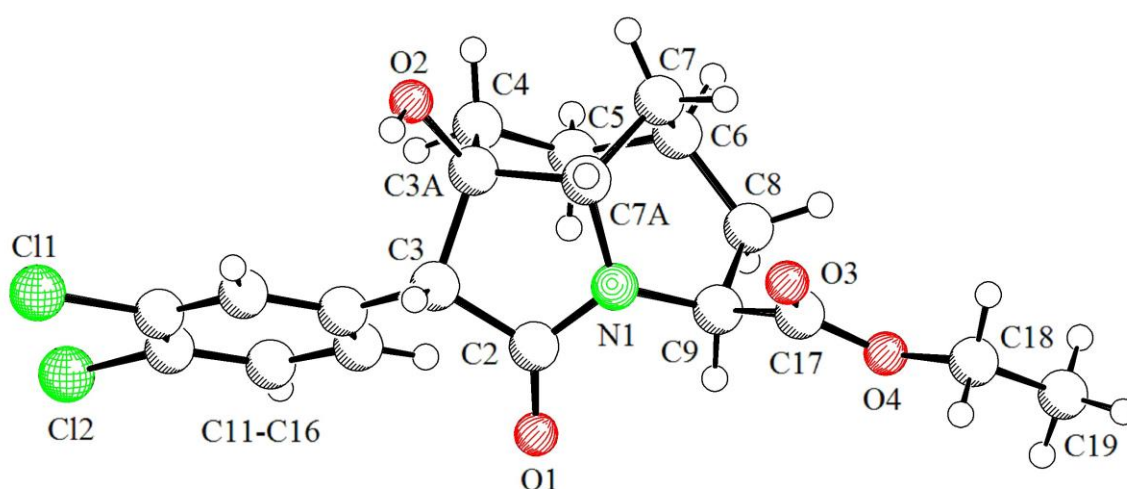
Table 19: Torsion angles (°) for **80**.

C10-N2-C1-C8	110.37(14)	C3-N2-C1-C8	-67.75(14)
C10-N2-C1-C9	-128.24(13)	C3-N2-C1-C9	53.64(15)
C10-N2-C3-C21	-90.60(14)	C1-N2-C3-C21	87.65(14)
C10-N2-C3-C4	138.72(12)	C1-N2-C3-C4	-43.03(15)
N2-C3-C4-C5	42.94(16)	C21-C3-C4-C5	-87.65(14)
C3-C4-C5-C9	-53.45(15)	C3-C4-C5-C6	69.12(15)
C9-C5-C6-C7	36.72(16)	C4-C5-C6-C7	-85.11(15)
C5-C6-C7-C8	-6.20(19)	C5-C6-C7-C26	175.22(12)
C26-C7-C8-O31	0.3(2)	C6-C7-C8-O31	-178.27(13)
C26-C7-C8-C1	-178.64(12)	C6-C7-C8-C1	2.7(2)
N2-C1-C8-O31	-87.22(14)	C9-C1-C8-O31	151.09(12)
N2-C1-C8-C7	91.90(15)	C9-C1-C8-C7	-29.80(18)
C4-C5-C9-C1	61.65(14)	C6-C5-C9-C1	-63.85(14)
N2-C1-C9-C5	-61.94(14)	C8-C1-C9-C5	59.79(14)
C3-N2-C10-O11	-4.41(19)	C1-N2-C10-O11	177.49(12)
C3-N2-C10-C12	176.10(11)	C1-N2-C10-C12	-2.00(19)
O11-C10-C12-C13	-109.55(14)	N2-C10-C12-C13	69.95(16)
C10-C12-C13-C14	22.58(18)	C10-C12-C13-C20	-158.51(13)
C20-C13-C14-C15	-0.91(19)	C12-C13-C14-C15	178.01(12)
C13-C14-C15-C17	1.8(2)	C13-C14-C15-Cl16	-178.22(10)
C14-C15-C17-C19	-1.4(2)	Cl16-C15-C17-C19	178.60(10)
C14-C15-C17-Cl18	177.70(10)	Cl16-C15-C17-Cl18	-2.27(16)
C15-C17-C19-C20	0.2(2)	Cl18-C17-C19-C20	-178.97(10)
C17-C19-C20-C13	0.7(2)	C14-C13-C20-C19	-0.3(2)
C12-C13-C20-C19	-179.28(12)	N2-C3-C21-O22	-162.04(13)
C4-C3-C21-O22	-32.19(18)	N2-C3-C21-O23	23.92(16)
C4-C3-C21-O23	153.77(11)	C8-C7-C26-O27	-5.7(2)
C6-C7-C26-O27	172.94(13)	C8-C7-C26-O28	173.12(12)
C6-C7-C26-O28	-8.23(18)	O22-C21-O23-C24	-3.50(19)
C3-C21-O23-C24	170.48(11)	C25-C24-O23-C21	79.98(15)
O27-C26-O28-C29	-2.6(5)	C7-C26-O28-C29	178.5(5)
O27-C26-O28-C29A	6.1(6)	C7-C26-O28-C29A	-172.8(6)
C26-O28-C29-C30	159.8(5)	C26-O28-C29A-C30A	-171.8(9)

Table 20: Hydrogen bond distances (Å) and angles (°) for **80**.

	Donor-H	Acceptor-H	Donor-Acceptor	Angle
O31-H31...O27	0.82(3)	1.87(2)	2.6108(16)	150.(2)

7.3.2 X-ray crystal structure of tricyclic alcohol **82**



SCHAKAL

A colorless needle-like specimen of $C_{19}H_{21}Cl_2NO_4$, approximate dimensions 0.018 mm x 0.057 mm x 0.264 mm, was used for the X-ray crystallographic analysis. The X-ray intensity data were measured on a Bruker D8 Venture Photon III Diffractometer system equipped with a micro focus tube $CuK\alpha$ ($CuK\alpha$, $\lambda = 1.54178 \text{ \AA}$) and a MX mirror monochromator.

A total of 1133 frames were collected. The total exposure time was 17.98 hours. The frames were integrated with the Bruker SAINT software package using a wide-frame algorithm. The integration of the data using a monoclinic unit cell yielded a total of 36830 reflections to a maximum θ angle of 65.08° (0.85 \AA resolution), of which 6089 were independent (average redundancy 6.049, completeness = 98.9%, $R_{int} = 87.44\%$, $R_{sig} = 48.96\%$) and 1500 (24.63%) were greater than $2\sigma(F^2)$. The final cell constants

of $a = 26.620(4)$ Å, $b = 6.3091(11)$ Å, $c = 22.468(3)$ Å, $\beta = 107.895(10)^\circ$, volume = $3590.9(10)$ Å³, are based upon the refinement of the XYZ-centroids of 845 reflections above $20 \sigma(I)$ with $6.979^\circ < 2\theta < 120.9^\circ$. Data were corrected for absorption effects using the Multi-Scan method (SADABS). The ratio of minimum to maximum apparent transmission was 0.765. The calculated minimum and maximum transmission coefficients (based on crystal size) are 0.4610 and 0.9400.

The structure was solved and refined using the Bruker SHELXTL Software Package, using the space group $P 1 21/c 1$, with $Z = 8$ for the formula unit, $C_{19}H_{21}Cl_2NO_4$. The final anisotropic full-matrix least-squares refinement on F^2 with 473 variables converged at $R1 = 10.50\%$, for the observed data and $wR2 = 31.55\%$ for all data. The goodness-of-fit was 0.907. The largest peak in the final difference electron density synthesis was $0.400 e^-/\text{Å}^3$ and the largest hole was $-0.465 e^-/\text{Å}^3$ with an RMS deviation of $0.103 e^-/\text{Å}^3$. On the basis of the final model, the calculated density was 1.473 g/cm^3 and $F(000)$, 1664 e^- .

Table 21: Sample and crystal data for **82**.

Identification code	dan10047	
Chemical formula	$C_{19}H_{21}Cl_2NO_4$	
Formula weight	398.27 g/mol	
Temperature	102(2) K	
Wavelength	1.54178 Å	
Crystal size	0.018 x 0.057 x 0.264 mm	
Crystal habit	colorless needle	
Crystal system	monoclinic	
Space group	$P 1 21/c 1$	
Unit cell dimensions	$a = 26.620(4)$ Å	$\alpha = 90^\circ$
	$b = 6.3091(11)$ Å	$\beta = 107.895(10)^\circ$
	$c = 22.468(3)$ Å	$\gamma = 90^\circ$
Volume	$3590.9(10)$ Å ³	
Z	8	

Density (calculated)	1.473 g/cm ³
Absorption coefficient	3.473 mm ⁻¹
F(000)	1664

Table 22: Data collection and structure refinement for **82**.

Diffractometer	Bruker D8 Venture Bruker D8 Venture Photon III Diffractometer
Radiation source	micro focus tube CuK α (CuK α , $\lambda = 1.54178 \text{ \AA}$)
Theta range for data collection	3.49 to 65.08°
Index ranges	-31 $\leq h \leq$ 31, -7 $\leq k \leq$ 7, -26 $\leq l \leq$ 26
Reflections collected	36830
Independent reflections	6089 [R(int) = 0.8744]
Coverage of independent reflections	98.9%
Absorption correction	Multi-Scan
Max. and min. transmission	0.9400 and 0.4610
Structure solution technique	direct methods
Structure solution program	SHELXT 2018/2 (Sheldrick, 2018)
Refinement method	Full-matrix least-squares on F ²
Refinement program	SHELXL-2018/3 (Sheldrick, 2018)
Function minimized	$\Sigma w(F_o^2 - F_c^2)^2$
Data / restraints / parameters	6089 / 0 / 473
Goodness-of-fit on F²	0.907
Final R indices	1500 data; $l > 2\sigma(l)$ R1 = 0.1050, wR2 = 0.1982 all data R1 = 0.3553, wR2 = 0.3155
Weighting scheme	$w = 1/[\sigma^2(F_o^2)]$ where $P = (F_o^2 + 2F_c^2)/3$
Largest diff. peak and hole	0.400 and -0.465 e \AA^{-3}

R.M.S. deviation from mean 0.103 eÅ⁻³

Table 23: Bond lengths (Å) for **82**.

C2-O1	1.227(17)	C2-N1	1.334(17)
C2-C3	1.52(2)	C3-C11	1.495(18)
C3-C3A	1.579(19)	C3-H3	1.0
C4-C5	1.511(18)	C4-C3A	1.535(19)
C4-H4A	0.99	C4-H4B	0.99
C5-C6	1.546(18)	C5-H5A	0.99
C5-H5B	0.99	C6-C8	1.530(17)
C6-C7	1.558(17)	C6-H6	1.0
C7-C7A	1.520(19)	C7-H7A	0.99
C7-H7B	0.99	C8-C9	1.554(19)
C8-H8A	0.99	C8-H8B	0.99
C9-N1	1.479(16)	C9-C17	1.531(19)
C9-H9	1.0	C11-C12	1.385(18)
C11-C16	1.419(18)	C12-C13	1.384(18)
C12-H12	0.95	C13-C14	1.388(18)
C13-C11	1.743(14)	C14-C15	1.402(18)
C14-C12	1.694(14)	C15-C16	1.402(18)
C15-H15	0.95	C16-H16	0.95
C17-O3	1.242(16)	C17-O4	1.324(17)
C18-O4	1.469(14)	C18-C19	1.536(19)
C18-H18A	0.99	C18-H18B	0.99
C19-H19A	0.98	C19-H19B	0.98
C19-H19C	0.98	C22-O5	1.228(16)
C22-N21	1.342(17)	C22-C23	1.548(19)
C23-C31	1.526(19)	C23-C23A	1.573(19)
C23-H23	1.0	C23A-O6	1.391(16)
C23A-C24	1.55(2)	C23A-C27A	1.57(2)
C24-C25	1.57(2)	C24-H24A	0.99
C24-H24B	0.99	C25-C26	1.50(2)
C25-H25A	0.99	C25-H25B	0.99
C26-C27	1.524(19)	C26-C28	1.56(2)
C26-H26	1.0	C27-C27A	1.516(19)

C27-H27A	0.99	C27-H27B	0.99
C27A-N21	1.446(17)	C27A-H27C	1.0
C28-C29	1.547(17)	C28-H28A	0.99
C28-H28B	0.99	C29-N21	1.482(16)
C29-C37	1.53(2)	C29-H29	1.0
C31-C36	1.395(19)	C31-C32	1.411(18)
C32-C33	1.390(19)	C32-H32	0.95
C33-C34	1.379(19)	C33-Cl3	1.743(13)
C34-C35	1.386(19)	C34-Cl4	1.753(14)
C35-C36	1.40(2)	C35-H35	0.95
C36-H36	0.95	C37-O7	1.210(17)
C37-O8	1.340(17)	C38-O8	1.438(16)
C38-C39	1.524(19)	C38-H38A	0.99
C38-H38B	0.99	C39-H39A	0.98
C39-H39B	0.98	C39-H39C	0.98
C3A-O2	1.418(16)	C3A-C7A	1.567(19)
C7A-N1	1.496(16)	C7A-H7A1	1.0
O2-H2	0.84	O6-H6A	0.84

Table 24: Bond angles (°) for **82**.

O1-C2-N1	127.1(15)	O1-C2-C3	123.5(12)
N1-C2-C3	109.3(14)	C11-C3-C2	118.6(12)
C11-C3-C3A	116.4(11)	C2-C3-C3A	102.2(12)
C11-C3-H3	106.2	C2-C3-H3	106.2
C3A-C3-H3	106.2	C5-C4-C3A	115.0(12)
C5-C4-H4A	108.5	C3A-C4-H4A	108.5
C5-C4-H4B	108.5	C3A-C4-H4B	108.5
H4A-C4-H4B	107.5	C4-C5-C6	116.1(13)
C4-C5-H5A	108.3	C6-C5-H5A	108.3
C4-C5-H5B	108.3	C6-C5-H5B	108.3
H5A-C5-H5B	107.4	C8-C6-C5	113.3(12)
C8-C6-C7	108.6(10)	C5-C6-C7	110.0(11)
C8-C6-H6	108.3	C5-C6-H6	108.3
C7-C6-H6	108.3	C7A-C7-C6	105.7(11)
C7A-C7-H7A	110.6	C6-C7-H7A	110.6

C7A-C7-H7B	110.6	C6-C7-H7B	110.6
H7A-C7-H7B	108.7	C6-C8-C9	112.5(11)
C6-C8-H8A	109.1	C9-C8-H8A	109.1
C6-C8-H8B	109.1	C9-C8-H8B	109.1
H8A-C8-H8B	107.8	N1-C9-C17	111.5(12)
N1-C9-C8	110.9(11)	C17-C9-C8	109.8(12)
N1-C9-H9	108.2	C17-C9-H9	108.2
C8-C9-H9	108.2	C12-C11-C16	119.6(13)
C12-C11-C3	121.7(14)	C16-C11-C3	118.4(13)
C13-C12-C11	120.6(14)	C13-C12-H12	119.7
C11-C12-H12	119.7	C12-C13-C14	122.4(13)
C12-C13-C11	116.8(12)	C14-C13-C11	120.9(11)
C13-C14-C15	116.3(13)	C13-C14-C12	122.4(11)
C15-C14-C12	121.3(11)	C14-C15-C16	123.4(14)
C14-C15-H15	118.3	C16-C15-H15	118.3
C15-C16-C11	117.5(13)	C15-C16-H16	121.2
C11-C16-H16	121.2	O3-C17-O4	126.3(14)
O3-C17-C9	124.5(14)	O4-C17-C9	109.1(13)
O4-C18-C19	103.4(11)	O4-C18-H18A	111.1
C19-C18-H18A	111.1	O4-C18-H18B	111.1
C19-C18-H18B	111.1	H18A-C18-H18B	109.0
C18-C19-H19A	109.5	C18-C19-H19B	109.5
H19A-C19-H19B	109.5	C18-C19-H19C	109.5
H19A-C19-H19C	109.5	H19B-C19-H19C	109.5
O5-C22-N21	127.3(14)	O5-C22-C23	127.1(13)
N21-C22-C23	105.5(13)	C31-C23-C22	115.6(13)
C31-C23-C23A	115.4(12)	C22-C23-C23A	100.8(11)
C31-C23-H23	108.2	C22-C23-H23	108.2
C23A-C23-H23	108.2	O6-C23A-C24	111.5(12)
O6-C23A-C27A	114.4(13)	C24-C23A-C27A	107.8(12)
O6-C23A-C23	114.3(12)	C24-C23A-C23	110.5(12)
C27A-C23A-C23	97.4(11)	C23A-C24-C25	116.3(12)
C23A-C24-H24A	108.2	C25-C24-H24A	108.2
C23A-C24-H24B	108.2	C25-C24-H24B	108.2
H24A-C24-H24B	107.4	C26-C25-C24	114.5(12)
C26-C25-H25A	108.6	C24-C25-H25A	108.6

C26-C25-H25B	108.6	C24-C25-H25B	108.6
H25A-C25-H25B	107.6	C25-C26-C27	108.3(13)
C25-C26-C28	113.4(14)	C27-C26-C28	110.8(12)
C25-C26-H26	108.1	C27-C26-H26	108.1
C28-C26-H26	108.1	C27A-C27-C26	107.8(13)
C27A-C27-H27A	110.1	C26-C27-H27A	110.1
C27A-C27-H27B	110.1	C26-C27-H27B	110.1
H27A-C27-H27B	108.5	N21-C27A-C27	113.4(12)
N21-C27A-C23A	101.8(12)	C27-C27A-C23A	116.0(13)
N21-C27A-H27C	108.4	C27-C27A-H27C	108.4
C23A-C27A-H27C	108.4	C29-C28-C26	113.8(12)
C29-C28-H28A	108.8	C26-C28-H28A	108.8
C29-C28-H28B	108.8	C26-C28-H28B	108.8
H28A-C28-H28B	107.7	N21-C29-C37	110.9(12)
N21-C29-C28	111.4(11)	C37-C29-C28	113.0(11)
N21-C29-H29	107.1	C37-C29-H29	107.1
C28-C29-H29	107.1	C36-C31-C32	119.4(13)
C36-C31-C23	124.1(14)	C32-C31-C23	116.5(14)
C33-C32-C31	119.1(14)	C33-C32-H32	120.5
C31-C32-H32	120.5	C34-C33-C32	120.6(13)
C34-C33-CI3	121.4(12)	C32-C33-CI3	117.9(13)
C33-C34-C35	121.5(13)	C33-C34-CI4	120.5(12)
C35-C34-CI4	118.0(12)	C34-C35-C36	118.2(14)
C34-C35-H35	120.9	C36-C35-H35	120.9
C31-C36-C35	121.2(15)	C31-C36-H36	119.4
C35-C36-H36	119.4	O7-C37-O8	123.7(14)
O7-C37-C29	126.3(14)	O8-C37-C29	110.1(14)
O8-C38-C39	106.0(12)	O8-C38-H38A	110.5
C39-C38-H38A	110.5	O8-C38-H38B	110.5
C39-C38-H38B	110.5	H38A-C38-H38B	108.7
C38-C39-H39A	109.5	C38-C39-H39B	109.5
H39A-C39-H39B	109.5	C38-C39-H39C	109.5
H39A-C39-H39C	109.5	H39B-C39-H39C	109.5
O2-C3A-C4	105.4(11)	O2-C3A-C7A	113.5(12)
C4-C3A-C7A	108.9(12)	O2-C3A-C3	113.7(12)
C4-C3A-C3	113.3(12)	C7A-C3A-C3	102.2(11)

N1-C7A-C7	111.0(11)	N1-C7A-C3A	101.5(11)
C7-C7A-C3A	112.9(11)	N1-C7A-H7A1	110.4
C7-C7A-H7A1	110.4	C3A-C7A-H7A1	110.4
C2-N1-C9	120.6(13)	C2-N1-C7A	114.0(13)
C9-N1-C7A	121.4(11)	C22-N21-C27A	114.3(12)
C22-N21-C29	119.8(13)	C27A-N21-C29	118.2(11)
C3A-O2-H2	109.5	C17-O4-C18	116.3(12)
C23A-O6-H6A	109.5	C37-O8-C38	115.9(12)

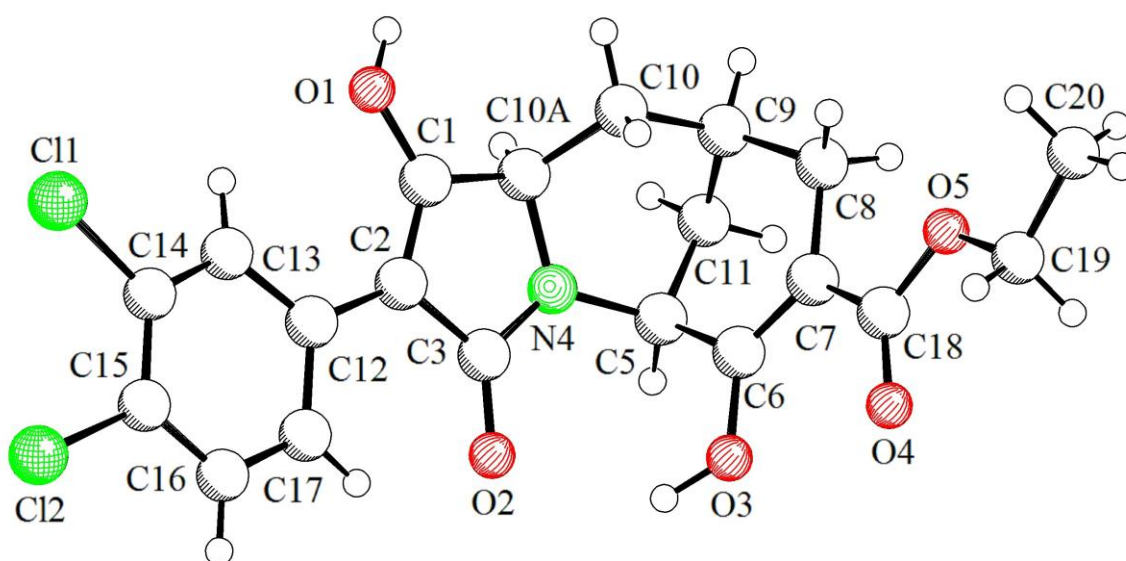
Table 25: Torsion angles (°) for **82**.

O1-C2-C3-C11	-26.(2)	N1-C2-C3-C11	150.2(12)
O1-C2-C3-C3A	-155.8(13)	N1-C2-C3-C3A	20.8(14)
C3A-C4-C5-C6	-51.0(18)	C4-C5-C6-C8	128.5(13)
C4-C5-C6-C7	6.8(16)	C8-C6-C7-C7A	-74.1(14)
C5-C6-C7-C7A	50.4(14)	C5-C6-C8-C9	-77.7(15)
C7-C6-C8-C9	44.8(16)	C6-C8-C9-N1	12.1(16)
C6-C8-C9-C17	-111.5(14)	C2-C3-C11-C12	153.5(13)
C3A-C3-C11-C12	-83.9(17)	C2-C3-C11-C16	-31.4(18)
C3A-C3-C11-C16	91.3(16)	C16-C11-C12-C13	2.(2)
C3-C11-C12-C13	177.4(13)	C11-C12-C13-C14	-2.(2)
C11-C12-C13-C11	178.2(11)	C12-C13-C14-C15	1.(2)
C11-C13-C14-C15	-179.4(10)	C12-C13-C14-C12	179.5(12)
C11-C13-C14-C12	-0.7(18)	C13-C14-C15-C16	0.(2)
C12-C14-C15-C16	-178.8(11)	C14-C15-C16-C11	1.(2)
C12-C11-C16-C15	-1.6(19)	C3-C11-C16-C15	-176.9(12)
N1-C9-C17-O3	-14.(2)	C8-C9-C17-O3	109.5(16)
N1-C9-C17-O4	168.2(11)	C8-C9-C17-O4	-68.5(15)
O5-C22-C23-C31	-23.(2)	N21-C22-C23-C31	156.2(12)
O5-C22-C23-C23A	-148.1(15)	N21-C22-C23-C23A	31.1(14)
C31-C23-C23A-O6	71.5(17)	C22-C23-C23A-O6	-163.2(12)
C31-C23-C23A-C24	-55.3(17)	C22-C23-C23A-C24	70.0(14)
C31-C23-C23A-C27A	-167.5(13)	C22-C23-C23A-C27A	-42.2(14)
O6-C23A-C24-C25	88.8(15)	C27A-C23A-C24-C25	-37.5(18)
C23-C23A-C24-C25	-142.9(13)	C23A-C24-C25-C26	45.(2)
C24-C25-C26-C27	-56.0(19)	C24-C25-C26-C28	67.4(18)

C25-C26-C27-C27A	63.7(16)	C28-C26-C27-C27A	-61.3(16)
C26-C27-C27A-N21	53.9(17)	C26-C27-C27A-C23A	-63.4(17)
O6-C23A-C27A-N21	160.6(11)	C24-C23A-C27A-N21	-74.8(13)
C23-C23A-C27A-N21	39.6(13)	O6-C23A-C27A-C27	-75.8(17)
C24-C23A-C27A-C27	48.8(17)	C23-C23A-C27A-C27	163.2(13)
C25-C26-C28-C29	-105.8(14)	C27-C26-C28-C29	16.2(17)
C26-C28-C29-N21	36.1(17)	C26-C28-C29-C37	-89.6(15)
C22-C23-C31-C36	-30.(2)	C23A-C23-C31-C36	87.3(18)
C22-C23-C31-C32	147.5(13)	C23A-C23-C31-C32	-95.2(16)
C36-C31-C32-C33	-1.(2)	C23-C31-C32-C33	-178.8(12)
C31-C32-C33-C34	2.(2)	C31-C32-C33-CI3	178.5(10)
C32-C33-C34-C35	-2.(2)	CI3-C33-C34-C35	-178.4(11)
C32-C33-C34-CI4	178.2(10)	CI3-C33-C34-CI4	1.3(18)
C33-C34-C35-C36	1.(2)	CI4-C34-C35-C36	-178.5(11)
C32-C31-C36-C35	1.(2)	C23-C31-C36-C35	178.3(13)
C34-C35-C36-C31	-1.(2)	N21-C29-C37-O7	-14.9(19)
C28-C29-C37-O7	111.0(16)	N21-C29-C37-O8	166.0(10)
C28-C29-C37-O8	-68.1(15)	C5-C4-C3A-O2	153.2(12)
C5-C4-C3A-C7A	31.1(18)	C5-C4-C3A-C3	-81.9(16)
C11-C3-C3A-O2	75.4(16)	C2-C3-C3A-O2	-153.8(11)
C11-C3-C3A-C4	-45.0(18)	C2-C3-C3A-C4	85.9(14)
C11-C3-C3A-C7A	-161.9(13)	C2-C3-C3A-C7A	-31.1(13)
C6-C7-C7A-N1	41.3(14)	C6-C7-C7A-C3A	-71.9(14)
O2-C3A-C7A-N1	153.0(11)	C4-C3A-C7A-N1	-89.9(13)
C3-C3A-C7A-N1	30.2(13)	O2-C3A-C7A-C7	-88.0(15)
C4-C3A-C7A-C7	29.1(16)	C3-C3A-C7A-C7	149.1(12)
O1-C2-N1-C9	18.(2)	C3-C2-N1-C9	-158.6(11)
O1-C2-N1-C7A	175.5(13)	C3-C2-N1-C7A	-0.9(15)
C17-C9-N1-C2	-128.2(13)	C8-C9-N1-C2	109.1(14)
C17-C9-N1-C7A	75.7(15)	C8-C9-N1-C7A	-47.0(16)
C7-C7A-N1-C2	-139.8(12)	C3A-C7A-N1-C2	-19.5(14)
C7-C7A-N1-C9	17.8(17)	C3A-C7A-N1-C9	138.1(12)
O5-C22-N21-C27A	174.1(14)	C23-C22-N21-C27A	-5.1(15)
O5-C22-N21-C29	25.(2)	C23-C22-N21-C29	-154.0(11)
C27-C27A-N21-C22	-148.6(13)	C23A-C27A-N21-C22	-23.2(15)
C27-C27A-N21-C29	0.8(19)	C23A-C27A-N21-C29	126.2(12)

C37-C29-N21-C22	-132.2(12)	C28-C29-N21-C22	101.0(14)
C37-C29-N21-C27A	80.1(15)	C28-C29-N21-C27A	-46.7(17)
O3-C17-O4-C18	1.(2)	C9-C17-O4-C18	178.9(11)
C19-C18-O4-C17	-172.1(11)	O7-C37-O8-C38	6.9(18)
C29-C37-O8-C38	-173.9(10)	C39-C38-O8-C37	-175.2(11)

7.3.3 X-ray crystal structure of tricyclic bis(enol) 84



SCHAKAL

A colorless plate-like specimen of $C_{20}H_{19}Cl_2NO_5$, approximate dimensions 0.031 mm x 0.038 mm x 0.090 mm, was used for the X-ray crystallographic analysis. The X-ray intensity data were measured on a Bruker D8 Venture Bruker D8 Venture Photon III Diffractometer system equipped with a micro focus tube $CuK\alpha$ ($CuK\alpha$, $\lambda = 1.54178 \text{ \AA}$) and a MX mirror monochromator.

A total of 1255 frames were collected. The total exposure time was 15.87 hours. The frames were integrated with the Bruker SAINT software package using a wide-frame algorithm. The integration of the data using a triclinic unit cell yielded a total of 21345 reflections to a maximum θ angle of 66.75° (0.84 \AA resolution), of which 3878 were independent (average redundancy 5.504, completeness = 99.9%, $R_{int} = 11.58\%$, R_{sig}

= 6.61%) and 2606 (67.20%) were greater than $2\sigma(F^2)$. The final cell constants of $a = 9.0833(2)$ Å, $b = 10.0462(2)$ Å, $c = 13.0327(3)$ Å, $\alpha = 91.222(2)^\circ$, $\beta = 109.426(2)^\circ$, $\gamma = 101.156(2)^\circ$, volume = $1095.64(4)$ Å³, are based upon the refinement of the XYZ-centroids of 3935 reflections above $20 \sigma(I)$ with $7.223^\circ < 2\theta < 133.1^\circ$. Data were corrected for absorption effects using the Multi-Scan method (SADABS). The ratio of minimum to maximum apparent transmission was 0.877. The calculated minimum and maximum transmission coefficients (based on crystal size) are 0.7790 and 0.9150.

The structure was solved and refined using the Bruker SHELXTL Software Package, using the space group P -1, with Z = 2 for the formula unit, C₂₀H₁₉Cl₂NO₅. The final anisotropic full-matrix least-squares refinement on F² with 330 variables converged at R1 = 5.56%, for the observed data and wR2 = 14.61% for all data. The goodness-of-fit was 1.019. The largest peak in the final difference electron density synthesis was 0.359 e⁻/Å³ and the largest hole was -0.468 e⁻/Å³ with an RMS deviation of 0.061 e⁻/Å³. On the basis of the final model, the calculated density was 1.286 g/cm³ and F(000), 440 e⁻.

Table 26: Sample and crystal data for **84**.

Identification code	dan10044	
Chemical formula	C ₂₀ H ₁₉ Cl ₂ NO ₅	
Formula weight	424.26 g/mol	
Temperature	101(2) K	
Wavelength	1.54178 Å	
Crystal size	0.031 x 0.038 x 0.090 mm	
Crystal habit	colorless plate	
Crystal system	triclinic	
Space group	P -1	
Unit cell dimensions	$a = 9.0833(2)$ Å	$\alpha = 91.222(2)^\circ$
	$b = 10.0462(2)$ Å	$\beta = 109.426(2)^\circ$
	$c = 13.0327(3)$ Å	$\gamma = 101.156(2)^\circ$
Volume	$1095.64(4)$ Å ³	

Z	2
Density (calculated)	1.286 g/cm ³
Absorption coefficient	2.918 mm ⁻¹
F(000)	440

Table 27: Data collection and structure refinement for **84**.

Diffractometer	Bruker D8 Venture Bruker D8 Venture Photon III Diffractometer
Radiation source	micro focus tube CuK α (CuK α , $\lambda = 1.54178 \text{ \AA}$)
Theta range for data collection	3.61 to 66.75°
Index ranges	-10 $\leq h \leq 10$, -11 $\leq k \leq 11$, -15 $\leq l \leq 15$
Reflections collected	21345
Independent reflections	3878 [R(int) = 0.1158]
Coverage of independent reflections	99.9%
Absorption correction	Multi-Scan
Max. and min. transmission	0.9150 and 0.7790
Structure solution technique	direct methods
Structure solution program	SHELXT 2018/2 (Sheldrick, 2018)
Refinement method	Full-matrix least-squares on F ²
Refinement program	SHELXL-2018/3 (Sheldrick, 2018)
Function minimized	$\Sigma w(F_o^2 - F_c^2)^2$
Data / restraints / parameters	3878 / 174 / 330
Goodness-of-fit on F²	1.019
Final R indices	2606 data; $l > 2\sigma(l)$ R1 = 0.0556, wR2 = 0.1263 all data R1 = 0.0923, wR2 = 0.1461
Weighting scheme	$w = 1/[\sigma^2(F_o^2) + (0.0594P)^2 + 1.0268P]$ where

	$P=(F_o^2+2F_c^2)/3$
Absolute structure parameter	0.000(14)
Extinction coefficient	0.0015(6)
Largest diff. peak and hole	0.359 and -0.468 eÅ ⁻³
R.M.S. deviation from mean	0.061 eÅ ⁻³

Table 28: Bond lengths (Å) for **84**.

N4-C3	1.359(4)	N4-C10A	1.450(4)
N4-C5	1.480(4)	O1-C1	1.342(4)
O1-H1	0.925(19)	O2-C3	1.232(4)
O3-C6	1.351(5)	O3-H3	0.95(2)
O3-H3A	0.94(2)	O4-C18	1.233(4)
O5-C18	1.347(4)	O5-C19	1.451(4)
C1-C2	1.351(4)	C1-C10A	1.496(4)
C2-C12	1.466(4)	C2-C3	1.492(4)
C5-C11	1.514(6)	C5-C6	1.532(5)
C5-H5	1.0	C6-C7	1.374(4)
C7-C18	1.439(4)	C7-C8	1.514(4)
C8-C9	1.524(5)	C8-H8A	0.99
C8-H8B	0.99	C9-C11	1.527(6)
C9-C10	1.558(5)	C9-H9	1.0
C10-C10A	1.523(5)	C10-H10A	0.99
C10-H10B	0.99	C10A-H10C	1.0
C11-H11A	0.99	C11-H11B	0.99
C12-C13	1.385(9)	C12-C17	1.406(9)
C12-C13A	1.410(10)	C12-C17A	1.421(10)
C13-C14	1.396(11)	C13-H13	0.95
C14-C15	1.391(12)	C14-Cl1	1.724(10)
C15-C16	1.392(10)	C15-Cl2	1.727(11)
C16-C17	1.382(10)	C16-H16	0.95
C17-H17	0.95	C13A-C14A	1.396(11)
C13A-H13A	0.95	C14A-C15A	1.389(17)
C14A-Cl1A	1.735(11)	C15A-C16A	1.373(16)
C15A-Cl2A	1.744(14)	C16A-C17A	1.385(11)

C16A-H16A	0.95	C17A-H17A	0.95
C19-C20	1.505(5)	C19-H19A	0.99
C19-H19B	0.99	C20-H20A	0.98
C20-H20B	0.98	C20-H20C	0.98

Table 29: Bond angles (°) for **84**.

C3-N4-C10A	112.9(2)	C3-N4-C5	126.5(3)
C10A-N4-C5	118.8(3)	C1-O1-H1	113.(3)
C6-O3-H3	122.(6)	C6-O3-H3A	124.(9)
C18-O5-C19	116.4(3)	O1-C1-C2	126.6(3)
O1-C1-C10A	120.8(3)	C2-C1-C10A	112.6(3)
C1-C2-C12	128.5(3)	C1-C2-C3	106.1(3)
C12-C2-C3	125.3(3)	O2-C3-N4	124.3(3)
O2-C3-C2	128.3(3)	N4-C3-C2	107.4(3)
N4-C5-C11	107.2(3)	N4-C5-C6	111.2(3)
C11-C5-C6	110.7(3)	N4-C5-H5	109.2
C11-C5-H5	109.2	C6-C5-H5	109.2
O3-C6-C7	125.0(3)	O3-C6-C5	114.0(3)
C7-C6-C5	121.0(3)	C6-C7-C18	119.7(3)
C6-C7-C8	122.0(3)	C18-C7-C8	118.3(3)
C7-C8-C9	112.3(3)	C7-C8-H8A	109.2
C9-C8-H8A	109.2	C7-C8-H8B	109.2
C9-C8-H8B	109.2	H8A-C8-H8B	107.9
C8-C9-C11	107.8(3)	C8-C9-C10	111.3(3)
C11-C9-C10	111.5(3)	C8-C9-H9	108.7
C11-C9-H9	108.7	C10-C9-H9	108.7
C10A-C10-C9	110.8(3)	C10A-C10-H10A	109.5
C9-C10-H10A	109.5	C10A-C10-H10B	109.5
C9-C10-H10B	109.5	H10A-C10-H10B	108.1
N4-C10A-C1	101.0(3)	N4-C10A-C10	109.6(3)
C1-C10A-C10	117.0(3)	N4-C10A-H10C	109.6
C1-C10A-H10C	109.6	C10-C10A-H10C	109.6
C5-C11-C9	107.6(3)	C5-C11-H11A	110.2
C9-C11-H11A	110.2	C5-C11-H11B	110.2
C9-C11-H11B	110.2	H11A-C11-H11B	108.5

C13-C12-C17	120.9(7)	C13A-C12-C17A	112.3(9)
C13-C12-C2	121.6(7)	C17-C12-C2	116.5(5)
C13A-C12-C2	119.1(7)	C17A-C12-C2	127.3(6)
C12-C13-C14	117.8(11)	C12-C13-H13	121.1
C14-C13-H13	121.1	C15-C14-C13	120.4(10)
C15-C14-C11	123.0(9)	C13-C14-C11	116.4(8)
C14-C15-C16	119.8(9)	C14-C15-C12	119.4(8)
C16-C15-C12	120.7(8)	C17-C16-C15	120.3(9)
C17-C16-H16	119.8	C15-C16-H16	119.8
C16-C17-C12	118.8(8)	C16-C17-H17	120.6
C12-C17-H17	120.6	C14A-C13A-C12	123.7(13)
C14A-C13A-H13A	118.2	C12-C13A-H13A	118.2
C15A-C14A-C13A	119.3(13)	C15A-C14A-C11A	119.0(10)
C13A-C14A-C11A	121.5(10)	C16A-C15A-C14A	118.2(12)
C16A-C15A-C12A	119.1(10)	C14A-C15A-C12A	122.7(10)
C15A-C16A-C17A	121.5(11)	C15A-C16A-H16A	119.3
C17A-C16A-H16A	119.3	C16A-C17A-C12	123.0(10)
C16A-C17A-H17A	118.5	C12-C17A-H17A	118.5
O4-C18-O5	121.0(3)	O4-C18-C7	125.9(3)
O5-C18-C7	113.1(3)	O5-C19-C20	106.4(3)
O5-C19-H19A	110.5	C20-C19-H19A	110.5
O5-C19-H19B	110.5	C20-C19-H19B	110.5
H19A-C19-H19B	108.6	C19-C20-H20A	109.5
C19-C20-H20B	109.5	H20A-C20-H20B	109.5
C19-C20-H20C	109.5	H20A-C20-H20C	109.5
H20B-C20-H20C	109.5		

Table 30: Torsion angles (°) for **84**.

O1-C1-C2-C12	0.2(5)	C10A-C1-C2-C12	179.9(3)
O1-C1-C2-C3	179.7(3)	C10A-C1-C2-C3	-0.6(4)
C10A-N4-C3-O2	179.7(3)	C5-N4-C3-O2	-15.9(5)
C10A-N4-C3-C2	0.0(4)	C5-N4-C3-C2	164.4(3)
C1-C2-C3-O2	-179.3(3)	C12-C2-C3-O2	0.2(5)
C1-C2-C3-N4	0.4(3)	C12-C2-C3-N4	179.9(3)
C3-N4-C5-C11	178.0(3)	C10A-N4-C5-C11	-18.4(4)

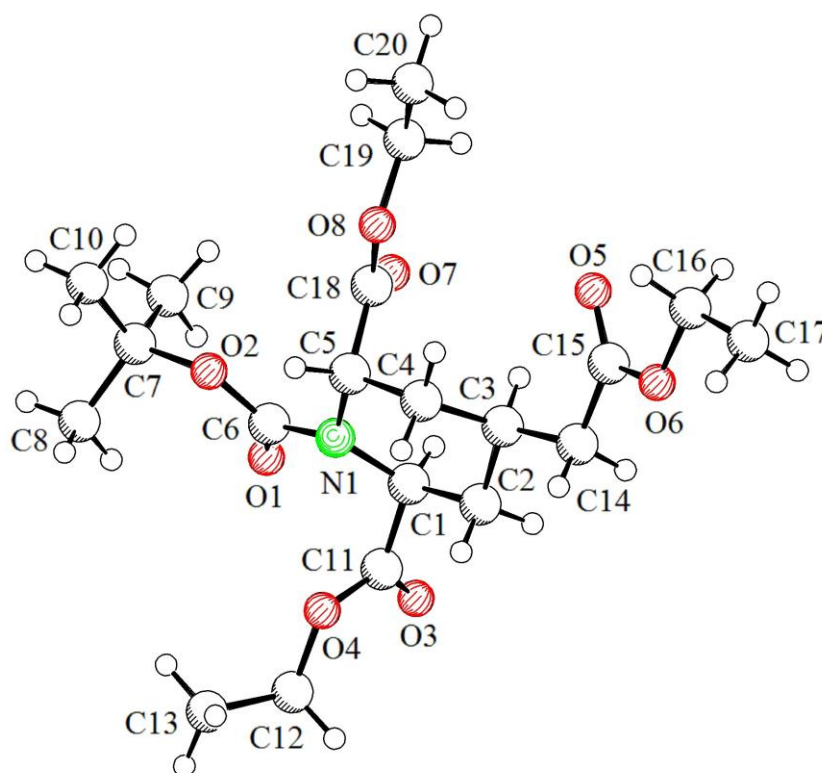
C3-N4-C5-C6	-60.9(4)	C10A-N4-C5-C6	102.7(4)
N4-C5-C6-O3	84.0(4)	C11-C5-C6-O3	-157.0(3)
N4-C5-C6-C7	-97.7(4)	C11-C5-C6-C7	21.3(4)
O3-C6-C7-C18	-3.1(5)	C5-C6-C7-C18	178.8(3)
O3-C6-C7-C8	177.3(3)	C5-C6-C7-C8	-0.9(5)
C6-C7-C8-C9	15.3(4)	C18-C7-C8-C9	-164.3(3)
C7-C8-C9-C11	-49.2(4)	C7-C8-C9-C10	73.4(4)
C8-C9-C10-C10A	-128.6(3)	C11-C9-C10-C10A	-8.2(4)
C3-N4-C10A-C1	-0.3(3)	C5-N4-C10A-C1	-166.0(3)
C3-N4-C10A-C10	123.7(3)	C5-N4-C10A-C10	-42.0(4)
O1-C1-C10A-N4	-179.7(3)	C2-C1-C10A-N4	0.6(4)
O1-C1-C10A-C10	61.4(4)	C2-C1-C10A-C10	-118.3(3)
C9-C10-C10A-N4	54.9(4)	C9-C10-C10A-C1	169.0(3)
N4-C5-C11-C9	66.1(4)	C6-C5-C11-C9	-55.3(4)
C8-C9-C11-C5	70.7(3)	C10-C9-C11-C5	-51.8(4)
C1-C2-C12-C13	11.2(12)	C3-C2-C12-C13	-168.2(12)
C1-C2-C12-C17	-180.0(7)	C3-C2-C12-C17	0.7(8)
C1-C2-C12-C13A	0.7(14)	C3-C2-C12-C13A	-178.7(13)
C1-C2-C12-C17A	-164.7(9)	C3-C2-C12-C17A	15.9(9)
C17-C12-C13-C14	17.(3)	C2-C12-C13-C14	-174.9(16)
C12-C13-C14-C15	-14.(3)	C12-C13-C14-C11	170.8(16)
C13-C14-C15-C16	6.(3)	C11-C14-C15-C16	-179.0(15)
C13-C14-C15-C12	-172.5(18)	C11-C14-C15-C12	2.(3)
C14-C15-C16-C17	-1.(2)	C12-C15-C16-C17	178.0(10)
C15-C16-C17-C12	3.1(17)	C13-C12-C17-C16	-11.4(18)
C2-C12-C17-C16	179.7(8)	C17A-C12-C13A-C14A	-17.(3)
C2-C12-C13A-C14A	175.(2)	C12-C13A-C14A-C15A	16.(4)
C12-C13A-C14A-C11A	-170.(2)	C13A-C14A-C15A-C16A	-7.(3)
C11A-C14A-C15A-C16A	178.1(15)	C13A-C14A-C15A-C12A	175.(2)
C11A-C14A-C15A-C12A	1.(3)	C14A-C15A-C16A-C17A	2.(2)
C12A-C15A-C16A-C17A	180.0(11)	C15A-C16A-C17A-C12	-5.(2)
C13A-C12-C17A-C16A	11.7(19)	C2-C12-C17A-C16A	178.0(9)
C19-O5-C18-O4	-1.7(4)	C19-O5-C18-C7	178.5(3)
C6-C7-C18-O4	4.3(5)	C8-C7-C18-O4	-176.1(3)
C6-C7-C18-O5	-175.9(3)	C8-C7-C18-O5	3.7(4)
C18-O5-C19-C20	-176.5(3)		

Table 31: Hydrogen bond distances (Å) and angles (°) for **84**.

	Donor-H	Acceptor-H	Donor-Acceptor	Angle
O1-H1...O4#1	0.925(19)	1.75(2)	2.621(3)	157.(4)
O3-H3A ^b ...O4	0.94(2)	2.04(13)	2.671(4)	122.(12)

Symmetry transformations used to generate equivalent atoms:
 #1 x-1, y, z

7.3.4 X-ray crystal structure of triester 144



SCHAKAL

A colorless plate-like specimen of $C_{20}H_{33}NO_8$, approximate dimensions 0.110 mm x 0.152 mm x 0.184 mm, was used for the X-ray crystallographic analysis. The X-ray intensity data were measured.

A total of 1460 frames were collected. The total exposure time was 19.34 hours. The frames were integrated with the Bruker SAINT software package using a wide-frame algorithm. The integration of the data using a triclinic unit cell yielded a total of 21978 reflections to a maximum θ angle of 68.60° (0.83 \AA resolution), of which 4032 were independent (average redundancy 5.451, completeness = 98.4%, $R_{\text{int}} = 3.89\%$, $R_{\text{sig}} =$

2.87%) and 3636 (90.18%) were greater than $2\sigma(F^2)$. The final cell constants of $a = 9.6207(3) \text{ \AA}$, $b = 10.1921(3) \text{ \AA}$, $c = 11.4218(4) \text{ \AA}$, $\alpha = 91.5380(10)^\circ$, $\beta = 90.4950(10)^\circ$, $\gamma = 97.6900(10)^\circ$, volume = $1109.41(6) \text{ \AA}^3$, are based upon the refinement of the XYZ-centroids of 9880 reflections above $20 \sigma(I)$ with $8.758^\circ < 2\theta < 137.0^\circ$. Data were corrected for absorption effects using the multi-scan method (SADABS). The ratio of minimum to maximum apparent transmission was 0.892. The calculated minimum and maximum transmission coefficients (based on crystal size) are 0.8670 and 0.9170.

The structure was solved and refined using the Bruker SHELXTL Software Package, using the space group P -1, with Z = 2 for the formula unit, $C_{20}H_{33}NO_8$. The final anisotropic full-matrix least-squares refinement on F^2 with 304 variables converged at $R1 = 3.54\%$, for the observed data and $wR2 = 8.55\%$ for all data. The goodness-of-fit was 1.048. The largest peak in the final difference electron density synthesis was $0.285 \text{ e}/\text{\AA}^3$ and the largest hole was $-0.318 \text{ e}/\text{\AA}^3$ with an RMS deviation of $0.65 \text{ e}/\text{\AA}^3$. On the basis of the final model, the calculated density was 1.244 g/cm^3 and $F(000)$, 448 e⁻.

Table 32: Sample and crystal data for **144**.

Identification code	DAN9602	
Chemical formula	$C_{20}H_{33}NO_8$	
Formula weight	415.47 g/mol	
Temperature	101(2) K	
Wavelength	1.54178 \AA	
Crystal size	0.110 x 0.152 x 0.184 mm	
Crystal habit	colorless plate	
Crystal system	triclinic	
Space group	P -1	
Unit cell dimensions	$a = 9.6207(3) \text{ \AA}$	$\alpha = 91.5380(10)^\circ$
	$b = 10.1921(3) \text{ \AA}$	$\beta = 90.4950(10)^\circ$
	$c = 11.4218(4) \text{ \AA}$	$\gamma = 97.6900(10)^\circ$
Volume	$1109.41(6) \text{ \AA}^3$	
Z	2	

Density (calculated)	1.244 g/cm ³
Absorption coefficient	0.798 mm ⁻¹
F(000)	448

Table 33: Data collection and structure refinement for **144**.

Theta range for data collection	4.38 to 68.60°
Index ranges	-11<=h<=11, -12<=k<=12, -13<=l<=13
Reflections collected	21978
Independent reflections	4032 [R(int) = 0.0389]
Coverage of independent reflections	98.4%
Absorption correction	multi-scan
Max. and min. transmission	0.9170 and 0.8670
Structure solution technique	direct methods
Structure solution program	SHELXL-2014/7 (Sheldrick, 2014)
Refinement method	Full-matrix least-squares on F ²
Refinement program	SHELXL-2014/7 (Sheldrick, 2014)
Function minimized	$\Sigma w(F_o^2 - F_c^2)^2$
Data / restraints / parameters	4032 / 78 / 304
Goodness-of-fit on F²	1.048
Final R indices	3636 data; l>2σ(l) R1 = 0.0354, wR2 = 0.0828 all data R1 = 0.0395, wR2 = 0.0855
Weighting scheme	w=1/[σ ² (F _o ²)+(0.0262P) ² +0.4918P]where P=(F _o ² +2F _c ²)/3
Largest diff. peak and hole	0.285 and -0.318 eÅ ⁻³
R.M.S. deviation from mean	0.65 eÅ ⁻³

Table 34: Bond lengths (Å) for **144**.

N1-C6	1.3771(15)	N1-C5	1.4654(14)
N1-C1	1.4749(15)	O1-C6	1.2124(14)
O2-C6	1.3447(15)	O2-C7	1.4860(14)
O3-C11	1.2043(15)	O4-C11	1.3391(15)
O4-C12	1.4557(14)	O5-C15	1.2062(16)
O6-C15	1.3359(15)	O6-C16	1.4680(17)
O7-C18	1.2007(16)	C1-C11	1.5218(16)
C1-C2	1.5342(16)	C1-H1	1.0
C2-C3	1.5221(16)	C2-H2A	0.99
C2-H2B	0.99	C3-C14	1.5237(16)
C3-C4	1.5249(17)	C3-H3	1.0
C4-C5	1.5312(16)	C4-H4A	0.99
C4-H4B	0.99	C5-C18	1.5280(16)
C5-H5	1.0	C7-C9	1.516(2)
C7-C10	1.5186(19)	C7-C8	1.5187(18)
C8-H8A	0.98	C8-H8B	0.98
C8-H8C	0.98	C9-H9A	0.98
C9-H9B	0.98	C9-H9C	0.98
C10-H10A	0.98	C10-H10B	0.98
C10-H10C	0.98	C12-C13A	1.459(13)
C12-C13	1.514(5)	C12-H12A	0.99
C12-H12B	0.99	C12-H12C	0.99
C12-H12D	0.99	C13-H13A	0.98
C13-H13B	0.98	C13-H13C	0.98
C13A-H13D	0.98	C13A-H13E	0.98
C13A-H13F	0.98	C14-C15	1.5132(18)
C14-H14A	0.99	C14-H14B	0.99
C16-C17	1.489(2)	C16-H16A	0.99
C16-H16B	0.99	C17-H17A	0.98
C17-H17B	0.98	C17-H17C	0.98
C18-O8	1.310(4)	C18-O8A	1.420(7)
O8-C19	1.455(4)	C19-C20	1.490(4)
C19-H19A	0.99	C19-H19B	0.99
C20-H20A	0.98	C20-H20B	0.98

C20-H20C	0.98	O8A-C19A	1.465(8)
C19A-C20A	1.488(6)	C19A-H19C	0.99
C19A-H19D	0.99	C20A-H20D	0.98
C20A-H20E	0.98	C20A-H20F	0.98

Table 35: Bond angles (°) for **144**.

C6-N1-C5	118.25(9)	C6-N1-C1	112.82(9)
C5-N1-C1	120.36(9)	C6-O2-C7	119.54(9)
C11-O4-C12	115.34(9)	C15-O6-C16	115.52(11)
N1-C1-C11	112.00(10)	N1-C1-C2	112.97(9)
C11-C1-C2	106.94(10)	N1-C1-H1	108.3
C11-C1-H1	108.3	C2-C1-H1	108.3
C3-C2-C1	111.69(10)	C3-C2-H2A	109.3
C1-C2-H2A	109.3	C3-C2-H2B	109.3
C1-C2-H2B	109.3	H2A-C2-H2B	107.9
C2-C3-C14	112.10(10)	C2-C3-C4	107.14(9)
C14-C3-C4	111.51(10)	C2-C3-H3	108.7
C14-C3-H3	108.7	C4-C3-H3	108.7
C3-C4-C5	111.04(9)	C3-C4-H4A	109.4
C5-C4-H4A	109.4	C3-C4-H4B	109.4
C5-C4-H4B	109.4	H4A-C4-H4B	108.0
N1-C5-C18	110.94(9)	N1-C5-C4	112.21(9)
C18-C5-C4	109.13(9)	N1-C5-H5	108.1
C18-C5-H5	108.1	C4-C5-H5	108.1
O1-C6-O2	125.55(11)	O1-C6-N1	123.05(11)
O2-C6-N1	111.38(9)	O2-C7-C9	109.86(11)
O2-C7-C10	101.77(9)	C9-C7-C10	110.89(12)
O2-C7-C8	109.96(10)	C9-C7-C8	113.16(11)
C10-C7-C8	110.61(12)	C7-C8-H8A	109.5
C7-C8-H8B	109.5	H8A-C8-H8B	109.5
C7-C8-H8C	109.5	H8A-C8-H8C	109.5
H8B-C8-H8C	109.5	C7-C9-H9A	109.5
C7-C9-H9B	109.5	H9A-C9-H9B	109.5
C7-C9-H9C	109.5	H9A-C9-H9C	109.5
H9B-C9-H9C	109.5	C7-C10-H10A	109.5

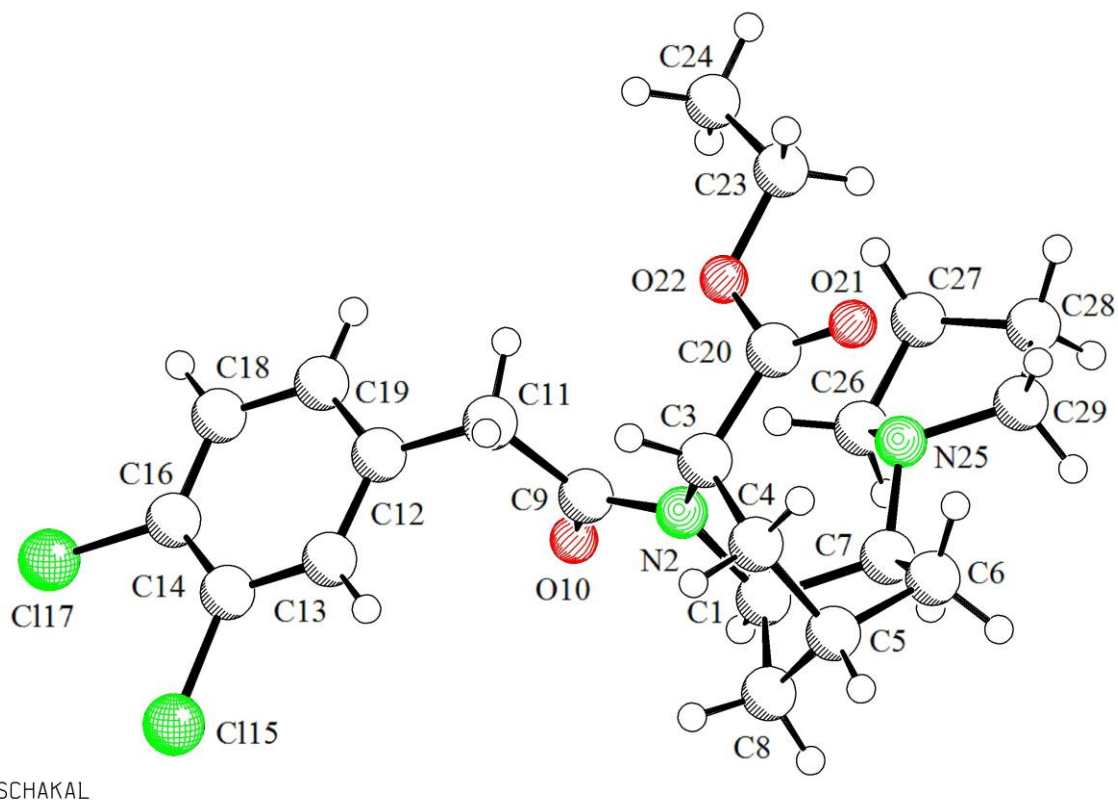
C7-C10-H10B	109.5	H10A-C10-H10B	109.5
C7-C10-H10C	109.5	H10A-C10-H10C	109.5
H10B-C10-H10C	109.5	O3-C11-O4	124.48(11)
O3-C11-C1	122.62(11)	O4-C11-C1	112.63(10)
O4-C12-C13A	110.6(8)	O4-C12-C13	106.4(3)
O4-C12-H12A	110.4	C13-C12-H12A	110.4
O4-C12-H12B	110.4	C13-C12-H12B	110.4
H12A-C12-H12B	108.6	O4-C12-H12C	109.5
C13A-C12-H12C	109.5	O4-C12-H12D	109.5
C13A-C12-H12D	109.5	H12C-C12-H12D	108.1
C12-C13-H13A	109.5	C12-C13-H13B	109.5
H13A-C13-H13B	109.5	C12-C13-H13C	109.5
H13A-C13-H13C	109.5	H13B-C13-H13C	109.5
C12-C13A-H13D	109.5	C12-C13A-H13E	109.5
H13D-C13A-H13E	109.5	C12-C13A-H13F	109.5
H13D-C13A-H13F	109.5	H13E-C13A-H13F	109.5
C15-C14-C3	112.28(10)	C15-C14-H14A	109.1
C3-C14-H14A	109.1	C15-C14-H14B	109.1
C3-C14-H14B	109.1	H14A-C14-H14B	107.9
O5-C15-O6	124.09(12)	O5-C15-C14	124.59(11)
O6-C15-C14	111.32(11)	O6-C16-C17	108.18(14)
O6-C16-H16A	110.1	C17-C16-H16A	110.1
O6-C16-H16B	110.1	C17-C16-H16B	110.1
H16A-C16-H16B	108.4	C16-C17-H17A	109.5
C16-C17-H17B	109.5	H17A-C17-H17B	109.5
C16-C17-H17C	109.5	H17A-C17-H17C	109.5
H17B-C17-H17C	109.5	O7-C18-O8	121.28(19)
O7-C18-O8A	130.2(3)	O7-C18-C5	125.37(11)
O8-C18-C5	112.88(19)	O8A-C18-C5	103.5(3)
C18-O8-C19	117.7(3)	O8-C19-C20	107.9(3)
O8-C19-H19A	110.1	C20-C19-H19A	110.1
O8-C19-H19B	110.1	C20-C19-H19B	110.1
H19A-C19-H19B	108.4	C19-C20-H20A	109.5
C19-C20-H20B	109.5	H20A-C20-H20B	109.5
C19-C20-H20C	109.5	H20A-C20-H20C	109.5
H20B-C20-H20C	109.5	C18-O8A-C19A	114.5(5)

O8A-C19A-C20A	110.8(4)	O8A-C19A-H19C	109.5
C20A-C19A-H19C	109.5	O8A-C19A-H19D	109.5
C20A-C19A-H19D	109.5	H19C-C19A-H19D	108.1
C19A-C20A-H20D	109.5	C19A-C20A-H20E	109.5
H20D-C20A-H20E	109.5	C19A-C20A-H20F	109.5
H20D-C20A-H20F	109.5	H20E-C20A-H20F	109.5

Table 36: Torsion angles (°) for **144**.

C6-N1-C1-C11	-55.69(13)	C5-N1-C1-C11	157.01(10)
C6-N1-C1-C2	-176.52(10)	C5-N1-C1-C2	36.18(14)
N1-C1-C2-C3	-47.09(13)	C11-C1-C2-C3	-170.75(10)
C1-C2-C3-C14	-176.56(10)	C1-C2-C3-C4	60.81(12)
C2-C3-C4-C5	-62.90(12)	C14-C3-C4-C5	174.10(9)
C6-N1-C5-C18	-61.33(13)	C1-N1-C5-C18	84.25(12)
C6-N1-C5-C4	176.31(10)	C1-N1-C5-C4	-38.11(14)
C3-C4-C5-N1	51.06(12)	C3-C4-C5-C18	-72.32(12)
C7-O2-C6-O1	-5.42(18)	C7-O2-C6-N1	176.10(10)
C5-N1-C6-O1	158.47(11)	C1-N1-C6-O1	10.42(16)
C5-N1-C6-O2	-23.00(14)	C1-N1-C6-O2	-171.05(9)
C6-O2-C7-C9	-59.79(14)	C6-O2-C7-C10	-177.34(11)
C6-O2-C7-C8	65.39(14)	C12-O4-C11-O3	-6.75(17)
C12-O4-C11-C1	179.08(9)	N1-C1-C11-O3	146.87(12)
C2-C1-C11-O3	-88.87(14)	N1-C1-C11-O4	-38.83(13)
C2-C1-C11-O4	85.43(12)	C11-O4-C12-C13A	-178.9(11)
C11-O4-C12-C13	-160.4(4)	C2-C3-C14-C15	171.23(10)
C4-C3-C14-C15	-68.64(13)	C16-O6-C15-O5	1.46(18)
C16-O6-C15-C14	-179.40(11)	C3-C14-C15-O5	-17.24(18)
C3-C14-C15-O6	163.62(10)	C15-O6-C16-C17	-175.43(12)
N1-C5-C18-O7	-13.65(17)	C4-C5-C18-O7	110.48(14)
N1-C5-C18-O8	174.19(19)	C4-C5-C18-O8	-61.7(2)
N1-C5-C18-O8A	156.3(3)	C4-C5-C18-O8A	-79.6(3)
O7-C18-O8-C19	2.9(4)	C5-C18-O8-C19	175.4(2)
C18-O8-C19-C20	-175.8(3)	O7-C18-O8A-C19A	-12.7(7)
C5-C18-O8A-C19A	178.0(4)	C18-O8A-C19A-C20A	-80.8(7)

7.3.5 X-ray crystal structure of bicyclic amine 143a



A colorless needle-like specimen of $C_{22}H_{28}Cl_2N_2O_3$, approximate dimensions 0.040 mm x 0.048 mm x 0.335 mm, was used for the X-ray crystallographic analysis. The X-ray intensity data were measured on a Bruker D8 Venture Bruker D8 Venture Photon III Diffractometer system equipped with a micro focus tube MoK α (MoK α , $\lambda = 0.71073 \text{ \AA}$) and a MX mirror monochromator.

A total of 250 frames were collected. The total exposure time was 2.43 hours. The frames were integrated with the Bruker SAINT software package using a narrow-frame algorithm. The integration of the data using an orthorhombic unit cell yielded a total of 25020 reflections to a maximum θ angle of 25.07° (0.84 \AA resolution), of which 3831 were independent (average redundancy 6.531, completeness = 99.7%, $R_{\text{int}} = 15.60\%$, $R_{\text{sig}} = 12.09\%$) and 2283 (59.59%) were greater than $2\sigma(F^2)$. The final cell constants of $a = 13.9618(14) \text{ \AA}$, $b = 8.2888(12) \text{ \AA}$, $c = 37.422(5) \text{ \AA}$, volume = $4330.7(10) \text{ \AA}^3$, are based upon the refinement of the XYZ-centroids of 1154 reflections above $20 \sigma(I)$ with $5.241^\circ < 2\theta < 44.95^\circ$. Data were corrected for absorption effects using the multi-scan method (SADABS). The ratio of minimum to maximum apparent transmission was 0.792. The calculated minimum and maximum transmission coefficients (based on crystal size) are 0.8990 and 0.9870.

The structure was solved and refined using the Bruker SHELXTL Software Package, using the space group Pbc_a , with $Z = 8$ for the formula unit, $C_{22}H_{28}Cl_2N_2O_3$. The final anisotropic full-matrix least-squares refinement on F^2 with 336 variables converged at $R1 = 6.05\%$, for the observed data and $wR2 = 16.70\%$ for all data. The goodness-of-fit was 1.033. The largest peak in the final difference electron density synthesis was $0.266 \text{ e}^-/\text{\AA}^3$ and the largest hole was $-0.280 \text{ e}^-/\text{\AA}^3$ with an RMS deviation of $0.066 \text{ e}^-/\text{\AA}^3$. On the basis of the final model, the calculated density was 1.348 g/cm^3 and $F(000)$, 1856 e^- .

Table 37: Sample and crystal data for **143a**.

Identification code	dan10043	
Chemical formula	$C_{22}H_{28}Cl_2N_2O_3$	
Formula weight	439.36 g/mol	
Temperature	101(2) K	
Wavelength	0.71073 \AA	
Crystal size	0.040 x 0.048 x 0.335 mm	
Crystal habit	colorless needle	
Crystal system	orthorhombic	
Space group	Pbc_a	
Unit cell dimensions	$a = 13.9618(14) \text{ \AA}$	$\alpha = 90^\circ$
	$b = 8.2888(12) \text{ \AA}$	$\beta = 90^\circ$
	$c = 37.422(5) \text{ \AA}$	$\gamma = 90^\circ$
Volume	$4330.7(10) \text{ \AA}^3$	
Z	8	
Density (calculated)	1.348 g/cm^3	
Absorption coefficient	0.326 mm^{-1}	
F(000)	1856	

Table 38: Data collection and structure refinement for **143a**.

Diffractometer	Bruker D8 Venture Bruker D8 Venture Photon III Diffractometer	
Radiation source	micro focus tube MoK α (MoK α , $\lambda = 0.71073 \text{ \AA}$)	
Theta range for data collection	2.62 to 25.07°	
Index ranges	-16 $\leq h \leq 16$, -9 $\leq k \leq 9$, -44 $\leq l \leq 44$	
Reflections collected	25020	
Independent reflections	3831 [R(int) = 0.1560]	
Coverage of independent reflections	99.7%	
Absorption correction	multi-scan	
Max. and min. transmission	0.9870 and 0.8990	
Structure solution technique	direct methods	
Structure solution program	SHELXT 2018/2 (Sheldrick, 2018)	
Refinement method	Full-matrix least-squares on F ²	
Refinement program	SHELXL-2018/3 (Sheldrick, 2018)	
Function minimized	$\Sigma w(F_o^2 - F_c^2)^2$	
Data / restraints / parameters	3831 / 231 / 336	
Goodness-of-fit on F²	1.033	
D/smax	0.001	
Final R indices	2283 data; I > 2 σ (I)	R1 = 0.0605, wR2 = 0.1366
	all data	R1 = 0.1121, wR2 = 0.1670
Weighting scheme	w=1/[$\sigma^2(F_o^2)+(0.0294P)^2+3.0023P$]where P=(F _o ² +2F _c ²)/3	
Largest diff. peak and hole	0.266 and -0.280 e \AA^{-3}	
R.M.S. deviation from mean	0.066 e \AA^{-3}	

Table 39: Bond lengths (Å) for **143a**.

C1-N2	1.475(4)	C1-C8	1.533(5)
C1-C7	1.541(5)	C1-H1	1.0
C3-N2	1.465(4)	C3-C4	1.536(5)
C3-C20	1.537(5)	C3-H3	1.0
C4-C5	1.525(6)	C4-H4A	0.99
C4-H4B	0.99	C5-C8	1.523(5)
C5-C6	1.542(5)	C5-H5	1.0
C6-C7	1.546(5)	C6-H6A	0.99
C6-H6B	0.99	C7-N25	1.446(5)
C7-H7	1.0	C8-H8A	0.99
C8-H8B	0.99	C9-O10	1.232(4)
C9-N2	1.361(4)	C9-C11	1.528(5)
C11-C12A	1.416(14)	C11-C12	1.497(5)
C11-H11A	0.99	C11-H11B	0.99
C11-H11C	0.99	C11-H11D	0.99
C12-C13	1.395(6)	C12-C19	1.396(6)
C13-C14	1.387(6)	C13-H13	0.95
C14-C16	1.391(6)	C14-Cl15	1.724(6)
C16-C18	1.373(7)	C16-Cl17	1.736(5)
C18-C19	1.390(6)	C18-H18	0.95
C19-H19	0.95	C12A-C19A	1.40(2)
C12A-C13A	1.405(15)	C13A-C14A	1.397(14)
C13A-H13A	0.95	C14A-C16A	1.391(14)
C14A-Cl15A	1.72(2)	C16A-C18A	1.397(14)
C16A-Cl17A	1.731(18)	C18A-C19A	1.391(15)
C18A-H18A	0.95	C19A-H19A	0.95
C20-O21	1.211(4)	C20-O22	1.345(5)
C23-O22	1.461(4)	C23-C24	1.488(6)
C23-H23A	0.99	C23-H23B	0.99
C24-H24A	0.98	C24-H24B	0.98
C24-H24C	0.98	C26-N25	1.478(5)
C26-C27	1.513(6)	C26-H26A	0.99
C26-H26B	0.99	C27-C28	1.520(7)
C27-H27A	0.99	C27-H27B	0.99

C28-C29	1.498(6)	C28-H28A	0.99
C28-H28B	0.99	C29-N25	1.485(5)
C29-H29A	0.99	C29-H29B	0.99

Table 40: Bond angles (°) for **143a**.

N2-C1-C8	108.0(3)	N2-C1-C7	114.0(3)
C8-C1-C7	101.9(3)	N2-C1-H1	110.8
C8-C1-H1	110.8	C7-C1-H1	110.8
N2-C3-C4	113.1(3)	N2-C3-C20	112.2(3)
C4-C3-C20	112.9(3)	N2-C3-H3	106.0
C4-C3-H3	106.0	C20-C3-H3	106.0
C5-C4-C3	113.9(3)	C5-C4-H4A	108.8
C3-C4-H4A	108.8	C5-C4-H4B	108.8
C3-C4-H4B	108.8	H4A-C4-H4B	107.7
C8-C5-C4	108.8(3)	C8-C5-C6	102.4(3)
C4-C5-C6	111.5(3)	C8-C5-H5	111.3
C4-C5-H5	111.3	C6-C5-H5	111.3
C5-C6-C7	105.2(3)	C5-C6-H6A	110.7
C7-C6-H6A	110.7	C5-C6-H6B	110.7
C7-C6-H6B	110.7	H6A-C6-H6B	108.8
N25-C7-C1	114.1(3)	N25-C7-C6	114.5(3)
C1-C7-C6	105.0(3)	N25-C7-H7	107.6
C1-C7-H7	107.6	C6-C7-H7	107.6
C5-C8-C1	100.4(3)	C5-C8-H8A	111.7
C1-C8-H8A	111.7	C5-C8-H8B	111.7
C1-C8-H8B	111.7	H8A-C8-H8B	109.5
O10-C9-N2	121.1(3)	O10-C9-C11	119.3(3)
N2-C9-C11	119.6(3)	C12A-C11-C9	115.(5)
C12-C11-C9	110.4(6)	C12-C11-H11A	109.6
C9-C11-H11A	109.6	C12-C11-H11B	109.6
C9-C11-H11B	109.6	H11A-C11-H11B	108.1
C12A-C11-H11C	108.5	C9-C11-H11C	108.5
C12A-C11-H11D	108.5	C9-C11-H11D	108.5
H11C-C11-H11D	107.5	C13-C12-C19	118.0(4)
C13-C12-C11	120.0(4)	C19-C12-C11	122.0(5)

C14-C13-C12	121.3(5)	C14-C13-H13	119.4
C12-C13-H13	119.4	C13-C14-C16	119.4(5)
C13-C14-C15	118.6(4)	C16-C14-C15	121.9(4)
C18-C16-C14	120.3(4)	C18-C16-C17	118.4(4)
C14-C16-C17	121.3(4)	C16-C18-C19	119.9(5)
C16-C18-H18	120.0	C19-C18-H18	120.0
C18-C19-C12	121.0(5)	C18-C19-H19	119.5
C12-C19-H19	119.5	C19A-C12A-C13A	118.4(19)
C19A-C12A-C11	118.(2)	C13A-C12A-C11	123.(2)
C14A-C13A-C12A	120.(2)	C14A-C13A-H13A	120.1
C12A-C13A-H13A	120.1	C16A-C14A-C13A	121.(2)
C16A-C14A-C15A	121.(2)	C13A-C14A-C15A	118.(2)
C14A-C16A-C18A	120.4(19)	C14A-C16A-C17A	125.(2)
C18A-C16A-C17A	114.(2)	C19A-C18A-C16A	118.(2)
C19A-C18A-H18A	120.9	C16A-C18A-H18A	120.9
C18A-C19A-C12A	122.(2)	C18A-C19A-H19A	119.0
C12A-C19A-H19A	119.0	O21-C20-O22	124.0(4)
O21-C20-C3	125.0(4)	O22-C20-C3	110.4(3)
O22-C23-C24	106.9(4)	O22-C23-H23A	110.3
C24-C23-H23A	110.3	O22-C23-H23B	110.3
C24-C23-H23B	110.3	H23A-C23-H23B	108.6
C23-C24-H24A	109.5	C23-C24-H24B	109.5
H24A-C24-H24B	109.5	C23-C24-H24C	109.5
H24A-C24-H24C	109.5	H24B-C24-H24C	109.5
N25-C26-C27	103.5(3)	N25-C26-H26A	111.1
C27-C26-H26A	111.1	N25-C26-H26B	111.1
C27-C26-H26B	111.1	H26A-C26-H26B	109.0
C26-C27-C28	102.9(4)	C26-C27-H27A	111.2
C28-C27-H27A	111.2	C26-C27-H27B	111.2
C28-C27-H27B	111.2	H27A-C27-H27B	109.1
C29-C28-C27	107.1(4)	C29-C28-H28A	110.3
C27-C28-H28A	110.3	C29-C28-H28B	110.3
C27-C28-H28B	110.3	H28A-C28-H28B	108.6
N25-C29-C28	105.8(4)	N25-C29-H29A	110.6
C28-C29-H29A	110.6	N25-C29-H29B	110.6
C28-C29-H29B	110.6	H29A-C29-H29B	108.7

C9-N2-C3	124.8(3)	C9-N2-C1	118.1(3)
C3-N2-C1	116.7(3)	C7-N25-C26	112.0(3)
C7-N25-C29	112.8(3)	C26-N25-C29	106.0(3)
C20-O22-C23	114.2(3)		

Table 41: Torsion angles (°) for **143a**.

N2-C3-C4-C5	33.5(4)	C20-C3-C4-C5	-95.2(4)
C3-C4-C5-C8	-53.8(4)	C3-C4-C5-C6	58.4(4)
C8-C5-C6-C7	28.3(4)	C4-C5-C6-C7	-87.9(4)
N2-C1-C7-N25	-40.3(4)	C8-C1-C7-N25	-156.5(3)
N2-C1-C7-C6	85.9(4)	C8-C1-C7-C6	-30.3(4)
C5-C6-C7-N25	127.3(3)	C5-C6-C7-C1	1.4(4)
C4-C5-C8-C1	70.9(4)	C6-C5-C8-C1	-47.2(4)
N2-C1-C8-C5	-72.4(3)	C7-C1-C8-C5	48.0(4)
O10-C9-C11-C12A	21.(3)	N2-C9-C11-C12A	-158.(3)
O10-C9-C11-C12	24.2(5)	N2-C9-C11-C12	-155.2(4)
C9-C11-C12-C13	69.8(9)	C9-C11-C12-C19	-110.3(8)
C19-C12-C13-C14	1.2(8)	C11-C12-C13-C14	-178.8(11)
C12-C13-C14-C16	0.0(9)	C12-C13-C14-CI15	178.1(10)
C13-C14-C16-C18	-2.0(10)	CI15-C14-C16-C18	179.9(12)
C13-C14-C16-CI17	177.0(11)	CI15-C14-C16-CI17	-1.0(12)
C14-C16-C18-C19	2.7(10)	CI17-C16-C18-C19	-176.3(11)
C16-C18-C19-C12	-1.4(8)	C13-C12-C19-C18	-0.6(7)
C11-C12-C19-C18	179.5(12)	C9-C11-C12A-C19A	71.(8)
C9-C11-C12A-C13A	-104.(7)	C19A-C12A-C13A-C14A	-3.(3)
C11-C12A-C13A-C14A	172.(11)	C12A-C13A-C14A-C16A	1.(3)
C12A-C13A-C14A-CI5A	173.(9)	C13A-C14A-C16A-C18A	-4.(6)
CI5A-C14A-C16A-C18A	-175.(9)	C13A-C14A-C16A-CI7A	165.(10)
CI5A-C14A-C16A-CI7A	-7.(11)	C14A-C16A-C18A-C19A	8.(8)
CI7A-C16A-C18A-C19A	-161.(10)	C16A-C18A-C19A-C12A	-11.(7)
C13A-C12A-C19A-C18A	8.(6)	C11-C12A-C19A-C18A	-167.(11)
N2-C3-C20-O21	-136.7(4)	C4-C3-C20-O21	-7.5(5)
N2-C3-C20-O22	51.9(4)	C4-C3-C20-O22	-178.8(3)
N25-C26-C27-C28	36.5(5)	C26-C27-C28-C29	-22.6(5)
C27-C28-C29-N25	0.3(5)	O10-C9-N2-C3	177.5(3)

C11-C9-N2-C3	-3.0(5)	O10-C9-N2-C1	-9.8(5)
C11-C9-N2-C1	169.7(3)	C4-C3-N2-C9	136.5(3)
C20-C3-N2-C9	-94.4(4)	C4-C3-N2-C1	-36.3(4)
C20-C3-N2-C1	92.9(4)	C8-C1-N2-C9	-115.2(3)
C7-C1-N2-C9	132.2(3)	C8-C1-N2-C3	58.0(4)
C7-C1-N2-C3	-54.5(4)	C1-C7-N25-C26	-61.9(4)
C6-C7-N25-C26	177.1(3)	C1-C7-N25-C29	178.6(3)
C6-C7-N25-C29	57.6(4)	C27-C26-N25-C7	-160.9(3)
C27-C26-N25-C29	-37.4(4)	C28-C29-N25-C7	145.9(4)
C28-C29-N25-C26	23.0(5)	O21-C20-O22-C23	6.3(6)
C3-C20-O22-C23	177.8(3)	C24-C23-O22-C20	-177.7(4)

7.4 Receptor binding studies

7.4.1 Materials

Guinea pig brains, rat brains and rat livers were commercially available (Harlan-Winkelmann, Borchon, Germany). Homogenizers: Elvehjem Potter (B. Braun Biotech International, Melsungen, Germany) and Soniprep[®] 150 (MSE, London, UK). Centrifuges: Cooling centrifuge Eppendorf 5424R (Eppendorf, Hamburg, Germany) and High-speed cooling centrifuge model Sorvall[®] RC-5C plus (Thermo Fisher Scientific, Langenselbold, Germany). Multiplates: standard 96 well multiplates (Diagonal, Münster, Germany). Shaker: self-made device with adjustable temperature and tumbling speed (scientific workshop of the institute). Harvester: MicroBeta[®] FilterMate 96 Harvester. Filter: Printed Filtermat Typ A and B. Scintillator: Meltilex[®] (Typ A or B) solid state scintillator. Scintillation analyzer: MicroBeta[®] Trilux (all Perkin Elmers LAS, Rodgau-Jügesheim, Germany).

7.4.2 Preparation of membrane homogenates from guinea pig

5 guinea pig brains were homogenized with the potter (500-800 rpm, 10 up and down strokes) in 6 volumes of cold 0.32 M sucrose. The suspension was centrifuged at 1,200 × g for 10 min at 4 °C. The supernatant was separated and centrifuged at 23,500 × g for 20 min at 4 °C. The pellet was resuspended in 5-6 volumes of buffer (50 mM TRIS, pH 7.4) and centrifuged again at 23,500 × g (20 min, 4 °C). This procedure was repeated twice. The final pellet was resuspended in 5-6 volumes of buffer and frozen (-80 °C) in 1.5 mL portions containing about 1.5 mg protein/mL.

7.4.3 Preparation of membrane homogenates from rat brain

5 rat brains (species: Sprague Dawley rats) were homogenized with the potter (500-800 rpm, 10 up and down strokes) in 6 volumes of cold 0.32 M sucrose. The suspension was centrifuged at 1,200 × g for 10 min at 4 °C. The supernatant was separated and centrifuged at 23,500 × g for 20 min at 4 °C. The pellet was resuspended in 5-6 volumes of buffer (50 mM TRIS, pH 7.4) and centrifuged again at 23,500 × g (20 min, 4 °C). This procedure was repeated twice. The final pellet was resuspended in 5-6 volumes of buffer and frozen (-80 °C) in 1.5 mL portions containing about 1.5 mg protein/mL.

7.4.4 Preparation of membrane homogenates from rat liver

Two rat livers were cut into small pieces and homogenized with the potter (500-800 rpm, 10 up and down strokes) in 6 volumes of cold 0.32 M sucrose. The suspension was centrifuged at $1,200 \times g$ for 10 min at 4 °C. The supernatant was separated and centrifuged at $31,000 \times g$ for 20 min at 4 °C. The pellet was resuspended in 5-6 volumes of buffer (50 mM TRIS, pH 8.0) and incubated at r.t. for 30 min. After the incubation, the suspension was centrifuged again at $31,000 \times g$ for 20 min at 4 °C. The final pellet was resuspended in 5-6 volumes of buffer and frozen (-80 °C) in 1.5 mL portions containing about 2 mg protein/mL.

7.4.5 Protein determination

The protein concentration was determined by the method of Bradford,^[lit] modified by Stoscheck.^[lit] The Bradford solution was prepared by dissolving 5 mg Coomassie Brilliant Blue G 250 in 2.5 mL of EtOH (95%, v/v). 10 mL deionized H₂O and 5 mL phosphoric acid (85%, m/v) were added to this solution, the mixture was stirred and filled to a total volume of 50 mL with deionized H₂O. The calibration was carried out using bovine serum albumin as a standard in 9 concentrations (0.1, 0.2, 0.4, 0.6, 0.8, 1.0, 1.5, 2.0 and 4.0 mg/mL). In a 96 well standard multiplate, 10 µL of the calibration solution or 10 µL of the membrane receptor preparation were mixed with 190 µL of the Bradford solution, respectively. After 5 min, the UV absorption of the protein-dye complex at $\lambda = 595 \text{ nm}$ was measured with a plate reader (Tecan Genios®, Tecan, Crailsheim, Germany).

7.4.6 General procedures for the binding assays

The test compound solutions were prepared by dissolving approximately 10 µmol (usually 2 - 4 mg) of test compound in DMSO so that a 10 nM stock solution was obtained. To obtain the required test solutions for the assay, the DMSO stock solution was diluted with the respective assay buffer. The filtermats were presoaked in 0.5% aqueous polyethylenimine solution for 2 h at r.t. before use. All binding experiments were carried out in duplicates in the 96 well multiplates. The concentrations given are the final concentration in the assay. Generally, the assays were performed by addition of 50 µL of the respective assay buffer, 50 µL of test compound solution in various concentrations (10^{-5} , 10^{-6} , 10^{-7} , 10^{-8} , 10^{-9} and 10^{-10} mol/L), 50 µL of the corresponding radioligand solution and 50 µL of the respective receptor preparation into each well of

the multiplate (total volume 100 μ L). The receptor preparation was always added at last. During the incubation, the multiplates were shaken at a speed of 500 - 600 rpm at the specified temperature. Unless otherwise noted, the assays were terminated after 120 min by rapid filtration using the harvester. During the filtration, each well was washed five times with 300 μ L of H₂O. Subsequently, the filtermats were dried at 95 °C. The solid scintillator was melted on the dried filtermats at a temperature of 95 °C for 5 min. After solidifying of the scintillator at r.t., the trapped radioactivity in the filtermats was measured with the scintillation analyzer. Each position on the filtermat corresponding to one well of the multiplate was measured for 5 min with the [³H]-counting protocol. The overall counting efficiency was 20%. The *IC*₅₀ values were calculated with the program GraphPad Prism[®] 3.0 (GraphPad Software, San Diego, CA, USA) by non-linear regression analysis. Subsequently, the *IC*₅₀ values were transformed into *K*_i values using the equation of Cheng and Prusoff.¹³⁴ The *K*_i values are given as mean value \pm SEM from three independent experiments.

7.4.7 Performance of the binding assays

KOR binding assay

The assay was performed with the radioligand [³H]U-69,593 (55 Ci/mmol, BIOTREND). The thawed guinea pig brain membrane preparation (about 100 μ g of the protein) was incubated with various concentrations of test compounds, 1 nM [³H]U-69,593, and TRIS-MgCl₂-buffer (50 mM TRIS, 8 mM MgCl₂, pH 7.4) at 37 °C. The non-specific binding was determined with 10 μ M unlabeled U-69,593. The *K*_d value of U-69,593 is 0.69 nM.^{52,147,148}

MOR binding assay

The assay was performed with the radioligand [³H]DAMGO (51 Ci/mmol, Perkin Elmer). The thawed guinea pig brain membrane preparation (about 100 μ g of the protein) was incubated with various concentrations of test compounds, 3 nM [³H]DAMGO, and TRIS-MgCl₂-buffer (50 mM TRIS, 8 mM MgCl₂, pH 7.4) at 37 °C. The non-specific binding was determined with 10 μ M unlabeled U-69,593. The *K*_d value of DAMGO is 0.57 nM.^{52,147,148}

DOR binding assay

The assay was performed with the radioligand [³H]DPDPE (69 Ci/mmol, BIOTREND). The thawed guinea pig brain membrane preparation (about 75 μ g of the protein) was

incubated with various concentrations of test compounds, 3 nM [³H]DPDPE, and TRIS-MgCl₂-buffer (50 mM TRIS, 8 mM MgCl₂, pH 7.4) supplemented with SIGMAFAST[®] protease inhibitor mix (Sigma Aldrich Biochemicals, Hamburg, Germany; 1 tablet dissolved in 100 mL of buffer) at 37 °C. The non-specific binding was determined with 10 μM unlabeled morphine. The K_d value of DPDPE is 0.65 nM.^{52,147,148}

σ₁ receptor binding assay

The assay was performed with the radioligand [³H]-(+)-pentazocine (22.0 Ci/mmol, Perkin Elmer). The thawed guinea pig brain membrane preparation (about 100 μg of the protein) was incubated with various concentrations of test compounds, 2 nM [³H]-(+)-pentazocine, and TRIS buffer (50 mM, pH 7.4) at 37 °C. The non-specific binding was determined with 10 μM unlabeled (+)-pentazocine. The K_d value of (+)-pentazocine is 2.9 nM.¹⁴⁰

σ₂ receptor binding assay

The assays were performed with the radioligand [³H]di-*o*-tolyguanidine (specific activity 50 Ci/mmol, ARC, St. Louis, MO, USA). The thawed rat liver membrane preparation (about 100 μg of the protein) was incubated with various concentrations of test compounds, 3 nM [³H]di-*o*-tolyguanidine and buffer containing (+)-pentazocine (500 nM (+)-pentazocine in TRIS buffer (50 mM TRIS, pH 8.0)) at r.t. The non-specific binding was determined with 10 μM unlabeled di-*o*-tolyguanidine. The K_d value of di-*o*-tolyguanidine is 17.9 nM.¹⁴¹

8. Appendices

8.1 List of abbreviations

\emptyset	diameter
$[\alpha]_{20}^D$	specific rotation [$\text{deg} \cdot \text{mL} \cdot \text{dm}^{-1} \cdot \text{g}^{-1}$]
δ	chemical shift
$\tilde{\nu}$	wave number
abs.	absolute
aliph	aliphatic
APCI	atmospheric pressure chemical ionization
aq	wässrig
arom	aromatic
Asp	aspartate
9-BBN	9-Borabicyclo[3.3.1]nonane
Boc	<i>tert</i> -butoxycarbonyl
calcd.	calculated
cAMP	cyclic adenosine monophosphate
CDCl_3	deuterated chloroform
CNS	central nervous system
COSY	$^1\text{H}/^1\text{H}$ correlation spectroscopy
cpm	counts per minute
4-DMAP	4-Dimethylaminopyridin
DAMGO	[D-Ala ² , N-CH ₃ Phe ⁴ , Gly-ol]-enkephalin
DEPT	distortionless enhancement by polarization transfer
DIPEA	<i>N</i> -ethyl- <i>N</i> -(propan-2-yl)propan-2-amine
DMF	<i>N,N</i> -dimethylformamide
DMP	Dess-Martin periodinane
DMSO-D_6	deuterated dimethyl sulfoxide
DPDPE	[D-Pen ² , D-Pen ⁵]-enkephalin

DTG	1,3-di- <i>o</i> -tolylguanidine
EC ₅₀	half maximal effective concentration
EDC	1-ethyl-3-(3-dimethylaminopropyl)carbodiimide
<i>ent</i>	enantiomeric
eq	equivalent
Et	ethyl
<i>et al.</i>	and others
EtOH	ethanol
Et ₂ O	diethyl ether
FT-IR	fourier transform infrared (-spectroscopy)
GPR	G Protein-coupled receptor
Gln	glutamine
gHMBC	heteronuclear multiple bond correlation
gHSQC	Heteronuclear single quantum correlation
HPLC	high performance liquid chromatography
HRMS	high resolution mass spectrometry
IC ₅₀	concentration of the test substance needed to inhibit 50% of the biological target
IR	infrared
<i>J</i>	coupling constant
<i>K_d</i>	dissociation constant
<i>K_i</i>	inhibition constant
<i>l</i>	length of the stationary phase
<i>L</i>	ligand
<i>L*</i>	radioligand
<i>M</i>	molar mass
mp	melting point
MS	mass spectrometry
<i>m/z</i>	mass to charge ratio
<i>n</i>	number of experiments

NaHMDS	sodium bis(trimethylsilyl)amide
NMR	nuclear magnetic resonance
PFA	paraformaldehyde
Ph	phenyl
ppm	parts per million
R	receptor
R_f	retention factor
RL	ligand-receptor-complex
RL*	radioligand-receptor-complex
RLU	relative luminescence units
rpm	round per minutes
r.t.	room temperature
SD	standard deviation
SEM	standard error of the mean
S _N 2	bimolecular nucleophilic substitution
T	test compound
<i>t</i>	tertiary
TBME	<i>tert</i> -butyl methyl ester
<i>t</i> -BuOCl	<i>tert</i> -butyl hypochlorite
TFA	trifluoroacetic acid
THF	tetrahydrofuran
TLC	thin layer chromatography
TM	transmembrane helix
TMS	tetramethylsilane
Tyr	tyrosine
t_R	retention time
TRIS	tris(hydroxymethyl)aminomethane
UV	ultraviolet
V	fraction size

8.2 NOESY spectra

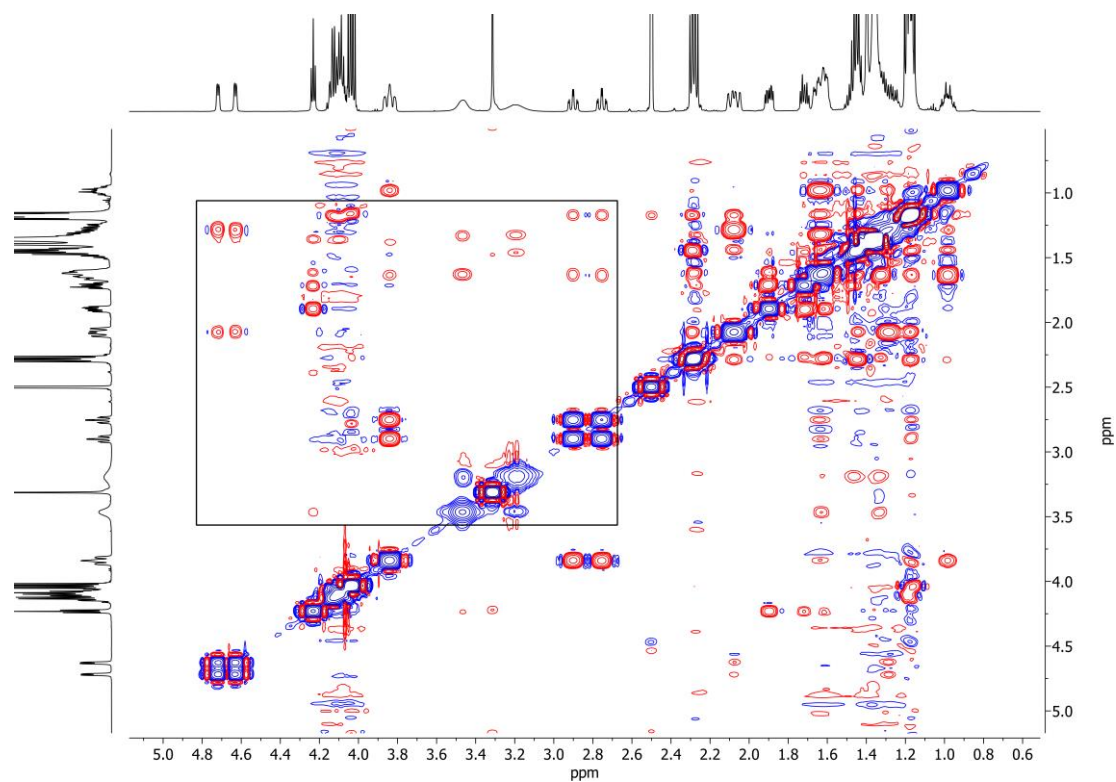


Figure S1: Complete NOESY spectrum of diester **37**.

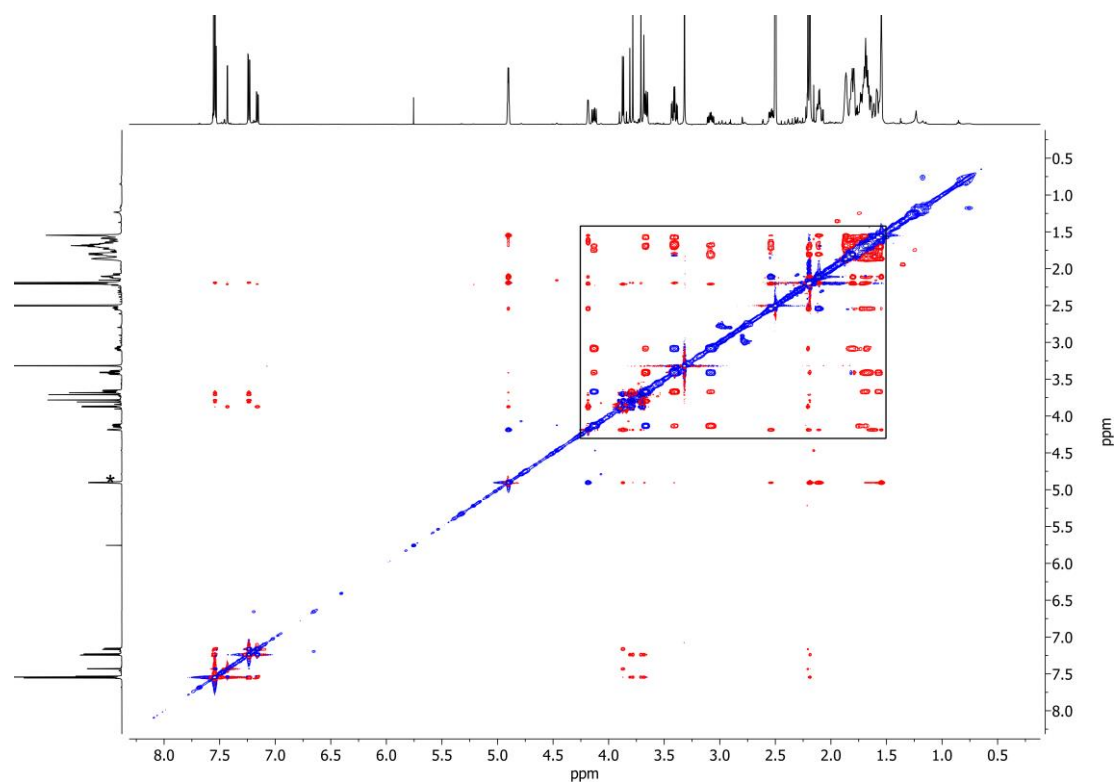


Figure S2: Complete NOESY spectrum of bicyclic amine **19b**.

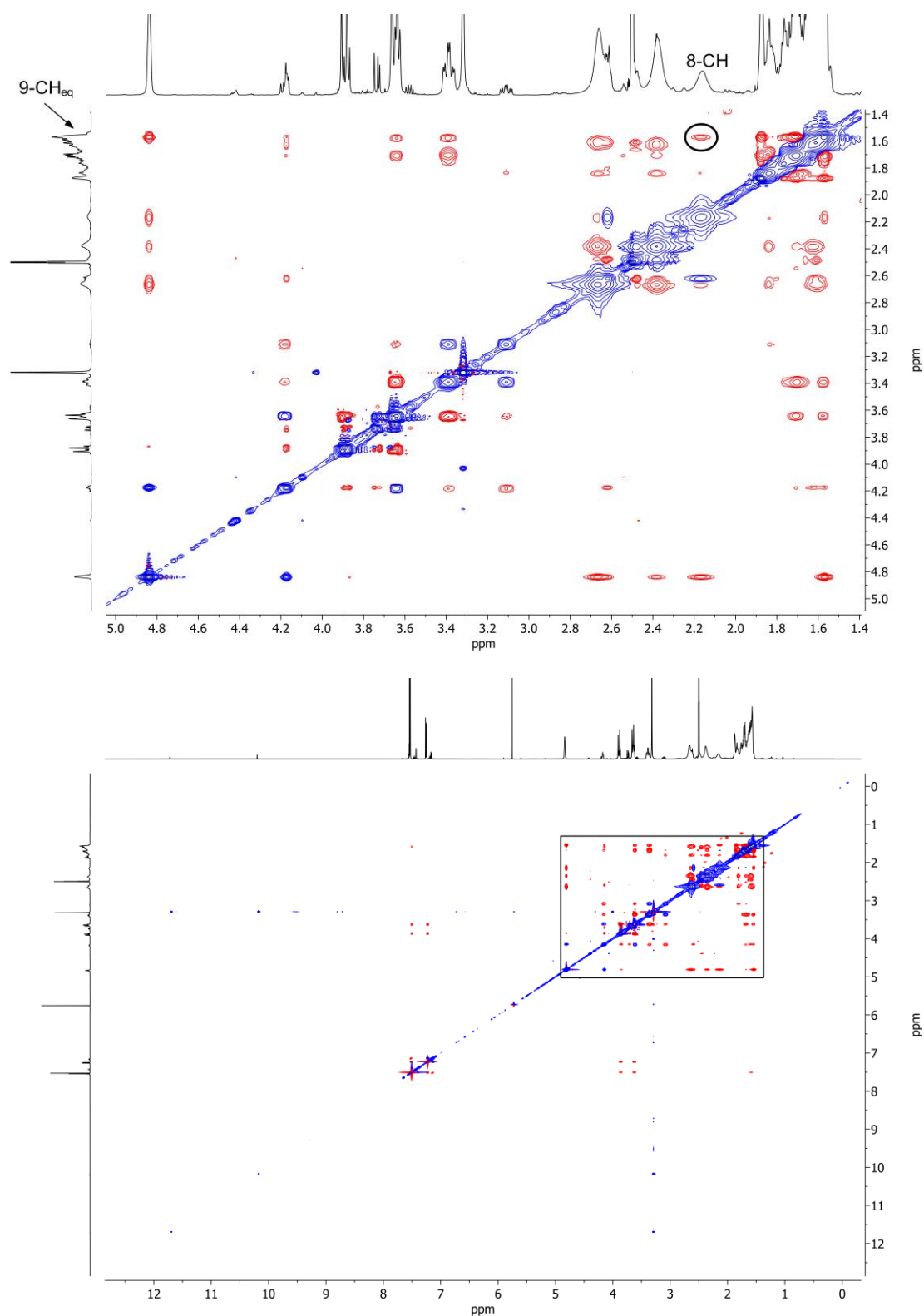


Figure S3: NOESY spectrum of bicyclic amine **19a**. Top: Magnification of the region of interest. Cross peak between 2.10 – 2.19 ppm (8-CH) and 1.51 – 1.64 ppm (9-CH_{eq}) for the major rotamer can be detected. The corresponding cross peaks are marked in black. Bottom: Complete NOESY spectrum.

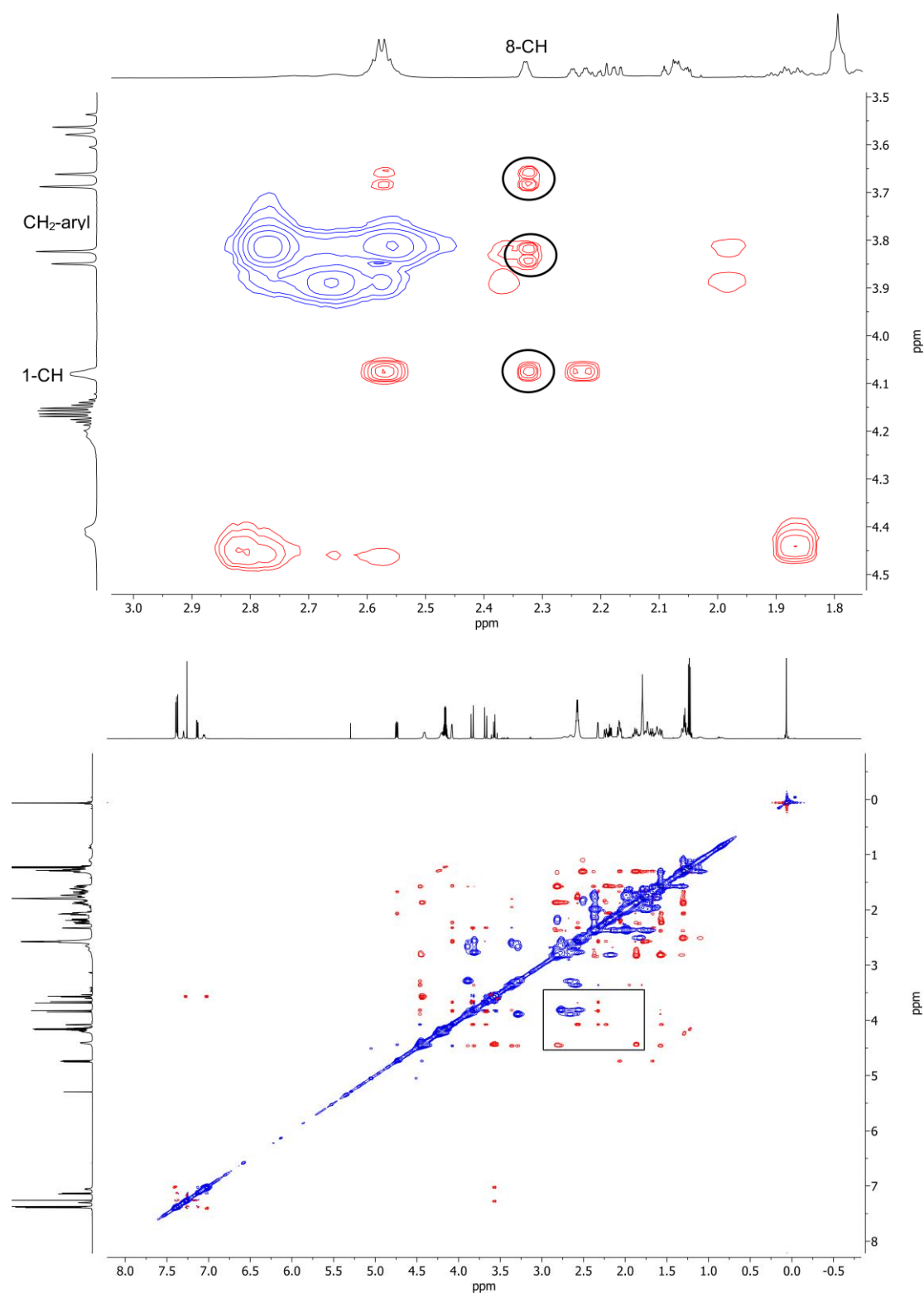


Figure S4: NOESY spectrum of bicyclic amine **20**. Top: Magnification of the region of interest. Cross peaks between 2.31 – 2.34 ppm (8-CH) and 4.08 ppm (1-CH), 3.84 ppm (CH₂-aryl) and 3.67 ppm (CH₂-aryl) for the major rotamer can be detected. The corresponding cross peaks are marked in black. Bottom: Complete NOESY spectrum.

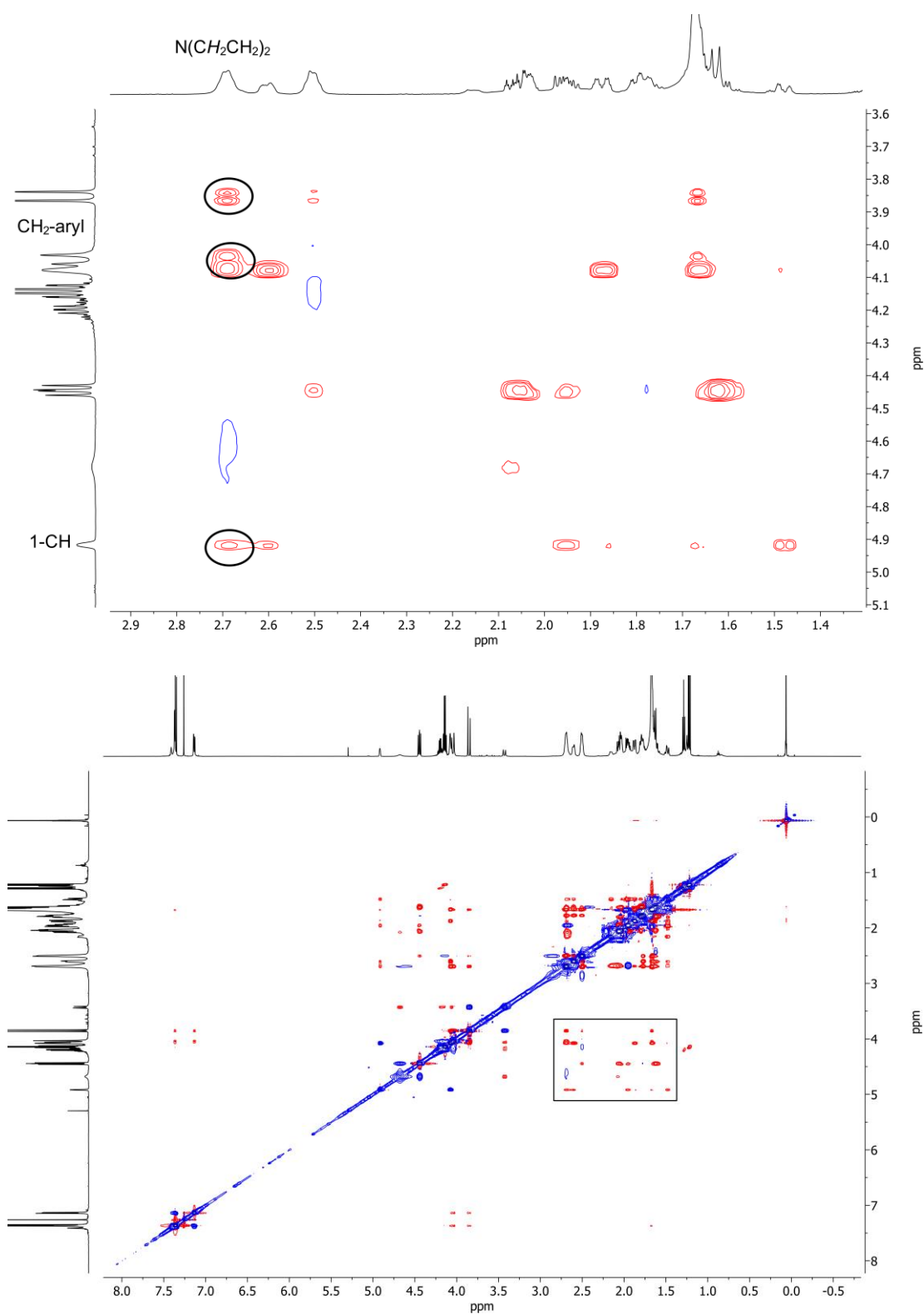


Figure S5: NOESY spectrum of bicyclic amine **21**. Top: Magnification of the region of interest. Cross peaks between 2.65 – 2.75 ppm ($N(CH_2CH_2)_2$) and 4.08 ppm (1-CH), 4.05 ppm (CH_2 -aryl) and 3.85 (CH_2 -aryl) for the major rotamer can be detected. The corresponding cross peaks are marked in black. Bottom: Complete NOESY spectrum.

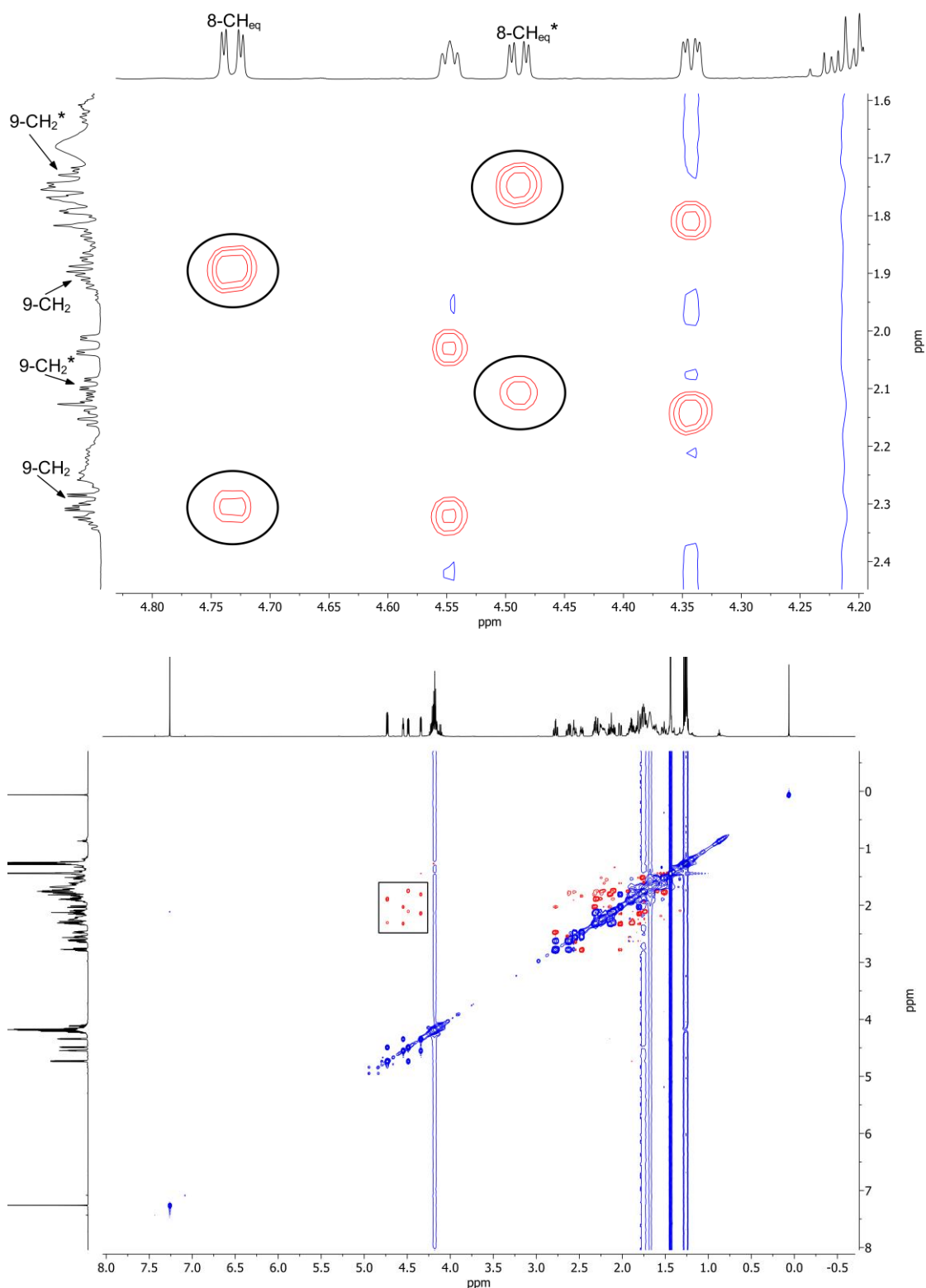


Figure S6: NOESY spectrum of bicyclic ketone **22**. Top: Magnification of the region of interest. Cross peaks between 4.73 ppm (8-CH_{eq}) and 2.27 – 2.35 ppm (9-CH₂) and 1.86 – 1.95 (9-CH₂) for the major rotamer and cross peaks between 4.49 ppm (8-CH_{eq}*) and 2.10 ppm (9-CH₂*) and 1.71 – 1.85 (9-CH₂*) for the minor rotamer can be detected. The corresponding cross peaks are marked in black. Bottom: Complete NOESY spectrum.

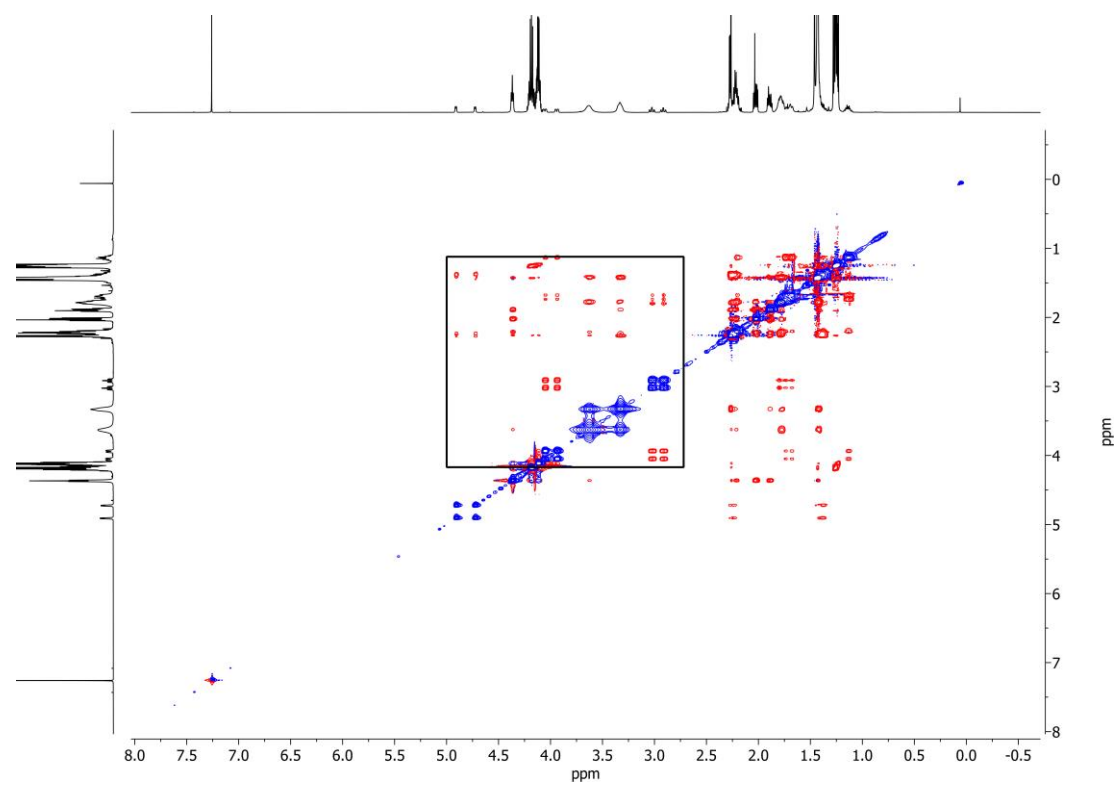


Figure S7: Complete NOESY spectrum of diester **115**.

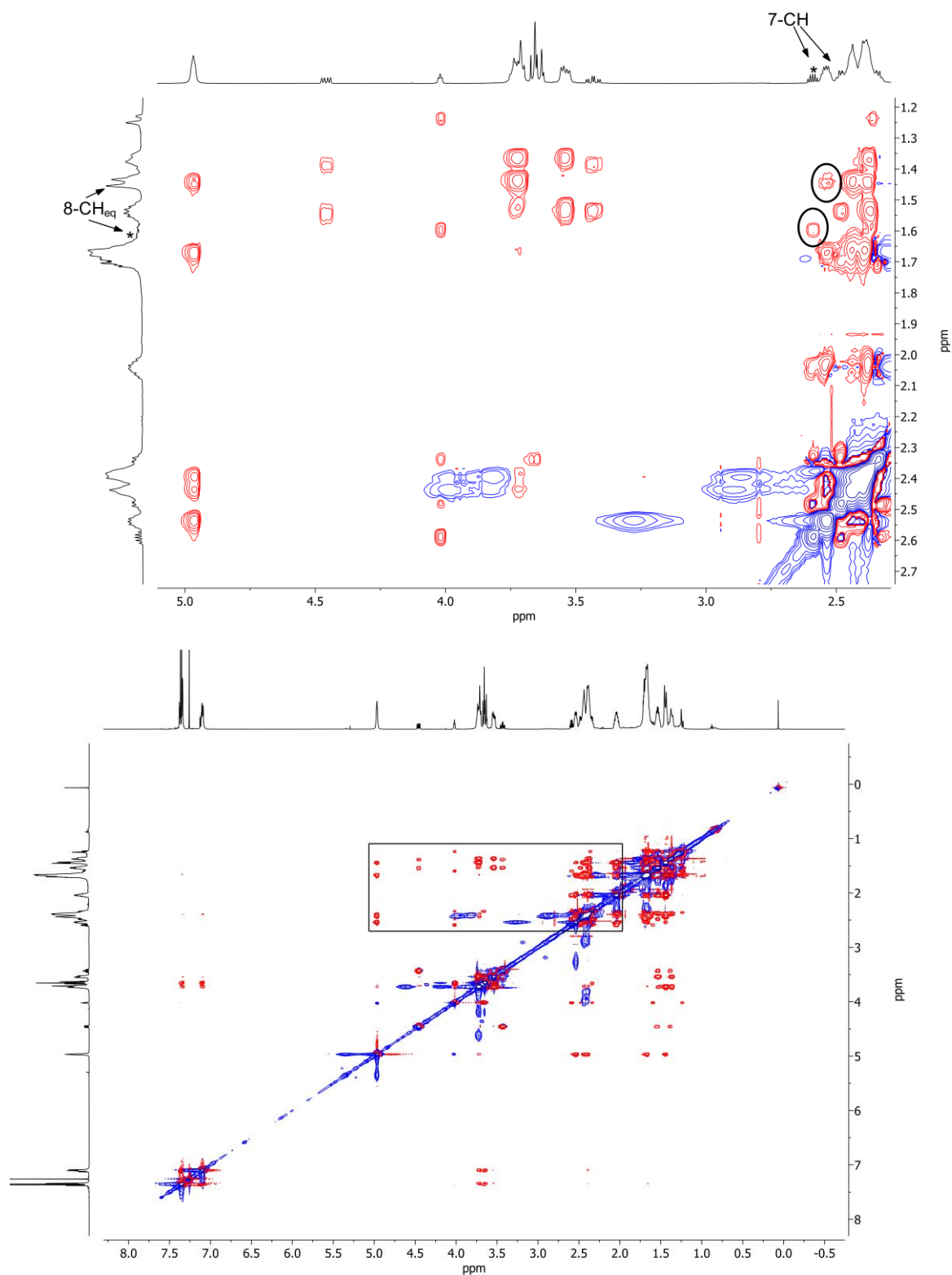


Figure S8: NOESY spectrum of bicyclic amine **23a**. Top: Magnification of the region of interest. A cross peak between 2.52 – 2.57 ppm (7-CH) and 1.41 – 1.47 ppm (8-CH_{eq}), for the major rotamer and a cross peak between 2.58 – 2.62 ppm (7-CH*) and 1.58 – 1.61 ppm (8-CH_{eq}*) for the minor rotamer can be detected. The corresponding cross peaks are marked in black. Bottom: Complete NOESY spectrum.

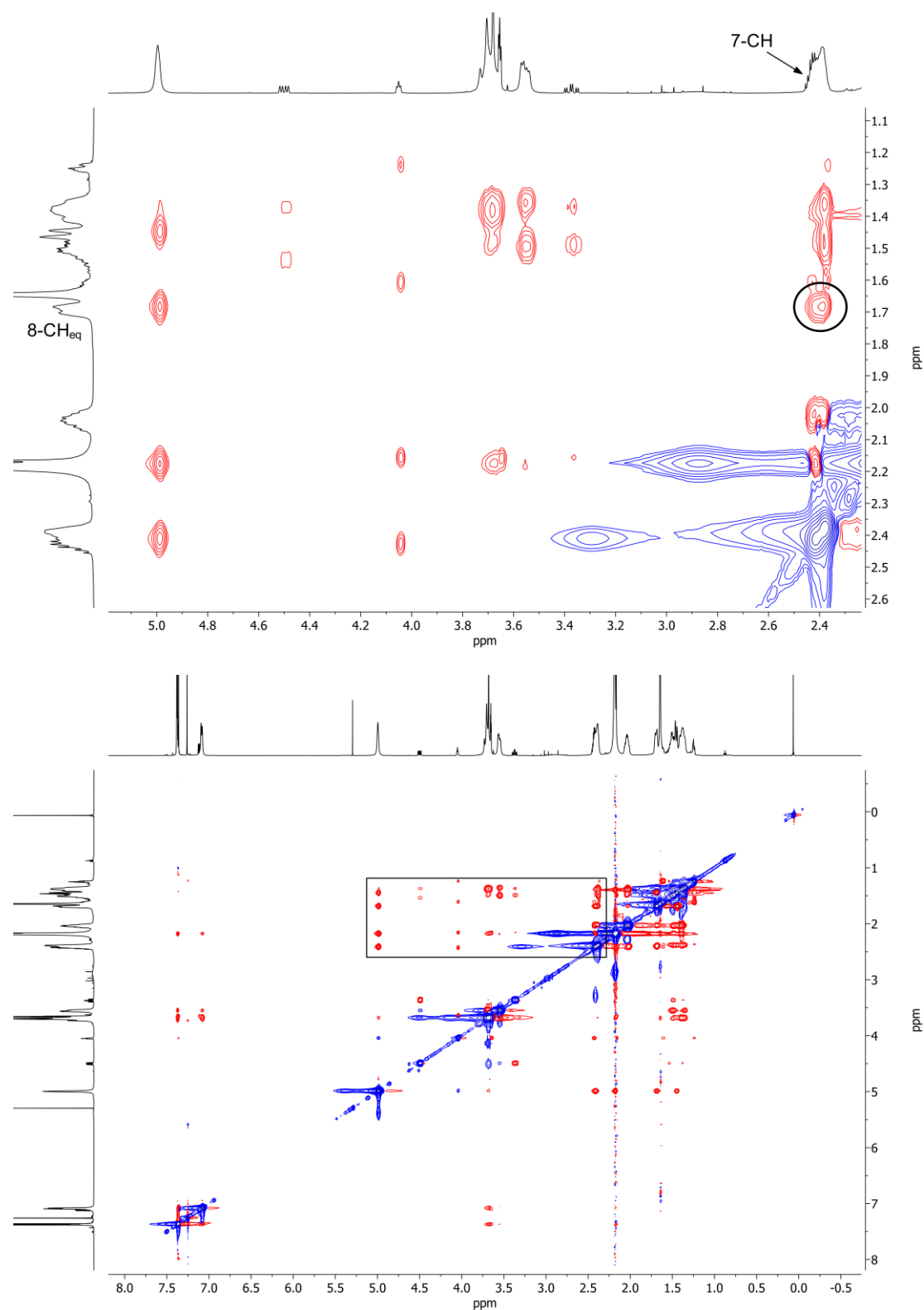


Figure S9: NOESY spectrum of bicyclic amine **23b**. Top: Magnification of the region of interest. A cross peak between 2.38 – 2.46 ppm (7-CH) and 1.66 – 1.72 ppm (8-CH_{eq}) for the major rotamer can be detected. The corresponding cross peak are marked in black. Bottom: Complete NOESY spectrum.

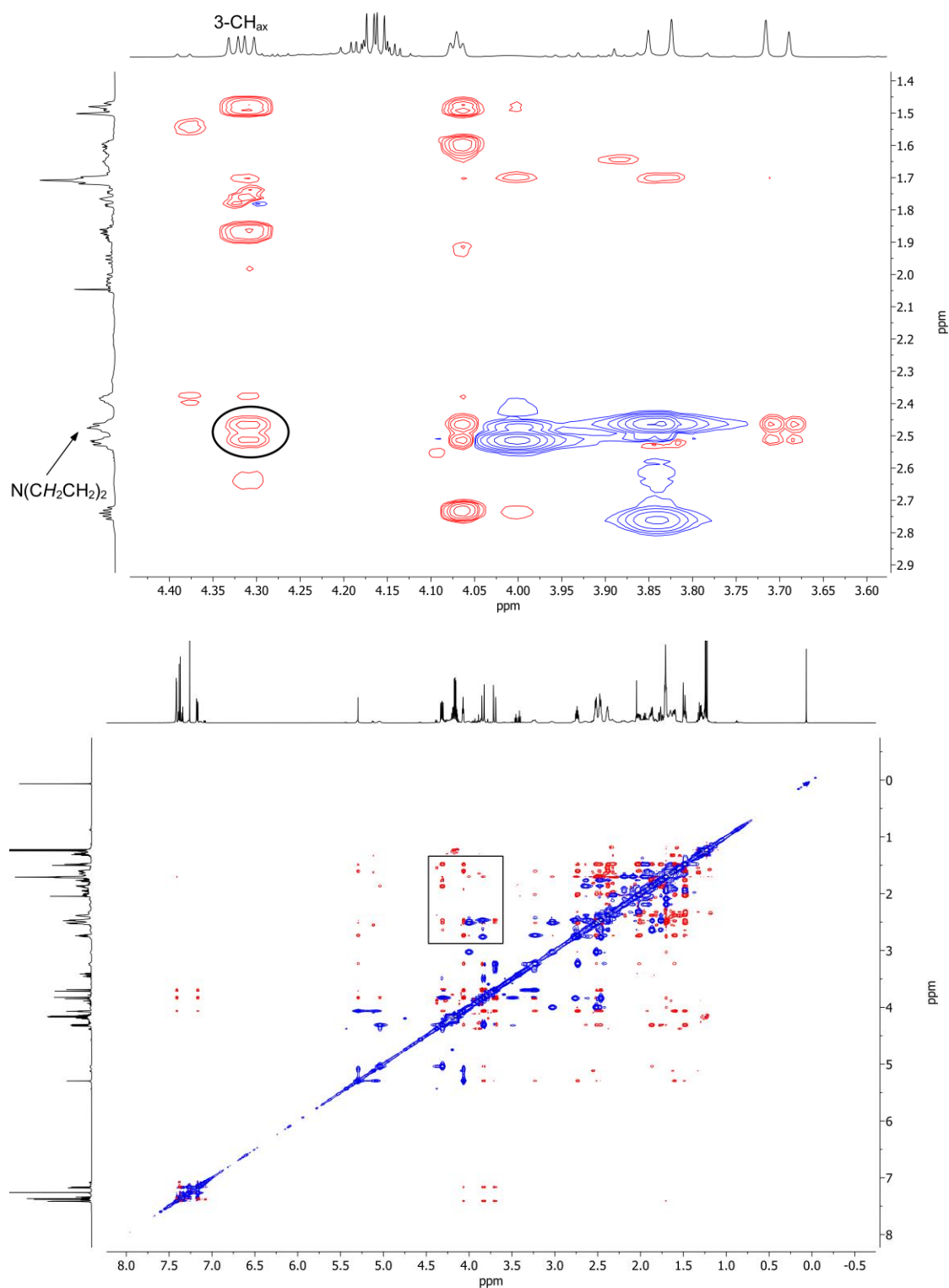


Figure S10: NOESY spectrum of bicyclic amine **142a**. Top: Magnification of the region of interest. A cross peak between 4.32 ppm (3-CH_{ax}) and 2.44 – 2.55 ppm (N(CH₂CH₂)₂) can be detected. The corresponding cross peak is marked in black. Bottom: Complete NOESY spectrum.

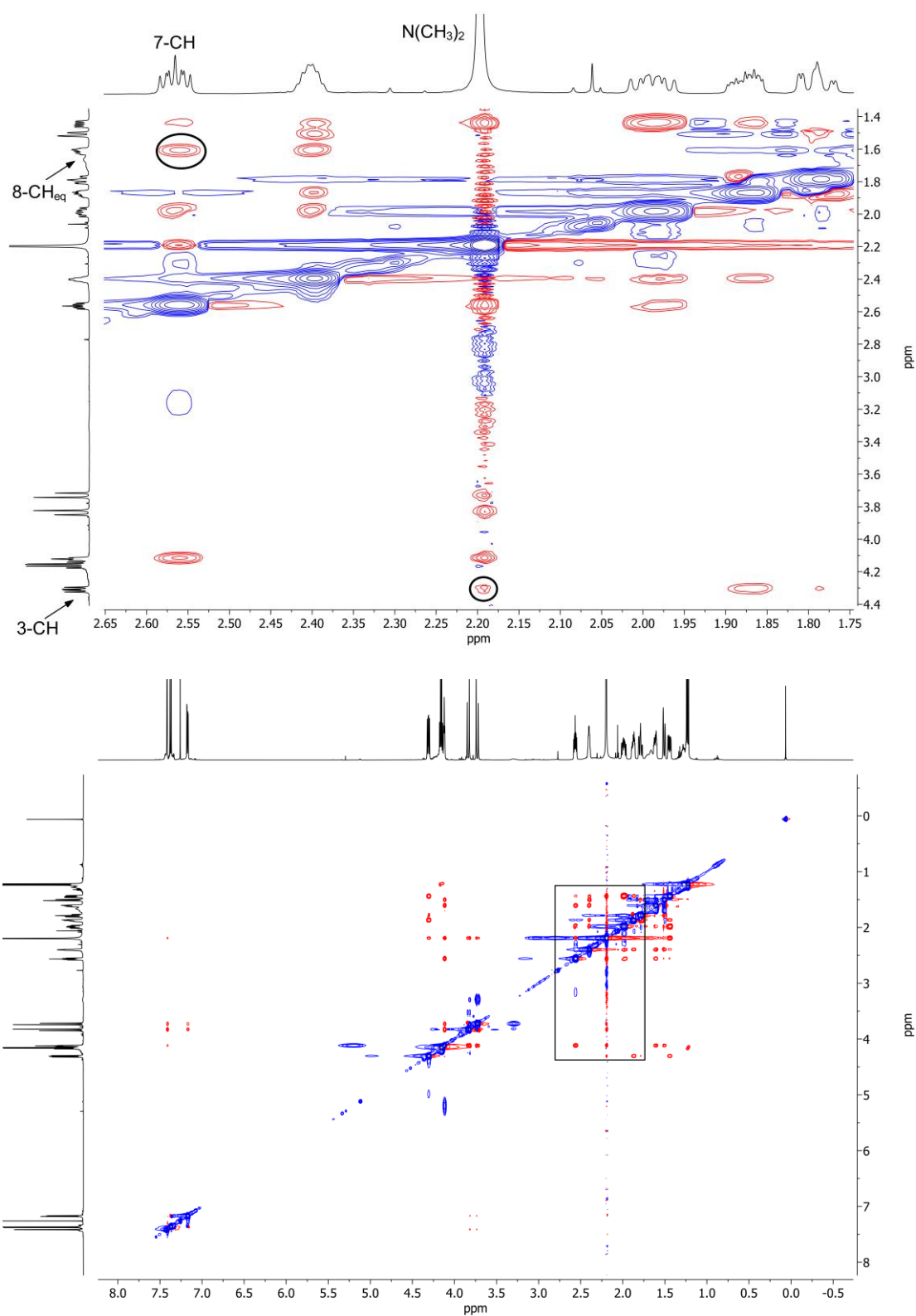


Figure S11: NOESY spectrum of bicyclic amine **142b**. Top: Magnification of the region of interest. Cross peaks between 2.57 ppm (7-CH) and 1.61 ppm (8-CH_{eq}) and between 2.20 ppm (N(CH₃)₂) and 4.31 ppm (3-CH) can be detected. The corresponding cross peaks are marked in black. Bottom: Complete NOESY spectrum.

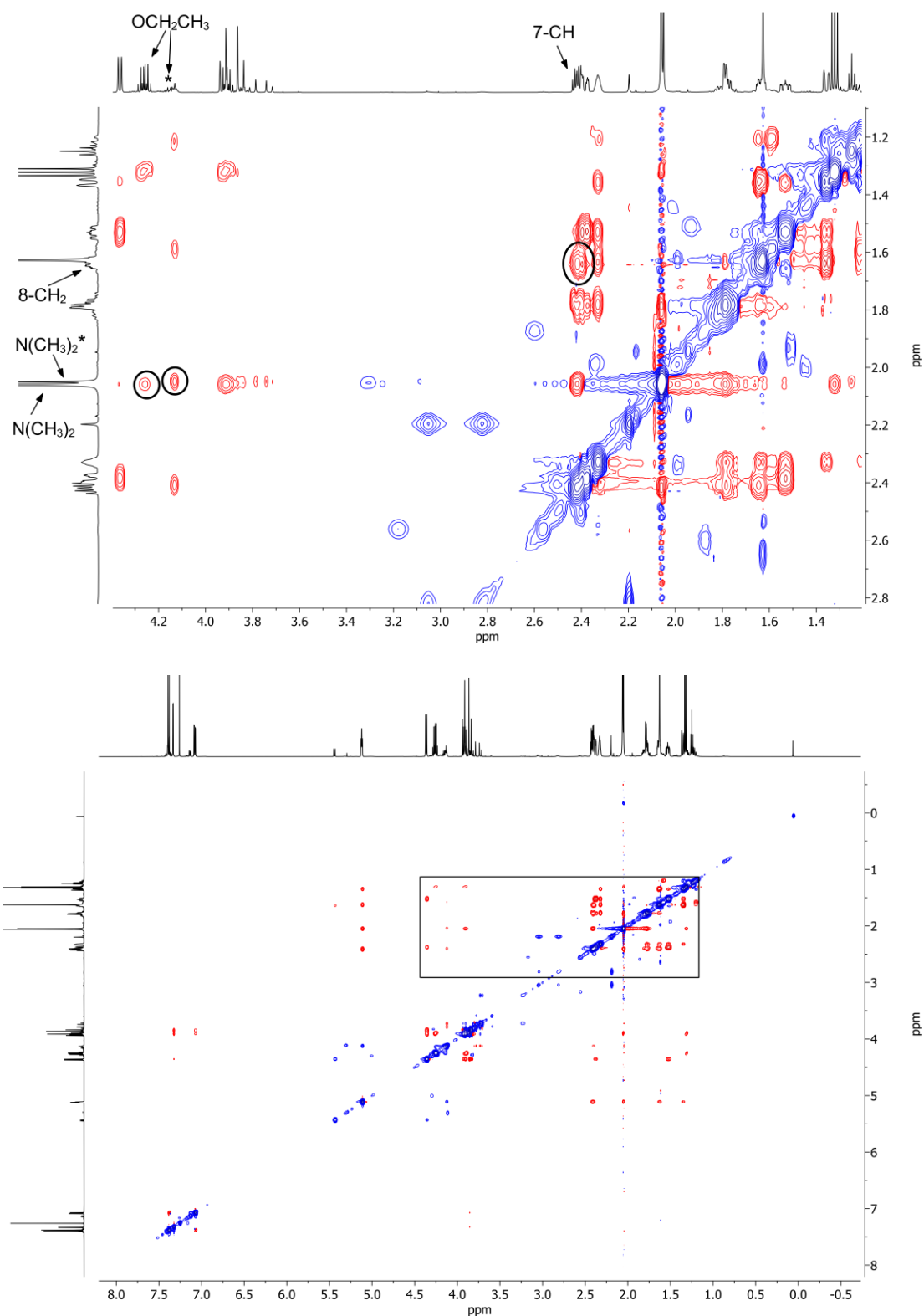


Figure S12: NOESY spectrum of bicyclic amine **143b**. Top: Magnification of the region of interest. Cross peaks between 2.36 – 2.45 ppm (7-CH) and 1.56 – 1.68 ppm (8-CH_{eq}) and between 4.26 ppm (OCH₂CH₃) and 2.06 ppm (N(CH₃)₂) for the major rotamer and a cross peak between 3.82 – 3.87 ppm (OCH₂CH₃*) and 2.05 ppm (N(CH₃)₂*) for the minor rotamer can be detected. The corresponding cross peaks are marked in black. Bottom: Complete NOESY spectrum.

8.3 Compound list

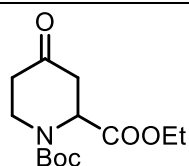
The following is the list of the compounds discussed in this work. The compounds are classified under:

Number: Nummer der Verbindung.

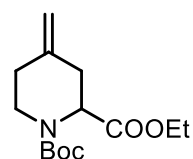
Page number: general section

Page number: experimental section

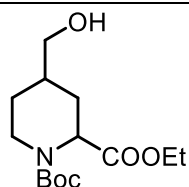
If possible, test compounds are denoted as **WMS 80-XX**.



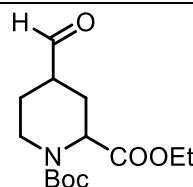
26a: 14, 120



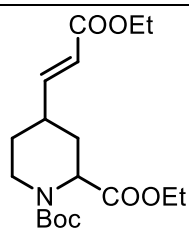
30: 16, 121



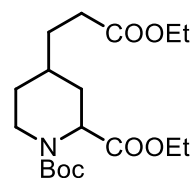
31: 16, 122



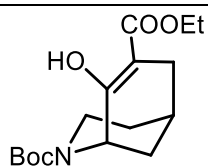
32: 16; 123



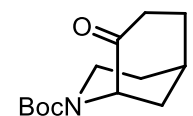
34: 17, 124



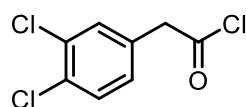
37: 19, 125



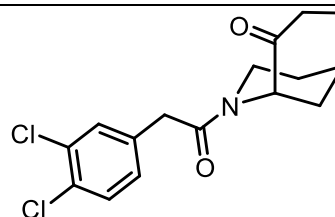
25: 21, 127



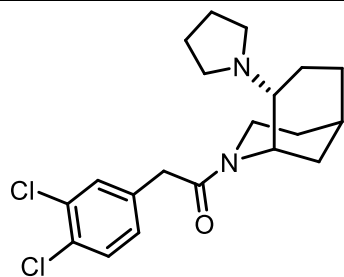
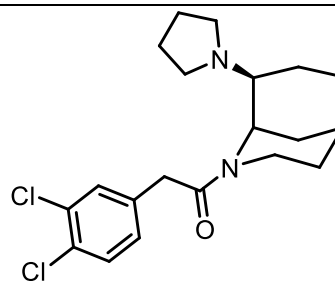
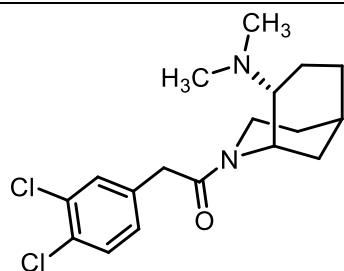
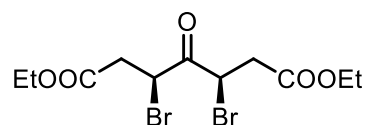
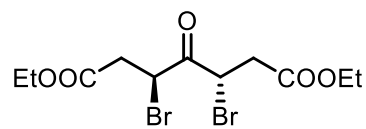
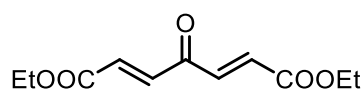
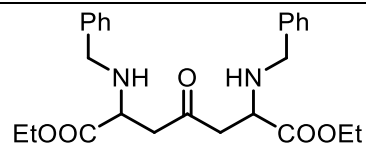
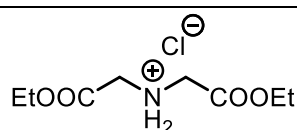
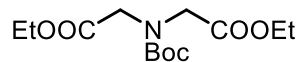
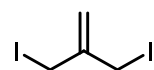
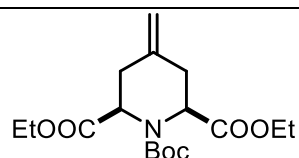
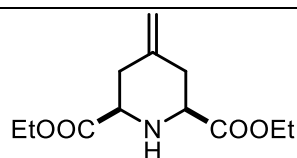
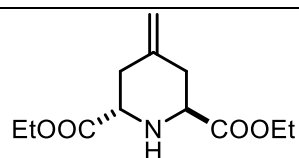
51: 27, 128

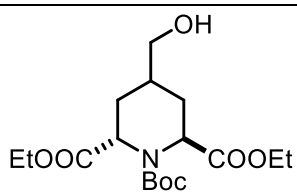
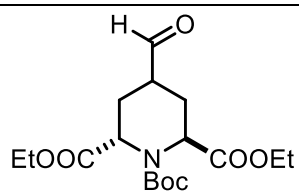
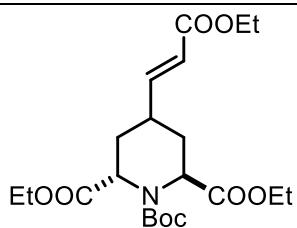
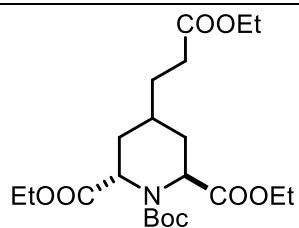
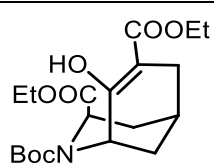
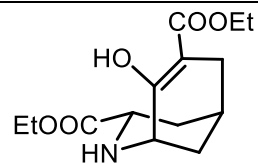
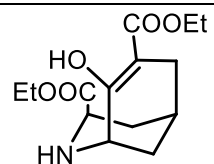
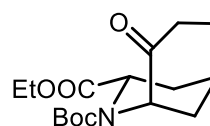
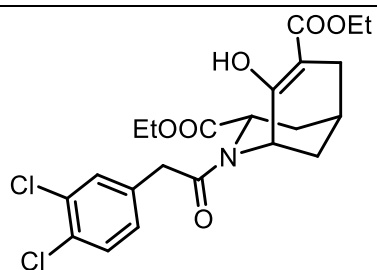
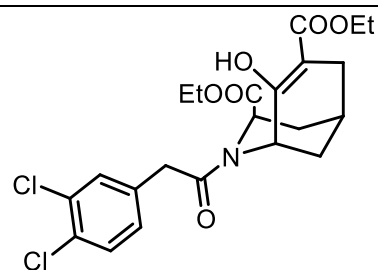
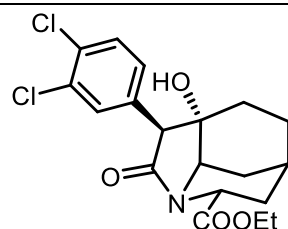
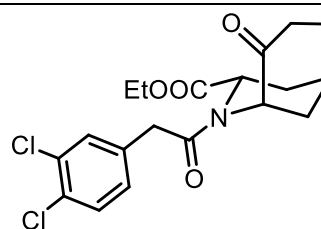


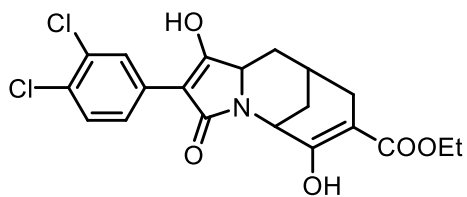
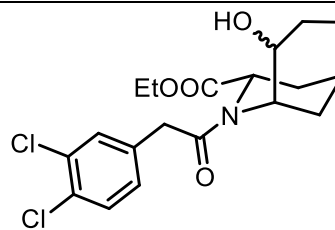
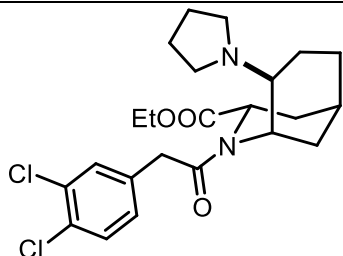
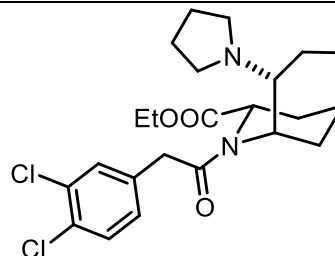
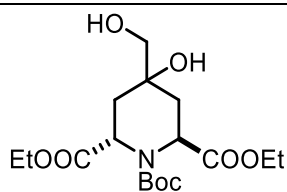
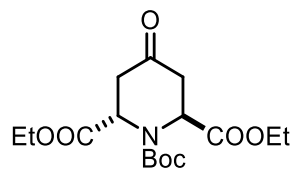
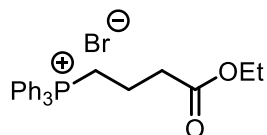
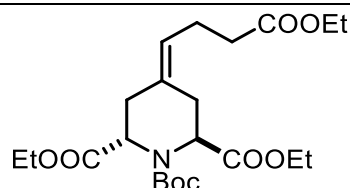
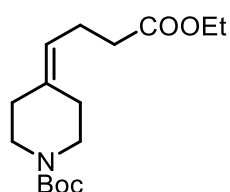
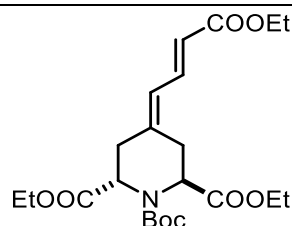
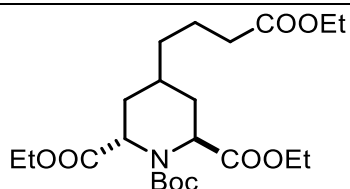
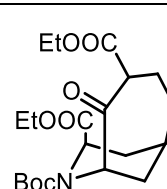
53: 28, 128

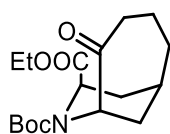
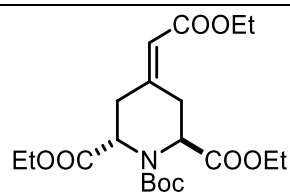
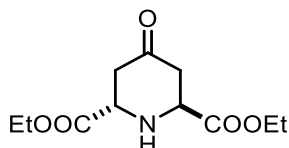
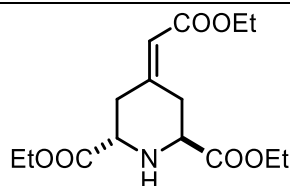
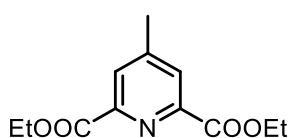
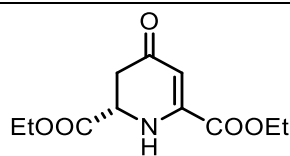
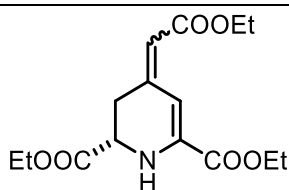
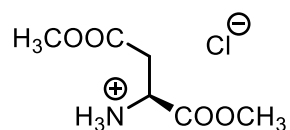
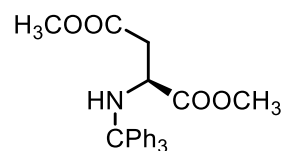
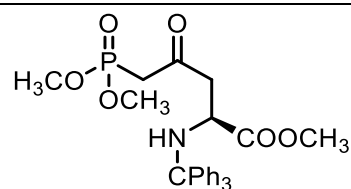
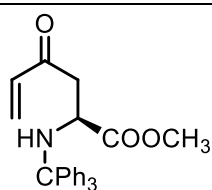
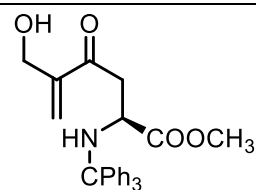
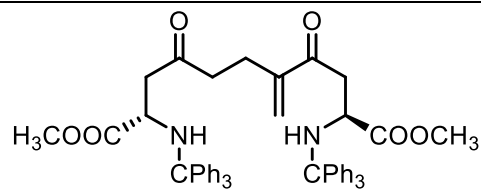
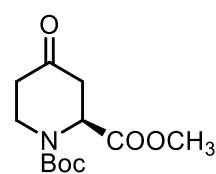


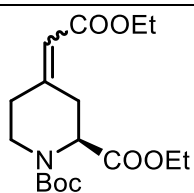
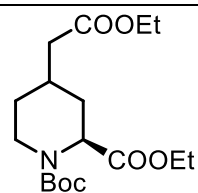
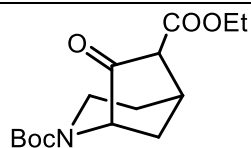
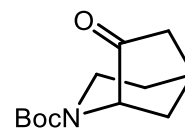
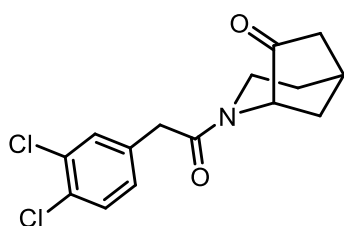
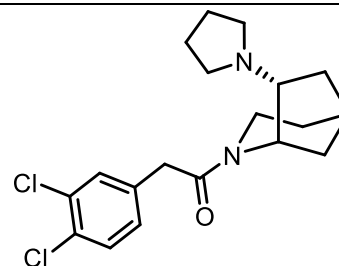
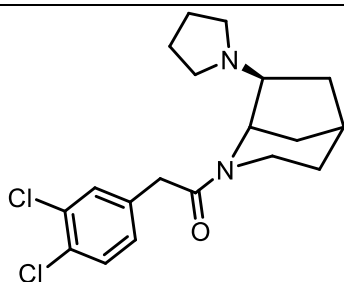
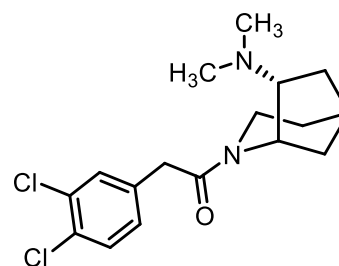
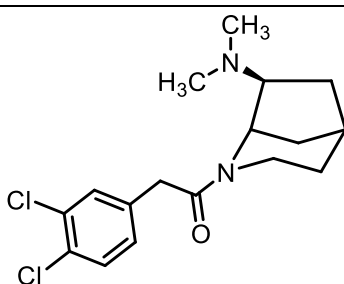
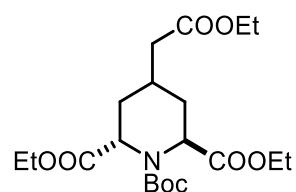
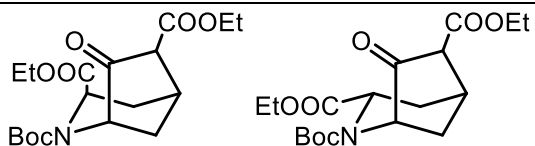
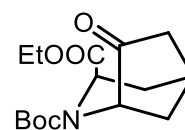
54: 28, 129

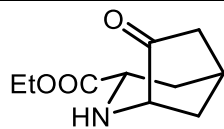
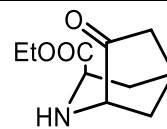
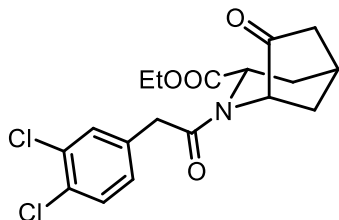
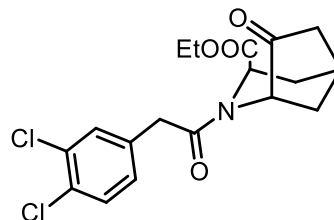
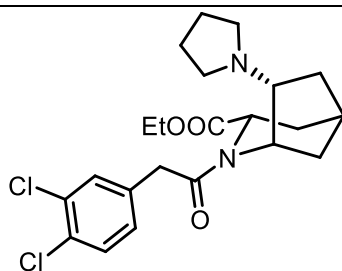
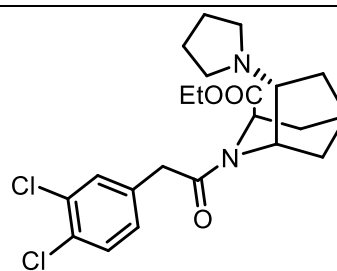
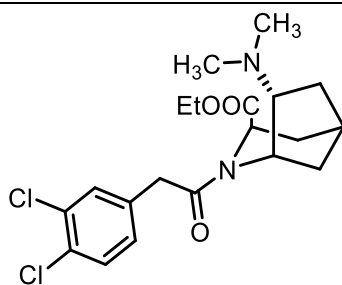
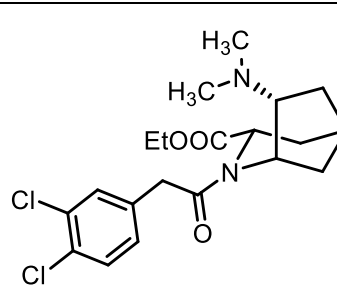
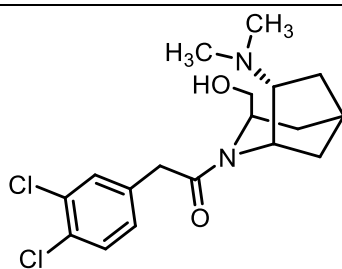
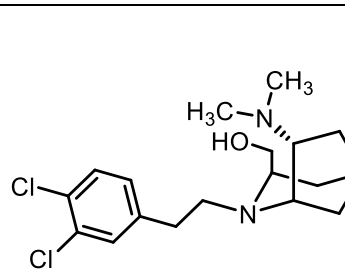
**19a:** 30, 130 (WMS 80-18)*ent*-**19a:** 34, 130 (WMS 80-19)**19b:** 30, 132 (WMS 80-14)**59:** 37, 133**60:** 37, 134**61:** 37, 135**64:** 39, 135**62a:** 39, 136**66:** 40, 137**56:** 40, 137**69:** 41, 138**70:** 41, 138

**71:** 43, 140**72:** 44, 141**73:** 44, 142**74:** 45, 143**75:** 45, 144**76:** 47, 145**77:** 47, 145**78:** 48, 146**79:** 49, 147**80:** 49, 148**82:** 51, 150 (WMS 80-08)**81:** 51, 150

**84:** 53, 152**86:** 55, 153**20:** 56, 154 (WMS 80-11)**21:** 56, 154 (WMS 80-12)**89:** 58, 157**87:** 58, 158**94:** 61, 159**95:** 61, 160**97:** 61, 161**99:** 62, 162**88:** 62, 163**100:** 63, 165

**22:** 63, 165**103:** 65, 166**104:** 66, 168**105:** 66, 168**111:** 67, 169**112:** 67, 170**113:** 67, 170**125:** 70, 171**121:** 70, 172**122:** 71, 173**123:** 72, 174**126:** 72, 174**130:** 73, 175**(S)-26b:** 74, 177

**135:** 75, 178**115:** 75, 180**136:** 78, 181**137:** 78, 183**139:** 79, 185**23a:** 80, 187 (**WMS 80-17**)*ent*-**23a:** 83, 188 (**WMS 80-16**)**23b:** 80, 189 (**WMS 80-06**)*ent*-**23b:** 83, 190 (**WMS 80-07**)**144:** 86, 192**145:** 87, 193**146:** 88, 194

**147:** 88, 195**148:** 88, 195**140:** 90, 197**141:** 90, 198**142a:** 91, 200**143a:** 91, 201 (WMS 80-04)**142b:** 94, 202 (WMS 80-09)**143b:** 94, 202 (WMS 80-13)**149:** 94, 204**150:** 95, 205

8.4 Bibliography

- (1) Loeser, J. D.; Melzack, R. Pain: An Overview. *Pain* **1999**, *353*, 1607–1609.
- (2) Stewart, W. F.; Ricci, J. A.; Chee, E.; Morganstein, D.; Lipton, R. Lost Productive Time and Cost Due to Common Pain Conditions in the US Workforce. *J. Am. Med. Assoc.* **2003**, *290* (18), 2443–2454.
- (3) Brooks, P. Use and Benefits of Nonsteroidal Anti-Inflammatory Drugs. *Am. J. Med.* **1998**, *104* (98), 9–13.
- (4) Courtwright, D. T. *Forces of Habit: Drugs and the Making of the Modern World*, 1st ed.; 2009.
- (5) Dhawan, B. N.; Cesselin, F.; Raghubir, R.; Reisine, T.; Bradley, P. B.; Portoghese, P. S.; Hamon, M. International Union of Pharmacology. XII. Classification of Opioid Receptors. *Pharmacol. Rev.* **1996**, *48* (4), 567–592.
- (6) Stein, C.; Machelska, H. Modulation of Peripheral Sensory Neurons by the Immune System: Implications for Pain Therapy. *Pharmacol. Rev.* **2011**, *63* (4), 860–881.
- (7) Martin, W. R. Opioid Antagonists. *Pharmacol. Rev.* **1967**, *19* (4), 463–521.
- (8) Terenius, L. Stereospecific Interaction Between Narcotic Analgesics and a Synaptic Plasma Membrane Fraction of Rat Cerebral Cortex. *Acta Pharmacol. Toxicol.* **1973**, *32*, 317–320.
- (9) Simon, E. J.; Hiller, J. M.; Edelman, I. Stereospecific Binding of the Potent Narcotic Analgesic [³H]Etorphine to Rat-Brain Homogenate. *Proc. Natl. Acad. Sci. U. S. A.* **1973**, *70* (7), 1947–1949.
- (10) Pert, C. B.; Snyder, S. H. Opiate Receptor: Demonstration in Nervous Tissue. *Science* **1973**, *179* (77), 1011–1014.
- (11) Martin, W. R. The Effects of Morphine- and Nalorphine-like Drugs in the Nondependent and Morphine-Dependent Chronic Spinal Dog. *J. Pharmacol. Exp. Ther.* **1976**, *197* (3), 517–532.
- (12) Lord, J. A. H.; Waterfield, A. A.; Hughes, J.; Kosterlitz, H. W. Endogenous Opioid Peptides: Multiple Agonists and Receptors. *Nature* **1977**, *267* (5611), 495–499.
- (13) Tam, S. W. Naloxone-Inaccessible σ Receptor in Rat Central Nervous System.

- Proc.Natl.Acad.Sci.U.S.A.* **1983**, *80* (21), 6703–6707.
- (14) Su, T. P.; London, E. D.; Jaffe, J. H. Steroid Binding at σ Receptors Suggests a Link Between Endocrine, Nervous, and Immune Systems. *Science* **1988**, *240*, 219–221.
- (15) Bunzow, J. R.; Saez, C.; Mortrud, M.; Bouvier, C.; Williams, J. T.; Low, M.; Grandy, D. K. Molecular Cloning and Tissue Distribution of a Putative Member of the Rat Opioid Receptor Gene Family That Is Not a μ , δ or κ Opioid Receptor Type. *FEBS Lett.* **1994**, *347*, 284–288.
- (16) Mollereau, C.; Parmentier, M.; Mailleux, P.; Butour, J. L.; Moisand, C.; Chalon, P.; Caput, D.; Vassart, G.; Meunier, J. C. ORL1, a Novel Member of the Opioid Receptor Family. *FEBS Lett.* **1994**, *341* (1), 33–38.
- (17) Calo', G.; Guerrini, R.; Rizzi, A.; Salvadori, S.; Regoli, D. Pharmacology of Nociceptin and Its Receptor: A Novel Therapeutic Target. *Br. J. Pharmacol.* **2000**, *129* (7), 1261–1283.
- (18) Palczewski, K.; Kumasaka, T.; Hori, T.; Behnke, C. A.; Motoshima, H.; Fox, B. A.; Le Trong, I.; Teller, D. C.; Okada, T.; Stenkamp, R. E.; Yamamoto, M.; Miyano, M. Crystal Structure of Rhodopsin: A G Protein-Coupled Receptor. *Science* **2000**, *289*, 739–745.
- (19) Waldhoer, M.; Bartlett, S. E.; Whistler, J. L. Opioid Receptors. *Annu. Rev. Biochem.* **2004**, *73*, 953–990.
- (20) Chen, Y.; Mestek, A.; Liu, J.; Yu, L. Molecular Cloning of a Rat κ Opioid Receptor Reveals Sequence Similarities to the μ and δ Opioid Receptors. *Biochem. J.* **1993**, *295* (3), 625–628.
- (21) Stewart, A.; Fisher, R. A. Introduction: G Protein-Coupled Receptors and RGS Proteins. In *Progress in Molecular Biology and Translational Science*; Elsevier B.V., 2015; Vol. 133, pp 1–11.
- (22) Childers, S. R. Opioid Receptor-Coupled Second Messenger Systems. *Life Sci.* **1991**, *48* (21), 1991–2003.
- (23) Miyake, M.; Christie, M. J.; North, R. A. Single Potassium Channels Opened by Opioids in Rat Locus Ceruleus Neurons. *Proc. Natl. Acad. Sci. U. S. A.* **1989**, *86* (9), 3419–3422.

- (24) Kieffer, B. L. *Recent Advances in Molecular Recognition and Signal Transduction of Active Peptides: Receptors for Opioid Peptides*; 1995; Vol. 15.
- (25) Bunzow, J. R.; Saez, C.; Mortrud, M.; Bouvier, C.; Williams, J. T.; Low, M.; Grandy, D. K. Molecular Cloning and Tissue Distribution of a Putative Member of the Rat Opioid Receptor Gene Family That Is Not a μ , δ or κ Opioid Receptor Type. *FEBS Lett.* **1994**, *347* (2–3), 284–288.
- (26) Vanderah, T. W. Delta and Kappa Opioid Receptors as Suitable Drug Targets for Pain. *Clin. J. Pain* **2010**, *26*, 10–15.
- (27) Chavkin, C. The Therapeutic Potential of κ -Opioids for Treatment of Pain and Addiction. *Neuropsychopharmacology* **2011**, *36* (1), 369–370.
- (28) Thomas, J. B.; Atkinson, R. N.; Rothman, R. B.; Fix, S. E.; Mascarella, S. W.; Vinson, N. A.; Xu, H.; Dersch, C. M.; Lu, Y. F.; Cantrell, B. E.; Zimmerman, D. M.; Carroll, F. I. Identification of the First *trans*-(3*R*,4*R*)-Dimethyl-4-(3-hydroxyphenyl)piperidine Derivative To Possess Highly Potent and Selective Opioid κ Receptor Antagonist Activity. *J. Med. Chem.* **2001**, *44* (17), 2687–2690.
- (29) Wu, H.; Wacker, D.; Mileni, M.; Katritch, V.; Han, G. W.; Vardy, E.; Liu, W.; Thompson, A. A.; Huang, X. P.; Carroll, F. I.; Mascarella, S. W.; Westkaemper, R. B.; Mosier, P. D.; Roth, B. L.; Cherezov, V.; Stevens, R. C. Structure of the Human κ -Opioid Receptor in Complex with JDTic. *Nature* **2012**, *485*, 327–332.
- (30) Che, T.; Majumdar, S.; Zaidi, S. A.; Ondachi, P.; McCorvy, J. D.; Wang, S.; Mosier, P. D.; Uprety, R.; Vardy, E.; Krumm, B. E.; Han, G. W.; Lee, M.-Y.; Pardon, E.; Steyaert, J.; Huang, X.-P.; Strachan, R. T.; Tribo, A. R.; Pasternak, G. W.; Carroll, F. I.; Stevens, R. C.; Cherezov, V.; Katritch, V.; Wacker, D.; Roth, B. L. Structure of the Nanobody-Stabilized Active State of the Kappa Opioid Receptor. *Cell* **2018**, *172*, 55–67.
- (31) Goldstein, A.; Tachibana, S.; Lowney, L. I.; Hunkapiller, M.; Hood, L. Dynorphin-(1-13), an Extraordinarily Potent Opioid Peptide. *Proc. Natl. Acad. Sci. U. S. A.* **1979**, *76* (12), 6666–6670.
- (32) Vanderah, T. W.; Largent-Milnes, T.; Lai, J.; Porreca, F.; Houghten, R. A.; Menzaghi, F.; Wisniewski, K.; Stalewski, J.; Sueiras-Diaz, J.; Galyean, R.; Schteingart, C.; Junien, J.-L.; Trojnar, J.; Rivière, P. J. M. Novel D-Amino Acid Tetrapeptides Produce Potent Antinociception by Selectively Acting at

- Peripheral κ -Opioid Receptors. *Eur. J. Pharmacol.* **2008**, *583* (1), 62–72.
- (33) Aldrich, J. V.; McLaughlin, J. P. Peptide Kappa Opioid Receptor Ligands: Potential for Drug Development. *AAPS J.* **2009**, *11* (2), 312–322.
- (34) Fishbane, S.; Jamal, A.; Munera, C.; Wen, W.; Menzaghi, F. A Phase 3 Trial of Difelikefalin in Hemodialysis Patients with Pruritus. *N. Engl. J. Med.* **2020**, *382* (3), 222–232.
- (35) Roth, B. L.; Baner, K.; Westkaemper, R.; Siebert, D.; Rice, K. C.; Steinberg, S. A.; Ernsberger, P.; Rothman, R. B. Salvinorin A: A Potent Naturally Occurring Nonnitrogenous κ Opioid Selective Agonist. *Proc. Natl. Acad. Sci. U. S. A.* **2002**, *99* (18), 11934–11939.
- (36) Béguin, C.; Richards, M. R.; Wang, Y.; Chen, Y.; Liu-Chen, L. Y.; Ma, Z.; Lee, D. Y. W.; Carlezon, W. A.; Cohen, B. M. Synthesis and in Vitro Pharmacological Evaluation of Salvinorin A Analogues Modified at C(2). *Bioorganic Med. Chem. Lett.* **2005**, *15* (11), 2761–2765.
- (37) Munro, T. A.; Duncan, K. K.; Xu, W.; Wang, Y.; Liu-Chen, L. Y.; Carlezon, W. A.; Cohen, B. M.; Béguin, C. Standard Protecting Groups Create Potent and Selective κ Opioids: Salvinorin B Alkoxymethyl Ethers. *Bioorganic Med. Chem.* **2008**, *16* (3), 1279–1286.
- (38) Nagase, H.; Hayakawa, J.; Kawamura, K.; Kawai, K.; Takezawa, Y.; Matsuura, H.; Tajima, C.; Endo, T. Discovery of a Structurally Novel Opioid κ -Agonist Derived from 4,5-Epoxymorphinan. *Chem. Pharm. Bull.* **1998**, *46* (2), 366–369.
- (39) Cowan, A.; Yosipovitch, G. *Pharmacology of Itch*, 1st ed.; 2015.
- (40) Fisher, J.; Ganelling, C. R. *Analogue-Based Drug Discovery*, 1st ed.; 2006.
- (41) Coursey, C. E. The Psychotomimetic Side Effects of Pentazocine. *Drug Intell. Clin. Pharm.* **1978**, *12* (6), 341–346.
- (42) Pasternak, G. W. *Foundations of Anesthesia*, 2nd ed.; Hemmings, H. C., Hopkins, P. M., Eds.; 2006.
- (43) Szmuszkovicz, J.; Von Voigtlander, P. F. Benzeneacetamide Amines: Structurally Novel Non-M μ Opioids. *J. Med. Chem.* **1982**, *25* (10), 1125–1126.
- (44) Von Voigtlander, P. F.; Lewis, R. A. U-50,488, a Selective Kappa Opioid Agonist: Comparison to Other Reputed Kappa Agonists. *Prog. Neuropsychopharmacol.*

- Biol. Psychiatry* **1982**, 6 (4–6), 467–470.
- (45) Gottschlich, R.; Krug, M.; Barber, A.; Devant, R. M. K-Opioid Activity of the Four Stereoisomers of the Peripherally Selective κ -Agonists, EMD 60 400 and EMD 61 753. *Chirality* **1994**, 6, 685–689.
- (46) Barber, A.; Bartoszyk, G. D.; Bender, H. M.; Gottschlich, R.; Greiner, H. E.; Harting, J.; Mauler, F.; Minck, K. -O; Murray, R. D.; Simon, M.; Seyfried, C. A. A Pharmacological Profile of the Novel, Peripherally-selective K-opioid Receptor Agonist, EMD 61753. *Br. J. Pharmacol.* **1994**, 113 (4), 1317–1327.
- (47) Camilleri, M. Novel Pharmacology: Asimadoline, a κ -Opioid Agonist, and Visceral Sensation. *Neurogastroenetal Motil* **2008**, 20 (9), 971–979.
- (48) Soeberdt, M.; Knie, U.; Abels, C.; Kiefmann, R. Asimadoline for Use in Treating Pulmonary Diseases, Vascular Diseases, and Sepsis. WO 2019122361, 2019.
- (49) Eguchi, M. Recent Advances in Selective Opioid Receptor Agonists and Antagonists. *Med. Res. Rev.* **2004**, 24 (2), 182–212.
- (50) de Costa, B. R.; Bowen, W. D.; Hellewell, S. B.; George, C.; Rothman, R. B.; Reid, A. A.; Walker, M.; Jacobson, A. E.; Rice, K. C. Alterations in the Stereochemistry of the κ -Selective Opioid Agonists U50,488 Result in High-Affinity σ Ligands. *J. Med. Chem.* **1998**, 32 (8), 1996–2002.
- (51) Naylor, A.; Judd, D. B.; Lloyd, J. E.; Scopes, D. I. C.; Hayes, A. G.; Birch, P. J. A Potent New Class of κ -Receptor Agonist: 4-Substituted 1-(Arylacetyl)-2-[(Dialkylamino)Methyl]Piperazines. *J. Med. Chem.* **1993**, 36 (15), 2075–2083.
- (52) Kracht, D.; Rack, E.; Schepmann, D.; Fröhlich, R.; Wünsch, B. Stereoselective Synthesis and Structure-Affinity Relationships of Bicyclic κ Receptor Agonists. *Org. Biomol. Chem.* **2010**, 8, 212–225.
- (53) Vecchietti, V.; Giordani, A.; Giardina, G.; Colle, R.; Clarke, G. D. (2S)-1-(Arylacetyl)-2-(Aminomethyl)Piperidine Derivatives: Novel, Highly Selective κ Opioid Analgesics. *J. Med. Chem.* **1991**, 34, 397–403.
- (54) Ilari, D.; Maskri, S.; Schepmann, D.; Köhler, J.; Daniliuc, C. G.; Koch, O.; Wünsch, B. Diastereoselective Synthesis of Conformationally Restricted KOR Agonists. *Org. Biomol. Chem.* **2021**.
- (55) Jackson, R. F. W.; Graham, L. J.; Rettle, A. B. Synthesis of Protected 4-

- Oxopipicolinic Acid and 4-Oxolysine Using a Palladium-Catalysed Coupling Process. *Tetrahedron Lett.* **1994**, *35*, 4417–4418.
- (56) Daly, M.; Cant, A. A.; Fowler, L. S.; Simpson, G. L.; Senn, H. M.; Sutherland, A. Switching the Stereochemical Outcome of 6-*Endo-Trig* Cyclizations; Synthesis of 2,6-*Cis*-6-Substituted 4-Oxopipicolinic Acids. *J. Org. Chem.* **2012**, *77*, 10001–10009.
- (57) Bousquet, Y.; Anderson, P. C.; Bogri, T.; Duceppe, J.-S.; Grenier, L.; Guse, I. Preparation of Enantiopure 4-Oxygenated Pipicolinic Acid Derivatives. *Tetrahedron* **1997**, *53*, 15671–15680.
- (58) Jung, M. E.; Shishido, K.; Light, L.; Davis, L. Preparation of Di- and Triacylimines and Their Use in the Synthesis of Nitrogen Heterocycles. *Tetrahedron Lett.* **1981**, *22*, 4607–4610.
- (59) Hermann, K.; Dreiding, A. S. Herstellung von Dihydro-, Tetrahydro- Und Hexahydrochelidamsäure-Derivaten. *Helv. Chim. Acta* **1976**, *59*, 626–642.
- (60) Einhorn, J.; Einhorn, C.; Pierre, J.-L. Dianions of N-Protected Iminodiacetic Acid Diesters: New Synthons with Broad Synthetic Potentialities. *Synlett* **1994**, *12*, 1023–1024.
- (61) Fowler, L. S.; Thomas, L. H.; Ellis, D.; Sutherland, A. A One-Pot, Reductive Amination/6-*Endo-Trig* Cyclisation for the Stereoselective Synthesis of 6-Substituted-4-Oxopipicolinic Acids. *Chem. Commun.* **2011**, *47*, 6569–6571.
- (62) Leeson, P. D.; Williams, B. J. Bicyclic Aminohydroxamates as Neuroprotective Agents. Pdf, 1990.
- (63) Fischer, E.; Speier, A. Darstellung Der Ester. *Chem. Ber.* **1895**, *28*, 3252–3258.
- (64) Clayden, J.; Greeves, N.; Warren, S. *Organic Chemistry*, 2nd ed.; 2012.
- (65) Sheehan, J. C.; Cruickshank, P. A.; Boshart, G. L. A Convenient Synthesis of Water-Soluble Carbodiimides. *J. Org. Chem.* **1961**, *26* (7), 2525–2528.
- (66) Aksnes, G. Alkaline Decomposition of Some Quaternary Phosphonium Compounds Containing Oxygen. *Acta Chem. Scand.* **1961**, *15*, 438–440.
- (67) Denney, D. B.; Chrisbacher Smith, L. Preparation and Reactions of Some Phosphobetaines. *Carbohydr. Res.* **1962**, *27*, 3404–3408.
- (68) Corey, H. S.; McCormick, J. R. D.; Swensen, W. E. The Wittig Reaction. I.

- Synthesis of β,γ -Unsaturated Acids. *J. Am. Chem. Soc.* **1964**, 86 (9), 1884–1885.
- (69) Balsamo, A.; Breschi, M.; Giannaccini, G.; Lapucci, A.; Lucacchini, A.; Macchia, B.; Manera, C.; Martini, C.; Martinotti, E.; Nencetti, S.; Rossello, A.; Scatizzi, R. Synthesis and β -Adrenergic Properties of Tetrahydronaphthalene Analogs of Dichloroisoproterenol. *Eur. J. Med. Chem.* **1993**, 28, 735–741.
- (70) Devkota, K.; Lohse, B.; Liu, Q.; Wang, M.-W.; Stærk, D.; Berthelsen, J.; Clausen, R. P. Analogues of the Natural Product Sinefungin as Inhibitors of EHMT1 and EHMT2. *ACS Med. Chem. Lett.* **2014**, 5, 293–297.
- (71) Lombardo, L.; Mander, L. N.; Turner, J. V. General Strategy for Gibberellin Synthesis: Total Syntheses of (\pm)-Gibberellin A₁ and Gibberlic Acid. *J. Am. Chem. Soc.* **1980**, 102, 6628–6629.
- (72) Brown, H. C.; Subba Rao, B. C. A New Technique for the Conversion of Olefins into Organoboranes and Related Alcohols. *J. Am. Chem. Soc.* **1956**, 78 (21), 5694–5695.
- (73) Brown, H. C.; Zweifel, G. A Stereospecific CIS Hydration of the Double Bond in Cyclic Derivatives. *J. Am. Chem. Soc.* **1959**, 81 (1), 247.
- (74) Brown, H. C. Hydroboration - a Powerful Synthetic Tool. *Tetrahedron* **1961**, 12 (3), 117–138.
- (75) Dess, D. B.; Martin, J. C. Readily Accessible 12-I-5 Oxidant for the Conversion of Primary and Secondary Alcohols to Aldehydes and Ketones. *J. Org. Chem.* **1983**, 48 (22), 4155–4156.
- (76) House, H. O.; Rasmusson, G. H. Stereoselective Synthesis of α -Substituted α,β -Unsaturated Esters. *J. Org. Chem.* **1960**, 26 (11), 4278–4281.
- (77) Schlosser, M.; Christmann, K. F. Mechanismus Und Stereochemie Der Wittig-Reaktion. *Justus Liebigs Ann. Chem.* **1967**, 708 (1), 1–35.
- (78) Vedejs, E.; Peterson, M. J. *Stereochemistry and Mechanism in the Wittig Reaction*; 1994; Vol. 21.
- (79) Dieckmann, W. Zur Kenntniss Der Ringbildung Aus Kohlenstoffketten. *Berichte der Dtsch. Chem. Gesellschaft* **1894**, 27 (1), 102–103.
- (80) Clemo, G. R.; Ramage, G. R. L1X.-The Lupin Alkaloids. Part IV. The Synthesis

- of Octahydropyridocoline. *J. Org. Chem.* **1931**, 437–442.
- (81) Clemo, G. R.; Metcalfe, T. P. 2-Ketoquinuclidine and a New Synthesis of Quinuclidine. *J. Org. Chem.* **1937**, 1989–1990.
- (82) Sternbach, L. H.; Kaiser, S. Antispasmodics. I. Bicyclic Basic Alcohols. *J. Am. Chem. Soc.* **1952**, 74, 2215–2218.
- (83) Martell, M. J.; Soine, T. O. Esters of Bicyclic Aminoalcohols as Potential Anticholinergics III. *J. Pharm. Sci.* **1963**, 52 (4), 331–336.
- (84) King, F. D.; Hadley, M. S.; Joiner, K. T.; Martin, R. T.; Sanger, G. J.; Smith, D. M.; Smith, G. E.; Smith, P.; Turner, D. H.; Watts, E. A. Substituted Benzamides with Conformationally Restricted Side Chains. 5. Azabicyclo[x,y,z] Derivatives as 5-HT₄ Receptor Agonists and Gastric Motility Stimulans. *J. Med. Chem.* **1993**, 36, 683–689.
- (85) Kim, M. G.; Bodor, E. T.; Wang, C.; Harden, T. K.; Kohn, H. C(8) Substituted 1-Azabicyclo[3.3.1]Non-3-Ones and C(8) Substituted 1-Azabicyclo [3.3.1]Nonan-4-Ones: Novel Muscarinic Receptor Antagonists. *J. Med. Chem.* **2003**, 46 (11), 2216–2226.
- (86) Kracht, D.; Saito, S.; Wünsch, B. Synthesis of 1,4-Diazabicyclo[3.3.1]Nonan-6-Ones. *Aust. J. Chem.* **2009**, 62, 1684–1689.
- (87) Ruggli, P. Über Einen Ring Mit Dreifacher Bindung. *Justus Liebigs Ann. Chem.* **1912**, 392 (1), 92–100.
- (88) Ziegler, K.; Ewald, L.; Seib, A. Zur Kenntnis Des “Dreiwertigen” Kohlenstoffs. XIV. Autoxydations- Und Zerfallsgeschwindigkeit Dissoziabler Äthane. *Justus Liebigs Ann. Chem.* **1933**, 504 (1), 182–189.
- (89) Hauser, C. R.; Renfrow, W. B. Certain Condensations Brought about by Bases. I. The Condensation of Ethyl Isobutyrate to Ethyl Isobutyryl-Isobutyrate. *J. Am. Chem. Soc.* **1937**, 59 (10), 1823–1826.
- (90) Schaefer, J. P.; Bloomfield, J. J. The Dieckmann Condensation (Including the Thorpe-Ziegler Condensation). *Org. React.* **1967**, 15, 1–203.
- (91) Carrick, W. L.; Fry, A. A Carbon-14 Isotope Effect Study of the Dieckmann Condensation of Diethyl Phenylene-Diacetate. *J. Am. Chem. Soc.* **1955**, 77 (16), 4381–4387.

- (92) Pedersen, K. J. The Ketonic Decomposition of Beta-Keto Carboxylic Acids. *J. Am. Chem. Soc.* **1929**, *51* (7), 2098–2107.
- (93) Ferris, J. P.; Miller, N. C. The Decarboxylation of β -Keto Acids. II. An Investigation of the Bredt Rule in Bicyclo[3.2.1]Octane Systems. *J. Am. Chem. Soc.* **1966**, *88* (15), 3522–3527.
- (94) Krapcho, A. P.; Ciganek, E. Chapter 1: The Krapcho Dealkoxycarbonylation Reaction of Esters with α -Electron-Withdrawing Substituents. *Org. React.* **2013**, *81*, 1–535.
- (95) Krapcho, A. P.; Glynn, G. A.; Grenon, B. J. The Decarboxylation of Geminal Dicarbethoxy Compounds. *Tetrahedron Lett.* **1967**, *3*, 215–217.
- (96) Krapcho, A. P.; Lovey, A. J. Decarbalkoxylations of Geminal Diesters, β -Keto Esters and α -Cyano Esters Effected by Sodium Chloride in Dimethyl Sulfoxide. *Tetrahedron Lett.* **1973**, *14* (12), 957–960.
- (97) Krapcho, A. P.; Jahngen, E. G. E.; Lovey, A. J. Decarbalkoxylations of Geminal Diesters and β -Keto Esters in Wet Dimethyl Sulfoxide. Effect of Sodium Chloride on the Decarbalkoxylation Rates of Mono- and Disubstituted Malonate Esters. *Tetrahedron Lett.* **1974**, *15* (13), 1091–1094.
- (98) Krapcho, A. P.; Weimaster, J. F.; Eldridge, J. M.; Jahngen, E. G. E.; Lovey, A. J.; Stephens, W. P. Synthetic Applications and Mechanism Studies of the Decarbalkoxylations of Geminal Diesters and Related Systems Effected in Me₂SO by Water and/or by Water with Added Salts. *J. Org. Chem.* **1978**, *43* (1), 138–147.
- (99) Schotten, C. Ueber Die Oxydation Des Piperidins. *Berichte der Dtsch. Chem. Gesellschaft* **1884**, *17* (2), 2544–2547.
- (100) Baumann, E. Ueber Eine Einfache Methode Der Darstellung von Benzoessäureäthern. *Berichte der Dtsch. Chem. Gesellschaft* **1886**, *19* (2), 3218–3222.
- (101) Marchionni, C.; Vogel, P.; Roversi, P. The Simultaneous Double Diels-Alder Addition of 1,1-Bis(3,5-Dimethylfur-2-Yl)Ethane; Toward a New, Asymmetric Synthesis of Long-Chain Polypropionate Fragments and Analogues. *Tetrahedron Lett.* **1996**, *37*, 4149–4152.

- (102) Radha Krishna, P.; Sreeshailam, A. A Stereoselective Formal Total Synthesis of (+)-Hyperaspine via a Tandem Aza-Michael Reaction. *Tetrahedron Lett.* **2007**, *48* (39), 6924–6927.
- (103) Finkelnstein, H. Darstellung Organischer Jodide Aus Den Entsprechenden Bromiden Und Chloriden. *Berichte der Dtsch. Chem. Gesellschaft* **1910**, *43* (2), 1528–1532.
- (104) John, J. P.; Jost, J.; Novikov, A. V. Synthesis of Plakortethers F and G. *J. Org. Chem.* **2009**, *74*, 6083–6091.
- (105) Burgess, J. *Metal Ions in Solution*, 1st ed.; Ellis Horwood: New York, 1978.
- (106) Karplus, M. Vicinal Proton Coupling in Nuclear Magnetic Resonance. *J. Am. Chem. Soc.* **1963**, *85* (15), 2870–2871.
- (107) Nourse, J. G. Pseudochirality. *J. Am. Chem. Soc.* **1975**, *97* (16), 4594–4601.
- (108) Gribble, G. W.; Ferguson, D. C. Reactions of Sodium Borohydride in Acidic Media. Selective Reduction of Aldehydes with Sodium Triacetoxyborohydride. *J. Chem. Soc. Chem. Commun.* **1975**, No. 13, 535–536.
- (109) Nutaitis, C. F.; Gribble, G. W. Chemoselective Reduction of Aldehydes with Tetra-n-Butylammonium Triacetoxyborohydride. *Tetrahedron Lett.* **1983**, *24* (40), 4287–4290.
- (110) Abdel-Magid, A. F.; Mehrman, S. J. A Review on the Use of Sodium Triacetoxyborohydride in the Reductive Amination of Ketones and Aldehydes. *Org. Process Res. Dev.* **2006**, *10* (5), 971–1031.
- (111) Evans, D. A.; T., C. K. The Directed Reduction of β -Hydroxy Ketones Employing $\text{Me}_4\text{NHB}(\text{OAc})_3$. *Tetrahedron Lett.* **1986**, *27* (49), 5939–5942.
- (112) Milas, N. A.; Sussman, S. The Hydroxylation of the Double Bond. *J. Am. Chem. Soc.* **1936**, *58*, 1302–1304.
- (113) Vanrheenen, V.; Kelly, R. C.; Cha, D. Y. An Improved Catalytic OsO_4 Oxidation of Olefins to *Cis*-1,2-Glycols Using Tertiary Amine Oxides as the Oxidant. *Tetrahedron Lett.* **1976**, *23*, 1973–1976.
- (114) Hentges, S. G.; Sharpless, K. B. Asymmetric Induction in the Reaction of Osmium Tetroxide with Olefins. *J. Org. Chem.* **1980**, *102* (12), 4263–4265.
- (115) Corey, E. J.; Jardine DaSilva, P.; Virgil, S.; Yuen, P.; Connell, R. D.

- Enantioselective Vicinal Hydroxylation of Terminal and *E*-1,2-Disubstituted Olefins by a Chiral Complex of Osmium Tetraoxide. An Effective Controller System and a Rational Mechanistic Model. *J. Am. Chem. Soc.* **1989**, *111*, 9243–9244.
- (116) Criegee, R. Osmiumsäure-ester Als Zwischenprodukte Bei Oxydationen. *Justus Liebigs Ann. Chem.* **1936**, *522* (1), 75–96.
- (117) Criegee, R.; Marchand, B.; Wonnowius, H. Zur Kenntnis Der Organischen Osmium-Verbindungen. *Justus Liebigs Ann. Chem.* **1942**, *559*, 99–133.
- (118) Varma, R. S.; Naicker, K. P. Ultrasound Accelerated Permanganate Oxidation: An Improved Procedure for the Synthesis of 1,2-*Cis* Diols from Olefins. *Tetrahedron Lett.* **1998**, *39*, 7463–7466.
- (119) Malaprade, L. Action of Polyalcohol on Periodic Acid. Analytical Application. *Bull. Soc. Chim. Fr.* **1928**, *43*, 683–696.
- (120) Criegee, R. Eine Oxydative Spaltung von Glykolen. *Berichte der Dtsch. Chem. Gesellschaft* **1931**, *64* (2), 260–266.
- (121) Pappo, R.; Allen, D. S.; Lemieux, R. U.; Johnson, W. S. Osmium Tetroxide-Catalyzed Periodate Oxidation of Olefinic Bonds. *J. Org. Chem.* **1956**, *21*, 478–479.
- (122) Braddock, D. C.; Cansell, G.; Hermitage, S. A. *Ortho*-Substituted Iodobenzenes as Novel Organocatalysts for Bromination of Alkenes. *Chem. Commun.* **2006**, No. 23, 2483–2485.
- (123) Horner, L.; Hoffmann, H.; Wippel, H. G. Phosphinoxyde Als Olefinierungsreagenzien. *Chem. Ber.* **1958**, *91* (1), 61–63.
- (124) Wadsworth, W. S.; Emmons, W. D. The Utility of Phosphonate Carbanions in Olefin Synthesis. *J. Am. Chem. Soc.* **1961**, *83* (7), 1733–1738.
- (125) Wadsworth, W. S. Synthetic Applications of Phosphoryl-Stabilized Anions. *Org. React.* **1977**, *25*, 73–253.
- (126) Dieckmann, W. Ueber Ein Ringförmiges Analogon Des Ketipinsäureesters. *Berichte der Dtsch. Chem. Gesellschaft* **1894**, *27* (1), 965–966.
- (127) Wissgott, U.; Bortlik, K. Prospects for New Natural Food Colorants. *Trends Food Sci. Technol.* **1996**, *7* (9), 298–302.

- (128) Gengatharan, A.; Dykes, G. A.; Choo, W. S. Betalains: Natural Plant Pigments with Potential Application in Functional Foods. *LWT - Food Sci. Technol.* **2015**, *64* (2), 645–649.
- (129) Delgado-Vargas, F.; Jiménez, A. R.; Paredes-López, O. Natural Pigments: Carotenoids, Anthocyanins, and Betalains - Characteristics, Biosynthesis, Processing, and Stability. *Crit. Rev. Food Sci. Nutr.* **2000**, *40* (3), 173–289.
- (130) Hilpert, H.; Dreiding, A. S. Über Die Totalsynthese Von Betalainen. *Helv. Chim. Acta* **1984**, *67*, 1547–1561.
- (131) Zhong, Y. L.; Zhou, H.; Gauthier, D. R.; Lee, J.; Askin, D.; Dolling, U. H.; Volante, R. P. Practical and Efficient Synthesis of *N*-Halo Compounds. *Tetrahedron Lett.* **2005**, *46* (7), 1099–1101.
- (132) Wang, J.; Liang, Y. L.; Qu, J. Boiling Water-Catalyzed Neutral and Selective *N*-Boc Deprotection. *Chem. Commun.* **2009**, No. 34, 5144–5146.
- (133) Brown, H. C.; Narasimhan, S.; Choi, Y. M. Selective Reductions. 30. Effect of Cation and Solvent on the Reactivity of Saline Borohydrides for Reduction of Carboxylic Esters. Improved Procedures for the Conversion of Esters to Alcohols by Metal Borohydrides. *J. Org. Chem.* **1982**, *47* (24), 4702–4708.
- (134) Cheng, Y.; Prusoff, W. H. Relationship between the Inhibition Constant (K_i) and the Concentration of Inhibitor Which Causes 50 per Cent Inhibition (I_{50}) of an Enzymatic Reaction. *Biochem. Pharmacol.* **1973**, *22* (23), 3099–3108.
- (135) Hunter, J. C.; Leighton, G. E.; Meecham, K. G.; Boyle, S. J.; Horwell, D. C.; Rees, D. C.; Hughes, J. CI-977, a Novel and Selective Agonist for the κ -Opioid Receptor. *Br. J. Pharmacol.* **1990**, *101* (1), 183–189.
- (136) Codd, E. E.; Shank, R. P.; Schupsky, J. J.; Raffa, R. B. Serotonin and Norepinephrine Uptake Inhibiting Activity of Centrally Acting Analgesics: Structural Determinants and Role in Antinociception. *J. Pharmacol. Exp. Ther.* **1995**, *274* (3), 1263–1270.
- (137) Mignat, C.; Wille, U.; Ziegler, A. Affinity Profiles of Morphine, Codeine, Dihydrocodeine and Their Glucuronides at Opioid Receptor Subtypes. *Life Sci.* **1995**, *56* (10), 793–799.
- (138) Varani, K.; Rizzi, A.; Calo', G.; Bigoni, R.; Toth, G.; Guerrini, R.; Gessi, S.;

- Salvadori, S.; Borea, P. A.; Regoli, D. Pharmacology of [Tyr¹]Nociceptin Analogs: Receptor Binding and Bioassay Studies. *Naunyn-Schmiedeberg's Arch Pharmacol* **1999**, *360*, 270–277.
- (139) Bourdier, T.; Poisnel, G.; Dhilly, M.; Delamare, J.; Henry, J.; Debruyne, D.; Barré, L. Synthesis and Biological Evaluation of N-Substituted Quinolinimides, as Potential Ligands for in Vivo Imaging Studies of δ -Opioid Receptors. *Bioconjug. Chem.* **2007**, *18* (2), 538–548.
- (140) DeHaven-Hudkins, D. L.; Fleissner, L. C.; Ford-Rice, F. Y. Characterization of the Binding of [3H](+)-Pentacozine to σ Recognition Sites in Guinea Pig Brain. *Eur. J. Pharmacol.* **1992**, *227* (4), 371–378.
- (141) Mach, R. H.; Smith, C. R.; Childers, S. R. Ibogaine Possesses a Selective Affinity for σ_2 Receptors. *Life Sci.* **1995**, *57* (4), 57–62.
- (142) Lever, J. R.; Gustafson, J. L.; Xu, R.; Allmon, R. L.; Lever, S. Z. σ_1 and σ_2 Receptor Binding Affinity and Selectivity of SA4503 and Fluoroethyl SA4503. *Synapse* **2006**, *59* (6), 350–358.
- (143) Molecular Operating Environment (MOE), 2019.01; Chemical Computing Group ULC, 1010 Sherbrooke St. West, Suite #910, Montreal, QC, H3A 2R7. 2019.
- (144) Lemaire-Audoire, S.; Vogel, P. Total, Asymmetric Synthesis of Ethyl D-Ido-4-Heptulosuronate Derivatives Starting from Diethyl 4-Oxopimelate. *Tetrahedron Asymmetry* **1999**, *10* (7), 1283–1293.
- (145) Gmeiner, P.; Feldman, P. L.; Chu-moyer, M. Y.; Rapoport, H. An Efficient and Practical Total Synthesis of (+)-Vincamine from L-Aspartic Acid. *J. Org. Chem.* **1990**, *55*, 3068–3074.
- (146) Rudisill, D. E.; Whitten, J. P. Synthesis of (R)-4-Oxo-5-Phosphonorvaline, an N-Methyl-D-Aspartic Acid Receptor Selective β -Keto Phosphonate. *Synthesis* **1994**, 851–854.
- (147) Geiger, C.; Zelenka, C.; Lehmkuhl, K.; Schepmann, D.; Englberger, W.; Wünsch, B. Conformationally Constrained κ Receptor Agonists: Stereoselective Synthesis and Pharmacological Evaluation of 6,8-Diazabicyclo[3.2.2]Nonane Derivatives. *J. Med. Chem.* **2010**, *53* (10), 4212–4222.
- (148) Wittig, C.; Schepmann, D.; Soeberdt, M.; Daniliuc, C. G.; Wünsch, B.

Stereoselective Synthesis of Conformationally Restricted KOR Agonists Based on the 2,5-Diazabicyclo[2.2.2]Octane Scaffold. *Org. Biomol. Chem.* **2017**, *15* (31), 6520–6540.

Curriculum vitae

Personal Data

Name	Hendrik Jonas
Date of birth	16.06.1993
Place of birth	Ochtrup, Germany
Nationality	german

Education

School

09/1999 – 07/2001	Grundschule auf dem Süsteresch, Schüttorf
09/2001 – 06/2012	Gymnasium Ochtrup
06/2012	Allgemeine Hochschulreife

University

10/2012 – 08/2015	Bachelor of Science, Westfälische Wilhelms Universität, Germany
10/2015 – 09/2017	Master of Science, Westfälische Wilhelms Universität, Germany
11/2017 – 09/2021	Joint PhD student in Medicinal Chemistry Dipt. Scienze e Tecnologie Biologiche Chimiche e Farmaceutiche, Università degli Studi di Palermo, Italy and Institut für Pharmazeutische und Medizinische Chemie, Westfälische Wilhelms Universität, Germany Supervisor: Prof.ssa Patrizia Diana Prof. Bernhard Wunsch
11/2017 – 10/2020	Scholarship, “Ministero dell’Istruzione, dell’Università e Ricerca – MIUR”, Italy
11/2020 – 10/2021	Scientific Assistant, Institut für Pharmazeutische und Medizinische Chemie, Münster, Germany
